# EVALUATION OF CORROSION PROTECTION SYSTEMS AND CORROSION TESTING METHODS FOR REINFORCING STEEL IN CONCRETE

By

Javier Balma

David Darwin

JoAnn P. Browning

Carl E. Locke, Jr.

A Report on Research Sponsored by

KANSAS DEPARTMENT OF TRANSPORTATION
Contract Nos. C1131 and C1281

GERDAU AMERISTEEL CORPORATION

SOUTH DAKOTA DEPARTMENT OF TRANSPORTATION
Project No. SD 2001-05

THE NATIONAL SCIENCE FOUNDATION
Research Grant No. CMS - 9812716

Structural Engineering and Engineering Materials
SM Report No. 76

**THE UNIVERSITY OF KANSAS CENTER FOR RESEARCH, INC.**

**LAWRENCE, KANSAS**

January 2005

# ABSTRACT

Corrosion protection systems for reinforcing steel in concrete and the laboratory methods used to compare these systems are evaluated. The systems evaluated include concrete with a low water-cement ratio, two corrosion inhibitors (Rheocrete 222+ and DCI-S), three microalloyed Thermex-treated steels, one conventional Thermex-treated steel, MMFX microcomposite steel, epoxy-coated steel, two duplex steels (2101 and 2205), and three heats of uncoated normalized steel, used as control specimens. The duplex steels were tested in both "as-rolled" and pickled conditions. The corrosion protection systems are evaluated using the rapid macrocell, Southern Exposure, and cracked beam tests. Some corrosion protection systems are also evaluated using the ASTM G 109 test. The corrosion rate, corrosion potential, and mat-to-mat resistance are used to compare the systems. An economic analysis is performed to determine the most cost-effective corrosion protection systems.

The degree of correlation between the Southern Exposure, cracked beam, and rapid macrocell tests is determined. The coefficient of variation is used to compare the variability in the corrosion rates and the total corrosion losses obtained using the different test methods. Impedance spectroscopy analysis is performed to obtain equivalent electrical circuits to represent the rapid macrocell and Southern Exposure tests.

Results show that microalloyed steel and conventional Thermex-treated steel show no improvement in corrosion resistance when compared to conventional normalized steel. In mortar or concrete with a low water-cement ratio, corrosion losses are lower than observed at higher water-cement ratios for either cracked or uncracked mortar or concrete. In uncracked mortar or concrete (rapid macrocell and Southern Exposure test) containing corrosion inhibitors, corrosion losses are lower than observed at the same water-cement ratio but with no inhibitor. For concrete containing inhibitors, with cracks above and parallel to the reinforcing steel (cracked beam test), Rheocrete 222+ improves the corrosion protection of the steel, while DCI-S does not.

MMFX microcomposite steel exhibits corrosion losses between 26 and 60% of the losses of conventional steel. Based on corrosion potentials, the two steels have a similar tendency to corrode. MMFX steel has a higher chloride corrosion threshold than conventional steel. Epoxy-coated steel, intentionally damaged by drilling four 3.2-mm ($^1/_8$-in.) diameter holes in the coating, exhibits low corrosion losses based on the total area of the bar, between 6 and 19% of that of uncoated conventional steel.

Pickled 2101 and 2205 duplex steels exhibit very good corrosion performance. The average corrosion losses for these steels ranged from 0.3 to 1.8% of the corrosion loss for conventional steel, and in most cases, the corrosion potentials indicated a very low tendency to corrode, even when exposed to high chloride concentrations. 2205 steel performs better than 2101 steel when tested in the same condition (pickled or non-pickled). For bars of the same type of steel, pickled bars exhibit lower corrosion rates than the bars that are not pickled. Based on present cost, decks containing pickled 2101 or 2205 steel are more cost effective than decks containing epoxy-coated or uncoated conventional steel.

Results from the rapid macrocell, Southern Exposure, and cracked beam tests show good correlation in most cases, and have similar variability in corrosion rates and losses. In general, total corrosion losses have less variability than corrosion rates.

**Key words:** chlorides, concrete, corrosion, duplex steel, epoxy-coated steel, macrocell, microalloyed steel, MMFX steel, potential, reinforcing steel, stainless steel

## ACKNOWLEDGEMENTS

This report is based on a thesis submitted by Javier Balma in partial fulfillment of the requirements of the Ph.D. degree. Major funding and material support for this research was provided by the Kansas Department of Transportation under Contract Nos. C1131 and C1281, with technical oversight by Dan Scherschligt, Gerdau AmeriSteel Corporation, the National Science Foundation under NSF Grant No. CMS – 9812716, the South Dakota Department of Transportation under project SD 2001-05, with supervision by the SD2001-05 Technical Panel, Dan Johnson (chair), Mark Clausen, Tom Gilsrud, Todd Hertel, Darin Hodges, David Huft, Darin Larson, and Paul Nelson, and the United States Department of Transportation Federal Highway Administration. Additional support for this project was provided by Dupont Corporation, 3M Corporation, Degussa, and LRM Industries.

## TABLE OF CONTENTS

## LIST OF TABLES

## LIST OF FIGURES

# CHAPTER 1

# INTRODUCTION

## 1.1. GENERAL

Corrosion of reinforcing steel in concrete is one of the major durability problems in reinforced concrete structures. The direct and indirect costs of repair and maintenance of concrete bridge decks damaged by corrosion of the reinforcing steel are summarized in a report by the Federal Highway Administration (FHWA) (Yunovich et al. 2002). "The annual direct cost of corrosion for highway bridges is estimated to be $6.43 billion to $10.15 billion, consisting of $3.79 billion to replace structurally deficient bridges over the next 10 years, $1.07 billion to $2.93 billion for maintenance and cost of capital for concrete bridge decks, $1.07 billion to $2.93 billion for maintenance and cost of capital for concrete substructure and superstructures (minus decks), and $0.50 billion for the maintenance painting cost of steel bridges. This gives an average annual cost of corrosion of $8.29 billion. Life-cycle analysis estimates indirect costs to the user due to traffic delays and lost productivity at more than 10 times the direct cost of corrosion." (Yunovich et al. 2002)

Due to the bare pavement policies implemented during the 1950s, deicing salts such as sodium chloride and calcium chloride are used on highways and bridges to keep them free of ice and snow. These chlorides can penetrate the concrete and attack the reinforcing steel, causing corrosion. Bridge decks are most likely to be damaged, but other elements, such as beams and piers, can also be affected due to runoff. Parking structures are also damaged due to corrosion of reinforcing steel in concrete (Weil 1988, Vincent and Rolf 1994). The use of deicing salts is not likely to

be discontinued. In fact, the use of deicing salts rose from 0.6 million tons in 1950 to 10.5 million tons in 1988 (Roberge 2000). Alternative deicing chemicals such as calcium magnesium acetate (CMA) can be used, but they have higher application rates and cost 10 times more than deicing salts (Roberge 2000). Structures in marine environments are also subjected to chloride-induced corrosion (Sagues et al. 1990).

Corrosion of reinforcing steel in concrete (see Section 1.2) causes cracking and spalling of the concrete due to the increased volume of corrosion products compared to the original steel. Loss of bond between the reinforcing steel and the concrete due to cracking of the concrete or severe corrosion (Amleh and Mirza 1999) and loss of steel area also reduce the strength of the member.

A wide variety of corrosion protection systems have been developed to protect reinforcing steel from corrosion. These include barriers that prevent chlorides from reaching the steel (overlays, sealers), electrochemical methods (cathodic protection), corrosion inhibitors in the concrete, and alternative reinforcing steels, such as stainless steel or epoxy-coated reinforcing bars (Kepler et al. 2000). Section 1.5 provides a description of the corrosion protection systems included in this study.

Several tests can be used to evaluate corrosion protection systems for reinforcing steel in concrete. These can simulate the conditions found in concrete bridge decks, where the top layer of steel is exposed to chlorides while the bottom layer of steel is free from chlorides. The monitoring methods used in these tests are described in Section 1.3.

In the current study, one rapid evaluation test, the corrosion macrocell test, and three bench-scale tests, the Southern Exposure (SE), cracked beam (CB), and ASTM G 109 tests, described in Chapter 2, are used to evaluate the effectiveness of corrosion protection systems. An economic analysis is also performed to compare the

costs of the most effective corrosion protection systems. A comparison between the results of the Southern Exposure, cracked beam, and rapid macrocell tests is performed. For the comparison, the corrosion rates and total corrosion losses for the Southern Exposure and cracked beam tests are plotted versus the same results for the rapid macrocell test to determine the degree of correlation between the tests. The results of the cracked beam test are also compared with those of the Southern Exposure test. The coefficient of variation is used to compare the variability of the corrosion rates and total corrosion losses for individual tests and to compare the variability of the results for the rapid macrocell, Southern Exposure and cracked beam tests. Electrochemical impedance spectroscopy is used to obtain an equivalent electronic circuit for the rapid macrocell and Southern Exposure tests. The balance of this chapter provides background for the tests performed in this study.

## 1.2. CORROSION OF STEEL IN CONCRETE

Metals are usually reduced from chemical compounds (minerals, ores), and a certain amount of energy is needed for this process. The corrosion process returns the metals to their original chemical compounds, releasing the same amount of energy, although at a different rate. Jones (1996) defines corrosion as "the destructive result of chemical reaction between a metal or metal alloy and its environment."

Steel corrosion products (rust) have a greater volume, three to five times more, than the original metal. This produces internal compressive stresses at the steel/mortar interface that produce tension in the surrounding material that results in cracking and spalling of concrete. As cracks grow, concrete permeability increases, allowing greater access of chlorides, oxygen, and water to the steel. The cracks can also cause significant loss of bond between the reinforcing steel and the concrete.

Corrosion of steel in concrete is an electrochemical process that involves the transfer of ions. Electrochemical corrosion requires four factors: an anode, a cathode, an electrolyte, and an electronic circuit. The anode and cathode form at different sites on the reinforcing steel. They can be located either on the same bar or on different bars. The electrolyte is usually the moisture in the concrete, and the electronic circuit between different bars is often provided by steel wire ties or chair supports. To protect the steel against corrosion, at least one of these factors must be eliminated.

The type of corrosion that occurs when the anode and the cathode are located on the same bar is called *microcell* corrosion. *Macrocell* corrosion occurs when the anode and the cathode are located on different bars that are connected electrically, such as two different layers of steel. Figure 1.1 illustrates the process of macrocell corrosion between two layers of steel, as occurs on a bridge deck.

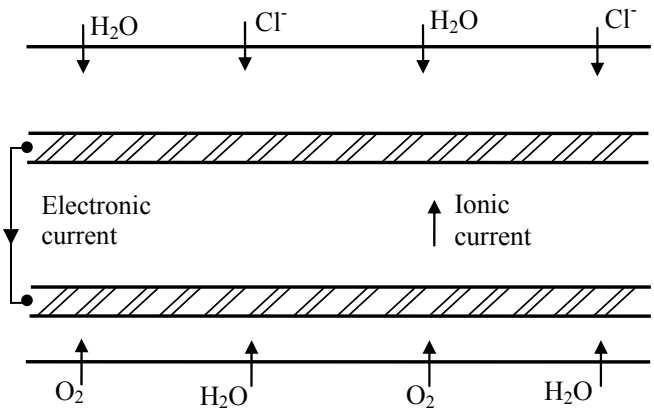


**Figure 1.1 –** Macrocell corrosion process

For reinforcing steel, when oxygen is present, iron is oxidized at the anode, causing ferrous ions to go into solution, and releasing electrons [Eq. (1.1)]. At the cathode, oxygen combines with water and the electrons released at the anode to form hydroxyl ions [Eq. (1.2)].

$$Fe \rightleftharpoons Fe^{2+} + 2e^{-} \quad (1.1)$$

$$^{1}/_{2}O_2 + H_2O + 2e^{-} \rightleftharpoons 2OH^{-} \quad (1.2)$$

The ferrous ions combine with hydroxyl ions to produce ferrous hydroxide [Eq. (1.3]), which is greenish-black in color. The ferrous hydroxide is oxidized in the presence of moisture and oxygen to produce ferric hydroxide [Eq. (1.4)], which is red-brown in color. The ferric hydroxide can dehydrate to form ferric oxide, which can be black or red in color, and is commonly known as rust [Eq. (1.5)].

$$Fe^{2+} + 2OH^{-} \longrightarrow Fe(OH)_2 \quad (1.3)$$

$$4Fe(OH)_2 + 2H_2O + O_2 \longrightarrow 4Fe(OH)_3 \quad (1.4)$$

$$2Fe(OH)_3 \longrightarrow Fe_2O_3 + 3H_2O \quad (1.5)$$

Reinforcing steel in concrete, however, is normally passive due to the high alkalinity of the cement paste (pH = 13.0 to 13.5). This high alkalinity leads to the formation of a γ-ferric oxide layer on the surface of the steel that protects it from corrosion.

$$2Fe(OH)_2 + {}^{1}/_{2}O_2 \longrightarrow 2\gamma\text{-}FeOOH + H_2O \quad (1.6)$$

This passive film can be destroyed by two mechanisms: (1) the presence of chloride ions, which results in a localized breakdown of the passive film, and (2) carbonation, which results in a decrease in the pH of the concrete, thus reducing the passivity.

For a concrete bridge deck or parking structure slab, chlorides typically enter from the top surface. Once the chlorides reach the top mat of steel, its electrochemical or corrosion potential will drop, becoming more negative. The potential of the bottom mat of steel will retain a more positive value. This difference in potential results in the formation of a galvanic cell that drives the corrosion process.

In the presence of chlorides, iron at the anode is oxidized as before [Eq. (1.1)] and the ferrous ions react with chloride ions to form a soluble iron-chloride complex [Eq. (1.7)]. The iron-chloride complex reacts with hydroxyl ions and forms ferrous hydroxide [Eq. (1.8)].

$$Fe^{2+} + Cl^{-} \longrightarrow [\text{FeCl complex}]^{+} \tag{1.7}$$

$$[\text{FeCl complex}]^{+} + 2OH^{-} \longrightarrow Fe(OH)_2 + Cl^{-} \tag{1.8}$$

The ferrous hydroxide is oxidized to ferric hydroxide that, in turn, dehydrates to form ferric oxide, as shown in Eqs. (1.4) and (1.5). At the cathode, hydroxyl ions are formed when oxygen combines with moisture and the electrons released at the anode, as before [Eq. (1.2)]. As demonstrated by Eqs. (1.7) and (1.8), the chloride ions are not consumed and remain available to continue contributing to corrosion. Chloride attack on reinforcing steel usually occurs as pitting corrosion. Pitting will continue to increase if the chloride content exceeds a specific concentration. This chloride threshold is believed to be dependent on the concentration of hydroxyl ions (Hausmann 1967, Kayyali and Haque 1995).

Chloride migration into concrete is usually modeled using Fick's Second Law of Diffusion, which is represented by

$$\frac{\partial C}{\partial t} = D_c \frac{\partial^2 C}{\partial x^2} \tag{1.9}$$

where

$C$ = chloride concentration

$D_c$ = diffusion coefficient

$t$ = time

$x$ = depth

The solution to Eq. (1.9) is:

$$C(x,t,C_0,D_c) = C_0\left[1 - erf\,\frac{x}{2\sqrt{tD_c}}\right] \tag{1.10}$$

where

$C_0$ = surface concentration

*erf* = error function

## 1.3 CORROSION MONITORING METHODS

The corrosion of metals can be evaluated using a number of methods. These include measuring corrosion potential, macrocell corrosion rate, linear polarization resistance, and electrochemical impedance spectroscopy (EIS). The following is a brief description of each method.

### 1.3.1 Corrosion Potential

The electrochemical potential of a metal is a measure of its thermodynamic state and its tendency to corrode. It is measured in volts. The more negative the potential, the higher the tendency to corrode. The potential serves as an indicator rather than as a direct measure of the corrosion rate. When a macrocell is formed, the driving force is the difference in potential between the anodic and cathodic sites. As the potential difference increases with all other variables constant, so does the corrosion rate, and the anode will always have a more negative potential than the cathode.

The corrosion potential of a bar is determined by measuring the potential difference between the bar and a reference electrode. A reference electrode "has a

relatively fixed value of potential, regardless of the environment" (Uhlig 1985) and often consists of a metal that is submerged in a solution containing its own ions. The reaction in the standard hydrogen electrode (SHE) [Eq. (1.11)] has been chosen to represent "zero potential". The reaction that occurs in a reference electrode is always known, as is its *half-cell potential* with respect to the standard hydrogen electrode.

$$2H^+ + 2e^- \rightleftharpoons H_2 \qquad (1.11)$$

The two most common reference electrodes are the saturated calomel electrode (SCE) and the copper-copper sulfate electrode (CSE). The differences in potential between the SHE and these two electrodes, as well as their half-cell reactions, are shown in Table 1.1.

**Table 1.1 –** Standard reference electrodes

| Electrode | Half-cell reaction | Potential vs. SHE (V) |
|---|---|---|
| Copper-copper sulfate (CSE) | $CuSO_4 + 2e^- \longrightarrow Cu + SO_4^{2-}$ | +0.318 |
| Saturated calomel (SCE) | $HgCl_2 + 2e^- \longrightarrow 2Hg + 2Cl^-$ | +0.241 |
| Standard hydrogen (SHE) | $2H^+ + 2e^- \longrightarrow H_2$ | 0.000 |

ASTM C 876 is used to evaluate the corrosion potential of uncoated reinforcing steel in concrete. Table 1.2 shows the probability of corrosion based on potential measurements, as presented in ASTM C 876.

**Table 1.2 –** Interpretation of half cell readings (ASTM C 876)

| Half-Cell Reading (V) | | Interpretation |
|---|---|---|
| CSE * | SCE * | |
| > -0.200 | > 0.125 | greater than 90% probability that corrosion is not occuring |
| -0.200 to -0.350 | -0.125 to -0.275 | corrosion activity is uncertain |
| < -0.350 | < -0.275 | greater than 90% probability that corrosion is occuring |

* **CSE**: copper-copper sulfate electrode, **SCE**: saturated calomel electrode

### 1.3.2 Macrocell Corrosion Rate

The corrosion rate of a reinforcing bar in a corrosion test where the corrosion current density has been measured can be obtained using Faraday's law, as shown in Eq. (1.12). The current density *i* can be obtained from a test where a macrocell has formed or from polarization resistance measurements, as explained below.

$$Rate = K\frac{ia}{nFD} \tag{1.12}$$

where *Rate* is given in μm/year, and

*K* = unit conversion factor = $31.5\times10^4$

*i* = current density, μA/cm$^2$ [*i* is equal to $i_m$ from Eq. (1.14) or $i_c$ from Eq. (1.15)]

*a* = atomic weight of the metal

For iron, *a* = 55.8 g/g-atom

*n* = number of ion equivalents exchanged

For iron, *n* = 2 equivalents

*F* = Faraday's constant

*F* = 96500 Coulombs/equivalent

*D* = density of the metal, g/cm$^3$

For iron, *D* = 7.87 g/cm$^3$

Using Eq. (1.12), the corrosion rate for iron can be expressed in terms of the corrosion current density as

$$Rate = 11.59i \tag{1.13}$$

In a test where a macrocell has formed, the current density can be obtained by measuring the voltage drop across a resistor that connects the anode and the cathode within the cell.

$$i_m = \frac{V}{RA} \tag{1.14}$$

where

$i_m$ = macrocell current density, μA/cm$^2$

$V$ = voltage drop across the resistor, mV

$R$ = resistance of the resistor, kΩ

$A$ = area of exposed metal at the anode bar, cm$^2$

### 1.3.3 Polarization Resistance

The corrosion current density can also be determined in a polarization resistance test. Polarization resistance is used to determine the microcell corrosion rate of a metal. A potentiostat is used to impose a range of potentials on the metal, usually –10 to +10 mV versus the open circuit corrosion potential, and measure the corresponding corrosion current. A polarization curve (Figure 1.2) is obtained and a portion of this curve is linear. The slope of the linear portion of the curve is called the polarization resistance $R_p$ and is proportional to the corrosion resistance of the metal.

The corrosion current density is given by the Stern-Geary relationship (Stern and Geary 1957):

$$i_c = \frac{B}{R_p} \tag{1.15}$$

where

$i_c$ = corrosion current density, μA/cm$^2$,

$R_p$ = polarization resistance (slope of linear portion of polarization curve), kΩ·cm$^2$.

$$B = \frac{\beta_a \beta_c}{2.303(\beta_a + \beta_c)} = \text{Stern-Geary constant, mV} \tag{1.16}$$

$\beta_a$ = anodic Tafel slope

$\beta_c$ = cathodic Tafel slope

The corrosion rate is then determined using Eq. (1.12).

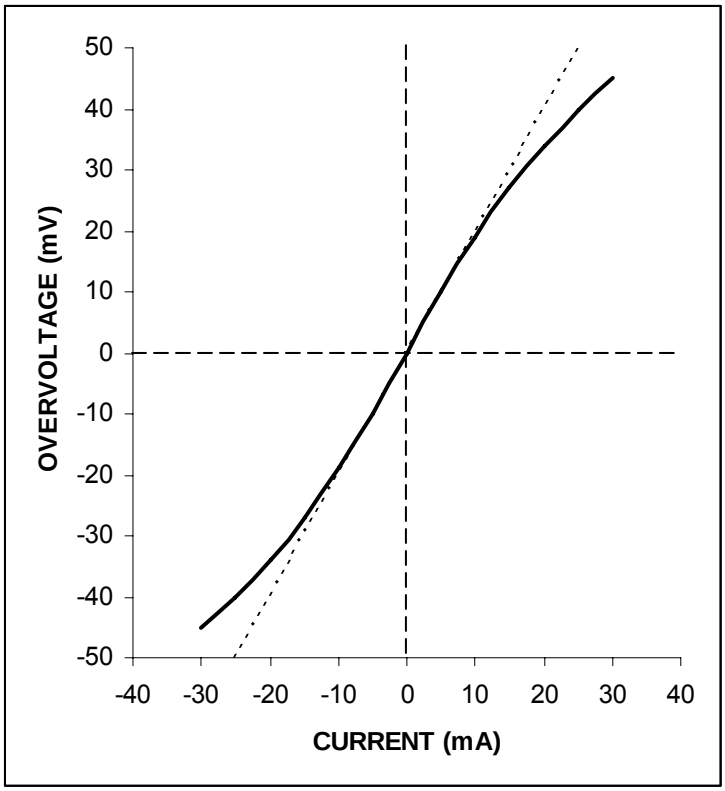


**Figure 1.2 –** Hypothetical polarization curve [adapted from Jones (1996)]

### 1.3.4 Electrochemical Impedance Spectroscopy (EIS)

In electrochemical impedance spectroscopy tests, a small-amplitude alternating potential is applied to an electrochemical cell over a range of frequencies and the current through the cell is measured. The impedance, or resistance to current flow, is measured. Any electrochemical cell can be modeled with an equivalent circuit consisting of a combination of resistors, capacitors, and inductors. The analysis of the electrochemical impedance data is performed to find an equivalent

circuit that fits the measured data. This section gives a description of the basic concepts of electrochemical impedance and its application to reinforced concrete.

#### 1.3.4.1 EIS Concepts

Ohm's Law defines impedance as the ratio between the voltage and the current.

$$Z = \frac{E}{I} \tag{1.17}$$

where

Z = impedance, ohms

E = voltage, volts

I = current, amps

The impedance is the resistance of the system to current flow. Table 1.3 shows the impedance provided and the relationship between current and voltage for common circuit elements. "In a potentiostated electrochemical cell, the input is the potential and the output is the current. Electrochemical cells are not linear. Doubling the voltage will not necessarily double the current." (Gamry 1999). If the amplitude of the excitation signal applied to the cell is small enough (1 to 10 mV), however, the response will be linear, since the signal will be confined to the linear portion of the current versus voltage curve. When a linear relationship exists between the input and the response, an equivalent circuit composed of resistors, capacitors, and inductors may be used to model the response.

**Table 1.3 –** Common circuit elements

| Element | Current vs. voltage | Impedance |
|---|---|---|
| Resistor | $E = IR$ | $Z = R$ |
| Inductor | $E = L\ \mathrm{d}i/\mathrm{d}t$ | $Z = \mathrm{j}\omega L$ |
| Capacitor | $E = C\ \mathrm{d}E/\mathrm{d}t$ | $Z = 1/\mathrm{j}\omega C$ |

where

$R$ = resistance
$L$ = inductance
$C$ = capacitance
$i$ = current
$E$ = potential
$\omega = 2\pi f$ = angular frequency, radians/second
$f$ = frequency, hertz
$\mathrm{j} = \sqrt{-1}$

Using the notation in Table 1.3 it is possible to represent impedance as a vector in the real-imaginary plane, as shown in Figure 1.3. The value of impedance is defined by the magnitude $|Z|$ and the angle its vector makes with the real positive axis $\phi$. Impedance can also be defined by the magnitudes of its real and imaginary components $Z'$ and $Z''$, respectively, where $Z' = Z\cos\phi$, and $Z'' = Z\sin\phi$. The magnitude, or modulus, of the impedance is given by $|Z| = \sqrt{(Z')^2 + (Z'')^2}$

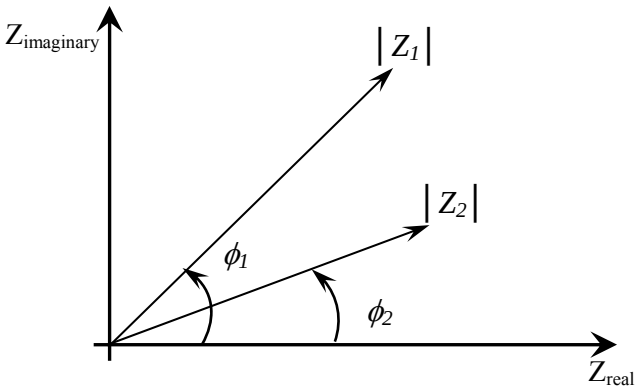


**Figure 1.3 –** Argand diagram

Under direct current (zero frequency), the impedance in a circuit is provided by resistors, while inductors act as short circuits and capacitors act as open circuits. When an alternating current is applied, the resistance to current flow is caused by all circuit elements (capacitors, inductors, and resistors). The applied AC voltage is in the form of a sine or cosine wave [Eq. (1.18)]. When the equivalent circuit is composed only of resistors, the measured current is also in the form of a sine or cosine wave, with the same frequency as the voltage, but with different amplitude and with no phase-shift. When the equivalent circuit contains capacitors or inductors, the measured current will exhibit a phase shift as well as a different amplitude [Eq. (1.19)].

$$E = E_o \cos(\omega t) \tag{1.18}$$

$$I = I_o \cos(\omega t - \phi) \tag{1.19}$$

where

$E_o$ = peak amplitude of the applied voltage

$I_o$ = peak amplitude of the response current

$\phi$ = phase angle

Therefore, the impedance can also be expressed as

$$Z = \frac{E}{I} = \frac{E_o \cos(\omega t)}{I_o \cos(\omega t - \phi)} = Z_o \frac{\cos(\omega t)}{\cos(\omega t - \phi)} \tag{1.20}$$

where $Z_o$ = impedance magnitude.

### 1.3.4.2 Equivalent Circuits

A number of standard equivalent circuits have been formulated. Figure 1.4 shows a Randles circuit, a simple circuit that is usually the starting point for more complex corrosion models. It consists of a resistor $R_s$, which represents the solution

resistance, in series with a resistor $R_{ct}$ and a capacitor $C_{dl}$ in parallel, which represent the double layer. The double layer is formed between the working electrode and the electrolyte surrounding it and consists of ions in the electrolyte that adhere to the surface of the working electrode.

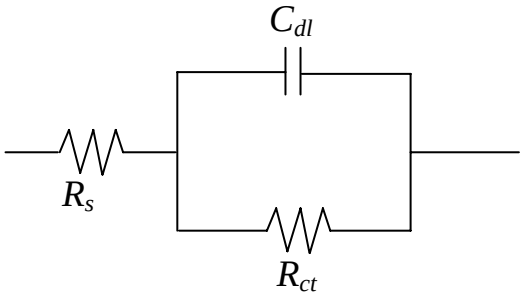


**Figure 1.4 –** Randles circuit

The solution resistance $R_s$ depends on the temperature, the type of ions, their concentration, and the geometry of the area through which the current is carried (Gamry 1999). For a uniform current, the solution resistance can be expressed as:

$$R_s = \rho \frac{l}{A} \tag{1.21}$$

where,

$\rho$ = solution resistivity

$l$, $A$ = length and area which define the geometry of the area through which the current is carried.

Electrochemical cells usually do not have a defined electrolyte area or a uniform current distribution. The determination of the current flow path and the area of the electrolyte represent key problems when calculating solution resistance.

The double layer capacitance $C_{dl}$ represents the corroding interface, and depends on many variables: electrode potential, ion concentration, type of ions, temperature, and roughness of the electrode, among others.

The resistor $R_{ct}$ represents the charge transfer resistance. When a reaction such as shown in Eq. (1.1) takes place, charge is transferred. For the case where the concentrations of the reactants in the bulk and at the electrode surface are the same, the overpotential (potential change from the open-circuit potential caused by the half-cell reaction) is very small, and the system is in equilibrium, the charge transfer resistance may be expressed as

$$R_{ct} = \frac{RT}{nFi_0} \tag{1.22}$$

where

$R$ = gas constant

$T$ = temperature

$n$ = number of electrons

$F$ = Faraday's constant

$i_0$ = exchange current density

The value of $R_{ct}$ is often related to that of the polarization resistance, which means that a decrease in $R_{ct}$ is associated with an increase in the corrosion rate [Eq. (1.15)]

The data obtained from electrochemical impedance spectroscopy is usually presented in two ways, using Nyquist and Bode plots. In a Nyquist plot (Figure 1.5), the real part of the impedance is plotted on the horizontal axis and the imaginary part of the impedance on the vertical axis. In a Nyquist plot, there is no indication of the frequency at which the data points are recorded. In a Bode plot (Figure 1.6), the log of the frequency is plotted on the horizontal axis, and the magnitude of the impedance

$|Z|$ and the phase shift $\phi$ are plotted on the vertical axis. Figures 1.5 and 1.6 show Nyquist and Bode plots for the Randles circuit shown in Figure 1.4.

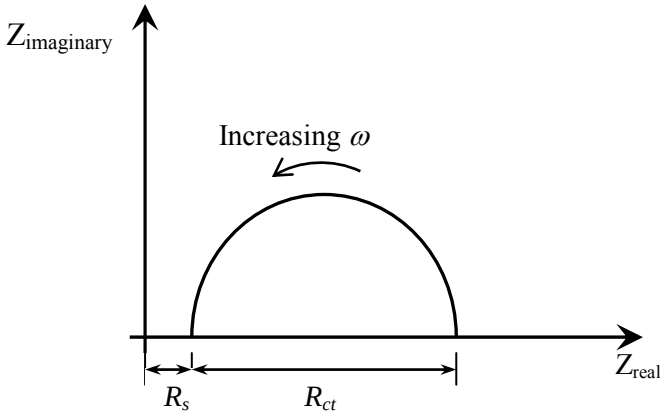


**Figure 1.5 –** Nyquist plot for Randles circuit

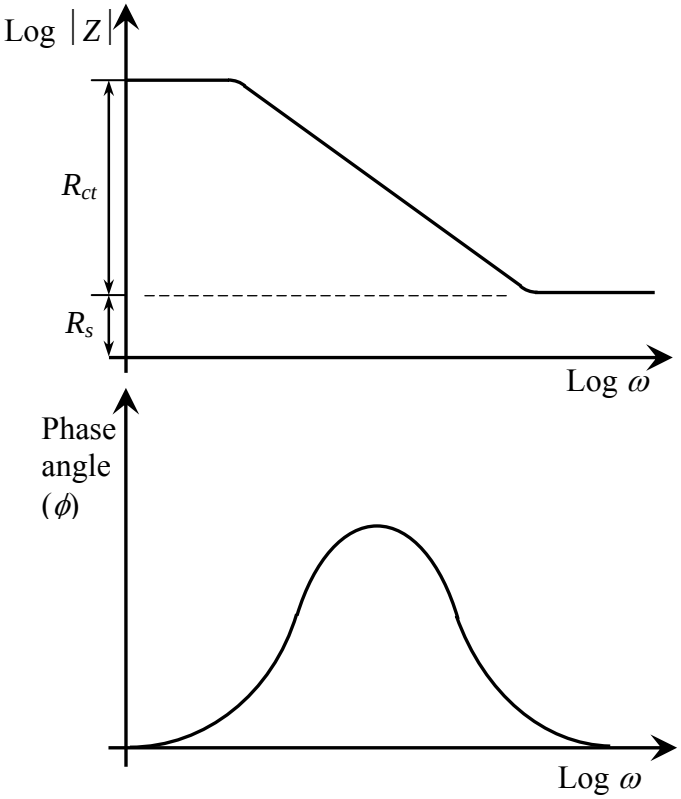


**Figure 1.6 –** Bode plot for Randles circuit

As shown in the two plots, at high frequencies, current flows easily through the capacitor, which acts like an open circuit, with no current flowing through $R_{ct}$. Thus, the impedance of the circuit is equal to the solution resistance $R_s$. At very low frequencies, the capacitor becomes fully charged and does not conduct current, and the magnitude of the impedance is equal to the sum of $R_s$ and $R_{ct}$. At intermediate frequencies, current flows through both $R_{ct}$ and $C_{dl}$. The semicircle obtained at intermediate frequencies (Figure 1.5), known as a capacitive arc, is determined by the impedance of the $R_{ct}$-$C_{dl}$ combination.

Research of steel-concrete systems performed using AC impedance shows behaviors different than that of the simple Randles circuit. First, more than one semicircle in the Nyquist plot (Figure 1.7a) has been observed. Several authors have suggested that a more accurate representation of the steel-concrete system should include more than one combination of capacitor and resistor, as shown in Figure 1.7b, where $R_f$ and $C_f$ are the resistance and capacitance of the surface film on the electrode.

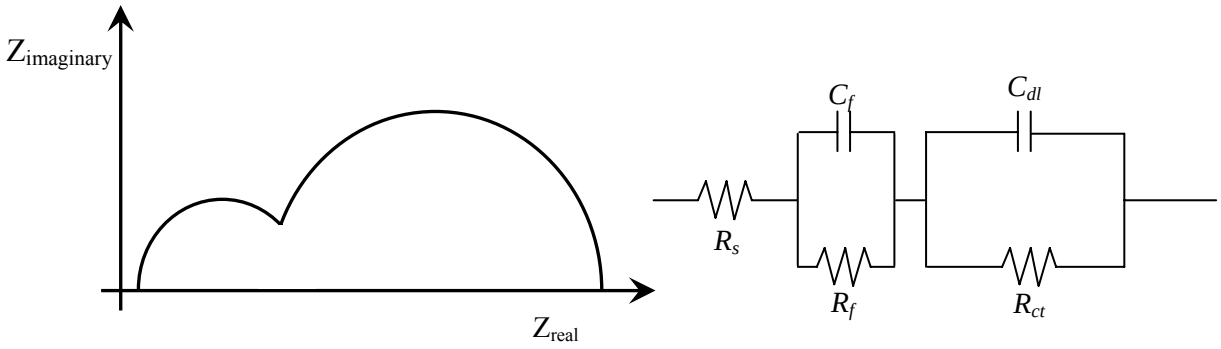


**Figure 1.7 –** (a) Nyquist plot showing two semicircles, (b) equivalent circuit used to model behavior in (a).

Second, the Nyquist diagram may contain a tail at very low frequencies (Figure 1.8a). This effect is related to diffusion control and is modeled with the addition of a Warburg impedance in series with the resistor in the Randles circuit (Figure 1.8b).

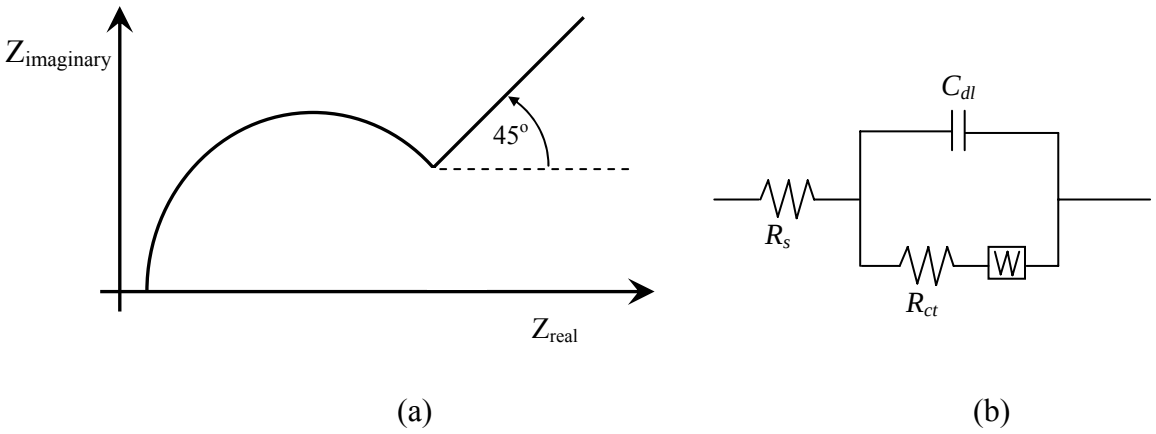


**Figure 1.8 –** (a) Nyquist plot showing low frequency tail, (b) equivalent circuit used to model behavior in (a).

A Warburg impedance is described by Eq. (1.23), where $\sigma$ is the Warburg coefficient [Eq. (1.24)]. As shown in Eq. 1.23, the real and imaginary parts of the Warburg impedance are equal and proportional to $1/\sqrt{\omega}$.

$$W = \frac{\sigma}{\sqrt{\omega}} - j\frac{\sigma}{\sqrt{\omega}} \tag{1.23}$$

$$\sigma = \frac{RT}{n^2 F^2 A\sqrt{2}}\left(\frac{1}{C_0^*\sqrt{D_0}} + \frac{1}{C_R^*\sqrt{D_R}}\right) \tag{1.24}$$

where

ω = angular frequency

$D_0$ = diffusion coefficient of the oxidant

$D_R$ = diffusion coefficient of the reductant

$A$ = surface area of the electrode

$n$ = number of moles of electrons transferred per mole of oxidized element ($n$ = 2 for oxidation of iron)

$C^*$ = bulk concentration of the diffusing species (moles/cm$^3$)

Because the real and imaginary parts of the Warburg impedance are equal, the Nyquist plot contains a 45$^o$ line at low frequencies, as shown in Figure 1.8a. At high frequencies, the Warburg impedance is very low since it describes a mass transfer process that involves ionic diffusion (Hladky et al. 1980).

Nyquist plots for real systems often tend to be depressed semicircles (Figure 1.9a). This has been explained as due to a non-ideal behavior of the capacitor and is attributed to the non-homogeneous surface of the electrode surface (Hladky et al. 1980). This is modeled by replacing the capacitor in the Randles circuit by a constant-phase element (CPE).

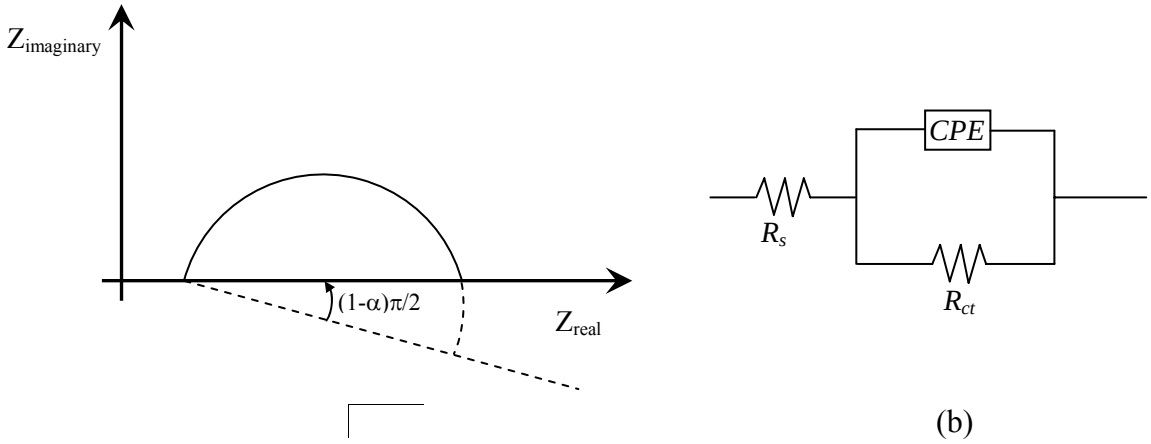


**Figure 1.9 –** (a) Nyquist plot showing depressed semicircle, (b) equivalent circuit used to model behavior in (a).

The impedance of a CPE has the form:

$$Z = \frac{A}{(j\omega)^{\alpha}} \tag{1.25}$$

For a capacitor, $A = 1/C$ ($C$ = capacitance) and $\alpha = 1$. For a CPE, the value of $\alpha$ is less than 1. The depressed semicircle is obtained by the rotation of the ideal semicircle in the Nyquist plot over an angle $(1-\alpha)\pi/2$ (Feliú et al. 1998).

For any given electrochemical cell, one or more of the different behaviors explained above may be observed. It is important to obtain an equivalent circuit that correctly models the data set, although there may be more than one equivalent circuit that provides a good fit and that can be used to model the response of the electrochemical cell (Feliú et al. 1998). Section 1.4.3 describes previous work on electrochemical impedance spectroscopy of steel in concrete and the different interpretations given by researchers to the results obtained from EIS tests.

## 1.4 TESTING METHODS

One rapid evaluation test, the corrosion macrocell test, and three bench-scale tests, the Southern Exposure, cracked beam, and ASTM G 109 tests, are used in the current study. These tests simulate the conditions found in concrete bridge decks subjected to deicing chemicals. The tests use corrosion potential and corrosion rate to evaluate the performance of the corrosion protection systems. Electrochemical impedance spectroscopy tests are performed on the specimens to determine an equivalent electronic circuit for each test. Full details of the specimens and testing procedures are given in Chapter 2. This section describes previous work related to the test methods used in this study.

### 1.4.1 Rapid Evaluation Tests

Rapid evaluation tests include the corrosion potential and corrosion macrocell test. These tests were developed by Martinez et al. (1990). Their research included the development and evaluation of a standard test specimen and the use of corrosion potential and corrosion macrocell tests to evaluate the effect of different concentrations of three deicing chemicals (calcium chloride, sodium chloride, and calcium magnesium acetate) on the corrosion of reinforcing steel cast in mortar.

The specimen used in the early rapid evaluation tests consisted of a 127 mm (5 in.) long, No. 13 [No. 4] reinforcing bar, embedded 76 mm (3 in.) into a 30 mm (1.2 in.) diameter cylinder. The thin mortar cover allowed the chlorides to reach the steel in a short period of time. Because only a portion of the steel is embedded in the mortar, this specimen is often referred to as a "lollipop" specimen. An epoxy band was applied to the steel in the region where it is first exposed (mortar-interface) to prevent crevice corrosion. In the corrosion potential test, a specimen was placed in a container with simulated concrete pore solution and a deicer. A saturated calomel electrode was placed in another container with saturated potassium chloride. A salt bridge connected the solution in both containers. In the corrosion macrocell test, two test specimens were placed in separate containers, one with simulated concrete pore solution and the other with simulated concrete pore solution and a deicer. The specimen in pore solution is referred to as the cathode and the specimen exposed to deicers is referred to as the anode. A salt bridge connected the solution in both containers, and the two specimens were electrically connected across a 100,000-ohm resistor.

The corrosion potential test provided more consistent results than the macrocell test. The high resistance used to connect the specimens in the macrocell

test limited the corrosion current, and a lower resistance was recommended for future tests. During the early stages of the testing period, some of the salt bridges did not function properly, so modifications to the methods used to fabricate the salt bridges were recommended.

The specimen configuration used by Martinez et al. (1990) was based on work performed by Yonezawa et al. (1988) in a study of the effect of chlorides on the corrosion of steel in concrete. A mild steel electrode, 8 mm (0.3 in.) in diameter, was partly embedded in a mortar cylinder that provided between 7 and 11.6 mm (0.28 and 0.46 in.) of cover. Specimens were placed in saturated calcium hydroxide with the addition of various concentrations of sodium chloride. Corrosion potential and linear polarization measurements were performed on the specimens. Results showed good correlation between the corrosion potential and linear polarization measurements.

The test specimens and the corrosion macrocell test developed by Martinez et al. (1990) have been modified in subsequent studies to improve the consistency and repeatability of the results. Changes include the use of a 10-ohm resistor instead of a 100,000-ohm resistor to increase the corrosion current between the specimens.

Smith et al. (1995) made several modifications to the test. The No. 13 [No. 4] bar was replaced by a No. 16 [No. 5] bar to reduce the mortar cover and lower the time to corrosion initiation. Three specimens were placed at the anode and the cathode. Compressed air, scrubbed to remove carbon dioxide, was bubbled into the cathode to prevent oxygen depletion. A visual inspection of the specimens revealed corrosion underneath the epoxy coating applied at the mortar interface. The use of a different epoxy was recommended.

Schwensen et al. (1995) evaluated microalloyed reinforcing steel, corrosion inhibitors, and deicers, and made additional modifications to the test. Four specimens

at the cathode and two specimens at the anode were used when evaluating steel in NaCl. For the evaluation of steel in $CaCl_2$ and CMA, two specimens were placed at the cathode with one at the anode. The use of two specimens at the cathode and one specimen at the anode was recommended for future research. Schwensen et al. (1995) also periodically recorded the open-circuit corrosion potential of the anode and cathode in the macrocell, and recommended that the separate corrosion potential test be discontinued since the same information could be obtained using the macrocell. The use of polarization resistance to obtain the microcell corrosion rate was also recommended.

Additional modifications to the macrocell test setup and specimens were made by Darwin et al. (2002). In the macrocell tests, corrosion products were observed on the exposed steel in the "lollipop" specimens and on the section of the bare bars not immersed in solution. This was attributed to the high humidity in the container, since the container is covered with a lid to limit evaporation. For this reason, the specimens were modified so that the reinforcing bar was completely embedded in the mortar cylinder. At the same time, the lid was lowered, and placed just above the level of the solution in the container. The resulting test, which runs for 15 weeks, has proven to provide consistent and reproducible results and is described in detail in Chapter 2. In research by Darwin et al. (2002) and Gong et al. (2002), it has provided reasonably good correlations with longer-term, larger-scale tests, a point that is specifically addressed in this study.

### 1.4.2 Bench-Scale Tests

Bench-scale specimens consist of small concrete slabs containing two mats of steel. The slabs are subjected to alternate ponding and drying cycles with a salt

solution. The macrocell current between the two mats of steel is measured to obtain the corrosion rate of the bars (Section 1.3.2). The corrosion potential of the top and bottom mats and the mat-to-mat resistance are also recorded.

The Southern Exposure (SE) specimen consists of a concrete slab, 305 mm (12 in.) long, 305 mm (12 in.) wide, and 178 mm (7 in.) high. The cracked beam (CB) specimen is the same length and height as the SE specimen, but one-half the width. A crack is simulated in the concrete, parallel or perpendicular to the reinforcing steel. In both specimens, a dam is placed around the top edge of the specimen. The ASTM G 109 specimen consists of a concrete slab, 279 mm (11 in.) long, 152 mm (6 in.) wide, and 114 mm (4.5 in.) high. A plexiglass dam is used to pond a solution on the top of the specimen over a region with dimensions of 76 × 150 mm (3 × 6 in.).

The Southern Exposure test was originally used by Pfeifer and Scali (1981) in a study to evaluate concrete sealers for bridges. The test was developed to simulate the exposure conditions in southern climates, thus the name Southern Exposure. A flexural crack was induced in some specimens to evaluate the behavior of cracked concrete. The specimens were subjected to a weekly ponding and drying cycle. The cycle for these tests consisted of ponding the specimens for 100 hours with a 15 percent NaCl solution followed by drying in a heat chamber at 100$^{o}$F for 68 hours. This weekly cycle was repeated 24 times.

The ASTM G 109 test was developed to evaluate the effect of chemical admixtures on the corrosion of metals in concrete and follows a cycle that includes ponding the specimens for two weeks. After this period, the specimens are allowed to dry for two weeks, and the cycle is repeated until a corrosion current between the two mats of steel of 10 μA (equivalent to a current density of 0.072 μA/cm$^2$ and a

corrosion rate of 0.83 μm/year for a No. 16 [No. 5] bar) is measured on at least one-half the specimens.

Lorentz et al. (1992) studied the impact of several variables on the corrosion of reinforcing steel in concrete with the use of the Southern Exposure specimen. These variables included the water-cement ratio (0.35 and 0.40), the use of silica fume (0, 7.5, and 10% by weight of cement), the percentage of entrained air (5 and 8%), and the type of reinforcing steel (plain and deformed) and coating (none, epoxy, epoxy with grit). The coating was intentionally damaged on some epoxy-coated specimens. The effect of cracks in the concrete was also studied using a specimen twice the length of the Southern Exposure specimen with cracks induced perpendicular to the reinforcing steel. The ponding and drying cycle used in the tests was "effective in establishing an environment in which the reinforcing steel could corrode." The cracked specimens showed corrosion currents that were two orders of magnitude higher than observed for uncracked specimens.

Nmai et al. (1994) used the Southern Exposure test to determine if sodium thiocyanate-based accelerating admixtures are safe for use in reinforced concrete structures. The temperature of the specimens during the drying period was maintained at 70°F instead of 100°F. Macrocell corrosion current between the two mats of steel and half-cell potentials of the top mat were recorded weekly. The specimens were broken after 52 weeks. Half-cell potential readings indicated times-to-corrosion that agreed with results obtained from macrocell currents.

The Southern Exposure and cracked beam tests were used at the University of Kansas in the evaluation of the corrosion resistance of microalloyed reinforcing steel (Senecal et al. 1995). The tests lasted for 48 weeks. A recommendation was made to extend the testing period for the bench-scale tests to two years to better evaluate the

corrosion behavior as affected by the deposition of corrosion products. A longer testing cycle, with one week of ponding and one week of drying, was also recommended for the SE and CB tests. The longer drying time would draw in more chlorides during the ponding cycle. Epoxy-coated wooden dams, attached to the concrete with silicone caulk, were used around the top edge of the specimens. The dams started leaking after 9 months due to seepage though the wood and loss of bond between the silicone and the wood. They recommended that a concrete dam be cast monolithically with the specimen to prevent leakage problems. Transverse cracks were induced in the cracked beam specimens by applying a three point bending load after a notch had been cut across the top center of the specimen. Recommendations for the improvement of the cracked beam specimens included (1) the use plastic inserts to form the cracks, (2) the reduction of the concentration of the salt solution from 15% to 3 or 4% to "provide more realistic conditions," and (3) the use of longitudinal cracks along the length of the bar.

Lorentz et al. (1992) used the Southern Exposure test to evaluate several variables on the corrosion of steel in concrete: water-cement ratio, addition of condensed silica fume, percentage of air entrained, type of reinforcing steel and coating, and the effect of cracks in the concrete. They used an integral concrete dam with the specimens. When the forms were stripped, some the the dams were damaged and had to be repaired with plexiglass attached to the top of the specimen with silicone caulk.

McDonald et al. (1998) used Southern Exposure and cracked beam tests to evaluate epoxy-coated, metal-clad, and solid metal reinforcing bars in concrete. In that study, modifications were made in the test procedures, including continuous ponding for 12 weeks after the first 12 weeks of cyclic ponding and drying and the

extension of the testing period to 96 weeks. A good correlation was observed between the mat-to-mat resistance and the corrosion performance of the bars. The results obtained from the tests were confirmed through linear polarization and AC impedance tests. The time required to interpret data from linear polarization and AC impedance tests was considered "very time-consuming and impractical for future large-scale tests."

### 1.4.3 Electrochemical Impedance Tests of Steel in Concrete

John et al. (1981) performed AC impedance measurements on concrete cubes containing four polished mild steel rods. The steel rods had different concrete covers [5, 10, and 15 mm (0.2, 0.4, and 0.6 in.)]. The specimens were immersed in either distilled water or artificial seawater. Other concrete cubes were cast with steel rods that had been pre-rusted by exposure in either salt spray or a humidity chamber. The samples with pre-rusted steel were immersed in seawater. Corrosion potentials of the rods were monitored regularly. Large scatter was observed between the four potential readings on each block, but general trends were identified. AC impedance measurements were obtained using two of the rods in each concrete cube as electrochemical probes. Measurements were obtained over a period of 5 months.

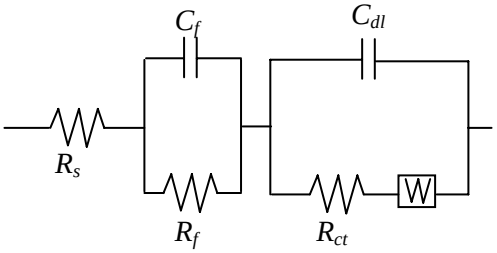


**Figure 1.10 –** Equivalent circuit used by John et al. (1981)

The electrochemical cells were modelled using the equivalent circuit shown in Figure 1.10. Just after immersion, the impedance results were similar for all samples. The Nyquist plots showed a large low frequency curve with a small "spur" at high frequencies. The form of the Nyquist plots was attributed to an RC network (a resistor and capacitor in parallel) with a large resistance and a large time constant ($\tau = R \times C$). After more than 50 days in solution, the size of the low frequency curve remained constant in size for the specimens immersed in seawater and had increased in size for the samples in distilled water. For the specimens immersed in seawater, the high frequency "spur" had also increased in size and "had taken the shape of a discernible curve." The curve had also shifted to the right due to an increase in the concrete resistance $R_s$. The curves for samples with pre-rusted steel showed the same shape of the high frequency "spur" during the first days in solution as the samples with polished steel after 50 days in solution. This curve also increased in size with time. The size of this "spur" was attributed to the resistance $R_f$ in Figure 1.10. After modeling the electrochemical cell with the equivalent circuit in Figure 1.10, it was determined that the impedance curve at low frequencies was affected by both a charge transfer process and a diffusion effect. The relative values of $R_{ct}$, $C_{dl}$ and the Warburg impedance were such that the curve was distorted and neither a charge-transfer semicircle nor a straight $45^o$ line was observed.

The corrosion behavior of mild steel under various conditions was evaluated by Srinivasan et al. (1987) using AC impedance techniques. The specimen consisted of a steel rod, 12 mm (0.5 in.) in diameter and 150 mm (5.9 in.) in length, embedded in a concrete cylinder. Exposure conditions included (1) specimens exposed to the atmosphere, (2) steel embedded in concrete with admixed chlorides, exposed to the atmosphere, (3) steel in concrete, exposed to salt spray, (4) steel embedded in

concrete, immersed in a 3% sodium chloride solution, and (5) steel coated with cement slurry and embedded in concrete with admixed chlorides.

For the specimens exposed to the atmosphere, a large low frequency curve was obtained in the Nyquist plot. This was attributed to capacitive behavior due to the formation of the passive film on the steel. The size and shape of the curves varied little during a 20 month period. The corrosion potential of the bars indicated that the steel was in a passive state, and visual inspection at the end of the test showed no signs of rust on the steel rods. The Nyquist plots for steel embedded in concrete with admixed chlorides showed distorted semicircles. The diameter of these semicircles decreased with time. The decrease in this diameter was attributed to an increase in the corrosion rate (see Section 1.3.4.1). The corrosion potentials of these samples indicated active corrosion, and visual inspection of the steel rods showed rust over 80% of the area. Samples exposed to salt spray showed a capacitive behavior similar to the samples exposed to the atmosphere, and samples immersed in sodium chloride exhibited behavior similar to that of samples in concrete with admixed chlorides.

EIS tests were performed by Hope et al. (1986) using 6.4 × 30 × 40 cm (2.5 × 12 × 16 in.) concrete slabs reinforced with three 13 mm (0.5 in.) diameter steel rods. Two sets of slabs were tested. The first set of slabs was prepared with 2.0% by weight of cement of admixed $CaCl_2 \cdot 2H_20$. A second set was prepared with an aggregate that contained 0.20% by weight of chloride. Linear polarization measurements were also taken.

The results for the slabs with admixed chlorides showed corrosion potentials of -0.550 V, indicating active corrosion, which was confirmed by visual examination of the bars after removal from the specimen. The Nyquist plots exhibited a semicircle at high frequencies and a line with a unit slope at lower frequencies. The slabs were

modeled with an equivalent circuit like the one shown in Figure 1.8b. Values for $R_s$ and $R_{ct}$ obtained were 86 and 11 ohms, respectively. The value of $R_{ct}$ was similar to the value obtained from polarization resistance of 13.3 ohms for $R_p$. The linear portion at low frequencies of the plots with a unit slope was attributed to the influence of diffusion of the reactants.

The impedance response for the slabs with the chloride contaminated aggregate differed from the response of the first set of slabs. A semicircle was also observed at high frequencies, but over a smaller range of frequencies. The plot was also linear at low frequencies, but the slope is higher than for the first set of slabs. The equivalent circuit used to model the second set of slabs is shown in Figure 1.11.

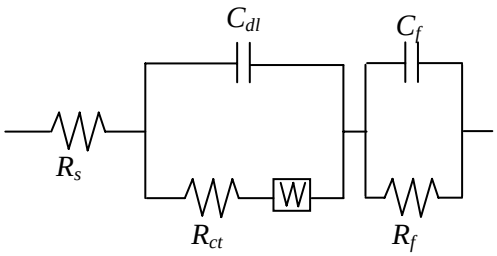


**Figure 1.11 –** Equivalent circuit used by Hope et al. (1986)

Hope et al. (1986) suggested that the behavior of this set was determined by the properties of a film on the surface of the bars and that the linear portion of the plots observed at low frequencies was a portion of a large semicircle determined by the combination of $C_f$ and $R_f$. Using this model, values for $R_{ct}$ (26 ohms) and $R_s$ (300 ohms) were obtained. The value of $R_f$ was not determined. Polarization resistance measurements gave a value of $R_p$ equal to 19 ohms.

Wenger et al. (1987) studied the results obtained from impedance measurements on concrete structures. AC impedance tests were performed on steel

rods embedded in mortar cylinders and reinforced concrete beams. In some samples, chlorides were admixed with the concrete. Nyquist plots were obtained for specimens with and without chlorides over a period of 2 years. The equivalent circuit shown in Figure 1.12 was used to model the specimens. The resistance $R_0$ was used to model the mortar, $R_1$ and $C_1$ were used to model the lime layer. The combination of $R_2$, $C_2$, $R_3$ and $C_3$ represents the metal-pore solution interface.

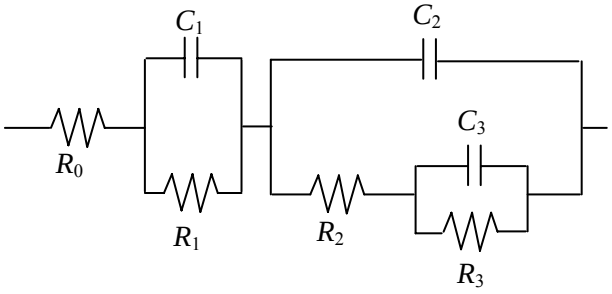


**Figure 1.12 –** Equivalent circuit used by Wenger et al. (1987)

For the cylindrical mortar samples, at high frequencies ($10^4$ – 10 Hz), a capacitive arc (Figure 1.5), formed by the impedance of a capacitor and resistance in parallel, was observed, for both active and passive reinforcement. This behavior was attributed to the precipitation of calcium hydroxide on the surface of the steel. When steel was passive, at low frequencies (10 – $10^{-4}$ Hz), only one capacitive arc was observed. For steel that was actively corroding, two arcs were observed. The authors proposed to use the size of the second capacitive arc to calculate the corrosion current. Although no description of the plots obtained for the concrete beams was given, it was mentioned that their interpretation was difficult. This was attributed to three factors: (1) the reinforcing bars were longer than the counter electrode, (2) the

complicated geometry of the reinforcing bars (working electrode), and (3) the formation of galvanic corrosion cells in the specimen.

## 1.5 CORROSION PROTECTION SYSTEMS

The service life of a concrete structure exposed to chlorides may be divided in two phases, as shown in Figure 1.13. The initiation phase is the period during which chlorides reach the reinforcing steel and break down the passive film, at time $t_0$. The propagation phase, which occurs over time $t_1$, is the period of active corrosion that ends when the structure reaches the end of its useful service life or must be repaired. Corrosion protection systems are designed to increase the length of one or both of these phases.

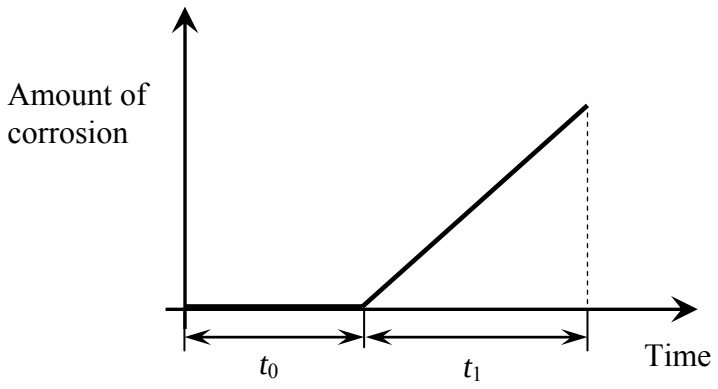


**Figure 1.13 –** Service life model of concrete structure subject to corrosion

Methods to increase $t_0$ or slow the initiation of corrosion include the use of corrosion inhibitors, low permeability concrete, overlays, waterproof membranes, concrete sealers, and alternative reinforcement, such as epoxy-coated or stainless steel bars. Methods to increase $t_1$ or reduce the corrosion rate include the use of corrosion

inhibitors, low permeability concrete, alternative reinforcement, and electrochemical methods, such as cathodic protection and chloride extraction.

The current study involves the evaluation of two corrosion inhibitors, one inorganic [calcium nitrite (DCI-S)] and one organic (Rheocrete 222$^{+}$), two duplex stainless steels, three micralloyed steels, one microcomposite steel, and the effect of variations in the water-cement ratio. This section gives a general explanation of these corrosion protection systems.

### 1.5.1 Corrosion Inhibitors

Corrosion inhibitors are chemical compounds that can help prevent or minimize the corrosion of the reinforcing steel in concrete without significantly changing the properties of concrete. They can have an effect on several factors in the corrosion process (Hansson et al. 1998):

1) the rate of chloride ingress
2) the degree to which the chlorides are chemically bound in the concrete cover
3) the chloride threshold of the reinforcing steel
4) the rate of ingress of dissolved oxygen
5) the electrical resistance of the concrete
6) the chemical composition of the electrolyte

Corrosion inhibitors are usually classified as anodic, cathodic or mixed (anodic and cathodic). Their classification depends on how they affect the corrosion process. Anodic inhibitors generally form an insoluble film on anodic surfaces to passivate the steel (Kepler et al. 2000). Mixed inhibitors block the reactions at the cathode and the anode. Research has been performed on a variety of potential

corrosion inhibitors. These include sodium and calcium nitrite, sodium benzoate, organic-based corrosion inhibiting admixtures (OCIA), and sodium and potassium chromate, among others. The current study evaluates two corrosion-inhibiting admixtures, DCI-S (calcium nitrite) and Rheocrete 222$^{+}$.

Calcium nitrite is considered to be an anodic inhibitor since it works to minimize the anodic reaction by reacting with ferrous ions to form a γ-ferric oxide, layer at the anode, as shown in Eq. (1.26)

$$Fe^{++} + OH^{-} + NO_2^{-} \longrightarrow NO\uparrow + \gamma\text{-}FeOOH \qquad (1.26)$$

Calcium nitrite competes with the chloride ions reacting with the steel, and in this way, increases the chloride concentration necessary to initiate corrosion. The type of reaction [Eq. (1.7) or (1.26)] that takes place will be determined by the relative concentration of chloride and nitrite ions. The chloride-nitrite ion ratio has to be below 1.5 for corrosion to be controlled (Berke and Rosenberg 1989). Calcium nitrite increases the compressive strength of concrete and acts as a set accelerator. A set retarder is usually added to the concrete to minimize its accelerating effects.

Darex Corrosion Inhibitor (DCI), manufactured by W. R. Grace, is composed of approximately 30% calcium nitrite and 70% water. The inhibitor evaluated in this study, DCI-S, is DCI plus a set retarder. The recommended dosage for DCI-S depends on the chloride exposure level and typically varies from 10 to 30 L/m$^3$ (2 to 6 gal/yd$^3$) of concrete.

Organic inhibitors include amines, esters, and sulfonates. They are classified as mixed corrosion inhibitors. Rheocrete 222$^{+}$, manufactured by Master Builders is a combination of amines and esters in water. This inhibitor protects the reinforcing steel in two ways: (1) forming a protective film on the steel surface and (2) reducing the penetration of chloride ions into the concrete. The recommended dosage is 5.0

$L/m^3$ (1 $gal/yd^3$) of concrete. This organic inhibitor reduces the compressive strength of concrete by 15 to 20% at 7 days (Darwin and Hadje-Ghaffari 1990).

Nmai et al. (1992) studied an organic corrosion-inhibiting admixture (OCIA), a combination of amines and esters in a water medium. Two corrosion tests were used in the study. The first test was similar to the Southern Exposure test; the only difference was that drying occured at room temperature instead of 100°F. Half-cell potentials, macrocell corrosion current, and mat-to-mat resistance were measured. The second test used precracked concrete reinforced with a single No. 13 [No. 4] bar to obtain a relationship between corrosion potential and time. Cracks were induced perpendicular to the reinforcing steel. These specimens were continuously ponded with a 6% NaCl solution. This test was later modified by adding a second layer of steel to allow measurements of the macrocell corrosion current. A calcium-nitrite based admixture was also evaluated using the cracked specimens.

Results from the uncracked specimens showed that the OCIA delayed the initiation of corrosion and showed lower corrosion currents once corrosion had initiated. For the cracked specimens containing one bar, the corrosion potential measurements showed initiation of corrosion after 5 days for the control specimens, after 30 days for the calcium-nitrite admixture specimens, and there were no signs of corrosion activity after 180 days for the OCIA specimens. For the cracked specimens with two layers of steel, the time to corrosion initiation was 6 days for untreated concrete, 17 and 39 days for concrete with the calcium-nitrite admixture, and 118 days for concrete containing OCIA. Tests also showed no significant effect of the organic inhibitor on the properties of plastic or hardened concrete.

A study by Senecal et al. (1995) included the evaluation of two corrosion inhibitors, Rheocrete 222 and DCI. The test methods included rapid corrosion potential and macrocell tests, and Southern Exposure and cracked beam tests. The inhibitors were evaluated using two microalloyed steels, one hot-rolled (CRSH) and the other Thermex-treated (CRST). The water-cement ratio was 0.5. This value is acceptable for organic inhibitors but is considered high for use with calcium nitrite (Berke et al. 1993). For CRSH steel, results from the Southern Exposure test showed similar corrosion rates for both inhibitors. Results for CRST steel showed higher corrosion rates for the specimens with calcium nitrite. Specimens with both inhibitors had lower corrosion rates than specimens without inhibitors.

Trepanier et al. (2001) tested four corrosion-inhibiting admixtures, two based on calcium nitrite and two organic inhibitors. Their commercial names were not specified. The time to corrosion initiation and the corrosion rates of steel in mortar were measured. Cylindrical mortar samples were cast with two water-cement ratios, 0.5 and 0.7. Batches included samples using three dosages of each inhibitor and a control sample. The corrosion potential of the bars was monitored and AC impedance tests were performed to obtain the corrosion rates. The four admixtures delayed the initiation of corrosion, with one of the calcium nitrite-based admixtures being the most effective. The effectiveness of the inhibitors increased with increasing dosage. The corrosion rates after initiation of corrosion were similar for all of the samples containing inhibitors. The control samples with a water-cement ratio of 0.5 showed higher corrosion rates than the specimens with inhibitors. The control samples with water-cement ratio of 0.7 showed lower corrosion rate than most of the samples with inhibitors. All of the samples showed large scatter in their results.

### 1.5.2 Alternative Reinforcement

Alternative reinforcement includes coated conventional steel bars or bars made of a material that is more corrosion-resistant than conventional steel. The development of corrosion resistant bars is based on alloying.

Coatings can be organic or metallic. Epoxy-coated steel is the main corrosion protection system used in bridges in the United States. Coatings create a barrier to the chloride ions and electrically isolate the steel. Metallic coatings can be either sacrificial or noble. Metals that have a more negative corrosion potential than conventional steel will act as sacrificial coatings. If the coating is broken, the sacrificial coating will corrode, protecting the conventional steel. Noble coatings have a more positive potential than conventional steel, which means that they are less likely to corrode in concrete than conventional reinforcing steel. If the coating is broken, the conventional steel will become anodic and will corrode. Metallic coatings include copper, zinc, stainless steel, nickel, and copper.

Stainless steels are those with a minimum of 12% chromium. They are divided according to their metallurgical structure into ferritic, ferritic-austenitic, martensitic, and austenitic. The most commonly used stainless steels for reinforcing bars have historically been 304, 316, and 316LN (Smith and Tullman 1999). These three types of steel are austenitic steels, which are low in carbon, with approximately 18% chromium and 8% nickel. Ferritic-austenitic steels are also called duplex steels. They contain 21-28% chromium and 1-8% nickel, and are also used as reinforcing steel. Ferritic steels have less than 17% chromium, and martensitic steels have carbon contents as high as 1.2% and 12 to 18% chromium. Neither has been used as concrete reinforcement.

The corrosion performance of reinforcing bars clad with 304 stainless steel was compared with that of conventional steel by Darwin et al. (1999) and Kahrs et al. (2001). The bars were evaluated using rapid corrosion potential and corrosion macrocell tests in which bare and mortar-embedded bars were exposed to a 1.6 m ion sodium chloride and simulated concrete pore solution. The corrosion rate of bare stainless steel clad bars was $^{1}/_{100}$ of the value observed for bare conventional steel bars. For mortar-embedded bars, the corrosion rate was $^{1}/_{20}$ to $^{1}/_{50}$ of the value observed for conventional steel. The results showed the importance of the method used to protect the ends of the bars from chlorides.

Clemeña and Virmani (2002) present the results of a study that compared the behavior of three solid stainless steel bars (316LN, 304, and 2205), stainless steel clad bars, and ASTM A 615 steel bars. Two 3 mm (0.12 in.) holes were drilled through the cladding to evaluate the effect of damage the performance of the clad bars. The specimens used in the study are similar to the Southern Exposure specimens, although smaller in size and with a 100 ohm resistor connecting the top and bottom mats of steel. The specimens were subjected to 3 days of ponding with a saturated NaCl solution followed by 4 days of drying at room temperature. Measurements included the macrocell current between top and bottom mat, open-circuit potential, and polarization resistance of each top bar. Pulverized concrete samples at the depth of the top mat of steel were obtained three times during the testing period from 10 randomly selected concrete blocks to determine the chloride ion concentrations.

After 2 years of exposure to the saturated NaCl solution solution, the specimens containing stainless steel clad bars and the specimens with solid stainless steel bars showed no signs of corrosion. The conventional steel bars started corroding early during the testing period. The chloride threshold for conventional steel was

estimated to be approximately 350 ppm ± 100 ppm (0.76 kg/m$^3$, 1.28 lb/yd$^3$) based on the average results. All of the other bars remained passive throughout the test period. At the end of the test period the chloride concentration at the level of the bars was approximately 5200 ppm ± 100 ppm (12.3 kg/m$^3$, 20.8 lb/yd$^3$), 15 times more than for conventional steel.

McDonald et al. (1998) used Southern Exposure and cracked beam tests to evaluate epoxy-coated, metal-clad, and solid metal reinforcing bars in concrete. The bars tested included conventional uncoated, epoxy-coated, galvanized, zinc-alloy, copper-clad, 304 stainless steel, and 316 stainless steel bars. Some specimens used conventional steel in the bottom mat to simulate structures in which corrosion-resistant steel is combined with conventional steel. In other specimens, corrosion-resistant steel was used in both top and bottom mats. The 304 stainless steel bars showed corrosion rates 1500 times less than conventional steel in both cracked and uncracked concrete, when used in both mats. Of the specimens with 304 stainless steel bars in the top mat and conventional steel in the bottom mat, half of them exhibited moderate to high corrosion rates, ranging from 3 to 100 times less than conventional steel. Specimens with 316 stainless steel bars had about 800 times less corrosion than conventional bars in both cracked and uncracked concrete, and with either stainless steel or conventional steel on the bottom mat.

Tata Steel Company in India originally developed a microalloyed steel with mechanical properties that are similar to those of conventional steel and with corrosion resistance that was claimed by the original developers to be three to five times better than conventional steel (Tata 1991). The alloying process is carried out "to affect the electrochemical behavior in such a way that either the corrosion potential increases or the critical current density decreases, so that the on-set of

anodic reaction gets lowered" (Tata 1991). These microalloyed steels have a carbon equivalent of 0.30 to 0.45%, and the alloys contain concentrations of chromium, copper and phosphorus that, while low, are significantly higher than used in conventional reinforcing steel. According to Tata (1991), the copper reacts with chlorides on the steel surface to form a layer of $CuCl_2 \cdot 3\ Cu(OH)_2$ that has low solubility and retards the corrosion process. Phosphorus oxides act as inhibitors and also slow the corrosion process. Chromium results in the formation of a spinel oxide layer ($FeO \cdot Cr_2O_3$) that is a poor conductor of electrons. Some of the steel is also heat treated by the Tempcore or Thermex process (tradenames), which involves quenching and tempering of the steel immediately after rolling. This process places the exterior of the bars in compression, reducing microcracks on the surface of the steel.

Four types of steel, hot-rolled conventional, Thermex-treated conventional, hot-rolled microalloyed, and Thermex-treated microalloyed steel, were evaluated at the University of Kansas (Senecal et al. 1995, Smith et al. 1995, Schwensen et al. 1995, Darwin 1995). In general, the Thermex-treated microalloyed steel had a macrocell corrosion rate equal to about one-half that of conventional steels in both the rapid macrocell and the Southern Exposure tests. The hot-rolled microalloyed steel showed higher corrosion rates than conventional steels in the bench-scale tests, but exhibited half the corrosion rate of conventional steel in the rapid macrocell test. The Thermex-treated conventional steel showed improved corrosion resistance compared to the hot-rolled conventional steel. All four types of steel showed similar corrosion potentials when exposed to the same concentrations of NaCl. Epoxy-coated, Thermex-treated microalloyed steel performed particularly well, when compared to conventional epoxy-coated steel (corroding at only about 10% of the rate). Based on

these observations, a recommendation was made to continue development of the new steel to be used as a superior epoxy-coated reinforcing steel.

Another study (Balma et al. 2002) evaluated three microalloyed Thermex-treated steels, one conventional Thermex-treated steel, and one conventional hot-rolled steel. Two of the microalloyed steels had phosphorus contents that exceeded the amounts allowed in ASTM specifications. The corrosion potentials of the steels indicated that the five steels had a similar tendency to corrode. Corrosion rates in the rapid macrocell test showed no advantage of the microalloyed steels over conventional steel. In the bench-scale tests, the microalloyed steel with regular phosphorus content had lower corrosion rates than conventional steel. After 70 weeks, it had 64% less corrosion loss in the G 109 test, 11% less corrosion loss in the Southern Exposure test, and 4% less corrosion loss in the cracked beam test, than conventional steel. This indicates that in cracked concrete both steels behave in a similar manner. The improved behavior observed in the bench-scale tests did not justify continued research on the steel for use by itself or as a superior epoxy-coated material.

A high-strength, low carbon, high-chromium (9%) alloy has been developed by MMFX Steel Corporation. The higher chromium content is believed to form a passive chromium oxide ($Cr_2O_3$) layer on the surface of the steel. The steel is microstructurally designed to minimize the formation of microgalvanic cells in the steel structure.

A report from Trejo (2002) presents preliminary results from a test program designed to determine the critical chloride threshold and corrosion rates for several types of reinforcing steel. The steel evaluated include ASTM A 615 conventional steel, ASTM A 706 low-alloy steel, 304 stainless steel, MMFX microcomposite steel,

and 316LN stainless steel. The critical chloride threshold was determined using the accelerated chloride threshold (ACT) test, developed by Trejo. ASTM G 109 tests were performed to obtain information on the corrosion rates of the steels.

Preliminary results from the ACT test gave an average critical chloride threshold of 0.6 kg/m$^3$ (1.0 lbs/yd$^3$) for ASTM A 615 steel, 5.2 kg/m$^3$ (8.8 lbs/yd$^3$) for the microcomposite steel, and 5.5 kg/m$^3$ (9.2 lbs/yd$^3$) for 304 stainless steel. Bars in the ASTM G 109 specimens had not started to corrode after 40 weeks.

Darwin et al. (2002) evaluated the corrosion properties of MMFX microcomposite steel. They determined that MMFX steel has a higher corrosion threshold and that it corrodes at a lower rate than conventional steel. When compared to epoxy-coated reinforcement (ECR) is was concluded that MMFX steel is less effective in preventing corrosion than ECR and that bridges constructed with MMFX steel would have a shorter life expectancy and higher cost than a bridge deck constructed with epoxy-coated steel.

### 1.5.3 Low Permeability Concrete

Low permeability concrete will slow the ingress of water, oxygen, and chloride ions, factors that are necessary for corrosion to occur. A lower permeability also reduces the electrical conductivity of the concrete. Factors that reduce the permeability are increased concrete cover over the reinforcing steel, lower water-cement ratios, and the use of mineral admixtures (pozzolans silica fume, blast-furnace slag, and fly ash). Sherman et al. (1996) reported the use of concretes with water-cement ratios of 0.30 and 0.32 that were practically impermeable. Crack surveys of bridge decks (Schmitt and Darwin 1995, 1999, Miller and Darwin 2000), however, indicate that at the cement contents normally associated with low permeability

contents, significant increases in cracking can be expected in reinforced concrete bridge decks, which defeats the purpose of the low permeability concrete.

## 1.6 OBJECTIVES AND SCOPE

The principal objectives of the current study are to evaluate the effectiveness of several corrosion protection systems and to compare the results obtained from the rapid macrocell test and the bench-scale tests.

The corrosion protection systems for reinforcing steel in concrete evaluated in this study are:

1) Two corrosion inhibitors, one with calcium nitrite (DCI-S) and one organic inhibitor (Rheocrete 222$^{+}$),
2) Concrete with two different water-cement ratios, 0.45 and 0.35.
3) Three microalloyed reinforcing steels
   - Microalloyed steel with a high phosphorus content, 0.117%, Thermex treated (CRPT1)
   - Microalloyed steel with a high phosphorus content, 0.100%, Thermex treated (CRPT2)
   - Microalloyed steel with normal phosphorus content, 0.017%, Thermex treated (CRT).
4) One conventional steel, Thermex treated (T)
5) MMFX Microcomposite steel
6) Epoxy-coated steel (ECR)
7) Two duplex stainless steels, 2101 and 2205, which were received in two conditions: (i) “as-rolled” and (ii) pickled, to remove the mill scale.

8) Three heats of conventional hot-rolled steel, N, N2 and N3, used as control specimens.

The rapid corrosion macrocell test (with and without mortar cover on the steel), and three bench-scale tests, the Southern Exposure, cracked beam, and ASTM G 109 tests are used to evaluate the corrosion protection systems. An economic analysis is performed to compare the costs of the most effective corrosion protection systems.

Between four and six specimens are evaluated for each test for each corrosion protection system, with the exception that the ASTM G 109 test was not used to evaluate MMFX, 2101 and 2205 steels.

Results for the three microalloyed steels and the conventional Thermex treated steel were previously reported by Balma et al. (2002). The results of the tests for microalloyed steel are presented since they are used for developing the correlations between the rapid evaluation and bench-scale tests. Test results for MMFX microcomposite steel were reported previously by Darwin et al. (2002) and Gong et al. (2002). At the time of the reports, the bench-scale tests were 26 and 40 weeks old, respectively. The present report covers the full 96-week test period.

A comparison between the results of the Southern Exposure, cracked beam, and rapid macrocell tests is performed. For the comparison, the corrosion rates and total corrosion losses for the Southern Exposure and cracked beam tests are plotted versus the same results for the rapid macrocell test to determine the degree of correlation between the tests. The results of the cracked beam test are also compared with those of the Southern Exposure test. The coefficient of variation is used to compare the variability of the corrosion rates and total corrosion losses for individual tests and to compare the variability of the results for the rapid macrocell, Southern

Exposure and cracked beam tests. Electrochemical impedance measurements are obtained from the different tests to obtain an equivalent circuit that represents each test.

# CHAPTER 2

# EXPERIMENTAL WORK

The corrosion macrocell, Southern Exposure, cracked beam, and ASTM G 109 tests are used to evaluate corrosion protection systems for reinforcing steel in concrete. Comparisons are made between the results obtained from the rapid macrocell and bench-scale tests. Electrochemical impedance tests are performed to determine equivalent circuits for these two tests. The materials tested include concrete containing corrosion inhibitors (DCI-S or Rheocrete 222+), concrete with water-cement ratios of 0.35 or 0.45, two duplex stainless steels (2101 and 2205), MMFX microcomposite steel, epoxy-coated steel, three Thermex-treated microalloyed steels, one Thermex-treated conventional steel, and three conventional, normalized steels as the control samples. This chapter describes the equipment, materials, and procedures used to prepare the specimens and to monitor and record corrosion behavior.

## 2.1 CORROSION PROTECTION SYSTEMS

The corrosion protection systems evaluated in this study are listed below. The chemical composition and mechanical properties of the reinforcing steels, as reported by the manufacturers, are given in Tables 2.1 and 2.2.

*Corrosion inhibitors*

Darex Corrosion Inhibitor (DCI-S), provided by W. R. Grace.

Rheocrete 222+, provided by Master Builders Technologies

*Reinforcing steels*

N1, N2, and N3: conventional steel, normalized.

T: conventional steel, Thermex treated.

CRPT1: microalloyed steel with a high phosphorus content (0.117%), Thermex treated (quenched and tempered).

CRPT2: microalloyed steel with a high phosphorus content (0.100%), Thermex treated.

CRT: microalloyed steel with normal phosphorus content (0.017%), Thermex treated.

MMFX: MMFX-2 microcomposite steel

ECR: Epoxy-coated steel with intentionally damaged coating.

2101(1) and 2101(2): Duplex stainless steel (21% chromium, 1% nickel)

2205: Duplex stainless steel (25% chromium, 5% nickel)

The duplex stainless steel labeled 2101(1) lacked boron; as a result, the bars were slightly deformed and showed small cracks on the surface. Tests on this steel were continued although the 2101(2) steel was received as a substitute.

The three duplex steels were received in two different conditions: (i) "as-rolled", and (ii) pickled, to remove the mill scale. The pickled bars are labeled 2101(1)p, 2101(2)p, and 2205p. The pickled bars were first blasted to a near white with stainless grit and then placed for 40 to 50 minutes in a solution of 25% nitric acid and 3 to 6% hydrofluoric acid. The temperature was maintained at 110 to 113 degrees Fahrenheit.

**Table 2.1 –** Chemical properties of reinforcing steel as provided by manufacturers.

| Designation | Heat No. | C | Mn | P | S | Si | Cr | Cu | Ni | Sn | Mo | V | Nb | N2 | Al | Cb | Ca |
|---|---|---|---|---|---|---|---|---|---|---|---|---|---|---|---|---|---|
| N | K0-5152 | 0.400 | 1.010 | 0.022 | 0.032 | 0.220 | 0.200 | 0.300 | 0.200 | 0.010 | 0.040 | 0.003 | - | - | - | - | - |
| N2 | | 0.420 | 0.960 | 0.014 | 0.040 | 0.200 | 0.140 | 0.300 | 0.100 | 0.009 | 0.019 | 0.002 | - | - | 0.001 | - | - |
| N3(1) | S44407 | 0.430 | 1.150 | 0.013 | 0.020 | 0.240 | 0.100 | 0.380 | 0.080 | 0.015 | 0.020 | 0.001 | - | - | - | 0.002 | 12 ppm |
| N3(2) | S44420 | 0.450 | 1.150 | 0.012 | 0.024 | 0.260 | 0.120 | 0.380 | 0.120 | 0.017 | 0.030 | 0.001 | - | - | - | 0.002 | 14 ppm |
| T | K0-0097 | 0.360 | 0.770 | 0.018 | 0.040 | 0.160 | 0.180 | 0.310 | 0.140 | 0.004 | 0.042 | 0.004 | - | - | - | - | - |
| CRPT1 | K9-1482 | 0.180 | 0.960 | 0.117 | 0.025 | 0.290 | 0.550 | 0.520 | 0.120 | 0.009 | 0.036 | 0.019 | - | - | - | - | - |
| CRPT2 | K9-6491 | 0.160 | 1.010 | 0.100 | 0.033 | 0.290 | 0.650 | 0.560 | 0.140 | 0.010 | 0.035 | 0.013 | - | - | - | - | - |
| CRT | K9-1481 | 0.190 | 0.940 | 0.017 | 0.031 | 0.390 | 0.710 | 0.450 | 0.110 | 0.009 | 0.040 | 0.002 | - | - | - | - | - |
| MMFX | | 0.060 | 0.460 | 0.010 | 0.011 | 0.230 | 9.130 | 0.100 | 0.080 | - | 0.020 | 0.018 | 0.007 | 118 ppm | - | - | - |
| 2205 | - | 0.020 | 1.370 | 0.023 | 0.001 | 0.420 | 22.270 | 0.300 | 4.880 | - | 3.260 | - | - | 0.192 | | | |
| 2101(1) | - | 0.032 | 4.990 | 0.023 | 0.001 | 0.490 | 21.330 | 0.350 | 1.530 | - | 0.130 | - | - | 0.222 | | | |
| 2101(2) | - | 0.030 | 4.900 | 0.019 | 0.001 | 0.770 | 21.420 | 0.350 | 1.520 | - | 0.330 | - | - | 0.237 | | | |

**Table 2.2 –** Physical properties of reinforcing steel as provided by manufacturers.

| Designation | Heat No. | Yield strength | | Tensile strength | | Elongation % in 203 mm (8 in.) | Bending | Deformation | | Weight | |
|---|---|---|---|---|---|---|---|---|---|---|---|
| | | (MPa) | (ksi) | (MPa) | (ksi) | | | (mm) | (in.) | (kg/m) | (lbs/ft) |
| N | K0-5152 | 466.6 | 67.7 | 774.0 | 112.3 | 13.00 | OK | 0.965 | 0.038 | 1.574 | 1.058 |
| N2 | | 467.1 | 67.7 | 745.1 | 108.1 | 15.00 | OK | 1.067 | 0.042 | 0.000 | |
| N3(1) | S44407 | 469.5 | 68.1 | 734.3 | 106.5 | 15.00 | OK | - | - | - | - |
| N3(2) | S44420 | 469.5 | 68.1 | 740.5 | 107.4 | 12.50 | OK | - | - | - | - |
| T | K0-0097 | 562.7 | 81.6 | 709.5 | 102.9 | 13.00 | OK | 1.067 | 0.042 | 1.484 | 0.997 |
| CRPT1 | K9-1482 | 616.1 | 89.4 | 769.6 | 111.6 | 13.00 | OK | 0.940/1.041 | 0.037/0.041 | 1.482/1.500 | 0.996/1.008 |
| CRPT2 | K9-6491 | 607.2 | 88.1 | 756.2 | 109.7 | 12.50 | OK | 0.991/1.067 | 0.039/0.042 | 1.473/1.586 | 0.990/1.066 |
| CRT | K9-1481 | 600.5 | 87.1 | 765.1 | 111.0 | 12.00 | OK | 1.016/1.067 | 0.040/0.042 | 1.476/1.500 | 0.992/1.008 |
| MMFX | 810737 | - | - | 1131.5 | 164.1 | 6.00 | - | - | - | - | - |
| 2205 | - | 490.2 | 71.1 | 742.6 | 107.7 | 32.20 | - | - | - | - | - |
| 2101(1) | - | 460.1 | 66.7 | 722.1 | 104.7 | 36.00 | - | - | - | - | - |
| 2101(2) | - | 519.2 | 75.3 | 760.9 | 110.3 | 35.60 | - | - | - | - | - |

## 2.2 RAPID MACROCELL TEST

The rapid macrocell test is used to determine the corrosion rate of the reinforcing steel. The reinforcing bars are tested with and without mortar cover in simulated concrete pore solution at two different sodium chloride (NaCl) ion concentrations (1.6 m and 6.04 m). Tests with the corrosion inhibitors and different water-cement ratios are performed at a 1.6 m NaCl ion concentration. The detailed test program is described in Section 2.2.4.

### 2.2.1 Test Procedure

Macrocell test specimens consist of an anode and a cathode, as shown in Figures 2.1 to 2.4. The cathode consists of two specimens in simulated concrete pore solution. The anode consists of one specimen in simulated concrete pore solution with sodium chloride (1.6 or 6.04 m NaCl ion concentration). The tests run for 15 weeks. Tests are performed on bare bars and bars embedded in mortar. The specimens with bars embedded in mortar were modified during the study, as described in Section 2.2.2 , in conjunction with a change in the test setup. For the earlier tests, a lid was placed on top of the container to limit evaporation, as shown in Figures 2.1 and 2.2. For latter tests, the lid was lowered and placed inside the container, just above the level of the solution, as shown in Figures 2.3 and 2.4. These modifications were made after corrosion products were observed in some tests, on bar surfaces that were not immersed in the solution. This corrosion was attributed to the high humidity inside the container. The changes were made to lower the humidity on the section of the bar not exposed directly to the solution.

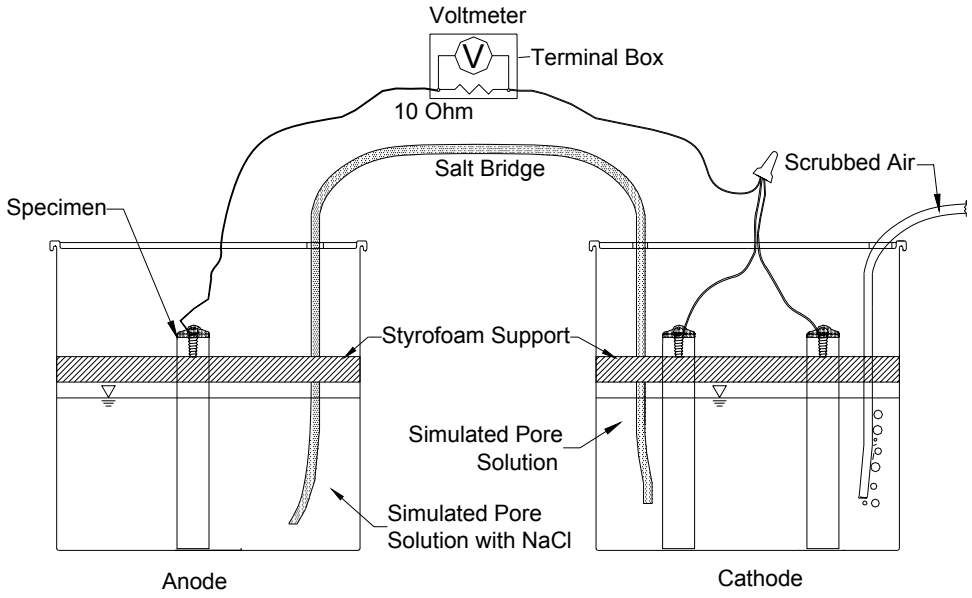


**Figure 2.1 –** Macrocell test setup with bare bars and lid on top of container

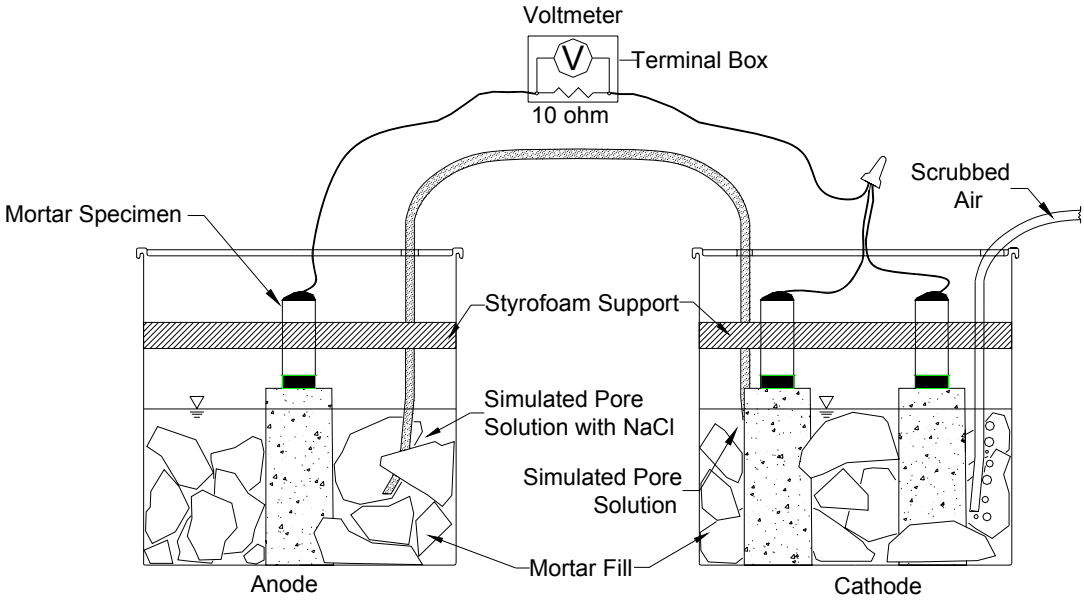


**Figure 2.2 –** Macrocell test setup with "lollipop" specimens and lid on top of container.

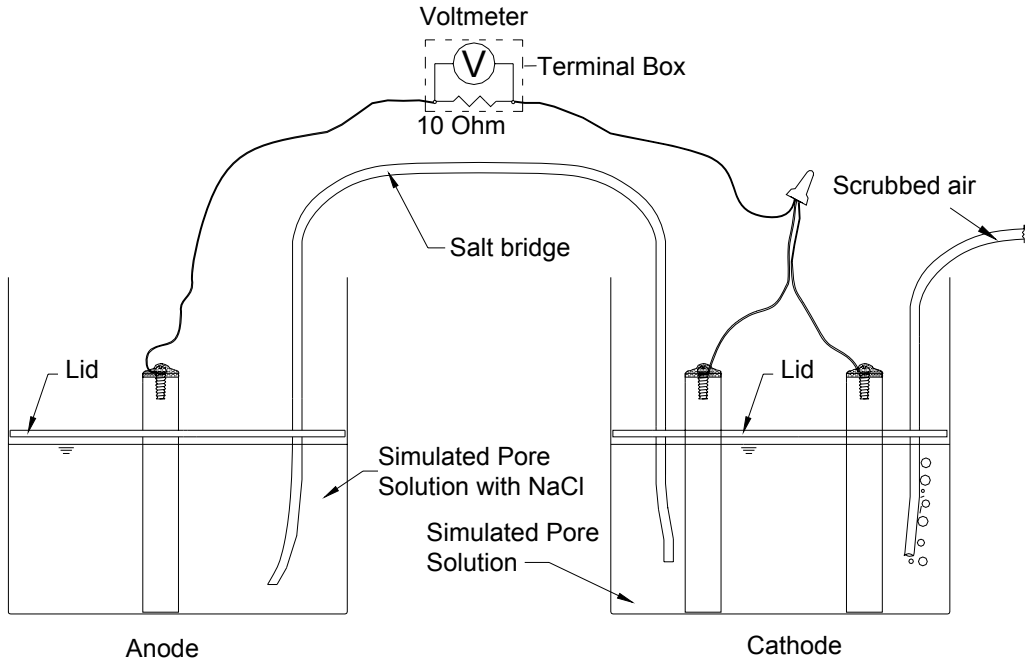


**Figure 2.3** – Macrocell test setup with bare bars and lid inside the container.

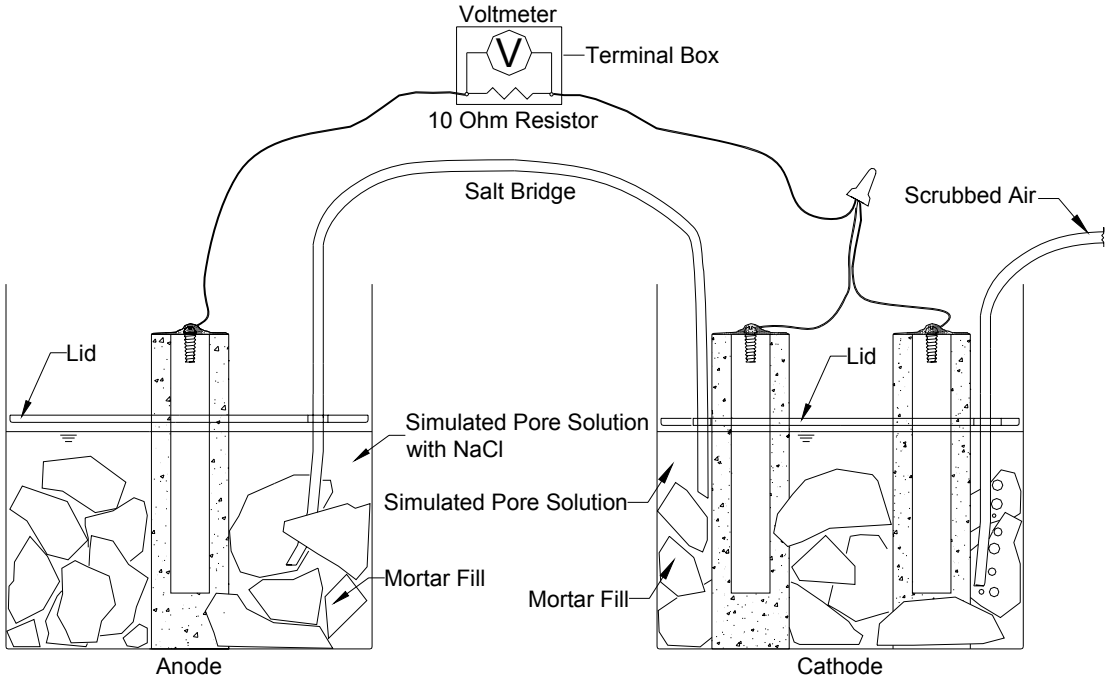


**Figure 2.4 –** Macrocell test setup with mortar-wrapped specimens and lid inside the container

For the earlier setup (Figures 2.1 and 2.2), at the anode, one specimen is placed in the center of a container. In the case of mortar-encased specimens, the specimen is surrounded with mortar fill. The top of the bar is supported with styrofoam. The simulated concrete pore solution with NaCl is added to the container to a depth exposing the lower 76 mm (3 in.) of the reinforcement to the solution – until the level of the solution is 51 mm (2 in.) from the top of the bar for bare specimens, and 13 mm ($^1/_2$ in.) from the top of the steel-mortar interface for mortar specimens. Holes are cut in the lids to introduce a salt bridge, calomel electrode, tubing from the air scrubber, and wire for the electrical connections. The free end of an insulated copper wire attached to the specimen is threaded through the container lid and then attached to a black binding post in a terminal box.

Two specimens are placed in another container to act as the cathode. Mortar-clad specimens are surrounded with mortar fill. The bars are held in place with the help of a styrofoam support. Simulated concrete pore solution is added to the container until the level of the solution is the same as it is at the anode. The free ends of copper wires attached to the cathode specimens are threaded through the container lid and then attached to a third wire that is attached to a red binding post in a terminal box. Air, scrubbed to remove $CO_2$, is bubbled into the solution surrounding the cathode specimens to provide enough oxygen for the cathodic reaction. A salt bridge connects the solutions surrounding the cathode and the anode.

For the later tests (Figures 2.3 and 2.4), the lid is placed inside of the container. To do this, the edges of the lids are cut off and additional holes are cut in the lid to hold the specimens in place. The solution is added to the containers until the level of the solution is 51 mm (2 in.) from the top of specimens. The lids are

placed 6 mm (¼ in.) above the solution. Since the lids support the bars, styrofoam supports are not needed. The rest of the setup is completed as before.

For both test configurations, the voltage drop is measured across a 10-ohm resistor that completes the macrocell circuit by connecting the black binding post to the red binding post in the terminal box. The negative terminal of the voltmeter is connected to the black binding post and the positive terminal of the voltmeter is connected to the red binding post.

As described in Chapter 1, the voltage drop obtained from the macrocell readings is converted to a corrosion rate (in μm/year) using the following equation:

$$Rate = 11.59i = \frac{11590V}{AR} \qquad (2.1)$$

where

$i$ = current density, μA/cm$^2$

$V$ = voltage drop across the resistor, V

$R$ = resistance of the resistor, kΩ

$A$ = area of exposed metal at the anode bar, cm$^2$

The total corrosion loss is obtained by integrating the corrosion rate.

After the voltage drop is measured, the anodes are disconnected from the terminal box. Two hours after being disconnected, the corrosion potential of the anode and the cathode are measured by placing a saturated calomel electrode in the solution surrounding the bar and connecting it to the positive terminal on the voltmeter, with the bar (cathode or anode) connected to the negative terminal of the voltmeter. Figure 2.5 shows the procedure for measuring the corrosion potential of the anode.

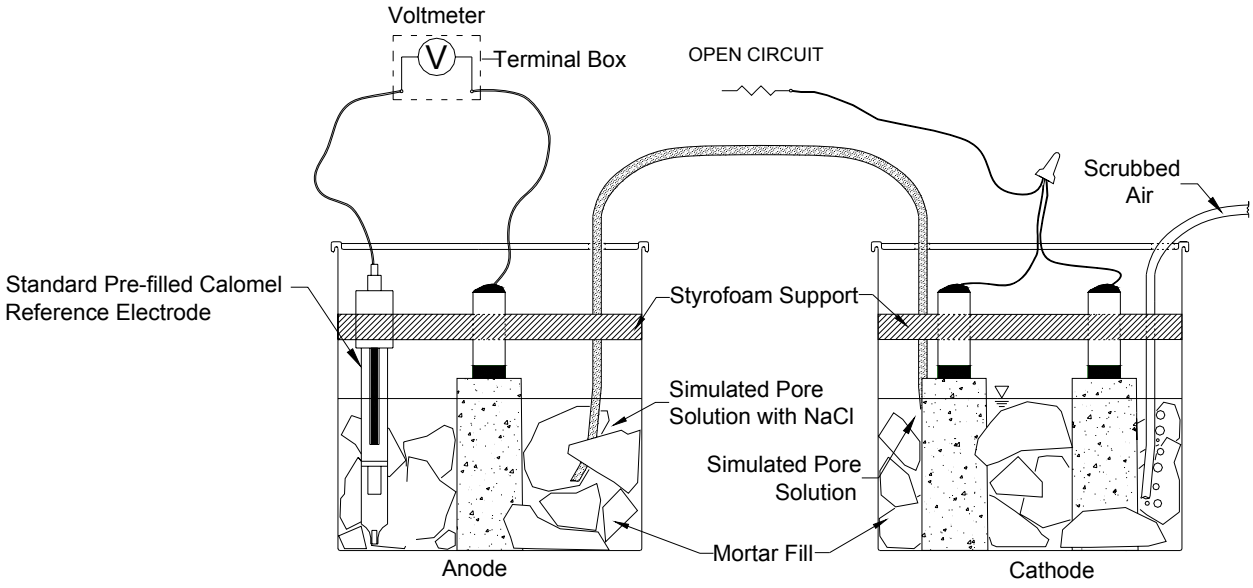


**Figure 2.5 –** Macrocell test setup for corrosion potential readings at the anode

### 2.2.2 Test Specimen Preparation

The specimens used in the rapid macrocell test consist of a 127 mm (5 in.) long, No. 16 [No. 5] reinforcing bar, either bare or embedded in mortar, as shown in Figure 2.6. Sharp edges on the bar ends are removed with a grinder, and the bar is drilled and tapped at one end to receive a 10-24 threaded bolt, 10 mm ($^3/_8$ in.) long, which is used to connect the copper wire.

The bar is then cleaned with acetone to remove oil or dust from the bar surface. Four 3.2 mm ($^1/_8$-in.) diameter holes are drilled on the coating of the ECR bars. For all other bars, sections of the bar that will be covered with epoxy are sandblasted to provide a better surface for the epoxy to adhere. These sections include the tapped end of the bar, and, for "lollipop" specimens, a 15 mm (0.60 in.) wide band centered 51 mm (2 in.) from the tapped end of the bar. Before sandblasting, sections of the bar that will not be sandblasted are covered with duct

tape. Some bars were completely sandblasted to evaluate the performance of bars were the mill scale has been removed. After sandblasting, the duct tape is removed and the bars are again cleaned with acetone to remove the sand. The epoxy is then applied, according to manufacturer's recommendations. All the epoxy-coated bars had epoxy-filled caps on the unthreaded end of the bar. Since the mill scale on the bars is believed to provide some corrosion protection, caps were used to protect the ends of some of the microalloyed steel specimens to prevent areas without mill scale from exposure to the deicing chemicals. In this case, a first coat of epoxy is applied to the unthreaded end of the bar. Two hours later, a cap if half-filled with epoxy, and the end of the bar is inserted into the cap. The epoxy and caps are applied at least 24 hours before casting the bar in mortar.

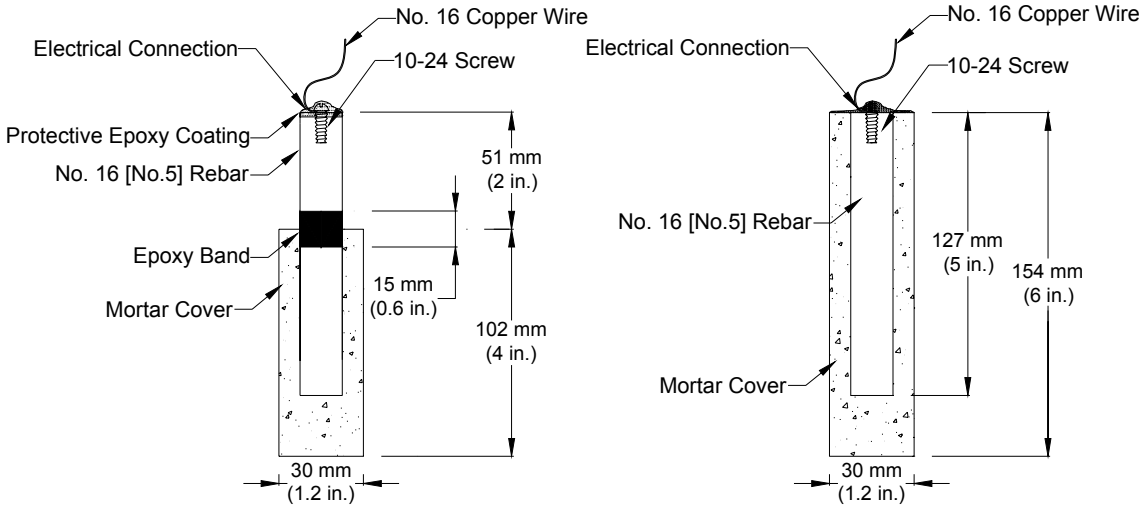


**Figure 2.6 –** Mortar specimens. (a) "Lollipop" specimen and (b) mortar-wrapped specimen.

*Mold Design and Assembly*

The mold design was developed by Martinez et al. (1990). The mold shown in Figure 2.7 is used to cast the "lollipop" specimens, and consists of the following commercially available materials:

(A) One laboratory grade No. 6 ½ rubber stopper with a centered 16 mm ($^5/_8$ in.) diameter hole.

(B) One laboratory grade No. 9 rubber stopper with a centered 16 mm ($^5/_8$ in.) diameter hole.

(C) One ASTM D 2466 32 mm (1¼ in.) to 32 mm (1¼ in.) PVC fitting, 42 mm (1.65 in.) internal diameter, shortened by 14 mm (0.55 in.) on one end.

(D) One ASTM D 2466 25.4 mm (1 in.) to 25.4 mm (1 in.) PVC fitting, 33 mm (1.3 in.) internal diameter. The fitting is turned in a lathe to 40.6 mm (1.6 in.) external diameter so that it will fit in PVC fitting (C).

(E) One ASTM D 2241 SDR 21 25.4 mm (1 in.) PVC pipe, 30 mm (1.18 in.) internal diameter and 102 mm (4 in.) long. The pipe is sliced longitudinally to allow for specimen removal. The slice is covered with a single layer of masking tape to avoid leakage during casting.

(F) Two pieces of $2 \times 8$ pressure treated lumber. Holes and recesses are bored into the flat surfaces to accept the specimen mold assembly and facilitate mortar placement.

(G) Four threaded rods.

The laboratory grade rubber stoppers, A and B, are used to hold the reinforcing bars in place and maintain uniform cover.

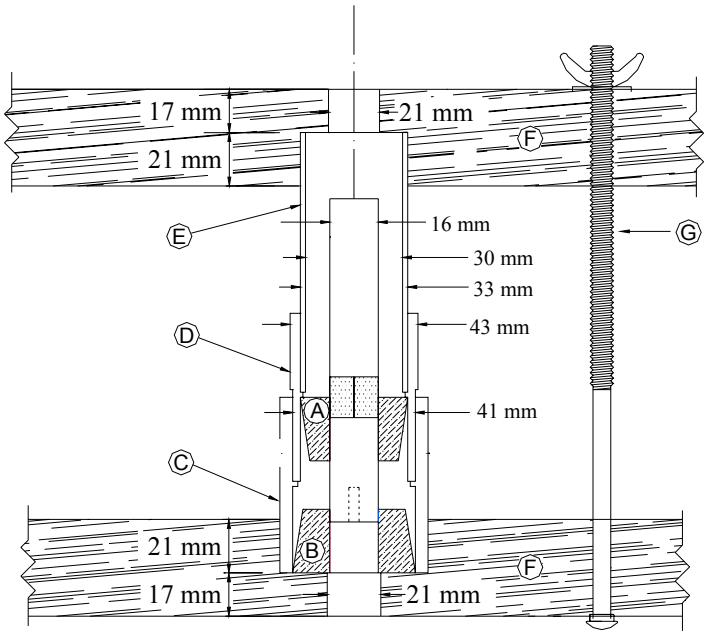


**Figure 2.7 –** Mold assembly for "lollipop" specimens

The molds for the "lollipop" specimens, Figure 2.7, are assembled as follows:

1) The tapped end of the reinforcing bar is inserted through the hole of the small rubber stopper, A, beginning at the widest end of the stopper. The distance between the untapped end of the bar and the rubber stopper is 76 mm (3 in.)
2) The rubber stopper, A, is inserted in the machined end of the small connector, D. The widest end of the small rubber stopper has to be in contact with the shoulder (an integral ring) on the internal surface of the small connector.
3) The large rubber stopper, B, is inserted in the cut end of the larger connector, C, until it makes contact with the shoulder on the inside surface of the connector.
4) The machined end of the small connector, D, is inserted in the free end of the large connector, C. At the same time, the tapped end of the reinforcing bar is inserted through the hole of the large rubber stopper, B.

5) The longitudinal slice along the side of the PVC pipe, E, is covered with masking tape. The pipe is then inserted in the free end of the small connector.
6) The assembled mold is inserted into the recesses in the top and bottom wooden pieces of the fixture, F. The threaded rods, G, are then inserted between the wooden boards. The rods are used to hold the molds together and center the reinforcing bars by tightening or loosening the nuts on the rods.

The mold used to cast the mortar-wrapped specimens is shown in Figure 2.8. For this case, the pipe, E, is 154 mm (6 in.) long instead of 102 mm (4 in.), the rubber stopper, B, and the connector, C, are no longer needed, and the rubber stopper, A, has a 4 mm ($^3/_{16}$ in.) diameter hole instead of a 16 mm ($^5/_8$ in.) diameter hole.

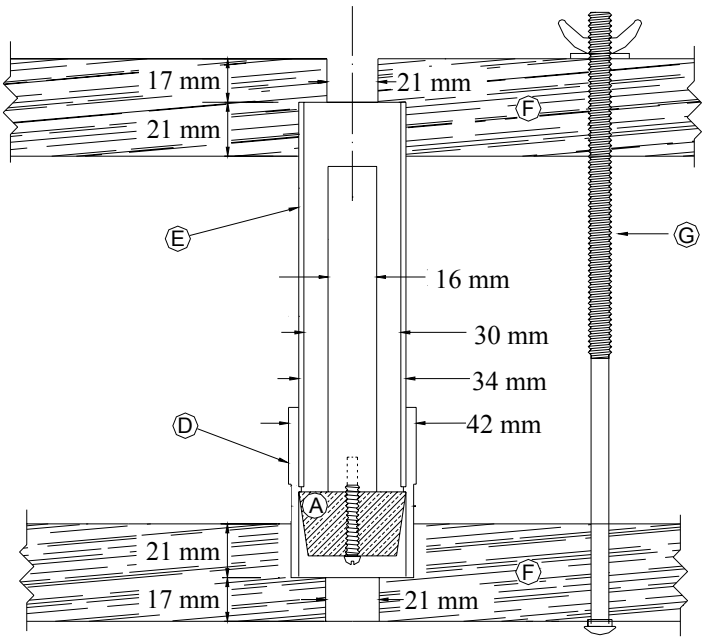


**Figure 2.8 –** Mold assembly for mortar-wrapped specimens

The molds for the mortar-wrapped specimens are assembled as follows (Figure 2.8):

1) A 10-24 $\times$38 mm ($1^1/_2$ in.) threaded bolt is inserted through the hole of the rubber stopper, A, beginning at the narrow end of the stopper. The bar is then bolted against the stopper.
2) The rubber stopper, A, is inserted in the machined end of the small connector, D. The widest end of the small rubber stopper has to be in contact with the shoulder (an integral ring) on the internal surface of the small connector.
3) The longitudinal slice along the side of the PVC pipe, E, is covered with masking tape. The pipe is then inserted in the free end of the small connector.
4) The assembled mold is inserted into the recesses in the top and bottom wooden pieces of the fixture, F. The threaded rods, G, are then inserted between the wooden boards. The rods are used to hold the molds together and center the reinforcing bars by tightening or loosening the nuts on the rods.

The "lollipop" specimens are cast in three layers. The mortar-wrapped specimens are cast in four layers. Each layer is rodded 25 times with a 2-mm (0.080-in.) diameter rod. The rod is allowed to penetrate the previous layer of mortar. After rodding, each layer is vibrated for 30 seconds on a vibrating table with amplitude of 0.15 mm (0.006 in.) and a frequency of 60 Hz.

The specimens are removed from the molds 24 hours after casting and placed in lime-saturated water for 13 days. After this period, the specimens are removed from the water, the tapped end of the specimen is dried with compressed air, and a 16-gage copper wire is attached to the specimen with a 10-24$\times$10 mm ($^3/_8$ in.) threaded bolt. The electrical connection is coated with epoxy according the

manufacturer's recommendations, to prevent crevice corrosion. The epoxy is allowed to dry for one day before the tests are started.

### 2.2.3 Materials and Equipment

The following equipment and materials are used in the rapid macrocell tests.

- *Voltmeter:* Hewlett Packard digital voltmeter, Model 3455A, with an impedance of 2MΩ. The voltmeter is used to measure the voltage drop across the resistor.
- *Multimeter:* Fluke 83 multimeter, with an impedance of 10MΩ. The multimeter is used to measure the corrosion potential of the specimens.
- *Mixer:* Hobart mixer, Model N-50. This mixer complies with ASTM C 305 and is used for mixing the mortar for the specimens used in the macrocell tests.
- *Saturated Calomel Electrode (SCE):* Fisher Scientific Catalog No. 13-620-52. The reference electrode is used to measure the corrosion potential of the bars.
- *Resistor:* A 10-ohm resistor is used to electronically connect the specimens at the anode and the cathode.
- *Terminal Box:* Terminal boxes are used to make the electrical connections between the test specimens. Each terminal box consists of a project box (from Radio Shack) with 5 pairs of binding posts (one red and one black). A 10-ohm resistor connects each pair of binding posts.
- *Wire:* 16-gage insulated copper wire is used to make the electrical connections to the bars.
- *Mortar:* The mortar is made with Portland Cement Type I (ASTM C 150), ASTM C 778 graded Ottawa sand, deionized water, and a corrosion inhibitor when applicable. The original mix design has a water-cement ratio of 0.50 and a sand-cement ratio of 2. This mix design is modified to obtain the mix designs with

water-cement ratios of 0.35 and 0.45. The water content is held constant and the cement content is modified to obtain the required water-cement ratio. When a corrosion inhibitor is used, the quantity of mix water is adjusted to account for the water in the inhibitor. The quantity of sand is determined to maintain the same volume of mortar. The mortar mix designs are shown in Table 2.3. The quantities shown are enough to prepare eight mortar specimens. The mortar is mixed in accordance with the requirements in ASTM C 305.

**Table 2.3 –** Mix design for mortar used in specimens for macrocell test

| Designation | w/c ratio | Water (g) | Cement (g) | Sand (g) | Rheocrete 222$^{+}$ (mL) | DCI-S (mL) |
|---|---|---|---|---|---|---|
| **50** | 0.50 | 400 | 800 | 1600 | - | - |
| **45** | 0.45 | 400 | 889 | 1526 | - | - |
| **45RH** | 0.45 | 396 | 889 | 1526 | 5.9 | - |
| **45DC** | 0.45 | 389 | 889 | 1526 | - | 17.6 |
| **35** | 0.35 | 400 | 1143 | 1315 | - | - |
| **35RH** | 0.35 | 396 | 1143 | 1315 | 6 | - |
| **35DC** | 0.35 | 389 | 1143 | 1315 | - | 17.9 |

a. *Mortar fill:* Mortar fill is used to surround the specimens with mortar cover. It is prepared using the same materials and mixing procedure as the mortar for the specimens. The fill is cast 25 mm (1 in.) deep on a metal baking sheet. The mortar fill in the container is crushed into 25 to 50 mm (1 to 2 in.) pieces prior to use.

b. *Epoxy coating:* Two different epoxies are used to cover the electrical connections on the reinforcing steel. 1) Nap Gard Rebar Patch Kit, manufactured by Herberts-O'Brien), and 2) Scothkote 323, manufactured by 3M. The epoxy coating is applied in accordance with manufacturer's recommendations.

c. *Concrete Pore Solution:* The simulated concrete pore solution is prepared based on the analysis by Farzammehr (1985) that indicates that one liter of pore solution contains 974.8 g of distilled water, 18.81 g of potassium hydroxide (KOH), 17.87 g of sodium hydroxide (NaOH), and 0.14 g of sodium chloride (NaCl). Following the procedures used by Senecal et al. (1995), Schwensen et al. (1995), Kahrs et al. (2001), Darwin et al. (2002), and Balma et al. (2002), NaCl is not used in the simulated pore solution in the current tests. The simulated concrete pore solution has a pH of 13.4.

d. *Sodium Chloride Solution:* The solutions containing sodium chloride (NaCl) are prepared by adding 45.6 or 249.8 g of NaCl to one liter of simulated concrete pore solution to obtain 1.6 and 6.04 molal ion concentration solutions, respectively.

e. *Salt bridges:* Salt bridges are used to provide an ionic path between the solutions surrounding the cathode and the anode. They are prepared following a procedure described by Steinbach and King (1950). A salt bridge consists of a flexible latex tube with an inner diameter of 10 mm ($^3/_8$ in.), filled with a gel. The gel is made using 4.5 g of agar, 30 g of potassium chloride (KCl), and 100 g of distilled water, enough to produce 4 salt bridges, each with a length of 0.6 m (2 ft). Salt bridges are prepared by mixing the constituents and heating them over a burner or hotplate for about 1 minute, or until the solution starts to thicken. The gel is poured into the latex tubes using a funnel. The salt bridges are then placed in boiling water for one hour, keeping the ends of the tubes out of the water. After boiling, the salt bridges are allowed to cool until firm. To provide an adequate ionic path, the gel in the salt bridge must be continuous, without any air bubbles.

f. *Air scrubber:* Air is bubbled into the simulated concrete pore solution surrounding the cathode in the macrocells to provide enough oxygen for the

cathodic reaction. An air scrubber is used to prevent carbonation of the pore solution by eliminating the carbon dioxide from the air. To prepare the air scrubber, a 5-gallon container is filled with a 1M sodium hydroxide solution. Compressed air is channeled into the scrubber and out to the specimens through latex tubing. The procedure for preparing the air scrubber is as follows:

1) Two barbed fittings are inserted on the top of the container.
2) A 1.5 m (5 ft) piece of plastic tubing is cut. On one end of the tubing, 1.2 m (4 ft) is perforated with a knife, making hundreds of holes to allow the air to produce small bubbles. The end of the tubing closest to the holes is sealed with a clamp.
3) The end with the holes is coiled at the bottom of the container and trap rock is used to hold down the tubing. The other end of the tubing is connected to the inside part of one of the barbed fittings.
4) The other side of the barbed fitting is connected to a plastic tube, which is connected to the compressed air outlet.
5) Another piece of plastic tubing is connected to the outside of the other barbed fitting. The air is distributed to the solution surrounding the cathodes using 0.3 m (1 ft) lengths of latex tubing and polypropylene T-shaped connectors.
6) Screw clamps are placed on the tubing to regulate the amount of air bubbled into each container.

Distilled water is periodically added to the container to replace water that is lost due to evaporation. The pH of the solution is checked every 2 months. Additional NaOH is added as needed.

### 2.2.4 Test Program

A summary of the test program for the rapid macrocell tests is presented in Tables 2.4 and 2.5 for bare and mortar-clad bars, respectively. Five or six specimens were evaluated for bare bars, and three to six specimens were evaluated for mortar-clad bars. Bare bars are used to evaluate the different types of steel in a 1.6 or 6.04 m ion NaCl and simulated concrete pore solution. Mortar-clad bars are used to evaluate the different types of steel, as well as conventional steel clad with mortar containing corrosion inhibitors (Rheocrete 222+ or DCI-S) and mortar with water-cement ratios of 0.35 or 0.45. A total of 139 tests with bare bars and 136 tests with mortar-clad bars were performed.

**Table 2.4 –** Test program for macrocell test with bare bars

| Specimen designation | NaCl ion concentration | Steel type | Number of tests |
|---|---|---|---|
| M-N | 1.6 m | N | 5 |
| M-T | 1.6 m | T | 5 |
| M-CRPT1 | 1.6 m | CRPT1 | 5 |
| M-CRPT2 | 1.6 m | CRPT2 | 5 |
| M-CRT | 1.6 m | CRT | 5 |
| M-2101(1) | 1.6 m | 2101(1) | 5 |
| M-2101(1)p | 1.6 m | 2101(1)p | 5 |
| M-2101(2) | 1.6 m | 2101(2) | 6 |
| M-2101(2)p | 1.6 m | 2101(2)p | 6 |
| M-2101(2)s | 1.6 m | 2101(2) | 6 |
| M-2205 | 1.6 m | 2205 | 5 |
| M-2205p | 1.6 m | 2205p | 5 |
| M-N3 | 1.6 m | N3 | 6 |
| M-MMFX(1) | 1.6 m | MMFX | 6 |
| M-MMFX(2) | 1.6 m | MMFX | 6 |
| M-MMFXb | 1.6 m | MMFX | 3 |
| M-N2h | 6.04 m | N2 | 5 |
| M-2101(1)h | 6.04 m | 2101(1) | 5 |
| M-2101(1)ph | 6.04 m | 2101(1)p | 5 |
| M-2101(2)h | 6.04 m | 2101(2) | 6 |
| M-2101(2)ph | 6.04 m | 2101(2)p | 6 |
| M-2101(2)sh | 6.04 m | 2101(2)s | 6 |
| M-2205h | 6.04 m | 2205 | 6 |
| M-2205ph | 6.04 m | 2205p | 5 |
| M-N3h | 6.04 m | N3 | 5 |
| M-MMFXsh | 6.04 m | MMFX | 6 |

* M - A

**M**: macrocell test

**A**: steel type → N, N2, and N3: conventional normalized steel, T: conventional, Thermex-treated steel, CRPT1: microalloyed steel with a high phosphorus content (0.117%), Thermex treated, CRPT2: microalloyed steel with a high phosphorus content (0.100%), Thermex treated, CRT: microalloyed steel with normal phosphorus content, Thermex treated, MMFX: MMFX-2 microcomposite steel, ECR: epoxy-coated steel, 2101(1) and 2101(2): Duplex stainless steel (21% chromium, 1% nickel), 2205: Duplex stainless steel (25% chromium, 5% nickel), p: pickled, s: sandblasted, b: bent bars at the anode, h: 6.04 m ion concentration

**Table 2.5 –** Test program for macrocell test with mortar specimens.

| Specimen designation | Type of specimen | NaCl ion concentration | Steel type | w/c ratio | Corrosion inhibitor | Number of tests |
|---|---|---|---|---|---|---|
| M-N-50 | Lollipop | 1.6 m | N | 0.50 | - | 5 |
| M-T-50 | Lollipop | 1.6 m | T | 0.50 | - | 5 |
| M-CRPT1-50 | Lollipop | 1.6 m | CRPT1 | 0.50 | - | 5 |
| M-CRPT2-50 | Lollipop | 1.6 m | CRPT2 | 0.50 | - | 5 |
| M-CRT-50 | Lollipop | 1.6 m | CRT | 0.50 | - | 5 |
| M-Nc-50 | Lollipop w/caps | 1.6 m | N | 0.50 | - | 4 |
| M-Tc-50 | Lollipop w/caps | 1.6 m | T | 0.50 | - | 4 |
| M-CRPT1c-50 | Lollipop w/caps | 1.6 m | CRPT1 | 0.50 | - | 4 |
| M-CRPT2c-50 | Lollipop w/caps | 1.6 m | CRPT2 | 0.50 | - | 4 |
| M-CRTc-50 | Lollipop w/caps | 1.6 m | CRT | 0.50 | - | 4 |
| M-N2-50 | Mortar-wrapped | 1.6 m | N2 | 0.50 | - | 5 |
| M-2101(1)-50 | Mortar-wrapped | 1.6 m | 2101(1) | 0.50 | - | 4 |
| M-2101(1)p-50 | Mortar-wrapped | 1.6 m | 2101(1)p | 0.50 | - | 4 |
| M-2101(2)-50 | Mortar-wrapped | 1.6 m | 2101(2) | 0.50 | - | 6 |
| M-2101(2)p-50 | Mortar-wrapped | 1.6 m | 2101(2)p | 0.50 | - | 6 |
| M-2205-50 | Mortar-wrapped | 1.6 m | 2205 | 0.50 | - | 6 |
| M-2205p-50 | Mortar-wrapped | 1.6 m | 2205p | 0.50 | - | 6 |
| M-N3-50 | Mortar-wrapped | 1.6 m | N3 | 0.50 | - | 6 |
| M-MMFX-50 | Mortar-wrapped | 1.6 m | MMFX | 0.50 | - | 6 |
| M-MMFX/N3-50 | Mortar-wrapped | 1.6 m | MMFX/N3 | 0.50 | - | 3 |
| M-N3/MMFX-50 | Mortar-wrapped | 1.6 m | N3/MMFX | 0.50 | - | 3 |
| M-ECR-50 | Mortar-wrapped | 1.6 m | ECR | 0.50 | - | 6 |
| M-N-45 | Lollipop | 1.6 m | N | 0.45 | - | 5 |
| M-N-RH45 | Lollipop | 1.6 m | N | 0.45 | Rheocrete 222+ | 5 |
| M-N-DC45 | Lollipop | 1.6 m | N | 0.45 | DCI-S | 5 |
| M-N-35 | Lollipop | 1.6 m | N | 0.35 | - | 5 |
| M-N-RH35 | Lollipop | 1.6 m | N | 0.35 | Rheocrete 222+ | 5 |
| M-N-DC35 | Lollipop | 1.6 m | N | 0.35 | DCI-S | 5 |

* M – A - B

**M**: macrocell test

**A**: steel type → N, N2, and N3: conventional normalized steel, T: conventional, Thermex-treated steel, CRPT1: CRPT1: microalloyed steel with a high phosphorus content (0.117%), Thermex treated, CRPT2: microalloyed steel with a high phosphorus content (0.100%), Thermex treated, CRT: microalloyed steel with normal phosphorus content, Thermex treated, MMFX: MMFX-2 microcomposite steel, ECR: epoxy-coated steel, 2101(1) and 2101(2): Duplex stainless steel (21% chromium, 1% nickel), 2205: Duplex stainless steel (25% chromium, 5% nickel), p: pickled, c: epoxy-coated caps on the end of the bar.

**B**: mix design → 50: water-cement ratio of 0.50 and no inhibitor, 45: water-cement ratio of 0.45 and no inhibitor, RH45: water-cement ratio of 0.45 and Rheocrete 222+, DC45: water-cement ratio of 0.45 and DCI-S, 35: water-cement ratio of 0.35 and no inhibitor, RH35: water-cement ratio of 0.35 and Rheocrete 222+, DC35: water-cement ratio of 0.35 and DCI-S.

## 2.3 BENCH-SCALE TESTS

Three bench-scale tests, the Southern Exposure, cracked beam, and ASTM G 109 tests, are used for this study. In each case, the testing period is 96 weeks. As in the corrosion macrocell test, the specimens are monitored by measuring the corrosion rate and corrosion potential of the bars. In addition, the mat-to-mat resistance is recorded.

### 2.3.1 Test Procedures

*Southern Exposure (SE)*

The Southern Exposure specimen (Figure 2.9) consists of a concrete slab, 305 mm (12 in.) long, 305 mm (12 in.) wide, and 178 mm (7 in.) high. The slab contains two mats of steel electrically connected across a 10-ohm resistor. The top mat of steel has two bars, and the bottom mat of steel has four bars. A concrete dam is cast around the top edge of the specimen at the same time as the specimen is cast. The top and bottom concrete cover is 25 mm (1 in.).

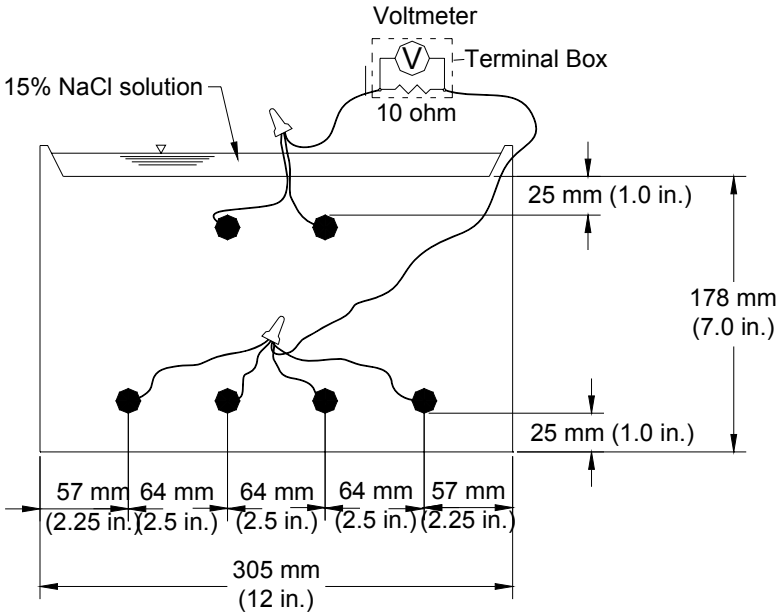


**Figure 2.9 –** Southern Exposure specimen

*Cracked Beam (CB)*

The cracked beam specimen (Figure 2.10a) is the same length and height as the Southern Exposure specimen, but half the width. It contains one bar in the top mat, electrically connected across a 10-ohm resistor to two bars in the bottom mat. A

crack is simulated in the concrete parallel to and above the top bar using a 0.30 mm (0.012 in.) stainless steel shim, 152 mm (6 in.) long, cast into the concrete and removed 24 hours after casting. As in the Southern Exposure specimen, the concrete cover to the top and bottom steel is 25 mm (1 in.). The width of the crack, 0.30 mm, is representative of typical crack widths observed in concrete bridge decks.

*ASTM G 109*

ASTM G 109 can be used to evaluate corrosion inhibitors for steel in concrete and to evaluate the corrosivity of admixtures in a chloride environment. The specimen (Figure 2.10b) has the following dimensions: 279 mm (11 in.) × 152 mm (6 in.) × 114 mm (4.5 in.). The specimen contains two layers of bars; the top layer has one bar with a 25 mm (1 in.) top concrete cover and the bottom layer contains 2 bars with a bottom concrete cover of 25 mm (1 in.). The two layers are electrically connected across a 100-ohm resistor. A plexiglass dam is used to pond a solution on the top of the specimen over a region with dimensions of 76 × 150 mm (3 × 6 in.).

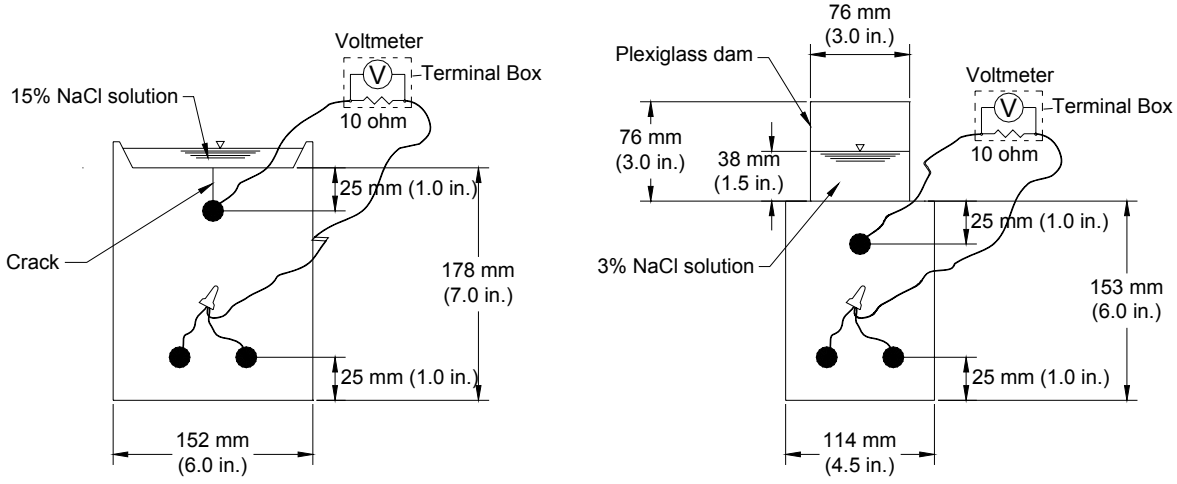


**Figure 2.10 –** (a) Cracked beam specimen and (b) ASTM G 109 specimen

*Test Procedure for Southern Exposure (SE) and Cracked Beam (CB) Tests*

The test procedure for the Southern Exposure and cracked beam specimens proceeds as follows:

1) On the first day, the specimens are ponded with a 15% NaCl solution at room temperature, 20 to 29°C (68 to 84°F). This solution is left on the specimen for 4 days.
2) On the fourth day, the voltage drop across the 10-ohm resistor connecting the two mats of steel is recorded for each specimen. The circuit is then disconnected and the mat-to-mat resistance is recorded. Two hours after disconnecting the specimens, the solution on top of the specimens is removed with a vacuum, and the corrosion potentials with respect to a copper-copper sulfate electrode (CSE) of the top and bottom mats of steel are recorded.
3) After the readings have been obtained, a heat tent is placed over the specimens, which maintains a temperature of 38 ± 2°C (100 ± 3°F). The specimens remain under the tent for three days.
4) After three days, the tent is removed and the specimens are again ponded with a 15% NaCl solution, and the cycle starts again.
5) This cycle is repeated for 12 weeks. The specimens are then subjected to 12 weeks of continuous ponding. During this period the solution is not removed and the specimens are not placed under the heat tents. Since the specimens are ponded, the corrosion potential during this period is taken with respect to a saturated calomel reference electrode (SCE) instead of a copper-copper sulfate electrode (CSE), since the SCE is more convenient when the electrode has to be immersed in solution.

After 12 weeks of continuous ponding, the drying and ponding cycle is repeated for 12 weeks, followed by 12 weeks of continuous ponding. This 24-week cycle is repeated to complete 96 weeks of testing.

*Test procedure for ASTM G 109 test*

The ponding and drying cycles in the G 109 test differ from those used in the Southern Exposure and cracked beam tests. For the G 109 test, the specimens are ponded with a 3% NaCl solution for two weeks. After two weeks the solution is removed with a vacuum and the specimens are allowed to dry for two weeks. This cycle is repeated for the full test period. The tests are performed at room temperature. The same readings as obtained for the Southern Exposure and cracked beam tests are taken weekly.

### 2.3.2 Test Specimen Preparation

The procedure for preparing the bench-scale specimens is as follows.

1) The bars are cut to the desired length, 305 mm (12 in.) for Southern Exposure and cracked beam specimens and 279 mm (11 in.) for G 109 specimens.
2) The sharp edges on the ends of the bars are removed with a grinder.
3) The ends of the bar are drilled and tapped to receive a 10-24 threaded bolt, 10 mm ($^3/_8$ in.) long. The bolt is used to hold the bars in place during casting and to make an electrical connection during the testing period.
4) The bars are then cleaned with acetone to remove dust and oil. The bars used in the G 109 test are pickled in a 10% sulfuric acid solution for 10 minutes and then dried and wire brushed. Four 3.2 mm ($^1/_8$ in.) diameter holes are drilled on the coating of the ECR bars.

5) Mineral oil is applied to the wooden forms prior to placing the bars in the forms.
6) For the cracked beam specimens, a 0.30 mm stainless steel shim is fixed on to the bottom part of the form so that the shim is located underneath and parallel to the top bar.
7) The bars are bolted into the forms.
8) The Southern Exposure and cracked beam specimens are cast upside down to allow for the integral concrete dam to be cast at the same time. The ASTM G 109 specimens are also cast upside down to provide a smooth surface for attaching the plexiglass dams.

The ASTM G 109 specimen in the present study deviates from the standard in three ways. First, the bars used are No. 16 [No. 5] bars instead of No. 13 [No. 4] bars. Second, the bars do not project out of the specimen, and third, electroplater's tape is not used to cover part of the bars, as described in the standard.

The specimens are prepared using the following procedure:

1) The concrete is mixed following the procedure in described in ASTM C 192.
2) The specimens are cast in two layers. Each layer is vibrated for 30 seconds on a vibrating table with an amplitude of 0.15 mm (0.006 in) and a frequency of 60 Hz. After the second layer is vibrated, the surface of the specimen is finished using a wooden float.
3) The specimens are cured in air for 24 hours.
4) After 24 hours, the Southern Exposure and cracked beam specimens are removed from the molds and the stainless steel shims are removed from the cracked beam specimens. The specimens are placed in a plastic bag with distilled water for 48

hours and then removed from the bags and cured in air for 25 days. After the first 24 hours, the G 109 specimens are removed from the molds and placed in a curing room, with a temperature of 23 ± 2°C (73.4 ± 3.6°F) and a relative humidity above 95%, for 26 days.

5) Several days before the testing period starts, 16-gage insulated copper wire is attached to the bars in the Southern Exposure and cracked beam specimens using 10-24 threaded bolts, 10 mm ($^3/_8$ in.) long. The sides of the specimens are then covered with epoxy, with emphasis on coating the electrical connections to prevent crevice corrosion or galvanic corrosion from occurring. The electrical connections are made to the bars in the G 109 specimens after the specimens have been removed from the curing room, one day before starting the tests.
6) The tops of the specimens are lightly sanded.
7) The specimens are supported on two pieces of wood, at least 13 mm (2 in.) thick, to allow air to flow under the specimens.
8) Plexiglass dams are attached to top of the G 109 specimens using superglue. The joints are sealed with silicone.
9) The top layer of steel is then connected to the outside red binding post on the terminal box, while the bottom layer of steel is connected to the outside black binding post, as illustrated in Figure 2.11.

### 2.3.3 Equipment and materials

The following equipment and materials are used in the bench-scale tests.

- *Resistor:* A 10-ohm resistor is used to electronically connect the top and bottom mats on the Southern Exposure and cracked beam specimens. A 100-ohm resistor

is used to electronically connect the top and bottom mats on the ASTM G 109 specimens.

- *Terminal Box:* As in the macrocell tests, a terminal box was prepared and used to make electrical connections between specimens. In this case, it was made up of a project box obtained from Radio Shack with 6 sets of 3 binding posts attached to it. Binding posts were either red or black. A sketch of the setup is shown in Figure 2.11. The appropriate resistor (10 ohms for SE and CB tests, and 100 ohms for G 109 test) is placed between the outside red binding post and the inner binding post. The top layer of steel is connected to the outside red binding post, while the bottom layer of steel is connected to the outside black binding post. A 16-gage insulated copper wire connects the outside black binding post to the inside binding post. This wire is disconnected from the inside binding post when an open circuit is required for measuring the corrosion potential of the bars.

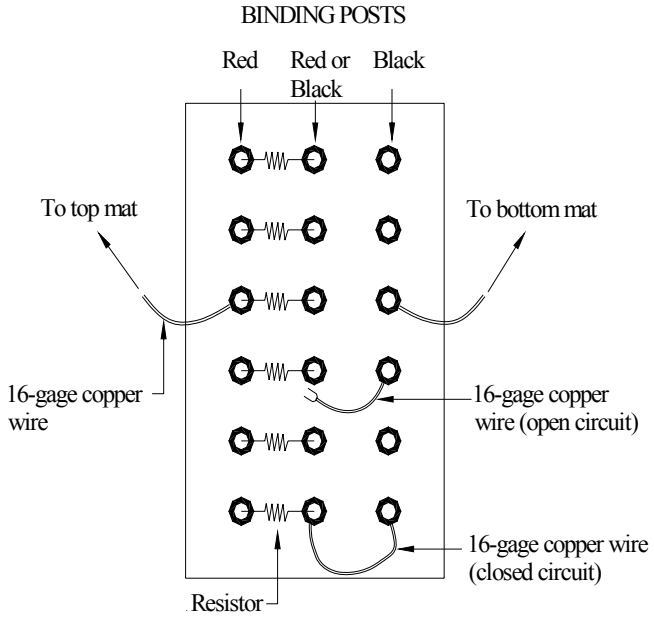


**Figure 2.11 –** Terminal box setup for bench-scale tests.

- *Saturatel Calomel Electrode (SCE):* Fisher Scientific Catalog No. 13-620-52. The saturated calomel electrode is used to take potential readings during the continuous ponding cycle.
- *Copper-copper sulfate electrode (CSE):* MC Miller Co. Electrode Model RE-5. The copper-copper sulfate electrode is used to take potential readings during the ponding and drying cycle.
- *Mixer:* Lancaster, counter current batch mixer, with a capacity of 0.06 $m^3$ (2 $ft^3$).
- *Epoxy:* Ceilgard 615 provided by Ceilcote. The epoxy is used to cover the sides of the specimens and the electrical connections to the specimen.
- *Concrete:* The concrete consists of Portland Type I cement, crushed limestone obtained from Fogle Quarry [¾ in. nominal maximum size, SG(SSD) = 2.58, absorption = 2.27%, unit weight = 1536 kg/$m^3$ (95.9 lb/$ft^3$)] as coarse aggregate , Kansas river sand (fineness modulus = 2.51, SG(SSD) = 2.60, absorption = 0.78%) as fine aggregate, tap water, vinsol resin as air-entraining agent, and Rheobuild 1000 as superplasticizer. When a corrosion inhibitor is used, the quantity of mix water is adjusted to account for the water in the inhibitor.

**Table 2.6 –** Mix design for concrete used in bench-scale specimens

| Designation | w/c ratio | Water (kg/$m^3$) | Cement (kg/$m^3$) | Coarse aggregate (kg/$m^3$) | Fine aggregate (kg/$m^3$) | Air-entraining agent (mL/$m^3$) | Rheocrete 222+ (mL/$m^3$) | DCI (mL/$m^3$) | S.P.* (mL/$m^3$) |
|---|---|---|---|---|---|---|---|---|---|
| **45** | 0.45 | 158 | 351 | 864 | 842 | 90 | - | - | - |
| **45RH** | 0.45 | 154 | 349 | 864 | 851 | 225 | 5000 | - | - |
| **45DC** | 0.45 | 145 | 342 | 864 | 848 | 88 | - | 15000 | - |
| **35** | 0.35 | 153 | 438 | 862 | 764 | 80 | - | - | 750 |
| **35RH** | 0.35 | 155 | 448 | 864 | 751 | 250 | 5000 | - | 760 |
| **35DC** | 0.35 | 147 | 445 | 864 | 761 | 85 | - | 15000 | 800 |

* S.P. = superplasticizer, Rheobuild 1000

The concrete has a slump of 3 in. and air content of 6.0%.

- *Voltmeter:* Hewlett Packard digital voltmeter, Model 3455A, with an impedance of 2MΩ. The voltmeter is used to measure the voltage drop across the resistor.
- *Multimeter:* Fluke 83 multimeter, with an impedance of 10MΩ. The multimeter is used to measure the corrosion potential of the specimens.
- *Ohmmeter:* Hewlett Packard digital milliohmmeter, Model 4338A.
- *Plexiglass:* Plexiglass with a wall thickness of 3 mm (0.125 in.) is used to build the plastic dams on top of the G 109 specimens.
- *Sulfuric acid:* A 10% solution by weight of sulfuric acid is used to pickle the bars for the ASTM G 109 test.

### 2.3.4 Test Program

A summary of the test program for the bench-scale tests is presented in Tables 2.7 and 2.9. Three to six specimens were evaluated for each type of steel, as well as for specimens with concrete containing corrosion inhibitors (Rheocrete 222+ or DCI-S) and concrete with water-cement ratios of 0.35 or 0.45. A total of 301 Southern Exposure, cracked beam, and ASTM G 109 tests were performed.

**Table 2.7 –** Test program for Southern Exposure tests.

| Specimen designation | Steel type | w/c ratio | Corrosion inhibitor | Number of tests |
|---|---|---|---|---|
| SE-N-45 | N | 0.45 | - | 6 |
| SE-T-45 | T | 0.45 | - | 6 |
| SE-CRPT1-45 | CRPT1 | 0.45 | - | 6 |
| SE-CRPT2-45 | CRPT2 | 0.45 | - | 6 |
| SE-CRT-45 | CRT | 0.45 | - | 6 |
| SE-N/CRPT1-45 | N/CRPT1 | 0.45 | - | 3 |
| SE-CRPT1/N-45 | CRPT1/N | 0.45 | - | 3 |
| SE-2101(1)-45 | 2101(1) | 0.45 | - | 6 |
| SE-2101(1)p-45 | 2101(1)p | 0.45 | - | 6 |
| SE-2101(2)-45 | 2101(2) | 0.45 | - | 6 |
| SE-2101(2)p-45 | 2101(2)p | 0.45 | - | 6 |
| SE-2205-45 | 2205 | 0.45 | - | 6 |
| SE-2205p-45 | 2205p | 0.45 | - | 6 |
| SE-2205/N2-45 | 2205/N2 | 0.45 | - | 3 |
| SE-N2/2205-45 | N2/2205 | 0.45 | - | 3 |
| SE-N3-45 | N3 | 0.45 | - | 6 |
| SE-MMFX-45 | MMFX | 0.45 | - | 6 |
| SE-MMFXb-45 | MMFX | 0.45 | - | 3 |
| SE-MMFX/N3-45 | MMFX/N3 | 0.45 | - | 3 |
| SE-N3/MMFX-45 | N3/MMFX | 0.45 | - | 3 |
| SE-ECR | ECR | 0.45 | - | 6 |
| SE-N-RH45 | N | 0.45 | Rheocrete 222+ | 3 |
| SE-N-DC45 | N | 0.45 | DCI-S | 3 |
| SE-N-35 | N | 0.35 | - | 3 |
| SE-N-RH35 | N | 0.35 | Rheocrete 222+ | 3 |
| SE-N-DC35 | N | 0.35 | DCI-S | 3 |
| SE-T-RH45 | T | 0.45 | Rheocrete 222+ | 3 |
| SE-T-DC45 | T | 0.45 | DCI-S | 3 |
| SE-T-35 | T | 0.35 | - | 3 |
| SE-T-RH35 | T | 0.35 | Rheocrete 222+ | 3 |
| SE-T-DC35 | T | 0.35 | DCI-S | 3 |

* SE – A - B

**SE**: Southern Exposure test

**A**: steel type → N, N2, and N3: conventional normalized steel, T: conventional, Thermex-treated steel, CRPT1: CRPT1: microalloyed steel with a high phosphorus content (0.117%), Thermex treated, CRPT2: microalloyed steel with a high phosphorus content (0.100%), Thermex treated, CRT: microalloyed steel with normal phosphorus content, Thermex treated, MMFX: MMFX-2 microcomposite steel, ECR: epoxy-coated steel, 2101(1) and 2101(2): Duplex stainless steel (21% chromium, 1% nickel), 2205: Duplex stainless steel (25% chromium, 5% nickel), p: pickled, b: bent bars on the top mat.

**B**: mix design → 45: water-cement ratio of 0.45 and no inhibitor, RH45: water-cement ratio of 0.45 and Rheocrete 222+, DC45: water-cement ratio of 0.45 and DCI-S, 35: water-cement ratio of 0.35 and no inhibitor, RH35: water-cement ratio of 0.35 and Rheocrete 222+, DC35: water-cement ratio of 0.35 and DCI-S.

**Table 2.8 –** Test program for cracked beam tests.

| Specimen designation | Steel type | w/c ratio | Corrosion inhibitor | Number of tests |
|---|---|---|---|---|
| CB-N-45 | N | 0.45 | - | 6 |
| CB-T-45 | T | 0.45 | - | 6 |
| CB-CRPT1-45 | CRPT1 | 0.45 | - | 6 |
| CB-CRPT2-45 | CRPT2 | 0.45 | - | 6 |
| CB-CRT-45 | CRT | 0.45 | - | 6 |
| CB-2101(1)-45 | 2101(1) | 0.45 | - | 3 |
| CB-2101(1)p-45 | 2101(1)p | 0.45 | - | 3 |
| CB-2101(2)-45 | 2101(2) | 0.45 | - | 6 |
| CB-2101(2)p-45 | 2101(2)p | 0.45 | - | 6 |
| CB-2205-45 | 2205 | 0.45 | - | 5 |
| CB-2205p-45 | 2205p | 0.45 | - | 5 |
| CB-N3-45 | N3 | 0.45 | - | 6 |
| CB-MMFX-45 | MMFX | 0.45 | - | 6 |
| CB-ECR | ECR | 0.45 | - | 6 |
| CB-N-RH45 | N | 0.45 | Rheocrete 222+ | 3 |
| CB-N-DC45 | N | 0.45 | DCI-S | 3 |
| CB-N-35 | N | 0.35 | - | 3 |
| CB-N-RH35 | N | 0.35 | Rheocrete 222+ | 3 |
| CB-N-DC35 | N | 0.35 | DCI-S | 3 |
| CB-T-RH45 | T | 0.45 | Rheocrete 222+ | 3 |
| CB-T-DC45 | T | 0.45 | DCI-S | 3 |
| CB-T-35 | T | 0.35 | - | 3 |
| CB-T-RH35 | T | 0.35 | Rheocrete 222+ | 3 |
| CB-T-DC35 | T | 0.35 | DCI-S | 3 |

* CB – A - B

**CB**: Cracked beam test

**A**: steel type → N and N3: conventional normalized steel, T: conventional, Thermex-treated steel, CRPT1: CRPT1: microalloyed steel with a high phosphorus content (0.117%), Thermex treated, CRPT2: microalloyed steel with a high phosphorus content (0.100%), Thermex treated, CRT: microalloyed steel with normal phosphorus content, Thermex treated, MMFX: MMFX-2 microcomposite steel, ECR: epoxy-coated steel, 2101(1) and 2101(2): Duplex stainless steel (21% chromium, 1% nickel), 2205: Duplex stainless steel (25% chromium, 5% nickel), p: pickled, b: bent bars on the top mat.

**B**: mix design → 45: water-cement ratio of 0.45 and no inhibitor, RH45: water-cement ratio of 0.45 and Rheocrete 222+, DC45: water-cement ratio of 0.45 and DCI-S, 35: water-cement ratio of 0.35 and no inhibitor, RH35: water-cement ratio of 0.35 and Rheocrete 222+, DC35: water-cement ratio of 0.35 and DCI-S.

**Table 2.9 –** Test program for ASTM G 109 tests.

| Specimen designation | Steel type | w/c ratio | Corrosion inhibitor | Number of tests |
|---|---|---|---|---|
| G-N-45 | N | 0.45 | - | 6 |
| G-T-45 | T | 0.45 | - | 6 |
| G-CRPT1-45 | CRPT1 | 0.45 | - | 6 |
| G-CRPT2-45 | CRPT2 | 0.45 | - | 6 |
| G-CRT-45 | CRT | 0.45 | - | 6 |
| G-N-RH45 | N | 0.45 | Rheocrete 222+ | 3 |
| G-N-DC45 | N | 0.45 | DCI-S | 3 |
| G-N-35 | N | 0.35 | - | 3 |
| G-N-RH35 | N | 0.35 | Rheocrete 222+ | 3 |
| G-N-DC35 | N | 0.35 | DCI-S | 3 |
| G-T-RH45 | T | 0.45 | Rheocrete 222+ | 3 |
| G-T-DC45 | T | 0.45 | DCI-S | 3 |
| G-T-35 | T | 0.35 | - | 3 |
| G-T-RH35 | T | 0.35 | Rheocrete 222+ | 3 |
| G-T-DC35 | T | 0.35 | DCI-S | 3 |

* G – A - B

**G**: ASTM G 109 test

**A**: steel type → N, N2, and N3: conventional normalized steel, T: conventional, Thermex-treated steel, CRPT1: CRPT1: microalloyed steel with a high phosphorus content (0.117%), Thermex treated, CRPT2: microalloyed steel with a high phosphorus content (0.100%), Thermex treated, CRT: microalloyed steel with normal phosphorus content, Thermex treated, MMFX: MMFX-2 microcomposite steel, ECR: epoxy-coated steel, 2101(1) and 2101(2): Duplex stainless steel (21% chromium, 1% nickel), 2205: Duplex stainless steel (25% chromium, 5% nickel), p: pickled, b: bent bars on the top mat.

**B**: mix design → 45: water-cement ratio of 0.45 and no inhibitor, RH45: water-cement ratio of 0.45 and Rheocrete 222+, DC45: water-cement ratio of 0.45 and DCI-S, 35: water-cement ratio of 0.35 and no inhibitor, RH35: water-cement ratio of 0.35 and Rheocrete 222+, DC35: water-cement ratio of 0.35 and DCI-S.

## 2.4 ELECTROCHEMICAL IMPEDANCE SPECTROSCOPY TESTS

AC impedance measurements are performed on the rapid macrocell mortar specimens and the Southern Exposure specimens to determine an equivalent circuit for each test. Based on the equivalent circuit, a theoretical correlation between the two tests is determined. The tests are performed using a PC4/750 Potentiostat and EIS300 Electrochemical Impedance Spectroscopy system, from Gamry Instruments.

Figure 2.12 shows a sample input screen from the EIS300 software.

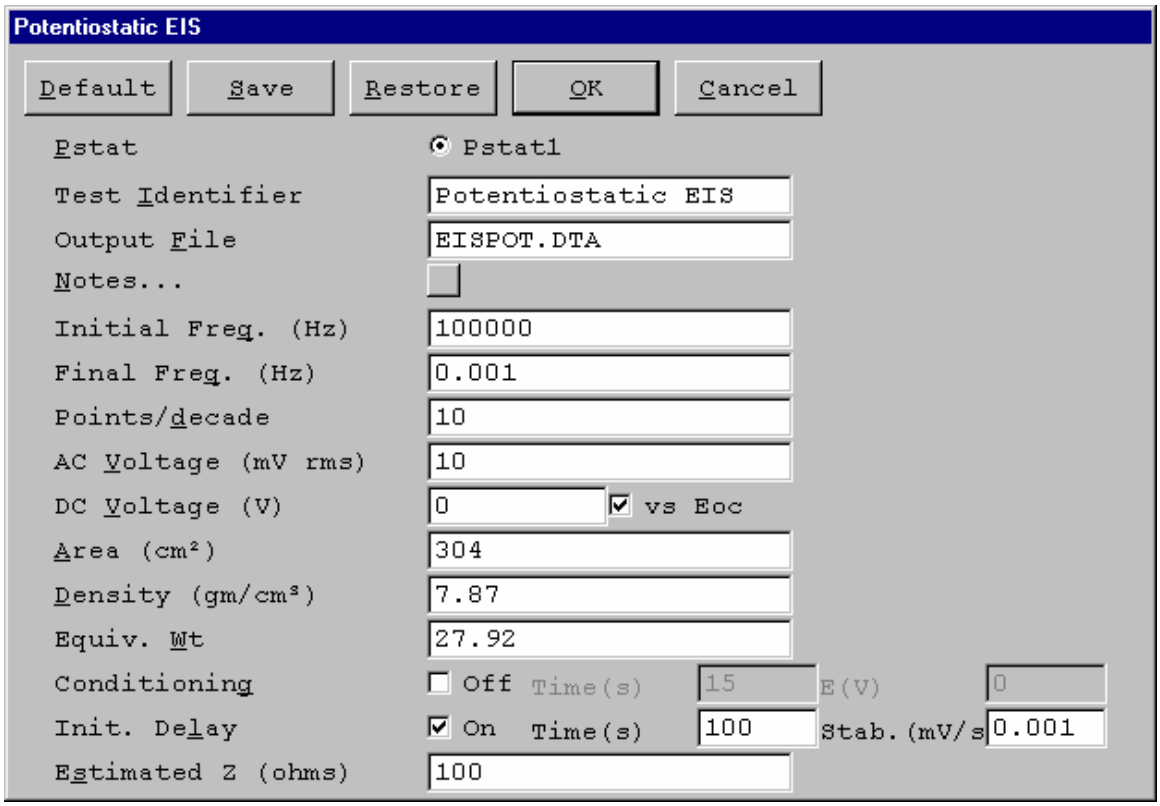


**Figure 2.12 –** Input screen for electrochemical impedance test

As shown in Figure 2.12, *Area* is the surface area of the sample in $cm^2$ exposed to the solution. *Density* and *Equiv. Wt.* are the density (in $g/cm^2$) and equivalent weight (atomic weight of an element divided by its valence), respectively. These three values are used for calculating the corrosion rate. *Initial Freq.* and *Final Freq.* define the starting and ending frequencies, respectively, for the scan. They can have values that range from 10 μHz to 100 kHz. *Points/decade* defines the density of the data that is collected in the impedance spectrum. *AC Voltage* is the amplitude of the AC signal applied to the cell during the scan. *DC Voltage* is used if a constant potential is applied to the cell during the scan. *Init. Delay* is set to ON to allow the open circuit potential of the sample to stabilize before the scan. *Time* is the time that the sample is held at open circuit before starting the scan. The delay is stopped if the

value for *Stab.* is reached before the *Time* is reached. The *Stab.* value allows the user to set a drift rate (change in open-circuit potential with respect to time) that represents a stable open-circuit potential, $E_{oc}$. If the absolute value of the drift rate falls below the specified value, the delay ends, even if the *Time* has not been reached. The *Estimated Z* parameter is a user-supplied estimate of the impedance of the cell at the *Initial Freq*. The EIS 300 system sets up the potentiostat to measure an impedance equal to *Estimated Z* and then measures the cell's impedance. *Conditioning* is used to insure the metal has a known surface condition at the start of the test. *Conditioning E* and *Conditioning Time* are the potential applied during the conditioning phase of the experiment and the length of time it is applied, respectively. The test parameters used in this study are shown in Figure 2.12. The value for *Area* is modified according to the sample being evaluated.

The tests are performed using a two electrode arrangement. In the macrocell test, the anode is used as the working electrode and the cathode is used as the counter and reference electrode. In the Southern Exposure test, the top mat of steel is the working electrode and the bottom mat of the steel is the counter and reference electrode.

The analysis of the impedance spectrum obtained is performed using the software provided with the EIS300 system. The user specifies the equivalent circuit used to model the electrochemical cell. The software makes use of a nonlinear least squares fitting (NLLS) algorithm to find the model (equivalent circuit) parameters that give the best fit between the model's impedance spectrum and the measured spectrum. The algorithm starts with initial estimates for the model's parameters and goes through a number of iterations. On each iteration the algorithm makes changes to one or more of the model's parameters and evaluates the corresponding fit. The

new values are accepted if the fit is improved, the old values are retained of the fit is not improved. The algorithm will stop making iterations when the goodness of fit reaches a given value or until a determined number of iterations is reached.

# CHAPTER 3

# EVALUATION OF CORROSION PROTECTION SYSTEMS

This chapter presents the results obtained from the rapid macrocell, Southern Exposure, cracked beam, and ASTM G 109 tests for the corrosion protection systems described in Section 2.1. Results for the rapid macrocell test include the corrosion rate, total corrosion loss, and corrosion potential of the anode and cathode with respect to a saturated calomel electrode. Results for the bench-scale tests include the corrosion rate, total corrosion loss, mat-to-mat resistance, and corrosion potential of the top and bottom mats of steel with respect to a copper-copper sulfate electrode. The Student's t-test is used to determine if there is a significant difference in the mean corrosion rates and losses for the different corrosion protection systems. The figures in this chapter show the average results. The individual test results are presented in Appendices A and B. Appendix A shows the results for the corrosion rates, losses and potentials. Appendix B shows the results for the mat-to-mat resistances. In many cases, the results show large scatter for the individual tests, as can be observed from the individual test results and the values of the standard deviation presented in this chapter. An economic analysis is performed, which includes the calculation of the present costs of bridge decks with different corrosion protection systems as well as the ratio of the premium of using duplex steel over the savings in repair costs when duplex steel is used instead of conventional uncoated or epoxy-coated steel.

For the results of the bench-scale tests, the results at week 70 of the test period were selected for comparison since some individual specimens exhibit unusual behavior after this period, which affects the average behavior. This unusual behavior

includes specimens with extremely high corrosion rates when compared to the other specimens in the same set and specimens that show drops in corrosion rate as the result of a more negative corrosion potential in the bottom mat of steel, which indicates that chlorides have reached the bottom mat of steel.

The work reported in this chapter shows that steel in specimens with mortar or concrete with a water-cement ratio of 0.35 or with corrosion inhibitors corrodes at a lower rate than in specimens with a water-cement ratio of 0.45 and no inhibitor. For samples in uncracked concrete (macrocell test with mortar specimens and Southern Exposure test), the corrosion losses of specimens with a water-cement ratio of 0.35 ranged from 7 to 60% of the corrosion loss of specimens with a water-cement ratio of 0.45. In the cracked beam test, the specimens with a water-cement ratio of 0.35 had corrosion losses that were 59% of the corrosion losses of specimens with a water-cement ratio of 0.45. The corrosion losses for specimens with corrosion inhibitors ranged from 1.3 to 68% of the corrosion losses of specimens with the same water-cement ratio and no inhibitor, in uncracked concrete. In the cracked beam test, the corrosion loss for specimens with corrosion inhibitors ranged between 51% and 179% of the corrosion losses of specimens with the same water-cement ratio and no inhibitor, indicating that, in cracked concrete, these corrosion protection systems are not as effective as they are in uncracked concrete.

The microalloyed steels (CRPT1, CRPT2, and CRT) showed no improvement in corrosion performance compared to conventional reinforcing steel. The corrosion potentials of the conventional and microalloyed steels indicated that they had a similar tendency to corrode. Corrosion rates in the rapid macrocell test showed no advantage of the microalloyed steels over conventional steel. In the bench-scale tests, only the microalloyed steel with regular phosphorus content, CRT, had lower

corrosion losses than conventional steel. After 70 weeks, corrosion losses for CRT steel were 90, 96 and 36% of the corrosion loss of conventional steel, in the Southern Exposure, cracked beam, and ASTM G 109 tests, respectively.

MMFX microcomposite steel had corrosion losses that ranged from 26 to 60% of the corrosion loss of conventional steel, while corrosion potentials indicated that they had a similar tendency to corrode.

Epoxy-coated steel had low corrosion losses based on the total area of the bar, with corrosion losses between 6 and 19% of that of uncoated conventional steel.

The 2101(2) and 2205 duplex steels evaluated in a pickled condition showed very good corrosion performance in all tests. The average corrosion losses for these steels ranged from 0.3 to 1.8% of the corrosion loss of conventional steel, and in most cases, the corrosion potentials indicated a very low tendency to corrode, even at high salt concentrations.

Based on present costs, the best options at discount rates of 2 and 4% are either a 216-mm or 230-mm deck containing 2101 pickled steel (2101p). At a 6% discount rate, the lowest cost option is a 230-mm deck containing epoxy-coated steel, when a time to first repair of 35 or 40 years is used. The ratio of the premium for using duplex steel over the savings in repair costs when duplex steel is used instead of conventional uncoated or epoxy-coated steel was also calculated. Based on the premium/savings ratio, a 216-mm deck containing 2101 pickled steel is still the best option at a discount rate of 2%. At a discount rate of 4%, some of the options using 2101 pickled steel have a premium/savings ratio below 50%, which is an acceptable value. At discount rate of 6%, the only option with a ratio lower than 50% is a 216-mm deck containing 2101p steel, when the lowest cost for the steel is used, and the deck containing epoxy-coated steel has a time to first repair of 30 years.

This chapter is divided into 8 sections. Section 3.1 presents a brief explanation of the Student's t-test, which was used to determine if the difference between the average of two samples was statistically significant. Section 3.2 presents a comparison of the results of specimens with conventional normalized steel. Section 3.3 presents the results for specimens with corrosion inhibitors and low water-cement ratio. Sections 3.4 through 3.7 present the results for microalloyed, MMFX microcomposite, epoxy-coated, and duplex stainless steels, respectively. Section 3.8 shows the results of the economic analysis performed to compare the costs of the most effective corrosion protection systems with those of uncoated conventional and epoxy-coated steel. Section 3.9 presents a discussion of the results.

## 3.1 STATISTICAL DIFFERENCE BETWEEN SAMPLES

The Student's t-test is used to evaluate if the difference of the means of two populations is statistically significant. In this study, the populations represent corrosion test results. This test is used when the sample size is small and the population standard deviations are unknown. Populations A and B have means $\mu_A$ and $\mu_B$, respectively. A sample of $n$ observations, $x_i$ ($i$ = 1 to $n$), is obtained from population A. This sample has a mean $\bar{x}$ and a standard deviation $s_x$. A sample of $m$ observations, $y_i$, is obtained from population B. This sample has a mean $\bar{y}$ and a standard deviation $s_y$. The difference between the population means $(\mu_A - \mu_B)$ is estimated by $(\bar{x} - \bar{y})$, and the standard error is estimated by Eq. (3.1).

$$\text{s.e.}(\bar{x} - \bar{y}) = \sqrt{\frac{s_x^2}{n} + \frac{s_y^2}{m}} \tag{3.1}$$

The standard error provides an indication of the accuracy of the estimated value. For smaller values of the standard error the estimate of the difference between the population means will be more accurate. The standard error is inversely proportional to the sample size, thus, the standard error decreases as the sample size increases.

A value known as the t-statistic ($t_{stat}$) is calculated from Eq. (3.2):

$$t_{stat} = \frac{\bar{x} - \bar{y}}{\sqrt{\frac{s_x^2}{n} + \frac{s_y^2}{m}}} \tag{3.2}$$

The value obtained for $t_{stat}$ is compared to the value obtained from the t-distribution, $t_{crit}$, which will depend on the level of significance, $\alpha$, and the number of degrees of freedom, $\nu$. The level of significance is the probability of rejecting the null hypothesis when it is actually true. The confidence level, *X%*, is equal to 1-$\alpha$ and measures the probability that the null hypothesis is accepted when it is true. For example, if $\alpha = 0.05$, there is a 5% probability of getting a result that indicates a difference in the means when they are actually equivalent. This translates to a confidence level of 95%. The number of degrees of freedom, $\nu$, is calculated from Eq. (3.3).

$$\nu = \frac{\left(\frac{s_x^2}{n} + \frac{s_y^2}{m}\right)}{\frac{s_x^4}{n^2(n-1)} + \frac{s_y^4}{m^2(m-1)}} \tag{3.3}$$

The values of $t_{crit}$ are tabulated in basic statistics books, and for this report the values were obtained with a Microsoft Excel spreadsheet. If the absolute value of $t_{stat}$ is greater than $t_{crit}$, then the null hypothesis ($\mu_A = \mu_B$) is rejected and the difference in the means is considered statistically different, at that level of significance. If the

absolute value of $t_{stat}$ is smaller than $t_{crit}$, then the null hypothesis is accepted and the difference in the means is considered not significant, at that level of significance.

Tables C.1 to C.14 in Appendix C show the results for the Student's t-test. The test was performed at four different levels of significance, 0.20, 0.10, 0.05, and 0.02 (confidence levels of 80, 90, 95, and 98%, respectively). Larger values of $\alpha$ give a higher probability of rejecting the null hypothesis. The tables show the materials and specimen types that are compared, the value of $t_{stat}$, and the value of $t_{crit}$ for each level of significance. A "Y" next to the value of $t_{crit}$ indicates that the difference in the means is significant, and an "N" indicates that the difference in the means is not significant. Results of the Student's t-test for the different corrosion protection systems are discussed in the corresponding section for each corrosion protection system.

## 3.2 CONVENTIONAL STEEL

The control samples for the macrocell and bench-scale tests were fabricated with three different heats of conventional steel, N, N2, and N3. This section presents the results of the rapid macrocell and bench-scale tests for specimens fabricated with conventional steel. The Student's t-test was used to determine if there is a significant difference between the corrosion rates and losses of the conventional steels.

Macrocell specimens with N steel (M-N and M-N-50) were evaluated using the test configuration shown in Figure 2.1, where the lid was placed on the top of the container. The mortar specimens containing N steel (M-N-50) were evaluated using a "lollipop" specimen, Figure 2.6(a). Corrosion products were observed on some of these bars on surfaces that were not immersed in the solution. This corrosion was attributed to the high humidity inside the container. All other specimens were

evaluated using the test configuration in Figure 2.3, where the edges of the lid were removed so that it could be placed inside of the container, just above the level of the solution, and mortar specimens were evaluated using the mortar-wrapped specimen shown in Figure 2.6(b).

Tables 3.1 and 3.2 show the corrosion rates and total corrosion losses, respectively, for specimens with conventional steel, and Tables C.1 and C.2 show the results of the Student's t-test. A large difference was observed between N steel and N2 and N3 steel for the macrocell with mortar specimens; N steel had a corrosion loss equal to 17% and 12% of the corrosion losses of N2 and N3 steel, respectively. For these specimens the difference in the mean corrosion rates and losses between N steel and either N2 or N3 steels was significant at $\alpha = 0.02$. In the Southern Exposure test, N steel had a corrosion rate equal to 45% that of N3 steel; this difference is significant at $\alpha = 0.10$. There is no statistically significant difference between N and N3 steel in the macrocell test with bare bars or in the cracked beam test.

Figures 3.1 and 3.2 show the average corrosion rates and total corrosion losses, respectively, of the macrocell tests for bare conventional steel. Both steels exhibit similar corrosion rates during the test period, with N steel showing consistently higher corrosion rates than N3 steel.

**Table 3.1 –** Average corrosion rates (in μm/year) for specimens with conventional steel.

| Specimen designation* | Specimen | | | | | | Average** | Standard deviation** |
|---|---|---|---|---|---|---|---|---|
| | 1 | 2 | 3 | 4 | 5 | 6 | | |
| **Macrocell test with bare bars in 1.6 m NaCl** | | | | | | | | |
| **M-N** | 54.59 | 56.17 | 12.28 | 37.20 | 40.79 | | 40.21 | 17.68 |
| **M-N3** | 52.60 | 0.26 | 67.77 | 40.17 | 32.43 | 22.08 | 35.88 | 23.61 |
| **Macrocell test with mortar specimens in 1.6 m NaCl** | | | | | | | | |
| **M-N-50** | 3.59 | 2.49 | 2.27 | 0.67 | 2.21 | | 2.25 | 1.04 |
| **M-N2-50** | 17.43 | 19.02 | 24.83 | 5.49 | 14.65 | | 16.28 | 7.09 |
| **M-N3-50** | 11.21 | 9.16 | 26.07 | 19.31 | 21.15 | 19.31 | 17.70 | 6.36 |
| **Southern Exposure test** | | | | | | | | |
| **SE-N-45** | 8.41 | 0.73 | 3.41 | 2.33 | 3.80 | 5.76 | 4.07 | 2.70 |
| **SE-N3-45** | 13.96 | 11.83 | 4.48 | 5.47 | 14.32 | 4.21 | 9.05 | 4.83 |
| **Cracked beam test** | | | | | | | | |
| **CB-N-45** | 9.55 | 4.55 | 2.22 | 3.92 | 17.61 | 6.22 | 7.34 | 5.61 |
| **CB-N3-45** | 20.37 | 1.70 | 23.30 | 1.58 | 5.28 | 2.31 | 9.09 | 10.01 |

* T - A - B
**T**: test → M: macrocell test, SE: Southern Exposure test, CB: cracked beam test
**A**: steel type → N, N2, and N3: conventional, normalized steel.
**B**: mix design → 50: water-cement ratio of 0.50 and no inhibitor, 45: water-cement ratio of 0.45 and no inhibitor.
** At week 15 for the macrocell test and week 70 for the Southern Exposure and cracked beam test.

**Table 3.2 –** Average corrosion losses (in μm) for specimens with conventional steel.

| Specimen designation* | Specimen | | | | | | Average** | Standard deviation** |
|---|---|---|---|---|---|---|---|---|
| | 1 | 2 | 3 | 4 | 5 | 6 | | |
| **Macrocell test with bare bars in 1.6 m NaCl** | | | | | | | | |
| **M-N** | 14.11 | 13.89 | 7.56 | 9.28 | 10.32 | | 11.03 | 2.88 |
| **M-N3** | 13.07 | 4.84 | 13.22 | 11.10 | 6.97 | 4.98 | 9.03 | 3.91 |
| **Macrocell test with mortar specimens in 1.6 m NaCl** | | | | | | | | |
| **M-N-50** | 1.05 | 0.72 | 0.53 | 0.40 | 0.51 | | 0.64 | 0.25 |
| **M-N2-50** | 4.04 | 2.95 | 2.22 | 3.75 | 6.21 | | 3.84 | 1.51 |
| **M-N3-50** | 5.54 | 5.08 | 7.01 | 5.21 | 4.79 | 5.12 | 5.46 | 0.80 |
| **Southern Exposure test** | | | | | | | | |
| **SE-N-45** | 7.13 | 8.89 | 6.90 | 3.02 | 4.19 | 4.56 | 5.78 | 2.21 |
| **SE-N3-45** | 9.80 | 13.01 | 2.50 | 5.90 | 8.65 | 3.95 | 7.30 | 3.92 |
| **Cracked beam test** | | | | | | | | |
| **CB-N-45** | 10.36 | 7.75 | 4.98 | 8.57 | 7.61 | 5.78 | 7.51 | 1.93 |
| **CB-N3-45** | 26.09 | 12.25 | 10.94 | 5.68 | 6.52 | 8.15 | 11.60 | 7.53 |

* T - A - B
**T**: test → M: macrocell test, SE: Southern Exposure test, CB: cracked beam test
**A**: steel type → N, N2, and N3: conventional, normalized steel.
**B**: mix design → 50: water-cement ratio of 0.50 and no inhibitor, 45: water-cement ratio of 0.45 and no inhibitor.
** At week 15 for the macrocell test and week 70 for the Southern Exposure and cracked beam test.

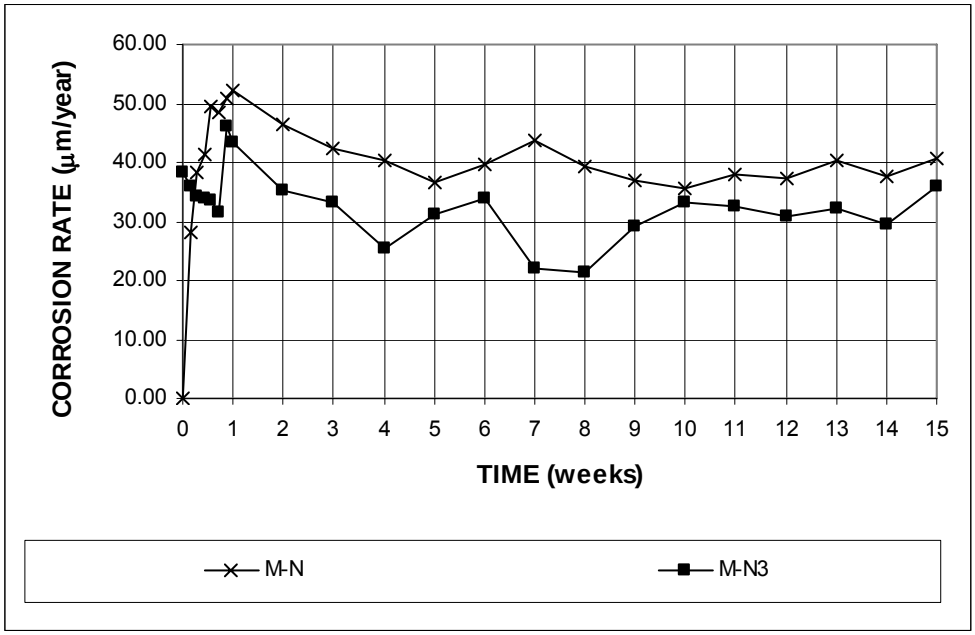


**Figure 3.1 –** Average corrosion rates as measured in the rapid macrocell test for bare conventional steel in 1.6 m ion NaCl and simulated concrete pore solution.

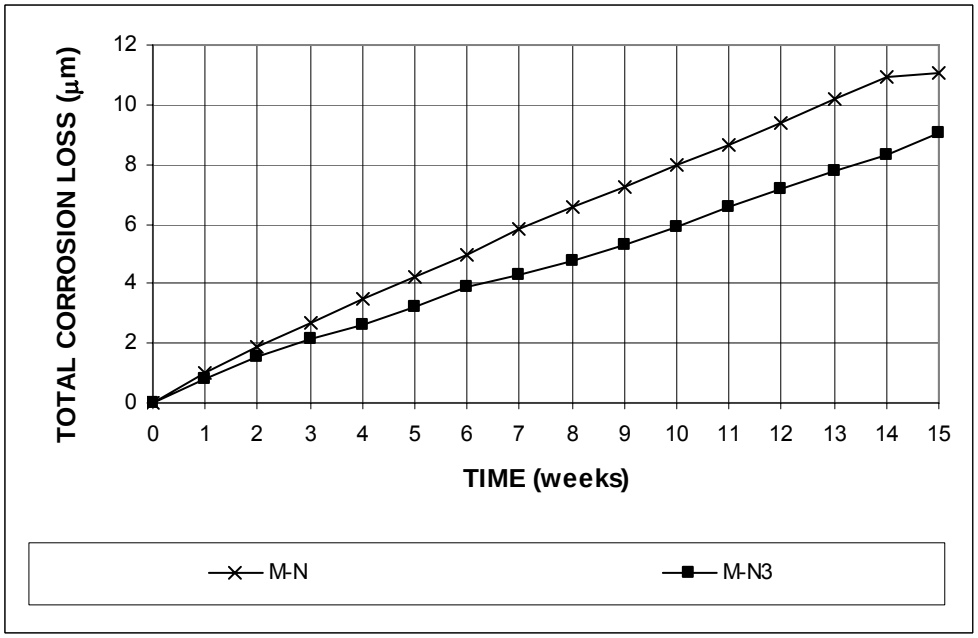


**Figure 3.2 –** Average corrosion losses as measured in the rapid macrocell test for bare conventional steel in 1.6 m ion NaCl and simulated concrete pore solution.

Figures 3.3 and 3.4 show the average corrosion rates and total corrosion losses, respectively, of the macrocell test with mortar specimens. The corrosion rate of N steel remained below 4 μm/year during the test period, while N2 and N3 steel reached corrosion rates above 10 μm/year at week 2 for N3 steel and at week 5 for N2 steel, and at some point during the test period reached values above 20 μm/year. As mentioned earlier in this section, the mortar specimen and test setup used to evaluate N steel was different from the ones used to evaluate N2 and N3 steel.

The average corrosion rates and total corrosion losses for the Southern Exposure tests are shown in Figures 3.5 and 3.6, respectively. The corrosion rates for both steels (Figure 3.5) increased with time at a similar rate during the first 45 weeks. After week 45, the corrosion rate of N steel dropped with time, while the corrosion rate of N3 steel continued to increase at a slow rate. The corrosion potentials of the top and bottom mats are shown in Figure 3.7. The corrosion potentials are very similar for both steels throughout the test period. The top and bottom mat potentials drop at a similar rate during the first weeks and both steels show a drop in the bottom mat potential near week 80.

Average corrosion rates and total corrosion losses for the cracked beam tests are shown in Figures 3.8 and 3.9, respectively. The corrosion rates for both steels are very similar during the test period, except for an increase in the corrosion rate of N3 steel between weeks 44 to 52. The corrosion potentials of the top and bottom mat are shown in Figure 3.10. Both steels show similar corrosion potentials during the test period, and both show a drop in the bottom mat potential after week 80, the latter likely due to a high chloride concentration in the concrete surrounding the bottom mat.

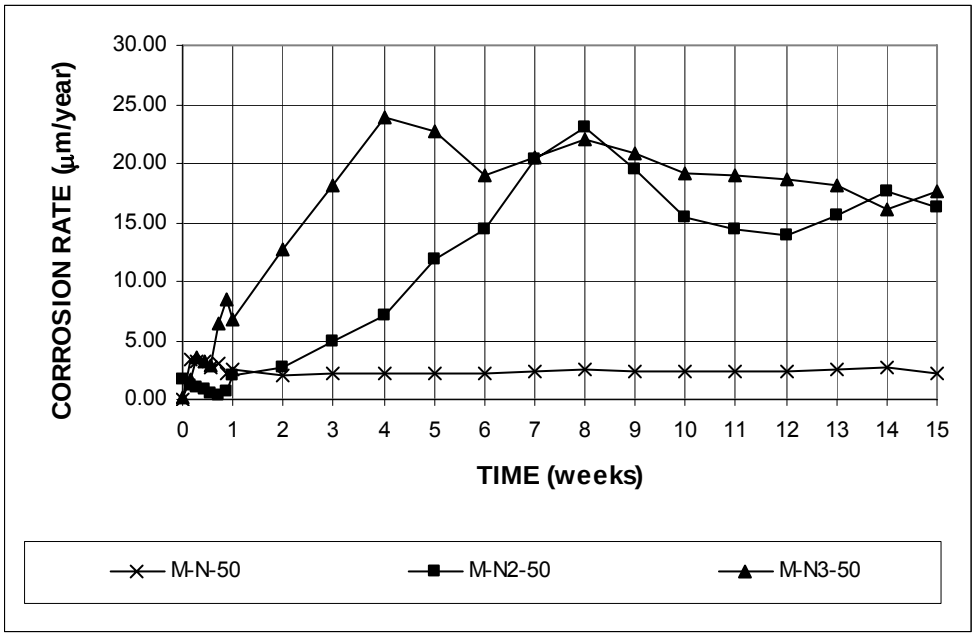


**Figure 3.3 –** Average corrosion rates as measured in the rapid macrocell test for mortar specimens in 1.6 m ion NaCl and simulated concrete pore solution for specimens with conventional steel.

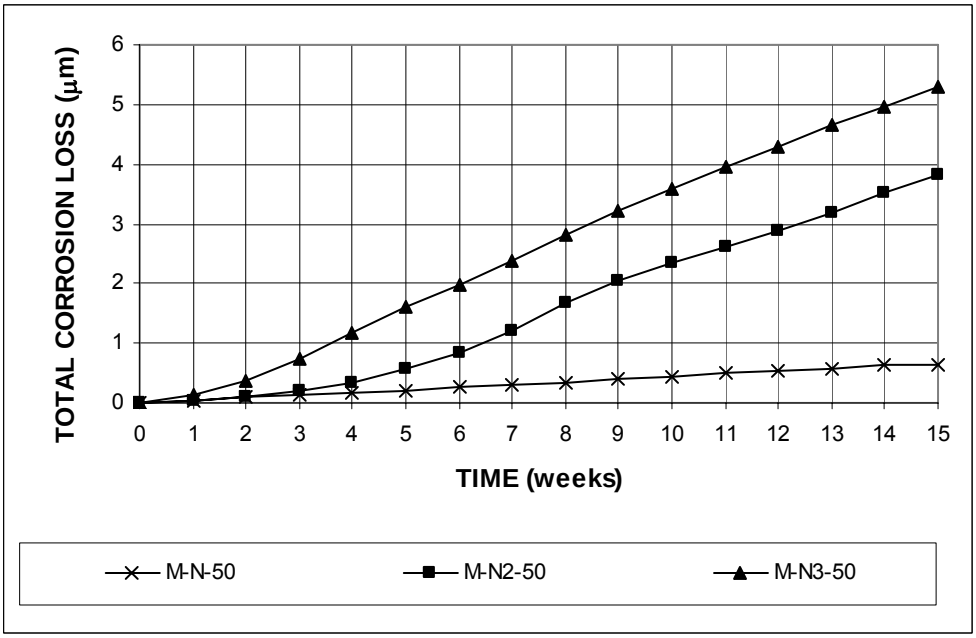


**Figure 3.4 –** Average corrosion losses as measured in the rapid macrocell test for mortar specimens in 1.6 m ion NaCl and simulated concrete pore solution for specimens with conventional steel.

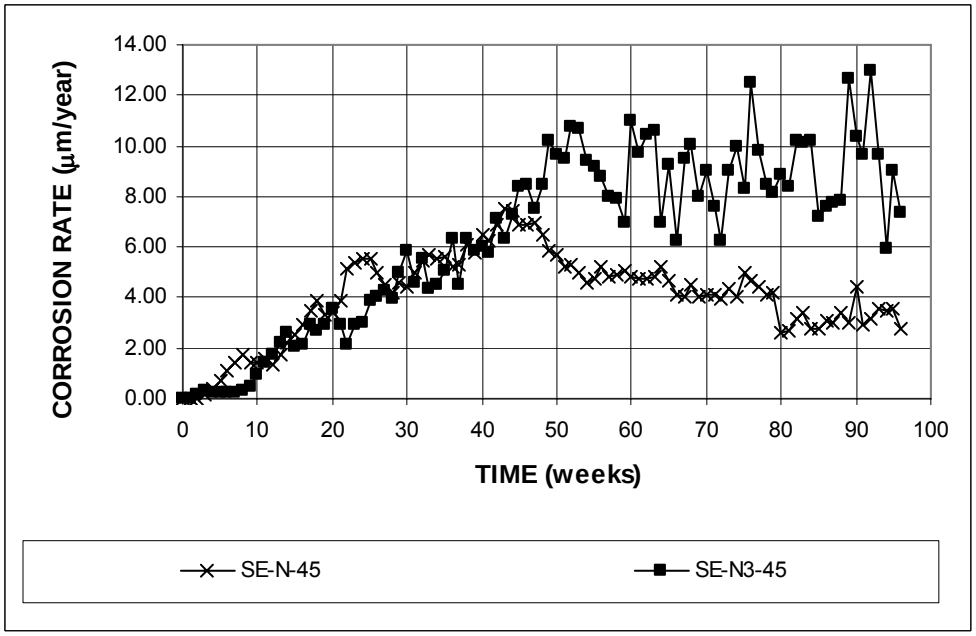


**Figure 3.5 –** Average corrosion rates as measured in the Southern Exposure test for specimens with conventional steel.

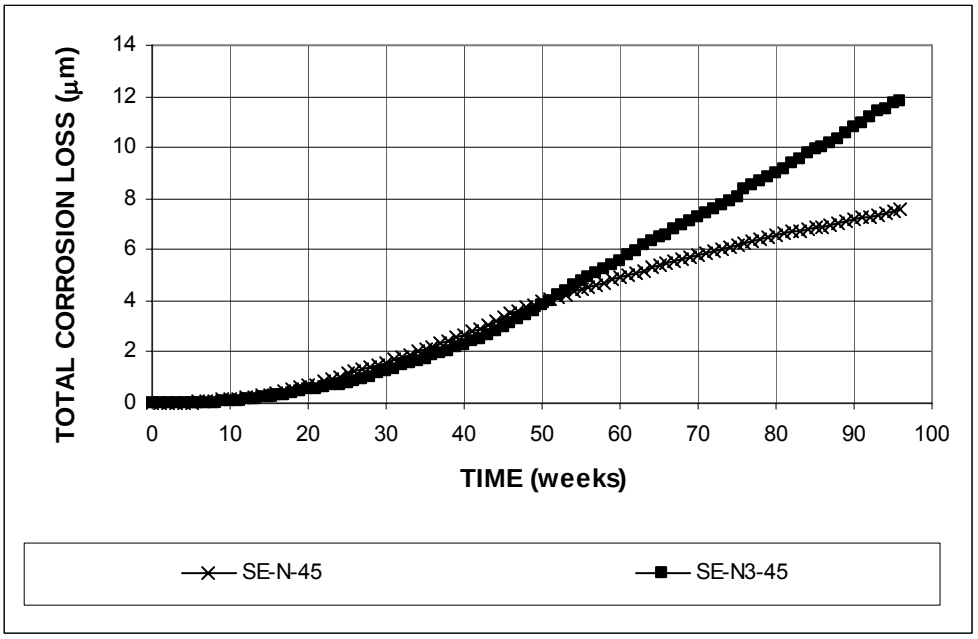


**Figure 3.6 –** Average corrosion losses as measured in the Southern Exposure test for specimens with conventional steel.

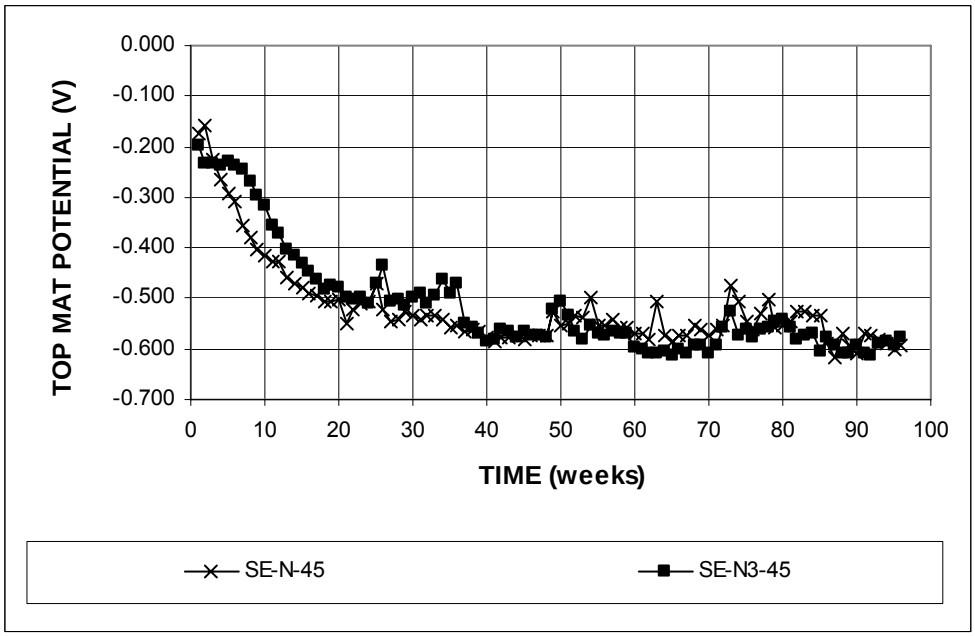


(a)

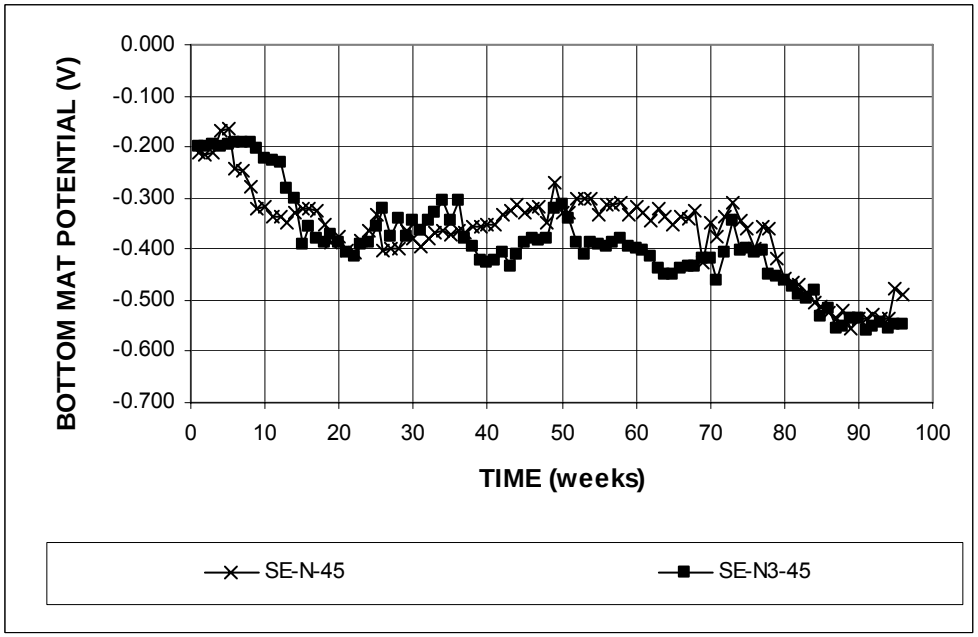


(b)

**Figure 3.7 –** (a) Average top mat corrosion potential and (b) average bottom mat corrosion potential with respect to copper-copper sulfate electrode as measured in the Southern Exposure test for specimens with conventional steel.

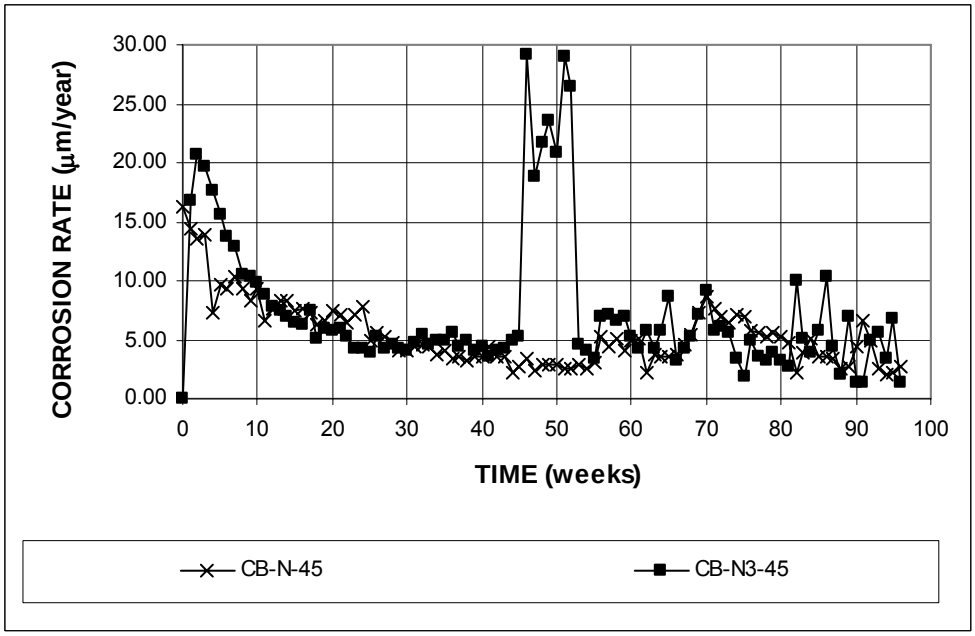


**Figure 3.8 –** Average corrosion rates as measured in the cracked beam test for specimens with conventional steel.

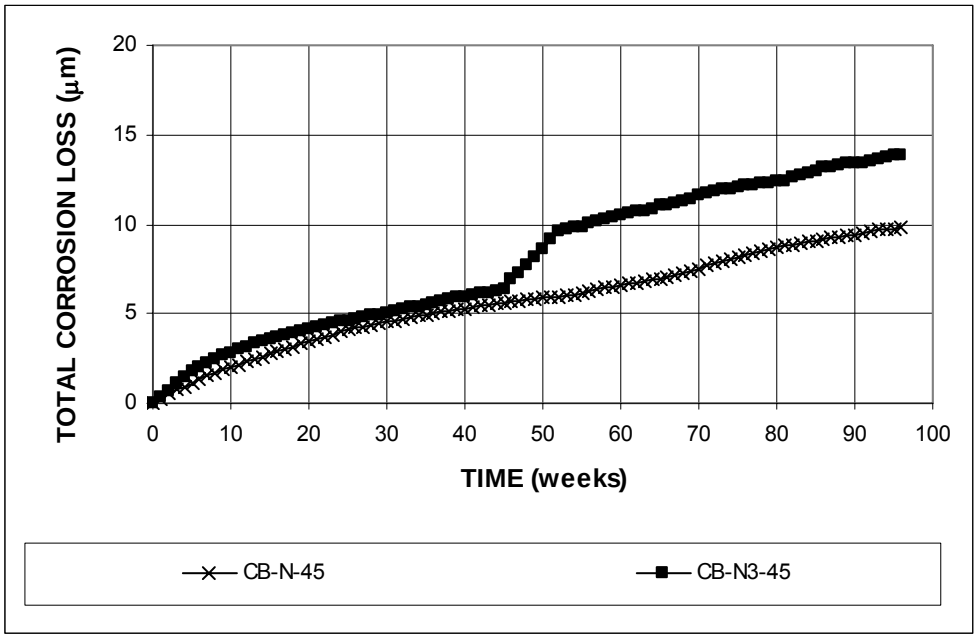


**Figure 3.9 –** Average corrosion losses as measured in the cracked beam test for specimens with conventional steel.

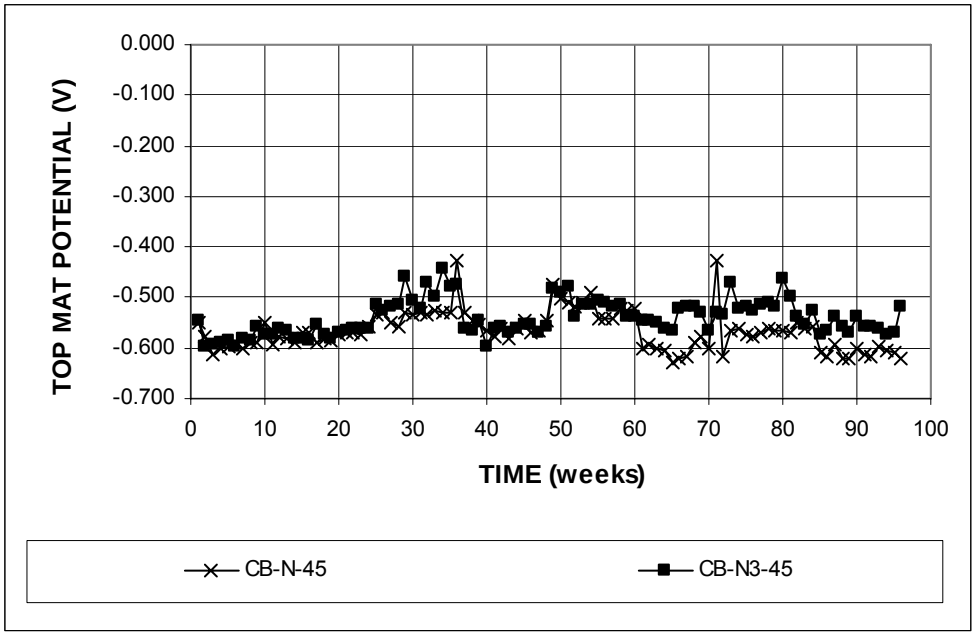


(a)

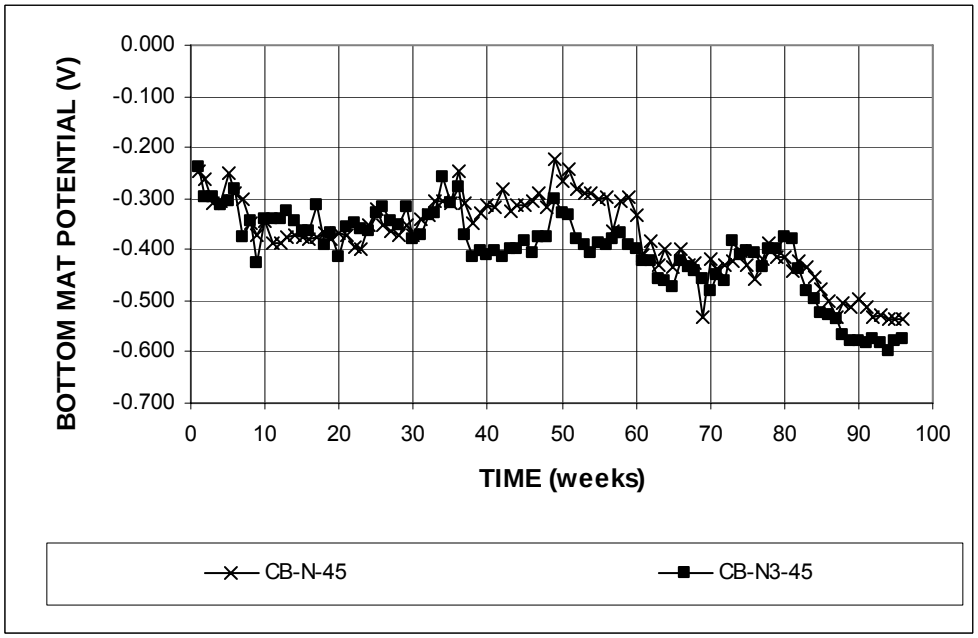


(b)

**Figure 3.10 –** (a) Average top mat corrosion potential and (b) average bottom mat corrosion potential with respect to copper-copper sulfate electrode as measured in the cracked beam test for specimens with conventional steel.

## 3.3 CORROSION INHIBITORS AND LOW WATER-CEMENT RATIO

This section describes the results for "lollipop" and bench-scale specimens prepared with concrete or mortar with water-cement ratios of 0.35 or 0.45 and with one of two corrosion inhibitors (Rheocrete 222+ or DCI-S). Macrocell specimens were evaluated using the test configuration shown in Figure 2.1, where the lid was placed on the top of the container.

### 3.3.1 Rapid Macrocell Test

Average corrosion rates for lollipop specimens in 1.6 m ion NaCl and simulated concrete pore solution are shown in Figure 3.11. Results show that the specimens with a water-cement ratio of 0.45 and no inhibitor (M-N-45) corroded at a higher rate than the other specimens during the second half of the test period. Specimens with a water-cement ratio of 0.35 and no inhibitor (M-N-35) had average corrosion rates that were higher than that of the specimens with corrosion inhibitors throughout the test period, and higher than M-N-45 during the first six weeks. Table 3.3 summarizes the average corrosion rates at week 15 and Table C.3 shows the results of the Student's t-test. Specimens M-N-45 had an average corrosion rate of 5.54 μm/year, followed by specimens M-N-35 with 1.85 μm/year, equal to 33% of the corrosion rate of M-N-45. The difference between M-N-45 and M-N-35 is significant at $\alpha = 0.10$. Specimens with a water-cement ratio of 0.45 and Rheocrete 222+ (M-N-RH45) had a corrosion rate of 1.50 μm/year, and specimens with a water-cement ratio of 0.45 and DCI-S (M-N-DC45) had a corrosion rate of 1.28 μm/year (27% and 23%, respectively, of the corrosion rate of M-N-45). The difference between M-N-45 and M-N-RH45 is significant at $\alpha = 0.10$, and the difference between M-N-45 and M-N-DC45 is significant at $\alpha = 0.05$. The specimens with the

lowest average corrosion rates were the specimens with a water-cement ratio of 0.35 and Rheocrete 222+ (M-N-RH35) with 0.23 μm/year, equal 12% of the corrosion rate of M-N-35. Specimens with a water-cement ratio of 0.35 and DCI-S (M-N-DC35) had an average corrosion rate at week 15 of 0.32 μm/year, equal 17% of the corrosion rates of M-N-35. The difference between M-N-35 and either M-N-RH35 or M-N-DC35 is significant at $\alpha = 0.20$.

The average total corrosion losses as a function of time are presented in Figure 3.12, and the total corrosion losses at week 15 are shown in Table 3.4. Results of the Student's t-test are presented in Table C.4. Specimens with a water-cement ratio of 0.45 and no inhibitor (M-N-45) had the highest total corrosion loss after 15 weeks, 0.87 μm, followed by specimens with a water-cement ratio of 0.35 and no inhibitor (M-N-35), 0.52 μm (60% of the corrosion loss of M-N-45). Specimens with a water-cement ratio of 0.45 and Rheocrete 222+ (M-N-RH45) had a corrosion loss of 0.15 μm, and specimens with a water-cement ratio of 0.45 and DCI-S (M-N-DC45) had a corrosion loss of 0.24 μm. These values are equal to 17 and 28%, respectively, of the corrosion loss of M-N-45. Statistically significant differences in the mean corrosion losses were obtained between M-N-45 and M-N-RH45 at $\alpha = 0.10$, and between M-N-45 and M-N-DC45 at $\alpha = 0.20$. The corrosion losses of specimens with a water-cement ratio of 0.35 and either Rheocrete 222+ or DCI-S (M-N-RH35 and M-N-DC35), were 0.23 and 0.15 μm, respectively. These values are equal to 44 and 29%, respectively, of the corrosion loss of M-N-35. The difference between M-N-35 and either M-N-RH35 or M-N-DC35 is not statistically significant.

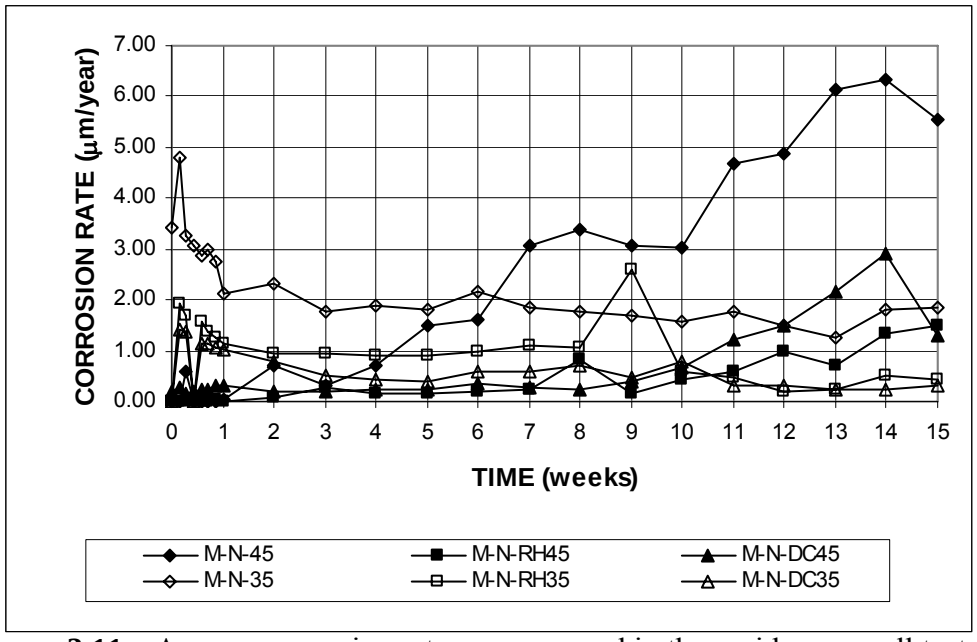


**Figure 3.11 –** Average corrosion rates as measured in the rapid macrocell test for lollipop specimens with and without corrosion inhibitors and water-cement ratios of 0.45 and 0.35 in 1.6 m ion NaCl and simulated concrete pore solution.

**Table 3.3 –** Average corrosion rates (in μm/year) at week 15 as measured in the rapid macrocell test for lollipop specimens with and without corrosion inhibitors and water-cement ratios of 0.45 and 0.35 in 1.6 m ion NaCl and simulated concrete pore solution.

| Specimen designation* | Specimen | | | | | Average | Standard deviation |
|---|---|---|---|---|---|---|---|
| | 1 | 2 | 3 | 4 | 5 | | |
| **"Lollipop" specimens in 1.6 m ion NaCl** | | | | | | | |
| **M-N-45** | 8.32 | 7.21 | 0.08 | 4.75 | 7.37 | 5.54 | 3.33 |
| **M-N-RH45** | 4.32 | 1.15 | 0.32 | 0.08 | 1.62 | 1.50 | 1.69 |
| **M-N-DC45** | 0.16 | 0.08 | 0.12 | 1.90 | 4.16 | 1.28 | 1.78 |
| **M-N-35** | 3.37 | 4.51 | 0.00 | 1.19 | 0.16 | 1.85 | 2.01 |
| **M-N-RH35** | 0.21 | 0.06 | 0.08 | 0.61 | 0.18 | 0.23 | 0.22 |
| **M-N-DC35** | 0.48 | 0.24 | 0.32 | 0.20 | 0.36 | 0.32 | 0.11 |

* M - A - B

**M**: macrocell test

**A**: steel type → N: conventional, normalized steel.

**B**: mix design → 45: water-cement ratio of 0.45 and no inhibitor, RH45: water-cement ratio of 0.45 and Rheocrete 222+, DC45: water-cement ratio of 0.45 and DCI-S, 35: water-cement ratio of 0.35 and no inhibitor, RH35: water-cement ratio of 0.35 and Rheocrete 222+, DC35: water-cement ratio of 0.35 and DCI-S.

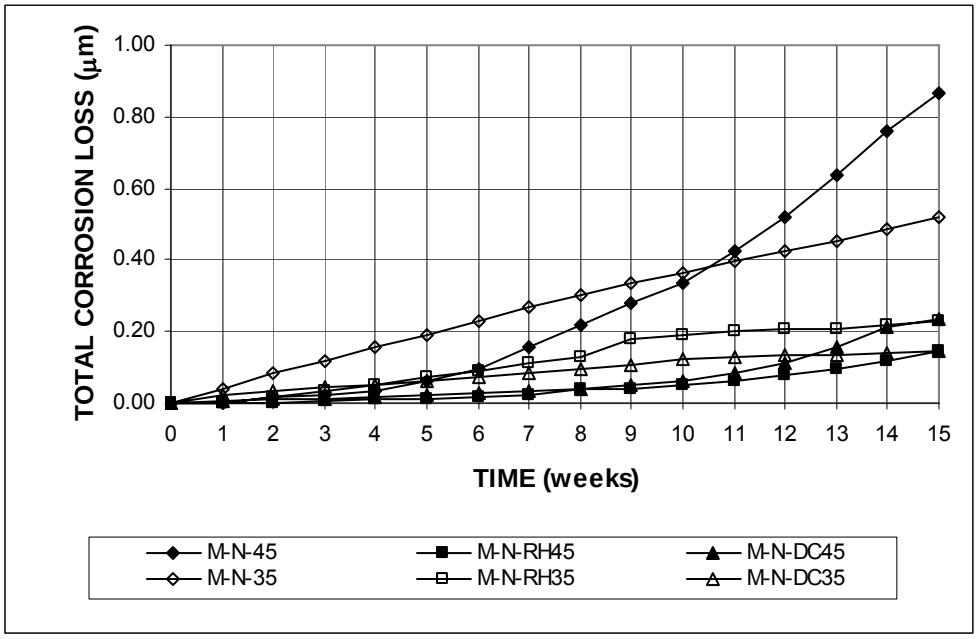


**Figure 3.12 –** Average total corrosion losses as measured in the rapid macrocell test for lollipop specimens with and without corrosion inhibitors and water-cement ratios of 0.45 and 0.35 in 1.6 m ion NaCl and simulated concrete pore solution.

**Table 3.4 –** Average total corrosion losses (in μm) at week 15 as measured in the rapid macrocell test for lollipop specimens with and without corrosion inhibitors and water-cement ratios of 0.45 and 0.35 in 1.6 m ion NaCl and simulated concrete pore solution.

| Specimen designation* | Specimen | | | | | Average | Standard deviation |
|---|---|---|---|---|---|---|---|
| | 1 | 2 | 3 | 4 | 5 | | |
| **"Lollipop" specimens in 1.6 m ion NaCl** | | | | | | | |
| **M-N-45** | 0.65 | 1.76 | 0.03 | 0.65 | 1.24 | 0.87 | 0.66 |
| **M-N-RH45** | 0.22 | 0.09 | 0.16 | 0.10 | 0.17 | 0.15 | 0.05 |
| **M-N-DC45** | 0.18 | 0.05 | 0.28 | 0.18 | 0.48 | 0.24 | 0.16 |
| **M-N-35** | 0.41 | 1.94 | 0.07 | 0.13 | 0.05 | 0.52 | 0.81 |
| **M-N-RH35** | 0.21 | 0.06 | 0.08 | 0.61 | 0.18 | 0.23 | 0.22 |
| **M-N-DC35** | 0.13 | 0.36 | 0.05 | 0.05 | 0.14 | 0.15 | 0.13 |

* M - A - B

**M**: macrocell test

**A**: steel type → N: conventional, normalized steel.

**B**: mix design → 45: water-cement ratio of 0.45 and no inhibitor, RH45: water-cement ratio of 0.45 and Rheocrete 222+, DC45: water-cement ratio of 0.45 and DCI-S, 35: water-cement ratio of 0.35 and no inhibitor, RH35: water-cement ratio of 0.35 and Rheocrete 222+, DC35: water-cement ratio of 0.35 and DCI-S.

The average corrosion potentials of the anodes and cathodes with respect to a saturated calomel electrode are shown in Figure 3.13. Except for specimens with a water-cement ratio of 0.45 and corrosion inhibitors (M-N-RH45 or M-N-DC45), the anode potential dropped below -0.275 V during the second week, indicating active corrosion. The anode potential dropped to values more negative than -0.275 V at week 8 for M-N-RH45 and at week 10 for M-N-DC45. The average anode potential for specimens with a water-cement ratio of 0.35 and Rheocrete 222+ (M-N-RH35) reached a value of approximately -0.350 V at week 9, but increased to -0.270 V at week 10. The cathode potential for all specimens remained between -0.125 and -0.300 V for the duration of the test, indicating that the bars remained passive, or that there was a low probability of corrosion.

### 3.3.2 Bench-Scale Tests

Bench-scale test results include specimens with both normalized and Thermex-treated conventional steel. The figures represent the average of six specimens for the samples without inhibitors and a water-cement ratio of 0.45, and three specimens for the remaining samples.

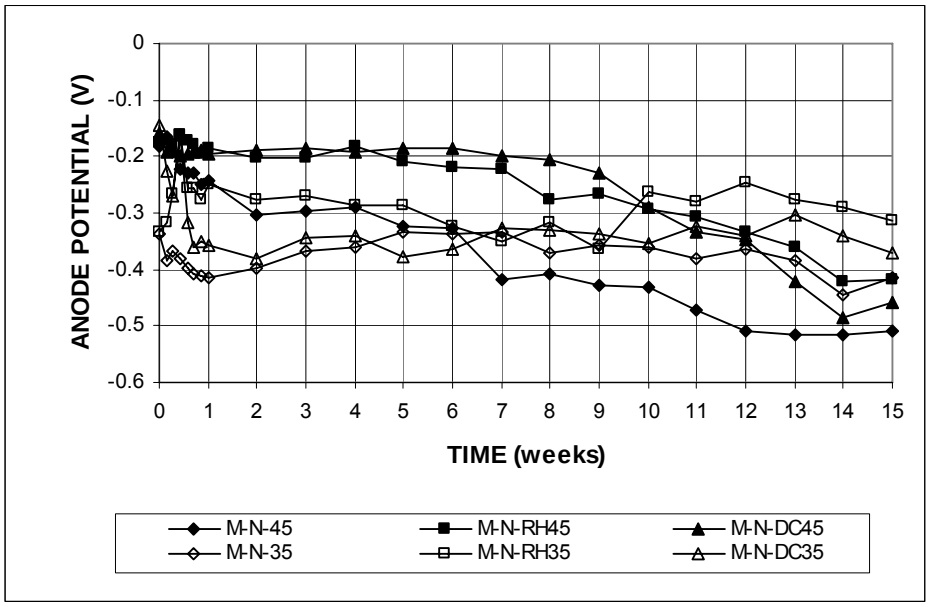


(a)

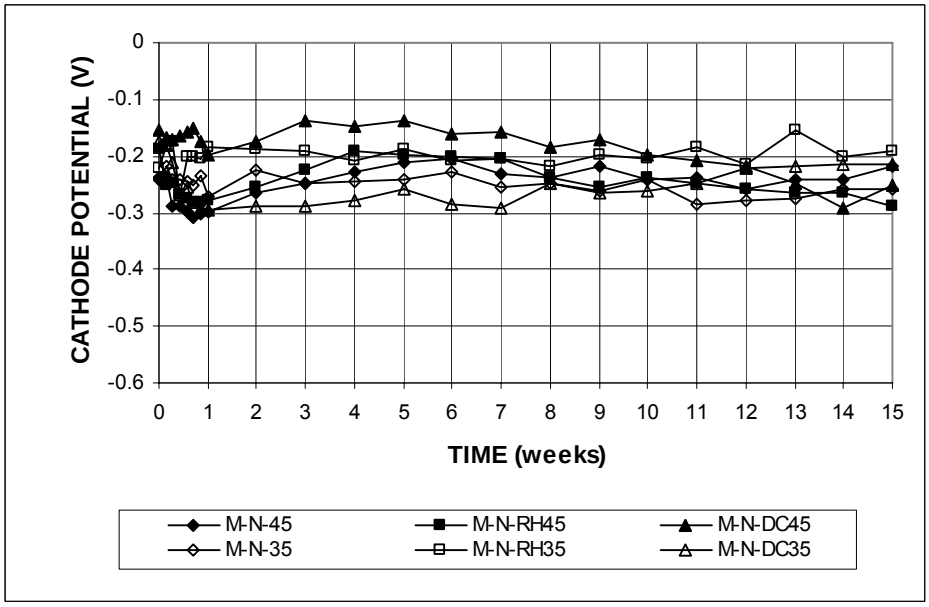


(b)

**Figure 3.13 –** (a) Average anode corrosion potentials and (b) average cathode corrosion potentials with respect to saturated calomel electrode as measured in the rapid macrocell test for lollipop specimens with and with and without corrosion inhibitors and water-cement ratios of 0.45 and 0.35 in 1.6 m ion NaCl and simulated concrete pore solution.

### 3.3.2.1 Southern Exposure Test

Figure 3.14 shows the average corrosion rates for the Southern Exposure specimens with ***conventional, normalized steel***. The specimens with no inhibitor and a water-cement ratio of 0.45 (SE-N-45) had the highest corrosion rates during the test period, with values as high as 7.6 μm/year. The remaining specimens had corrosion rates below 2.0 μm/year, with the exception of the specimens with a water-cement ratio of 0.45 and DCI-S (SE-N-DC45), which had a corrosion rate between 2.0 and 3.0 μm/year between weeks 47 and 54. Table 3.5 shows the average corrosion rates at week 70 and Table C.3 shows the results of the Student's t-test for the mean values. Specimens SE-N-45 had an average corrosion rate of 4.07 μm/year followed by specimens with a water-cement ratio of 0.35 and no inhibitor (SE-N-35) at 1.17 μm/year, equal to 29% of the corrosion rate of SE-N-45. The difference in the mean corrosion rates between these two specimens is significant at $\alpha = 0.10$. Specimens with a water-cement ratio of 0.45 and Rheocrete 222+ (SE-N-RH45) had a corrosion rate of 0.68 μm/year and specimens with a water-cement ratio of 0.45 and DCI-S (SE-N-DC45) had a corrosion rate of 0.86 μm/year. These values correspond to 17% and 21%, respectively, of the corrosion rate of the control specimens, SE-N-45. The difference in the average corrosion rates between SE-N-45 and either SE-N-RH45 or SE-N-DC45 is significant at $\alpha = 0.05$. Specimens with a water-cement ratio of 0.35 and Rheocrete 222+ (SE-N-RH35) had the lowest corrosion rate, 0.04 μm/year, equal to 2.4% of the corrosion rate of SE-N-35. The difference in the average corrosion rates of SE-N-35 and SE-N-RH35 is significant at $\alpha = 0.20$. The specimens with a water-cement ratio of 0.35 containing DCI-S had a corrosion rate of 0.60 μm/year, equal to 51% of the corrosion rate of SE-N-35. The difference in the average

corrosion rates of SE-N-35 and SE-N-DC35, however, is not statistically significant due to the high scatter in the small number of tests.

Figure 3.15 shows the average total corrosion losses for the test period and Table 3.6 summarizes the average total corrosion losses at week 70. Results of the Student's t-test are presented in Table C.4. Specimens with a water-cement ratio of 0.45 and no inhibitor (SE-N-45) had an average total corrosion loss of 5.78 μm. Specimens with a water-cement ratio of 0.35 and no inhibitor (SE-N-35) had an average total corrosion loss of 0.71 μm, equal to 12% of that of SE-N-45. Specimens with a water-cement ratio of 0.45 and Rheocrete 222+ (SE-N-RH45) had an average corrosion loss of 0.51 μm, and specimens with a water-cement ratio of 0.45 and DCI-S (SE-N-DC45) had an average corrosion loss of 0.95 μm, which correspond to 9% and 16%, respectively, of the corrosion loss of SE-N-45. The difference in the average corrosion losses between SE-N-45 and either SE-N-RH45, SE-N-DC45 or SE-N-35 is significant at $\alpha = 0.02$. Specimens with a water-cement ratio of 0.35 and Rheocrete 222+ (SE-N-RH35) had an average corrosion loss of 0.10 μm, and specimens with a water-cement ratio of 0.35 and DCI-S (SE-N-DC35) had an average corrosion loss of 0.24 μm. These values are equal to 14% and 34%, respectively, of the corrosion loss of SE-N-35. The difference in the average corrosion losses between SE-N-35 and SE-N-RH35 is significant at $\alpha = 0.20$, and the difference in the average corrosion losses between SE-N-35 and SE-N-DC35 is not statistically significant.

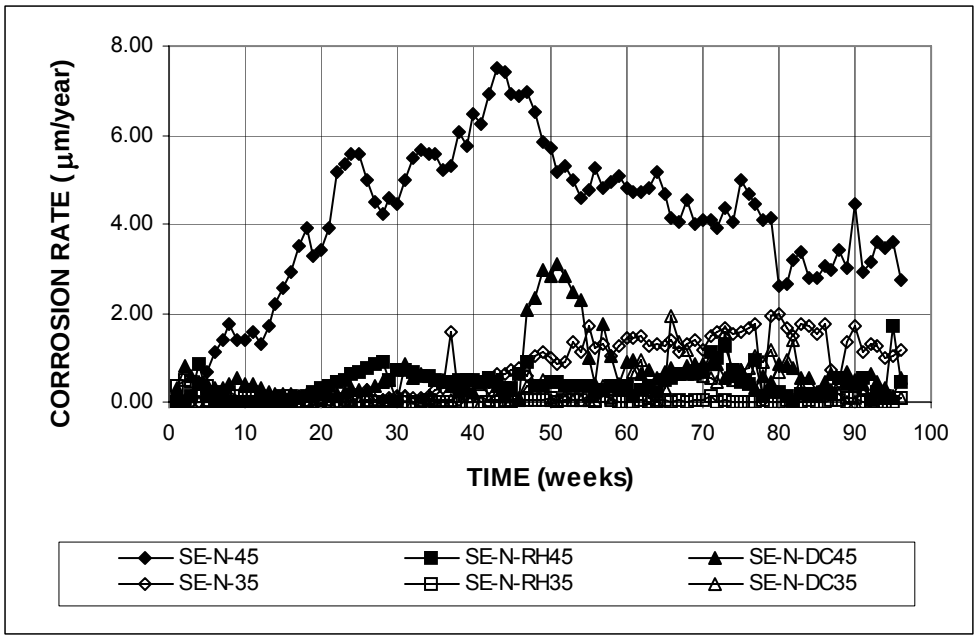


**Figure 3.14 –** Average corrosion rates as measured in the Southern Exposure test for specimens with and without corrosion inhibitors and water-cement ratios of 0.45 and 0.35. Specimens with conventional, normalized steel.

**Table 3.5 –** Average corrosion rates (in µm/year) at week 70 as measured in the Southern Exposure test for specimens with and without corrosion inhibitors and water-cement ratios of 0.45 and 0.35. Specimens with conventional, normalized steel.

| Specimen designation* | Specimen | | | | | | Average | Standard deviation |
|---|---|---|---|---|---|---|---|---|
| | 1 | 2 | 3 | 4 | 5 | 6 | | |
| **Southern Exposure test** | | | | | | | | |
| **SE-N-45** | 8.41 | 0.73 | 3.41 | 2.33 | 3.80 | 5.76 | 4.07 | 2.70 |
| **SE-N-RH45** | 1.01 | 0.54 | 0.48 | | | | 0.68 | 0.29 |
| **SE-N-DC45** | 1.52 | 0.87 | 0.20 | | | | 0.86 | 0.66 |
| **SE-N-35** | 2.04 | 1.38 | 0.09 | | | | 1.17 | 0.99 |
| **SE-N-RH35** | 0.04 | 0.03 | 0.06 | | | | 0.04 | 0.02 |
| **SE-N-DC35** | 0.25 | 0.31 | 1.24 | | | | 0.60 | 0.55 |

* SE - A - B

**SE**: Southern Exposure test

**A**: steel type → N: conventional, normalized steel.

**B**: mix design → 45: water-cement ratio of 0.45 and no inhibitor, RH45: water-cement ratio of 0.45 and Rheocrete 222+, DC45: water-cement ratio of 0.45 and DCI-S, 35: water-cement ratio of 0.35 and no inhibitor, RH35: water-cement ratio of 0.35 and Rheocrete 222+, DC35: water-cement ratio of 0.35 and DCI-S.

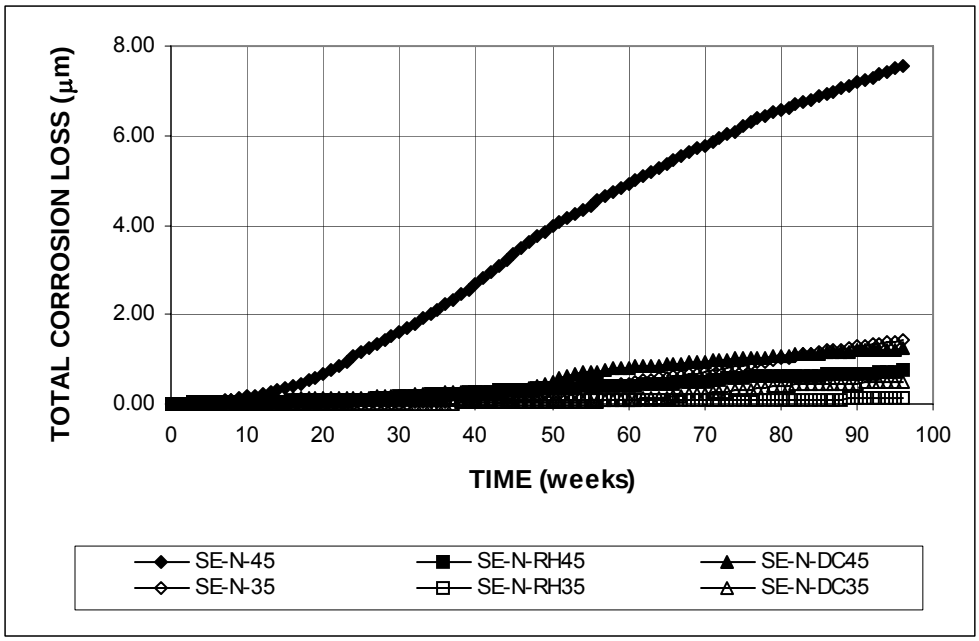


**Figure 3.15 –** Average total corrosion losses as measured in the Southern Exposure test for specimens with and without corrosion inhibitors and water-cement ratios of 0.45 and 0.35. Specimens with conventional, normalized steel.

**Table 3.6 –** Average total corrosion losses (in µm) at week 70 as measured in the Southern Exposure test for specimens with and without corrosion inhibitors and water-cement ratios of 0.45 and 0.35. Specimens with conventional, normalized steel.

| Specimen designation* | Specimen | | | | | | Average | Standard deviation |
|---|---|---|---|---|---|---|---|---|
| | 1 | 2 | 3 | 4 | 5 | 6 | | |
| **Southern Exposure test** | | | | | | | | |
| **SE-N-45** | 7.13 | 8.89 | 6.90 | 3.02 | 4.19 | 4.56 | 5.78 | 2.21 |
| **SE-N-RH45** | 1.05 | 0.22 | 0.26 | | | | 0.51 | 0.47 |
| **SE-N-DC45** | 1.98 | 0.68 | 0.21 | | | | 0.95 | 0.91 |
| **SE-N-35** | 1.18 | 0.83 | 0.14 | | | | 0.71 | 0.53 |
| **SE-N-RH35** | 0.02 | 0.25 | 0.03 | | | | 0.10 | 0.13 |
| **SE-N-DC35** | 0.09 | 0.34 | 0.28 | | | | 0.24 | 0.13 |

* SE - A - B

**SE**: Southern Exposure test

**A**: steel type → N: conventional, normalized steel.

**B**: mix design → 45: water-cement ratio of 0.45 and no inhibitor, RH45: water-cement ratio of 0.45 and Rheocrete 222+, DC45: water-cement ratio of 0.45 and DCI-S, 35: water-cement ratio of 0.35 and no inhibitor, RH35: water-cement ratio of 0.35 and Rheocrete 222+, DC35: water-cement ratio of 0.35 and DCI-S.

Figure 3.16 shows the corrosion potential of the top and bottom mats of steel with respect to a copper-copper sulfate electrode for the specimens with conventional, normalized steel. Specimens with a water-cement ratio of 0.45 and no inhibitor (SE-N-45) show active corrosion on the top mat, at week 7, followed by specimens with a water-cement ratio of 0.45 and Rheocrete 222+ (SE-N-RH45) at week 26, and specimens with a water-cement ratio of 0.45 and DCI-S (SE-N-DC45) at week 37. At week 70, all specimens, with the exception of specimens with a water-cement ratio of 0.35 and corrosion inhibitors (SE-N-RH35 and SE-N-DC35), had a corrosion potential of the top mat that was more negative than -0.350 V.

Figure 3.6(b) shows that for the first half of the test period, specimens with a water-cement ratio of 0.35 had a corrosion potential of the bottom mat that was more positive than -0.200 V, which indicates a passive condition. During this same period, specimens with a water-cement ratio of 0.45 had bottom mat corrosion potentials that ranged from -0.200 to -0.400 V. At week 70, all specimens had a corrosion potential of the bottom mat that was between -0.200 and -0.350 V, indicating a low probability of corrosion. The bottom mat potentials for specimens SE-N-45 dropped to values below -0.400 V at week 79, which indicates a high probability of corrosion, and that chlorides had reached the bottom mat of steel.

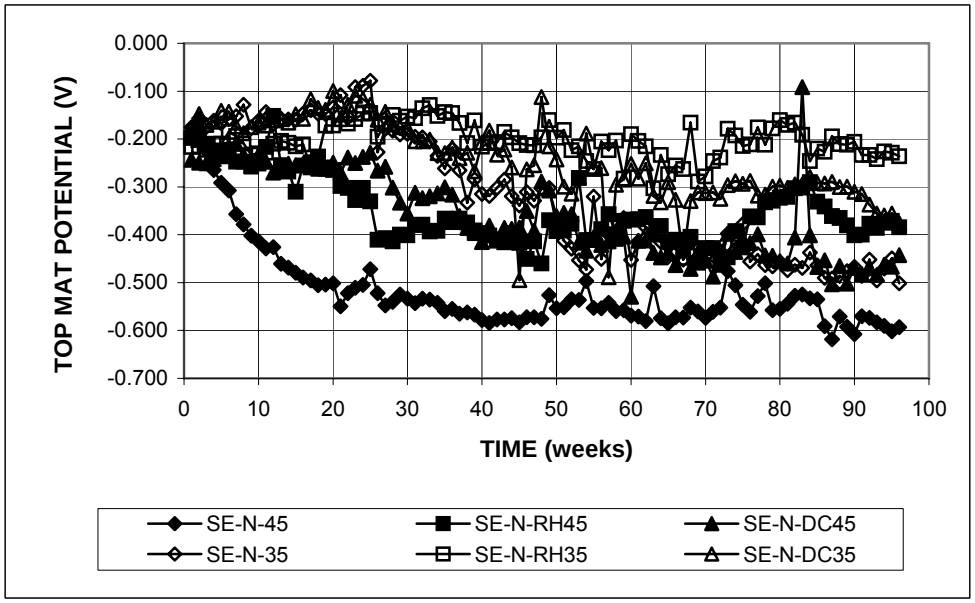


(a)

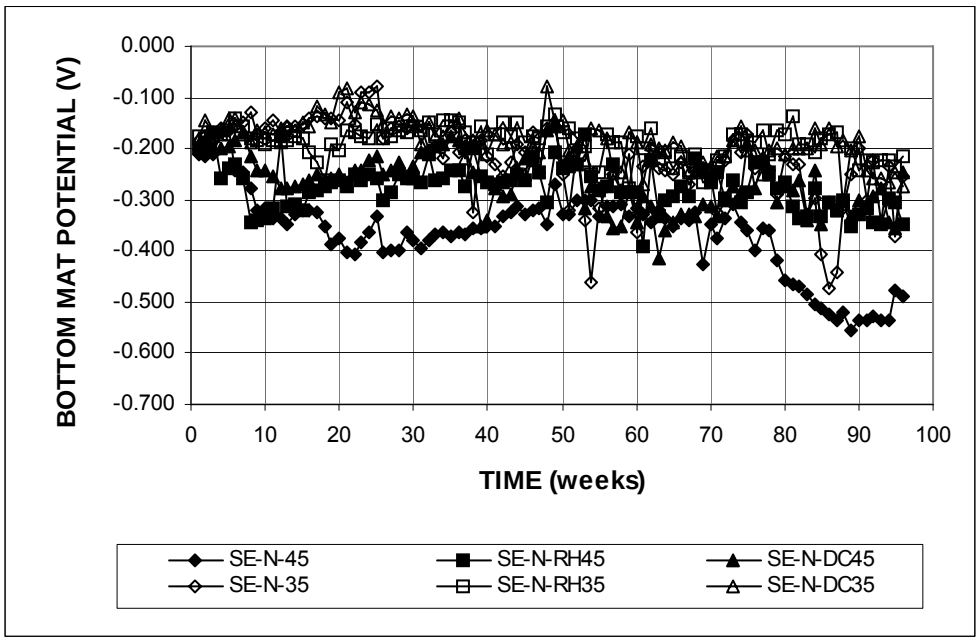


(b)

**Figure 3.16 –** (a) Average top mat corrosion potentials and (b) average bottom mat corrosion potentials with respect to copper-copper sulfate electrode as measured in the Southern Exposure test for specimens with and without corrosion inhibitors and water-cement ratios of 0.45 and 0.35. Specimens with conventional, normalized steel.

Figure 3.17 shows the average mat-to-mat resistances for specimens with conventional, normalized steel. The average mat-to-mat resistances had values of approximately 150 ohms for all specimens at the start of the test period and increased with time at a similar rate for all specimens during the first 30 weeks. After week 30, the mat-to-mat resistance of specimens SE-N-RH45 and SE-N-DC45 increased at a higher rate than for the rest of the specimens. At week 70, specimens with a water-cement ratio of 0.45 and corrosion inhibitors (SE-N-RH45 and SE-N-DC45) had the highest mat-to-mat resistances, with values above 1500 ohms. The remaining specimens had a mat-to-mat resistance below 1000 ohms. The mat-to-mat resistance increases with time due to the formation of corrosion products on the surface of the bars. The drop in the average mat-to-mat resistance for specimens M-N-45 after week 80 indicates the formation of cracks in the specimens.

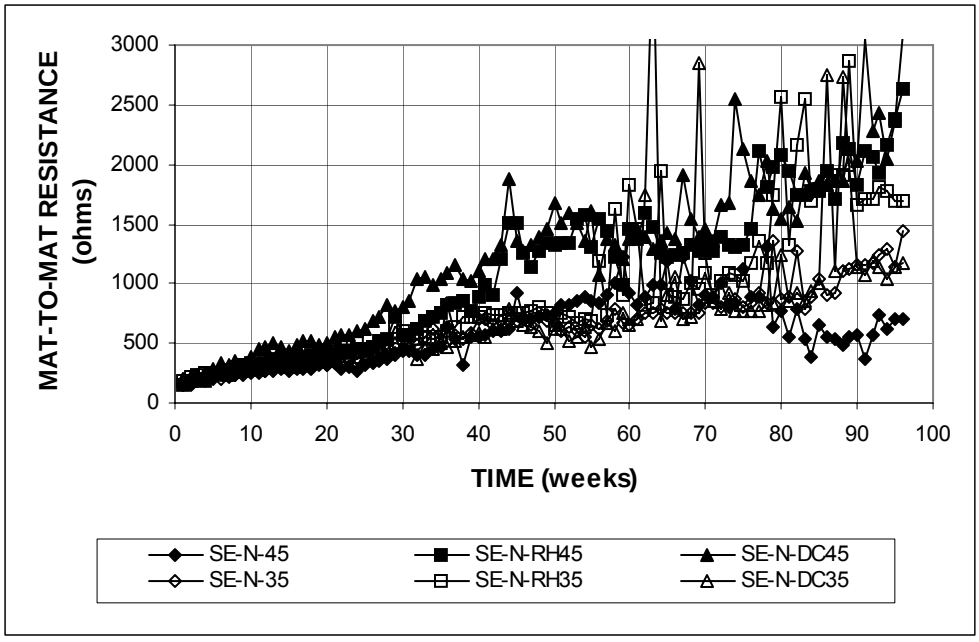


**Figure 3.17 –** Average mat-to-mat resistances as measured in the Southern Exposure test for specimens with and without corrosion inhibitors and water-cement ratios of 0.45 and 0.35. Specimens with conventional, normalized steel.

Evaluation of the test specimens after the 96-week test period indicated the presence of corrosion products on most of the bars in the top mat. Figure 3.18 shows the top bars for a specimen with a water-cement ratio of 0.45 and Rheocrete 222+ and Figure 3.19 shows the top bars for a specimen with a water-cement ratio of 0.45 and DCI-S.

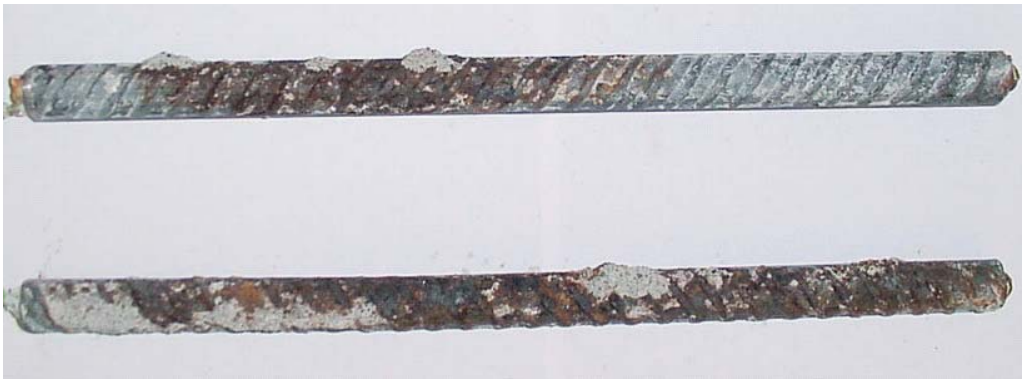

**Figure 3.18 –** Top bars from Southern Exposure specimen with conventional, normalized steel, a water-cement ratio of 0.45 and Rheocrete 222+ at week 96.

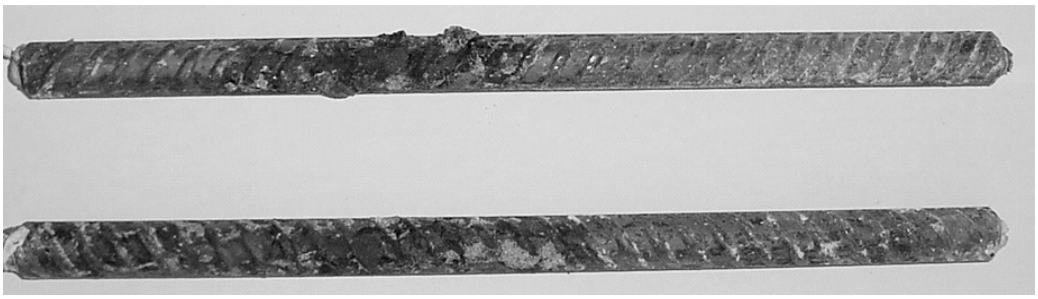

**Figure 3.19 –** Top bars from Southern Exposure specimen with conventional, normalized steel, a water-cement ratio of 0.45 and DCI-S at week 96.

The average corrosion rates versus time for the specimens with ***Thermex-treated conventional steel*** are presented in Figure 3.20. The specimens with a water-cement ratio of 0.45 and no inhibitor (SE-T-45) had the highest average corrosion rate, while all of the specimens with a water-cement ratio of 0.35 had corrosion rates

of nearly zero throughout the test period. Table 3.7 shows the average corrosion rates at week 70 and Table C.3 shows the results of the Student's t-test. The specimens with a water-cement ratio of 0.45 had corrosion rates of 9.76, 0.44, and 1.68 μm/year for specimens with no inhibitor (SE-T-45), specimens with Rheocrete 222+ (SE-T-RH45), and specimens with DCI-S (SE-T-DC45), respectively. The difference in the average corrosion rates between SE-T-45 and either SE-T-RH45 or SE-T-DC45 is significant at $\alpha = 0.20$. Specimens with a water-cement ratio of 0.35 had corrosion rates lower than 0.02 μm/year, corresponding to 0.2% of the corrosion rate of SE-T-45. The difference in the average corrosion rates between SE-T-45 and SE-T-35 is significant at $\alpha = 0.10$.

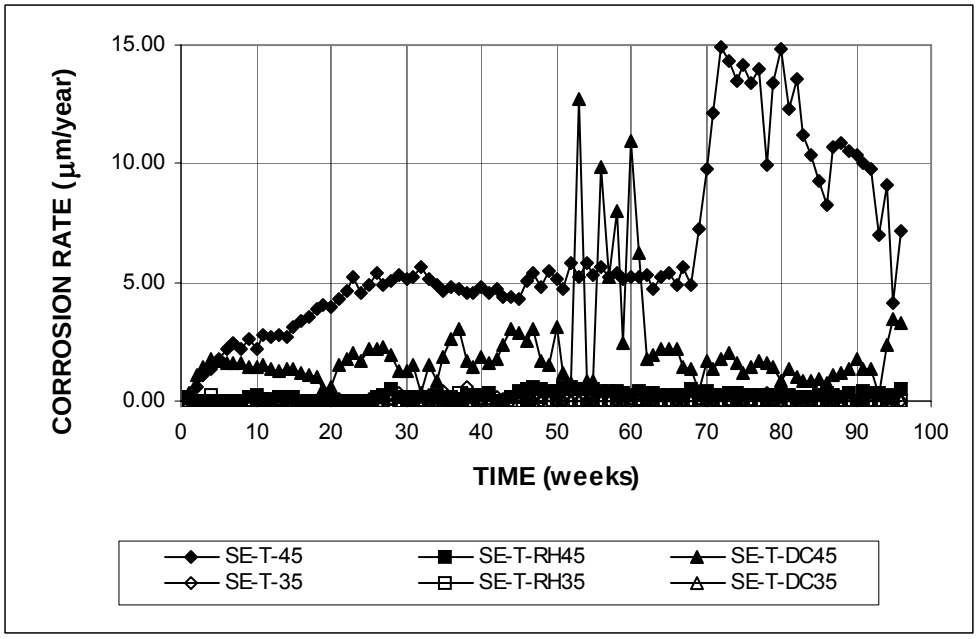


**Figure 3.20 –** Average corrosion rates as measured in the Southern Exposure test for specimens with and without corrosion inhibitors and water-cement ratios of 0.45 and 0.35. Specimens with Thermex-treated conventional steel.

**Table 3.7 –** Average corrosion rates (in μm/year) at week 70 as measured in the Southern Exposure test for specimens with and without corrosion inhibitors and water-cement ratios of 0.45 and 0.35. Specimens with Thermex-treated conventional steel.

| Specimen designation* | Specimen | | | | | | Average | Standard deviation |
|---|---|---|---|---|---|---|---|---|
| | 1 | 2 | 3 | 4 | 5 | 6 | | |
| **Southern Exposure test** | | | | | | | | |
| **SE-T-45** | 10.70 | 2.44 | 4.98 | 32.63 | 1.30 | 6.51 | 9.76 | 11.68 |
| **SE-T-RH45** | 0.01 | 0.33 | 0.97 | | | | 0.44 | 0.49 |
| **SE-T-DC45** | 3.98 | 0.00 | 1.05 | | | | 1.68 | 2.06 |
| **SE-T-35** | 0.00 | 0.00 | 0.02 | | | | 0.01 | 0.01 |
| **SE-T-RH35** | 0.00 | 0.00 | 0.04 | | | | 0.02 | 0.02 |
| **SE-T-DC35** | 0.01 | 0.01 | 0.01 | | | | 0.01 | 0.00 |

* SE - A - B
**SE**: Southern Exposure test
**A**: steel type → T: Thermex-treated conventional steel.
**B**: mix design → 45: water-cement ratio of 0.45 and no inhibitor, RH45: water-cement ratio of 0.45 and Rheocrete 222+, DC45: water-cement ratio of 0.45 and DCI-S, 35: water-cement ratio of 0.35 and no inhibitor, RH35: water-cement ratio of 0.35 and Rheocrete 222+, DC35: water-cement ratio of 0.35 and DCI-S.

Figure 3.21 shows the average total corrosion losses versus time for specimens with Thermex-treated conventional steel. Table 3.8 shows the average total corrosion losses at week 70 and Table C.4 shows the results of the Student's t-test. After 70 weeks, the average total corrosion loss for specimens with a water-cement ratio of 0.45 and no inhibitor (SE-T-45) was 5.92 μm. Specimens with a water-cement ratio of 0.45 and DCI-S (SE-T-DC45) had an average total corrosion loss of 3.03 μm, equal to 51% of the corrosion loss of SE-T-45, and specimens with a water-cement ratio of 0.45 and Rheocrete 222+ (SE-T-RH45) had an average total corrosion loss of 0.30 μm, equal to 5% of the corrosion loss of SE-T-45. The difference in the average corrosion losses between SE-T-45 and SE-T-RH45 is significant at $\alpha = 0.02$. and the difference in the average corrosion losses between SE-T-45 and SE-T-DC45 is significant at $\alpha = 0.20$. The specimens with a water-cement ratio of 0.35 had corrosion losses below 0.09 μm after 70 weeks, corresponding to 1.5% of the average corrosion loss of SE-T-45. The difference in the average

corrosion losses between SE-T-45 and SE-T-35 is significant at $\alpha = 0.02$. There is no statistically significant difference between the corrosion losses of SE-T-35 and SE-T-RH35, and there is a significant difference at $\alpha = 0.20$ between the average corrosion losses of SE-T-35 and SE-T-DC35.

When the results obtained from the specimens with conventional normalized and conventional Thermex-treated steel are averaged, the specimens with a water-cement ratio of 0.35 and no inhibitor exhibited an average total corrosion loss equal to 7% of the corrosion loss of specimens with a water-cement ratio of 0.45 and no inhibitor. Specimens with a water-cement ratio of 0.45 and corrosion inhibitors had corrosion losses equal to 7% and 68% for specimens with Rheocrete 222+ and DCI-S, respectively, of that of specimens with a water-cement ratio of 0.45 and no inhibitor. The specimens with a water-cement ratio of 0.35 and corrosion inhibitors had the lowest average corrosion losses, with values equal to 1.3% and 4% for specimens with Rheocrete 222+ and DCI-S, respectively, of the corrosion losses exhibited by specimens with a water-cement ratio of 0.35 and no inhibitor.

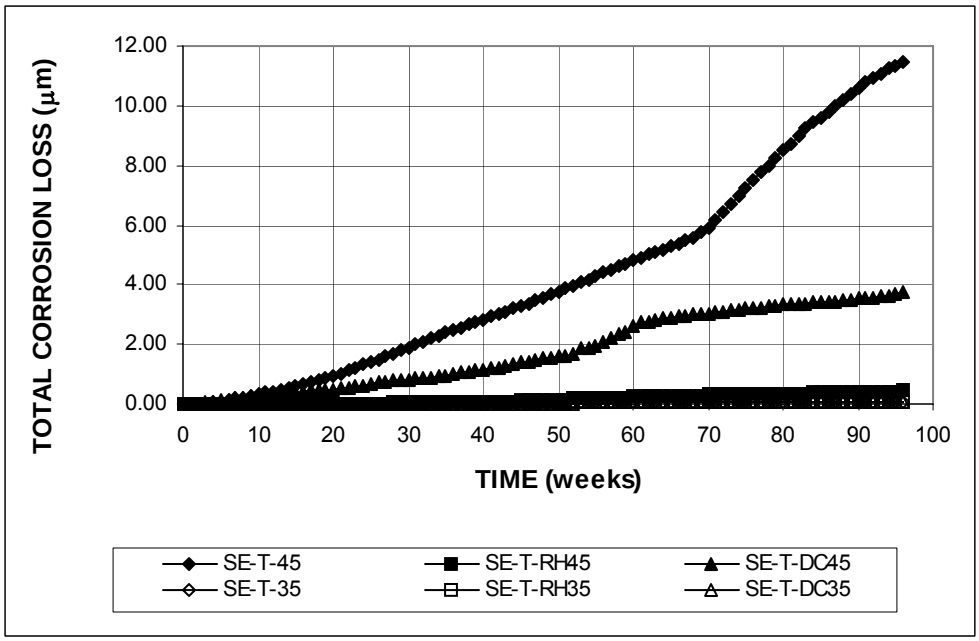


**Figure 3.21 –** Average total corrosion losses as measured in the Southern Exposure test for specimens with and without corrosion inhibitors and water-cement ratios of 0.45 and 0.35. Specimens with Thermex-treated conventional steel.

**Table 3.8 –** Average total corrosion losses (in μm) at week 70 as measured in the Southern Exposure test for specimens with and without corrosion inhibitors and water-cement ratios of 0.45 and 0.35. Specimens with Thermex-treated conventional steel.

| Specimen designation* | Specimen | | | | | | Average | Standard deviation |
|---|---|---|---|---|---|---|---|---|
| | 1 | 2 | 3 | 4 | 5 | 6 | | |
| **Southern Exposure test** | | | | | | | | |
| **SE-T-45** | 11.50 | 4.92 | 5.35 | 5.15 | 0.93 | 7.66 | 5.92 | 3.49 |
| **SE-T-RH45** | 0.04 | 0.39 | 0.47 | | | | 0.30 | 0.23 |
| **SE-T-DC45** | 5.66 | 1.84 | 1.59 | | | | 3.03 | 2.28 |
| **SE-T-35** | 0.06 | 0.12 | 0.09 | | | | 0.09 | 0.03 |
| **SE-T-RH35** | 0.09 | 0.03 | 0.05 | | | | 0.05 | 0.03 |
| **SE-T-DC35** | 0.02 | 0.01 | 0.08 | | | | 0.04 | 0.04 |

* SE - A - B

**SE**: Southern Exposure test

**A**: steel type → T: Thermex-treated conventional steel.

**B**: mix design → 45: water-cement ratio of 0.45 and no inhibitor, RH45: water-cement ratio of 0.45 and Rheocrete 222+, DC45: water-cement ratio of 0.45 and DCI-S, 35: water-cement ratio of 0.35 and no inhibitor, RH35: water-cement ratio of 0.35 and Rheocrete 222+, DC35: water-cement ratio of 0.35 and DCI-S.

The average corrosion potentials of the top mat and bottom mats of steel with respect to a copper-copper sulfate electrode are shown in Figure 3.22. Specimens with a water-cement ratio of 0.45 and no inhibitor (SE-T-45) and specimens with a water-cement ratio of 0.45 and DCI-S (SE-T-DC45) were undergoing active corrosion in the top mat during the first weeks of testing. At week 70, all specimens with a water-cement ratio of 0.45 had a top mat corrosion potential that was more negative than -0.350 V, indicating active corrosion, while all specimens with a water-cement ratio of 0.35 had a top mat corrosion potential that was more positive than -0.200 V, indicating a high probability that corrosion was not occurring. Results for the bottom mat indicate that all of the specimens with a water-cement ratio of 0.35 were passive, with potentials that were more positive than -0.200 V, while specimens with a water-cement ratio of 0.45 had bottom mat corrosion potentials between -0.200 and -0.350 V, indicating a low probability of corrosion.

Figure 3.23 shows the average mat-to-mat resistances for specimens with Thermex-treated conventional steel. The average mat-to-mat resistances had values between 200 and 400 ohms at the start of the test period, and increased with time due to the formation of corrosion products on the surface of the bars. At week 70, specimens with no inhibitors (SE-T-45 and SE-T-35) had the highest mat-to-mat resistance, with values close to 2000 ohms. Specimens with a water-cement ratio of 0.45 and DCI-S had a mat-to-mat resistance of 1250 ohms, and the remaining specimens had mat-to-mat resistances below 1000 ohms.

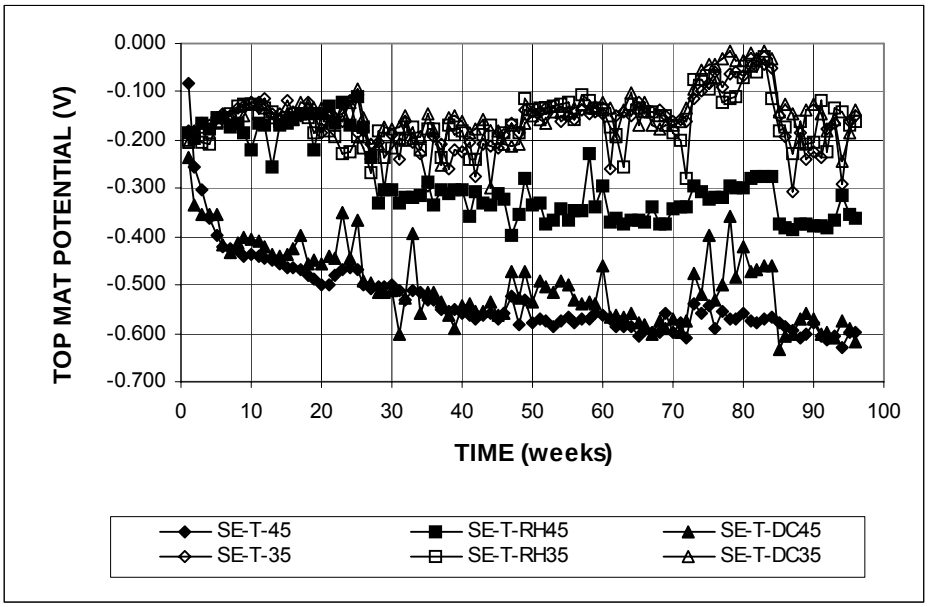


(a)

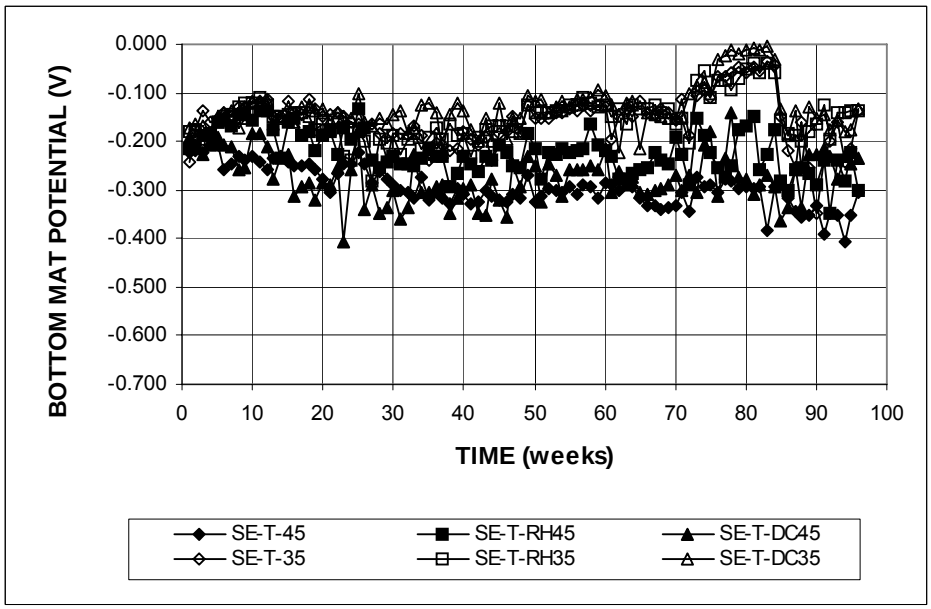


(b)

**Figure 3.22 –** (a) Average top mat corrosion potentials and (b) average bottom mat corrosion potentials with respect to copper-copper sulfate electrode as measured in the Southern Exposure test for specimens with and without corrosion inhibitors and water-cement ratios of 0.45 and 0.35. Specimens with Thermex-treated conventional steel.

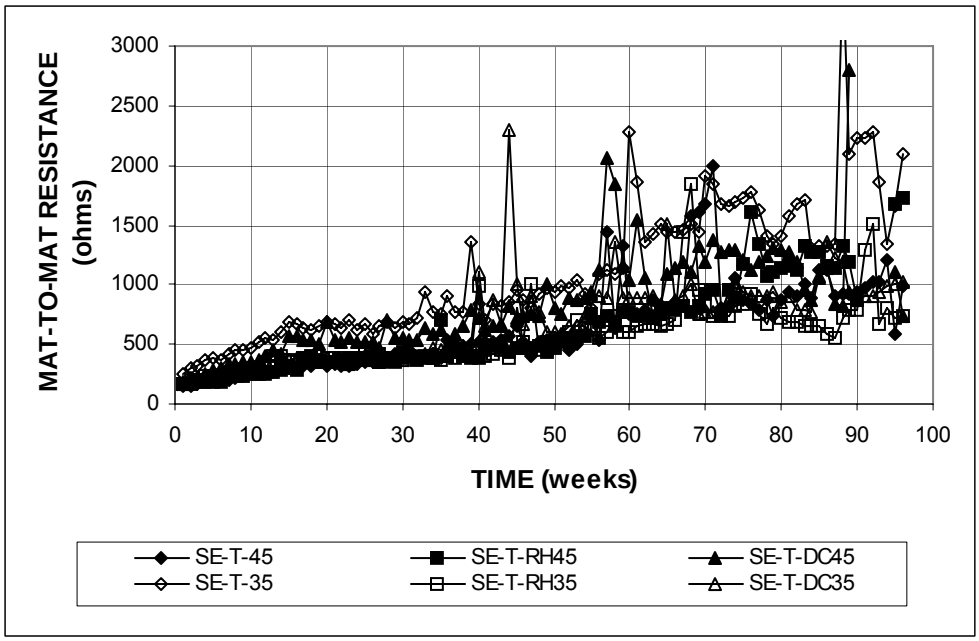


**Figure 3.23 –** Average mat-to-mat resistances as measured in the Southern Exposure test for specimens with and without corrosion inhibitors and water-cement ratios of 0.45 and 0.35. Specimens with Thermex-treated conventional steel.

### 3.3.2.2 Cracked Beam Test

Figure 3.24 shows the average corrosion rates as a function of time for specimens with ***conventional, normalized steel***. The average corrosion rates at week 70 are summarized in Table 3.9 and results of the Student's t-test are presented in Table C.3. The specimens had similar corrosion rates throughout the test period, with the exception of those specimens with a water-cement ratio of 0.35 and DCI inhibitor (CB-N-DC35), which had a big increase in the corrosion rate after week 45, and specimens with a water-cement ratio of 0.45 and DCI inhibitor (CB-N-DC45), which showed increased corrosion rates between weeks 47 and 56. As shown in Table 3.9, the increased average corrosion rate for specimens CB-N-DC35 reflects a high corrosion rate in all three specimens. The increase in the average corrosion rate for

specimens CB-N-DC45 reflects an increased corrosion rate in only one of the three specimens, as shown in Figure A.164(a).

During the first weeks of the tests, the average corrosion rates exceeded 15 μm/year for all specimens and then dropped with time, reaching values below 5 μm/year after week 30. The high values during the initial weeks result because the cracks in the specimens provide a direct path for the chlorides to the steel. The reduction in the corrosion rates with time result from the formation of corrosion products, which can seal the crack and limit the ingress of chlorides and oxygen. As shown in Table 3.9, the average corrosion rate at week 70 was 7.34 μm/year for specimens with a water-cement ratio of 0.45 and no inhibitor (CB-N-45). For specimens with a water-cement ratio of 0.35 and no inhibitor (CB-N-35) the corrosion rate was 1.99 μm/year, equal to 27% of the corrosion rate of specimens CB-N-45. The difference in the average corrosion rates between CB-N-45 and CB-N-35 is significant at $\alpha = 0.10$. Specimens with a water cement ratio of 0.45 and Rheocrete 222+ (CB-N-RH45) and specimens with a water-cement ratio of 0.45 and DCI-S (CB-N-DC45) had corrosion rates of 1.89 and 1.92 μm/year, respectively, corresponding to approximately 26% of the corrosion rate of CB-N-45. The difference in the average corrosion rates between CB-N-45 and either CB-N-RH45 or CB-N-DC45 is statistically significant at $\alpha = 0.10$. Specimens with a water-cement ratio of 0.35 and Rheocrete 222+ (CB-N-RH35) had a corrosion rate of 2.82 μm/year, which is higher than the average corrosion rate of CB-N-35. The difference in the corrosion rates of CB-N-35 and CB-N-RH35 is not statistically significant. As mentioned above, specimens CB-N-DC35 showed extremely high corrosion rates, with an average of 36.37 μm/year at week 70. The difference in the corrosion rates of CB-N-35 and CB-N-DC35 is significant at $\alpha = 0.20$.

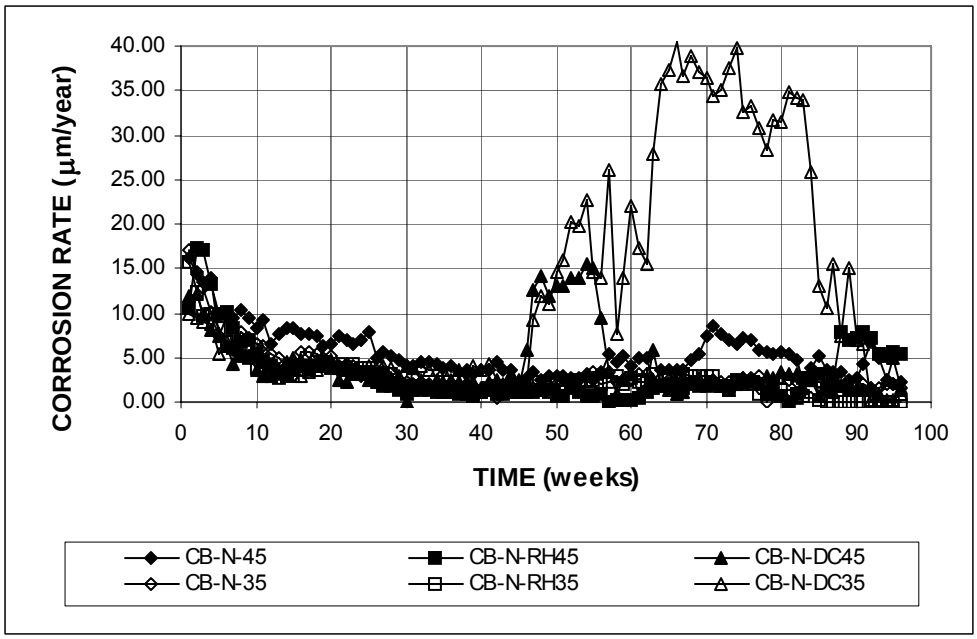


**Figure 3.24 –** Average corrosion rates as measured in the cracked beam test for specimens with and without corrosion inhibitors and water-cement ratios of 0.45 and 0.35. Specimens with conventional, normalized steel.

**Table 3.9 –** Average corrosion rates (in µm/year) at week 70 as measured in the cracked beam test for specimens with and without corrosion inhibitors and water-cement ratios of 0.45 and 0.35. Specimens with conventional, normalized steel.

| Specimen designation* | Specimen | | | | | | Average | Standard deviation |
|---|---|---|---|---|---|---|---|---|
| | 1 | 2 | 3 | 4 | 5 | 6 | | |
| **Cracked beam test** | | | | | | | | |
| **CB-N-45** | 9.55 | 4.55 | 2.22 | 3.92 | 17.61 | 6.22 | 7.34 | 5.61 |
| **CB-N-RH45** | 3.00 | 1.60 | 1.07 | | | | 1.89 | 1.00 |
| **CB-N-DC45** | 2.33 | 0.78 | 2.65 | | | | 1.92 | 1.00 |
| **CB-N-35** | 3.08 | 1.46 | 1.42 | | | | 1.99 | 0.95 |
| **CB-N-RH35** | 1.68 | 1.64 | 5.16 | | | | 2.82 | 2.02 |
| **CB-N-DC35** | 49.20 | 45.08 | 14.82 | | | | 36.37 | 18.77 |

* CB - A - B

**CB**: cracked beam test

**A**: steel type → N: conventional, normalized steel.

**B**: mix design → 45: water-cement ratio of 0.45 and no inhibitor, RH45: water-cement ratio of 0.45 and Rheocrete 222+, DC45: water-cement ratio of 0.45 and DCI-S, 35: water-cement ratio of 0.35 and no inhibitor, RH35: water-cement ratio of 0.35 and Rheocrete 222+, DC35: water-cement ratio of 0.35 and DCI-S.

Figure 3.25 shows the average total corrosion losses versus time for specimens with conventional normalized steel and Table 3.10 summarizes the losses at week 70. Table C.4 presents the results of the Student's t-test. As shown in Table 3.10, specimens with a water-cement ratio of 0.35 and DCI-S (CB-N-DC35) had a total corrosion loss of 14.35 μm, while specimens with a water-cement ratio of 0.45 and no inhibitor (CB-N-45) had a total corrosion loss of 7.51 μm. For specimens with a water-cement ratio of 0.45 and Rheocrete 222+ (CB-N-RH45) and specimens with a water-cement ratio of 0.45 and DCI-S (CB-N-DC45), the average total corrosion losses were 4.13 and 6.59 μm/year, respectively, equal to 55% and 87% of the corrosion loss of CB-N-45. The difference in the average corrosion losses between CB-N-45 and CB-N-RH45 is significant at $\alpha = 0.02$, while the difference in the average corrosion losses between CB-N-45 and CB-N-DC45 is not statistically significant. The total corrosion loss for specimens with a water-cement ratio of 0.35 and no inhibitor (CB-N-35) was 5.10 μm, which is equal to 68% of the corrosion loss of CB-N-45. The difference in the average corrosion losses between CB-N-45 and CB-N-35 is significant at $\alpha = 0.05$. Specimens with a water-cement ratio of 0.35 and Rheocrete 222+ (CB-N-RH35) had a corrosion loss of 4.47 μm, equal to 88% of the average total corrosion loss of CB-N-35. The difference in the average corrosion losses between CB-N-35 and CB-N-RH35 is not statistically significant.

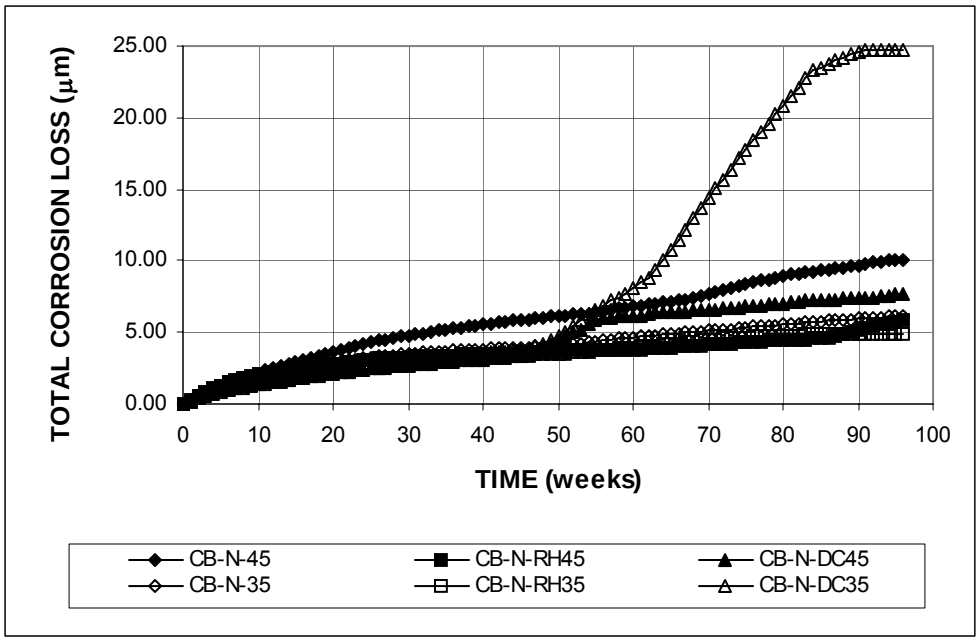


**Figure 3.25 –** Average total corrosion losses as measured in the cracked beam test for specimens with and without corrosion inhibitors and water-cement ratios of 0.45 and 0.35. Specimens with conventional, normalized steel.

**Table 3.10 –** Average total corrosion losses (in μm) at week 70 as measured in the cracked beam test for specimens with and without corrosion inhibitors and water-cement ratios of 0.45 and 0.35. Specimens with conventional, normalized steel.

| Specimen designation* | Specimen | | | | | | Average | Standard deviation |
|---|---|---|---|---|---|---|---|---|
| | 1 | 2 | 3 | 4 | 5 | 6 | | |
| **Cracked beam test** | | | | | | | | |
| **CB-N-45** | 10.36 | 7.75 | 4.98 | 8.57 | 7.61 | 5.78 | 7.51 | 1.93 |
| **CB-N-RH45** | 4.52 | 4.14 | 3.72 | | | | 4.13 | 0.40 |
| **CB-N-DC45** | 8.11 | 7.10 | 4.56 | | | | 6.59 | 1.83 |
| **CB-N-35** | 5.63 | 4.78 | 4.89 | | | | 5.10 | 0.46 |
| **CB-N-RH35** | 4.02 | 4.09 | 5.29 | | | | 4.47 | 0.71 |
| **CB-N-DC35** | 12.73 | 21.54 | 8.78 | | | | 14.35 | 6.53 |

* CB - A - B

**CB**: cracked beam test

**A**: steel type → N: conventional, normalized steel.

**B**: mix design → 45: water-cement ratio of 0.45 and no inhibitor, RH45: water-cement ratio of 0.45 and Rheocrete 222+, DC45: water-cement ratio of 0.45 and DCI-S, 35: water-cement ratio of 0.35 and no inhibitor, RH35: water-cement ratio of 0.35 and Rheocrete 222+, DC35: water-cement ratio of 0.35 and DCI-S.

Figure 3.26 shows the average corrosion potentials of the top and bottom mats of steel with respect to a copper-copper sulfate electrode. For the top mat of steel, all specimens had a corrosion potential that was more negative than -0.400 V, which indicates that the bars were actively corroding, starting the first week of the tests. The presence of the cracks in the specimen allows the ingress of enough chlorides to initiate corrosion of the top mat of steel during the first week of the test. The average corrosion potentials of the bottom mat for all specimens remained between -0.200 and -0.350 V, indicating a low probability for corrosion, except for specimens CB-N-45, which showed active corrosion between weeks 8 to 35 and after week 80, specimens CB-N-RH45 from weeks 50 to 70, and specimens CB-N-DC45 after week 78.

Figure 3.27 shows the average mat-to-mat resistances for cracked beam specimens, which had values of approximately 300 ohms for all specimens at the start of the test period, and increased with time at a similar rate for all specimens, with little scatter during the first 40 weeks. At week 70, specimens with a water-cement ratio of 0.35 and inhibitors (CB-N-RH45 and CB-N-DC45) had the highest mat-to-mat resistances, with values above 2500 ohms. Specimens with a water-cement ratio of 0.35 and no inhibitor (CB-T-35) had a mat-to-mat resistance of 2200 ohms. The specimens with a water-cement ratio of 0.45 had mat-to-mat resistances below 1600 ohms. The drop in the average mat-to-mat resistance of specimens CB-N-45 indicates the formation of cracks in the specimens.

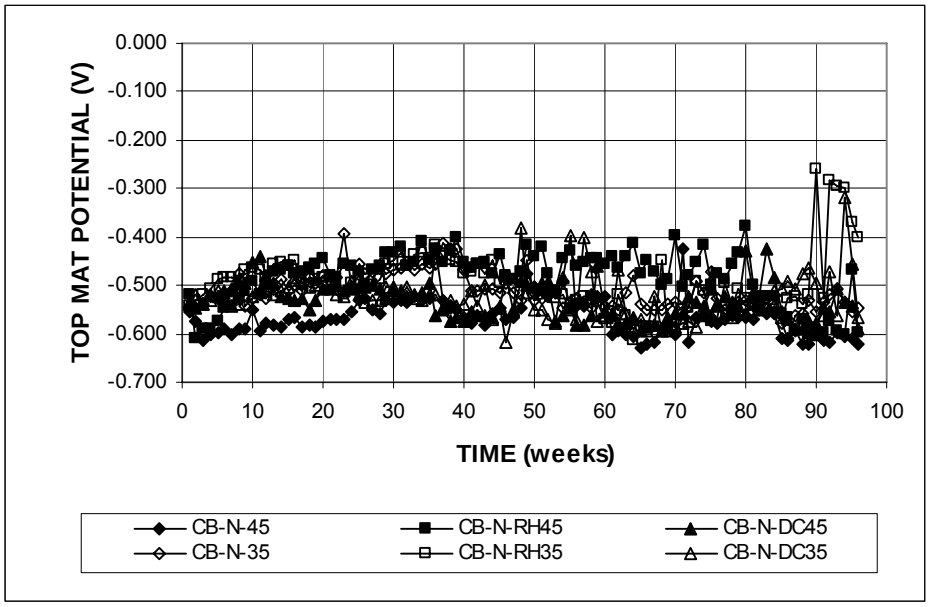


(a)

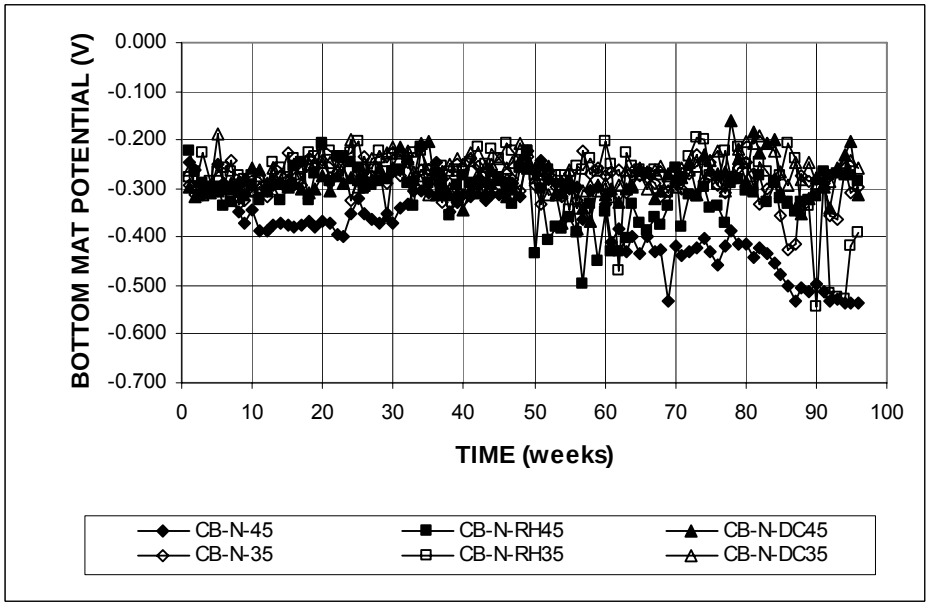


(b)

**Figure 3.26 –** (a) Average top mat corrosion potential and (b) average bottom mat corrosion potential with respect to copper-copper sulfate electrode as measured in the cracked beam test for specimens with and without corrosion inhibitors and water-cement ratios of 0.45 and 0.35. Specimens with conventional, normalized steel.

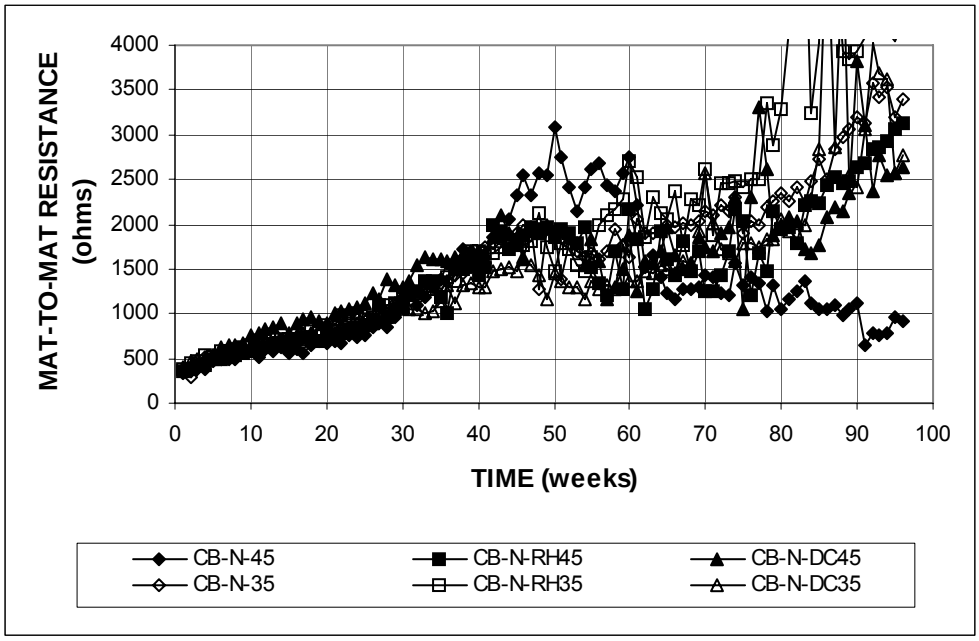


**Figure 3.27 –** Average mat-to-mat resistances as measured in the cracked beam test for specimens with and without corrosion inhibitors and water-cement ratios of 0.45 and 0.35. Specimens with conventional, normalized steel.

The average corrosion rates versus time for cracked beam specimens with ***Thermex-treated conventional steel*** are presented in Figure 3.28. During the first 5 weeks, the corrosion rate jumped to values above 7 μm/year for all specimens and dropped with time after week 5. Specimens with a water-cement ratio of 0.45 and DCI-S (CB-T-DC45) showed extremely high corrosion rates during the first 49 weeks, reaching values above 30 μm/year during the first 9 weeks, and then dropped to values similar to the rest of the specimens. These high average corrosion rates were dominated by one specimen, which had corrosion rates as high as 94 μm/year, and which remained above 20 μm/year during the first 49 weeks, as shown in Figure A.175(a). The corrosion rates for this specimen dropped to values of approximately 2.50 μm/year at week 50, and remained below this value for the rest of the test period.

Specimens with a water-cement ratio of 0.45 and no inhibitor (CB-T-45) had a higher corrosion rate than the remaining specimens, with the exception of CB-T-DC45, throughout the test period. Table 3.11 summarizes the average corrosion rate at week 70 and Table C.3 shows the results of the Student's t-test. The average corrosion rate for specimens with a water-cement ratio of 0.45 and no inhibitor (CB-T-45) was 5.07 μm/year. Specimens with a water-cement ratio of 0.35 and no inhibitor (CB-T-35) had a corrosion rate of 1.13 μm/year, which corresponds to 27% of the corrosion rate of CB-T-45, with the difference in the averages being significant at $\alpha = 0.10$. The average corrosion rates for specimens CB-T-RH45 and CB-T-DC45 were 0.79 and 0.82 μm/year, respectively. The difference in the average corrosion rates between CB-T-45 and either CB-T-RH45 or CB-T-DC45 is statistically significant at $\alpha = 0.05$. The average corrosion rates for specimens CB-T-RH35 and CB-T-DC35 were 0.79 and 0.67 μm/year, respectively. The difference in the average corrosion rates between CB-T-35 and CB-T-RH35 is statistically significant at $\alpha = 0.05$, as is the difference between CB-T-35 and CB-T-DC35.

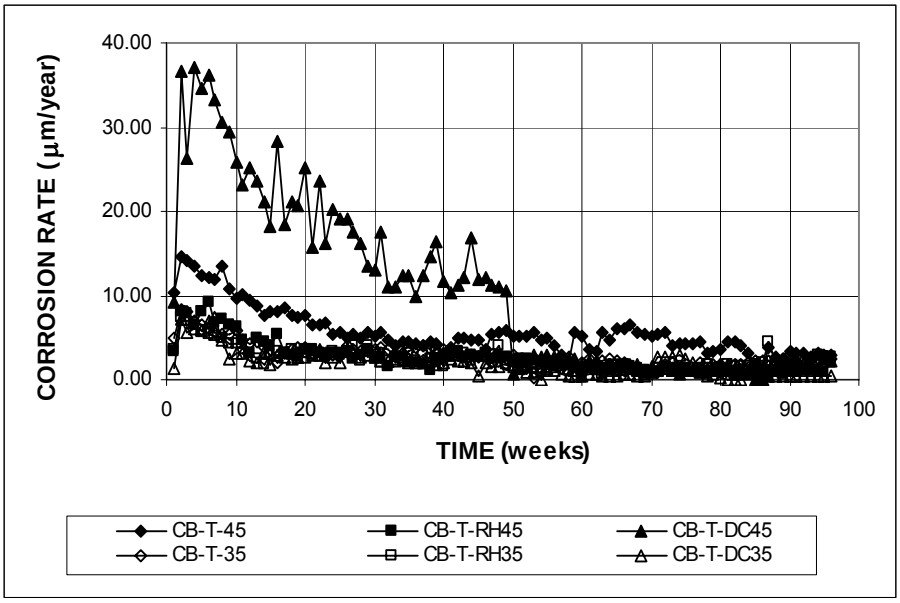


**Figure 3.28 –** Average corrosion rates as measured in the cracked beam test for specimens with and without corrosion inhibitors and water-cement ratios of 0.45 and 0.35. Specimens with Thermex-treated conventional steel.

**Table 3.11 –** Average corrosion rates (in µm/year) at week 70 as measured in the cracked beam test for specimens with and without corrosion inhibitors and water-cement ratios of 0.45 and 0.35. Specimens with Thermex-treated conventional steel.

| Specimen designation* | Specimen | | | | | | Average | Standard deviation |
|---|---|---|---|---|---|---|---|---|
| | 1 | 2 | 3 | 4 | 5 | 6 | | |
| **Cracked beam test** | | | | | | | | |
| **CB-T-45** | 9.43 | 3.14 | 2.27 | 9.85 | 4.16 | 1.57 | 5.07 | 3.65 |
| **CB-T-RH45** | 1.49 | 0.03 | 0.85 | | | | 0.79 | 0.73 |
| **CB-T-DC45** | 0.02 | 1.39 | 1.06 | | | | 0.82 | 0.71 |
| **CB-T-35** | 0.00 | 2.13 | 1.27 | | | | 1.13 | 1.07 |
| **CB-T-RH35** | 0.44 | 0.47 | 1.48 | | | | 0.79 | 0.59 |
| **CB-T-DC35** | 0.03 | 0.46 | 1.51 | | | | 0.67 | 0.76 |

* CB - A - B

**CB**: cracked beam test

**A**: steel type → T: Thermex-treated conventional steel.

**B**: mix design → 45: water-cement ratio of 0.45 and no inhibitor, RH45: water-cement ratio of 0.45 and Rheocrete 222+, DC45: water-cement ratio of 0.45 and DCI-S, 35: water-cement ratio of 0.35 and no inhibitor, RH35: water-cement ratio of 0.35 and Rheocrete 222+, DC35: water-cement ratio of 0.35 and DCI-S.

Figure 3.29 shows the average total corrosion losses versus time for specimens with Thermex-treated conventional steel, and Table 3.12 summarizes the losses at week 70. Table C.4 presents the results of the Student's t-test. Specimens with a water-cement ratio of 0.45 and no inhibitor (CB-T-45) had an average total corrosion loss of 8.72 μm, while specimens with a water-cement ratio of 0.35 and no inhibitor (CB-T-35) had an average total corrosion loss of 4.42 μm (51% of the corrosion loss of CB-T-45). The difference in the average corrosion losses between CB-T-45 and CB-T-35 is significant at $\alpha = 0.02$. Specimens with a water-cement ratio of 0.35 and DCI-S (CB-T-DC35) had the lowest corrosion loss, 2.73 μm, which corresponds to 62% of the corrosion loss of CB-T-35. Due to the high corrosion rates during the first 50 weeks, specimens with a water-cement ratio of 0.45 and DCI-S (CB-T-DC45) had a corrosion loss of 18.58 μm at week 70, mainly due to the high average corrosion rates of one of the specimens during the first 49 weeks. Specimens with Rheocrete 222+ had average total corrosion losses of 4.20 and 3.67 μm, for specimens with water-cement ratios of 0.45 and 0.35, respectively. The difference in the average corrosion losses between CB-T-45 and CB-T-RH45 is significant at $\alpha = 0.02$, while the difference in the average corrosion losses between CB-T-35 and CB-T-RH35 is not significant.

The results for specimens CB-T-DC35 are quite different from that of specimens CB-N-DC35 (Figures 3.24 and 3.25 and Tables 3.9 and 3.10). This is an indication of the wide variations that can be obtained with this test.

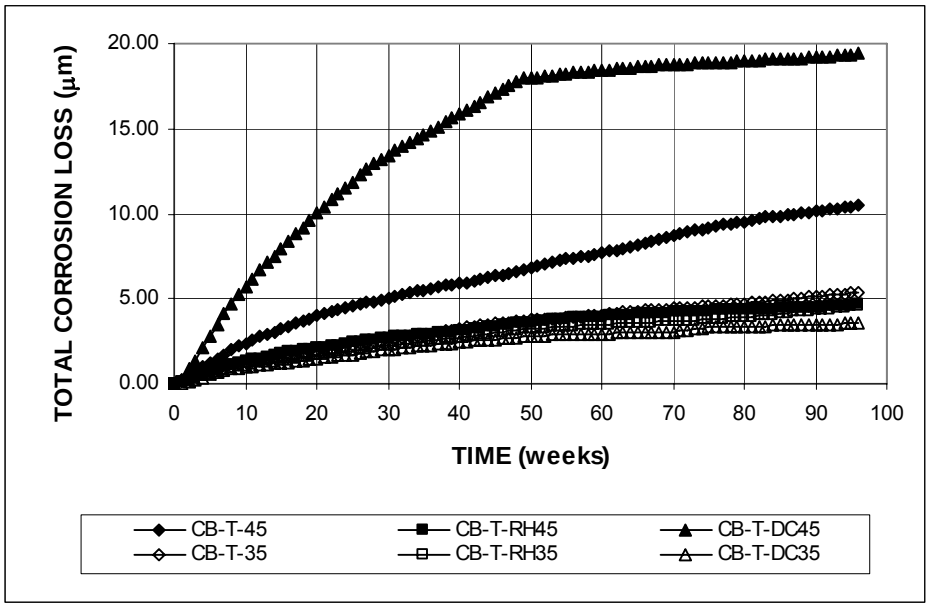


**Figure 3.29 –** Average total corrosion losses as measured in the cracked beam test for specimens with and without corrosion inhibitors and water-cement ratios of 0.45 and 0.35.Specimens with Thermex-treated conventional steel.

**Table 3.12 –** Average total corrosion losses (in μm) at week 70 as measured in the cracked beam test for specimens with and without corrosion inhibitors and water-cement ratios of 0.45 and 0.35. Specimens with Thermex-treated conventional steel.

| Specimen designation* | Specimen | | | | | | Average | Standard deviation |
|---|---|---|---|---|---|---|---|---|
| | 1 | 2 | 3 | 4 | 5 | 6 | | |
| **Cracked beam test** | | | | | | | | |
| **CB-T-45** | 9.59 | 7.42 | 8.86 | 10.96 | 10.48 | 4.99 | 8.72 | 2.21 |
| **CB-T-RH45** | 5.02 | 5.05 | 2.52 | | | | 4.20 | 1.45 |
| **CB-T-DC45** | 7.70 | 2.77 | 45.28 | | | | 18.58 | 23.25 |
| **CB-T-35** | 4.99 | 4.77 | 3.52 | | | | 4.42 | 0.79 |
| **CB-T-RH35** | 2.05 | 6.36 | 2.60 | | | | 3.67 | 2.35 |
| **CB-T-DC35** | 2.37 | 2.75 | 3.06 | | | | 2.73 | 0.35 |

* CB - A - B
**CB**: cracked beam test
**A**: steel type → T: Thermex-treated conventional steel.
**B**: mix design → 45: water-cement ratio of 0.45 and no inhibitor, RH45: water-cement ratio of 0.45 and Rheocrete 222+, DC45: water-cement ratio of 0.45 and DCI-S, 35: water-cement ratio of 0.35 and no inhibitor, RH35: water-cement ratio of 0.35 and Rheocrete 222+, DC35: water-cement ratio of 0.35 and DCI-S.

When the results obtained from specimens fabricated with conventional normalized and conventional Thermex-treated steel are averaged, the average corrosion losses for specimens with a water-cement ratio of 0.35 and no inhibitor are 59% of the corrosion losses of specimens with a water-cement ratio of 0.45 and no inhibitor. For specimens with a water-cement ratio of 0.45, the corrosion losses were 51% and 155% for specimens with Rheocrete 222+ and DCI-S, respectively, of the corrosion loss of specimens with no inhibitors. For specimens with a water-cement ratio of 0.35, the corrosion losses were 86% and 179% for specimens with Rheocrete 222+ and DCI-S, respectively, of the corrosion loss of specimens with no inhibitors.

Figure 3.30 shows the average corrosion potentials of the top and bottom mats of steel with respect to a copper-copper sulfate electrode. All specimens showed corrosion potentials of the top mat of steel that were more negative than -0.400 V, indicating active corrosion, starting at week 1. The corrosion potentials of the bottom mat remained between -0.200 and -0.350 V, indicating a low probability of corrosion, for all specimens, except those with a water-cement ratio of 0.45 and no inhibitor (CB-T-45), which had corrosion potentials of the bottom mat that were more negative than -0.350 V, indicating active corrosion.

Figure 3.31 shows the average mat-to-mat resistances for specimens with Thermex-treated conventional steel. At the start of the test period, values ranged from 200 to 600 ohms. At week 70, specimens with a water-cement ratio of 0.35 and DCI-S (CB-T-DC35) had a mat-to-mat resistance above 5000 ohms. The remaining specimens had mat-to-mat resistances below 3000 ohms.

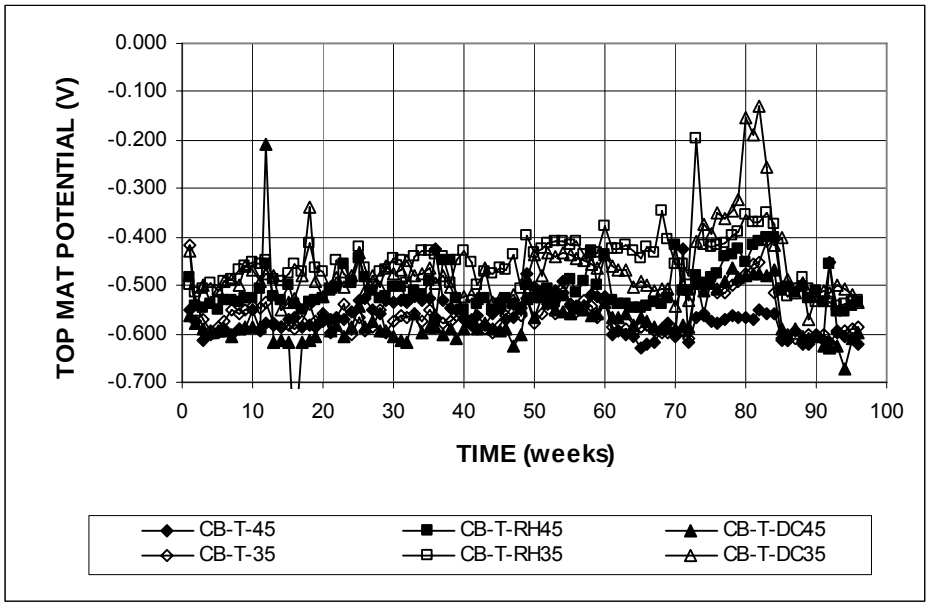


(a)

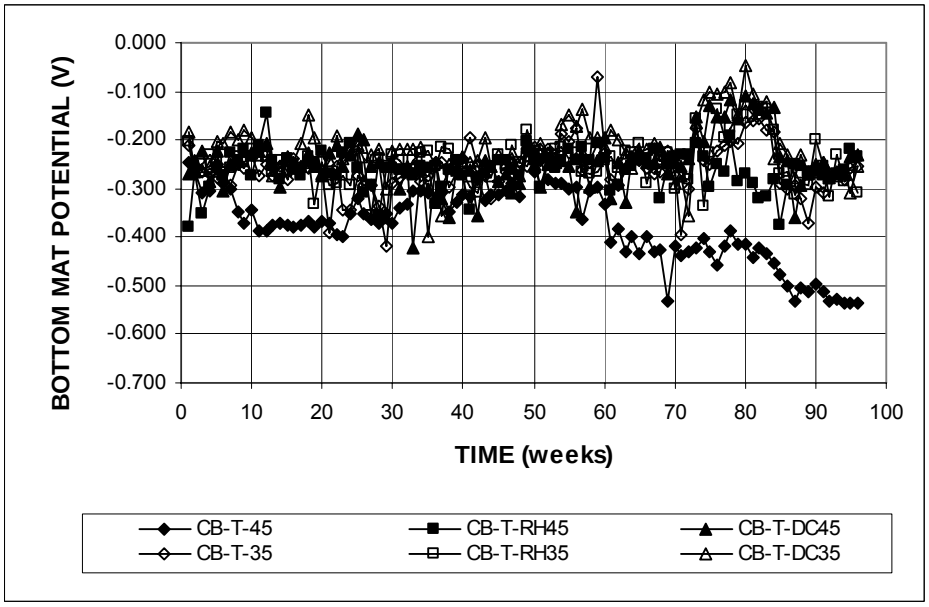


(b)

**Figure 3.30 –** (a) Average top mat corrosion potentials and (b) average bottom mat corrosion potentials with respect to copper-copper sulfate electrode as measured in the cracked beam test for specimens with and without corrosion inhibitors and water-cement ratios of 0.45 and 0.35. Specimens with Thermex-treated conventional steel.

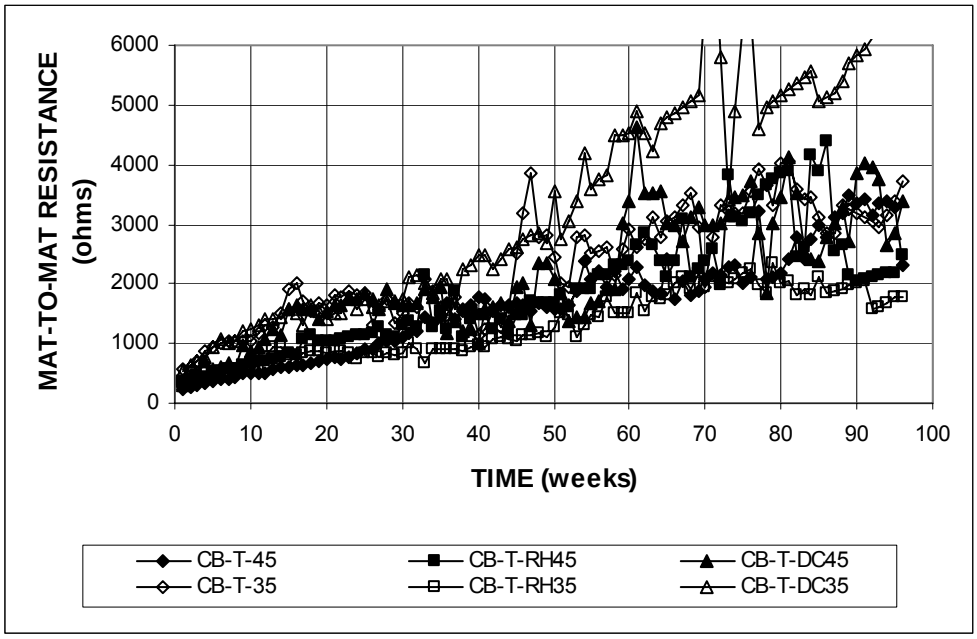


**Figure 3.31 –** Average mat-to-mat resistances as measured in the cracked beam test for specimens with and without corrosion inhibitors and water-cement ratios of 0.45 and 0.35. Specimens with Thermex-treated conventional steel.

### 3.3.2.3 ASTM G 109 Test

The average corrosion rates versus time in the ASTM G 109 tests are presented in Figures 3.32 and 3.33 for specimens with conventional, normalized steel and Thermex-treated conventional steel, respectively. Significant corrosion rates were obtained for the specimens containing N and T steel with a water-cement ratio of 0.45 and no inhibitor (G-N-45 and G-T-45, respectively), and for specimens with N and T steel, a water-cement ratio of 0.45 and DCI-S inhibitor (G-N-DC45 and G-T-DC45, respectively), although the corrosion rates were much lower for the latter. Specimens G-N-45 and G-T-45 started corroding after 17 and 21 weeks, respectively. The corrosion rate of specimens G-N-45 reached values above 4 μm/year, but after week 72, it dropped to below 2.2 μm/year. Specimens G-N-DC45 started corroding

at week 42 and had corrosion rates between 0.25 and 0.50 μm/year from week 42 to week 96. Specimens G-T-DC45 showed no corrosion for the first 80 weeks, and had a corrosion rate of about 0.25 μm/year for the last 16 weeks of the test period. Table 3.13 shows the average corrosion rates at week 70 and Table C.3 shows the results of the Student's t-test. The average corrosion rates were 3.80 μm/year for G-N-45, 2.85 μm/year for G-T-45, and 0.39 μm/year for G-N-DC45. The difference in the average corrosion rates between G-N-45 and either G-N-RH45, G-N-DC45 or G-N-35 is significant at $\alpha = 0.10$. The difference in the average corrosion rates between G-T-45 and G-T-RH45, G-T-DC45 or G-T-35 is also significant at $\alpha = 0.10$. The rest of the specimens showed no corrosion. The fact that low corrosion activity was observed for most specimens in the ASTM G 109 test is attributed to the lower salt concentration of the solution ponded over the specimens and to the less aggressive ponding and drying cycle to which the specimens are subjected, compared to the other bench-scale tests. These two factors reduce the rate at which chlorides penetrate the concrete.

The average total corrosion losses as a function of time for the ASTM G 109 specimens are shown in Figures 3.34 and 3.35, for normalized and Thermex-treated conventional steels, respectively. The average total corrosion losses at week 70 are summarized in Table 3.14 and the results of the Student's t-test are shown in Table C.4. For specimens with a water-cement ratio of 0.45 and no inhibitor, the average total corrosion losses at week 70 were equal to 2.61 and 1.60 μm for specimens with conventional, normalized steel (G-N-45) and Thermex-treated conventional steel (G-T-45), respectively. Specimens with N steel, a water-cement ratio of 0.45, and DCI-S (G-N-DC45) had a corrosion loss of 0.15 μm, equal to 6% of the corrosion loss of G-N-45, and specimens with T steel, a water-cement ratio of 0.35 and no

inhibitor (G-T-35) had a corrosion loss of 0.08 μm, equal to 5% of the corrosion loss of G-T-45. The remaining specimens had corrosion losses below 0.02 μm. The difference in the average corrosion loss of G-N-45 and either G-N-RH45, G-N-DC45, or G-N-35 is significant at $\alpha = 0.02$, while the difference in the average corrosion loss of G-T-45 and G-T-RH45, G-T-DC45, or G-T-35 is significant at $\alpha = 0.20$.

**Table 3.13 –** Average corrosion rates (in μm/year) at week 70 as measured in the ASTM G 109 test for specimens with and without corrosion inhibitors and water-cement ratios of 0.45 and 0.35.

| Specimen designation* | Specimen | | | | | | Average | Standard deviation |
|---|---|---|---|---|---|---|---|---|
| | 1 | 2 | 3 | 4 | 5 | 6 | | |
| **ASTM G 109 test** | | | | | | | | |
| **G-N-45** | 3.37 | 0.99 | 1.21 | 0.00 | 9.64 | 7.61 | 3.80 | 3.94 |
| **G-N-RH45** | 0.00 | 0.00 | 0.00 | | | | 0.00 | 0.00 |
| **G-N-DC45** | 0.00 | 0.28 | 0.91 | | | | 0.39 | 0.46 |
| **G-N-35** | 0.00 | 0.00 | 0.00 | | | | 0.00 | 0.00 |
| **G-N-RH35** | 0.00 | 0.00 | 0.00 | | | | 0.00 | 0.00 |
| **G-N-DC35** | 0.00 | 0.00 | 0.00 | | | | 0.00 | 0.00 |
| **G-T-45** | 0.00 | 0.00 | 2.13 | 8.30 | 4.59 | 2.07 | 2.85 | 3.16 |
| **G-T-RH45** | 0.00 | 0.00 | 0.00 | | | | 0.00 | 0.00 |
| **G-T-DC45** | 0.01 | 0.01 | 0.00 | | | | 0.01 | 0.00 |
| **G-T-35** | 0.00 | 0.00 | 0.00 | | | | 0.00 | 0.00 |
| **G-T-RH35** | 0.00 | 0.00 | 0.00 | | | | 0.00 | 0.00 |
| **G-T-DC35** | 0.00 | 0.00 | 0.00 | | | | 0.00 | 0.00 |

* G - A - B

**G**: ASTM G 109 test

**A**: steel type → N: conventional, normalized steel, T: Thermex-treated conventional steel.

**B**: mix design → 45: water-cement ratio of 0.45 and no inhibitor, RH45: water-cement ratio of 0.45 and Rheocrete 222+, DC45: water-cement ratio of 0.45 and DCI-S, 35: water-cement ratio of 0.35 and no inhibitor, RH35: water-cement ratio of 0.35 and Rheocrete 222+, DC35: water-cement ratio of 0.35 and DCI-S.

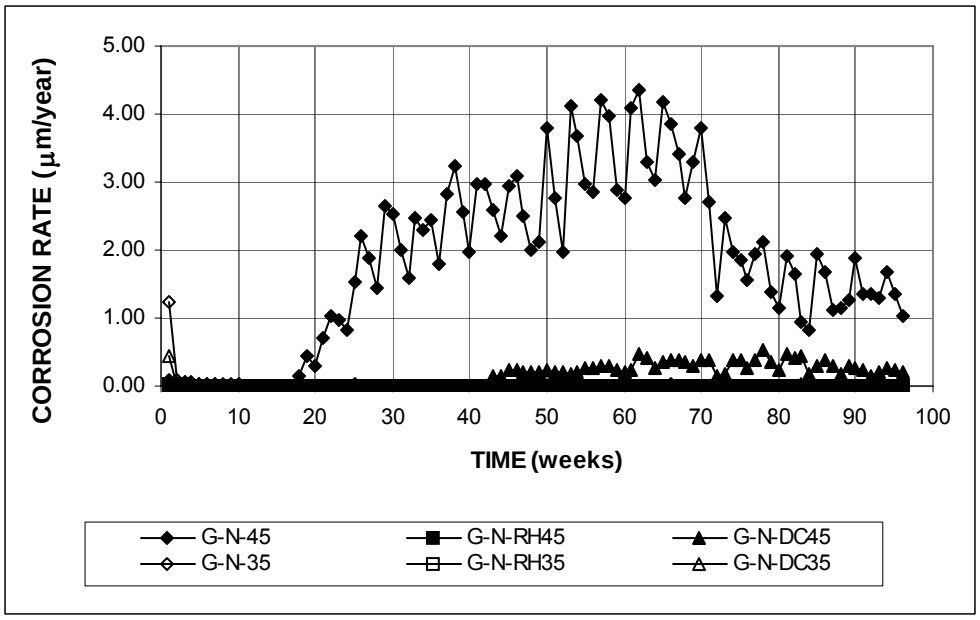


**Figure 3.32 –** Average corrosion rates as measured in the ASTM G 109 test for specimens with and without corrosion inhibitors and water-cement ratios of 0.45 and 0.35. Specimens with conventional, normalized steel.

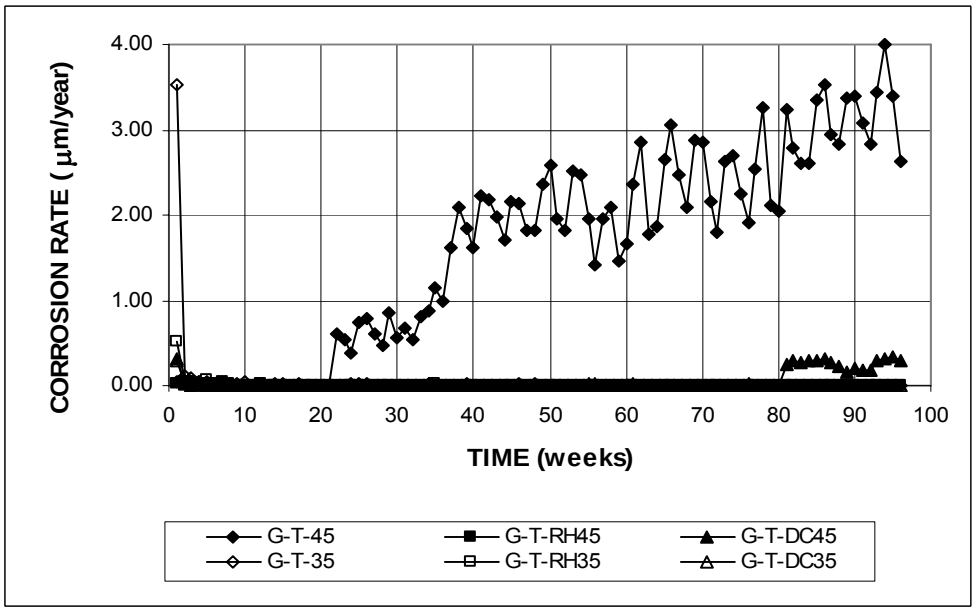


**Figure 3.33 –** Average corrosion rates as measured in the ASTM G 109 test for specimens with and without corrosion inhibitors and water-cement ratios of 0.45 and 0.35. Specimens with Thermex-treated conventional steel.

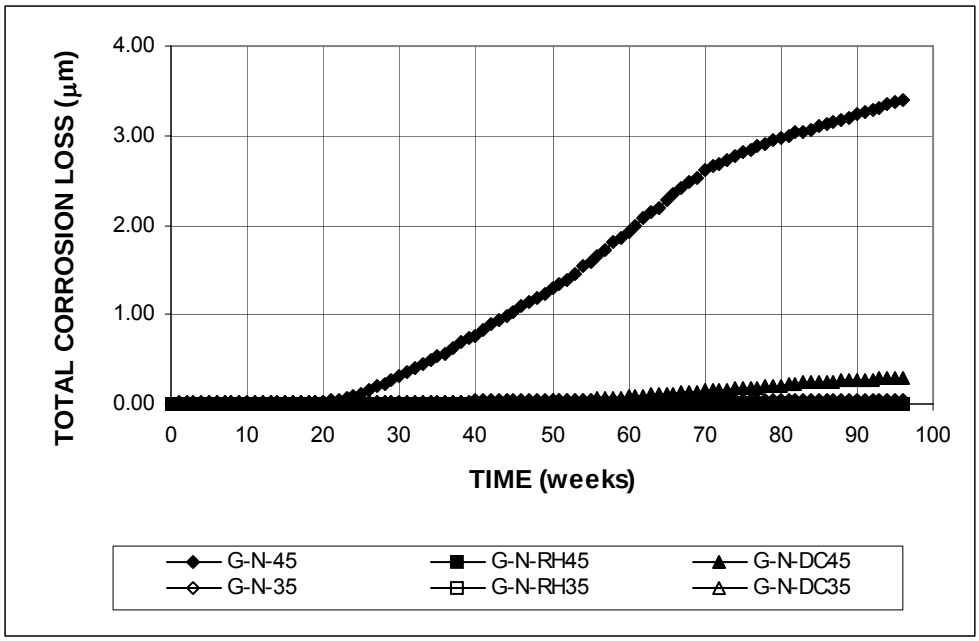


**Figure 3.34 –**Average total corrosion losses as measured in the ASTM G 109 test for specimens with and without corrosion inhibitors and water-cement ratios of 0.45 and 0.35. Specimens with conventional, normalized steel.

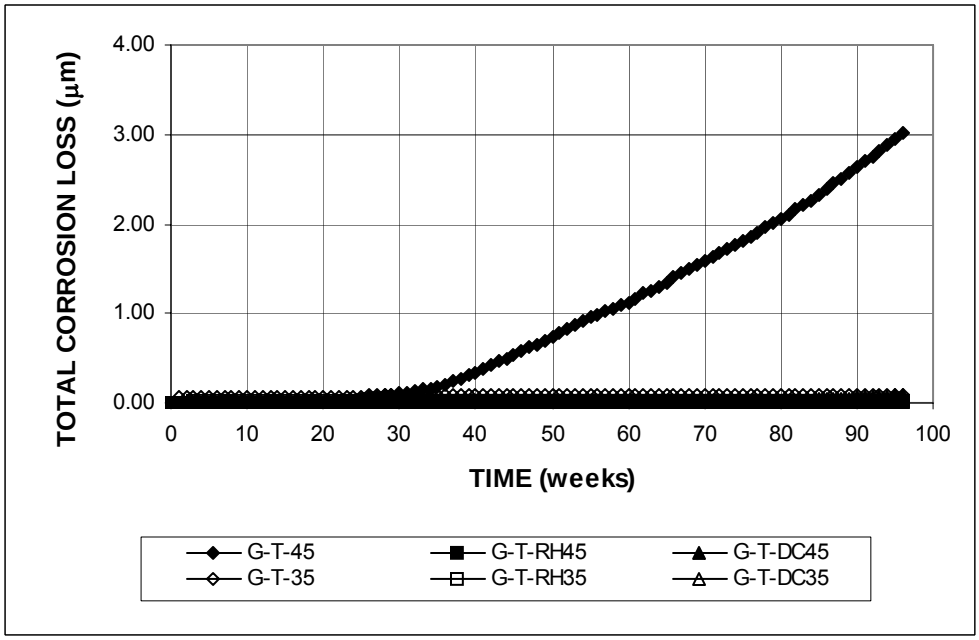


**Figure 3.35 –** Average total corrosion losses as measured in the ASTM G 109 test for specimens with and without corrosion inhibitors and water-cement ratios of 0.45 and 0.35. Specimens with Thermex-treated conventional steel.

**Table 3.14 –** Average total corrosion losses (in μm) at week 70 as measured in the ASTM G 109 test for specimens with and without corrosion inhibitors and water-cement ratios of 0.45 and 0.35.

| Specimen designation* | Specimen | | | | | | Average | Standard deviation |
|---|---|---|---|---|---|---|---|---|
| | 1 | 2 | 3 | 4 | 5 | 6 | | |
| **ASTM G 109 test** | | | | | | | | |
| **G-N-45** | 2.92 | 1.45 | 1.03 | 3.05 | 4.19 | 3.01 | 2.61 | 1.17 |
| **G-N-RH45** | 0.00 | 0.00 | 0.00 | | | | 0.00 | 0.00 |
| **G-N-DC45** | 0.00 | 0.09 | 0.35 | | | | 0.15 | 0.18 |
| **G-N-35** | 0.02 | 0.05 | 0.04 | | | | 0.04 | 0.02 |
| **G-N-RH35** | 0.01 | 0.00 | 0.00 | | | | 0.00 | 0.00 |
| **G-N-DC35** | 0.02 | 0.02 | 0.01 | | | | 0.02 | 0.01 |
| **G-T-45** | 0.01 | 0.00 | 0.34 | 6.71 | 0.69 | 1.84 | 1.60 | 2.60 |
| **G-T-RH45** | 0.00 | 0.01 | 0.00 | | | | 0.01 | 0.00 |
| **G-T-DC45** | 0.01 | 0.01 | 0.01 | | | | 0.01 | 0.00 |
| **G-T-35** | 0.17 | 0.01 | 0.06 | | | | 0.08 | 0.08 |
| **G-T-RH35** | 0.01 | 0.01 | 0.03 | | | | 0.02 | 0.01 |
| **G-T-DC35** | 0.02 | 0.02 | 0.00 | | | | 0.01 | 0.01 |

* G - A - B

**G**: ASTM G 109 test

**A**: steel type → N: conventional, normalized steel, T: Thermex-treated conventional steel.

**B**: mix design → 45: water-cement ratio of 0.45 and no inhibitor, RH45: water-cement ratio of 0.45 and Rheocrete 222+, DC45: water-cement ratio of 0.45 and DCI-S, 35: water-cement ratio of 0.35 and no inhibitor, RH35: water-cement ratio of 0.35 and Rheocrete 222+, DC35: water-cement ratio of 0.35 and DCI-S.

The average corrosion potentials of the top and bottom mats of steel with respect to a copper-copper-sulfate electrode are shown in Figures 3.36 and 3.37 for specimens with normalized and Thermex-treated conventional steel, respectively. Active corrosion of the top mat of steel, indicated by corrosion potentials more negative than -0.350 V, was observed for specimens with a water-cement ratio of 0.45 and no inhibitor (G-N-45 and G-T-45). Specimens with N steel, a water-cement ratio of 0.45, and DCI-S (G-N-DC45) had a top mat corrosion potential of approximately -0.310 V at week 70, indicating a low probability for corrosion, but at week 75, the potential dropped to values more negative than -0.400 V, indicating active corrosion. Specimens with T steel, a water-cement ratio of 0.45, and DCI-S (G-T-DC45) had top mat corrosion potentials that were more positive than -0.150 V for the first 80 weeks, but at the end of the test period had corrosion potentials that were more negative than

-0.400 V, indicating active corrosion. The rest of the specimens had corrosion potentials indicating a passive condition in the top mat throughout the test period. All specimens had corrosion potentials that indicated a passive condition of the bottom mat of steel, with the exception of G-N-45, which had bottom mat potentials of approximately -0.300 V after week 48. Specimens G-N-DC45 and G-T-45 showed bottom mat corrosion potentials around -0.200 V, while the remaining specimens had bottom mat corrosion potentials that were more positive than -0.150 V after week 50.

Figures 3.38 and 3.39 show the average mat-to-mat resistances for specimens with normalized and Thermex-treated conventional steel, respectively. For specimens with N steel, the average mat-to-mat resistance during the first week was approximately 200 ohms for all specimens, with little scatter. By week 70, the mat-to-mat resistances had increased to values between 1000 and 2000 ohms for all specimens, with the highest value for specimens with a water-cement ratio of 0.45 and corrosion inhibitors (G-N-RH45 and G-N-DC45).

For specimens with T steel, the average mat-to-mat resistances at week 1 were between 100 and 300 ohms. Specimens with a water-cement ratio of 0.35 and no inhibitor (G-T-35) showed consistently higher values than the other specimens throughout the test period. At week 70, the mat-to-mat resistance ranged from 1000 to 1800 ohms.

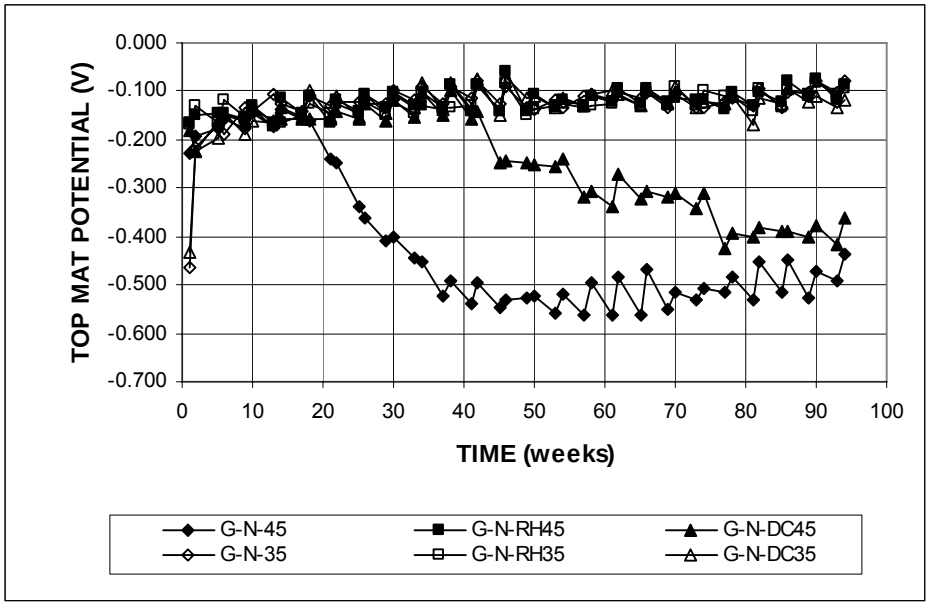


(a)

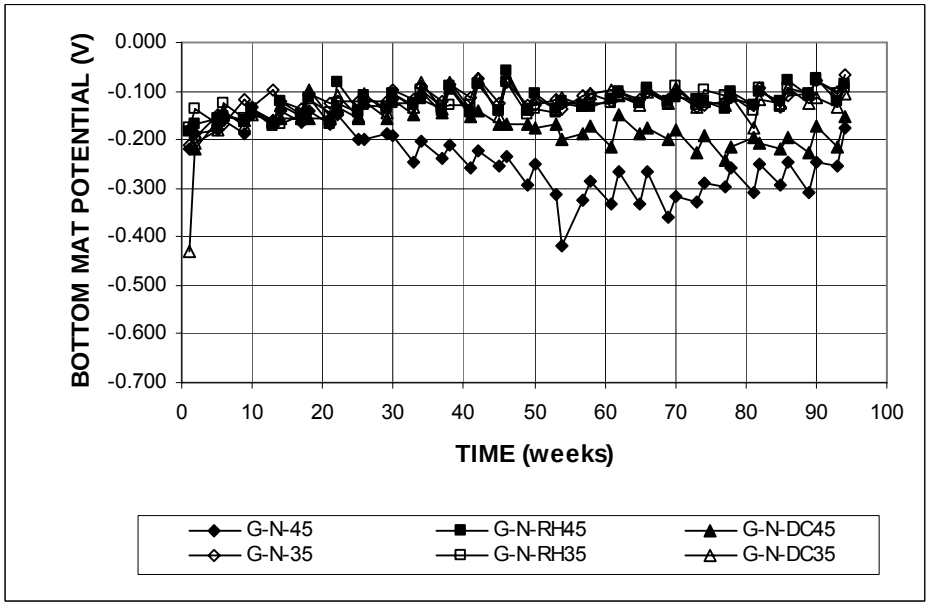


(b)

**Figure 3.36 –** (a) Average top mat corrosion potentials and (b) average bottom mat corrosion potentials with respect to copper-copper sulfate electrode as measured in the ASTM G 109 test for specimens with and without corrosion inhibitors and water-cement ratios of 0.45 and 0.35. Specimens with conventional, normalized steel.

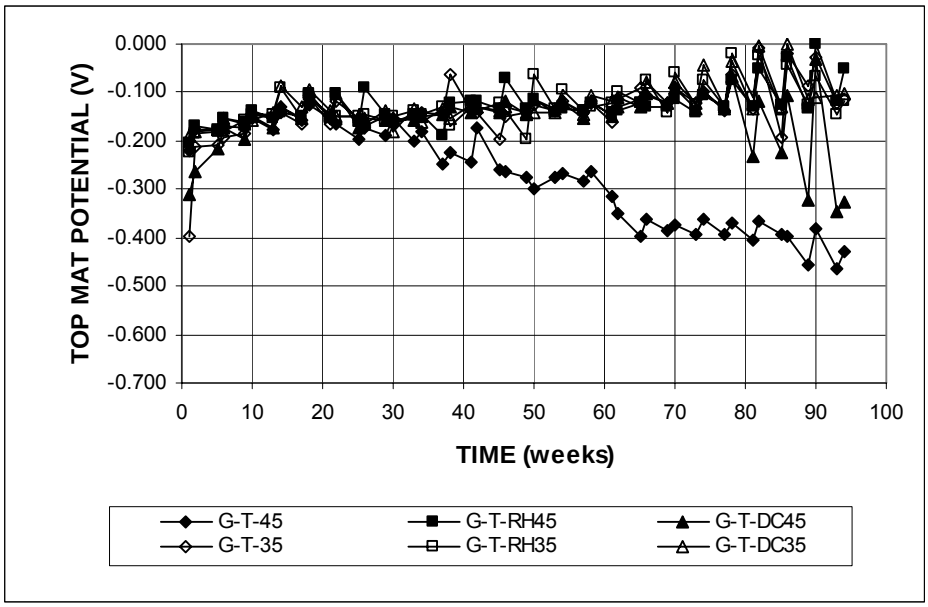


(a)

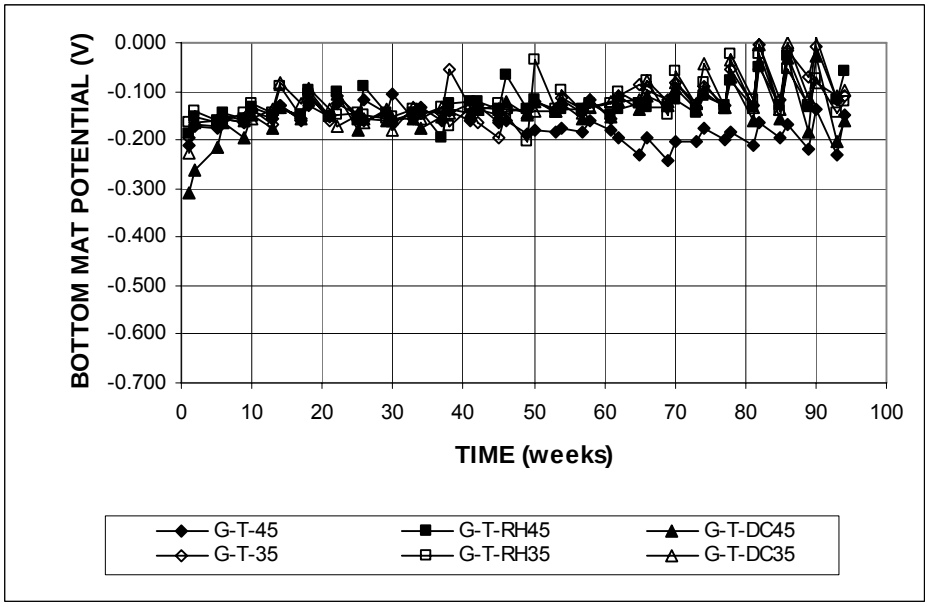


(b)

**Figure 3.37 –** (a) Average top mat corrosion potentials and (b) average bottom mat corrosion potentials with respect to copper-copper sulfate electrode as measured in the ASTM G 109 test for specimens with and without corrosion inhibitors and water-cement ratios of 0.45 and 0.35. Specimens with Thermex-treated conventional steel.

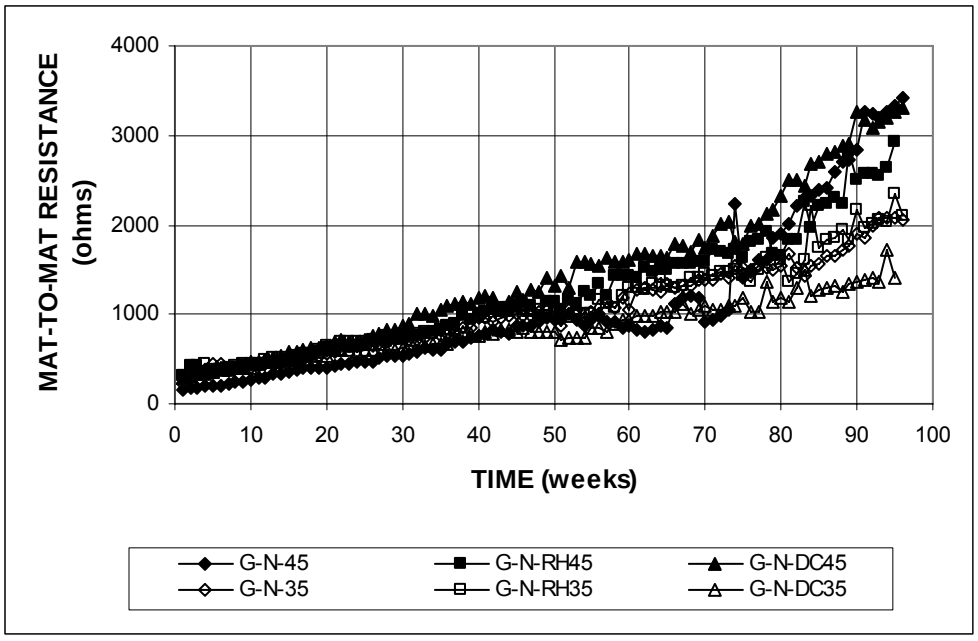


**Figure 3.38 –** Average mat-to-mat resistances as measured in the ASTM G 109 test for specimens with and without corrosion inhibitors and water-cement ratios of 0.45 and 0.35. Specimens with conventional, normalized steel.

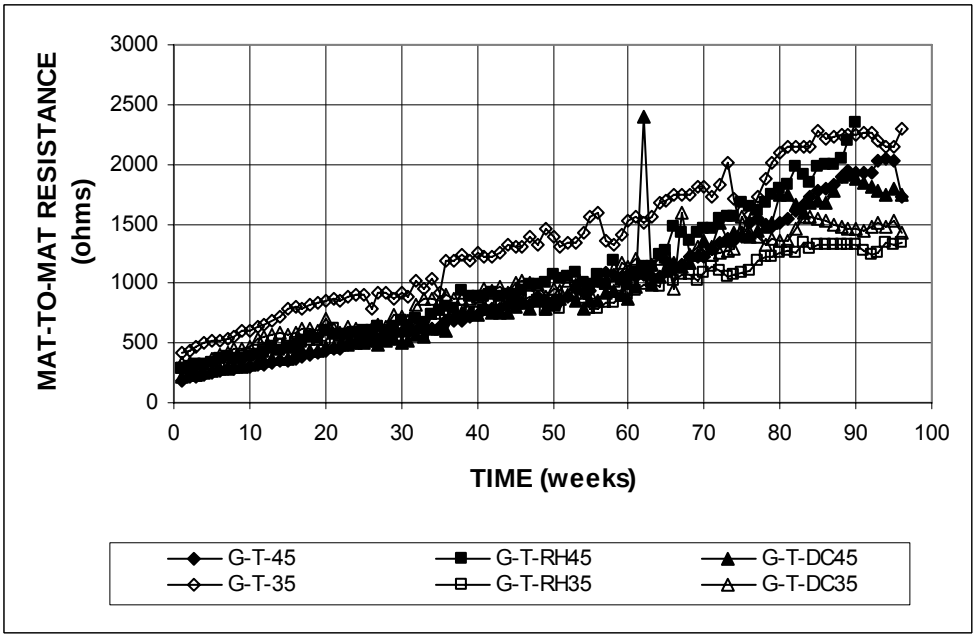


**Figure 3.39 –** Average mat-to-mat resistances as measured in the ASTM G 109 test for specimens with and without corrosion inhibitors and water-cement ratios of 0.45 and 0.35. Specimens with Thermex-treated conventional steel.

## 3.4 MICROALLOYED STEEL

This section presents the results of the macrocell tests using bare and "lollipop" specimens, and the bench-scale tests (Southern Exposure, cracked beam, and ASTM G 109) for five different steels: conventional, normalized steel (N); Thermex-treated conventional steel (T); Thermex-treated microalloyed steel with a high phosphorus content, 0.117%, (CRPT1); Thermex-treated microalloyed steel with a high phosphorus content, 0.100%, (CRPT2); and Thermex-treated microalloyed steel with normal phosphorus content, 0.017%, (CRT). The Southern Exposure tests also include specimens with a combination of conventional and microalloyed steels; CRPT1 steel was chosen as the microalloyed steel for these tests because, at the time the decision was made, initial results (through 17 weeks) from the Southern Exposure tests (Figure 3.46) indicated better corrosion performance of this steel when compared to the two other microalloyed steels. The results of these tests were previously reported by Balma et al. (2002) and are presented here because they are used to correlate the performance of the rapid macrocell and bench-scale tests.

### 3.4.1 Rapid Macrocell Test

The macrocell tests were performed on bare bars and lollipop specimens in 1.6 m ion NaCl and simulated concrete pore solution. The mortar in the lollipop specimens had a water-cement ratio of 0.50. The bars for the mortar specimens were prepared with and without epoxy-filled caps on the ends of the bars to protect them from corrosion. Macrocell specimens were evaluated using the test configuration in Figure 2.1, where the lid was placed on the top of the container. Corrosion potentials of the anodes and the cathodes were not measured for the macrocell test. Readings were taken daily for 100 days.

### 3.4.1.1 Bare Bars

For bare bars in 1.6 m ion NaCl and simulated concrete pore solution, the average corrosion rates as a function of time are presented in Figure 3.40. Corrosion rates ranged from 20 to 60 μm/year. T steel shows lower corrosion rates than the rest of the steels during the first 11 weeks. Table 3.15 summarizes the average corrosion rates at day 100 and Table C.5 shows the results of the Student's t-test. As shown in Table 3.15, CRPT1 had the highest corrosion rate, 49.26 μm/year, while N and T steel had average corrosion rates of 40.18 and 29.11 μm/year, respectively. CRT and CRPT1 steels had corrosion rates of 45.36 and 37.44 μm/year, respectively. The difference in the average corrosion rates between N steel and the remaining steels is not statistically significant.

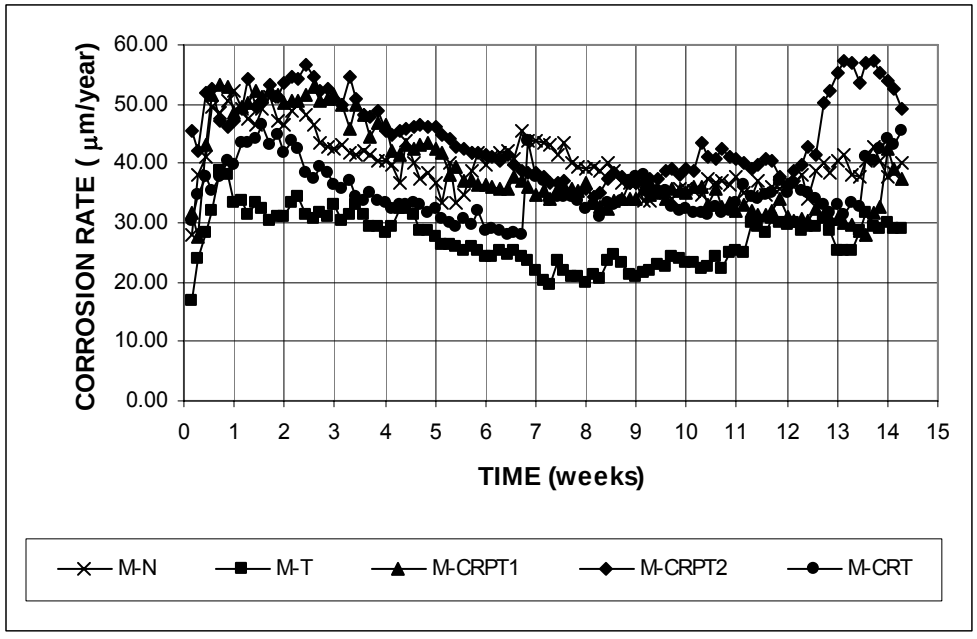


**Figure 3.40 –** Average corrosion rates as measured in the rapid macrocell test for bare conventional and microalloyed steel bars in 1.6 m ion NaCl and simulated concrete pore solution.

**Table 3.15 –** Average corrosion rates (in μm/year) at day 100 as measured in the rapid macrocell test for bare conventional and microalloyed steel bars in a 1.6 m ion NaCl and simulated concrete pore solution.

| Specimen designation* | Steel type | Specimen | | | | | Average | Standard deviation |
|---|---|---|---|---|---|---|---|---|
| | | 1 | 2 | 3 | 4 | 5 | | |
| **Bare bars in 1.6 m NaCl** | | | | | | | | |
| **M-N** | **N** | 54.59 | 56.17 | 12.28 | 37.20 | 40.79 | 40.21 | 17.68 |
| **M-T** | **T** | 48.52 | 26.57 | 26.10 | 8.35 | 42.06 | 30.32 | 15.68 |
| **M-CRPT1** | **CRPT1** | 26.27 | 37.52 | 64.70 | 21.51 | 37.09 | 37.42 | 16.75 |
| **M-CRPT2** | **CRPT2** | 45.77 | 77.69 | 26.10 | 53.67 | 43.93 | 49.43 | 18.74 |
| **M-CRT** | **CRT** | 74.56 | 42.08 | 35.94 | 44.01 | 27.60 | 44.84 | 17.80 |

* M - A - B
**M**: macrocell test
**A**: steel type → N: conventional, normalized steel, T: Thermex-treated conventional steel, CRPT1: Thermex-treated microalloyed steel with a high phosphorus content (0.117%), CRPT2: Thermex-treated microalloyed steel with a high phosphorus content (0.100%), CRT: Thermex treated microalloyed steel with normal phosphorus content (0.017%).

The average total corrosion losses during the test period are shown in Figure 3.41 and the losses at day 100 are summarized in Table 3.16. Results of the Student's t-test are shown in Table C.6. As shown in Table 3.16, Thermex-treated conventional steel (T) had the lowest corrosion loss, 7.77 μm, and conventional, normalized steel (N) had a total corrosion loss of 11.03 μm, with the difference in the means being statistically significant at $\alpha = 0.10$. CRT steel had a corrosion loss of 9.53 μm, equal to 86% of the corrosion loss of N steel, but the difference is not statistically significant. CRPT1 and CRPT2 had corrosion losses of 10.63 and 12.29 μm, respectively.

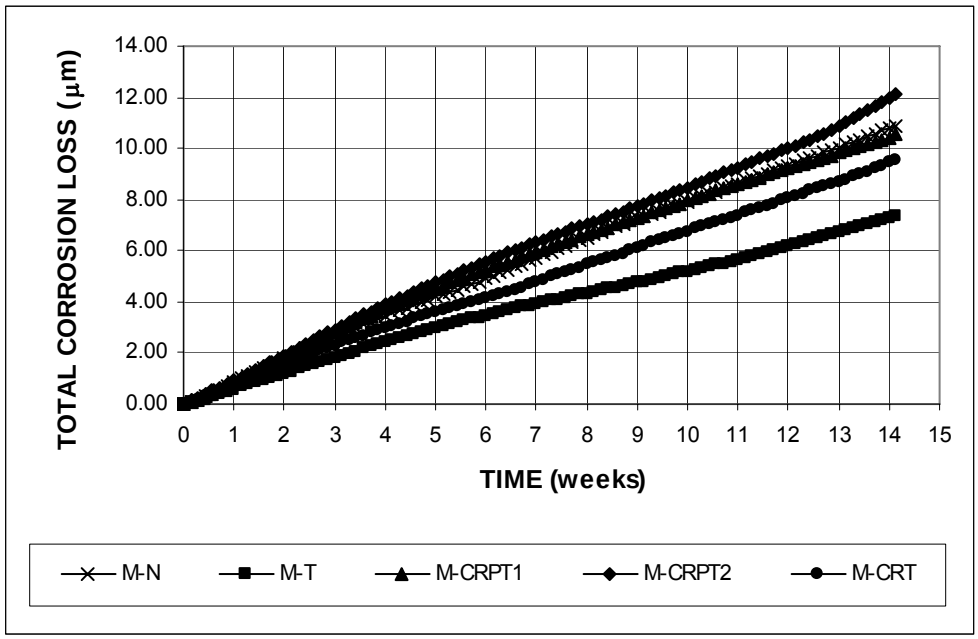


**Figure 3.41 –** Average total corrosion losses as measured in the rapid macrocell test for bare conventional and microalloyed steel bars in 1.6 m ion NaCl and simulated concrete pore solution.

**Table 3.16 –** Average total corrosion losses (in μm) at day 100 as measured in the rapid macrocell test for bare conventional and microalloyed steel bars in 1.6 m ion NaCl and simulated concrete pore solution.

| Specimen designation* | Steel type | Specimen | | | | | Average | Standard deviation |
|---|---|---|---|---|---|---|---|---|
| | | 1 | 2 | 3 | 4 | 5 | | |
| **Bare bars in 1.6 m NaCl** | | | | | | | | |
| **M-N** | **N** | 14.11 | 13.89 | 7.56 | 9.28 | 10.32 | 11.03 | 2.88 |
| **M-T** | **T** | 7.84 | 9.38 | 8.05 | 4.02 | 9.56 | 7.77 | 2.23 |
| **M-CRPT1** | **CRPT1** | 8.86 | 11.98 | 10.41 | 8.99 | 12.92 | 10.63 | 1.80 |
| **M-CRPT2** | **CRPT2** | 11.61 | 14.85 | 10.48 | 13.39 | 11.10 | 12.29 | 1.80 |
| **M-CRT** | **CRT** | 8.63 | 8.45 | 9.70 | 11.22 | 9.68 | 9.53 | 1.11 |

* M - A

**M**: macrocell test

**A**: steel type → N: conventional, normalized steel, T: Thermex-treated conventional steel, CRPT1: Thermex-treated microalloyed steel with a high phosphorus content (0.117%), CRPT2: Thermex-treated microalloyed steel with a high phosphorus content (0.100%), CRT: Thermex treated microalloyed steel with normal phosphorus content (0.017%).

### 3.4.1.2 "Lollipop" Specimens

Figure 3.42 shows the average corrosion rates versus time for lollipop specimens with epoxy-filled caps on the ends of the bars. The corrosion rate of T steel remained around 2 μm/year during most of the test period, lower than the rest of the steels, which had corrosion rates above 3 μm/year during most of the test period. Table 3.17 shows the average corrosion rates at day 100. T steel had the lowest average corrosion rate, 2.77 μm/year, while N steel had an average corrosion rate of 3.33 μm/year. The other three steels had higher average corrosion rates (5.03, 3.96, and 5.63 μm/year) than N and T steel.

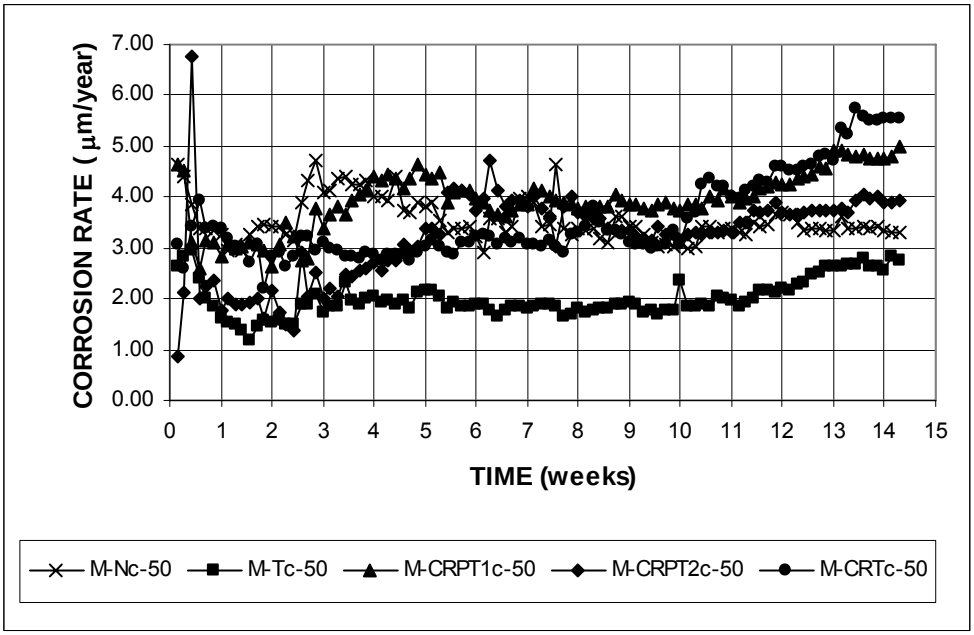


**Figure 3.42 –** Average corrosion rates as measured in the rapid macrocell test for lollipop specimens with conventional and microalloyed steel bars with epoxy-filled caps on the ends in 1.6 m ion NaCl and simulated concrete pore solution.

**Table 3.17 –** Average corrosion rates (in μm/year) at day 100 as measured in the rapid macrocell test for lollipop specimens with conventional and microalloyed steel bars with epoxy-filled caps on the ends, in a 1.6 m ion NaCl and simulated concrete pore solution.

| Specimen designation* | Steel type | Specimen | | | | Average | Standard deviation |
|---|---|---|---|---|---|---|---|
| | | 1 | 2 | 3 | 4 | | |
| **"Lollipop" specimens with caps in 1.6 m ion NaCl** | | | | | | | |
| **M-Nc-50** | **N** | 3.47 | 3.80 | 0.63 | 5.43 | 3.33 | 2.00 |
| **M-Tc-50** | **T** | 3.72 | 3.41 | 2.94 | 1.00 | 2.77 | 1.22 |
| **M-CPRT1c-50** | **CRPT1** | 4.37 | 7.66 | 5.04 | 3.05 | 5.03 | 1.94 |
| **M-CRPT2c-50** | **CRPT2** | 5.66 | 2.66 | 4.02 | 3.49 | 3.96 | 1.27 |
| **M-CRTc-50** | **CRT** | 4.46 | 4.79 | 3.84 | 9.41 | 5.63 | 2.55 |

* M - A - B

**M**: macrocell test

**A**: steel type → N: conventional, normalized steel, T: Thermex-treated conventional steel, CRPT1: Thermex-treated microalloyed steel with a high phosphorus content (0.117%), CRPT2: Thermex-treated microalloyed steel with a high phosphorus content (0.100%), CRT: Thermex treated microalloyed steel with normal phosphorus content (0.017%), c: epoxy-filled cap on the end of the bar.

**B**: mix design → 50: water-cement ratio of 0.50 and no inhibitor.

Figure 3.43 shows the average total corrosion losses during the test period. The average corrosion losses summarized in Table 3.18 show that, after 100 days, N steel had a corrosion loss of 0.97 μm and T steel had a corrosion loss of 0.55 μm. The microalloyed steels had corrosion losses of 1.08, 0.88, and 0.98 μm for CRPT1, CRPT2, and CRT, respectively. Results for the Student's t-test are presented in Table C.6 and show no significant difference in the average corrosion losses between N steel and the remaining steels.

The average corrosion rates versus time for lollipop specimens without epoxy-filled caps on the ends of the bars are presented in Figure 3.44. N steel had a lower corrosion rate than the rest of the steels throughout the test period. The average corrosion rates at day 100 are presented in Table 3.18. Conventional steel, N, had the lowest average corrosion rate at 2.25 μm/year. The rest of the steel had corrosion rates ranging from 3.03 to 3.44 μm/year.

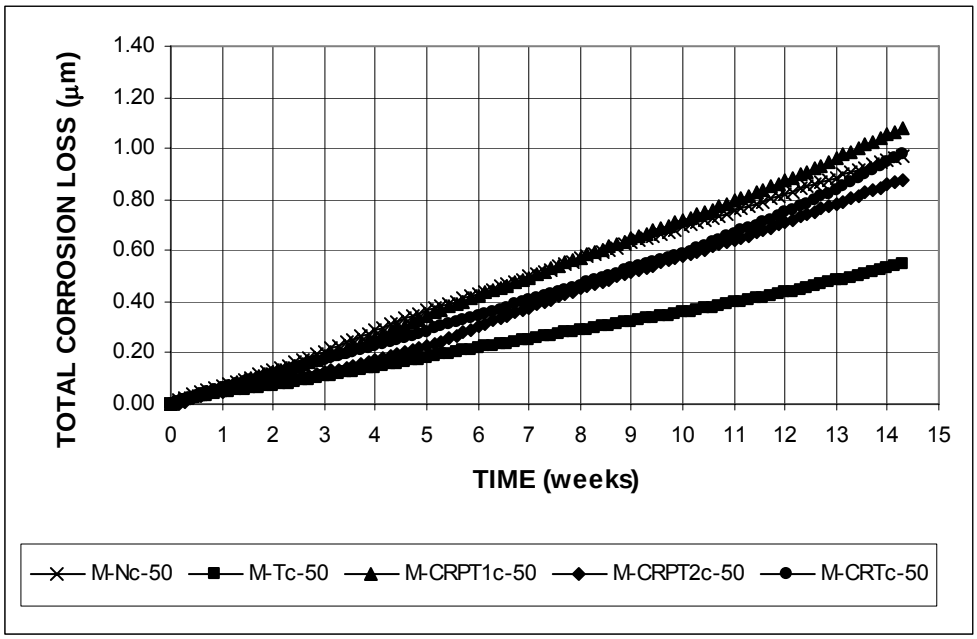


**Figure 3.43 –** Average total corrosion losses as measured in the rapid macrocell test for lollipop specimens with conventional and microalloyed steel bars with epoxy-filled caps on the end, in 1.6 m ion NaCl and simulated concrete pore solution.

**Table 3.18 –** Average total corrosion losses (in µm) at day 100 as measured in the rapid macrocell test of lollipop specimens with conventional and microalloyed steel bars with epoxy-filled caps on the ends, in a 1.6 m ion NaCl and simulated concrete pore solution.

| Specimen designation* | Steel type | Specimen | | | | Average | Standard deviation |
|---|---|---|---|---|---|---|---|
| | | 1 | 2 | 3 | 4 | | |
| **"Lollipop" specimens with caps in 1.6 m ion NaCl** | | | | | | | |
| **M-Nc-50** | **N** | 0.95 | 1.48 | 0.23 | 1.24 | 0.97 | 0.54 |
| **M-Tc-50** | **T** | 0.79 | 0.44 | 0.86 | 0.11 | 0.55 | 0.35 |
| **M-CPRT1c-50** | **CRPT1** | 0.92 | 1.52 | 1.06 | 0.84 | 1.08 | 0.30 |
| **M-CRPT2c-50** | **CRPT2** | 1.27 | 0.59 | 0.96 | 0.71 | 0.88 | 0.30 |
| **M-CRTc-50** | **CRT** | 1.14 | 0.97 | 0.54 | 1.28 | 0.98 | 0.32 |

* M - A - B

**M**: macrocell test

**A**: steel type → N: conventional, normalized steel, T: Thermex-treated conventional steel, CRPT1: Thermex-treated microalloyed steel with a high phosphorus content (0.117%), CRPT2: Thermex-treated microalloyed steel with a high phosphorus content (0.100%), CRT: Thermex treated microalloyed steel with normal phosphorus content (0.017%), c: epoxy-filled cap on the end of the bar.

**B**: mix design → 50: water-cement ratio of 0.50 and no inhibitor.

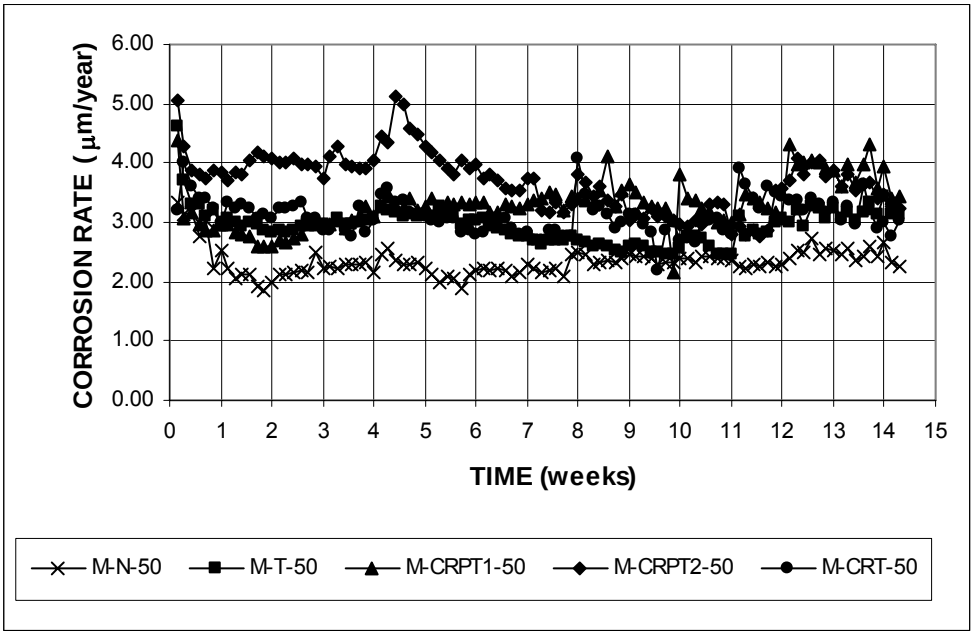


**Figure 3.44 –** Average corrosion rates as measured in the rapid macrocell test for lollipop specimens with conventional and microalloyed steel without epoxy-filled caps on the ends in 1.6 m ion NaCl and simulated concrete pore solution.

**Table 3.19 –** Average corrosion rates (in μm/year) at day 100 as measured in the rapid macrocell test for lollipop specimens with conventional and microalloyed steel bars without epoxy-filled caps on the ends in a 1.6 m ion NaCl and simulated concrete pore solution.

| Specimen designation* | Steel type | Specimen | | | | | Average | Standard deviation |
|---|---|---|---|---|---|---|---|---|
| | | 1 | 2 | 3 | 4 | 5 | | |
| **"Lollipop" specimens without caps in 1.6 m ion NaCl** | | | | | | | | |
| **M-N-50** | **N** | 3.59 | 2.49 | 2.27 | 0.67 | 2.21 | 2.25 | 1.04 |
| **M-T-50** | **T** | 4.65 | 3.41 | 2.81 | 3.85 | 1.03 | 3.15 | 1.36 |
| **M-CPRT1-50** | **CRPT1** | 6.56 | 3.21 | 2.86 | 0.35 | 4.21 | 3.44 | 2.25 |
| **M-CRPT2-50** | **CRPT2** | 3.68 | 2.76 | 4.95 | 3.81 | 0.93 | 3.23 | 1.50 |
| **M-CRT-50** | **CRT** | 3.49 | 4.73 | 3.61 | 0.64 | 2.66 | 3.03 | 1.52 |

* M - A - B

**M**: macrocell test

**A**: steel type → N: conventional, normalized steel, T: Thermex-treated conventional steel, CRPT1: Thermex-treated microalloyed steel with a high phosphorus content (0.117%), CRPT2: Thermex-treated microalloyed steel with a high phosphorus content (0.100%), CRT: Thermex treated microalloyed steel with normal phosphorus content (0.017%).

**B**: mix design → 50: water-cement ratio of 0.50 and no inhibitor.

The average total corrosion losses during the test period are shown in Figure 3.45, and the total corrosion losses at day 100 are summarized in Table 3.20 for the specimens without epoxy-filled caps on the ends. After 100 days, N and T steel had corrosion losses of 0.64 and 0.81 μm, respectively. The three microalloyed steels had corrosion losses of 0.90, 1.01, and 0.85 μm. None of the differences in the corrosion losses is statistically significant (Table C.6).

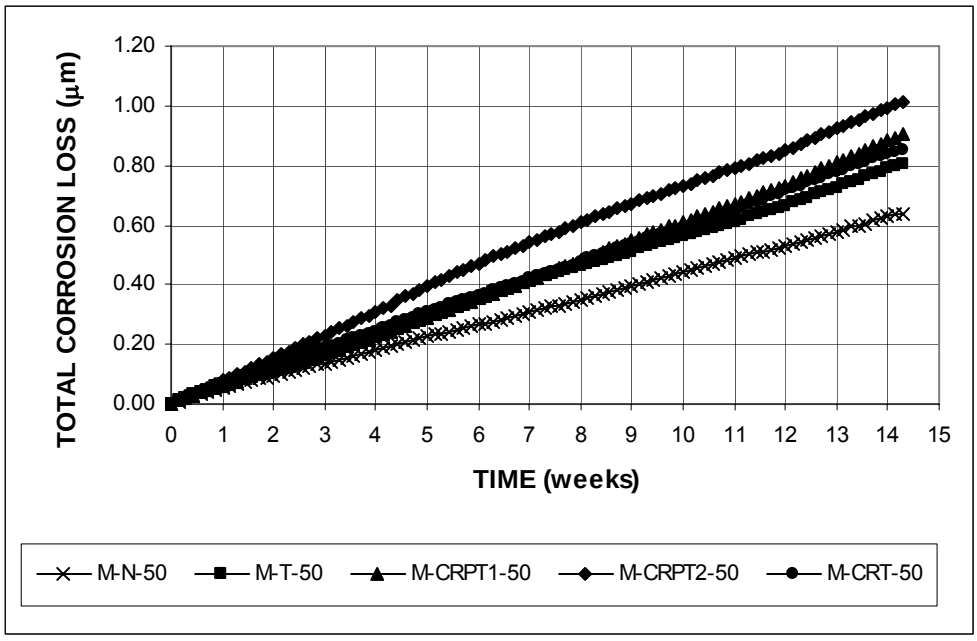


**Figure 3.45 –** Average total corrosion losses as measured in the rapid macrocell test for lollipop specimens with conventional and microalloyed steel bars without epoxy-filled caps on the ends, in 1.6 m ion NaCl and simulated concrete pore solution.

**Table 3.20 –** Average total corrosion losses (in μm) at day 100 as measured in the rapid macrocell test for lollipop specimens with conventional and microalloyed steel bars without epoxy-filled caps on the ends in a 1.6 m ion NaCl and simulated concrete pore solution.

| Specimen designation* | Steel type | Specimen | | | | | Average | Standard deviation |
|---|---|---|---|---|---|---|---|---|
| | | 1 | 2 | 3 | 4 | 5 | | |
| "Lollipop" specimens without caps in 1.6 m ion NaCl | | | | | | | | |
| M-N-50 | N | 1.05 | 0.72 | 0.53 | 0.40 | 0.51 | 0.64 | 0.25 |
| M-T-50 | T | 1.23 | 0.80 | 0.79 | 1.06 | 0.16 | 0.81 | 0.41 |
| M-CPRT1-50 | CRPT1 | 1.58 | 1.03 | 0.18 | 0.53 | 1.19 | 0.90 | 0.55 |
| M-CRPT2-50 | CRPT2 | 1.03 | 0.57 | 1.54 | 1.44 | 0.45 | 1.01 | 0.49 |
| M-CRT-50 | CRT | 1.02 | 1.19 | 1.20 | 0.06 | 0.80 | 0.85 | 0.47 |

* M - A - B
**M**: macrocell test
**A**: steel type → N: conventional, normalized steel, T: Thermex-treated conventional steel, CRPT1: Thermex-treated microalloyed steel with a high phosphorus content (0.117%), CRPT2: Thermex-treated microalloyed steel with a high phosphorus content (0.100%), CRT: Thermex treated microalloyed steel with normal phosphorus content (0.017%).
**B**: mix design → 50: water-cement ratio of 0.50 and no inhibitor.

### 3.4.2 Bench-Scale Tests

Southern Exposure, cracked beam, and ASTM G 109 tests were used to evaluate the microalloyed steels and the accompanying conventional steel. The concrete had a water-cement ratio of 0.45 and no inhibitor. Six specimens were used for each test for each of the five steels. As mentioned before, specimens containing both conventional and CRPT1 steel were also evaluated.

#### 3.4.2.1 Southern Exposure Test

The average corrosion rates as a function of time are presented in Figure 3.46 for the Southern Exposure tests. The corrosion rates increased with time at a similar manner for all steels during the first 30 weeks. T steel showed greatly increased corrosion rates starting at week 70. The average corrosion rates at week 70 are summarized in Table 3.21 and the results of the Student's t-test are shown in Table C.5. N steel had the lowest average corrosion rate, 4.07 μm/year, while T steel had

the highest average corrosion rate, 9.76 μm/year. CRPT1, CRPT2, and CRT had average corrosion rates of 4.14, 6.43, and 4.14 μm/year, respectively. The specimens with both N and CRPT1 steel showed corrosion rates of 4.96 and 6.65 μm/year, with the lower value for specimens with N steel on the top mat of steel.

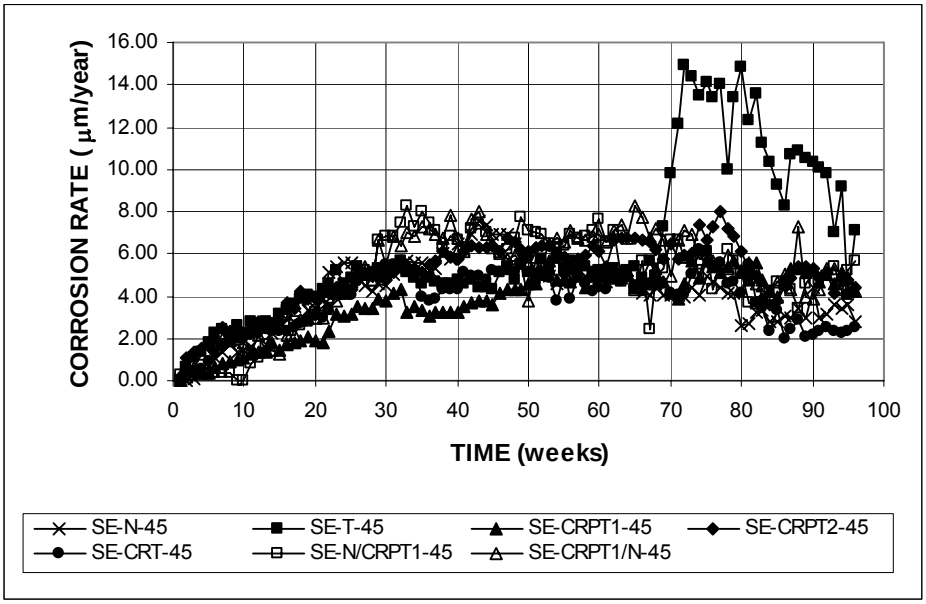


**Figure 3.46 –** Average corrosion rates as measured in the Southern Exposure test for specimens with conventional and microalloyed steel

**Table 3.21 –** Average corrosion rates (in μm/year) at week 70 as measured in the Southern Exposure test for specimens with conventional and microalloyed steel.

| Specimen designation* | Steel type | Specimen | | | | | | Average | Standard deviation |
|---|---|---|---|---|---|---|---|---|---|
| | | 1 | 2 | 3 | 4 | 5 | 6 | | |
| **Southern Exposure test** | | | | | | | | | |
| **SE-N-45** | **N** | 8.41 | 0.73 | 3.41 | 2.33 | 3.80 | 5.76 | 4.07 | 2.70 |
| **SE-T-45** | **T** | 10.70 | 2.44 | 4.98 | 32.63 | 1.30 | 6.51 | 9.76 | 11.68 |
| **SE-CRPT1-45** | **CRPT1** | 4.36 | 1.30 | 10.06 | 6.94 | 0.05 | 2.13 | 4.14 | 3.79 |
| **SE-CRPT2-45** | **CRPT2** | 7.56 | 4.90 | 13.28 | 7.20 | 3.41 | 2.25 | 6.43 | 3.94 |
| **SE-CRT-45** | **CRT** | 3.78 | 6.96 | 6.70 | 1.46 | 5.03 | 0.91 | 4.14 | 2.57 |
| **SE-N/CRPT1-45** | **N/CRPT1** | 3.75 | 9.58 | 9.54 | 4.39 | 6.47 | 6.18 | 6.65 | 2.48 |
| **SE-CRPT1/N/45** | **CRPT1/N** | 9.58 | 0.21 | 5.06 | 4.56 | 3.71 | 6.61 | 4.96 | 3.11 |

* SE - A - B

**SE**: Southern Exposure test

**A**: steel type → N: conventional, normalized steel, T: Thermex-treated conventional steel, CRPT1: Thermex-treated microalloyed steel with a high phosphorus content (0.117%), CRPT2: Thermex-treated microalloyed steel with a high phosphorus content (0.100%), CRT: Thermex treated microalloyed steel with normal phosphorus content (0.017%), N/CRPT1: N steel in the top mat and CRPT1 steel in the bottom mat, CRPT1/N: CRPT1 steel in the top mat and N steel in the bottom mat.

**B**: mix design → 45: water-cement ratio of 0.45 and no inhibitor.

Figure 3.47 shows the average total corrosion losses throughout the test period, and Table 3.22 summarizes the total corrosion losses at week 70. CRPT1 and CRT steel had the lowest corrosion losses at 4.34 and 5.18 μm, respectively. These values correspond to 75% and 90%, respectively, of the corrosion loss of N steel, which had a loss of 5.78 μm. The difference in the average corrosion rates of N and CRT steel is not significant. CRPT2 has the highest corrosion loss, 6.50 μm, while T steel had a corrosion loss of 5.92 μm. As a result of the increased average corrosion rate exhibited by T steel after week 70, by the end of the test period T steel had the highest total corrosion loss, with values above 11.5 μm, while the remaining steels had losses below 10 μm. None of the differences in the corrosion losses is statistically significant (Table C.6).

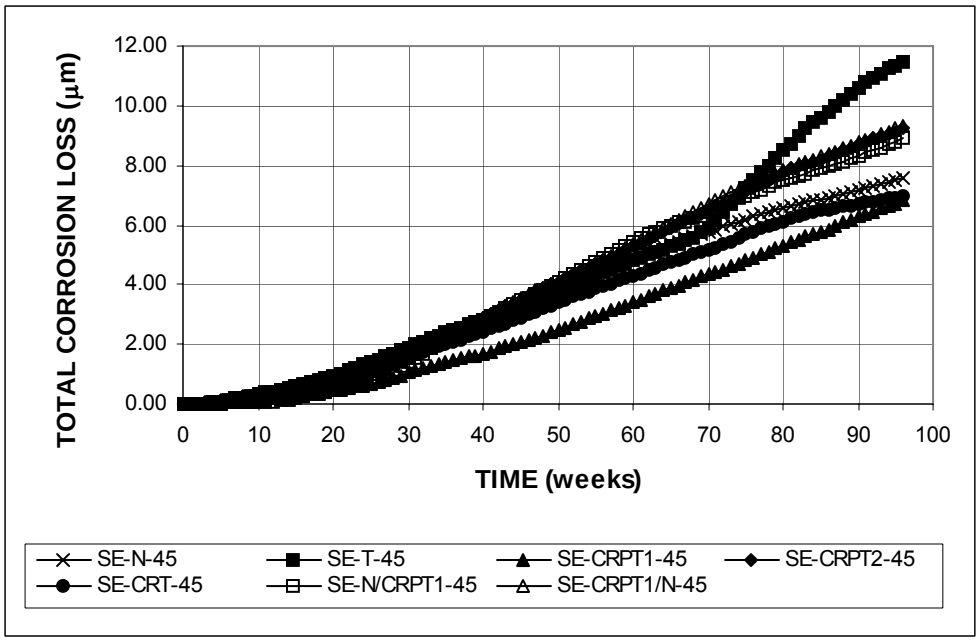


**Figure 3.47 –** Average total corrosion losses as measured in the Southern Exposure test for specimens with conventional and microalloyed steel.

**Table 3.22 –** Average total corrosion losses (in μm) at week 70 as measured in the Southern Exposure test for specimens with conventional and microalloyed steel.

| Specimen designation* | Steel type | Specimen | | | | | | Average | Standard deviation |
|---|---|---|---|---|---|---|---|---|---|
| | | 1 | 2 | 3 | 4 | 5 | 6 | | |
| **Southern Exposure test** | | | | | | | | | |
| **SE-N-45** | **N** | 7.13 | 8.89 | 6.90 | 3.02 | 4.19 | 4.56 | 5.78 | 2.21 |
| **SE-T-45** | **T** | 11.50 | 4.92 | 5.35 | 5.15 | 0.93 | 7.66 | 5.92 | 3.49 |
| **SE-CRPT1-45** | **CRPT1** | 3.96 | 3.15 | 7.95 | 7.90 | 1.43 | 1.64 | 4.34 | 2.94 |
| **SE-CRPT2-45** | **CRPT2** | 8.22 | 4.56 | 13.06 | 6.95 | 4.79 | 1.40 | 6.50 | 3.97 |
| **SE-CRT-45** | **CRT** | 8.31 | 7.45 | 7.68 | 1.39 | 5.09 | 1.14 | 5.18 | 3.22 |
| **SE-N/CRPT1-45** | **N/CRPT1** | 6.00 | 3.92 | 4.72 | 7.62 | 7.95 | 8.45 | 6.44 | 1.85 |
| **SE-CRPT1/N/45** | **CRPT1/N** | 6.05 | 6.00 | 2.84 | 4.46 | 9.14 | 11.58 | 6.68 | 3.18 |

* SE - A - B

**SE**: Southern Exposure test

**A**: steel type → N: conventional, normalized steel, T: Thermex-treated conventional steel, CRPT1: Thermex-treated microalloyed steel with a high phosphorus content (0.117%), CRPT2: Thermex-treated microalloyed steel with a high phosphorus content (0.100%), CRT: Thermex treated microalloyed steel with normal phosphorus content (0.017%), N/CRPT1: N steel in the top mat and CRPT1 steel in the bottom mat, CRPT1/N: CRPT1 steel in the top mat and N steel in the bottom mat.

**B**: mix design → 45: water-cement ratio of 0.45 and no inhibitor.

Figure 3.48 shows the average corrosion potentials of the top and bottom mats of steel with respect to a copper-copper sulfate electrode. After 25 weeks, all of the specimens had an average corrosion potential of the top mat that was more negative than -0.350 V, which indicates active corrosion. At week 70, the average corrosion potentials of the top mat were more negative than -0.475 V for all specimens. The average corrosion potentials of the bottom mat were between -0.200 and -0.400 V during the test period. For the more negative potentials, there is a high probability that corrosion is occurring. For specimens with N steel, there is a big drop in potential of the bottom mat at week 79, which indicates that chlorides had reached the bottom mat.

Figure 3.49 shows the average mat-to-mat resistances for the Southern Exposure specimens. At week 1, values are approximately 150 ohms for all specimens and there is little scatter during the first 30 weeks. By week 70, the results show large scatter between the different specimens and the values range from 500 ohms for SE-CRPT1/N-45 to 1800 ohms for SE-CRPT1-45.

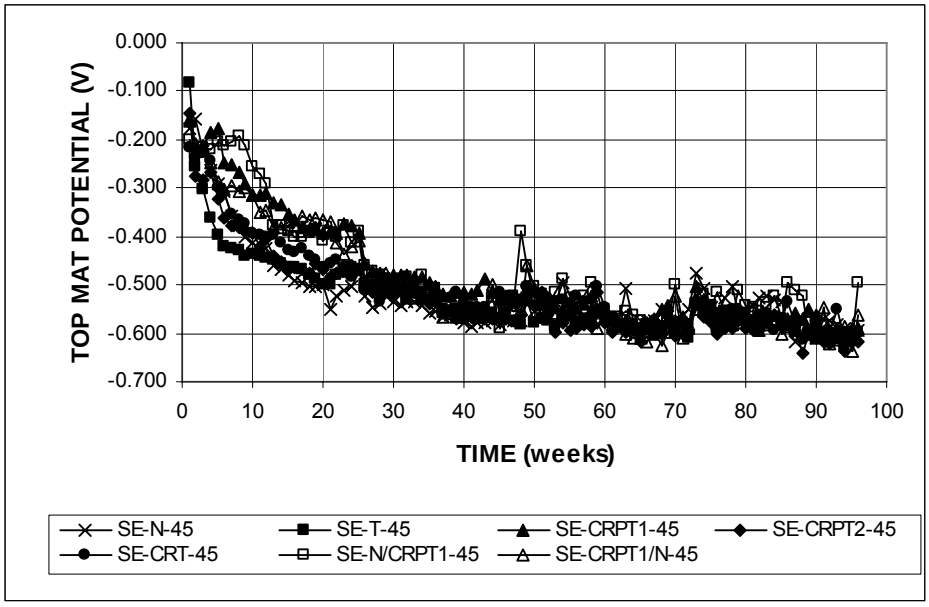


(a)

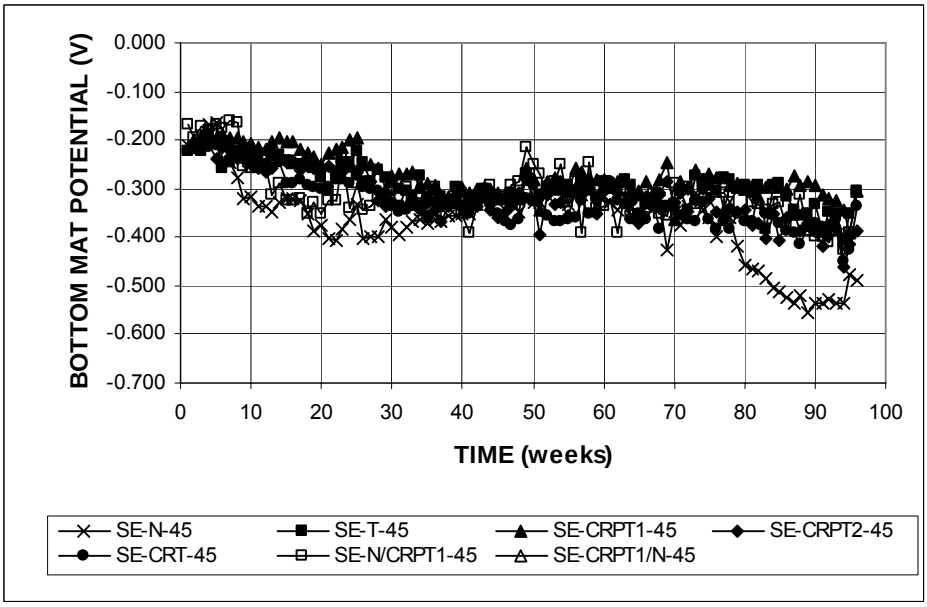


(b)

**Figure 3.48 –** (a) Average top mat corrosion potentials and (b) bottom mat corrosion potentials with respect to copper-copper sulfate electrode as measured in the Southern Exposure test for specimens with conventional and microalloyed steel.

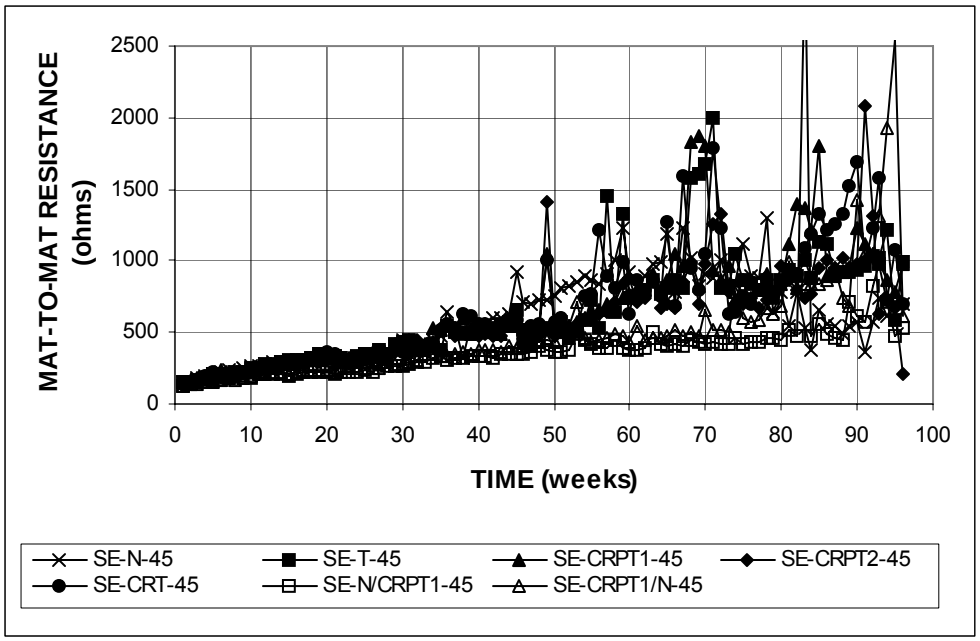


**Figure 3.49 –** Average mat-to-mat resistances as measured in the Southern Exposure test for specimens with conventional and microalloyed steel.

### 3.4.2.2 Cracked Beam Test

The average corrosion rates versus time for the cracked beam specimens with microalloyed steel are presented in Figure 3.50. The corrosion rates during the first 10 weeks remained above 8 μm/year for all steels. The corrosion rates dropped with time, and by week 30, all steels had corrosion rates below 6 μm/year. Table 3.23 shows the average corrosion rates at week 70 and Table C.5 shows the results of the Student's t-test. N steel had the highest corrosion rate at 7.34 μm/year, followed by T steel at 5.07 μm/year. CRPT2 and CRT had the lowest average corrosion rates, 4.08 μm/year, corresponding to 56% of the rate for N steel. The difference in the average corrosion rates between N steel and any of the other steels is not statistically significant.

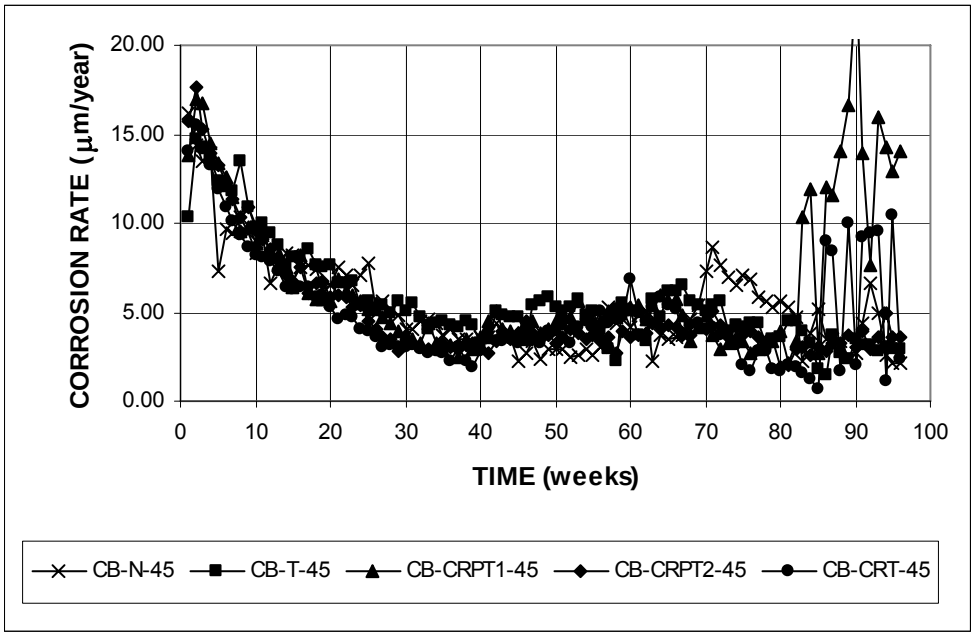


**Figure 3.50 –** Average corrosion rates as measured in the cracked beam test for specimens with conventional and microalloyed steel.

**Table 3.23 –** Average corrosion rates (in μm/year) for weeks at week 70 as measured in the cracked beam test for specimens with conventional and microalloyed steel.

| Specimen designation* | Steel type | Specimen | | | | | | Average | Standard deviation |
|---|---|---|---|---|---|---|---|---|---|
| | | 1 | 2 | 3 | 4 | 5 | 6 | | |
| **Cracked beam test** | | | | | | | | | |
| **CB-N-45** | **N** | 9.55 | 4.55 | 2.22 | 3.92 | 17.61 | 6.22 | 7.34 | 5.61 |
| **CB-T-45** | **T** | 9.43 | 3.14 | 2.27 | 9.85 | 4.16 | 1.57 | 5.07 | 3.65 |
| **CB-CRPT1-45** | **CRPT1** | 2.41 | 1.50 | 1.00 | 6.88 | 12.27 | 4.93 | 4.83 | 4.27 |
| **CB-CRPT2-45** | **CRPT2** | 1.54 | 1.64 | 0.56 | 9.61 | 1.76 | 9.39 | 4.08 | 4.22 |
| **CB-CRT-45** | **CRT** | 1.01 | 4.69 | 1.46 | 6.44 | 6.48 | 4.39 | 4.08 | 2.37 |

* CB - A - B

**CB**: cracked beam test

**A**: steel type → N: conventional, normalized steel, T: Thermex-treated conventional steel, CRPT1: Thermex-treated microalloyed steel with a high phosphorus content (0.117%), CRPT2: Thermex-treated microalloyed steel with a high phosphorus content (0.100%), CRT: Thermex treated microalloyed steel with normal phosphorus content (0.017%).

**B**: mix design → 45: water-cement ratio of 0.45 and no inhibitor.

Figure 3.51 shows the average total corrosion losses throughout the test period. Table 3.24 summarizes the average total corrosion losses at week 70 and Table C.6 shows the results of the Student's t-test. After 70 weeks, N and T steels had average total corrosion losses of 7.51 and 8.72 μm, respectively, while CRPT1 and CRPT2 had losses of 8.17 and 7.50 μm, respectively. CRT has the lowest corrosion loss, 7.24 μm, equal to 96% of the corrosion loss for N steel. The difference in the average corrosion loss of N and CRT steel is not statistically significant.

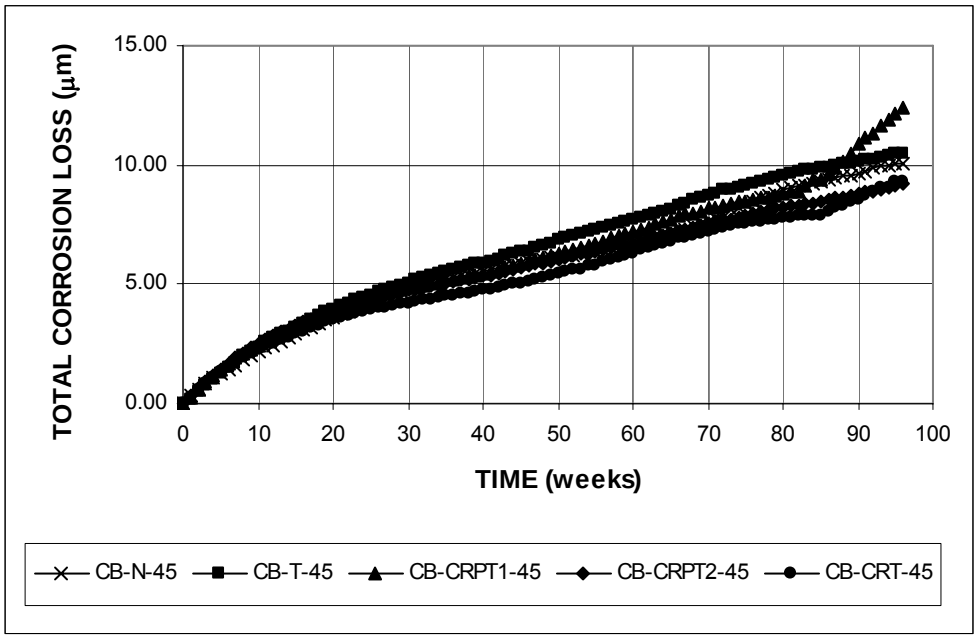


**Figure 3.51 –** Average total corrosion losses as measured in the cracked beam test for specimens with conventional and microalloyed steel.

**Table 3.24 –** Average total corrosion losses (in μm) at week 70 as measured in the cracked beam test for specimens with conventional and microalloyed steel.

| Specimen designation* | Steel type | Specimen | | | | | | Average | Standard deviation |
|---|---|---|---|---|---|---|---|---|---|
| | | 1 | 2 | 3 | 4 | 5 | 6 | | |
| **Cracked beam test** | | | | | | | | | |
| **CB-N-45** | **N** | 10.36 | 7.75 | 4.98 | 8.57 | 7.61 | 5.78 | 7.51 | 1.93 |
| **CB-T-45** | **T** | 9.59 | 7.42 | 8.86 | 10.96 | 10.48 | 4.99 | 8.72 | 2.21 |
| **CB-CRPT1-45** | **CRPT1** | 9.08 | 5.80 | 5.17 | 12.34 | 9.67 | 6.97 | 8.17 | 2.70 |
| **CB-CRPT2-45** | **CRPT2** | 7.20 | 5.96 | 4.14 | 13.04 | 5.79 | 8.88 | 7.50 | 3.14 |
| **CB-CRT-45** | **CRT** | 7.66 | 8.72 | 8.17 | 7.50 | 7.24 | 7.47 | 7.79 | 0.55 |

* CB - A - B
**CB**: cracked beam test
**A**: steel type → N: conventional, normalized steel, T: Thermex-treated conventional steel, CRPT1: Thermex-treated microalloyed steel with a high phosphorus content (0.117%), CRPT2: Thermex-treated microalloyed steel with a high phosphorus content (0.100%), CRT: Thermex treated microalloyed steel with normal phosphorus content (0.017%).
**B**: mix design → 45: water-cement ratio of 0.45 and no inhibitor.

The average corrosion potentials of the top and bottom mats of steel with respect to a copper-copper sulfate electrode are shown in Figure 3.52. The corrosion potentials of the top mat were more negative than -0.500 V for all specimens starting at week 1, indicating active corrosion. For the bottom mat, the corrosion potentials remained more positive than -0.350 V for the first 60 weeks for all but N steel. After 70 weeks, the corrosion potentials of the bottom mat ranged from -0.300 to -0.440 V, indicating that chlorides had reached that layer of steel, initiating corrosion.

Figure 3.53 shows the average mat-to-mat resistances for the cracked beam specimens. At week 1, values for all steels ranged from 250 to 325 ohms. Conventional, normalized steel, N, showed a drop in mat-to-mat resistance after week 60 due to cracking of the specimen. At week 70, N steel had the lowest mat-to-mat resistance with 1400 ohms. The remaining specimens had mat-to-mat resistances between 2000 and 2500 ohms.

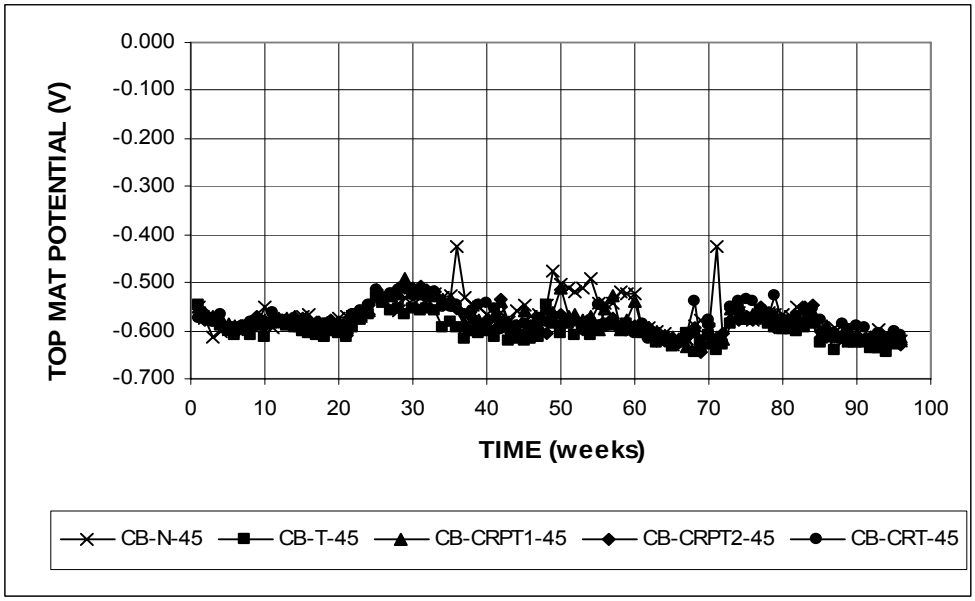


(a)

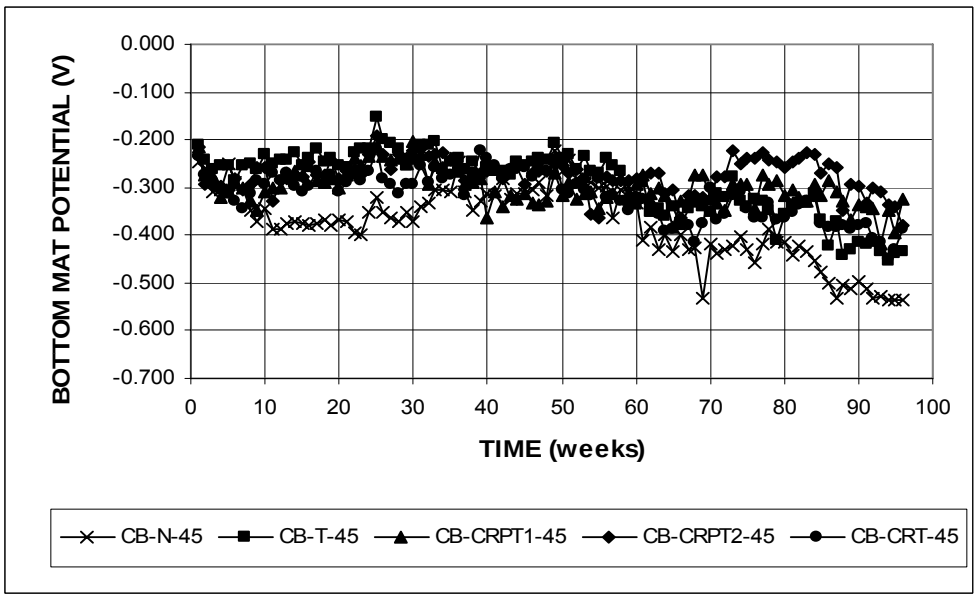


(b)

**Figure 3.52 –** (a) Average top mat corrosion potentials and (b) average bottom mat corrosion potentials with respect to copper-copper sulfate electrode as measured in the cracked beam test for specimens with conventional and microalloyed steel.

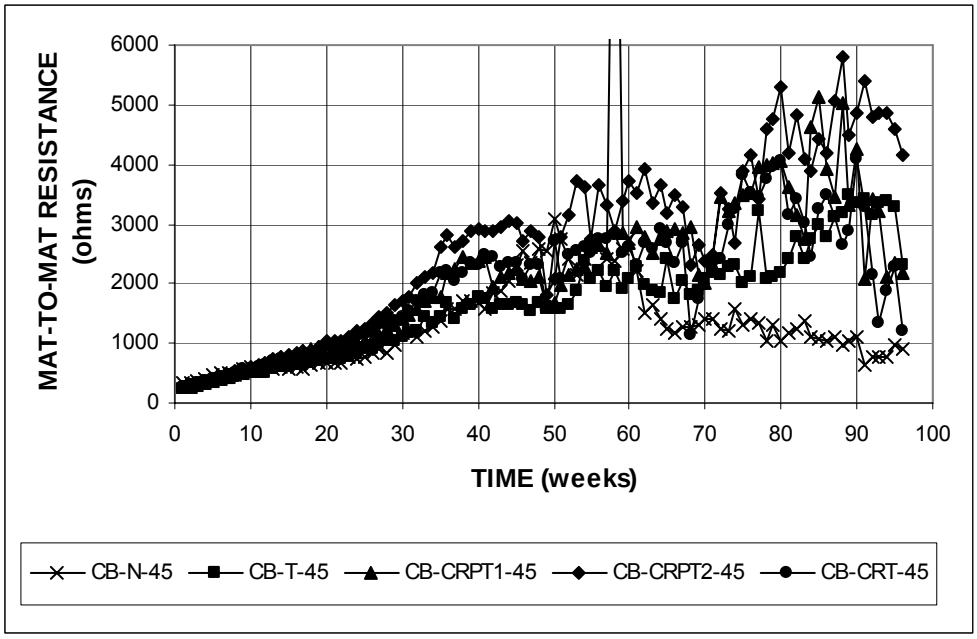


**Figure 3.53 –** Average mat-to-mat resistances as measured in the cracked beam test for specimens with conventional and microalloyed steel.

### 3.4.2.3 ASTM G 109 Test

Figure 3.54 shows the average corrosion rates versus time for microalloyed steels in the ASTM G 109 test. The corrosion rates remained close to zero for the first 15 weeks for all steels. N steel is the first to show an increase in the corrosion rate, at week 18, followed by T and CRPT2 steels at week 22, and CRPT1 steel at week 30. CRT started corroding last, at week 35, which might indicate a higher corrosion threshold. The average corrosion rates at week 70 are summarized in Table 3.25 and the results of the Student's t-test are shown in Table C.5. Corrosion rates obtained were 3.83 and 2.85 μm/year for N and T steel, respectively. CRT had a corrosion rate of 3.01 μm/year, equal to 79% of the corrosion rate of N steel, but higher than the corrosion rate for T steel. CRPT1 and CRPT2 steel had average

corrosion rates of 3.92 and 3.40 μm/year, respectively. The difference in the average corrosion rate between N and CRT steel is not statistically significant.

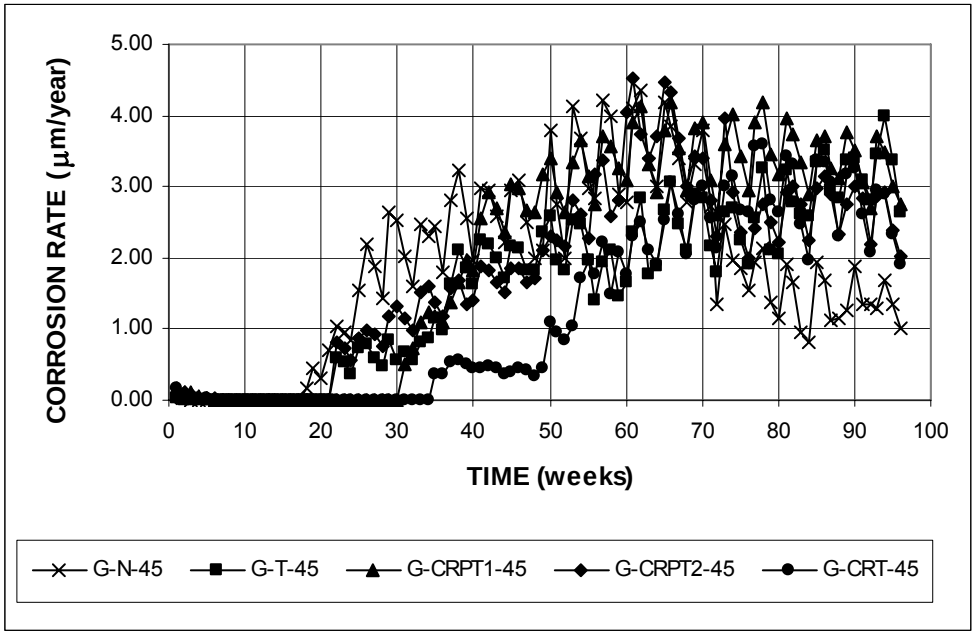


**Figure 3.54 –** Average corrosion rates as measured in the ASTM G 109 test for specimens with conventional and microalloyed steel.

**Table 3.25 –** Average corrosion rates (in μm/year) at week 70 as measured in the ASTM G 109 test for specimens with conventional and microalloyed steel.

| Specimen designation* | Steel type | Specimen | | | | | | Average | Standard deviation |
|---|---|---|---|---|---|---|---|---|---|
| | | 1 | 2 | 3 | 4 | 5 | 6 | | |
| **ASTM G 109 test** | | | | | | | | | |
| **G-N-45** | **N** | 3.37 | 0.99 | 1.21 | 0.00 | 9.64 | 7.61 | 3.80 | 3.94 |
| **G-T-45** | **T** | 0.00 | 0.00 | 2.13 | 8.30 | 4.59 | 2.07 | 2.85 | 3.16 |
| **G-CRPT1-45** | **CRPT1** | 1.48 | 1.91 | 0.00 | 10.72 | 4.51 | 4.88 | 3.92 | 3.82 |
| **G-CRPT2-45** | **CRPT2** | 1.92 | 2.70 | 2.68 | 11.15 | 1.98 | 0.00 | 3.40 | 3.92 |
| **G-CRT-45** | **CRT** | 2.08 | 1.96 | 0.50 | 6.90 | 2.43 | 4.17 | 3.01 | 2.24 |

* G - A - B

**G**: ASTM G-109 test

**A**: steel type → N: conventional, normalized steel, T: Thermex-treated conventional steel, CRPT1: Thermex-treated microalloyed steel with a high phosphorus content (0.117%), CRPT2: Thermex-treated microalloyed steel with a high phosphorus content (0.100%), CRT: Thermex treated microalloyed steel with normal phosphorus content (0.017%).

**B**: mix design → 45: water-cement ratio of 0.45 and no inhibitor.

The average total corrosion losses versus time are presented in Figure 3.55 and the values at week 70 are summarized in Table 3.26. The results of the Student's t-test are shown in Table C.6. At week 70, CRT had the lowest corrosion loss, with a value of 0.94 μm, equal to 36% of the corrosion loss of N steel (2.61 μm). The difference in the average corrosion losses between N and CRT steel is significant at $\alpha = 0.02$. CRPT1 and CRPT2 showed corrosion losses of 2.12 and 2.05 μm, equal to 81 and 79% of the corrosion loss for N steel, respectively. T steel had an average total corrosion loss of 1.60 μm/year, or 61% of the loss for N steel. The difference in the average corrosion losses between N and the remaining steels is not statistically significant.

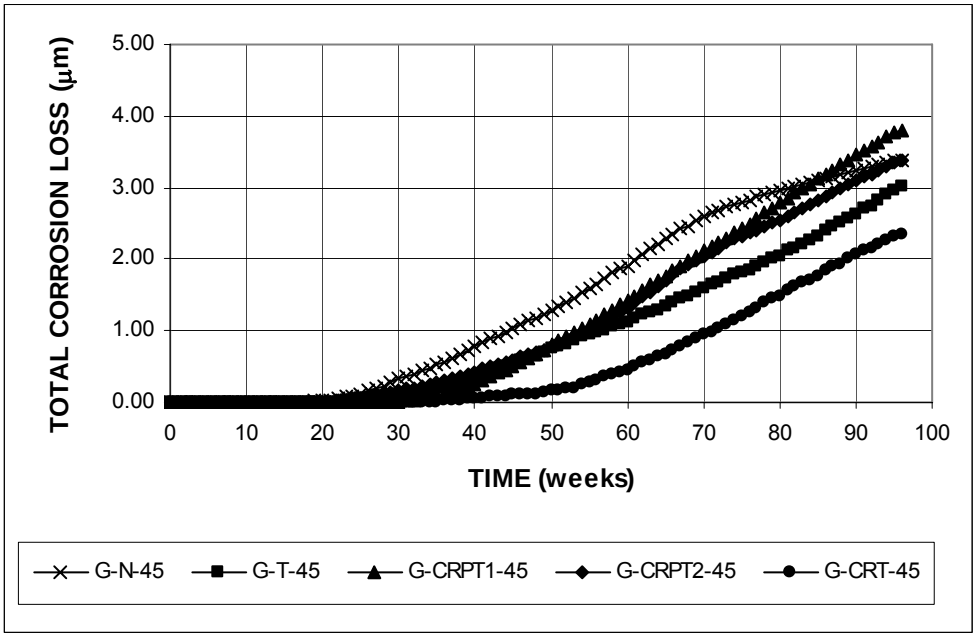


**Figure 3.55 –** Average total corrosion losses as measured in the ASTM G 109 test for specimens with conventional and microalloyed steel.

**Table 3.26 –** Average total corrosion losses (in μm) at week 70 as measured in the ASTM G 109 test for specimens with conventional and microalloyed steel.

| Specimen designation* | Steel type | Specimen | | | | | | Average | Standard deviation |
|---|---|---|---|---|---|---|---|---|---|
| | | 1 | 2 | 3 | 4 | 5 | 6 | | |
| **ASTM G 109 test** | | | | | | | | | |
| **G-N-45** | **N** | 2.92 | 1.45 | 1.03 | 3.05 | 4.19 | 3.01 | 2.61 | 1.17 |
| **G-T-45** | **T** | 0.01 | 0.00 | 0.34 | 6.71 | 0.69 | 1.84 | 1.60 | 2.60 |
| **G-CRPT1-45** | **CRPT1** | 0.38 | 0.34 | 0.01 | 6.82 | 2.07 | 3.08 | 2.12 | 2.59 |
| **G-CRPT2-45** | **CRPT2** | 0.46 | 0.51 | 0.94 | 8.95 | 1.38 | 0.04 | 2.05 | 3.41 |
| **G-CRT-45** | **CRT** | 0.65 | 0.21 | 0.01 | 1.77 | 1.85 | 1.14 | 0.94 | 0.78 |

* G - A - B

**G**: ASTM G-109 test

**A**: steel type → N: conventional, normalized steel, T: Thermex-treated conventional steel, CRPT1: Thermex-treated microalloyed steel with a high phosphorus content (0.117%), CRPT2: Thermex-treated microalloyed steel with a high phosphorus content (0.100%), CRT: Thermex treated microalloyed steel with normal phosphorus content (0.017%).

**B**: mix design → 45: water-cement ratio of 0.45 and no inhibitor.

The average corrosion potentials of the top and bottom mats of steel with respect to a copper-copper sulfate electrode are presented in Figure 3.56. Results show that during the first 19 weeks, all values were more positive than -0.200 V, indicating a passive condition. At week 21, the average corrosion potential of the top mat for N steel dropped to more negative values. The corrosion potentials of the other steels started dropping after week 35. The average corrosion potentials of the top mat at week 70 were more negative than -0.350 V for all steels, indicating a high probability that corrosion was occurring. For the bottom mat of steel, the corrosion potential for all steels, with the exception of N steel, remained more positive than -0.300 V through the test period, indicating a low probability for corrosion.

The average mat-to-mat resistances for the G 109 test are shown in Figure 3.57. Values ranged from 150 ohms, for N steel, to 220 ohms, for CRPT2 steel, at week 1. Values remain fairly close between the different steels throughout the test period, except for N steel, which shows an increase in the mat-to-mat resistance after week 75. At week 70, the mat-to-mat resistances ranged from 1100 to 1280 ohms.

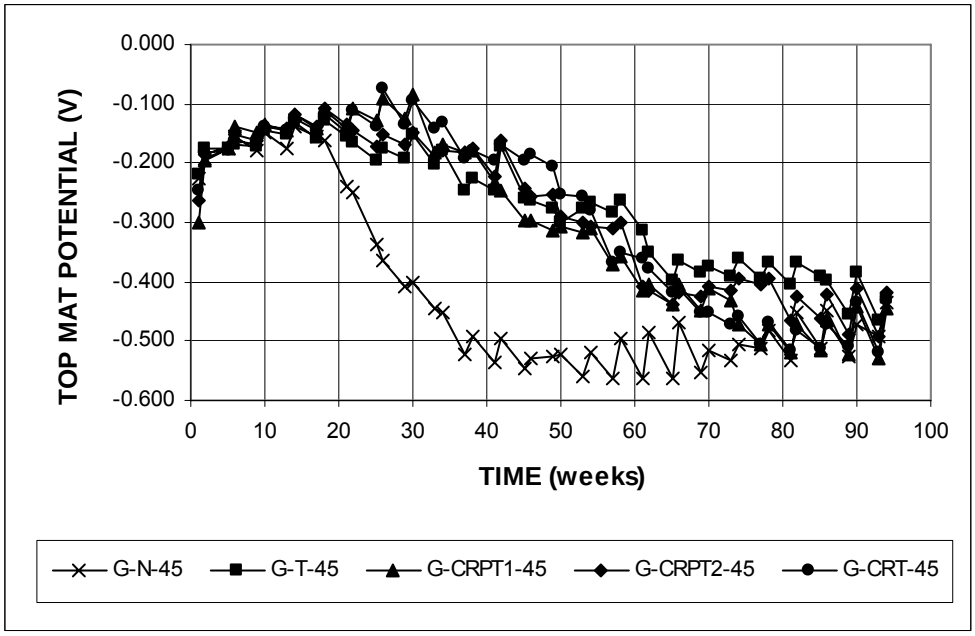


(a)

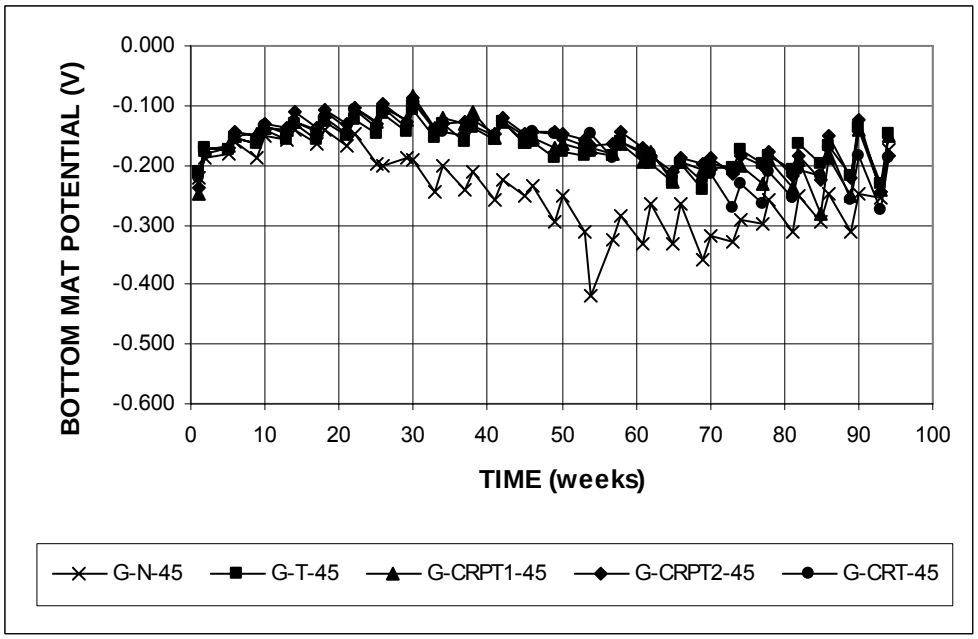


(b)

**Figure 3.56 –** (a) Average top mat corrosion potentials and (b) average bottom mat corrosion potentials with respect to copper-copper sulfate electrode as measured in the ASTM G 109 test. Specimens with conventional and microalloyed steel.

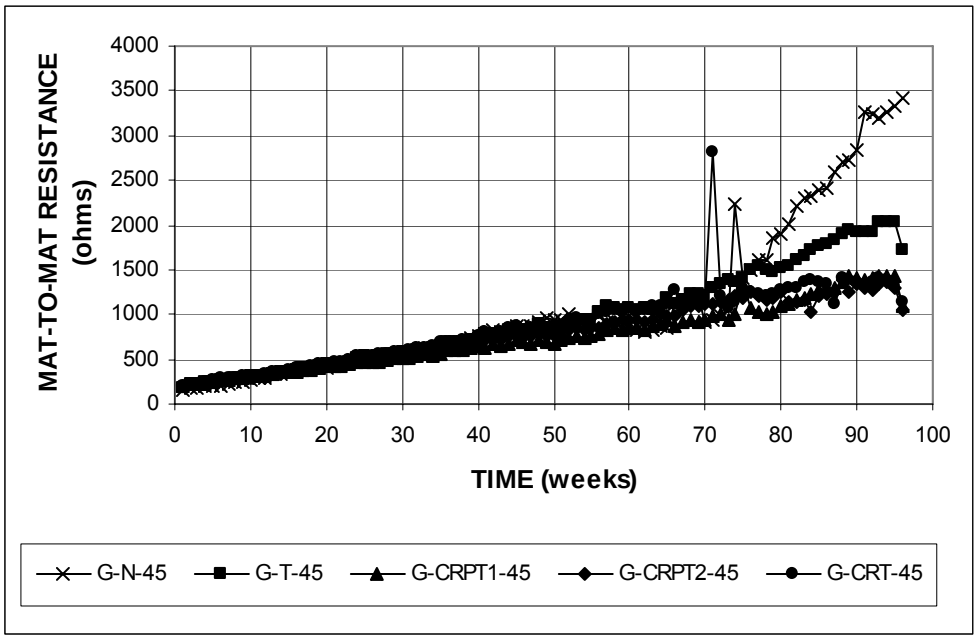


**Figure 3.57 –** Average mat-to-mat resistances as measured in the ASTM G 109 test for specimens with conventional and microalloyed steel.

## 3.5 MMFX MICROCOMPOSITE STEEL

This section describes the results of the macrocell and bench-scale tests for specimens containing MMFX microcomposite steel. Combinations of conventional and MMFX steel are also evaluated. Preliminary test results for MMFX microcomposite steel were reported previously by Darwin et al. (2002) and Gong et al. (2002). At the time of the latter report, the bench-scale tests were 40 weeks old. The present report covers the full 96-week test period.

### 3.5.1 Rapid Macrocell Test

Macrocell tests of MMFX microcomposite steel were performed on bare bars in 1.6 and 6.04 m ion NaCl and simulated concrete pore solution and on mortar-wrapped specimens in 1.6 m ion NaCl and simulated concrete pore solution. The mortar-wrapped specimens had a water-cement ratio of 0.50. In addition to testing

MMFX steel alone, the macrocell tests with mortar-wrapped specimens were also used to evaluate the effect of combining conventional steel with MMFX steel (M-N3/MMFX-50 and M-MMFX/N3-50).

#### 3.5.1.1 Bare Bars

Specimens labeled MMFX(1) were evaluated using the test configuration shown in Figure 2.1, where the lid was placed on the top of the container. Corrosion products were observed on some of these bars on surfaces that were not immersed in the solution. This corrosion was attributed to the high humidity inside the container. All other bare specimens were evaluated using the test configuration in Figure 2.3, where the edges of the lid were removed so that it could be placed inside of the container, just above the level of the solution. The Student's t-test (Table C.7 and C.8) was used to compare if the difference in the mean corrosion rates and losses between MMFX bars evaluated using the two different configurations, MMFX(1) and MMFX(2) was significant. The difference in the corrosion rates at week 15 was not significant, but the difference in the corrosion losses at week 15 was significant at $\alpha = 0.02$.

The average corrosion rates as a function of time are shown in Figure 3.58. Conventional steel (N3) had the highest corrosion rate during the test period. The No. 19 [No. 6] MMFX bars (MMFX#19) showed similar values to N3 steel after week 9. The average corrosion rates for MMFX(1) reached values of 30 μm/year at week 2, and decreased with time, reaching values below 15 μm/year at week 13. The remaining specimens [MMFX(2), MMFXb, and MMFXs] had average corrosion rates below 15 μm/year throughout the test period. The average corrosion rates at week 15 are summarized in Table 3.27 and results of the Student's t-test are shown in

Table C.7. Conventional steel, N3, had the highest average corrosion rate, 35.88 μm/year, followed by MMFX#19, 29.16 μm/year. The corrosion rates for the other MMFX bars ranged between 8.87 and 16.61 μm/year, corresponding to 25% and 46%, respectively, of the corrosion rate of conventional steel. The difference in the average corrosion rates between N3 and MMFX(2) samples is significant at $\alpha = 0.20$.

The average total corrosion losses versus time are presented in Figure 3.59 and the values at week 15 are summarized in Table 3.28. Results of the Student's t-test are presented in Table C.8. At week 15, the total corrosion loss for conventional steel was 9.03 μm, while the values for MMFX bars ranged from 1.74 μm for bent bars to 6 μm for No. 19 [No. 6] bars. The average corrosion loss for the 24 No. 16 [No. 5] MMFX straight bars was 3.13 μm, corresponding to 35% of the corrosion loss of conventional steel. The difference in the average corrosion losses between N3 and MMFX(2) samples is significant at $\alpha = 0.02$.

**Table 3.27 –** Average corrosion rates (in μm/year) at week 15 as measured in the rapid macrocell test with bare bars in 1.6 m ion NaCl and simulated concrete pore solution for specimens with conventional and MMFX microcomposite steel.

| Specimen designation* | Steel type | Specimen | | | | | | Average | Standard deviation |
|---|---|---|---|---|---|---|---|---|---|
| | | 1 | 2 | 3 | 4 | 5 | 6 | | |
| **Bare bars in 1.6 m NaCl** | | | | | | | | | |
| **M-N3** | **N3** | 52.60 | 0.26 | 67.77 | 40.17 | 32.43 | 22.08 | 35.88 | 23.61 |
| **M-MMFX(1)** | **MMFX** | 14.50 | 5.03 | 9.66 | 5.92 | 12.48 | 22.41 | 11.67 | 6.41 |
| **M-MMFX(2)** | **MMFX** | 11.74 | 8.71 | 22.83 | 12.68 | 21.29 | 22.42 | 16.61 | 6.26 |
| **M-MMFXs** | **MMFXs** | 6.31 | 20.13 | 13.86 | 21.87 | 10.77 | 4.58 | 12.92 | 7.08 |
| **M-MMFXb** | **MMFXb** | 8.09 | 16.38 | 6.44 | 6.48 | 8.54 | 7.26 | 8.87 | 3.78 |
| **M-MMFX#19** | **MMFX#19** | 35.42 | 27.66 | 31.59 | 19.24 | 34.61 | 26.44 | 29.16 | 6.05 |

* M - A
**M**: macrocell test
**A**: steel type → N3: conventional, normalized steel, MMFX: MMFX-2 microcomposite steel, s: sandblasted, b: bent bars at the anode.

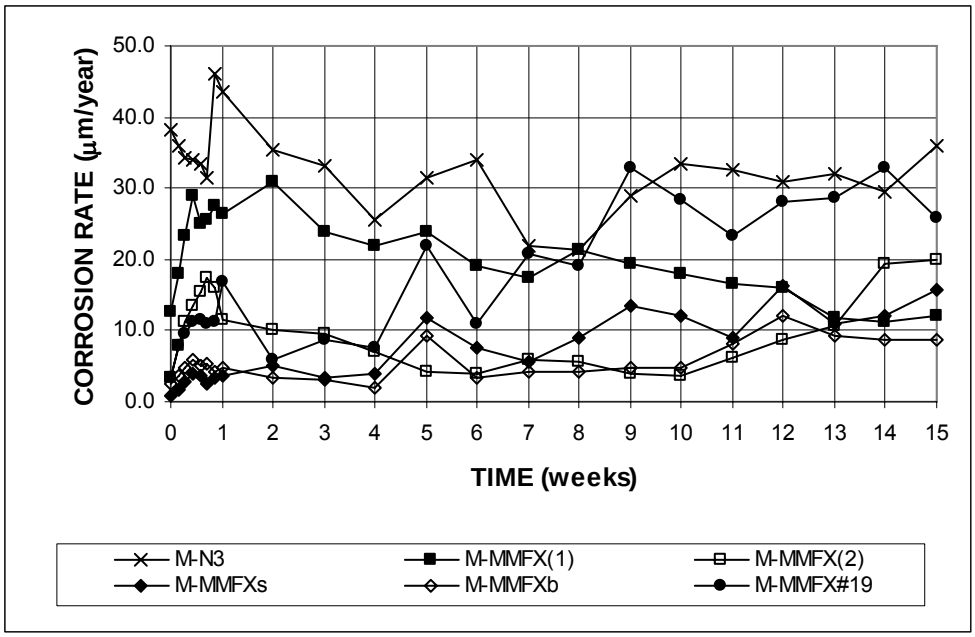


**Figure 3.58 –** Average corrosion rates as measured in the rapid macrocell test for bare bars in 1.6 m ion NaCl and simulated concrete pore solution for specimens with conventional and MMFX microcomposite steel.

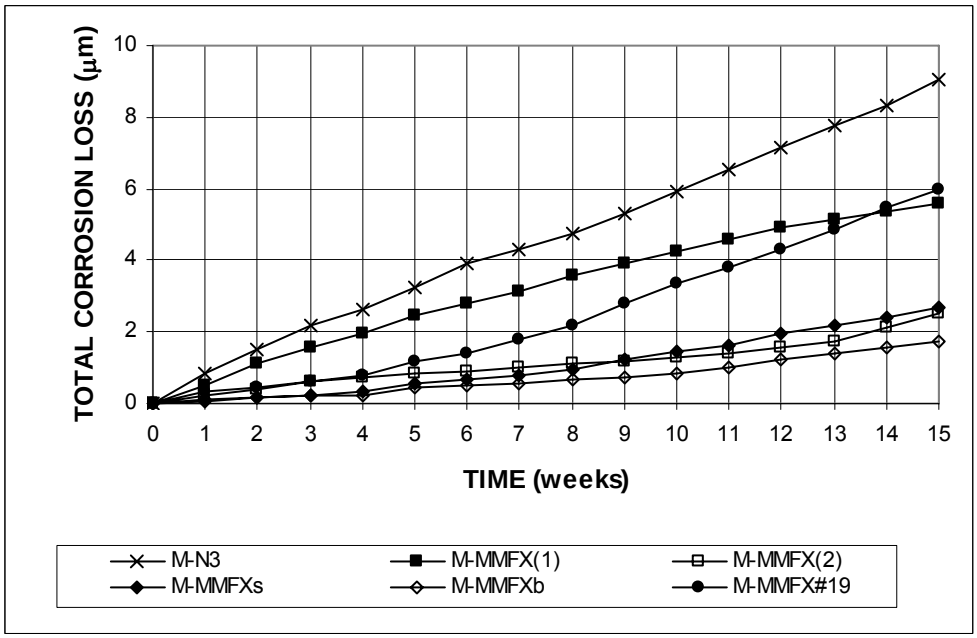


**Figure 3.59 –** Average total corrosion losses as measured in the rapid macrocell test for bare bars in 1.6 m ion NaCl and simulated concrete pore solution for specimens with conventional and MMFX microcomposite steel.

**Table 3.28 –** Average total corrosion losses (in μm) at week 15 as measured in the rapid macrocell test with bare bars in 1.6 m ion NaCl and simulated concrete pore solution for specimens with conventional and MMFX microcomposite steel.

| Specimen designation* | Steel type | Specimen | | | | | | Average | Standard deviation |
|---|---|---|---|---|---|---|---|---|---|
| | | 1 | 2 | 3 | 4 | 5 | 6 | | |
| **Bare bars in 1.6 m NaCl** | | | | | | | | | |
| **M-N3** | **N3** | 13.07 | 4.84 | 13.22 | 11.10 | 6.97 | 4.98 | 9.03 | 3.91 |
| **M-MMFX(1)** | **MMFX** | 7.26 | 4.78 | 6.20 | 4.90 | 3.64 | 6.66 | 5.57 | 1.36 |
| **M-MMFX(2)** | **MMFX** | 3.10 | 2.10 | 3.26 | 1.13 | 1.63 | 3.84 | 2.51 | 1.05 |
| **M-MMFXs** | **MMFXs** | 1.96 | 2.63 | 3.23 | 3.29 | 2.86 | 2.14 | 2.69 | 0.55 |
| **M-MMFXb** | **MMFXb** | 1.51 | 2.76 | 1.20 | 1.46 | 1.51 | 1.99 | 1.74 | 0.56 |
| **M-MMFX#19** | **MMFX#19** | 9.85 | 5.83 | 5.19 | 3.60 | 6.17 | 5.36 | 6.00 | 2.09 |

* M - A
**M**: macrocell test
**A**: steel type → N3: conventional, normalized steel, MMFX: MMFX-2 microcomposite steel, s: sandblasted, b: bent bars at the anode.

The average corrosion potentials of the anodes and cathodes with respect to a saturated calomel electrode are presented in Figure 3.60. The anode potentials were more negative than -0.275 V, indicating active corrosion throughout the test period. The corrosion potential of the cathodes remained more positive than -0.200 V, indicating a passive condition.

For the specimens from group MMFX(1), corrosion products were observed primarily above the surface of the solution, as shown in Figure 3.61. For specimens from group MMFX(2), the corrosion products were observed below the surface of the solution, as shown in Figure 3.62. Corrosion products were observed above and below the surface of the solution for bare conventional steel evaluated with the same test setup as group MMFX(2), as shown in Figure 3.63.

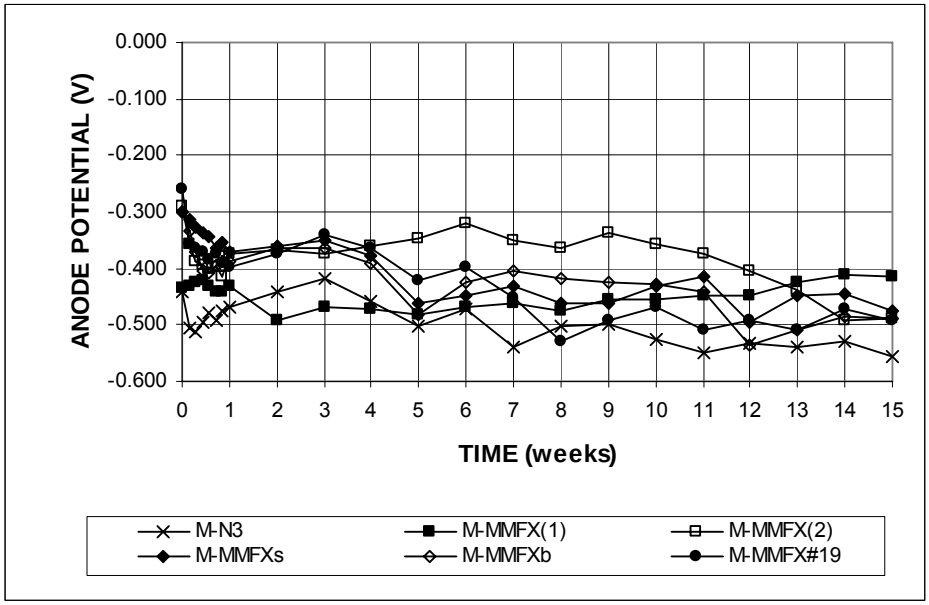


(a)

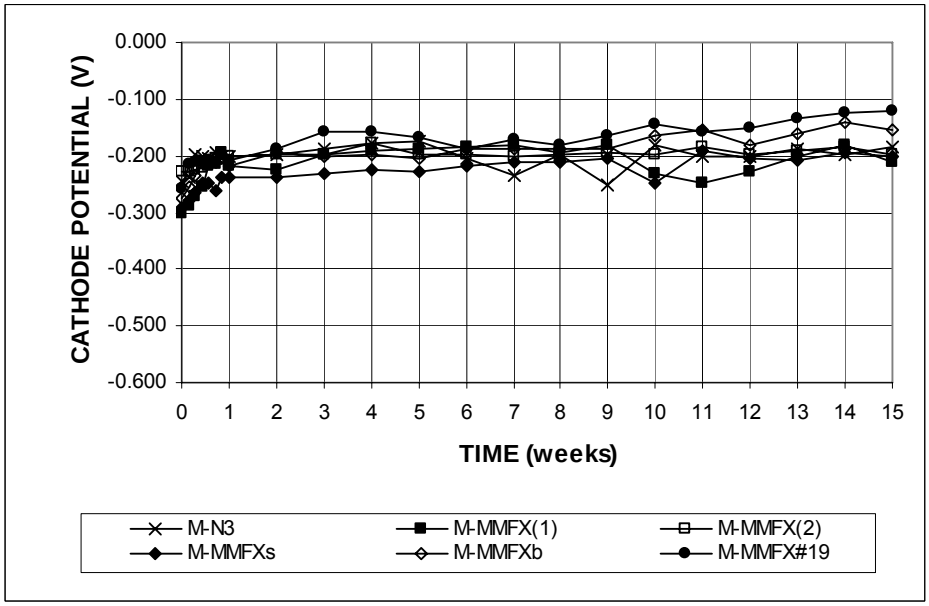


(b)

**Figure 3.60 –** (a) Average anode corrosion potentials and (b) average cathode corrosion potentials with respect to saturated calomel electrode as measured in the rapid macrocell test. Bare bars in 1.6 m ion NaCl and simulated concrete pore solution for specimens with conventional and MMFX microcomposite steel.

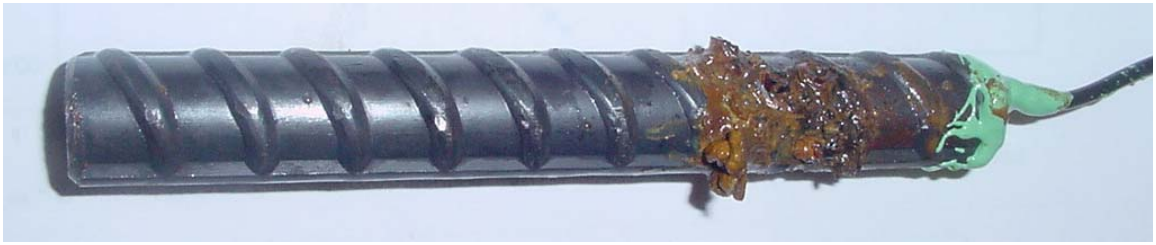

**Figure 3.61 –** Bare MMFX steel anode bar from group MMFX(1) showing corrosion products that formed above the surface of the solution at week 15.

**Figure 3.62 –** Bare MMFX steel anode bar from group MMFX(2), showing corrosion products that formed below the surface of the solution at week 15.

**Figure 3.63 –** Bare conventional steel (N3) anode bar showing corrosion products that formed above and below the surface of the solution at week 15.

The average corrosion rates and average total corrosion losses as a function of time for conventional and sandblasted MMFX bars exposed to a 6.04 m ion NaCl and simulated concrete pore solution are shown in Figures 3.64 and 3.65, respectively. Both steels corroded at similar rates during most of the test period. Tables 3.29 and 3.30 summarize the average corrosion rates and the total corrosion loss at week 15, respectively. Tables C.7 and C.8 show the results of the Student's t-test for the

average corrosion rates and losses, respectively. The average corrosion rates at the end of the test period were 25.46 μm/year for N3 steel and 42.50 μm/year for MMFX steel. Corrosion losses after 15 weeks were 9.63 and 9.68 μm for conventional and MMFX steels, respectively. The difference in the average corrosion rates is significant at $\alpha = 0.05$, but the difference in the corrosion losses is not significant. When compared to specimens exposed to a 1.6 m ion NaCl and simulated concrete pore solution, conventional steel had a lower corrosion rate at week 15 for the specimens exposed to a higher NaCl ion concentration, although for the first 6 weeks, the corrosion rates were higher. For sandblasted MMFX steel, the corrosion rates were much higher for the specimens in the 6.04 m NaCl ion solution throughout the test period.

**Table 3.29 –** Average corrosion rates (in μm/year) at week 15 as measured in the rapid macrocell test with bare bars in 6.04 m ion NaCl and simulated concrete pore solution for specimens with conventional and MMFX microcomposite steel.

| Specimen designation* | Steel type | Specimen | | | | | | Average | Standard deviation |
|---|---|---|---|---|---|---|---|---|---|
| | | 1 | 2 | 3 | 4 | 5 | 6 | | |
| **Bare bars in 6.04 m NaCl** | | | | | | | | | |
| **M-N3h** | **N3** | 33.87 | 37.80 | 12.17 | 24.51 | 18.96 | | 25.46 | 10.52 |
| **M-MMFXsh** | **MMFXs** | 53.02 | 30.81 | 50.13 | 34.49 | 49.94 | 36.62 | 42.50 | 9.59 |

* M - A
**M**: macrocell test
**A**: steel type → N3: conventional, normalized steel, MMFX: MMFX-2 microcomposite steel, s: sandblasted, h: 6.04 m ion NaCl concentration.

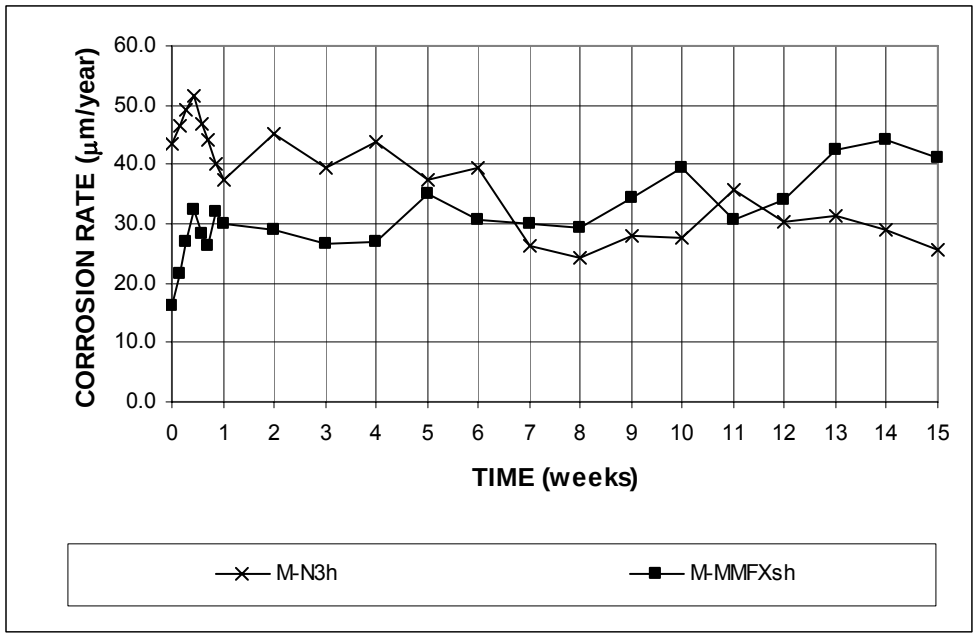


**Figure 3.64 –** Average corrosion rates as measured in the rapid macrocell test for bare bars in 6.04 m ion NaCl and simulated concrete pore solution for specimens with conventional and MMFX microcomposite steel.

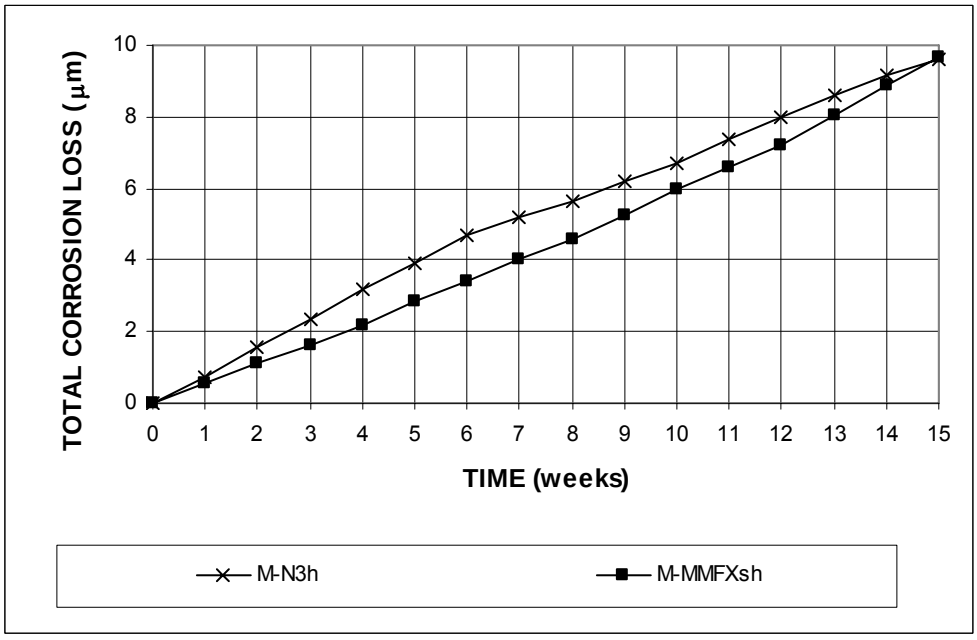


**Figure 3.65 –** Average total corrosion losses as measured in the rapid macrocell test for bare bars in 6.04 m ion NaCl and simulated concrete pore solution for specimens with conventional and MMFX microcomposite steel.

**Table 3.30 –** Average total corrosion losses (in μm) at week 15 as measured in the rapid macrocell test with bare bars in 6.04 m ion NaCl and simulated concrete pore solution for specimens with conventional and MMFX microcomposite steel.

| Specimen designation* | Steel type | Specimen | | | | | | Average | Standard deviation |
|---|---|---|---|---|---|---|---|---|---|
| | | 1 | 2 | 3 | 4 | 5 | 6 | | |
| **Bare bars in 6.04 m NaCl** | | | | | | | | | |
| **M-N3h** | **N3** | 12.16 | 11.53 | 6.83 | 9.19 | 8.46 | | 9.63 | 2.20 |
| **M-MMFXsh** | **MMFXs** | 13.71 | 7.92 | 10.75 | 4.96 | 8.96 | 11.78 | 9.68 | 3.09 |

* M - A
**M**: macrocell test
**A**: steel type → N3: conventional, normalized steel, MMFX: MMFX-2 microcomposite steel, s: sandblasted, b: bent bars at the anode.

The average corrosion potentials of the anodes and the cathodes with respect to a saturated calomel electrode are shown in Figure 3.66. The values were similar for both steels. The anode potentials remained around -0.500 V for both steels, indicating a high tendency to corrode. The cathode potentials remained at values close to -0.200 V for both steels, indicating a low probability for corrosion.

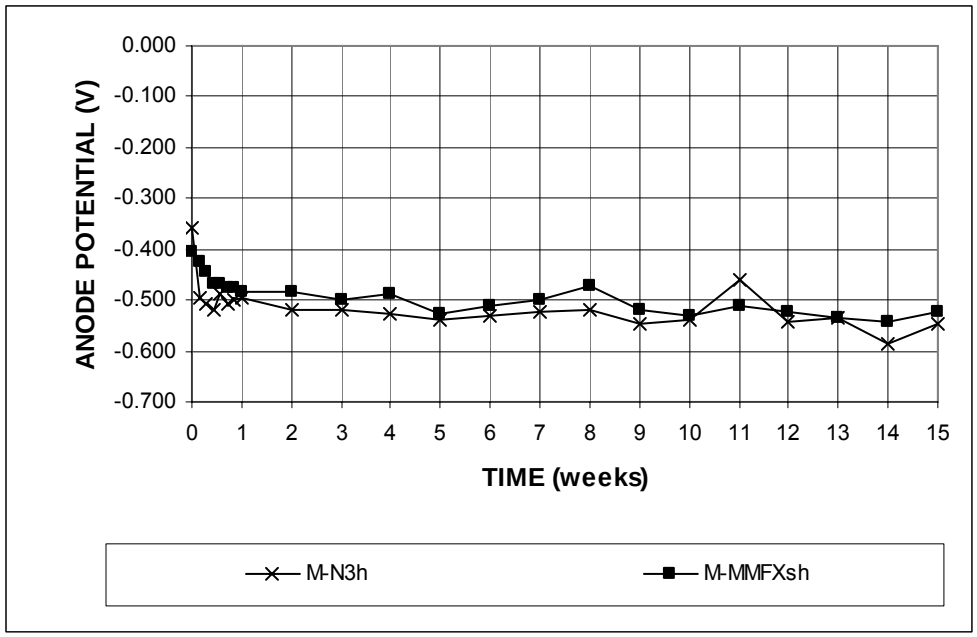


(a)

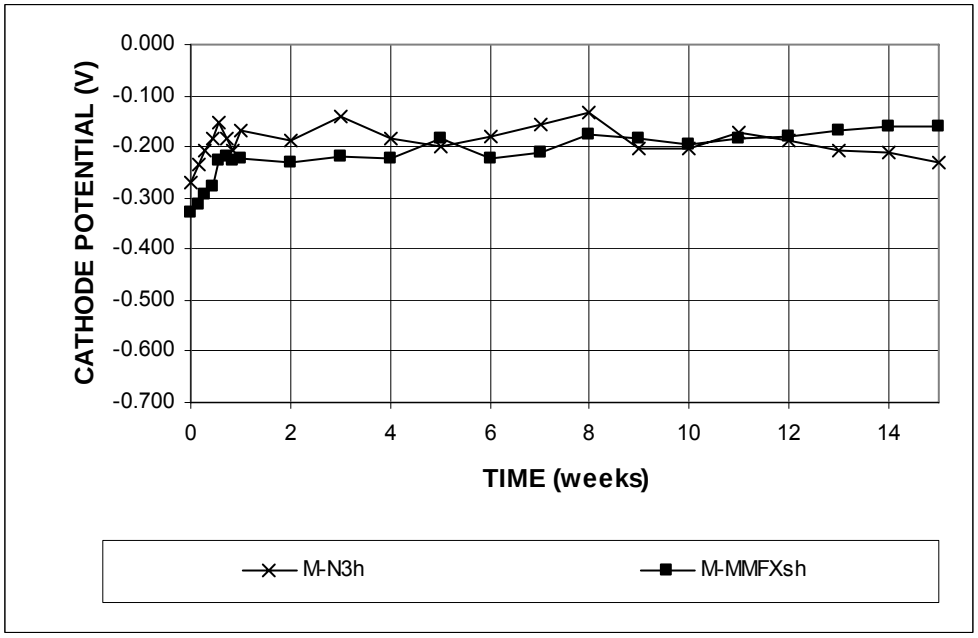


(b)

**Figure 3.66 –** (a) Average anode corrosion potentials and (b) average cathode corrosion potentials with respect to saturated calomel electrode as measured in the rapid macrocell test for bare bars in 6.04 m ion NaCl and simulated concrete pore solution for specimens with conventional and MMFX microcomposite steel.

### 3.5.1.2 Mortar-Wrapped Specimens

Figure 3.67 shows the average corrosion rates versus time for mortar-wrapped bars in 1.6 m ion NaCl and simulated concrete pore solution. Conventional steel exhibited the highest corrosion rate throughout the test period. The specimens with conventional steel at the anode and MMFX at the cathode (M-N3/MMFX-50) had a higher corrosion rate than specimens with MMFX at the anode (M-MMFX-50 and M-MMFX/N3-50) for the first 11 weeks. Table 3.31 shows the average corrosion rates at week 15 and Table C.7 shows the results of the Student's t-test. Conventional steel (N3) had a corrosion rate of 17.7 μm/year. Specimens with conventional steel at the anode and MMFX steel at the cathode (M-N3/MMFX-50) had a corrosion rate of 12.05 μm/year. The difference in the average corrosion rates between M-N3-50 and M-N3/MMFX-50 is significant at $\alpha$ = 0.20. The second highest corrosion rate occurred for the tests with MMFX steel at the anode and conventional steel at the cathode (M-MMFX/N3-50), with a corrosion rate of 12.98 μm/year. The specimens with MMFX steel at the anode and cathode (M-MMFX-50) had the lowest average corrosion rates in the group, 10.59 μm/year, equal to 60% of the corrosion rate for the macrocell with conventional steel at the anode and cathode (M-N3-50). The difference in the average corrosion rates between M-N3-50 and M-MMFX-50 is significant at $\alpha$ = 0.05. The lower corrosion rate for the specimens with MMFX at the cathode seems to indicate that MMFX steel limits the activity at the cathode.

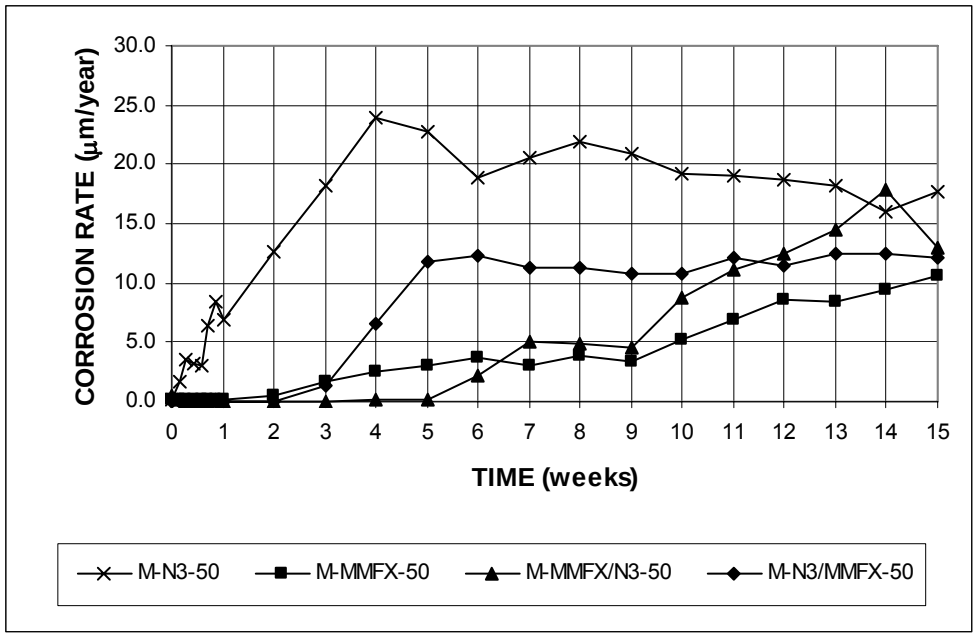


**Figure 3.67 –** Average corrosion rates as measured in the rapid macrocell test for mortar-wrapped specimens in 1.6 m ion NaCl and simulated concrete pore solution for specimens with conventional and MMFX microcomposite steel.

**Table 3.31 –** Average corrosion rates (in μm/year) at week 15 as measured in the rapid macrocell test for mortar-wrapped specimens in 1.6 m ion NaCl and simulated concrete pore solution for specimens with conventional and MMFX microcomposite steel.

| Specimen designation* | Steel type | Specimen | | | | | | Average | Standard deviation |
|---|---|---|---|---|---|---|---|---|---|
| | | 1 | 2 | 3 | 4 | 5 | 6 | | |
| **Mortar-wrapped specimens in 1.6 m NaCl** | | | | | | | | | |
| **M-N3-50** | **N3** | 11.21 | 9.16 | 26.07 | 19.31 | 21.15 | 19.31 | 17.70 | 6.36 |
| **M-MMFX-50** | **MMFX** | 8.87 | 17.37 | 10.12 | 9.54 | 11.68 | 5.98 | 10.59 | 3.81 |
| **M-MMFX/N3-50** | **MMFX/N3** | 15.20 | 11.44 | 12.28 | | | | 12.98 | 1.97 |
| **M-N3/MMFX-50** | **N3/MMFX** | 15.03 | 10.58 | 10.55 | | | | 12.05 | 2.58 |

* M - A - B
**M**: macrocell test
**A**: steel type → N3: conventional, normalized steel, MMFX: MMFX-2 microcomposite steel
**B**: mix design → 50: water-cement ratio of 0.50 and no inhibitor.

The average total corrosion losses throughout the test period are shown in Figure 3.68, and the average total corrosion losses at week 15 are presented in Table 3.32. The results of the Student's t-test are shown in Table C.8. After 15 weeks,

specimens with conventional steel at the anode and cathode (M-N3-50) had a corrosion loss of 5.46 μm. Specimens with conventional steel at the anode and MMFX at the cathode (M-N3/MMFX-50) had a loss of 2.63 μm, while specimens with MMFX steel at the anode and conventional steel at the cathode (M-MMFX/N3-50) had a loss of 1.82 μm. The difference in the average corrosion loss between specimens M-N3-50 and M-N3/MMFX-50 is significant at $\alpha = 0.02$. Specimens with MMFX steel at the anode and cathode (M-MMFX-50) had the lowest corrosion loss, 1.37 μm, corresponding to 25% of the total loss of M-N3-50. The difference in the average corrosion loss between specimens M-N3-50 and M-MMFX-50 is significant at $\alpha = 0.02$.

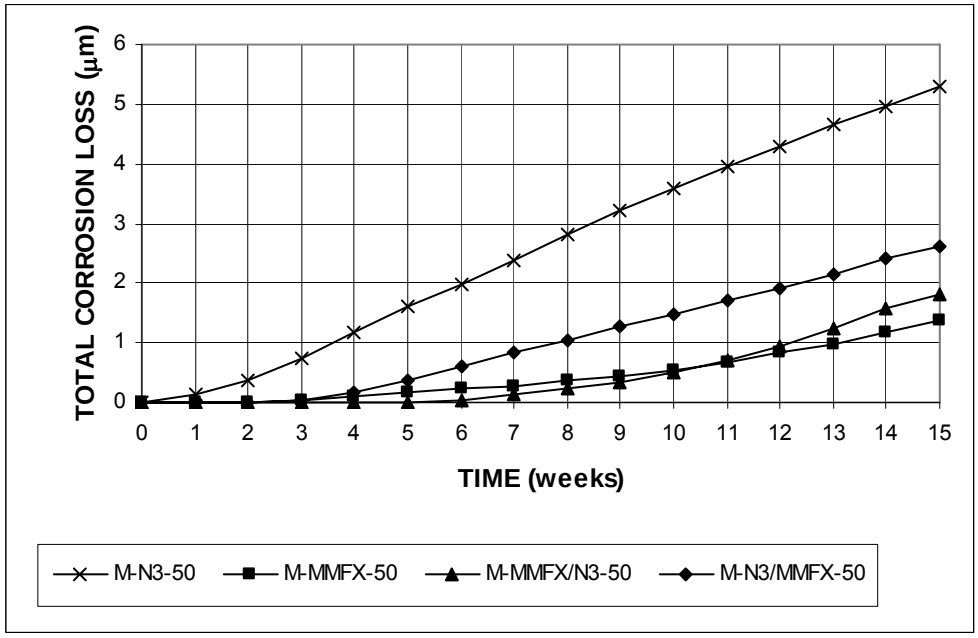


**Figure 3.68 –** Average total corrosion losses as measured in the rapid macrocell test for mortar-wrapped specimens in 1.6 m ion NaCl and simulated concrete pore solution for specimens with conventional and MMFX microcomposite steel.

**Table 3.32 –** Average total corrosion losses (in μm) at week 15 as measured in the rapid macrocell test for mortar-wrapped specimens in 1.6 m ion NaCl and simulated concrete pore solution for specimens with conventional and MMFX microcomposite steel.

| Specimen designation* | Steel type | Specimen | | | | | | Average | Standard deviation |
|---|---|---|---|---|---|---|---|---|---|
| | | 1 | 2 | 3 | 4 | 5 | 6 | | |
| **Mortar-wrapped specimens in 1.6 m NaCl** | | | | | | | | | |
| **M-N3-50** | **N3** | 5.54 | 5.08 | 7.01 | 5.21 | 4.79 | 5.12 | 5.46 | 0.80 |
| **M-MMFX-50** | **MMFX** | 2.18 | 0.56 | 1.88 | 0.99 | 1.68 | 0.93 | 1.37 | 0.63 |
| **M-MMFX/N3-50** | **MMFX/N3** | 1.60 | 1.75 | 2.11 | | | | 1.82 | 0.26 |
| **M-N3/MMFX-50** | **N3/MMFX** | 3.33 | 2.21 | 2.35 | | | | 2.63 | 0.61 |

* M - A - B
**M**: macrocell test
**A**: steel type → N3: conventional, normalized steel, MMFX: MMFX-2 microcomposite steel.
**B**: mix design → 50: water-cement ratio of 0.50 and no inhibitor.

Figure 3.69 shows the average corrosion potentials of the anodes and cathodes with respect to a saturated calomel electrode. The corrosion potential of the anode dropped below -0.275 V at week 2 for conventional steel, and at week 4 for MMFX steel. After 15 weeks, the anode potentials ranged from -0.500 to -0.610 V, indicating active corrosion for all specimens. The cathode potential remained more positive than -0.200 V for MMFX steel, indicating a passive condition. For the remaining tests, the cathode potentials were between -0.250 and -0.300 V, indicating a low probability of corrosion.

After 15 weeks of testing, the mortar cover was removed from the bars. Corrosion products were observed on both the conventional and MMFX steel bars at the anode, as shown in Figures 3.70 and 3.71, respectively.

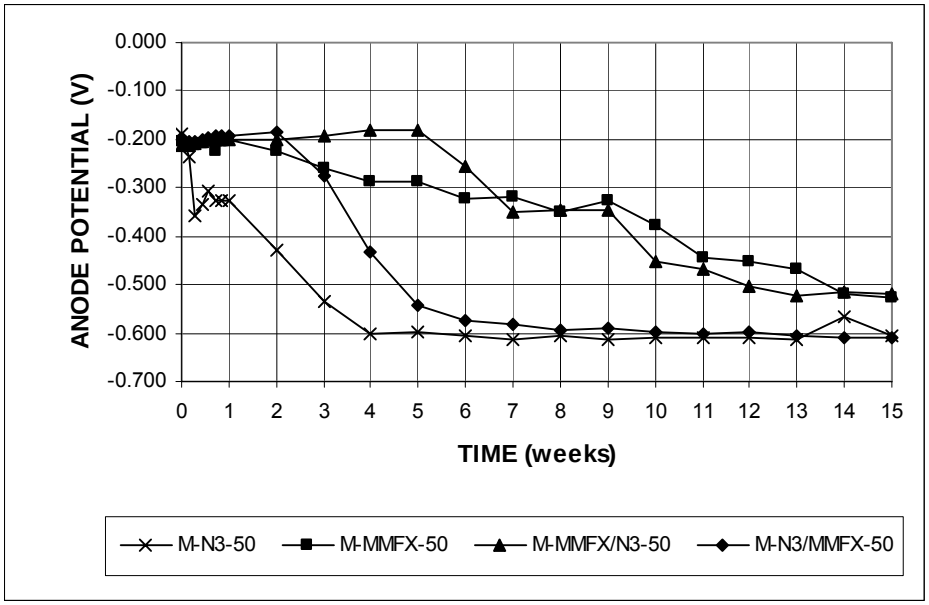


(a)

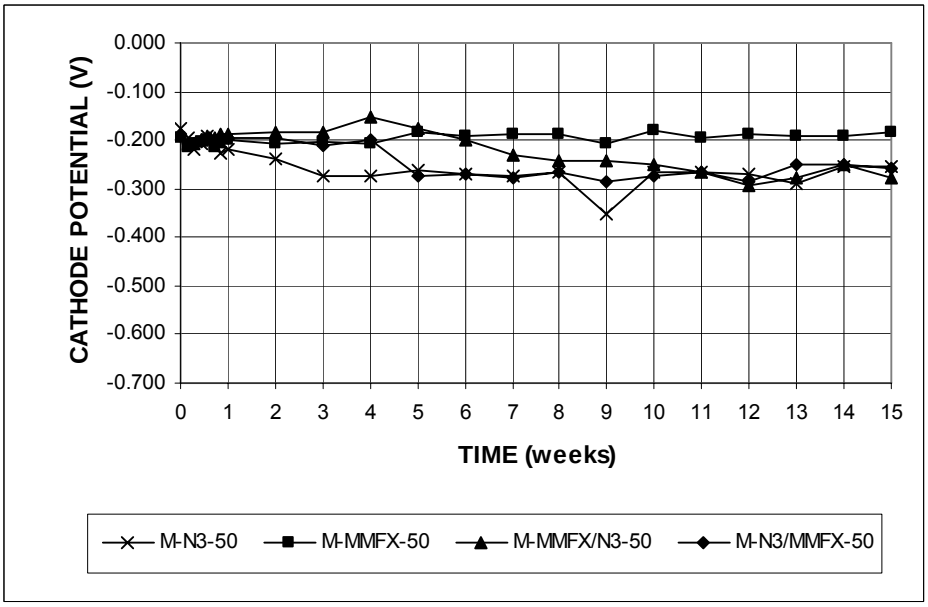


(b)

**Figure 3.69 –** (a) Average anode corrosion potentials and (b) average cathode corrosion potentials with respect to saturated calomel electrode as measured in the rapid macrocell test for mortar-wrapped specimens in 1.6 m ion NaCl and simulated concrete pore solution for specimens with conventional and MMFX microcomposite steel.

**Figure 3.70 –** Corrosion products on conventional steel anode after removal of mortar cover at week 15.

**Figure 3.71 –** Corrosion products on MMFX steel anode after removal of mortar cover at week 15.

### 3.5.2 Bench-Scale Tests

Southern Exposure and cracked beam tests were used to evaluate MMFX microcomposite steel. The concrete had a water-cement ratio of 0.45 and no inhibitor. In addition to testing MMFX steel alone, specimens with a combination of MMFX and conventional steel and specimens with bent MMFX steel in the top mat were also evaluated.

#### 3.5.2.1 Southern Exposure Test

The average corrosion rates versus time are shown in Figure 3.72. Specimens with bent MMFX bars in the top mat (SE-MMFXb-45) had the highest corrosion rate during the first 15 weeks, and the lowest corrosion rates during the last 40 weeks. After week 30, specimens with conventional steel in the top and bottom mats (SE-N3-45) showed higher corrosion rates than the other specimens. The average corrosion rates at week 70 are summarized in Table 3.33 and the results of the

Student's t-test are presented in Table C.7. Conventional steel (SE-N3-45) had an average corrosion rate of 9.05 μm/year. The specimens with MMFX steel in the top and bottom mats (SE-MMFX-45) had an average corrosion rate of 2.44 μm/year, equal to 27% of the corrosion rate of SE-N3-45. The difference in the average corrosion rates between SE-N3-45 and SE-MMFX-45 is significant at $\alpha = 0.05$. The specimens with bent MMFX bars on the top mat exhibited a corrosion rate at week 70 of 1.34 μm/year. The specimens with conventional steel in the top mat and MMFX steel in the bottom mat (SE-N3/MMFX-45) had a corrosion rate of 3.07 μm/year, one third of the corrosion rate of the specimens with conventional steel in the top and bottom mat. The difference in the average corrosion rate between SE-N3-45 and SE-N3/MMFX-45 is significant at $\alpha = 0.05$. The specimens with MMFX in the top mat and conventional steel in the bottom mat (SE-MMFX/N3-45) had a corrosion rate of 2.65 μm/year, slightly higher than the specimens with MMFX steel in the top and bottom mat. As mentioned before, MMFX seems to limit the activity in the bottom mat (cathode).

Figure 3.73 shows the average total corrosion losses during the test period, and Table 3.34 summarizes the average total corrosion losses at week 70. Table C.8 presents the results of the Student's t-test. Conventional steel (SE-N3-45) had a corrosion loss of 7.30 μm, and MMFX steel (SE-MMFX-45) had a corrosion loss of 1.89 μm, corresponding to 26% of that obtained for conventional steel. The difference in the average corrosion loss of SE-N3-45 and SE-MMFX-45 is significant at $\alpha = 0.05$. Specimens with bent MMFX bars on the top mat (SE-MMFXb-45) had an average corrosion loss of 4.61 μm (63% of SE-N3-45), while specimens with MMFX steel on the top mat and conventional steel on the bottom mat (SE-MMFX/N3-45) had a corrosion loss of 2.17 μm. The specimens with

conventional steel in the top mat and MMFX steel in the bottom mat (SE-N3/MMX-45) had an average corrosion loss of 4.77 μm. The difference in the average corrosion rate between SE-N3-45 and SE-N3/MMFX-45 is not statistically significant.

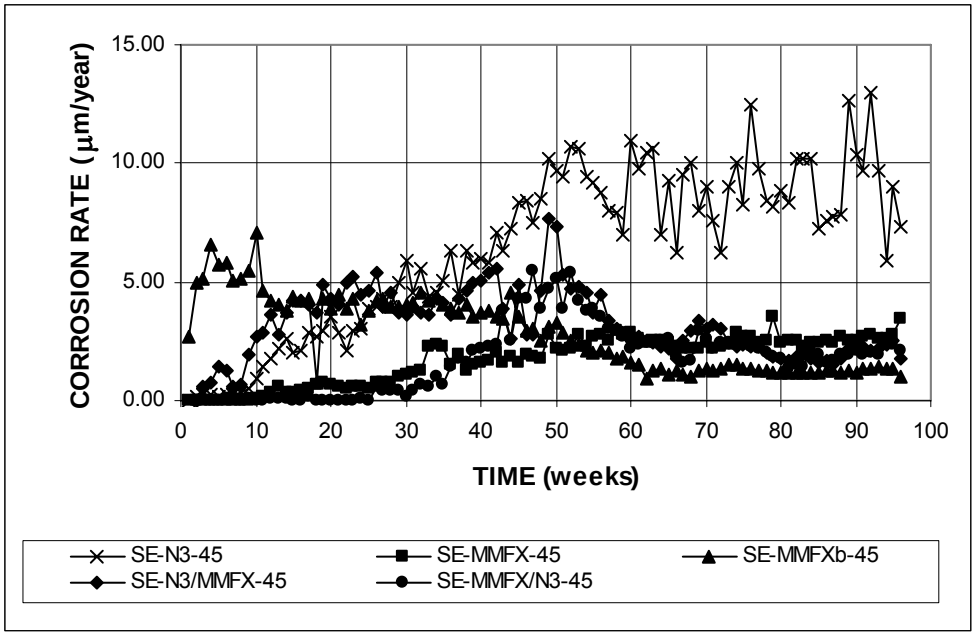


**Figure 3.72 –** Average corrosion rates as measured in the Southern Exposure test for specimens with conventional and MMFX microcomposite steel.

**Table 3.33 –** Average corrosion rates (in μm/year) at week 70 as measured in the Southern Exposure test for specimens with conventional and MMFX microcomposite steel.

| Specimen designation* | Steel type | Specimen | | | | | | Average | Standard deviation |
|---|---|---|---|---|---|---|---|---|---|
| | | 1 | 2 | 3 | 4 | 5 | 6 | | |
| **Southern Exposure test** | | | | | | | | | |
| **SE-N3-45** | **N3** | 13.96 | 11.83 | 4.48 | 5.47 | 14.32 | 4.21 | 9.05 | 4.83 |
| **SE-MMFX-45** | **MMFX** | 3.82 | 1.84 | 2.91 | 1.75 | 2.69 | 1.66 | 2.44 | 0.85 |
| **SE-MMFXb-45** | **MMFXb** | 1.30 | 1.09 | 1.63 | | | | 1.34 | 0.27 |
| **SE-MMFX/N3-45** | **MMFX/N3** | 1.82 | 2.88 | 3.26 | | | | 2.65 | 0.74 |
| **SE-N3/MMFX-45** | **N3/MMFX** | 1.72 | 3.40 | 4.11 | | | | 3.07 | 1.23 |

* SE - A - B
**SE**: Southern Exposure test
**A**: steel type → N3: conventional, normalized steel, MMFX: MMFX-2 microcomposite steel, b: bent bars on the top mat.
**B**: mix design → 45: water-cement ratio of 0.45 and no inhibitor.

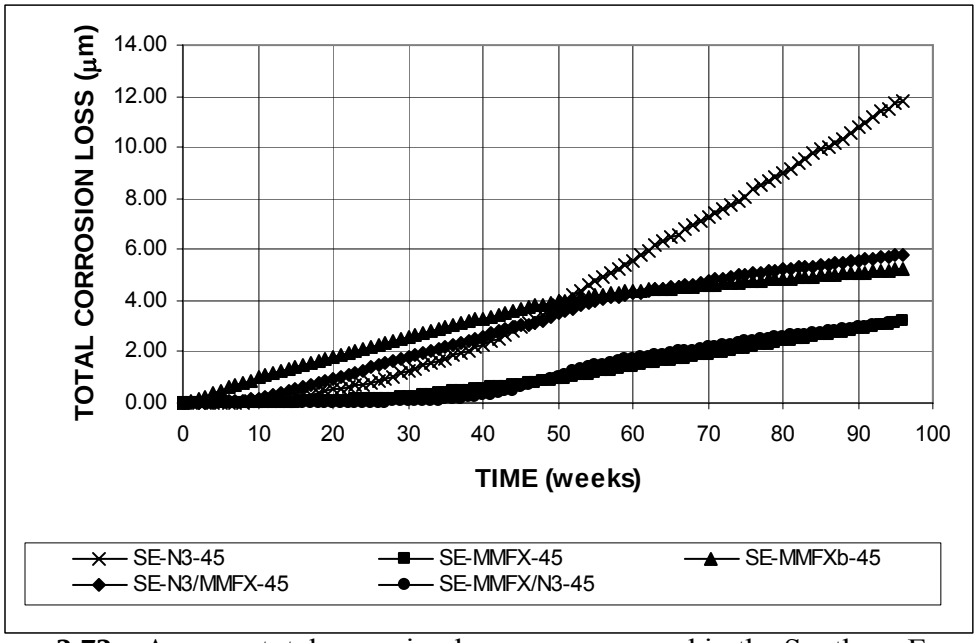


**Figure 3.73 –** Average total corrosion losses as measured in the Southern Exposure test for specimens with conventional and MMFX microcomposite steel.

**Table 3.34 –** Average total corrosion losses (in μm) at week 70 as measured in the Southern Exposure test for specimens with conventional and MMFX microcomposite steel.

| Specimen designation* | Steel type | Specimen | | | | | | Average | Standard deviation |
|---|---|---|---|---|---|---|---|---|---|
| | | 1 | 2 | 3 | 4 | 5 | 6 | | |
| **Southern Exposure test** | | | | | | | | | |
| **SE-N3-45** | **N3** | 9.80 | 13.01 | 2.50 | 5.90 | 8.65 | 3.95 | 7.30 | 3.92 |
| **SE-MMFX-45** | **MMFX** | 2.98 | 1.79 | 2.76 | 1.47 | 1.70 | 0.65 | 1.89 | 0.86 |
| **SE-MMFXb-45** | **MMFXb** | 4.96 | 3.31 | 5.54 | | | | 4.61 | 1.16 |
| **SE-MMFX/N3-45** | **MMFX/N3** | 1.88 | 2.41 | 2.23 | | | | 2.17 | 0.27 |
| **SE-N3/MMFX-45** | **N3/MMFX** | 2.72 | 5.09 | 6.49 | | | | 4.77 | 1.91 |

* SE - A - B
**SE**: Southern Exposure test
**A**: steel type → N3: conventional, normalized steel, MMFX: MMFX-2 microcomposite steel, b: bent bars on the top mat.
**B**: mix design → 45: water-cement ratio of 0.45 and no inhibitor.

The average corrosion potentials of the top and bottom mats of steel with respect to a saturated calomel electrode are presented in Figure 3.74. The top mat corrosion potential for the MMFX bent bars became more negative than -0.350 V during the first week. Active corrosion was observed for specimens with

conventional steel in the top and bottom mats (SE-N3-45) at week 11 and for specimens with straight MMFX bars in the top and bottom mats (SE-MMFX-45) at week 18. By week 70, all specimens had corrosion potentials for the top mat that were more negative than -0.500 V, indicating active corrosion.

The average corrosion potentials for the bottom mat became more negative than -0.350 V for specimens SE-N3-45 and SE-MMFX/N3-45 after week 14. Specimens with N3 in the top mat and MMFX steel in the bottom mat (SE-N3/MMFX-45) showed active corrosion of the bottom mat at week 38.

Figure 3.75 shows the average mat-to-mat resistances for the Southern Exposure specimens. The average mat-to-mat resistances at week 1 were between 100 and 200 ohms for all specimens. During the first 40 weeks, the mat-to-mat resistances increased at a slow rate for all specimens. After week 40, the mat-to-mat resistances increased at a higher rate. At week 70, specimens with bent MMFX bars in the top mat had the highest mat-to-mat resistance, with values above 1500 ohms. The remaining specimens had mat-to-mat resistances below 1000 ohms. Specimens with conventional steel in the top and bottom mat had the lowest mat-to-mat resistances. The mat-to-mat resistance of specimens with conventional steel dropped at week 75 due to the formation of cracks in the specimen.

After the 96-week test period, the bars were removed from the concrete and inspected. The MMFX steel bars showed corrosion products on the bars from the top mat, as shown in Figure 3.76. Corrosion products were also observed on conventional steel bars from the top mat of steel.

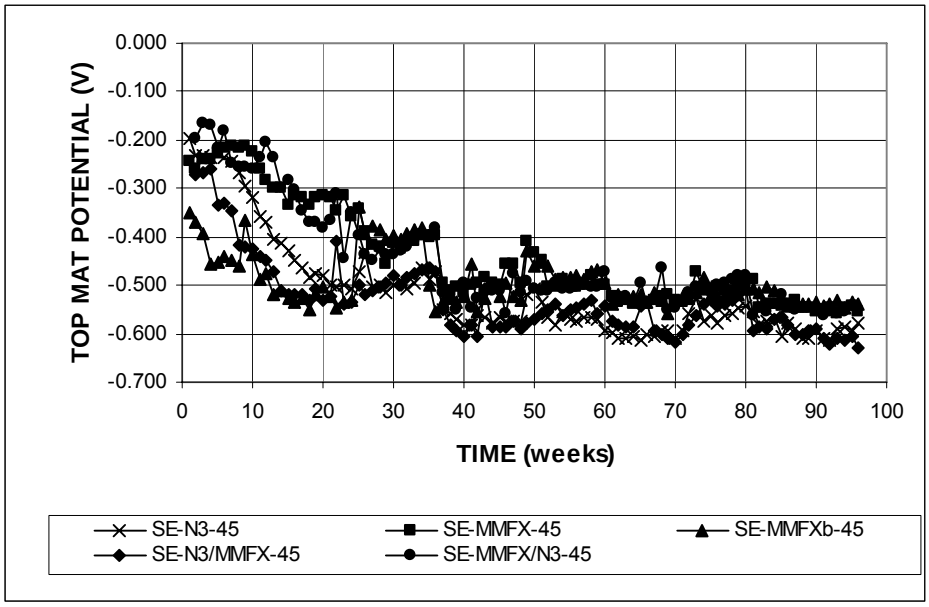


(a)

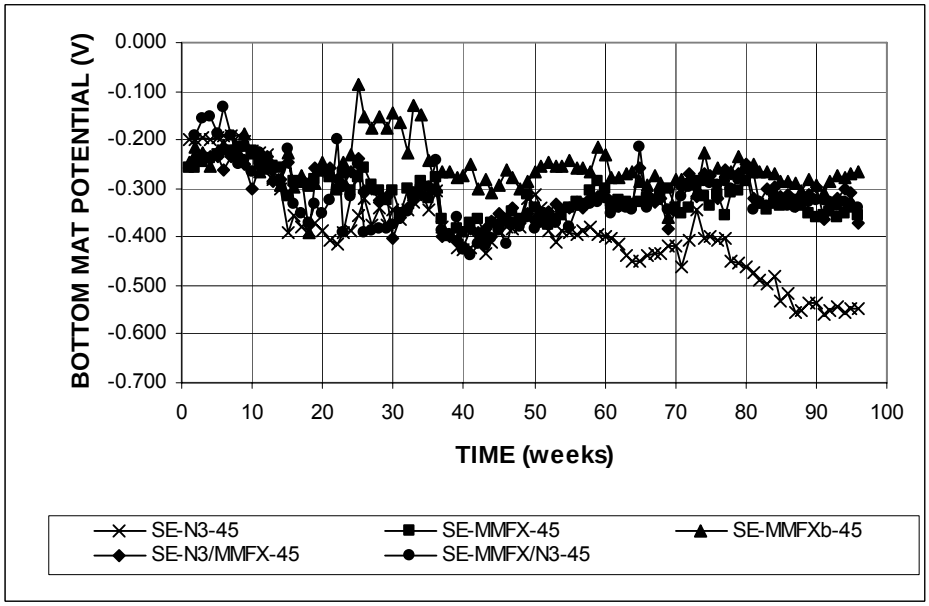


(b)

**Figure 3.74 –** (a) Average top mat corrosion potentials and (b) average bottom mat corrosion potentials with respect to copper-copper sulfate electrode as measured in the Southern Exposure test for specimens with conventional and MMFX microcomposite steel.

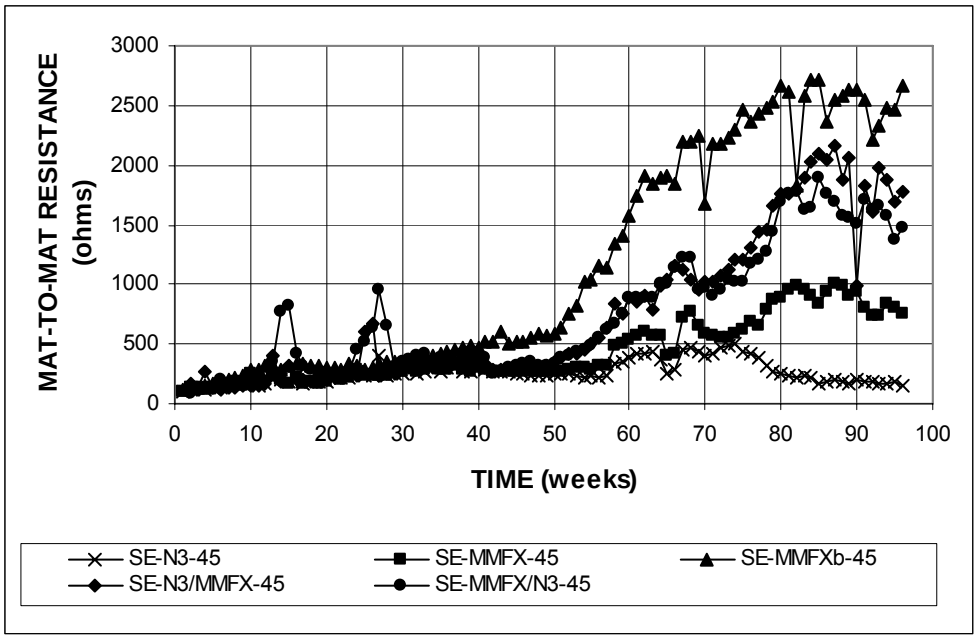


**Figure 3.75 –** Average mat-to-mat resistances as measured in the Southern Exposure test for specimens with conventional and MMFX microcomposite steel.

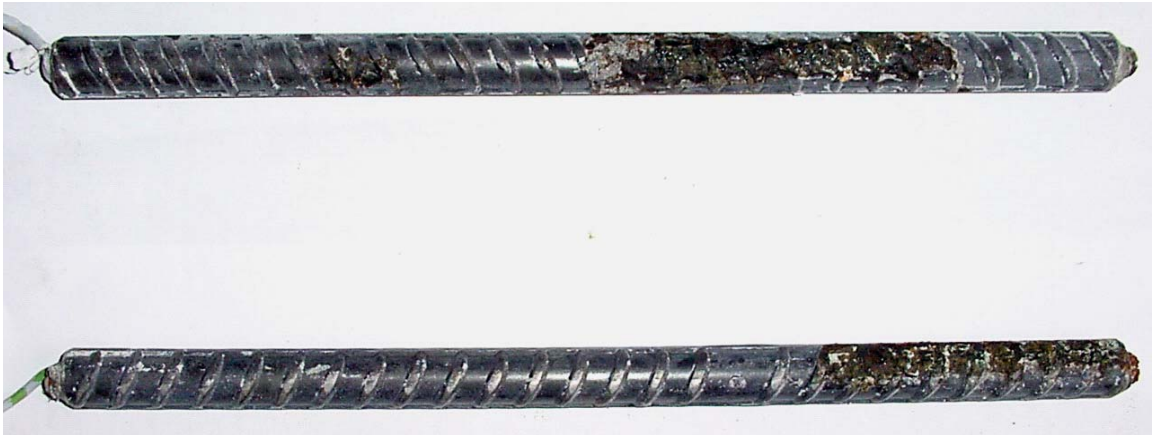

**Figure 3.76 -** Corrosion products on MMFX microcomposite steel bars from top mat of a Southern Exposure specimen, at week 96.

### 3.5.2.2 Cracked Beam Test

Figure 3.77 shows the average corrosion rates as a function of time for the cracked beam test. During the first 9 weeks, conventional steel had corrosion rates higher than 10 μm/year. After week 9, its corrosion rates ranged from 2 to 10 μm/year, with a jump to values above 20 μm/year between weeks 44 and 53. MMFX steel had corrosion rates below 5 μm/year. Table 3.34 shows the average corrosion rates at week 70. Conventional steel had a corrosion rate of 9.09 μm/year while MMFX steel had a corrosion rate of 2.25 μm/year, corresponding to 25% of that of conventional steel. The Student's t-test (Table C.7) shows that the difference in the average corrosion rates is significant at $\alpha = 0.20$.

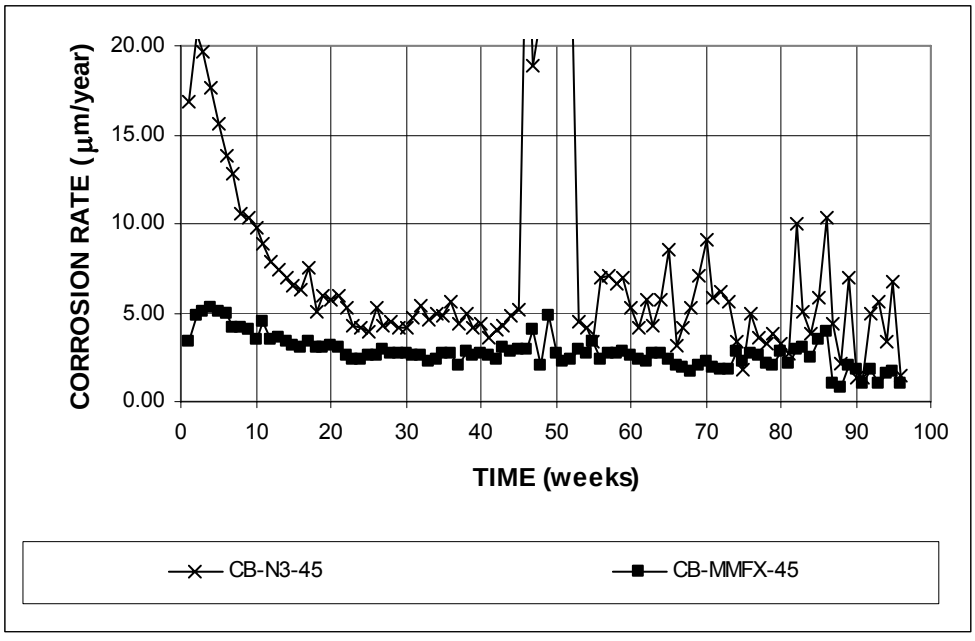


**Figure 3.77 –** Average corrosion rates as measured in the cracked beam test for specimens with conventional and MMFX microcomposite steel.

**Table 3.35 –** Average corrosion rates (in μm/year) at week 70 as measured in the cracked beam test for specimens with conventional and MMFX microcomposite steel.

| Specimen designation* | Steel type | Specimen | | | | | | Average | Standard deviation |
|---|---|---|---|---|---|---|---|---|---|
| | | 1 | 2 | 3 | 4 | 5 | 6 | | |
| **Cracked beam test** | | | | | | | | | |
| **CB-N3-45** | **N3** | 20.37 | 1.70 | 23.30 | 1.58 | 5.28 | 2.31 | 9.09 | 10.01 |
| **CB-MMFX-45** | **MMFX** | 3.55 | 2.77 | 1.39 | 2.67 | 2.13 | 0.97 | 2.25 | 0.95 |

* CB - A - B
**CB**: cracked beam test
**A**: steel type → N3: conventional, normalized steel, MMFX: MMFX-2 microcomposite steel.
**B**: mix design → 45: water-cement ratio of 0.45 and no inhibitor.

Figure 3.78 shows the average total corrosion losses during the test period. The average total corrosion losses after 70 weeks, shown in Table 3.36 were 11.6 and 4.03 μm for conventional and MMFX steel, respectively. MMFX steel had a total corrosion loss equal to 35% of the value for conventional steel. The difference in the average corrosion losses is significant at $\alpha$ = 0.10, according to results from the Student's t-test presented in Table C.8.

**Table 3.36 –** Average total corrosion losses (in μm) at week 70 as measured in the cracked beam test for specimens with conventional and MMFX microcomposite steel.

| Specimen designation* | Steel type | Specimen | | | | | | Average | Standard deviation |
|---|---|---|---|---|---|---|---|---|---|
| | | 1 | 2 | 3 | 4 | 5 | 6 | | |
| **Cracked beam test** | | | | | | | | | |
| **CB-N3-45** | **N3** | 26.09 | 12.25 | 10.94 | 5.68 | 6.52 | 8.15 | 11.60 | 7.53 |
| **CB-MMFX-45** | **MMFX** | 4.94 | 2.61 | 3.73 | 5.18 | 4.65 | 3.04 | 4.03 | 1.06 |

* CB - A - B
**CB**: cracked beam test
**A**: steel type → N3: conventional, normalized steel, MMFX: MMFX-2 microcomposite steel.
**B**: mix design → 45: water-cement ratio of 0.45 and no inhibitor.

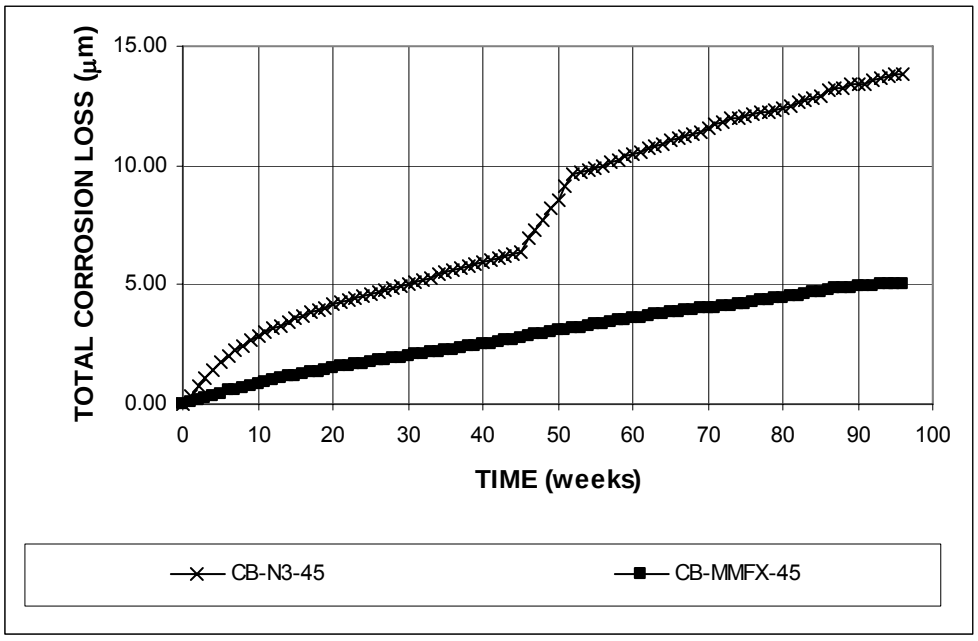


**Figure 3.78 –** Average total corrosion losses as measured in the cracked beam test for specimens with conventional and MMFX microcomposite steel.

The average corrosion potentials of the top and bottom mats of steel with respect to a copper-copper sulfate electrode are shown in Figure 3.79. The corrosion potentials of the top mat remained between -0.400 and -0.600 V for the test period, indicating active corrosion. The average corrosion potentials of the bottom mat for both steels ranged from -0.200 to -0.400 V for the first 60 weeks. Values close to -0.350 V indicate the probable presence of chlorides in the bottom mat. This is attributed to easy access of chlorides due to the presence of the crack. After week 60, the corrosion potential of the bottom mat dropped for conventional steel, and by the end of the test period, it reached values close to -0.600 V.

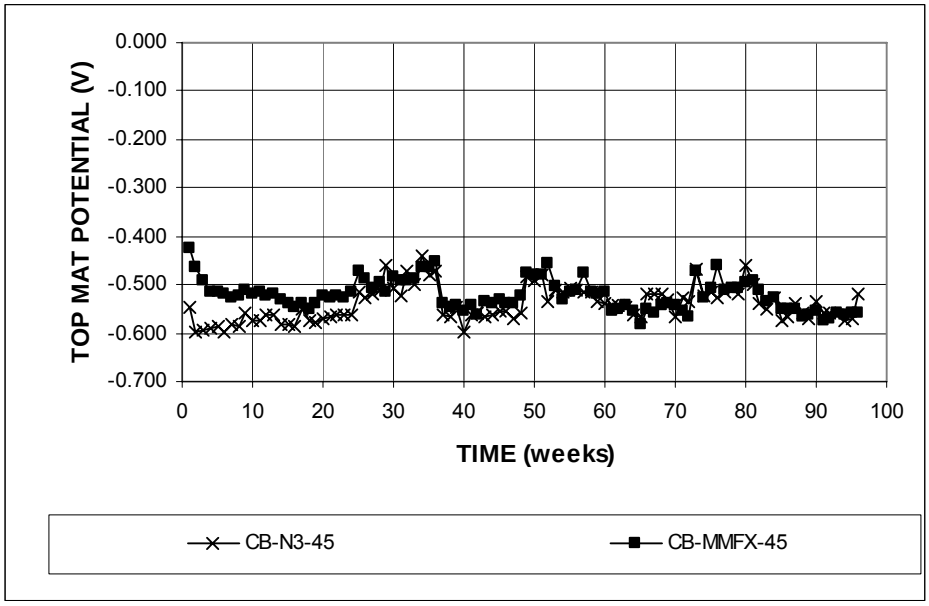


(a)

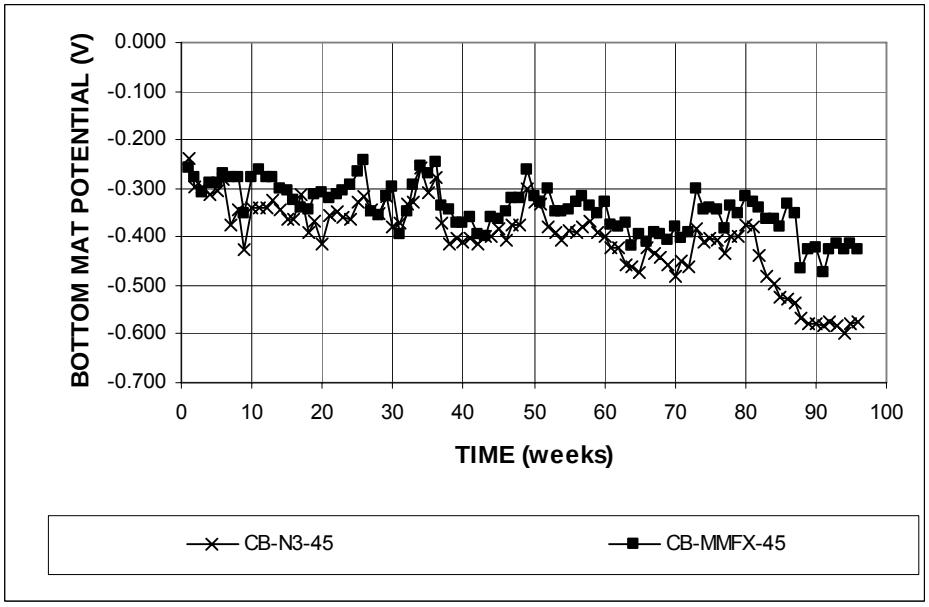


(b)

**Figure 3.79 –** (a) Average top mat corrosion potentials and (b) average bottom mat corrosion potentials with respect to copper-copper sulfate electrode as measured in the cracked beam test for specimens with conventional and MMFX microcomposite steel.

Figure 3.80 shows the average mat-to-mat resistances for cracked beam specimens with conventional and MMFX steel. Conventional steel had lower mat-to-mat resistances than MMFX steel throughout the test period. By week 70, the mat-to-mat resistance for conventional steel was approximately 1000 ohms, while the mat-to-mat resistance for MMFX steel was approximately 1400 ohms.

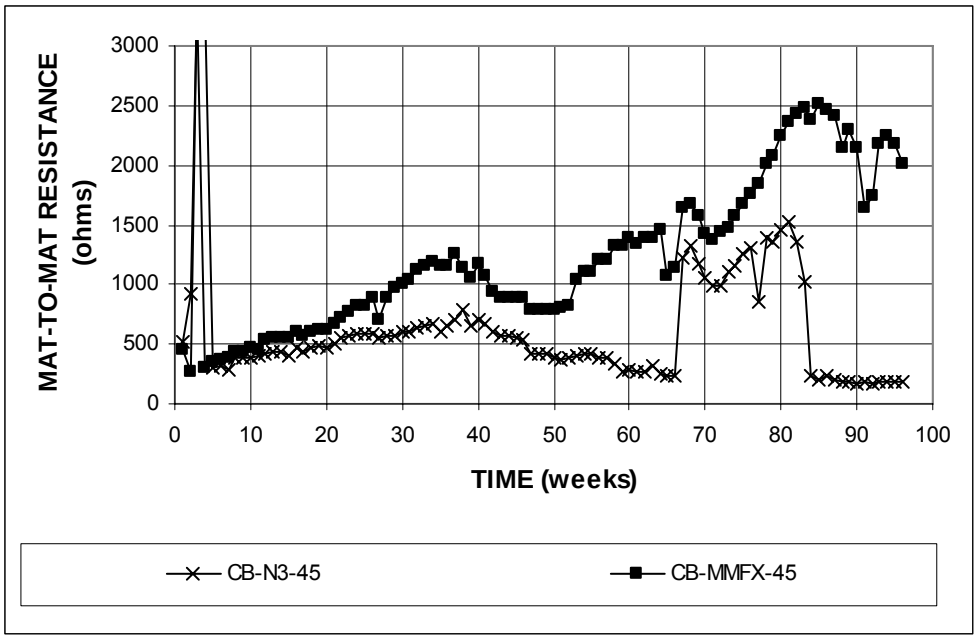


**Figure 3.80 –** Average mat-to-mat resistances as measured in the cracked beam test for specimens with conventional and MMFX microcomposite steel.

## 3.6 EPOXY-COATED STEEL

Test results for epoxy-coated steel were reported previously by Darwin et al. (2002) and Gong et al. (2002). At the time of the latter report, the bench-scale tests were 40 weeks old. The present report covers the full 96-week test period.

### 3.6.1 Rapid Macrocell Test

Mortar-wrapped specimens were used to evaluate the epoxy-coated steel with the rapid macrocell test. The mortar had a water-cement ratio of 0.50. Uncoated steel was used in the cathodes. The epoxy coating was intentionally damaged by drilling four 3.2-mm ($^1/_8$-in.) diameter holes through the coating on each epoxy-coated bar.

Figure 3.81 shows the average corrosion rates. Figure 3.81(b) expands the vertical axis in Figure 3.81(a). The corrosion rates for the epoxy-coated bars were calculated based on both the exposed area of the four 3.2-mm ($^1/_8$-in.) diameter holes drilled in the epoxy (M-ECR-50[1]) and the total area of the bars exposed to solution (M-ECR-50[2]). Table 3.37 summarizes the average corrosion rates at week 15 and Table C.9 shows the results of the Student's t-test.

For the exposed area of steel, the average corrosion rate reached values as high as 532 μm/year at week 15, as shown in Figure 3.81(a) and Table 3.37. For the total bar area exposed to the solution, the average corrosion rates were below those of conventional steel. At 15 weeks, the epoxy-coated bars had an average corrosion rate of 5.31 μm/year based on the total area exposed to solution (M-ECR-50[2]), or 30% of the corrosion rate of conventional steel, 17.70 μm/year. The difference in the average corrosion rates of M-N3-50 and M-ECR-50[2] is significant at $\alpha = 0.02$.

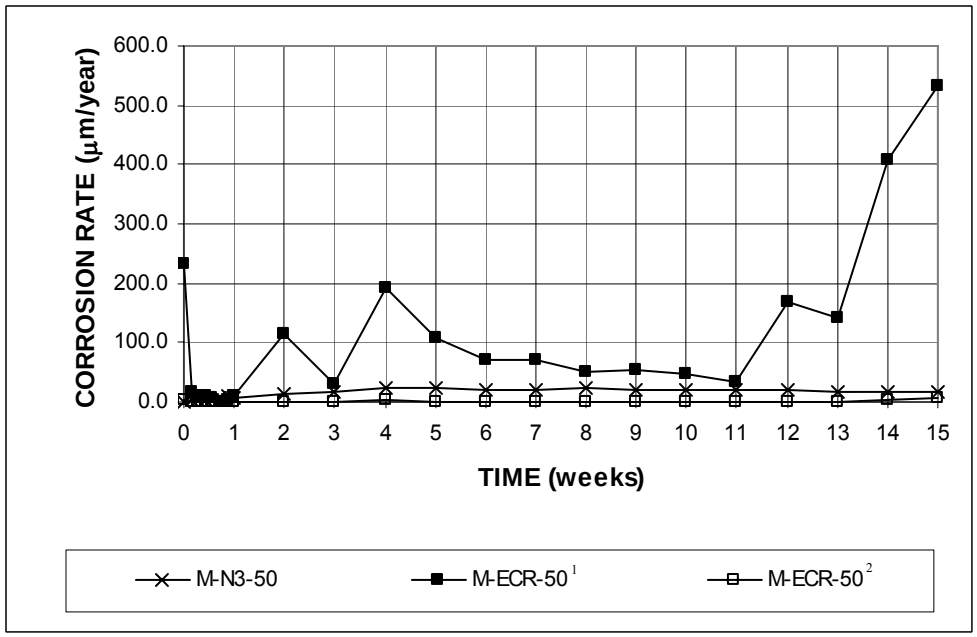


(a)

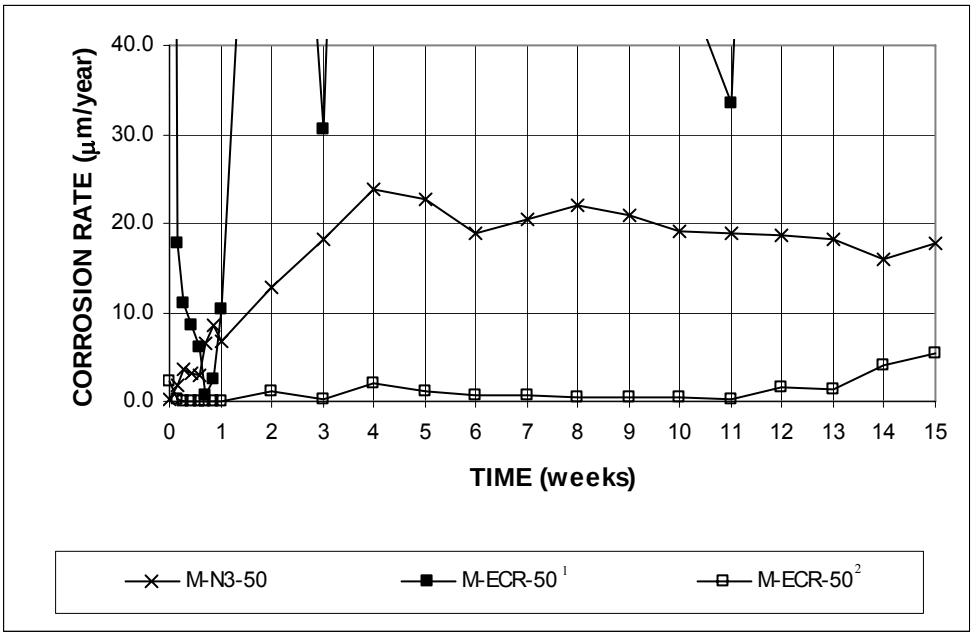


(b)

[1] Based on exposed area, four 3.2-mm (1/8-in.) diameter holes in epoxy
[2] Based on total area of bar exposed to solution

**Figure 3.81 –** Average corrosion rates as measured in the rapid macrocell test for mortar-wrapped specimens in 1.6 m ion NaCl and simulated concrete pore solution for specimens with uncoated conventional and epoxy-coated.

**Table 3.37 –** Average corrosion rates (in μm/year) at week 15 as measured in the rapid macrocell test for mortar-wrapped specimens in 1.6 m ion NaCl and simulated concrete pore solution for specimens with uncoated conventional and epoxy-coated steel.

| Specimen designation* | Steel type | Specimen | | | | | | Average | Standard deviation |
|---|---|---|---|---|---|---|---|---|---|
| | | 1 | 2 | 3 | 4 | 5 | 6 | | |
| **Mortar-wrapped specimens in 1.6 m NaCl** | | | | | | | | | |
| **M-N3-50** | **N3** | 11.21 | 9.16 | 26.07 | 19.31 | 21.15 | 19.31 | 17.70 | 6.36 |
| **M-ECR-50** [1] | **ECR** | 3.65 | 1841.62 | 76.73 | 646.76 | 621.18 | 0.00 | 531.66 | 707.91 |
| **M-ECR-50** [2] | **ECR** | 0.04 | 18.40 | 0.77 | 6.46 | 6.21 | 0.00 | 5.31 | 7.07 |

* M - A - B
**M**: macrocell test
**A**: steel type → N3: conventional, normalized steel, ECR: epoxy-coated steel
**B**: mix design → 50: water-cement ratio of 0.50 and no inhibitor.
[1] Based on exposed area, four 3.2-mm (1/8-in.) diameter holes in epoxy
[2] Based on total area of bar exposed to solution

The average total corrosion losses versus time are shown in Figure 3.82. Figure 3.82(b) expands the vertical axis of Figure 3.82(a). Table 3.38 summarizes the average total corrosion losses at week 15 and Table C.10 shows the results of the Student's t-test. The total corrosion loss was 9.63 μm for uncoated conventional steel compared to 0.39 μm for epoxy-coated bars based on the total area exposed to the solution (M-ECR-50[2]), which is equal to 6% of the corrosion loss of uncoated steel. The difference in the average corrosion losses of M-N3-50 and is significant at $\alpha = 0.02$. The total corrosion loss for the epoxy-coated bars, based on the area of the four holes (M-ECR-50[1]) was 39.89 μm.

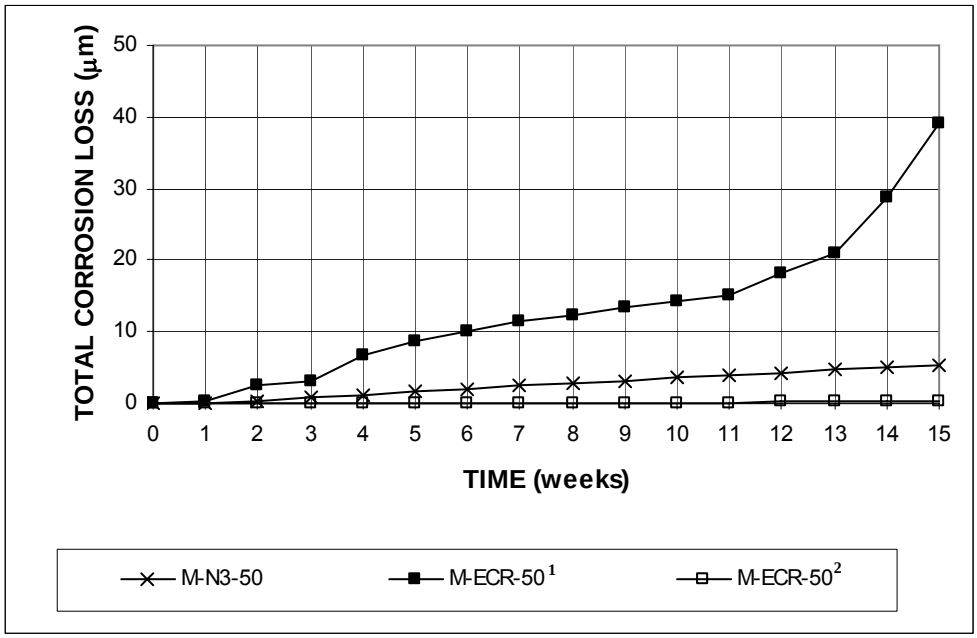


(a)

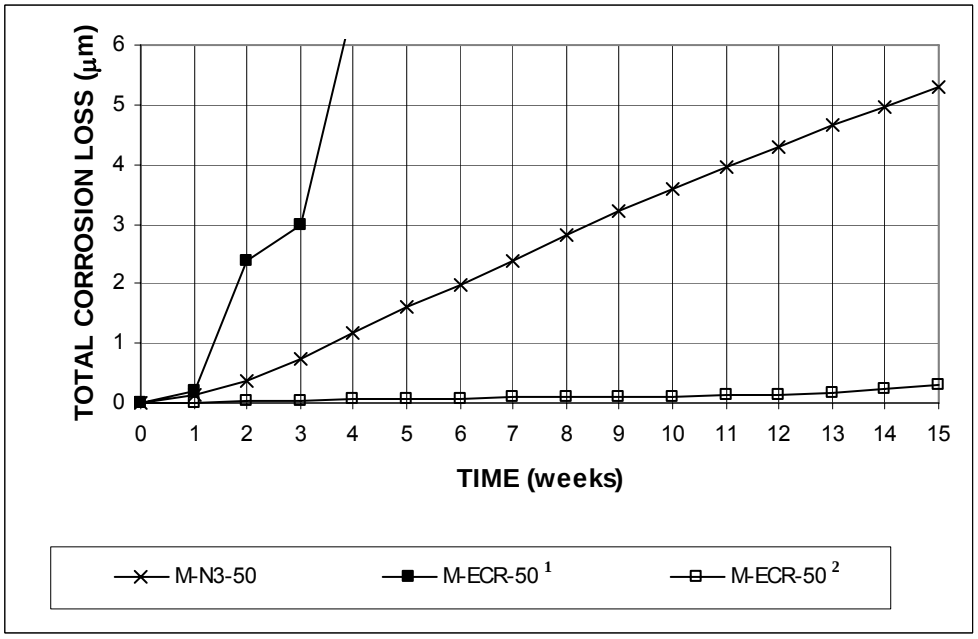


(b)

[1] Based on exposed area, four 3.2-mm (1/8-in.) diameter holes in epoxy
[2] Based on total area of bar exposed to solution

**Figure 3.82 –** Average total corrosion losses as measured in the rapid macrocell test for mortar-wrapped specimens in 1.6 m ion NaCl and simulated concrete pore solution for specimens with uncoated conventional and epoxy-coated steel.

**Table 3.38 –** Average total corrosion losses (in μm) at week 15 as measured in the rapid macrocell test for mortar-wrapped bars in 1.6 m ion NaCl and simulated concrete pore solution for specimens with uncoated conventional and epoxy-coated steel.

| Specimen designation* | Steel type | Specimen | | | | | | Average | Standard deviation |
|---|---|---|---|---|---|---|---|---|---|
| | | 1 | 2 | 3 | 4 | 5 | 6 | | |
| **Mortar-wrapped specimens in 1.6 m NaCl** | | | | | | | | | |
| **M-N3-50** | **N3** | 5.54 | 5.08 | 7.01 | 5.21 | 4.79 | 5.12 | 5.46 | 0.80 |
| **M-ECR-50** [1] | **ECR** | 2.18 | 130.70 | 10.26 | 63.87 | 28.81 | 3.51 | 39.89 | 50.14 |
| **M-ECR-50** [2] | **ECR** | 0.01 | 1.30 | 0.09 | 0.63 | 0.28 | 0.02 | 0.39 | 0.50 |

* M - A - B
**M**: macrocell test
**A**: steel type → N3: conventional, normalized steel, ECR: epoxy-coated steel
**B**: mix design → 50: water-cement ratio of 0.50 and no inhibitor.
[1] Based on exposed area, four 3.2-mm (1/8-in.) diameter holes in epoxy
[2] Based on total area of bar exposed to solution

The average corrosion potentials of the anodes and the cathodes with respect to a saturated calomel electrode are shown in Figure 3.83. Conventional steel had corrosion potentials as low as -0.600 V at week 4. The corrosion potential of the epoxy-coated bars remained near -0.300 V for most of the test period, but dropped to values close to -0.500 V at week 14. The corrosion potential for the conventional steel cathodes remained close to -0.275 V. For the epoxy-coated bars, the cathode potential remained near -0.200 V, indicating a more passive condition.

After the 15-week test period, the mortar was removed, and the bars were inspected. Three of the six epoxy-coated anodes exhibited corrosion products at the holes in the epoxy, while the other three anodes exhibited no corrosion products, as shown in Figures 3.84 and 3.85.

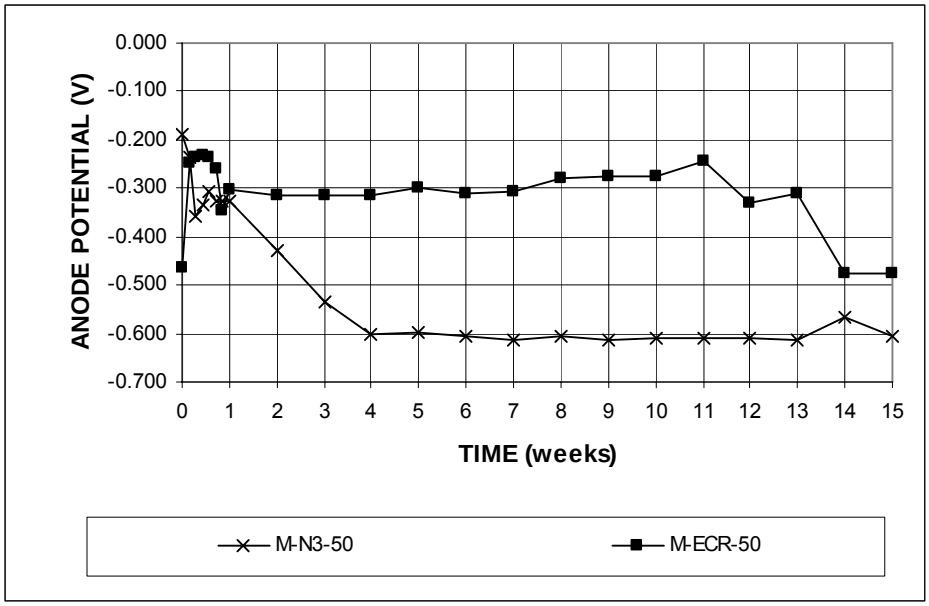


(a)

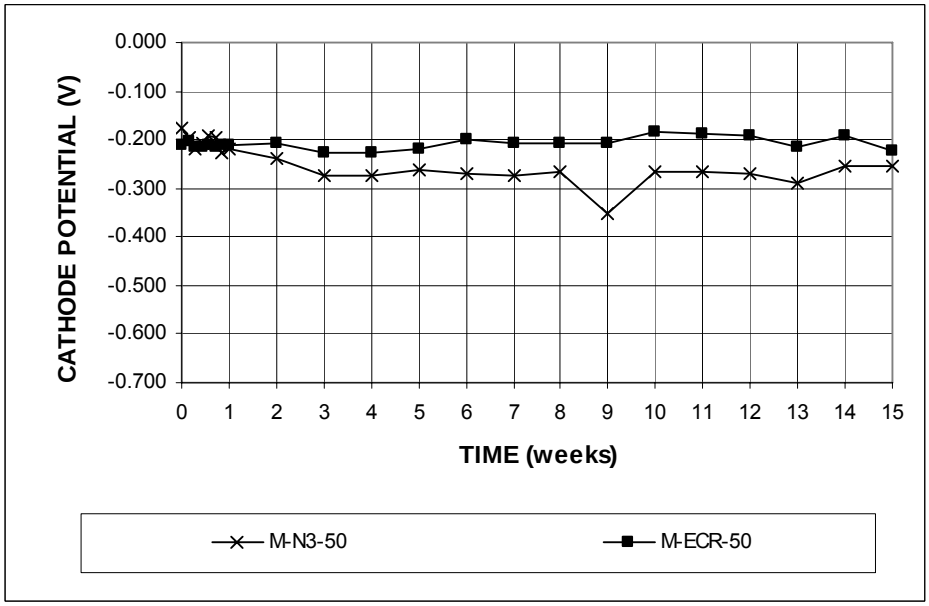


(b)

**Figure 3.83 –** (a) Average anode corrosion potentials and (b) average cathode corrosion potentials, with respect to saturated calomel electrode as measured in the rapid macrocell test. Mortar-wrapped specimens in 1.6 m ion NaCl and simulated concrete pore solution for specimens with uncoated conventional and epoxy-coated steel.

**Figure 3.84 –** Corrosion products on exposed steel on epoxy-coated anode bars after removal of mortar cover at week 15.

**Figure 3.85 –** Epoxy-coated anode bars with no corrosion products after removal of mortar cover at week 15.

### 3.6.2 Bench-Scale Tests

Southern Exposure and cracked beam tests were used to evaluate the epoxy-coated steel. The concrete had a water-cement ratio of 0.45 and no inhibitor. Uncoated steel was used in the bottom mats of the specimens. The epoxy coating was intentionally damaged by drilling four 3.2-mm ($^1/_8$-in.) diameter holes through the coating on each epoxy-coated bar.

#### 3.6.2.1 Southern Exposure Test

Figure 3.86 shows the average corrosion rates versus time for conventional and epoxy-coated steel in the Southern Exposure test. The corrosion rates of conventional steel increased gradually, and by week 70, the corrosion rate was 9.05 μm/year, as shown in Table 3.39. For the epoxy-coated bars, when the corrosion rate was calculated based on the exposed area (SE-ECR-45[1]), the corrosion rate at week 70 was 477 μm/year. When the corrosion rate was calculated based on the total area of the bars (SE-ECR-45[2]), the corrosion rate was 0.72 μm/year, corresponding to 8% of the corrosion rate of conventional steel. The difference in the average corrosion rates of SE-N3-45 and SE-ECR-45[2] is significant at $\alpha = 0.02$, as shown in Table C.9.

The average total corrosion losses as a function of time are shown in Figure 3.87, and the values at week 70 are summarized in Table 3.40. At week 70, conventional steel had a corrosion loss of 7.30 μm. The average corrosion loss for epoxy-coated steel was 229 μm, based on the exposed area of steel (SE-ECR-45[1]), and 0.31 μm based on the total area of the bars (SE-ECR-45[2]), equal to 4% of the corrosion loss of the uncoated bars. The difference in the average corrosion losses of SE-N3-45 and SE-ECR-45[2] is significant at $\alpha = 0.02$, as shown in Table C.10.

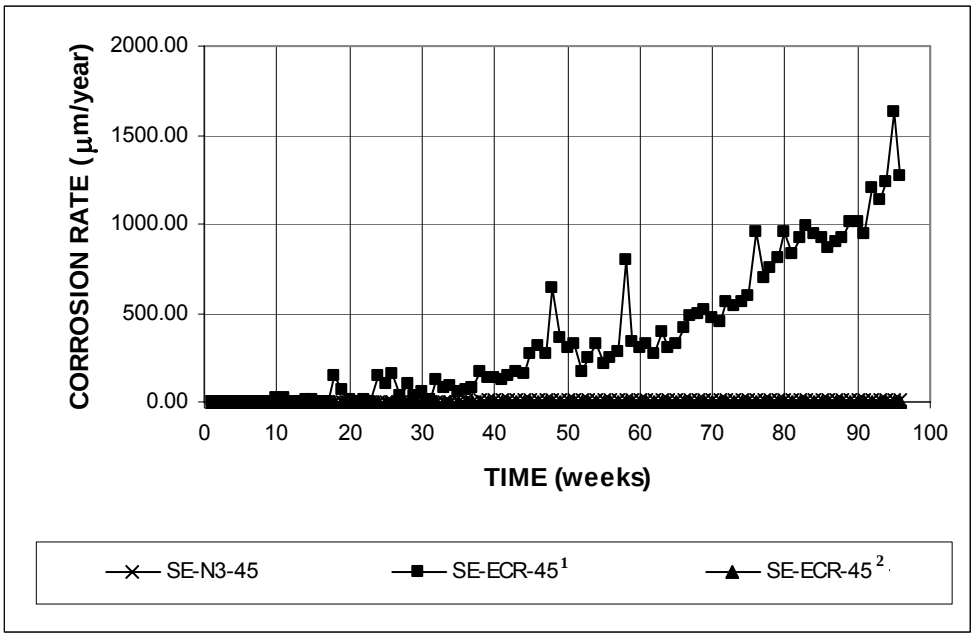


(a)

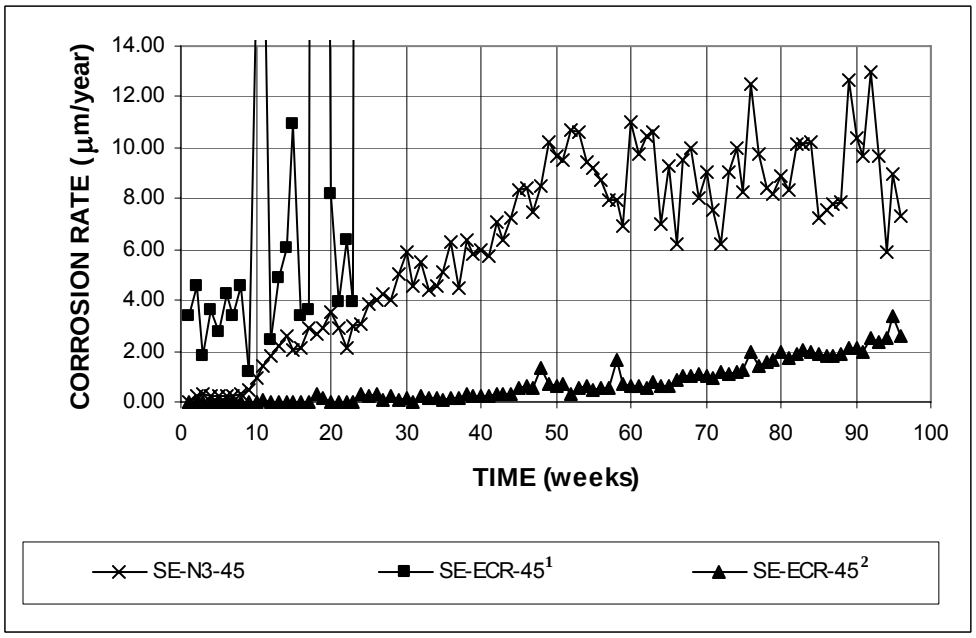


(b)

[1] Based on exposed area, four 3.2-mm (1/8-in.) diameter holes in epoxy
[2] Based on total area of bar exposed to solution

**Figure 3.86 –** Average corrosion rates as measured in the Southern Exposure test for specimens with uncoated conventional and epoxy-coated steel.

**Table 3.39 –** Average corrosion rates (in μm/year) at week 70 as measured in the Southern Exposure test for specimens with uncoated conventional and epoxy-coated steel.

| Specimen designation* | Steel type | Specimen | | | | | | Average | Standard deviation |
|---|---|---|---|---|---|---|---|---|---|
| | | 1 | 2 | 3 | 4 | 5 | 6 | | |
| **Southern Exposure test** | | | | | | | | | |
| **SE-N3-45** | **N3** | 13.96 | 11.83 | 4.48 | 5.47 | 14.32 | 4.21 | 9.05 | 4.83 |
| **SE-ECR-45** [1] | **ECR** | 777 | 723 | 414 | 816 | 33 | 99 | 476.93 | 349.24 |
| **SE-ECR-45** [2] | **ECR** | 1.61 | 1.49 | 0.86 | 1.69 | 0.07 | 0.20 | 0.99 | 0.72 |

* SE - A - B
**SE**: Southern Exposure test
**A**: steel type → N3: conventional, normalized steel, ECR: epoxy-coated steel
**B**: mix design → 45: water-cement ratio of 0.45 and no inhibitor.
[1] Based on exposed area, four 3.2-mm (1/8-in.) diameter holes in epoxy
[2] Based on total area of bar exposed to solution

**Table 3.40 –** Average total corrosion losses (in μm) at week 70 as measured in the Southern Exposure test for specimens with uncoated conventional and epoxy-coated steel.

| Specimen designation* | Steel type | Specimen | | | | | | Average | Standard deviation |
|---|---|---|---|---|---|---|---|---|---|
| | | 1 | 2 | 3 | 4 | 5 | 6 | | |
| **Southern Exposure test** | | | | | | | | | |
| **SE-N3-45** | **N3** | 9.80 | 13.01 | 2.50 | 5.90 | 8.65 | 3.95 | 7.30 | 3.92 |
| **SE-ECR-45** [1] | **ECR** | 412 | 418 | 153 | 210 | 77 | 102 | 228.64 | 151.47 |
| **SE-ECR-45** [2] | **ECR** | 0.85 | 0.86 | 0.32 | 0.43 | 0.16 | 0.21 | 0.47 | 0.31 |

* SE - A - B
**SE**: Southern Exposure test
**A**: steel type → N3: conventional, normalized steel, ECR: epoxy-coated steel
**B**: mix design → 45: water-cement ratio of 0.45 and no inhibitor.
[1] Based on exposed area, four 3.2-mm (1/8-in.) diameter holes in epoxy
[2] Based on total area of bar exposed to solution

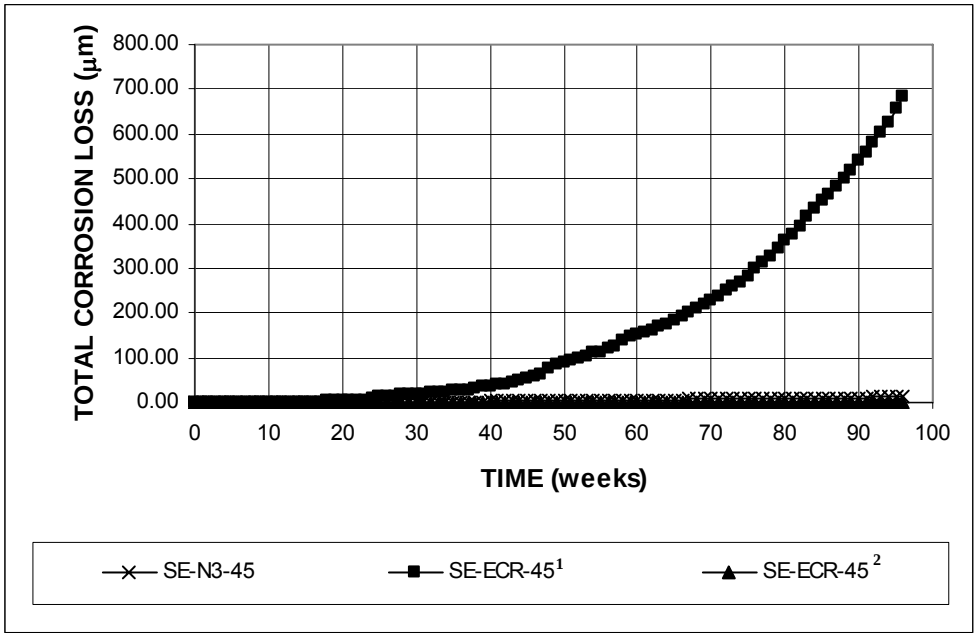


(a)

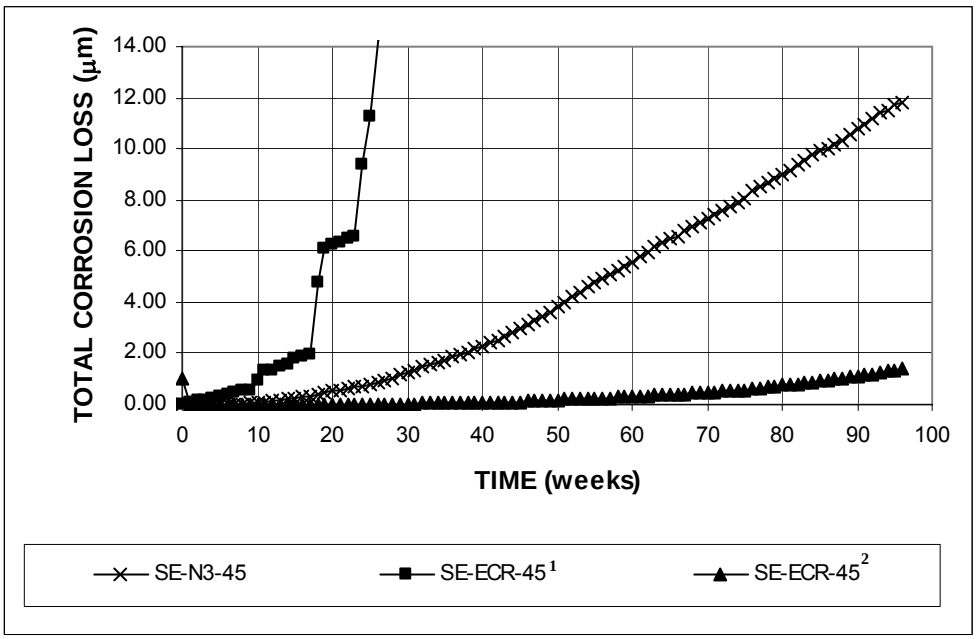


(b)

[1] Based on exposed area, four 3.2-mm (1/8-in.) diameter holes in epoxy
[2] Based on total area of bar exposed to solution

**Figure 3.87 –** Average total corrosion losses as measured in the Southern Exposure test for specimens with uncoated conventional and epoxy-coated steel.

Figure 3.88 shows the average corrosion potentials of the top and bottom mats of steel with respect to a copper-copper sulfate electrode. For both steels, the corrosion potential of the top mat was above -0.225 V during the first weeks of the test, and then dropped with time. At week 70, the corrosion potential of the top mat was more negative than -0.500 V for both steels, indicating active corrosion. For the bottom mat, corrosion potentials dropped at a lower rate than for the top mat, and by week 70, the corrosion potentials were between -0.350 V and -0.450 V. These values are also considered an indication of active corrosion. After week 70, the average bottom mat corrosion potential of specimens with epoxy-coated steel increased to values around -0.300 V, while the bottom mat corrosion potential of specimens with conventional steel decreased to values below -0.500 V.

Figure 3.89 shows the average mat-to-mat resistances for conventional and epoxy-coated steel. The mat-to-mat resistance for conventional steel remained below 500 ohms, while for epoxy-coated steel, it ranged from 1000 to 1700 ohms. This high resistance is caused by the epoxy coating. As noted earlier, the specimens with conventional steel showed a drop in the average mat-to-mat resistance at week 75 due to the formation of cracks in the specimen.

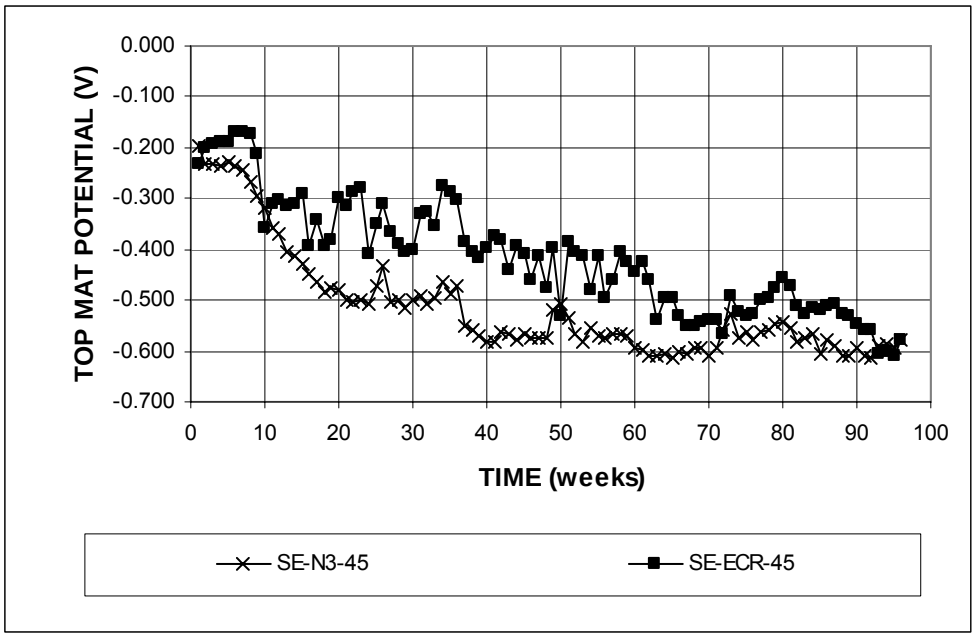


(a)

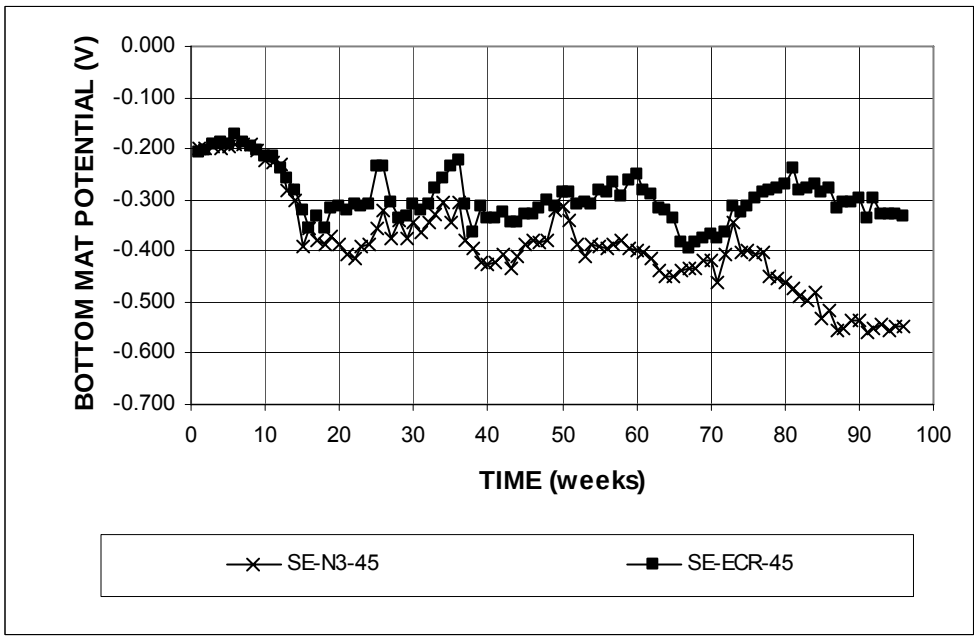


(b)

**Figure 3.88 –** (a) Average top mat corrosion potentials and (b) average bottom mat corrosion potentials, with respect to copper-copper sulfate electrode as measured in the Southern Exposure test for specimens with uncoated conventional and epoxy-coated steel.

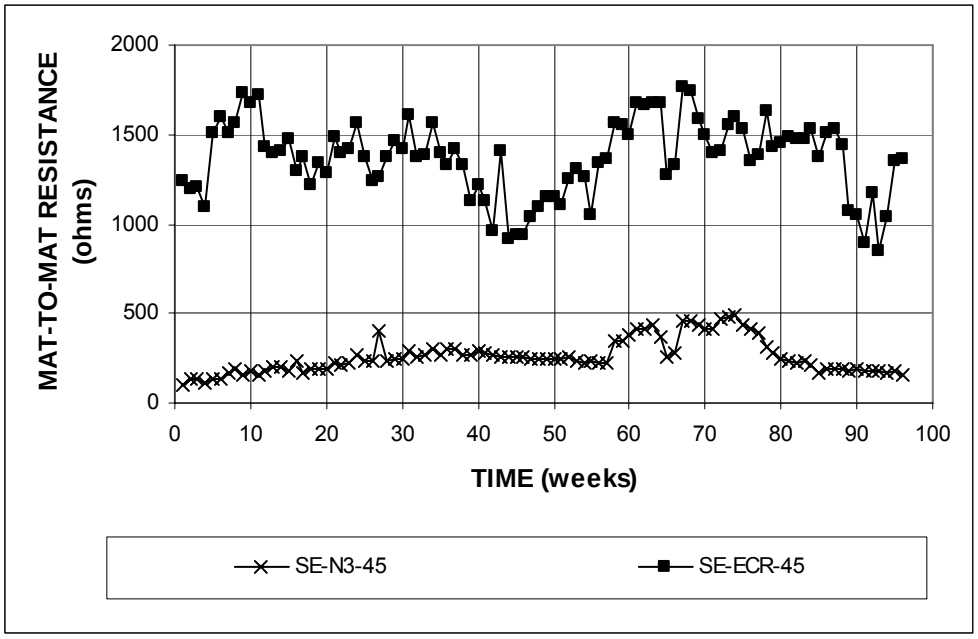


**Figure 3.89 –** Average mat-to-mat resistances as measured in the Southern Exposure test for specimens with uncoated conventional and epoxy-coated steel.

### 3.6.2.2 Cracked Beam Test

The average corrosion rates versus time for the cracked beam tests of conventional and epoxy-coated steel are shown in Figure 3.90. Conventional steel had a corrosion rate that was above 15 μm/year during the first 5 weeks and that ranged from 2 to 10 μm/year after week 10, with a jump to values above 20 μm/year between weeks 46 and 52. Based on the exposed area of steel in the epoxy-coated bars, the corrosion rate for most of the test period ranged from 400 to 1200 μm/year, with higher values at the beginning and end of the test period; based on the total area of steel, the corrosion rates were below 4 μm/year during the test period. Table 3.41 summarizes the corrosion rates at week 70 and Table C.9 shows the results of the Student's t-test. Conventional steel had a corrosion rate of 9.09 μm/year, while epoxy-coated bars had a corrosion rate of 1.79 μm/year, based on the total area of the bars (CB-ECR-45[2]), corresponding to 20% of the corrosion rate of the uncoated steel.

The difference in the average corrosion rates of CB-N3-45 and CB-ECR-45[2] is significant at $\alpha = 0.20$. A corrosion rate of 870 μm/year was obtained for epoxy-coated bars based on the exposed area of steel (CB-ECR-45[1]).

Figure 3.91 shows the average total corrosion losses versus time for the conventional and epoxy coated bars. Table 3.42 summarizes the average total corrosion losses through week 70, at which time conventional steel had a corrosion loss of 11.60 μm, compared with 2.26 μm for epoxy-coated bars based on the total area of the bars (CB-ECR-45[2]). The latter is equal to 19% of the corrosion loss of conventional steel. The difference in the average corrosion losses of CB-N3-45 and CB-ECR-45[2] is significant at $\alpha = 0.05$, as shown in Table C.10. The average total corrosion loss for the epoxy-coated bars based on the exposed area of steel (CB-ECR-45[1]) was 1094 μm. The high corrosion losses at the exposed steel areas in all of the tests emphasize the potential negative impact of combining epoxy-coated steel (which is likely to be damaged during construction) with uncoated steel, as has been done in some bridge decks.

**Table 3.41 –** Average corrosion rates (in μm/year) at week 70 as measured in the cracked beam test for specimens with uncoated conventional and epoxy-coated steel.

| Specimen designation* | Steel type | Specimen | | | | | | Average | Standard deviation |
|---|---|---|---|---|---|---|---|---|---|
| | | 1 | 2 | 3 | 4 | 5 | 6 | | |
| **Cracked beam test** | | | | | | | | | |
| **CB-N3-45** | **N3** | 20.37 | 1.70 | 23.30 | 1.58 | 5.28 | 2.31 | 9.09 | 10.01 |
| **CB-ECR-45** [1] | **ECR** | 2131 | 439 | 976 | 859 | 29 | 786 | 869.89 | 707.27 |
| **CB-ECR-45** [2] | **ECR** | 4.40 | 0.90 | 2.01 | 1.77 | 0.06 | 1.62 | 1.79 | 1.46 |

* CB - A - B
**CB**: cracked beam test
**A**: steel type → N3: conventional, normalized steel, ECR: epoxy-coated steel
**B**: mix design → 45: water-cement ratio of 0.45 and no inhibitor.
[1] Based on exposed area, four 3.2-mm (1/8-in.) diameter holes in epoxy
[2] Based on total area of bar exposed to solution

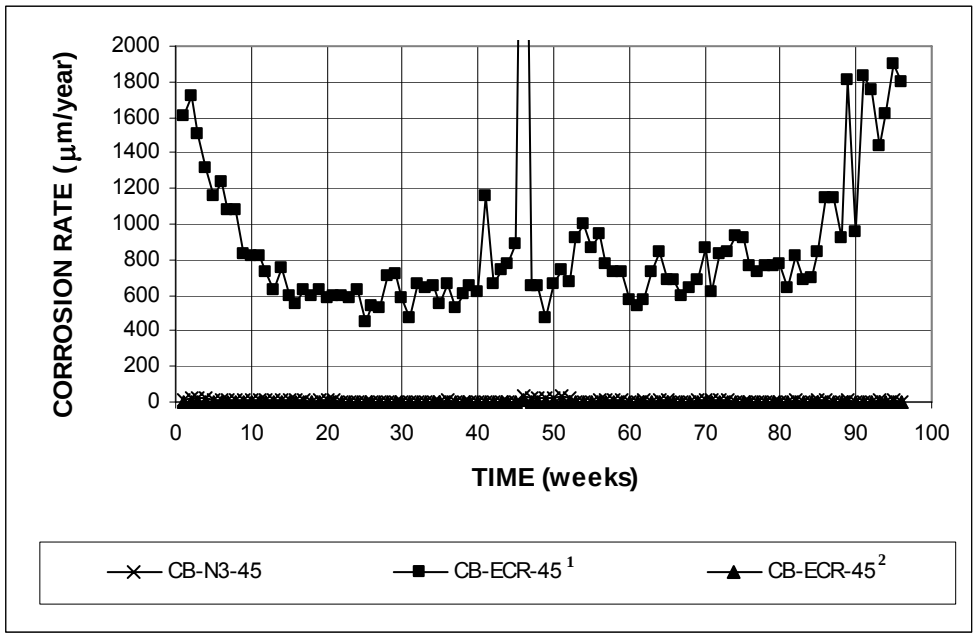


(a)

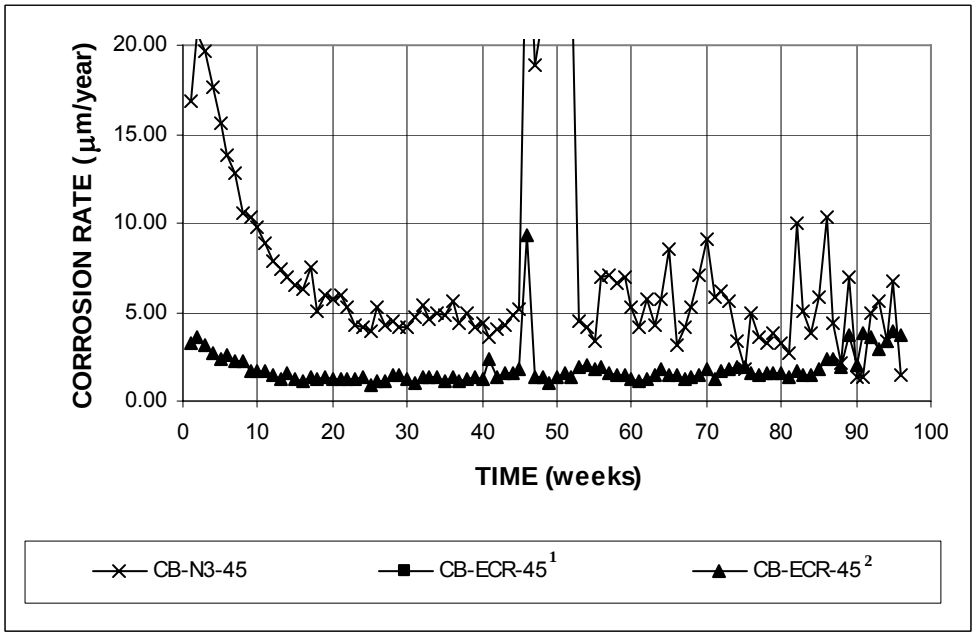


(b)

[1] Based on exposed area, four 3.2-mm (1/8-in.) diameter holes in epoxy
[2] Based on total area of bar exposed to solution

**Figure 3.90 –** Average corrosion rates as measured in the cracked beam test for specimens with uncoated conventional and epoxy-coated steel.

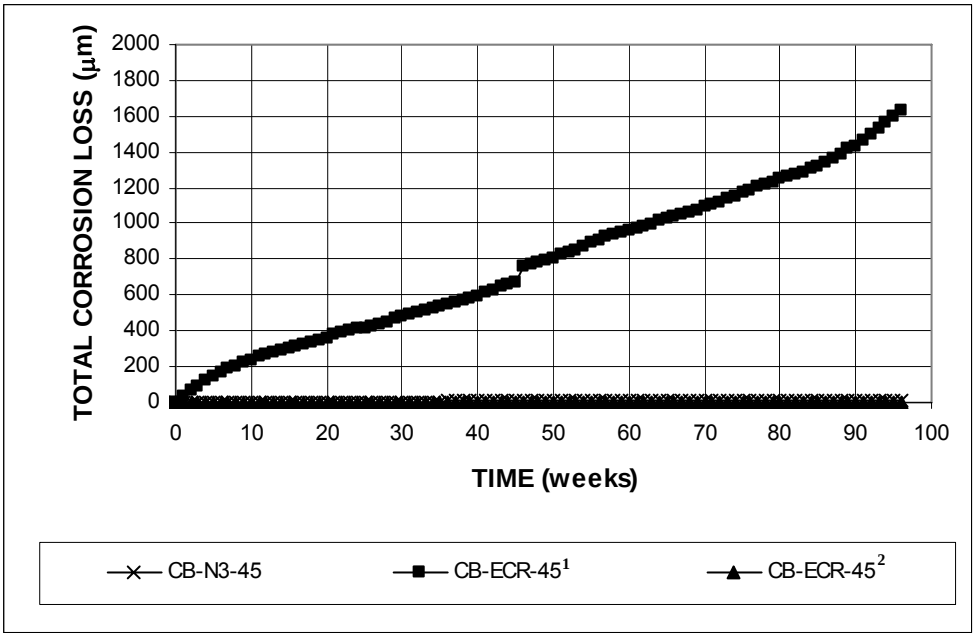


(a)

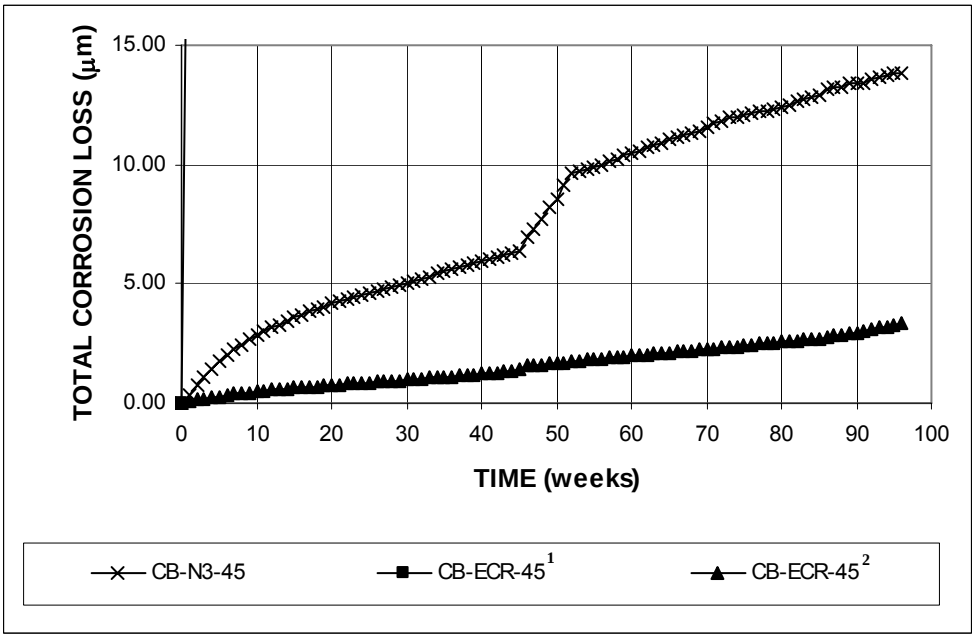


(b)

[1] Based on exposed area, four 3.2-mm (1/8-in.) diameter holes in epoxy
[2] Based on total area of bar exposed to solution

**Figure 3.91 –** Average total corrosion losses as measured in the cracked beam test for specimens with uncoated conventional and epoxy-coated steel.

**Table 3.42 –** Average total corrosion losses (in μm) at week 70 as measured in the cracked beam test for specimens with uncoated conventional and epoxy-coated steel.

| Specimen designation* | Steel type | Specimen | | | | | | Average | Standard deviation |
|---|---|---|---|---|---|---|---|---|---|
| | | 1 | 2 | 3 | 4 | 5 | 6 | | |
| **Cracked beam test** | | | | | | | | | |
| **CB-N3-45** | **N3** | 26.09 | 12.25 | 10.94 | 5.68 | 6.52 | 8.15 | 11.60 | 7.53 |
| **CB-ECR-45** [1] | **ECR** | 2215 | 708 | 1347 | 1748 | 208 | 340 | 1094.20 | 806.22 |
| **CB-ECR-45** [2] | **ECR** | 4.57 | 1.46 | 2.78 | 3.61 | 0.43 | 0.70 | 2.26 | 1.66 |

* CB - A - B
**CB**: cracked beam test
**A**: steel type → N3: conventional, normalized steel, ECR: epoxy-coated steel
**B**: mix design → 45: water-cement ratio of 0.45 and no inhibitor.
[1] Based on exposed area, four 3.2-mm (1/8-in.) diameter holes in epoxy
[2] Based on total area of bar exposed to solution

The average corrosion potentials of the top and bottom mats of steel with respect to a copper-copper sulfate electrode are shown in Figure 3.92. The corrosion potentials for both types of bars were similar throughout the test period. The potentials for the top mat were consistently negative than -0.400 V, indicating active corrosion. For the bottom mat, the corrosion potential started around -0.250 V, indicating a low probability for corrosion; by week 70, however, it had dropped to values below -0.400 V, indicating active corrosion. At week 82, the bottom mat potential for the uncoated steel dropped, and by week 85 it had values that were more negative than -0.500 V, indicating a significant chloride content at the level of the bottom mat.

The average mat-to-mat resistances are presented in Figure 3.93. For conventional steel, the mat-to-mat resistance remained below 1000 ohms for most of the test period, with values above 1000 ohms from week 68 to week 73. For the epoxy-coated bars, the mat-to-mat resistance started at approximately 800 ohms and increase up to values of 4000 ohms by week 70.

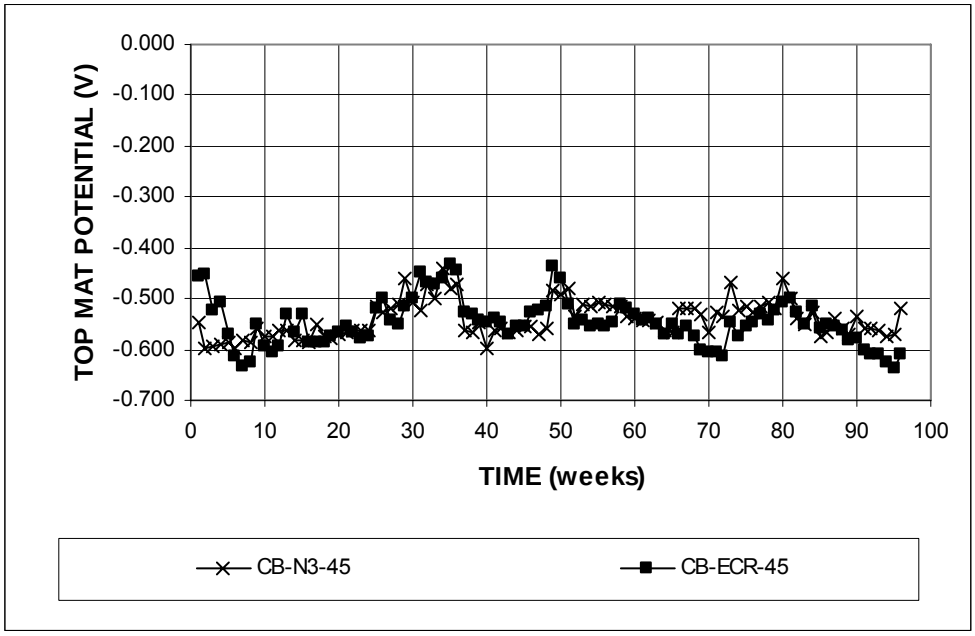


(a)

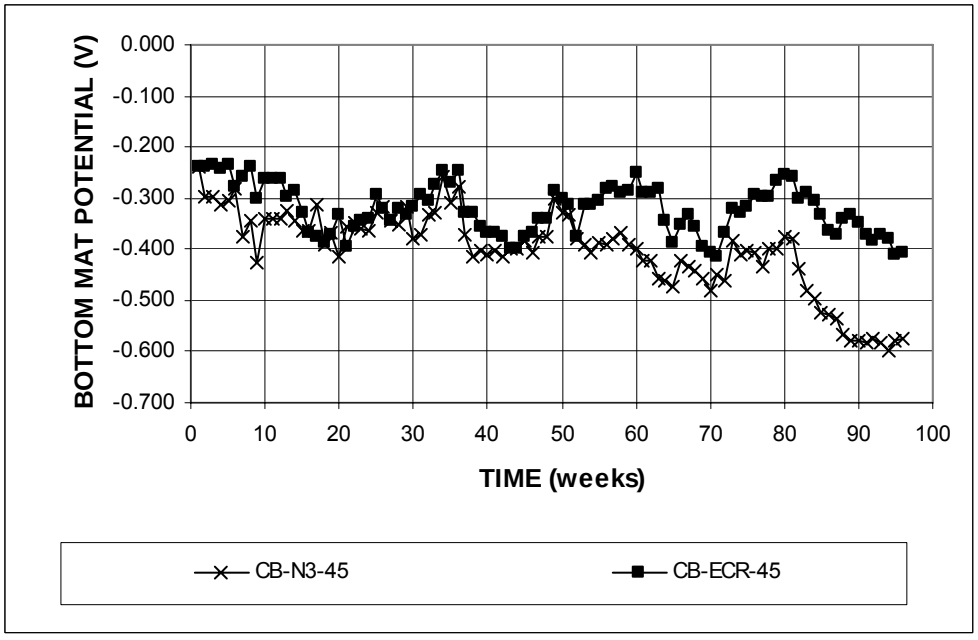


(b)

**Figure 3.92 –** (a) Average top mat corrosion potentials and (b) average bottom mat corrosion potentials, with respect to copper-copper sulfate electrode as measured in the cracked beam test for specimens with uncoated conventional and epoxy-coated steel.

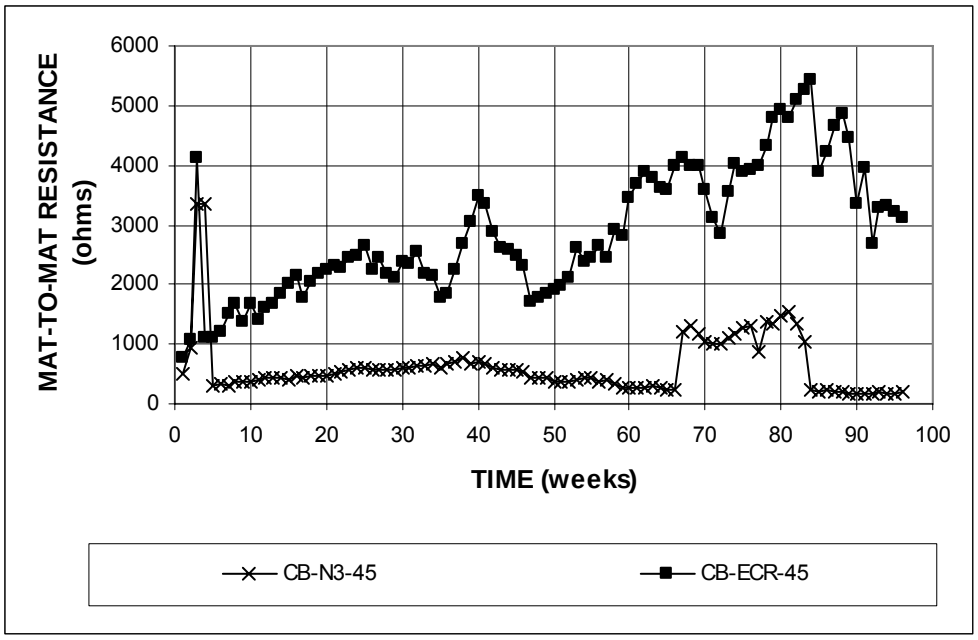


**Figure 3.93 –** Average mat-to-mat resistances as measured in the cracked beam test for specimens with uncoated conventional and epoxy-coated steel.

## 3.7 DUPLEX STAINLESS STEELS

This section describes the results of the macrocell and bench-scale tests for the duplex steels listed in Section 2.2. The steels include 2205 (22% chromium and 5% nickel) and two heats of 2101 (21% chromium and 1% nickel). The steels were tested in both the "as-rolled" and pickled condition. In the latter case, pickling was used to remove the mill scale from the bar surface. As described in Section 2.1, the duplex stainless steel bars labeled 2101(1) lacked boron, and as a result, the bars were slightly deformed and showed small cracks on the surface. The duplex steel labeled 2101(2) steel was received as a replacement. In addition to testing in an as-rolled and pickled condition, the 2101(2) steel was tested after sandblasting to remove the mill scale and is designated 2101(2)s.

### 3.7.1 Rapid Macrocell Test

Bare steel specimens were used to evaluate the steel in 1.6 and 6.04 m ion NaCl and simulated concrete pore solution. Mortar-wrapped specimens were used to evaluate the steels in a 1.6 m ion NaCl and simulated concrete pore solution. The mortar had a water-cement ratio of 0.50.

#### 3.7.1.1 Bare Bars

Figure 3.94 shows the average corrosion rates versus time for bare bars in the 1.6 m ion NaCl solution. Conventional steel has the highest corrosion rate during the test period, with the sandblasted 2101(2) steel exhibiting similar corrosion rates to conventional steel between weeks 4 and 10. 2101(2) steel shows a jump in the average corrosion rate at week 12, caused by a jump in one of the specimens, which had corrosion rates above 1.5 μm/year from weeks 12 to 14. 2205 steel also shows a jump in the average corrosion rate at week 9 [Figure 3.94(b)]. In this case, it was caused by a jump in the corrosion rate of one of the specimens at that week. The corrosion rate returned to the previous lower values at week 10. The remaining specimens remained below 0.25 μm/year. Table 3.43 summarizes the average corrosion rates at week 15 and Table C.11 shows the results of the Student's t-test. As shown in Table 3.43, at the end of the test period, conventional steel had a corrosion rate of 35.88 μm/year, while 2101(2)s steel had a corrosion rate of 11.78 μm/year. The lowest corrosion rates were exhibited by 2205p and 2101(2)p steels, at 0.09 and 0.04 μm/year, respectively. These values correspond to 0.25% and 0.10%, respectively, of the corrosion rate of conventional steel. The remaining steels had corrosion rates between 0.13 and 3.05 μm/year. The difference in the average corrosion rates of N3 and 2101(2)s is statistically significant at $\alpha = 0.20$, and the

difference in the average corrosion rates of N3 compared to the remaining steels is significant at $\alpha = 0.02$. Overall, 2205 steel had lower corrosion rates than 2101(1) and 2101(2) steels when evaluated in the same condition (i.e. pickled or non-pickled). Bars that were pickled had lower corrosion rates than bars of the same steel that were not pickled. Table C.12 shows the results of the Student's t-test for comparing the average corrosion rates of pickled bars versus non-pickled bars. The results indicate that the difference in the average corrosion rates between 2205 and 2205p steel is not significant, while the difference in the average corrosion rates between 2101(1) and 2101(1)p steel is significant at $\alpha = 0.02$. For 2101(2) steel, the difference in the corrosion rates between the pickled and non-pickled bars is significant at $\alpha = 0.05$. Since 2101(2)p and 2205p had the lowest average corrosion rates, the Student's t-test was also performed to determine if their means could be considered equal. The results show that there is a significant difference in their mean corrosion rates at $\alpha = 0.05$.

**Table 3.43 –** Average corrosion rates (in μm/year) at week 15 as measured in the rapid macrocell test for bare bars in 1.6 m ion NaCl and simulated concrete pore solution for specimens with conventional and duplex stainless steel.

| Specimen designation* | Steel type | Specimen | | | | | | Average | Standard deviation |
|---|---|---|---|---|---|---|---|---|---|
| | | 1 | 2 | 3 | 4 | 5 | 6 | | |
| **Bare bars in 1.6 m NaCl** | | | | | | | | | |
| **M-N3** | **N3** | 52.60 | 0.26 | 67.77 | 40.17 | 32.43 | 22.08 | 35.88 | 23.61 |
| **M-2205** | **2205** | 0.12 | 0.29 | 0.09 | 0.03 | 0.12 | | 0.13 | 0.10 |
| **M-2205p** | **2205p** | 0.09 | 0.06 | 0.14 | 0.09 | 0.09 | | 0.09 | 0.03 |
| **M-2101(1)** | **2101(1)** | 3.12 | 1.73 | 1.42 | 2.17 | 3.53 | | 2.39 | 0.90 |
| **M-2101(1)p** | **2101(1)p** | 0.43 | 0.00 | 0.00 | 0.23 | 0.20 | | 0.17 | 0.18 |
| **M-2101(2)** | **2101(2)** | 0.06 | 6.79 | 1.68 | 3.44 | 4.02 | 2.31 | 3.05 | 2.30 |
| **M-2101(2)p** | **2101(2)p** | 0.06 | 0.03 | 0.00 | 0.00 | 0.06 | 0.09 | 0.04 | 0.03 |
| **M-2101(2)s** | **2101(2)s** | 0.49 | 0.12 | 0.14 | 8.03 | 59.42 | 2.49 | 11.78 | 23.53 |

* M - A
**M**: macrocell test
**A**: steel type → N3: conventional, normalized steel, 2101(1) and 2101(2): Duplex stainless steel (21% chromium, 1% nickel), 2205: Duplex stainless steel (25% chromium, 5% nickel), p: pickled, s: sandblasted.

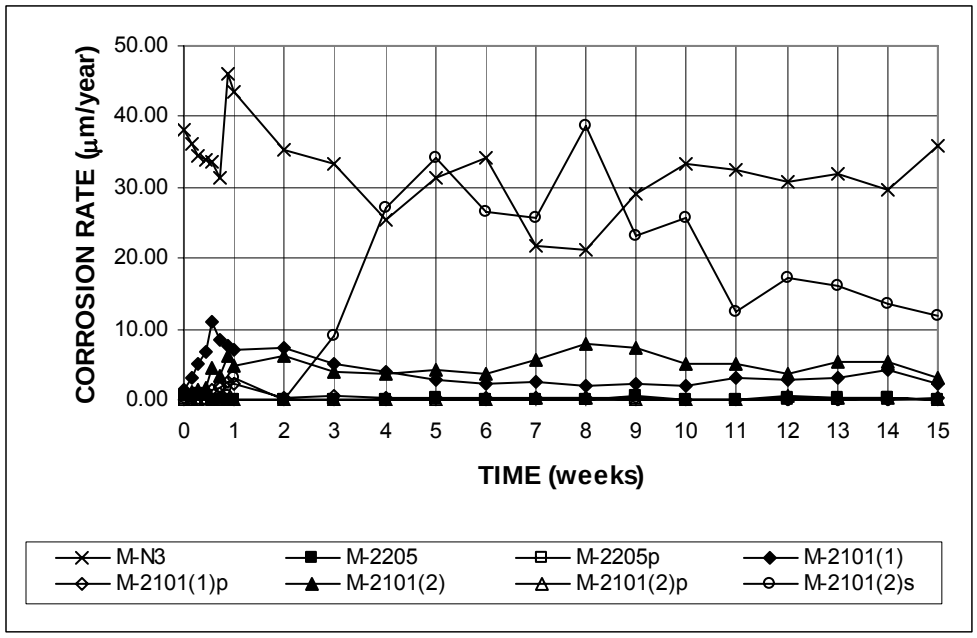


(a)

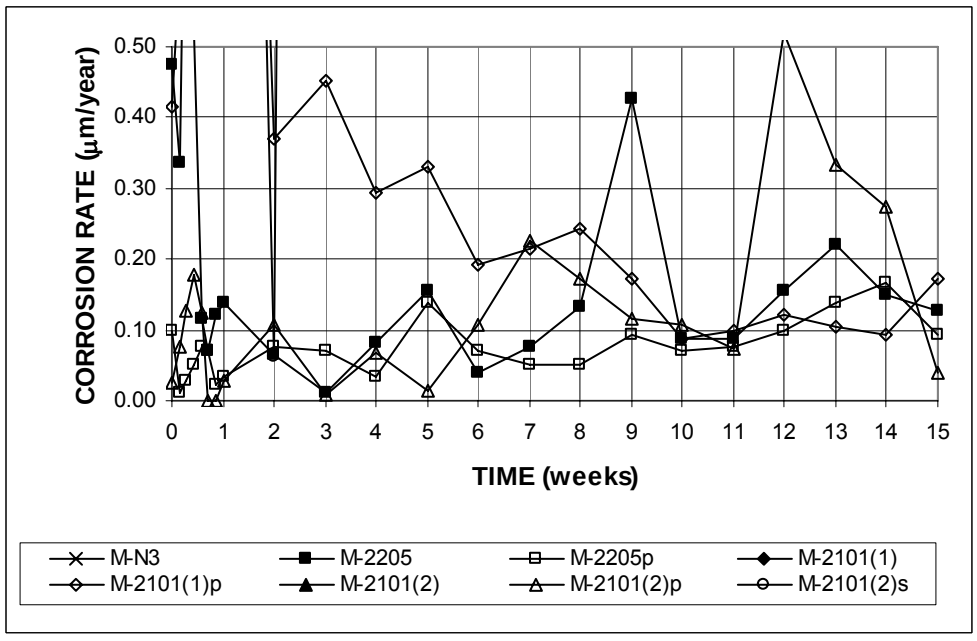


(b)

**Figure 3.94 –** Average corrosion rates as measured in the rapid macrocell test for bare bars in 1.6 m ion NaCl and simulated concrete pore solution for specimens with conventional and duplex stainless steel.

The average total corrosion losses versus time are shown in Figure 3.95, and the values at week 15 are summarized in Table 3.44. Results of the Student's t-test are presented in Table C.13. After 15 weeks, conventional steel had undergone the highest corrosion loss, 9.03 μm, followed by 2101(2)s at 5.48 μm. The lowest corrosion losses occurred for 2205p steel at 0.02 μm (0.2% of the corrosion loss of conventional steel) and 2205 and 2101(2)p steels with losses of 0.04 μm (0.4% of the corrosion loss of conventional steel). The non-pickled 2101 steels had corrosion losses of 1.01 and 1.45 μm for 2101(1) and 2101(2) steel, respectively. The difference in the corrosion losses of N3 and 2101(2)s is not statistically significant. The difference in the corrosion losses of N3 with the remaining steels is significant at $\alpha$ = 0.02. The use of sandblasting to remove the mill scale on the bars is not effective. The sandblasted bars had corrosion rates and losses that were much higher than the bars that were tested with mill scale or pickled. The difference in the corrosion loss of pickled and non-pickled bars was also evaluated (Table C.14). Results show that the difference between 2101(1) and 2101(1)p, and 2205 and 2205p, is significant at $\alpha$ = 0.20, while the difference between 2101(2) and 2101(2)p is significant at $\alpha$ = 0.02. Since 2205p and 2101(2)p steels had the lowest corrosion rates and losses, they were compared with the Student's t-test and the results show that the difference in the corrosion losses of 2205p and 2101(2)p is not statistically significant.

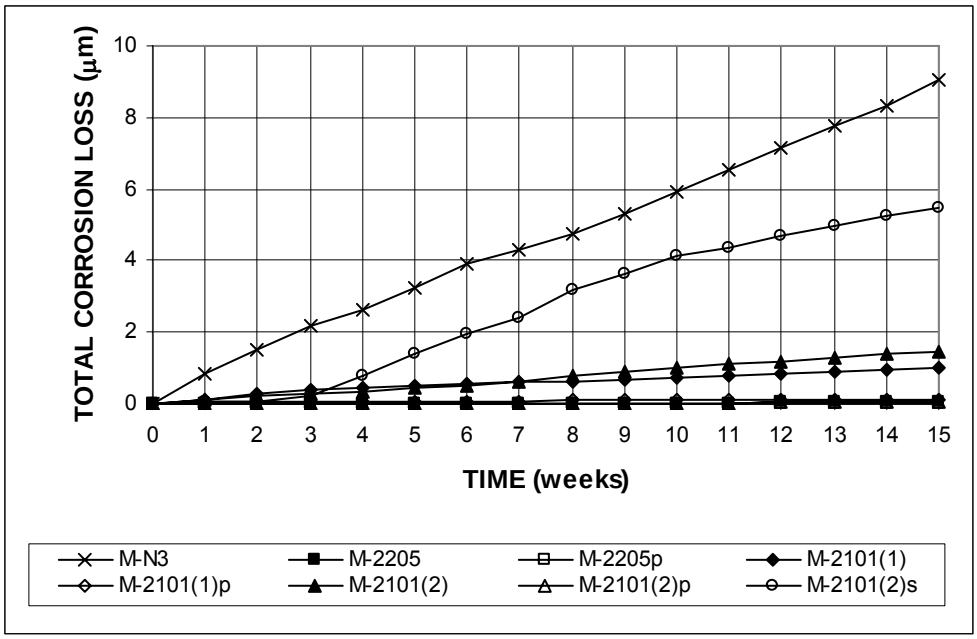


(a)

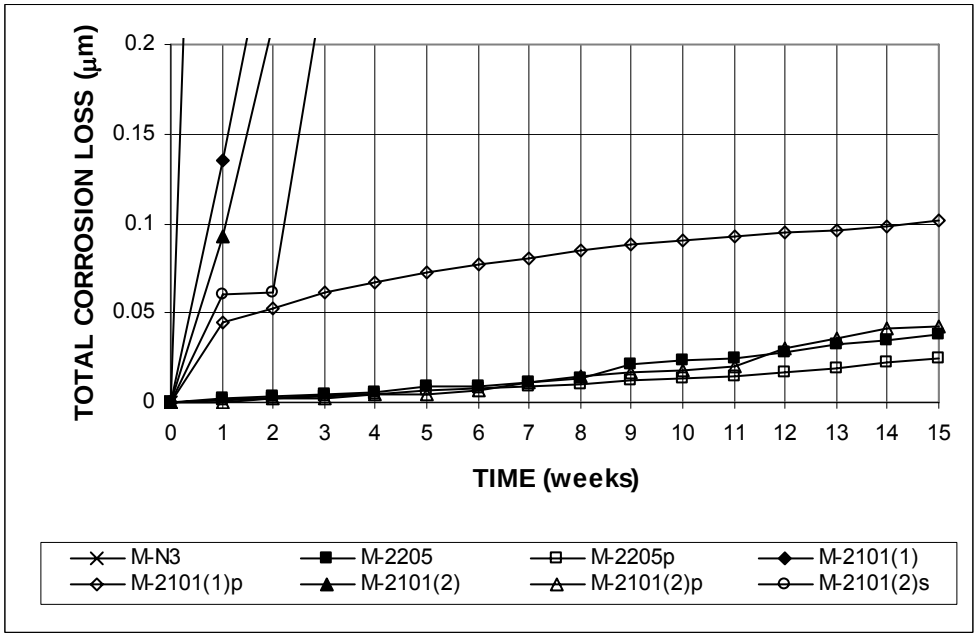


(b)

**Figure 3.95 –** Average total corrosion losses as measured in the rapid macrocell test for bare bars in 1.6 m ion NaCl and simulated concrete pore solution for specimens with conventional and duplex stainless steel.

**Table 3.44 –** Average total corrosion losses (in μm) at week 15 as measured in the rapid macrocell test for bare bars in 1.6 m ion NaCl and simulated concrete pore solution for specimens with conventional and duplex stainless steel.

| Specimen designation* | Steel type | Specimen | | | | | | Average | Standard deviation |
|---|---|---|---|---|---|---|---|---|---|
| | | 1 | 2 | 3 | 4 | 5 | 6 | | |
| **Bare bars in 1.6 m NaCl** | | | | | | | | | |
| **M-N3** | **N3** | 13.07 | 4.84 | 13.22 | 11.10 | 6.97 | 4.98 | 9.03 | 3.91 |
| **M-2205** | **2205** | 0.03 | 0.03 | 0.03 | 0.06 | 0.03 | | 0.04 | 0.01 |
| **M-2205p** | **2205p** | 0.03 | 0.02 | 0.03 | 0.02 | 0.02 | | 0.02 | 0.00 |
| **M-2101(1)** | **2101(1)** | 0.67 | 0.69 | 0.32 | 0.55 | 2.85 | | 1.01 | 1.04 |
| **M-2101(1)p** | **2101(1)p** | 0.17 | 0.05 | 0.01 | 0.17 | 0.12 | | 0.10 | 0.07 |
| **M-2101(2)** | **2101(2)** | 1.40 | 1.57 | 1.29 | 0.81 | 1.58 | 2.04 | 1.45 | 0.40 |
| **M-2101(2)p** | **2101(2)p** | 0.04 | 0.01 | 0.02 | 0.03 | 0.02 | 0.13 | 0.04 | 0.04 |
| **M-2101(2)s** | **2101(2)s** | 0.40 | 0.45 | 1.58 | 12.10 | 12.86 | 5.47 | 5.48 | 5.74 |

* M - A
**M**: macrocell test
**A**: steel type → N3: conventional, normalized steel, 2101(1) and 2101(2): Duplex stainless steel (21% chromium, 1% nickel), 2205: Duplex stainless steel (25% chromium, 5% nickel), p: pickled, s: sandblasted.

The average anode and cathode potentials with respect to a saturated calomel electrode are shown in Figure 3.96. Conventional steel had an anode potential that was more negative than -0.400 V throughout the test period, indicating active corrosion. Steels 2101(1), 2101(2), and 2101(2)s had anode potentials between -0.200 and -0.300 V. The remaining steels had anode potentials that were more positive than -0.175 V, indicating a low probability for corrosion. All steels had cathode potentials that were more positive than -0.200 V, and the corrosion potentials became more positive with time, with the exception of conventional steel, which remained at -0.200 V.

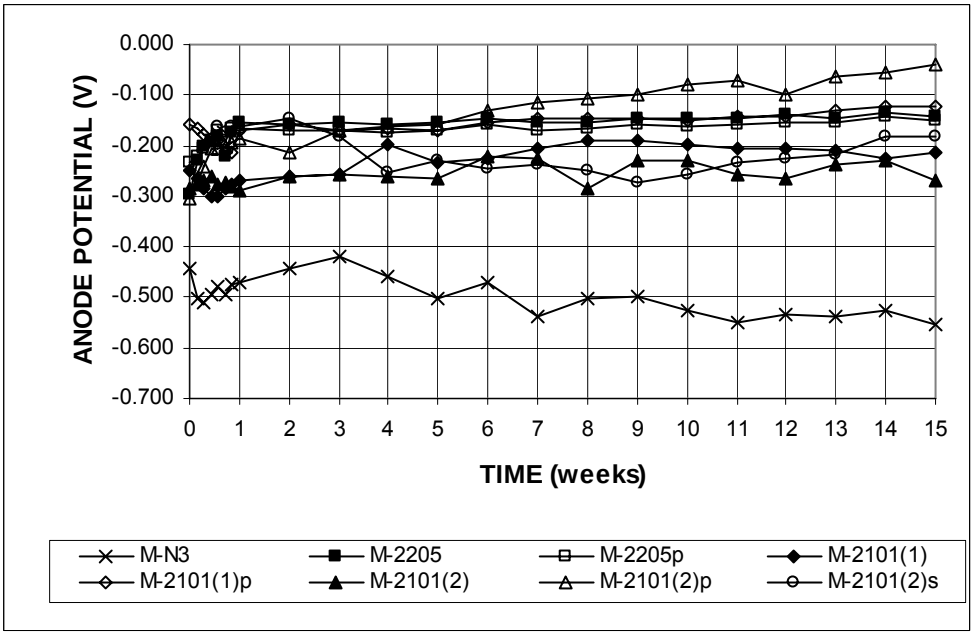


(a)

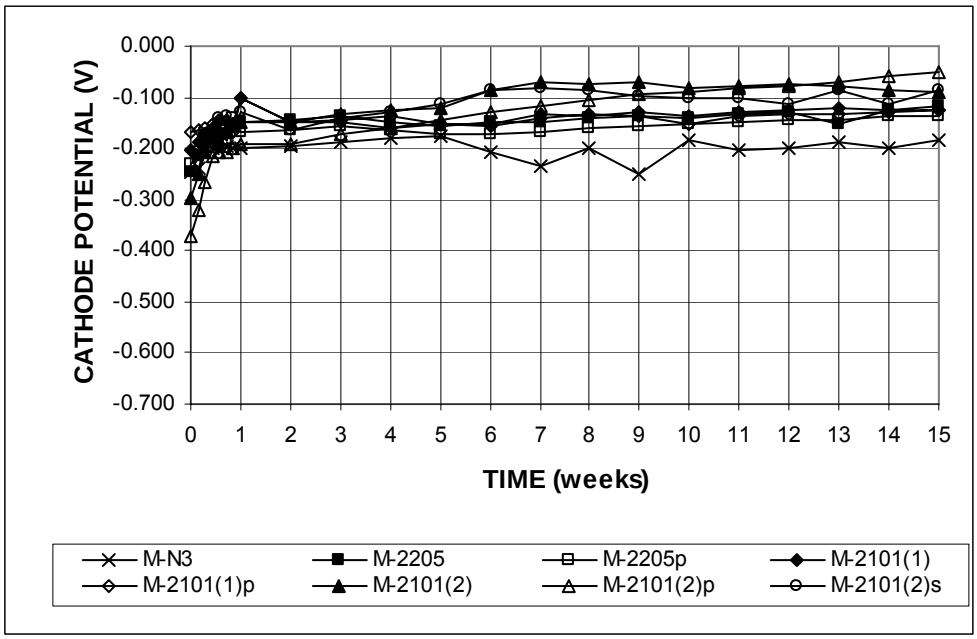


(b)

**Figure 3.96 –** (a) Average anode corrosion potentials and (b) average cathode corrosion potentials, with respect to saturated calomel electrode as measured in the rapid macrocell test for bare bars in 1.6 m ion NaCl and simulated concrete pore solution for specimens with conventional and duplex stainless steel.

Figure 3.97 shows the average corrosion rates versus time for bare bars in 6.04 m ion NaCl and simulated concrete pore solution. Conventional steel, N3, and 2101(2)s had the highest average corrosion rates, with values above 20 μm/year during the test period. 2101(1) and 2101(2) had corrosion rates between 10 and 20 μm/year. The corrosion rate for 2101(1)p was approximately 8 μm/year for the first 4 weeks and dropped to about 5 μm/year for the rest of the test period. The average corrosion rate for 2101(2)p steel was below 0.25 μm/year for the first 6 weeks and increased to values as high as 2 μm/year at week 12. The corrosion rate for 2205 steel was below 0.25 μm/year for the first 5 weeks and increased to values as high as 3.8 μm/year later in the test period, while for 2205p, the corrosion rates remained below 0.30 μm/year throughout the test period. Table 3.45 shows the average corrosion rates at week 15 and Tables C.11 and C.12 show the results of the Student's t-test. Conventional steel had the highest corrosion rate at 25.46 μm/year, followed by 2101(2)s at 22.83 μm/year. The difference in the average corrosion rates of N3 and 2101(2)s is not statistically significant. 2205p steel had the lowest corrosion rate at 0.28 μm/year, equal to 1.0% of the corrosion rate of conventional steel. 2101(1) and 2101(2) steel had corrosion rates of 13.61 and 11.04 μm/year, respectively. 2101(1)p steel had a corrosion rate of 4.46 μm/year (18% of the corrosion rate of conventional steel) and 2101(2)p had a corrosion rate of 0.96 μm/year (4% of the corrosion rate of conventional steel). The difference in the average corrosion rate between conventional steel and either 2205, 2205p, 2101(1)p, and 2101(2)p steels is significant at $\alpha = 0.02$. The differences between 2205 and 2205p, and between 2101(2) and 2101(2)p are also significant at $\alpha = 0.02$, while the difference between 2101(1) and 2101(1) is significant at $\alpha = 0.05$. The difference between 2205p and 2101(2)p steel is not statistically significant.

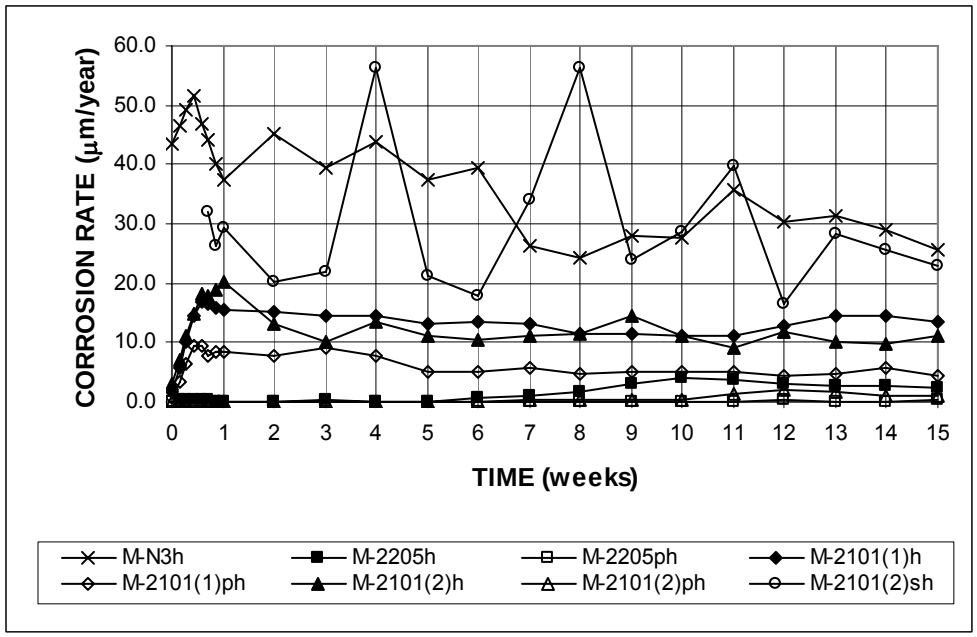


(a)

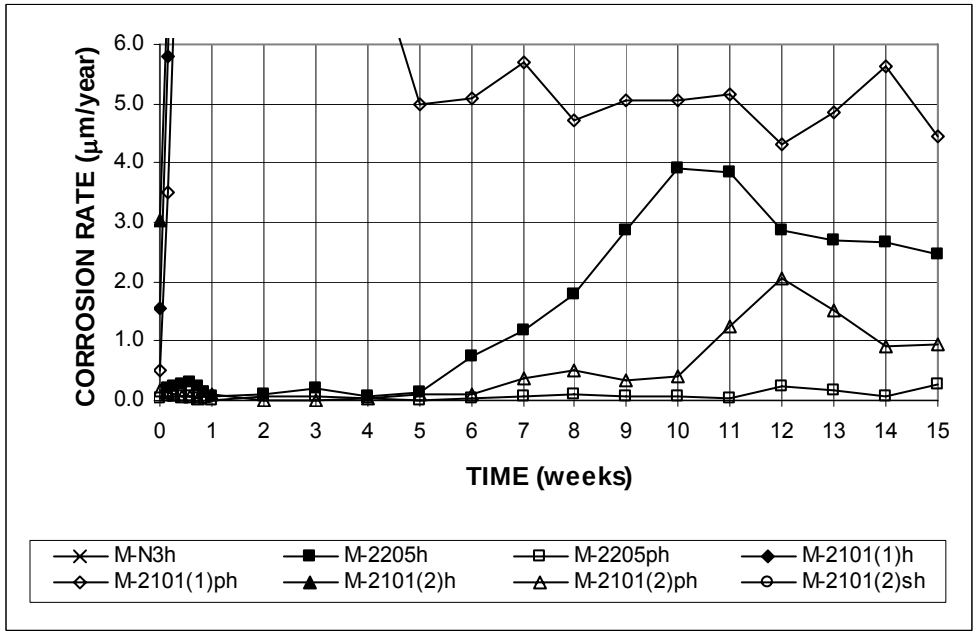


(b)

**Figure 3.97 –** Average corrosion rates as measured in the rapid macrocell test for bare bars in 6.04 m ion NaCl and simulated concrete pore solution for specimens with conventional and duplex stainless steel.

**Table 3.45 –** Average corrosion rates (in μm/year) at week 15 as measured in the rapid macrocell test for bare bars in 6.04 m ion NaCl and simulated concrete pore solution for specimens with conventional and duplex stainless steel.

| Specimen designation* | Steel type | Specimen | | | | | | Average | Standard deviation |
|---|---|---|---|---|---|---|---|---|---|
| | | 1 | 2 | 3 | 4 | 5 | 6 | | |
| **Bare bars in 6.04 m NaCl** | | | | | | | | | |
| **M-N3h** | **N3** | 33.87 | 37.80 | 12.17 | 24.51 | 18.96 | | 25.46 | 10.52 |
| **M-2205h** | **2205** | 2.40 | 1.24 | 2.69 | 2.80 | 2.92 | 2.77 | 2.47 | 0.63 |
| **M-2205ph** | **2205p** | 0.14 | 0.20 | 0.23 | 0.40 | 0.43 | | 0.28 | 0.13 |
| **M-2101(1)h** | **2101(1)** | 20.72 | 10.86 | 15.51 | 4.06 | 16.88 | | 13.61 | 6.40 |
| **M-2101(1)ph** | **2101(1)p** | 2.63 | 3.03 | 2.08 | 9.13 | 5.40 | | 4.46 | 2.91 |
| **M-2101(2)h** | **2101(2)** | 7.20 | 12.72 | 11.59 | 11.21 | 13.15 | 10.38 | 11.04 | 2.14 |
| **M-2101(2)ph** | **2101(2)p** | 3.47 | 0.23 | 0.00 | 0.00 | 1.82 | 0.23 | 0.96 | 1.41 |
| **M-2101(2)sh** | **2101(2)s** | 9.39 | 56.47 | 41.53 | 13.73 | 5.20 | 10.66 | 22.83 | 20.99 |

* M - A
**M**: macrocell test
**A**: steel type → N and N2: conventional, normalized steel, 2101(1) and 2101(2): Duplex stainless steel (21% chromium, 1% nickel), 2205: Duplex stainless steel (25% chromium, 5% nickel), p: pickled, s: sandblasted, h: 6.04 m ion concentration.

Figure 3.98 shows the average total corrosion losses for the test period and Table 3.46 summarizes average the total corrosion losses at week 15. Conventional steel had the highest total corrosion loss after 15 weeks at 9.63 μm, followed by 2101(2)s steel at 8.51 μm. The lowest corrosion losses were for 2205p steel at 0.03 μm, equal to 0.3% of the corrosion loss of conventional steel, and 2101(2)p steel at 0.17 μm, equal to 1.8% of the corrosion loss of conventional steel. 2101(1)p steel had a corrosion loss of 1.70 μm, corresponding to 18% of the corrosion loss of conventional steel. 2101(1) and 2101(2) steel had corrosion losses of 3.43 and 3.84 μm/year, respectively, equal to about 40% of the corrosion loss of conventional steel. Tables C.13 and C.14 show the results of the Student's t-test. The difference in the average corrosion losses of conventional and all duplex steels, with the exception of 2101(2)s, is significant at $\alpha = 0.02$. When comparing pickled versus non-pickled steels, there is a significant difference at $\alpha = 0.02$ between the pickled and the non-pickled samples for the three duplex steels. The two steels with the lowest corrosion

losses, 2101(2)p and 2205p, were also compared with the Student's t-test, and it showed that the difference is significant at $\alpha = 0.02$.

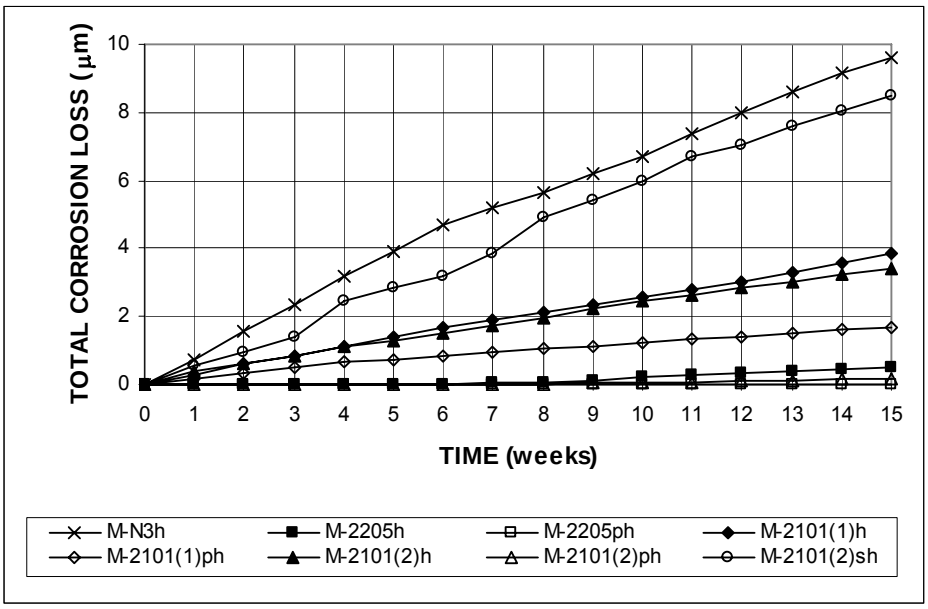


(a)

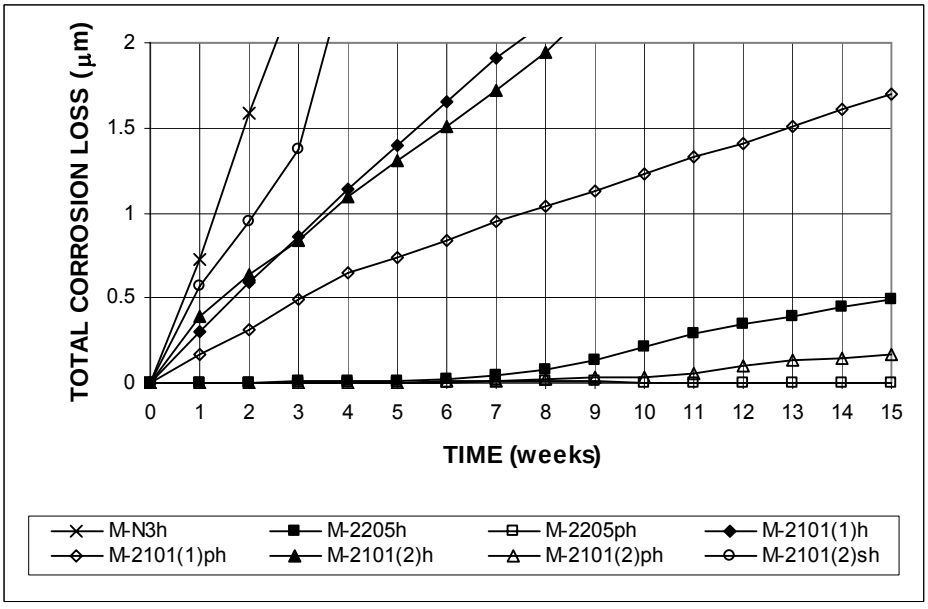


(b)

**Figure 3.98 –** Average total corrosion losses as measured in the rapid macrocell test for bare bars in 6.04 m ion NaCl and simulated concrete pore solution for specimens with conventional and duplex stainless steel.

**Table 3.46 –** Average total corrosion losses (in μm) at week 15 as measured in the rapid macrocell test for bare bars in 6.04 m ion NaCl and simulated concrete pore solution for specimens with conventional and duplex stainless steel.

| Specimen designation* | Steel type | Specimen | | | | | | Average | Standard deviation |
|---|---|---|---|---|---|---|---|---|---|
| | | 1 | 2 | 3 | 4 | 5 | 6 | | |
| **Bare bars in 6.04 m NaCl** | | | | | | | | | |
| **M-N3h** | **N3** | 12.16 | 11.53 | 6.83 | 9.19 | 8.46 | | 9.63 | 2.20 |
| **M-2205h** | **2205** | 0.50 | 0.34 | 0.52 | 0.34 | 0.61 | 0.64 | 0.49 | 0.13 |
| **M-2205ph** | **2205p** | 0.02 | 0.03 | 0.02 | 0.02 | 0.05 | | 0.03 | 0.01 |
| **M-2101(1)h** | **2101(1)** | 3.85 | 3.48 | 4.38 | 2.03 | 5.46 | | 3.84 | 1.26 |
| **M-2101(1)ph** | **2101(1)p** | 0.84 | 1.36 | 1.38 | 3.16 | 1.76 | | 1.70 | 0.88 |
| **M-2101(2)h** | **2101(2)** | 2.28 | 3.83 | 3.80 | 3.78 | 3.24 | 3.64 | 3.43 | 0.60 |
| **M-2101(2)ph** | **2101(2)p** | 0.25 | 0.18 | 0.00 | 0.14 | 0.28 | 0.14 | 0.17 | 0.10 |
| **M-2101(2)sh** | **2101(2)s** | 7.61 | 15.81 | 19.87 | 2.41 | 2.24 | 3.12 | 8.51 | 7.60 |

* M - A
**M**: macrocell test
**A**: steel type → N and N2: conventional, normalized steel, 2101(1) and 2101(2): Duplex stainless steel (21% chromium, 1% nickel), 2205: Duplex stainless steel (25% chromium, 5% nickel), p: pickled, s: sandblasted, h: 6.04 m ion concentration.

The average corrosion potentials of the anodes and cathodes with respect to a saturated calomel electrode are presented in Figure 3.99. The anode potentials indicated active corrosion for conventional, 2101(1), 2101(1)p, 2101(2), and 2101(2)s steels by the second week of the test. The anode potential for 2205 steel was more positive than -0.150 V during the first 6 weeks and dropped to values between -0.200 and -0.220 V at week 9. The anode potential for 2205p steel remained around -0.150 V throughout the test period. During the first weeks, the cathode potentials remained between -0.125 and -0.200 V for all steels, indicating that the steel was not fully passivated. For 2205 and 2101(2) steel, the cathode potentials became more positive and reached values above -0.100 V by week 10.

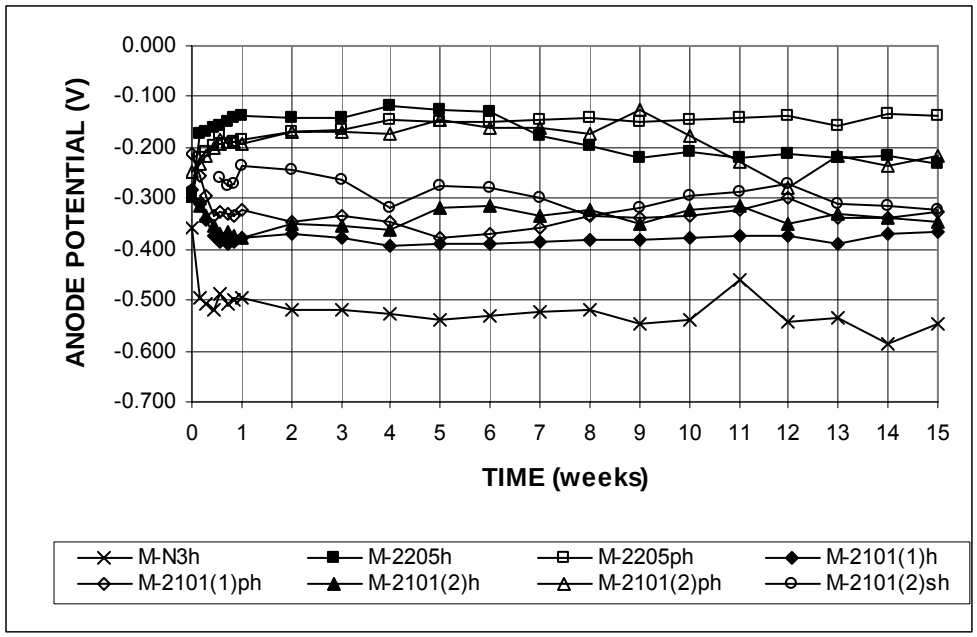


(a)

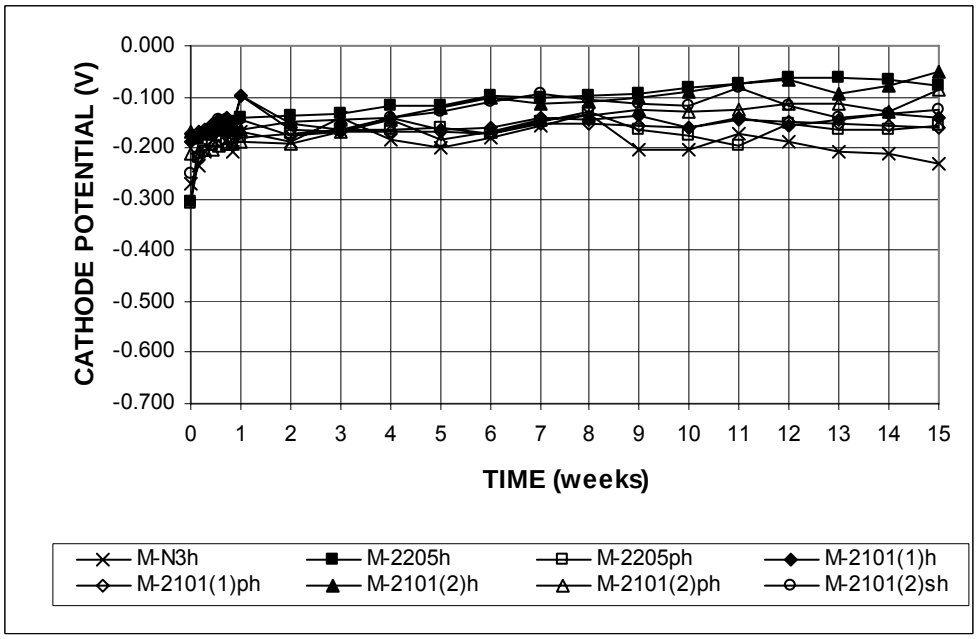


(b)

**Figure 3.99 –** (a) Average anode corrosion potentials and (b) average cathode corrosion potentials, with respect to saturated calomel electrode as measured in the rapid macrocell test for bare bars in 6.04 m ion NaCl and simulated concrete pore solution for specimens with conventional and duplex stainless steel.

Corrosion products were observed on stainless steel bars that showed significant corrosion losses. Figures 3.100, 3.101, 3.102, and 3.104 show the corrosion products on 2101(1), 2101(1)p, 2101(2), and 2205 bars, respectively, exposed to 6.04 m ion NaCl and simulated concrete pore solution. Figure 3.102 shows the corrosion products on 2205 steel exposed to 6.04 m ion NaCl and simulated concrete pore solution. Figure 3.103 shows two 2101(2)p anode bars exposed to 6.04 m ion NaCl and simulated concrete pore solution, one of the bars shows corrosion products while the other bar remains clean. Figure 3.105 shows that anode bars of 2205p steel exposed to the same solution did not have corrosion products.

**Figure 3.100 –** Corrosion products on 2101(1) anode bars in 6.04 m ion NaCl and simulated concrete pore solution at week 15.

**Figure 3.101 –** 2101(1)p anode bars in 6.04 m ion NaCl and simulated concrete pore solution showing small amounts of corrosion products at week 15.

**Figure 3.102 –** Corrosion products on 2101(2) anode bars in 6.04 m ion NaCl and simulated concrete pore solution at week 15.

**Figure 3.103 –** 2101(2)p anode bars in 6.04 m ion NaCl and simulated concrete pore solution showing small amounts of corrosion products on one of the bars, at week 15.

**Figure 3.104 –** 2205 anode bars in 6.04 m ion NaCl and simulated concrete pore solution showing some corrosion products at week 15.

**Figure 3.105 –** 2205p anode bars in 6.04 m ion NaCl and simulated concrete pore solution showing no corrosion products at week 15.

### 3.7.1.2 Mortar-Wrapped Specimens

The average corrosion rates versus time for the mortar-wrapped specimens are presented in Figure 3.106. Conventional steel had the highest corrosion rate during the test period, with 2101(1) and 2101(2) steels also showing significant corrosion rates. The average corrosion rates for 2205, 2205p, 2101(1)p, and 2101(2)p steels remained below 0.20 μm/year throughout the test period. Table 3.47 shows the average corrosion rates at week 15 and Tables C.11 and C.12 show the results of the Student's t-test. Conventional steel had an average corrosion rate of 16.28 μm/year, while 2101(1) and 2101(2) steels had corrosion rates of 8.68 and 5.11 μm/year, respectively. The rest of the duplex steels had corrosion rates below 0.11 μm/year, corresponding to 0.7% of the rate for conventional steel. The difference in the average corrosion rates of conventional steel and the duplex steels is significant at

$\alpha$ = 0.02, except for 2101(1), which is significant at $\alpha$ = 0.20. When comparing pickled versus non-pickled steels, the difference between 2101(1) and 2101(1)p is significant at $\alpha$ = 0.10, and the difference between 2101(2) and 2101(2)p is significant at $\alpha$ = 0.02. There is no statistically significant difference between 2205 and 2205p, or between 2205p and 2101(2)p.

Figure 3.107 shows the average total corrosion losses versus time and Table 3.48 summarizes the average total corrosion losses at week 15. As shown in Table 3.48, after 15 weeks, conventional steel had a corrosion loss of 3.84 μm, followed by 2101(1) and 2101(2) steels with losses of 0.99 and 0.80 μm, respectively. The rest of the duplex steels had corrosion losses lower than 0.03 μm, equal to 0.8% of the corrosion loss of conventional steel. Tables C.13 and C.14 show the results of the Student's t-test. The results show that the difference in the average corrosion losses between conventional and the duplex steels is significant at $\alpha$ = 0.02. The difference between 2101(1) and 2101(1)p is significant at $\alpha$ = 0.10, and the difference between 2101(2) and 2101(2)p is significant at $\alpha$ = 0.02. There is no statistically significant difference between 2205 and 2205p, or between 2205p and 2101(2)p.

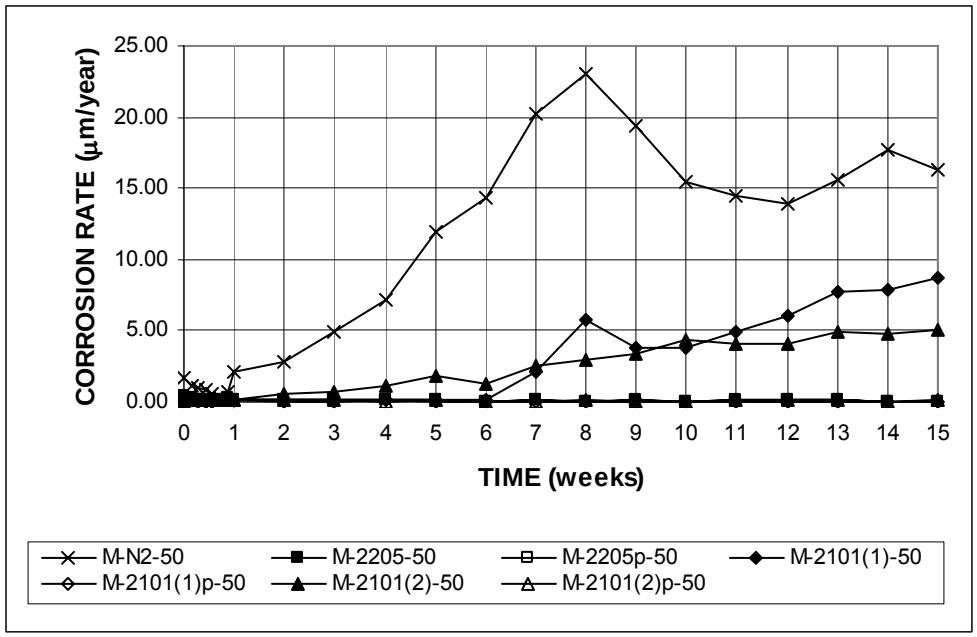


(a)

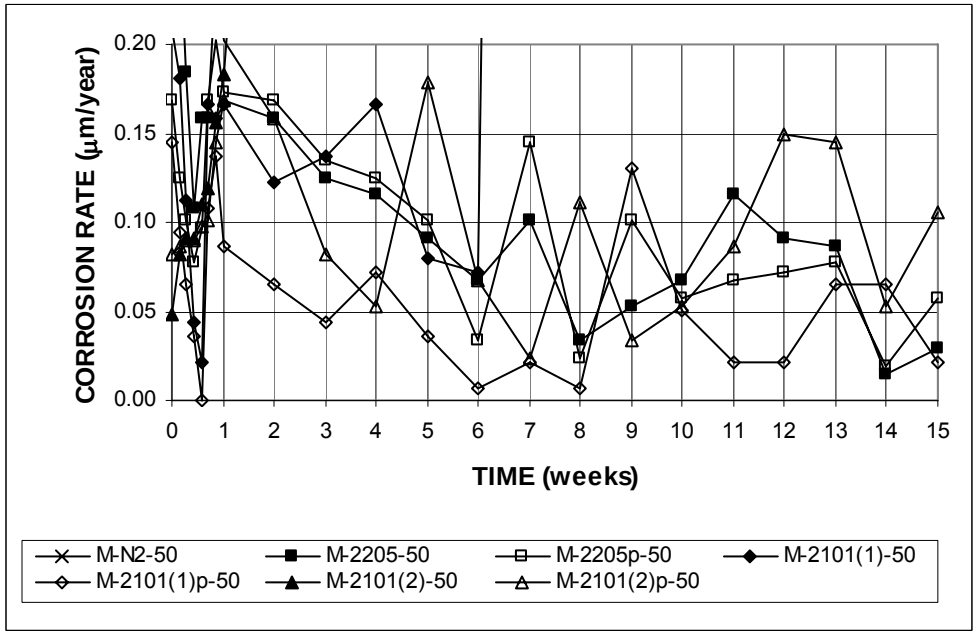


(b)

**Figure 3.106 –** Average corrosion rates as measured in the rapid macrocell test for mortar-wrapped specimens in 1.6 m ion NaCl and simulated concrete pore solution for specimens with conventional and duplex stainless steel.

**Table 3.47 –** Average corrosion rates (in μm/year) at week 15 as measured in the rapid macrocell test for mortar-wrapped specimens in 1.6 m ion NaCl and simulated concrete pore solution for specimens with conventional and duplex stainless steel.

| Specimen designation* | Steel type | Specimen | | | | | | Average | Standard deviation |
|---|---|---|---|---|---|---|---|---|---|
| | | 1 | 2 | 3 | 4 | 5 | 6 | | |
| **Mortar-wrapped specimens in 1.6 m NaCl** | | | | | | | | | |
| **M-N2-50** | **N2** | 17.43 | 19.02 | 24.83 | 5.49 | 14.65 | | 16.28 | 7.09 |
| **M-2205-50** | **2205** | 0.06 | 0.03 | 0.00 | 0.03 | 0.06 | 0.00 | 0.03 | 0.03 |
| **M-2205p-50** | **2205p** | 0.09 | 0.00 | 0.00 | 0.12 | 0.14 | 0.00 | 0.06 | 0.07 |
| **M-2101(1)-50** | **2101(1)** | 9.13 | 13.06 | 11.56 | 0.95 | | | 8.68 | 5.40 |
| **M-2101(1)p-50** | **2101(1)p** | 0.00 | 0.00 | 0.03 | 0.06 | | | 0.02 | 0.03 |
| **M-2101(2)-50** | **2101(2)** | 5.52 | 4.91 | 5.81 | 3.76 | 8.87 | 1.76 | 5.11 | 2.36 |
| **M-2101(2)p-50** | **2101(2)p** | 0.09 | 0.03 | 0.12 | 0.03 | 0.17 | 0.20 | 0.11 | 0.07 |

* M - A - B

**M**: macrocell test

**A**: steel type → N2: conventional, normalized steel, 2101(1) and 2101(2): Duplex stainless steel (21% chromium, 1% nickel), 2205: Duplex stainless steel (25% chromium, 5% nickel), p: pickled.

**B**: mix design → 50: water-cement ratio of 0.50 and no inhibitor.

**Table 3.48 –** Average total corrosion losses (in μm) at week 15 as measured in the rapid macrocell test for mortar-wrapped specimens in 1.6 m ion NaCl and simulated concrete pore solution for specimens with conventional and duplex stainless steel.

| Specimen designation* | Steel type | Specimen | | | | | | Average | Standard deviation |
|---|---|---|---|---|---|---|---|---|---|
| | | 1 | 2 | 3 | 4 | 5 | 6 | | |
| **Mortar-wrapped specimens in 1.6 m NaCl** | | | | | | | | | |
| **M-N2-50** | **N2** | 4.04 | 2.95 | 2.22 | 3.75 | 6.21 | | 3.84 | 1.51 |
| **M-2205-50** | **2205** | 0.03 | 0.03 | 0.02 | 0.02 | 0.03 | 0.02 | 0.03 | 0.01 |
| **M-2205p-50** | **2205p** | 0.04 | 0.03 | 0.02 | 0.02 | 0.02 | 0.02 | 0.03 | 0.01 |
| **M-2101(1)-50** | **2101(1)** | 0.76 | 1.95 | 0.93 | 0.32 | | | 0.99 | 0.69 |
| **M-2101(1)p-50** | **2101(1)p** | 0.01 | 0.00 | 0.02 | 0.02 | | | 0.01 | 0.01 |
| **M-2101(2)-50** | **2101(2)** | 1.15 | 0.51 | 0.77 | 0.54 | 1.21 | 0.64 | 0.80 | 0.31 |
| **M-2101(2)p-50** | **2101(2)p** | 0.02 | 0.02 | 0.03 | 0.02 | 0.04 | 0.03 | 0.03 | 0.01 |

* M - A - B

**M**: macrocell test

**A**: steel type → N2: conventional, normalized steel, 2101(1) and 2101(2): Duplex stainless steel (21% chromium, 1% nickel), 2205: Duplex stainless steel (25% chromium, 5% nickel), p: pickled.

**B**: mix design → 50: water-cement ratio of 0.50 and no inhibitor.

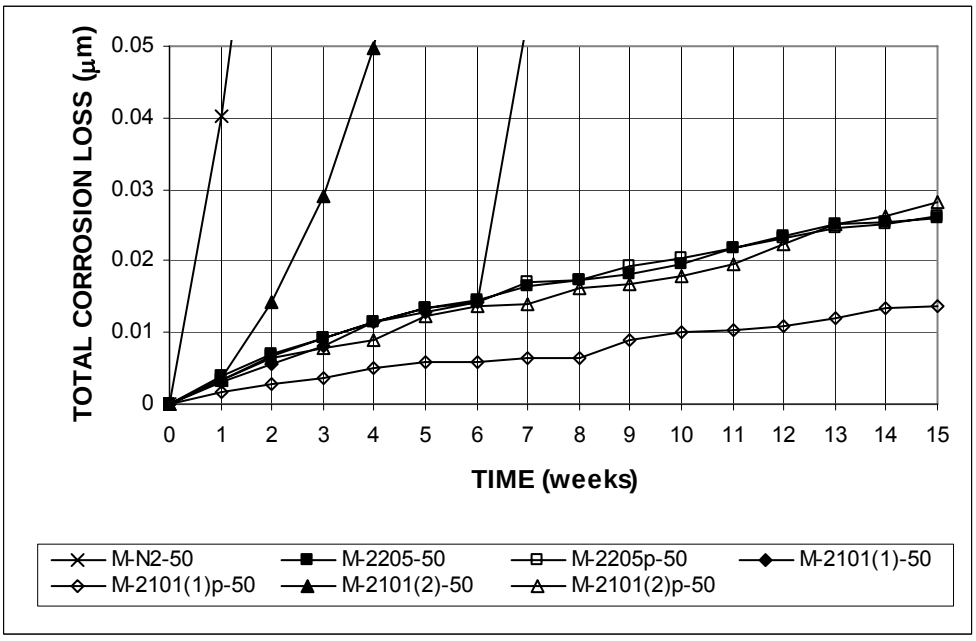


(a)

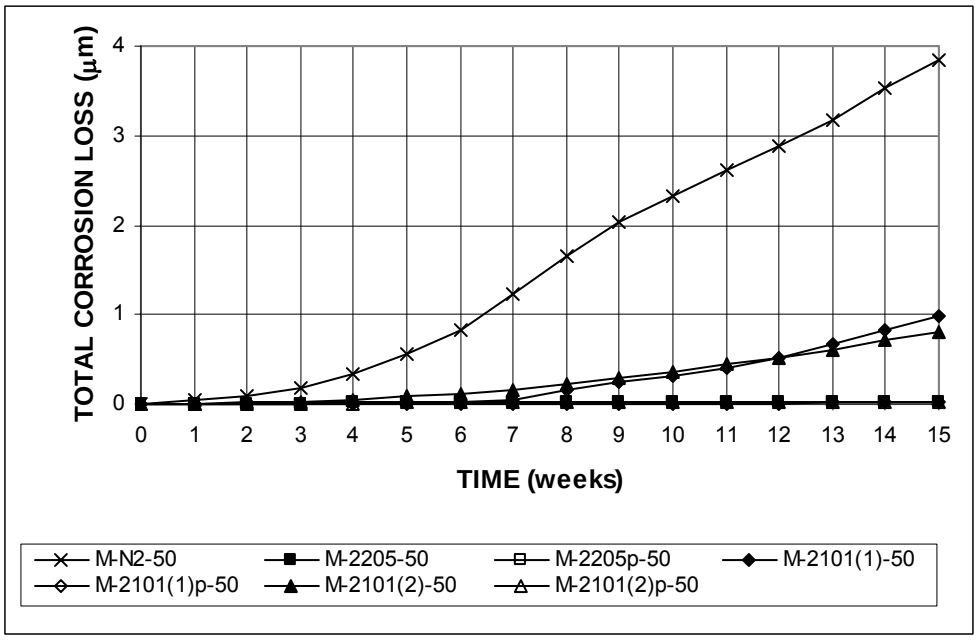


(b)

**Figure 3.107 –** Average total corrosion losses as measured in the rapid macrocell test for mortar-wrapped specimens in 1.6 m ion NaCl and simulated concrete pore solution for specimens with conventional and duplex stainless steel.

The average anode and cathode potentials with respect to a saturated calomel electrode are shown in Figure 3.108. The anode potential for conventional, 2101(1), and 2101(2) steels at the end of the test period indicated active corrosion. All other steels had anode potentials that were more positive than -0.125 V, indicating a passive condition. Cathode potentials for all steels indicated a passive condition, with the exception of conventional steel, which had cathode potentials between -0.150 and -0.250 V, indicating that the steel was not fully passivated.

Corrosion products were observed on 2101(1) and 2101(2) anode bars after the mortar cover was removed at week 15, as shown in Figures 3.109 and 3.111, respectively. No corrosion products were observed on 2101(1)p, 2101(2)p, 2205 and 2205p, as shown in Figures 3.110, 3.112, 3.113, and 3.114, respectively.

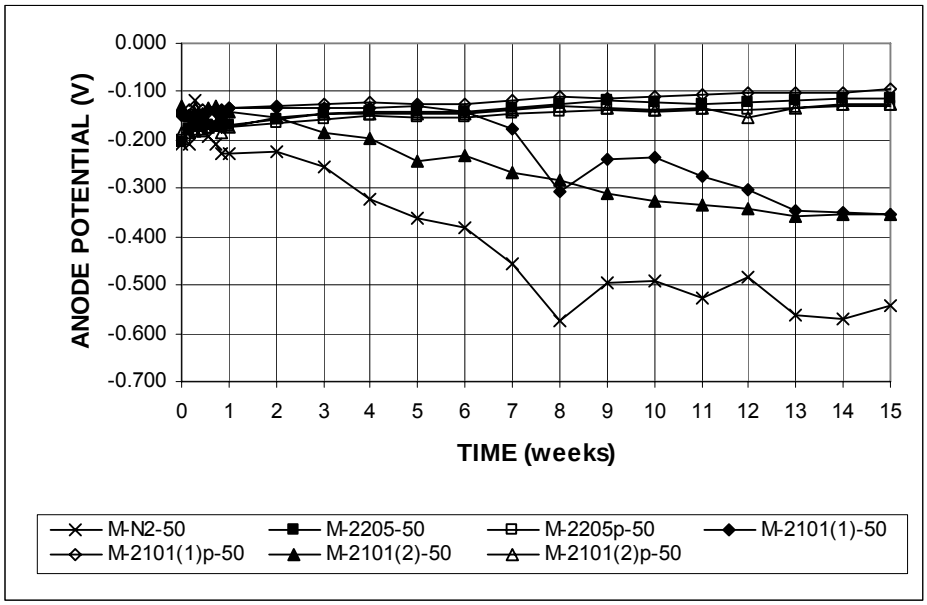


(a)

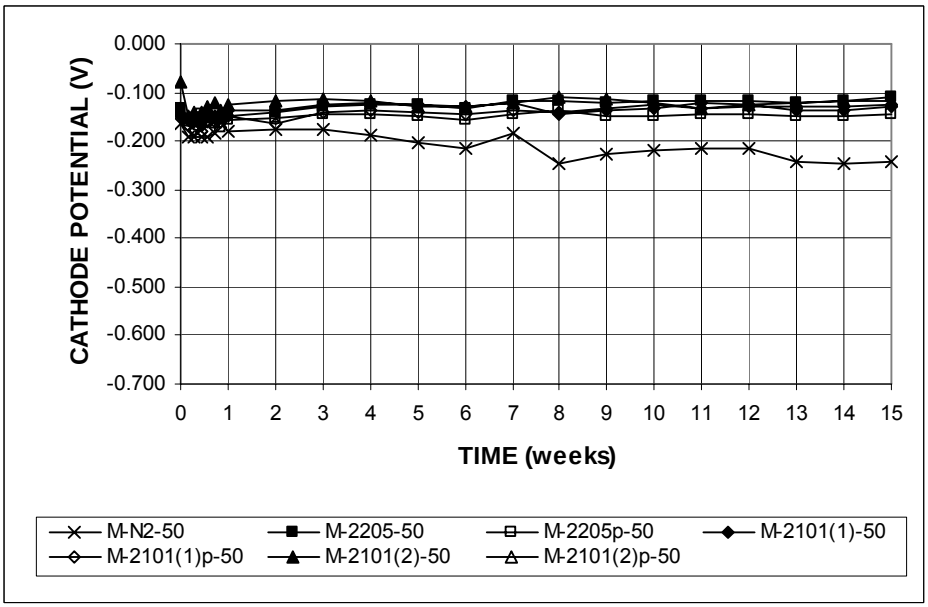


(b)

**Figure 3.108 –** (a) Average anode corrosion potentials and (b) average cathode corrosion potentials, with respect to saturated calomel electrode as measured in the rapid macrocell test for mortar-wrapped specimens in 1.6 m ion NaCl and simulated concrete pore solution for specimens with conventional and duplex stainless steel.

**Figure 3.109 –** Corrosion products on 2101(1) anode bars after removal of mortar cover at week 15.

**Figure 3.110 –** 2101(1)p anode bars after removal of mortar cover at week 15 showing no corrosion products.

**Figure 3.111 –** Corrosion products on 2101(2) anode bars after removal of mortar cover at week 15.

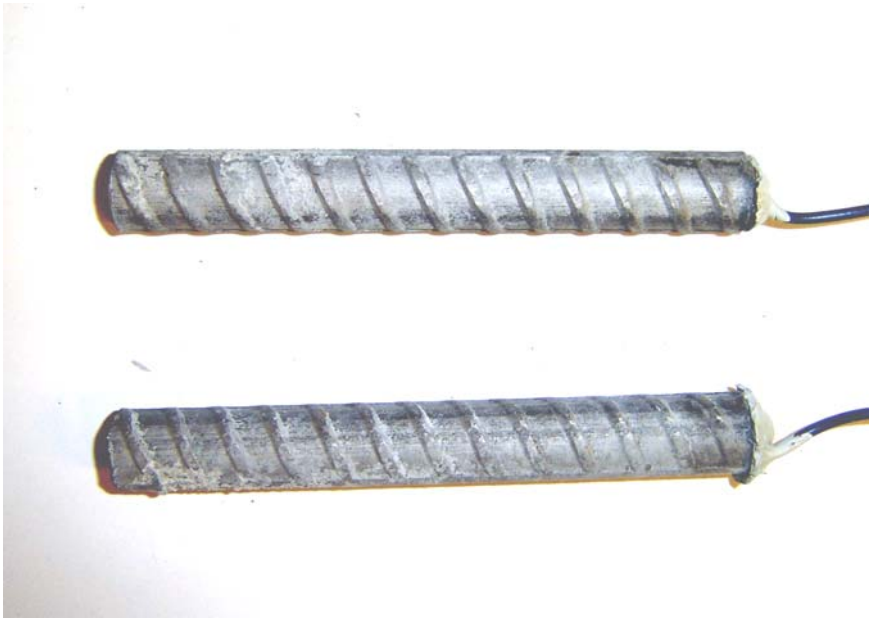

**Figure 3.112 –** 2101(2)p anode bars after removal of mortar cover at week 15 showing no corrosion products.

**Figure 3.113 –** 2205 anode bars after removal of mortar cover at week 15 showing no corrosion products.

**Figure 3.114 –** 2205p anode bars after removal of mortar cover at week 15 showing no corrosion products.

### 3.7.2 Bench-Scale Tests

The Southern Exposure and the cracked beam tests were also used to evaluate the duplex steels. The specimens were fabricated using concrete with a water-cement ratio of 0.45 and no inhibitor. In addition to the specimens with duplex steel on the top and bottom mats of steel, specimens with a combination of 2205 and conventional steel were also evaluated. As described earlier, the duplex stainless steel bars labeled 2101(1) were defective due to a lack of boron, which resulted in slightly deformed bars that had small cracks on the surface.

#### 3.7.2.1 Southern Exposure Test

The average corrosion rates are shown in Figures 3.115 and 3.116. Figure 3.115 shows the results for specimens with the same steel on the top and bottom mat, and Figure 3.116 shows the results for specimens with a combination of conventional and 2205 steel. Conventional steel and 2101(1) steel had the highest corrosion rates. 2101(1)p steel also showed significant corrosion rates during the second half of the test period. Specimens with conventional steel in the top mat and 2205 steel in the bottom mat had corrosion rates that were similar to specimens with conventional steel in the top and bottom mats. As shown in Table 3.49, conventional steel had the highest corrosion rate, at 4.07 μm/year, followed by 2101(1) steel at 3.16 μm/year. The lowest average corrosion rate was for 2101(2)p steel, with a corrosion rate of zero, followed by 2205 and 2205p steels, at 0.02 μm/year. Specimens with a combination of conventional and duplex steel had a corrosion rate of 3.63 μm/year for the specimens with conventional steel in the top mat (SE-N2/2205-45), and 0.10 μm/year for the specimens with conventional steel in the bottom mat (SE-2205/N2-45). Tables C.11 and C.12 show the results of the Student's t-test. The

difference in the average corrosion rates between conventional steel and either 2205, 2205p, or 2101(2)p is significant at $\alpha$ = 0.02, while the difference between conventional and either 2101(1)p or 2101(2) is significant at $\alpha$ = 0.05. When comparing pickled versus non-pickled steels, the differences between 2101(1) and 2101(1)p and between 2101(2) and 2101(2)p are significant at $\alpha$ = 0.20.

**Table 3.49 –** Average corrosion rates (in μm/year) at week 70 as measured in the Southern Exposure test for specimens with conventional and duplex stainless steel.

| Specimen designation* | Steel type | Specimen | | | | | | Average | Standard deviation |
|---|---|---|---|---|---|---|---|---|---|
| | | 1 | 2 | 3 | 4 | 5 | 6 | | |
| **Southern Exposure test** | | | | | | | | | |
| **SE-N-45** | **N** | 8.41 | 0.73 | 3.41 | 2.33 | 3.80 | 5.76 | 4.07 | 2.70 |
| **SE-2205-45** | **2205** | 0.04 | 0.04 | 0.01 | 0.00 | 0.00 | | 0.02 | 0.02 |
| **SE-2205p-45** | **2205p** | 0.10 | 0.00 | 0.01 | 0.00 | 0.00 | | 0.02 | 0.04 |
| **SE-2101(1)-45** | **2101(1)** | 1.42 | 4.44 | 3.62 | | | | 3.16 | 1.56 |
| **SE-2101(1)p-45** | **2101(1)p** | 0.03 | 2.27 | 0.23 | | | | 0.85 | 1.24 |
| **SE-2101(2)-45** | **2101(2)** | 0.00 | 0.00 | 0.00 | 0.75 | 1.02 | | 0.35 | 0.49 |
| **SE-2101(2)p-45** | **2101(2)p** | 0.01 | 0.00 | 0.00 | 0.00 | 0.00 | | 0.00 | 0.00 |
| **SE-N2/2205-45** | **N2/2205** | 2.77 | 2.71 | 5.40 | | | | 3.63 | 1.53 |
| **SE-2205/N2-45** | **2205/N2** | 0.13 | 0.00 | 0.17 | | | | 0.10 | 0.09 |

* SE - A - B

**SE**: Southern Exposure test

**A**: steel type → N, N2: conventional, normalized steel, 2101(1) and 2101(2): duplex stainless steel (21% chromium, 1% nickel), 2205: duplex stainless steel (25% chromium, 5% nickel), N2/2205: N2 steel in the top mat and 2205 steel in the bottom mat, 2205/N2: 2205 steel in the top mat and N2 steel in the bottom mat, p: pickled.

**B**: mix design → 45: water-cement ratio of 0.45 and no inhibitor.

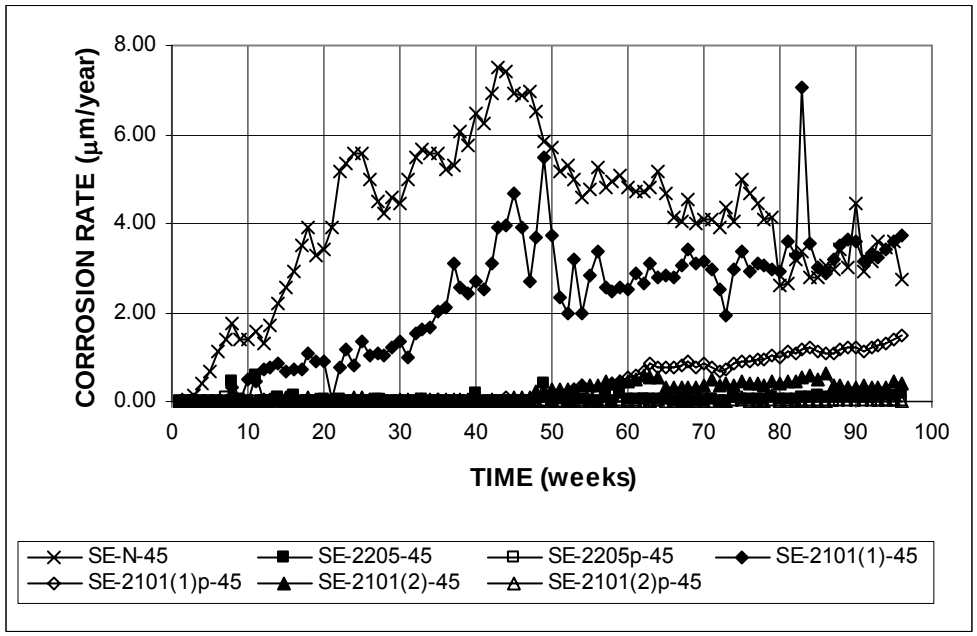


(a)

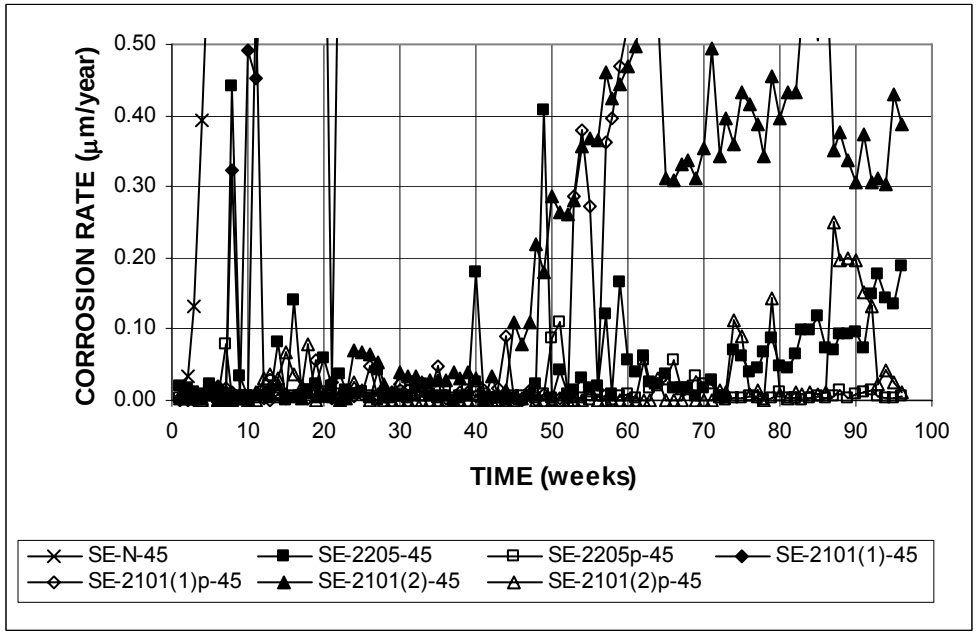


(b)

**Figure 3.115 –** Average corrosion rates as measured in the Southern Exposure test for specimens with conventional and duplex stainless steel.

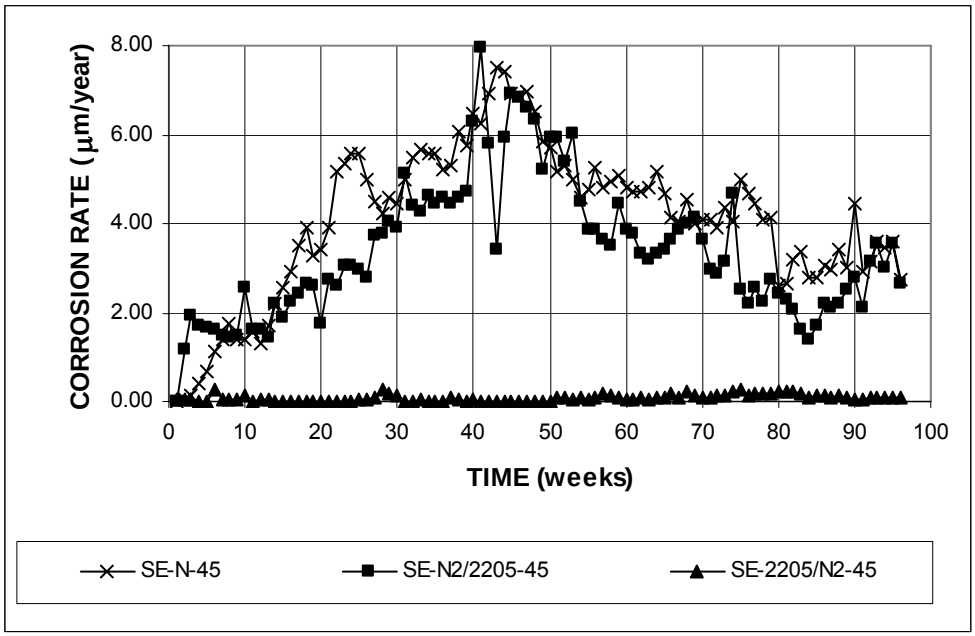


**Figure 3.116 –** Average corrosion rates as measured in the Southern Exposure test for specimens with conventional steel and a combination of conventional and duplex stainless steel.

Figures 3.117 and 3.118 show the average total corrosion losses versus time for the duplex stainless steels. Figure 3.117 shows the results for specimens with the same steel on the top and bottom mat, and Figure 3.118 shows the results for specimens with a combination of conventional and 2205 steel. As shown in Table 3.50, specimens containing conventional steel had an average corrosion loss of 5.78 μm after 70 weeks, and specimens with conventional steel in the top mat and 2205 steel in the bottom mat (SE-N2/2205-45) had a corrosion loss of 4.96 μm/year. Significant corrosion losses were also obtained by specimens containing 2101(1) steel, at 2.55μm. 2101(2)p and 2205p steels exhibited the lowest corrosion losses, with 0.01 and 0.02 μm, respectively. These values are less than 0.3% of the corrosion loss of conventional steel. 2101(1)p steel had a low corrosion loss, 0.21 μm, while the specimens with 2205 steel in the top mat and conventional steel in the bottom mat

had a corrosion loss of 0.07 μm, similar to the specimens with 2205 steel in the top and bottom mats. Results of the Student's t-test are shown in Tables C.13 and C.14. The difference in the average corrosion losses between conventional and the duplex steel is significant at $\alpha = 0.02$, except for 2101(1), where the difference is significant at $\alpha = 0.05$. The differences between 2101(1) and 2101(1)p and between 2101(2) and 2101(2)p are significant at $\alpha = 0.10$. There is no statistically significant difference between 2205 and 2205p, or between 2205p and 2101(2)p.

**Table 3.50 –** Average total corrosion losses (in μm) at week 70 as measured in the Southern Exposure test for specimens with conventional and duplex stainless steel.

| Specimen designation* | Steel type | Specimen | | | | | | Average | Standard deviation |
|---|---|---|---|---|---|---|---|---|---|
| | | 1 | 2 | 3 | 4 | 5 | 6 | | |
| **Southern Exposure test** | | | | | | | | | |
| **SE-N-45** | **N** | 7.13 | 8.89 | 6.90 | 3.02 | 4.19 | 4.56 | 5.78 | 2.21 |
| **SE-2205-45** | **2205** | 0.02 | 0.08 | 0.19 | 0.00 | 0.00 | | 0.06 | 0.08 |
| **SE-2205p-45** | **2205p** | 0.02 | 0.02 | 0.02 | 0.01 | 0.01 | | 0.02 | 0.01 |
| **SE-2101(1)-45** | **2101(!)** | 1.24 | 2.69 | 3.72 | | | | 2.55 | 1.24 |
| **SE-2101(1)p-45** | **2101(1)p** | 0.02 | 0.60 | 0.02 | | | | 0.21 | 0.33 |
| **SE-2101(2)-45** | **2101(2)** | 0.22 | 0.04 | 0.00 | 0.21 | 0.46 | | 0.19 | 0.18 |
| **SE-2101(2)p-45** | **2101(20p** | 0.01 | 0.01 | 0.02 | 0.01 | 0.01 | | 0.01 | 0.00 |
| **SE-N2/2205-45** | **N2/2205** | 3.35 | 4.56 | 6.97 | | | | 4.96 | 1.84 |
| **SE-2205/N2-45** | **2205/N2** | 0.04 | 0.03 | 0.15 | | | | 0.07 | 0.07 |

* SE - A - B

**SE**: Southern Exposure test

**A**: steel type → N, N2: conventional, normalized steel, 2101(1) and 2101(2): duplex stainless steel (21% chromium, 1% nickel), 2205: duplex stainless steel (25% chromium, 5% nickel), N2/2205: N2 steel in the top mat and 2205 in the bottom mat, 2205/N2: 2205 steel in the top mat and N2 steel in the bottom mat, p: pickled.

**B**: mix design → 45: water-cement ratio of 0.45 and no inhibitor.

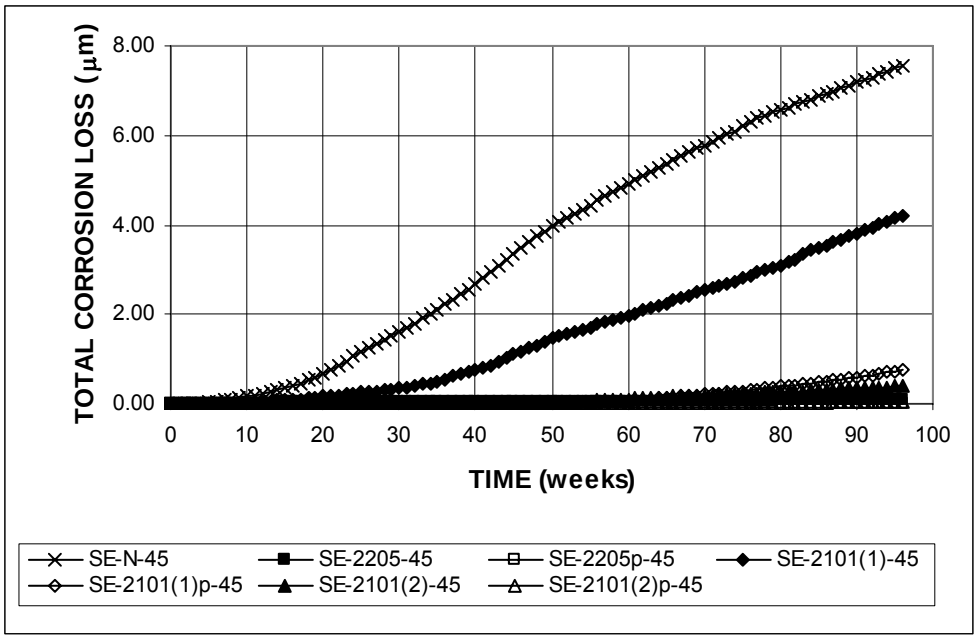


(a)

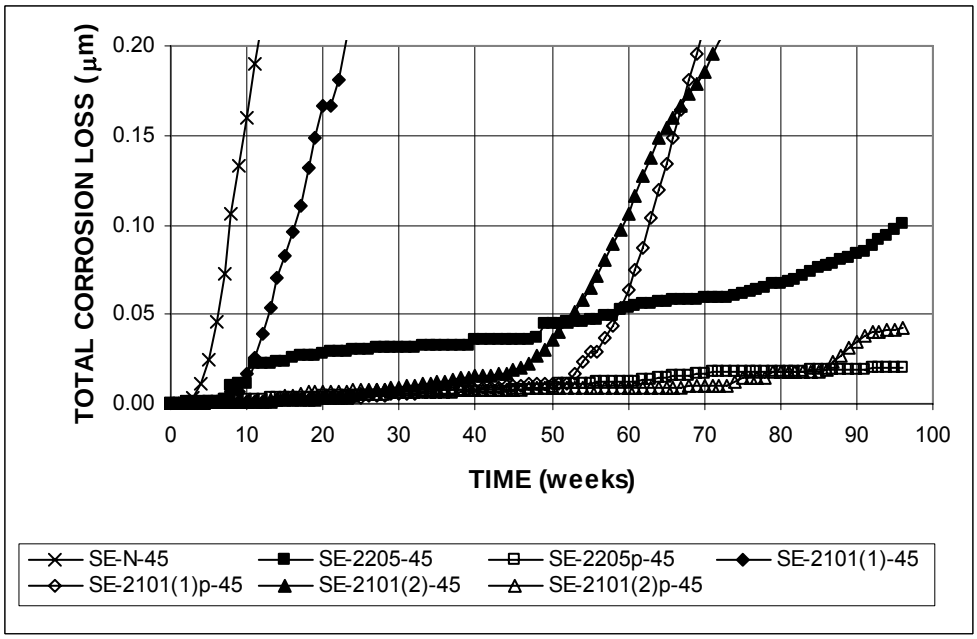


(b)

**Figure 3.117 –** Average total corrosion losses as measured in the Southern Exposure test for specimens with conventional and duplex stainless steel.

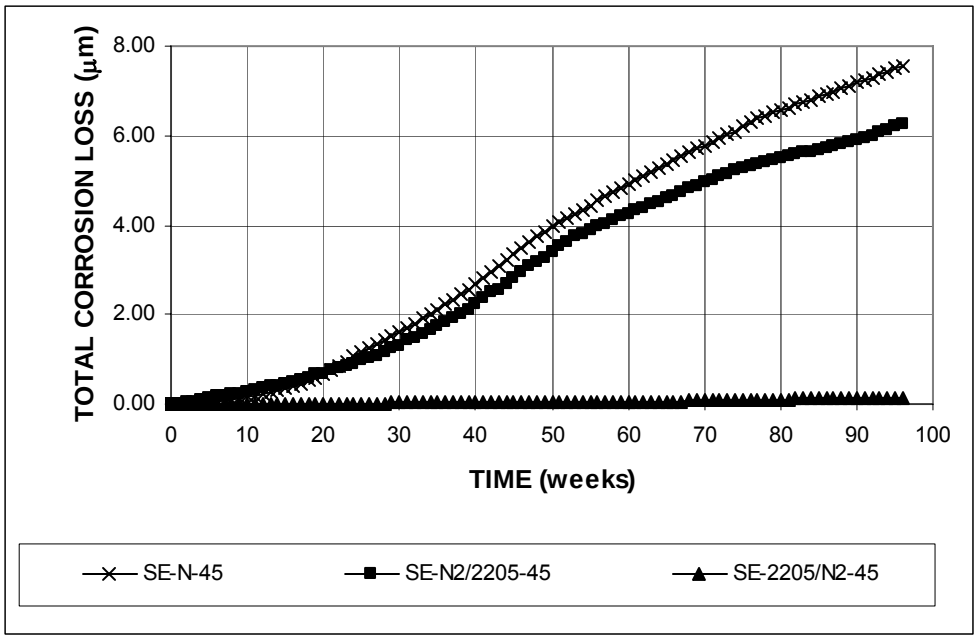


**Figure 3.118 –** Average total corrosion losses as measured in the Southern Exposure test for specimens with conventional steel and a combination of conventional and duplex stainless steel.

The average corrosion potentials of the top and bottom mats of steel with respect to a copper-copper sulfate electrode are shown in Figures 3.119 and 3.120. Figure 3.119 shows the results for specimens with the same steel on the top and bottom mat, and Figure 3.120 shows the results for specimens with a combination of conventional and 2205 steel. Conventional steel showed active corrosion in the top mat at week 8, followed by 2101(1) steel at week 37, and 2101(1)p and 2101(2) steels at week 70. The remaining specimens had top mat corrosion potentials that were above -0.250 V, with the exception of specimens containing 2205 steel in the top mat and conventional steel in the bottom mat (SE-2205/N2-45), which had corrosion potentials of approximately -0.300 V.

The bottom mat corrosion potential for all steels remained more positive than -0.300 V during the test period, with the exception of conventional steel, which showed active corrosion on the bottom mat starting in week 10, and 2101(1) steel which had corrosion potentials below -0.300 V between weeks 60 and 75, and after week 90.

Figures 3.121 and 3.122 show the average mat-to-mat resistances for the Southern Exposure specimens containing duplex steel. Figure 3.121 shows the results for specimens with the same steel on the top and bottom mat, and Figure 3.122 shows the results for specimens with a combination of conventional and 2205 steel. The mat-to-mat resistance for all steels was approximately 200 ohms at the start of the test period. The values increased at a similar rate for all specimens during the first 30 weeks. By week 70, 2205 steel had the highest mat-to-mat resistance, with values above 1200 ohms, while 2101(1) steel had the lowest mat-to-mat resistance, with values below 400 ohms. The mat-to-mat resistances of the remaining steels were between 600 and 800 ohms at week 70.

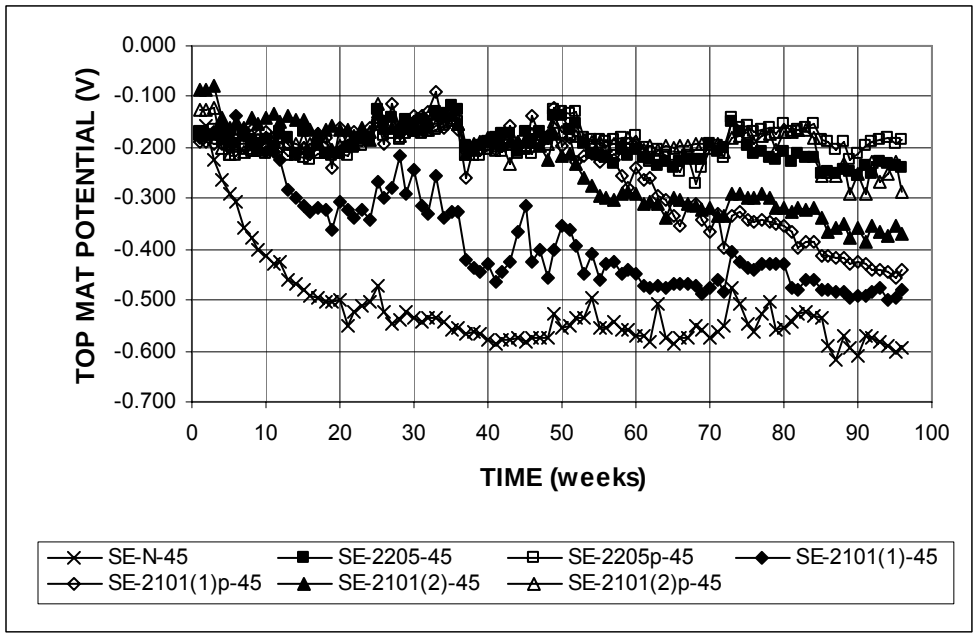


(a)

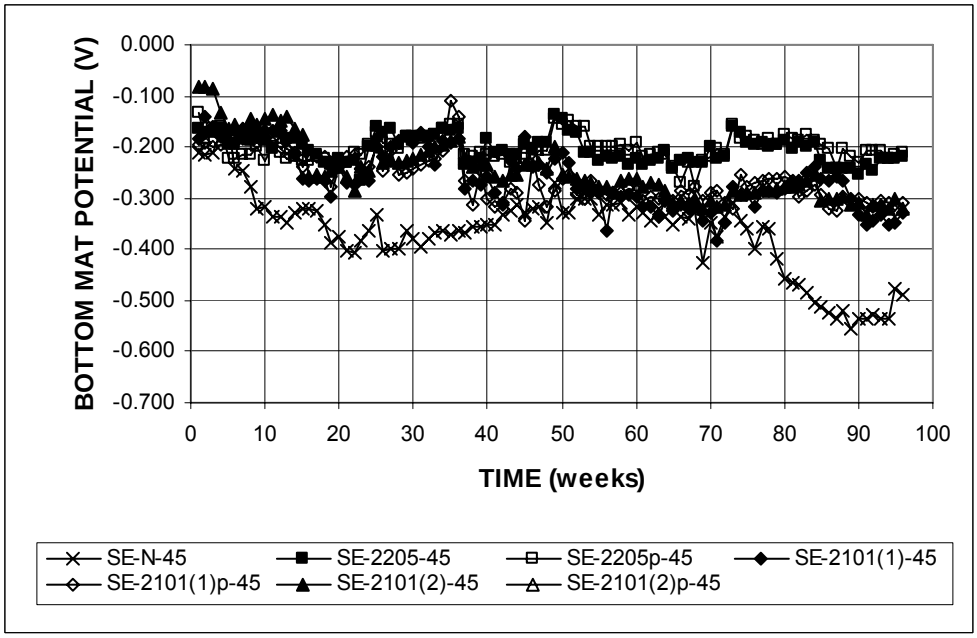


(b)

**Figure 3.119 –** (a) Average top mat corrosion potentials and (b) average bottom mat corrosion potentials, with respect to copper-copper sulfate electrode as measured in the Southern Exposure test for specimens with conventional and duplex stainless steel.

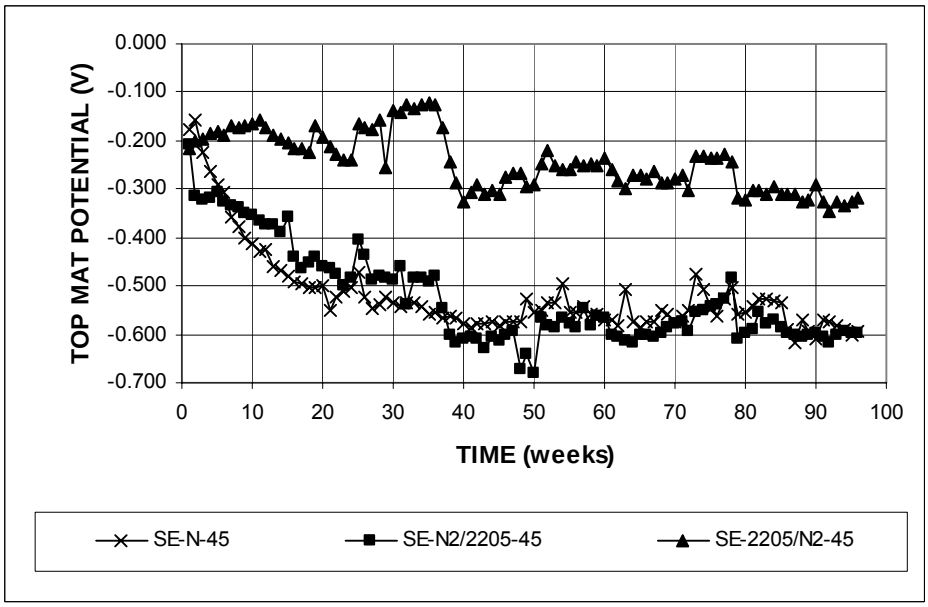


(a)

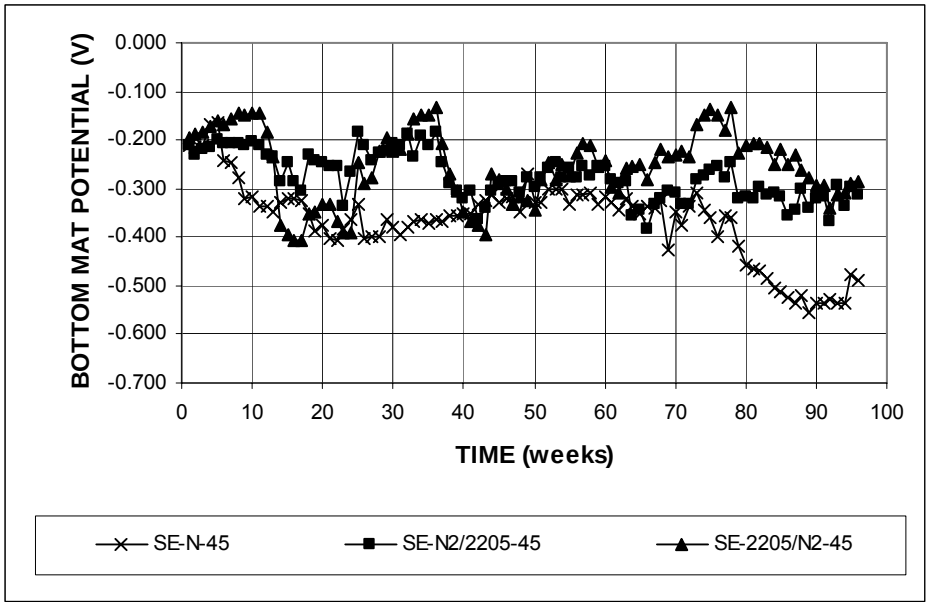


(b)

**Figure 3.120 –** (a) Average top mat corrosion potentials and (b) average bottom mat corrosion potentials, with respect to copper-copper sulfate electrode as measured in the Southern Exposure test for specimens with conventional steel and a combination of conventional and duplex stainless steel.

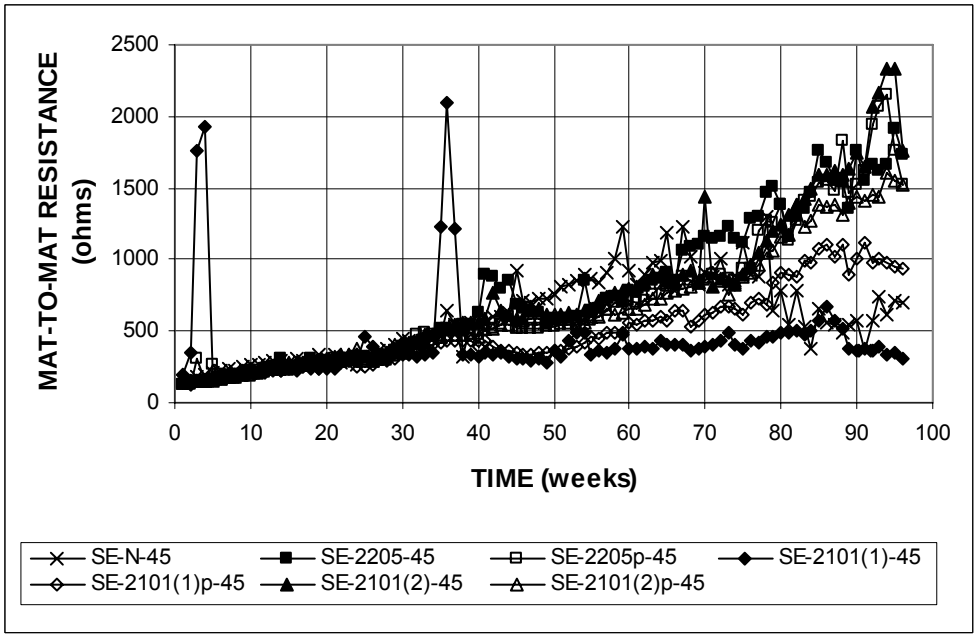


**Figure 3.121 –** Average mat-to-mat resistances as measured in the Southern Exposure test for specimens with conventional and duplex stainless steel.

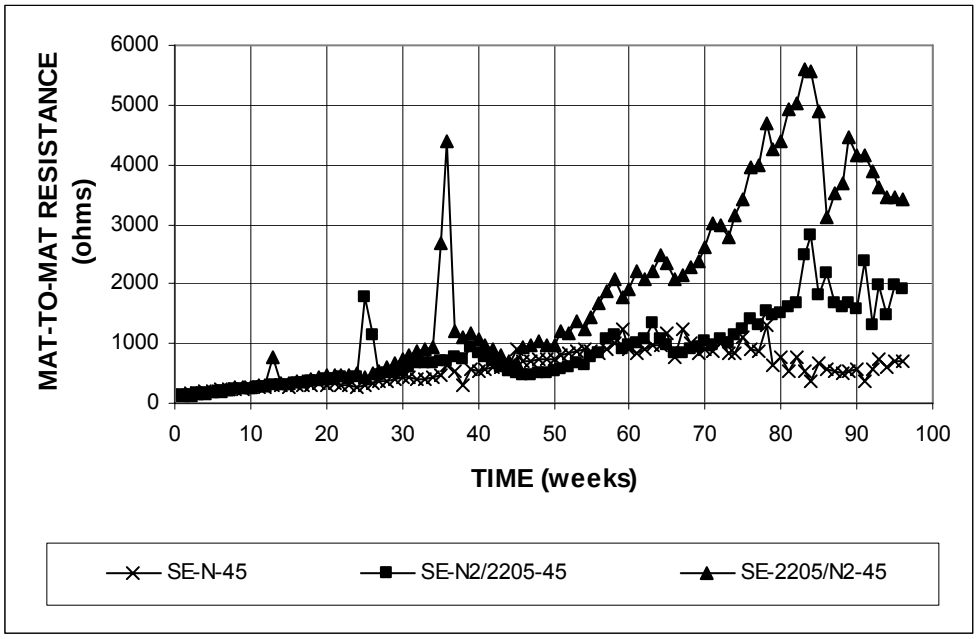


**Figure 3.122 –** Average mat-to-mat resistances as measured in the Southern Exposure test for specimens with a combination of conventional and duplex stainless steel.

### 3.7.2.2 Cracked Beam Test

Figure 3.123 shows the average corrosion rates for the duplex stainless steels. Conventional, 2101(1), and 2101(2) steels show significantly higher corrosion rates than the remaining steels. As shown in Table 3.51, at week 70, conventional steel had the highest corrosion rate at 7.34 μm/year. 2101(1) and 2101(2) steels also had relatively high corrosion rates of 0.87 and 0.70 μm/year, respectively. The lowest corrosion rates occurred for 2101(2)p and 2205p, at 0.02 and 0.08 μm/year, respectively. These values correspond to 0.2% and 1.0%, respectively, of the corrosion rate of conventional steel. Tables C.11 and C.12 show the results of the Student's t-test. The difference in the average corrosion rates between conventional and the duplex steels is significant at $\alpha = 0.05$, while the difference between 2101(2) and 2101(2)p is significant at $\alpha = 0.02$. There is no statistically significant difference between 2205 and 2205p, 2101(1) and 2101(1)p, or 2101(2)p and 2205p.

**Table 3.51 –** Average corrosion rates (in μm/year) at week 70 as measured in the cracked beam test for specimens with conventional and duplex stainless steel.

| Specimen designation* | Steel type | Specimen | | | | | | Average | Standard deviation |
|---|---|---|---|---|---|---|---|---|---|
| | | 1 | 2 | 3 | 4 | 5 | 6 | | |
| **Cracked beam test** | | | | | | | | | |
| **CB-N-45** | **N** | 9.55 | 4.55 | 2.22 | 3.92 | 17.61 | 6.22 | 7.34 | 5.61 |
| **CB-2205-45** | **2205** | 0.15 | 0.34 | 0.05 | 0.02 | 0.00 | | 0.11 | 0.14 |
| **CB-2205p-45** | **2205p** | 0.05 | 0.34 | 0.01 | 0.00 | 0.00 | | 0.08 | 0.15 |
| **CB-2101(1)-45** | **2101(1)** | 1.71 | 0.70 | 0.19 | | | | 0.87 | 0.77 |
| **CB-2101(1)p-45** | **2101(1)p** | 0.21 | 0.17 | 0.07 | | | | 0.15 | 0.07 |
| **CB-2101(2)-45** | **2101(2)** | 0.47 | 0.52 | 0.56 | 1.10 | 0.82 | | 0.70 | 0.27 |
| **CB-2101(2)p-45** | **2101(2)p** | 0.05 | 0.00 | 0.03 | 0.00 | 0.00 | | 0.02 | 0.02 |

* CB - A - B
**CB**: Cracked beam test
**A**: steel type → N: conventional, normalized steel, 2101(1) and 2101(2): duplex stainless steel (21% chromium, 1% nickel), 2205: duplex stainless steel (25% chromium, 5% nickel), p: pickled.
**B**: mix design → 45: water-cement ratio of 0.45 and no inhibitor.

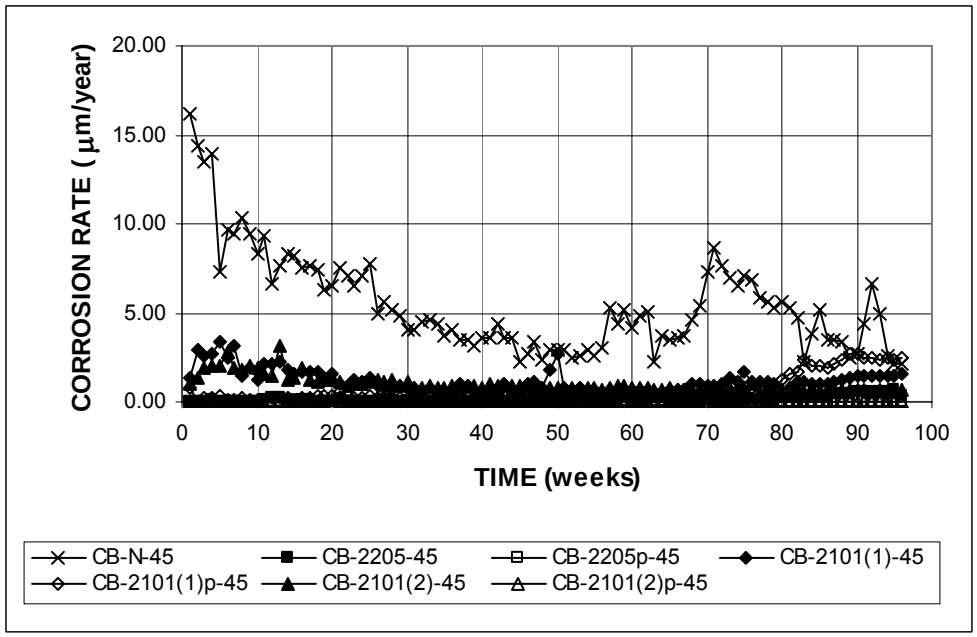


(a)

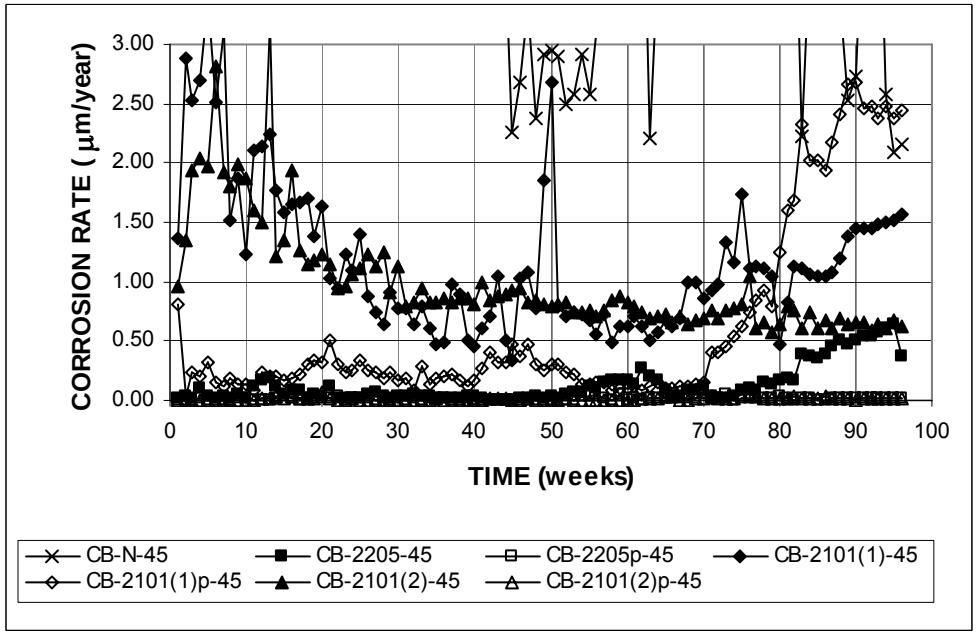


(b)

**Figure 3.123 –** Average corrosion rates as measured in the cracked beam test for specimens with conventional and duplex stainless steel.

Figure 3.124 shows the average corrosion losses versus time and Table 3.52 summarizes the total corrosion losses at week 70 for cracked beam specimens with duplex stainless steels. The lowest corrosion losses were for 2101(2)p and 2205p steels, which had corrosion losses of 0.01 and 0.02 μm, respectively, after 70 weeks. These values are equal to less than 0.3% of the corrosion loss of conventional steel, which had a total corrosion loss of 7.52 μm. Significant corrosion losses were also obtained for 2101(1) and 2101(2), at 3.15 and 2.96 μm, respectively. Tables C.12 and C.14 show the results of the Student's t-test. The difference in the average corrosion losses between conventional steel and the duplex steels is significant at $\alpha$ = 0.02. The differences between 2205 and 2205p and between 2101(1) and 2101(1)p are significant at $\alpha$ = 0.10, while the difference between 2101(2) and 2101(2)p is significant at $\alpha$ = 0.02. There is no statistically significant difference between the losses for 2205p and 2101(2)p.

**Table 3.52 –** Average total corrosion losses (in μm) at week 70 as measured in the cracked beam test for specimens with conventional and duplex stainless steel.

| Specimen designation* | Steel type | Specimen | | | | | | Average | Standard deviation |
|---|---|---|---|---|---|---|---|---|---|
| | | 1 | 2 | 3 | 4 | 5 | 6 | | |
| **Cracked beam test** | | | | | | | | | |
| **CB-N-45** | **N** | 10.36 | 7.75 | 4.98 | 8.57 | 7.61 | 5.78 | 7.51 | 1.93 |
| **CB-2205-45** | **2205** | 0.10 | 0.18 | 0.06 | 0.06 | 0.03 | | 0.08 | 0.06 |
| **CB-2205p-45** | **2205p** | 0.02 | 0.03 | 0.01 | 0.01 | 0.01 | | 0.02 | 0.01 |
| **CB-2101(1)-45** | **2101(1)** | 1.45 | 2.17 | 1.10 | | | | 1.57 | 0.54 |
| **CB-2101(1)p-45** | **2101(1)p** | 0.23 | 0.49 | 0.17 | | | | 0.30 | 0.17 |
| **CB-2101(2)-45** | **2101(2)** | 1.51 | 1.21 | 1.53 | 1.51 | 1.66 | | 1.48 | 0.16 |
| **CB-2101(2)p-45** | **2101(2)p** | 0.02 | 0.01 | 0.02 | 0.01 | 0.01 | | 0.01 | 0.01 |

* CB - A - B

**CB**: Cracked beam test

**A**: steel type → N: conventional, normalized steel, 2101(1) and 2101(2): duplex stainless steel (21% chromium, 1% nickel), 2205: duplex stainless steel (25% chromium, 5% nickel), p: pickled.

**B**: mix design → 45: water-cement ratio of 0.45 and no inhibitor.

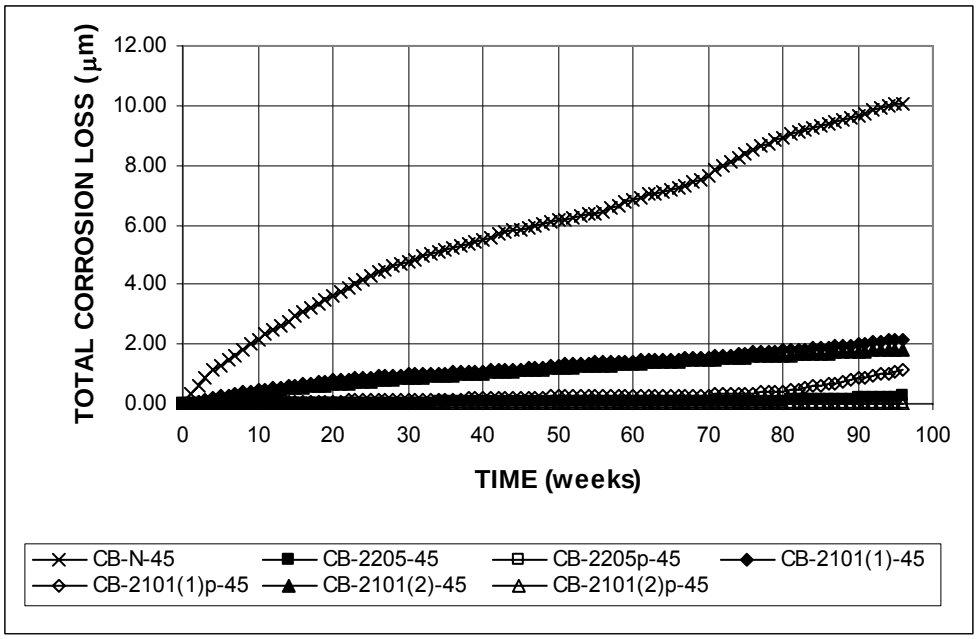


(a)

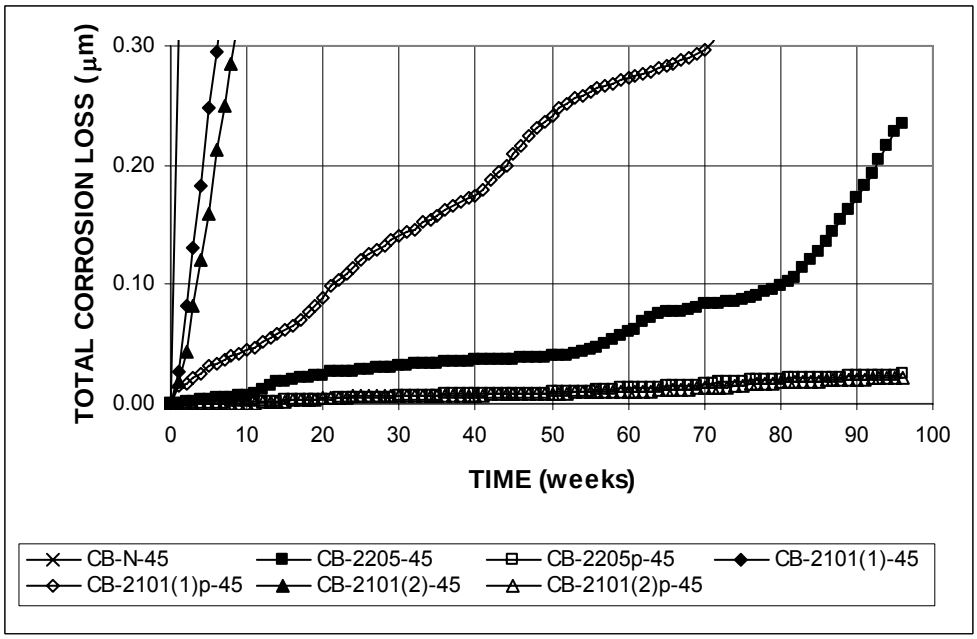


(b)

**Figure 3.124 –** Average total corrosion losses as measured in the cracked beam test for specimens with conventional and duplex stainless steel.

The average corrosion potentials of the top and bottom mats of steel with respect to a copper-copper sulfate electrode are shown in Figure 3.125. The corrosion potential of the top mat for conventional steel was more negative than -0.600 V starting at week 1, indicating a high tendency to corrode. 2101(1), 2101(2), and 2101(1)p steels also showed a high probability of corrosion, with corrosion potentials for the top mat that were more negative than -0.400 V. The top mat potential for the other steels remained more positive than -0.300 V, indicating a lower tendency to corrode, although one specimen of 2101(2)p steel [CB-2101(2)p-45-1] had corrosion potentials as low as –0.450 V after week 63, as shown in Figure A.203(a). The bottom mat corrosion potential for all steels was more positive than -0.300 V, with the exception of conventional steel, which had an average bottom mat corrosion potential that dropped below -0.350 V after week 8.

The average mat-to-mat resistances for the duplex steels in the cracked beam test are shown in Figure 3.126. All steels had a similar mat-to-mat resistance during the first 30 weeks. By week 70, however, there was a large scatter in the results; 2205, 2101(1) and 2101(1)p steels had average mat-to-mat resistances above 4000 ohms, while conventional steel had an average mat-to-mat resistance of approximately 1500 ohms. The remaining steels had average mat-to-mat resistances that ranged between 2000 and 3000 ohms.

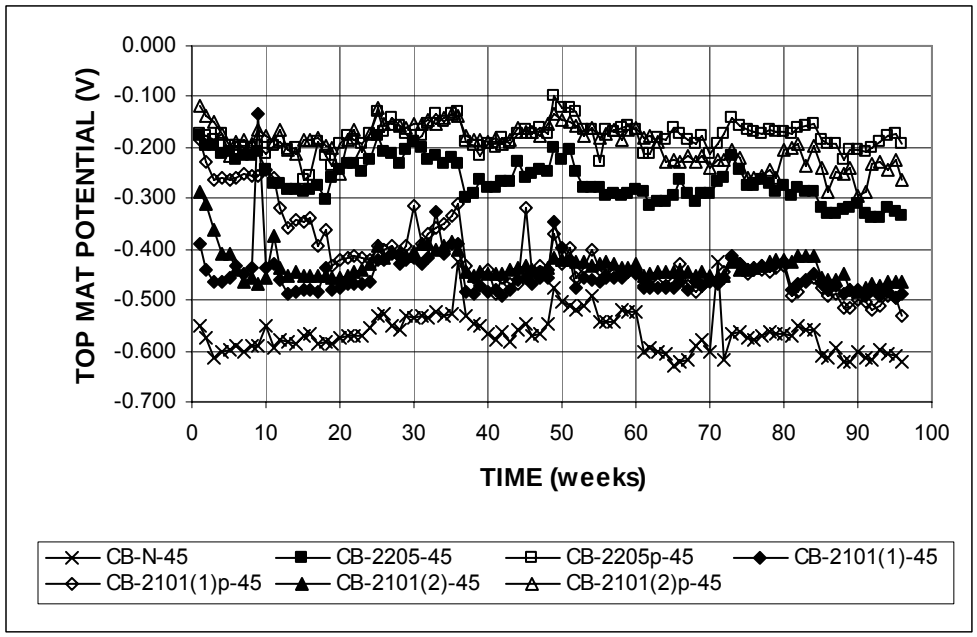


(a)

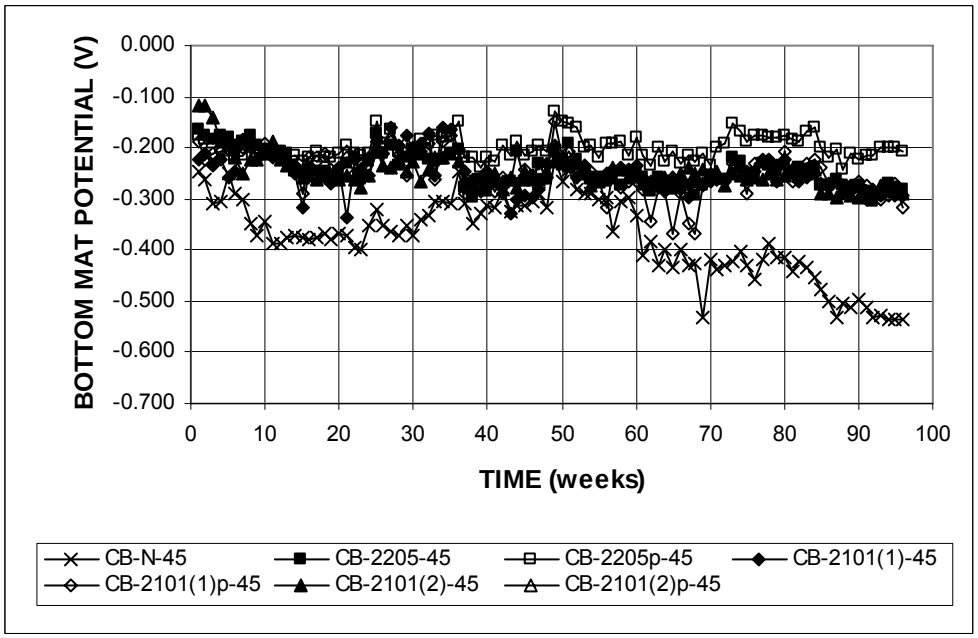


(b)

**Figure 3.125 –** (a) Average top mat corrosion potentials and (b) average bottom mat corrosion potentials, with respect to copper-copper sulfate electrode as measured in the cracked beam test for specimens with conventional and duplex stainless steel.

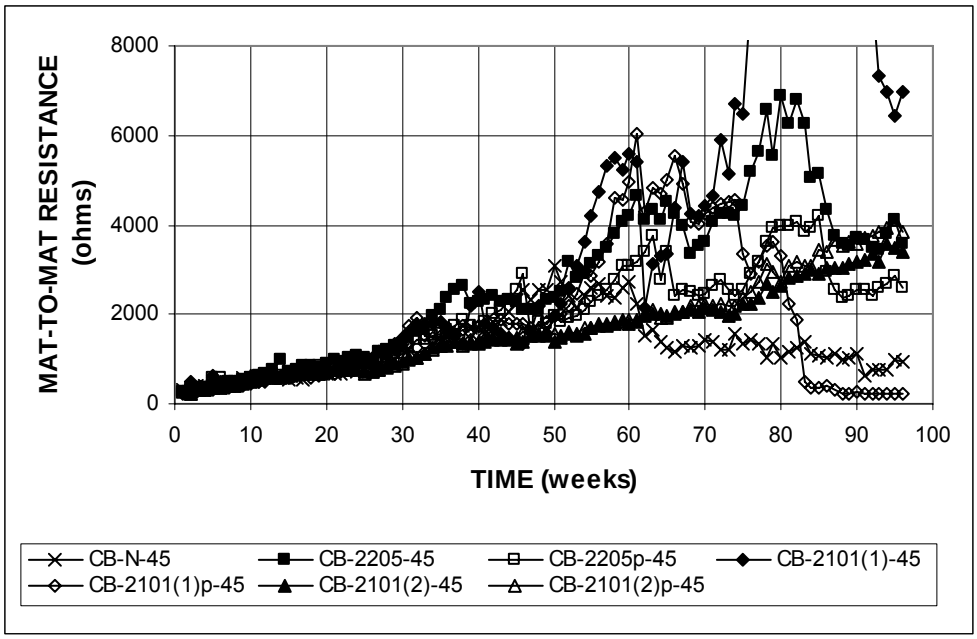


**Figure 3.126 –** Average mat-to-mat resistances as measured in the Southern Exposure test for specimens with conventional and duplex stainless steel.

The reinforcing bars were removed from the concrete specimens after the 96-week test period. Inspection of the bars used in the top mat of the specimens showed corrosion products on the 2101(1), 2101(1)p, 2101(2) and 2205 bars, as shown in Figure 3.127 to 3.130. The 2101(2)p pickled bar of the cracked beam specimen [CB-2101(2)p-45-1], which showed a drop in corrosion potential at week 63, also showed some corrosion products, as shown in Figure 3.131. The remaining 2101(2)p bars showed no corrosion products, as shown in Figure 3.132, and looked as clean as the 2205p bars, shown in Figure 3.133.

**Figure 3.127 –** Corrosion products on 2101(1) steel bar from top mat of cracked beam specimens at week 96.

**Figure 3.128 –** Corrosion products on 2101(1)p steel bar from top mat of cracked beam specimens at week 96.

**Figure 3.129 –** Corrosion products on 2101(2) steel bar from top mat of cracked beam specimen, at week 96.

**Figure 3.130 –** Corrosion products on 2205 steel bar from top mat of cracked beam specimen, at week 96

**Figure 3.131 –** Corrosion products on bars used on top mat of cracked beam specimen CB-2101(2)p-45-1, at week 96.

**Figure 3.132 –** 2101(2)p bar used on top mat of cracked beam specimen, showing no corrosion products, at week 96.

**Figure 3.133 –** 2205p bar used on top mat of cracked beam specimen, showing no corrosion products, at week 96.

## 3.8 ECONOMIC ANALYSIS

Based on the results obtained from the corrosion tests, it was determined that 2205 and 2101 steels in a pickled condition would provide the best corrosion protection. An economic analysis was performed to compare the present cost of bridge decks built with conventional, epoxy-coated, 2101 pickled (2101p), and 2205 pickled (2205p) steel, following the procedures used by Kepler et al. (2000) and Darwin et al. (2002). The present cost takes into consideration the cost of a new bridge deck as well as repair costs during the economic life of the structure, which is taken as 75 years. To perform an economic analysis, it is necessary to first determine the time to first repair of the bridge deck.

### 3.8.1 Time to First Repair

The time to first repair of the structure includes the time required for corrosion initiation and the time it takes for the corrosion products to produce cracking and spalling of the concrete cover. The time to first repair of bridges constructed with the different corrosion protection systems was determined based on experience from the

Kansas Department of Transportation (KDOT), the South Dakota Department of Transportation (SDDOT) and on the results obtained from testing performed at the University of Kansas.

For uncoated conventional and epoxy-coated steel, the time to first repair was obtained from values provided by KDOT and SDDOT (Darwin et al. 2002). According to KDOT, the time to first repair for bridges containing uncoated conventional steel is 25 years, while for bridges containing epoxy-coated steel the time to first repair is 30 years. According to SDDOT, the time to first repair for bridges containing uncoated conventional steel is 10 under harsh conditions and 25 years under arid conditions. For epoxy-coated reinforcement, the SDDOT estimate is 40 years.

For other corrosion protection systems, the time to first repair can be estimated based on three factors:

1) the chloride content required for corrosion initiation, referred to as the chloride corrosion threshold.
2) the time required to reach the chloride corrosion threshold, and
3) the time required to reach a total corrosion loss of 25 μm, which is the amount of corrosion products with a volume that will crack the concrete (Pfeifer 2000).

For 2101(2)p and 2205p steel, the chloride content for corrosion initiation has not been obtained since specimens containing these two steels did not show signs of significant corrosion during the duration of the tests. At the measured average rates of corrosion, these systems will not reach a total corrosion loss of 25 μm for over 300 years. It is assumed that the life expectancy of bridge decks with these two steels is more than 75 years.

### 3.8.2 Cost Effectiveness

A "typical" 230-mm (9-in.) bridge deck is used to evaluate the cost effectiveness of the corrosion protection systems. A 216-mm bridge deck is also used with stainless steel since it is assumed that a decrease in concrete cover can be accepted. A 191-mm concrete subdeck with a 38-mm silica fume concrete overlay (SFO) containing epoxy-coated steel is also included in the evaluation since it is the most common bridge deck type used by KDOT for high-traffic, high-salt exposure conditions. The analysis includes the cost of the new bridge, as well as the cost of repairs over the service life of the bridge. The time to first repair is obtained as mentioned in the previous section. Additional repairs are expected at 25-year cycles following the first repair, based on KDOT estimates.

The cost of concrete, \$475.30/$m^3$, was obtained from average bid items obtained from KDOT for the years 2000 to 2003. Based on data from Kepler et al. (2000), the average density of reinforcing steel is 143 kg/$m^3$. The costs of materials, fabrication, delivery, and placement were obtained from manufacturers and fabricators in 2004. The costs for uncoated conventional steel and epoxy-coated steel are \$0.55/kg (\$0.25/lb) and \$0.68/kg (\$0.31/lb) at the mill, respectively. The cost for fabrication, delivery, and placement is \$1.30/kg (\$0.59/lb) and \$1.41/kg (\$0.64/lb) for uncoated and epoxy-coated steel, respectively. This gives a total in-place cost of \$1.85/kg (\$0.84/lb) for uncoated conventional steel and \$2.09/kg (\$0.95/lb) for epoxy-coated steel. The cost of 2205 pickled steel at the mill was obtained in two different ways. First, a price between \$4.51/kg (\$2.05/lb) and \$5.50/kg (\$2.50/lb) at the mill was obtained from a manufacturer, Carpenter Technologies. Second, a price of \$3.74/kg (\$1.70/lb) had been obtained previously from a manufacturer, and based on recent increases in price for chromium, nickel, molybdenum, and scrap steel, an

increase in price of $0.22/kg ($0.10/lb) was calculated, giving a price of $3.96/kg ($1.80/lb). The three different prices for 2205 pickled steel are used in the analysis: $3.96/kg, $4.51/kg, and $5.50/kg. The difference in cost between 2101 and 2205 pickled steels was calculated based on current costs of chromium, nickel, molybdenum, and scrap steel and the composition of the steels. Current costs for raw materials are $1.58/kg ($0.72/lb) for chromium, $14.63/kg ($6.65/lb) for nickel, $34.10/kg ($15.50/lb) for molybdenum, and $0.28/kg, ($0.13/lb) for scrap steel. The difference in cost between 2101 and 2205 pickled steels based on the cost of the raw materials is $1.50/kg ($0.68/lb), giving prices for 2101 pickled steel of $2.46/kg ($1.12/lb), $3.01/kg ($1.37/lb) and $4.00/kg ($1.82/lb) at the mill. The cost for fabrication, delivery and placement of stainless steel is $1.39/kg ($0.63/lb), based on the same fabrication cost as conventional steel and the same delivery and placement cost as epoxy-coated steel. This gives total in-place costs of $5.35/kg ($2.43/lb), $5.90/kg ($2.68/lb) and $6.89/kg ($3.13/lb) for 2205 pickled steel, and $3.85/kg ($1.75/lb), $4.40/kg ($2.00/lb) and $5.39/kg ($2.45/lb) for 2101 pickled steel. All costs are transformed into a cost in dollars per square meter, as shown below.

*230-mm concrete deck*

$$\frac{\$475.30}{\mathrm{m}^3} \times \frac{0.230\,\mathrm{m}^3}{\mathrm{m}^2} = \$109.32/\mathrm{m}^2$$

*216-mm concrete deck*

$$\frac{\$475.30}{\mathrm{m}^3} \times \frac{0.216\,\mathrm{m}^3}{\mathrm{m}^2} = \$102.66/\mathrm{m}^2$$

*191-mm concrete deck + 38-mm silica fume overlay*

$$\frac{\$475.30}{\mathrm{m}^3} \times \frac{0.191\,\mathrm{m}^3}{\mathrm{m}^2} + \$43.61/\mathrm{m}^2 = \$134.39/\mathrm{m}^2$$

*Conventional steel*

$$\frac{\$1.85}{\mathrm{kg}} \times \frac{143\,\mathrm{kg}}{\mathrm{m}^3} \times \frac{0.230\,\mathrm{m}^3}{\mathrm{m}^2} = \$60.85/\mathrm{m}^2$$

*Epoxy-coated steel*

$$\frac{\$2.09}{\text{kg}} \times \frac{143\,\text{kg}}{\text{m}^3} \times \frac{0.230\,\text{m}^3}{\text{m}^2} = \$68.74/\text{m}^2$$

*2205 pickled steel (low end)*

$$\frac{\$5.35}{\text{kg}} \times \frac{143\,\text{kg}}{\text{m}^3} \times \frac{0.230\,\text{m}^3}{\text{m}^2} = \$175.96/\text{m}^2$$

*2205 pickled steel (middle value)*

$$\frac{\$5.90}{\text{kg}} \times \frac{143\,\text{kg}}{\text{m}^3} \times \frac{0.230\,\text{m}^3}{\text{m}^2} = \$194.05/\text{m}^2$$

*2205 pickled steel (high end)*

$$\frac{\$6.89}{\text{kg}} \times \frac{143\,\text{kg}}{\text{m}^3} \times \frac{0.230\,\text{m}^3}{\text{m}^2} = \$226.61/\text{m}^2$$

*2101 pickled steel (low end)*

$$\frac{\$3.85}{\text{kg}} \times \frac{143\,\text{kg}}{\text{m}^3} \times \frac{0.230\,\text{m}^3}{\text{m}^2} = \$126.63/\text{m}^2$$

*2101 pickled steel (middle value)*

$$\frac{\$4.40}{\text{kg}} \times \frac{143\,\text{kg}}{\text{m}^3} \times \frac{0.230\,\text{m}^3}{\text{m}^2} = \$144.72/\text{m}^2$$

*2101 pickled steel (high end)*

$$\frac{\$5.39}{\text{kg}} \times \frac{143\,\text{kg}}{\text{m}^3} \times \frac{0.230\,\text{m}^3}{\text{m}^2} = \$177.28/\text{m}^2$$

Based on information obtained from KDOT for bridges that received repairs in 1999 and reported by Kepler et al. (2000), 6% of the total deck received full depth repair, and 22% of the total deck received partial depth repair. The cost of repairs for bridge decks is calculated based on the average low-bid costs reported by KDOT for the years 2000-2003. The costs of full-depth and partial-depth repair are $\$380.30/\text{m}^2$ and $\$125.77/\text{m}^2$, respectively. Other costs include machine preparation ($\$13.13/\text{m}^2$), a 38-mm silica fume overlay ($\$43.61/\text{m}^2$), and incidental costs ($\$154.89/\text{m}^2$). Based on these costs, the average cost of repair is $\$262.34/\text{m}^2$ as shown below.

$$0.22 \times \frac{\$125.77}{\text{m}^2} + 0.06 \times \frac{\$380.30}{\text{m}^2} + \frac{\$13.13}{\text{m}^2} + \frac{\$43.61}{\text{m}^2} + \frac{\$154.89}{\text{m}^2} + = \$262.34/\text{m}^2$$

The cost comparison is performed based on the cost of the new bridge deck plus the present value of the costs of repairs over the 75-year economic life of the structure. Discount rates of 2, 4 and 6% are used. The present value is calculated using Eq. (3.4):

$$P = F \times (1+i)^{-n} \tag{3.4}$$

where

$P$ = present value

$F$ = cost of repair

$i$ = discount rate (%/100)

$n$ = time to repair (in years)

Table 3.53 shows the results of the economic analysis for the different options. The new deck cost of a 230-mm bridge deck reinforced with conventional steel is \$170.17/m$^2$, while the cost of the same deck reinforced with epoxy-coated steel is \$178.06/m$^2$. The new deck costs of a 230-mm bridge deck reinforced with 2205p steel are \$285.28/m$^2$, \$303.37/m$^2$, and \$335.93/m$^2$, depending on the cost of the steel, as mentioned earlier. The new deck costs of a 230-mm bridge deck reinforced with 2101p steel are \$235.95/m$^2$, \$254.04/m$^2$, and \$286.60/m$^2$, depending on the cost of the steel. The use of a 216-mm bridge deck instead of a 230-mm bridge deck reduces the new deck price by \$6.32/m$^2$. Decks containing 2101p steel are \$49.32/m$^2$ cheaper than decks containing 2205p steel.

**Table 3.53 -** Economic analysis for bridge decks containing conventional uncoated, epoxy-coated, and duplex stainless steel.

| Option | Type of deck | Type of steel | Cost of deck ($/m$^2$) | Cost of steel ($/m$^2$) | Total cost ($/m$^2$) | Cost of repair 1 ($/m$^2$) | Time to repair 1 (years) | Cost of repair 2 ($/m$^2$) | Time to repair 2 (years) | Cost of repair 3 ($/m$^2$) | Time to repair 3 (years) | Present cost i = 2% ($/m$^2$) | Present cost i = 4% ($/m$^2$) | Present cost i = 6% ($/m$^2$) |
|---|---|---|---|---|---|---|---|---|---|---|---|---|---|---|
| 1 | 230-mm | Black | $109.32 | $60.85 | $170.17 | $262.34 | 10 | $262.34 | 35 | $262.34 | 60 | $596.51 | $438.82 | $358.74 |
| 2 | | | | | | | 25 | | 50 | | | $427.54 | $305.49 | $245.54 |
| 3 | 230-mm | ECR | $109.32 | $68.74 | $178.06 | $262.34 | 30 | $262.34 | 55 | | | $411.17 | $289.29 | $234.38 |
| 4 | | | | | | | 35 | | 60 | | | $389.19 | $269.48 | $220.14 |
| 5 | | | | | | | 40 | | 65 | | | $369.29 | $253.20 | $209.51 |
| 6 | 191-mm + | | | | | | 30 | | 55 | | | $436.24 | $314.36 | $259.45 |
| 7 | 38-mm SFO | ECR | $134.39 | $68.74 | $203.13 | $262.34 | 35 | $262.34 | 60 | | | $414.26 | $294.55 | $245.21 |
| 8 | | | | | | | 40 | | 65 | | | $394.36 | $278.27 | $234.58 |
| 9 | 230-mm | 2205p | $109.32 | $175.96 | $285.28 | | | | | | | $285.28 | $285.28 | $285.28 |
| 10 | | | | $194.05 | $303.37 | | | | | | | $303.37 | $303.37 | $303.37 |
| 11 | | | | $226.61 | $335.93 | | | | | | | $335.93 | $335.93 | $335.93 |
| 12 | 230-mm | 2101p | $109.32 | $126.63 | $235.95 | | | | | | | $235.95 | $235.95 | $235.95 |
| 13 | | | | $144.72 | $254.04 | | | | | | | $254.04 | $254.04 | $254.04 |
| 14 | | | | $177.28 | $286.60 | | | | | | | $286.60 | $286.60 | $286.60 |
| 15 | 216-mm | 2205p | $102.60 | $175.96 | $278.56 | | | | | | | $278.56 | $278.56 | $278.56 |
| 16 | | | | $194.05 | $296.65 | | | | | | | $296.65 | $296.65 | $296.65 |
| 17 | | | | $226.61 | $329.21 | | | | | | | $329.21 | $329.21 | $329.21 |
| 18 | 216-mm | 2101p | $102.60 | $126.63 | $229.23 | | | | | | | $229.23 | $229.23 | $229.23 |
| 19 | | | | $144.72 | $247.32 | | | | | | | $247.32 | $247.32 | $247.32 |
| 20 | | | | $177.28 | $279.88 | | | | | | | $279.88 | $279.88 | $279.88 |

At discount rates of 2% and 4%, the lowest cost option is a 216-mm deck containing 2101 pickled steel, with a present cost of $229.23/m$^2$. If a 230-mm bridge deck is used, the cost of a deck with 2101 pickled steel is still lower than decks with epoxy-coated steel, at $235.95/m$^2$. These values were obtained using the low end of the price for 2101p steel. If the high end of the price is used, 2101p steel still has a lower present cost, at $279.88/m$^2$ and $286.60/m$^2$, for the 216 and 230-mm bridge decks, respectively. At a 6% discount rate, the lowest cost option is a 230-mm deck containing epoxy-coated steel, with present costs of $209.51/m$^2$ and $220.14/m$^2$ for 40 and 35 years of time to first repair, respectively. The 191-mm concrete bridge deck with a 38-mm silica fume overlay containing epoxy-coated bars has a present cost of $234.58 at a 6% discount rate and 40 years of time to first repair. This value is higher than the initial cost of 2101p steel at the low end, $229.23/m$^2$. The cost of a 216-mm deck containing 2205p steel is $329.21 at the low end. This value is lower than that of the decks with epoxy-coated steel at a discount rate of 2%, but higher than at discount rates of 4 and 6%.

Although the present cost provides a good comparison, a better indicator of the cost effectiveness is the ratio of the premium for using duplex steel over the savings in repair costs. The savings in repair costs are the present value of the bridge deck including repairs over the life of the structure minus the cost of the new bridge deck and are shown in Table 3.54. The premiums for duplex steel, shown in Tables 3.55 and 3.56, are the cost of new decks containing duplex steel minus the cost of a new deck containing epoxy-coated steel. Ratios of premium/savings are shown in Tables 3.55 and 3.56. Ratios below 50% are considered satisfactory.

**Table 3.54 –** Savings in repair costs for decks with conventional uncoated and epoxy-coated steel if duplex steel is used as a replacement.

| Option | Type of deck | Type of steel | Savings in repair costs i = 2% ($/m$^2$) | i = 4% ($/m$^2$) | i = 6% ($/m$^2$) |
|---|---|---|---|---|---|
| 1 | 230-mm | Black | $426.34 | $268.65 | $188.57 |
| 2 | | | $427.54 | $305.49 | $245.54 |
| 3 | 230-mm | ECR | $233.11 | $111.23 | $56.32 |
| 4 | | | $211.13 | $91.42 | $42.08 |
| 5 | | | $191.23 | $75.14 | $31.45 |
| 6 | 191-mm + 38-mm SFO | ECR | $233.11 | $111.23 | $56.32 |
| 7 | | | $211.13 | $91.42 | $42.08 |
| 8 | | | $191.23 | $75.14 | $31.45 |

Table 3.55 shows the ratios of premium for duplex steel over savings in repair costs for decks containing duplex steel versus a 230-mm deck containing epoxy-coated steel. The lowest premium/savings ratio indicates the best option. At a 2% discount rate, a 216-mm deck containing 2101p steel has a maximum premium/savings ratio of 53% for the high-end cost of 2101p and a time to first repair of 40 years for the deck containing epoxy-coated steel. For the low-end cost of 2101p and a time to first repair of 40 years for the deck containing epoxy-coated steel, the ratio is 22%. If the duplex steel is placed in a 230-mm deck instead of a 216-mm deck, the maximum premium/savings ratio is 57%. For decks containing 2205p steel, premium/savings ratios of 50% and lower were obtained for a 230-mm deck when compared to a deck containing epoxy-coated steel with an time to first repair of 30 years, and for a 216-mm deck when compared to a deck containing epoxy-coated steel with a time to first repair of 30 or 35 years. At a discount rate of 4%, only the option of a 216-mm deck containing 2101p steel has a premium/savings ratio lower than 50%. At a discount rate of 6%, the lowest premium/savings ratio is 91%.

Table 3.56 shows the ratios of premium for duplex steel over savings in repair costs for decks containing duplex steel versus a 191-mm deck with a 38-mm silica

fume overlay (SFO) containing epoxy-coated steel. Since the cost of the 191-mm deck with the silica fume overlay is more than the 230-mm deck, the premium/savings ratios are lower in this case. At a discount rate of 2%, a 216-mm deck containing 2101p steel has a maximum premium/savings ratio of 40% for the high-end cost of 2101p and a time to first repair of 40 years for the deck containing epoxy-coated steel. For the low-end cost of 2101p and a time to first repair of 40 years for the deck containing epoxy-coated steel, the ratio is 11%. For a 230-mm deck containing 2101p steel the premium/savings ratio ranges from 14% to 44%. For decks containing 2205p steel, the premium/savings ratio ranges from 35% to 69% for a 216-mm deck and from 32% to 66% for a 230-mm deck. At discount rates of 4%, for decks containing 2101p steel, the premium/savings ratio has values as low as 23% for a 216-mm deck and 30% for a 230-mm deck. For decks containing 2205p steel, all options have ratios higher than 68%. At a discount rate of 6%, the only option with a ratio of 50% is a 216-mm deck containing 2101p steel, when the low-end cost for the steel is used and the deck containing epoxy-coated steel has a time to first repair of 30 years.

**Table 3.55 –** Premium/savings ratio for decks containing duplex steel versus a 230-mm deck containing epoxy-coated steel.

| Decks compared | Options* | | Premium for duplex steel | Ratio Premium/Savings i = 2% ($/m$^2$) | i = 4% ($/m$^2$) | i = 6% ($/m$^2$) |
|---|---|---|---|---|---|---|
| | **9** | **3** | 107.22 | 46% | 96% | 190% |
| **230-mm deck** | **9** | **4** | 107.22 | 51% | 117% | 255% |
| **containing 2205p** | **9** | **5** | 107.22 | 56% | 143% | 341% |
| **vs.** | **10** | **3** | 125.31 | 54% | 113% | 223% |
| **230-mm deck** | **10** | **4** | 125.31 | 59% | 137% | 298% |
| **containing ECR** | **10** | **5** | 125.31 | 66% | 167% | 398% |
| | **11** | **3** | 157.87 | 68% | 142% | 280% |
| | **11** | **4** | 157.87 | 75% | 173% | 375% |
| | **11** | **5** | 157.87 | 83% | 210% | 502% |
| | **12** | **3** | 57.89 | 25% | 52% | 103% |
| **230-mm deck** | **12** | **4** | 57.89 | 27% | 63% | 138% |
| **containing 2101p** | **12** | **5** | 57.89 | 30% | 77% | 184% |
| **vs.** | **13** | **3** | 75.98 | 33% | 68% | 135% |
| **230-mm deck** | **13** | **4** | 75.98 | 36% | 83% | 181% |
| **containing ECR** | **13** | **5** | 75.98 | 40% | 101% | 242% |
| | **14** | **3** | 108.54 | 47% | 98% | 193% |
| | **14** | **4** | 108.54 | 51% | 119% | 258% |
| | **14** | **5** | 108.54 | 57% | 144% | 345% |
| | **15** | **3** | 100.50 | 43% | 90% | 178% |
| **216-mm deck** | **15** | **4** | 100.50 | 48% | 110% | 239% |
| **containing 2205p** | **15** | **5** | 100.50 | 53% | 134% | 320% |
| **vs.** | **16** | **3** | 118.59 | 56% | 130% | 282% |
| **230-mm deck** | **16** | **4** | 118.59 | 62% | 158% | 377% |
| **containing ECR** | **16** | **5** | 118.59 | 51% | 107% | 211% |
| | **17** | **3** | 151.15 | 65% | 136% | 268% |
| | **17** | **4** | 151.15 | 72% | 165% | 359% |
| | **17** | **5** | 151.15 | 79% | 201% | 481% |
| | **18** | **3** | 51.17 | 22% | 46% | 91% |
| **216-mm deck** | **18** | **4** | 51.17 | 24% | 56% | 122% |
| **containing 2101p** | **18** | **5** | 51.17 | 27% | 68% | 163% |
| **vs.** | **19** | **3** | 69.26 | 30% | 62% | 123% |
| **230-mm deck** | **19** | **4** | 69.26 | 33% | 76% | 165% |
| **containing ECR** | **19** | **5** | 69.26 | 36% | 92% | 220% |
| | **20** | **3** | 101.82 | 44% | 92% | 181% |
| | **20** | **4** | 101.82 | 48% | 111% | 242% |
| | **20** | **5** | 101.82 | 53% | 136% | 324% |

* see Table 3.53

**Table 3.56 –** Premium/savings ratio for decks containing duplex steel versus a 216-mm concrete + 38-mm SFO deck containing epoxy-coated steel.

| Decks compared | Options* | | Premium for duplex steel | Ratio Premium/Savings i = 2% ($/m$^2$) | i = 4% ($/m$^2$) | i = 6% ($/m$^2$) |
|---|---|---|---|---|---|---|
| | **9** | **6** | 82.15 | 35% | 74% | 146% |
| **230-mm deck** | **9** | **7** | 82.15 | 39% | 90% | 195% |
| **containing 2205p** | **9** | **8** | 82.15 | 43% | 109% | 261% |
| **vs.** | **10** | **6** | 100.24 | 43% | 90% | 178% |
| **191-mm +** | **10** | **7** | 100.24 | 47% | 110% | 238% |
| **38-mm SFO** | **10** | **8** | 100.24 | 52% | 133% | 319% |
| **containing ECR** | **11** | **6** | 132.80 | 57% | 119% | 236% |
| | **11** | **7** | 132.80 | 63% | 145% | 316% |
| | **11** | **8** | 132.80 | 69% | 177% | 422% |
| | **12** | **6** | 32.82 | 14% | 30% | 58% |
| **230-mm deck** | **12** | **7** | 32.82 | 16% | 36% | 78% |
| **containing 2101p** | **12** | **8** | 32.82 | 17% | 44% | 104% |
| **vs.** | **13** | **6** | 50.91 | 22% | 46% | 90% |
| **191-mm +** | **13** | **7** | 50.91 | 24% | 56% | 121% |
| **38-mm SFO** | **13** | **8** | 50.91 | 27% | 68% | 162% |
| **containing ECR** | **14** | **6** | 83.47 | 36% | 75% | 148% |
| | **14** | **7** | 83.47 | 40% | 91% | 198% |
| | **14** | **8** | 83.47 | 44% | 111% | 265% |
| | **15** | **6** | 75.43 | 32% | 68% | 134% |
| **216-mm deck** | **15** | **7** | 75.43 | 36% | 83% | 179% |
| **containing 2205p** | **15** | **8** | 75.43 | 39% | 100% | 240% |
| **vs.** | **16** | **6** | 93.52 | 40% | 84% | 166% |
| **191-mm +** | **16** | **7** | 93.52 | 44% | 102% | 222% |
| **38-mm SFO** | **16** | **8** | 93.52 | 49% | 124% | 297% |
| **containing ECR** | **17** | **6** | 126.08 | 54% | 113% | 224% |
| | **17** | **7** | 126.08 | 60% | 138% | 300% |
| | **17** | **8** | 126.08 | 66% | 168% | 401% |
| | **18** | **6** | 26.10 | 11% | 23% | 46% |
| **216-mm deck** | **18** | **7** | 26.10 | 12% | 29% | 62% |
| **containing 2101p** | **18** | **8** | 26.10 | 14% | 35% | 83% |
| **vs.** | **19** | **6** | 44.19 | 19% | 40% | 78% |
| **191-mm +** | **19** | **7** | 44.19 | 21% | 48% | 105% |
| **38-mm SFO** | **19** | **8** | 44.19 | 23% | 59% | 141% |
| **containing ECR** | **20** | **6** | 76.75 | 33% | 69% | 136% |
| | **20** | **7** | 76.75 | 36% | 84% | 182% |
| | **20** | **8** | 76.75 | 40% | 102% | 244% |

* see Table 3.53

## 3.9 DISCUSSION OF RESULTS

### 3.9.1 Summary of Results

The use of a low water-cement ratio and corrosion inhibitors seems to improve the corrosion protection of the steel in uncracked concrete, such as the Southern Exposure test. In cracked concrete, the use of a low water-cement ratio and corrosion inhibitors is not as effective, and in some cases these specimens showed higher corrosion losses than the control samples.

The microalloyed steels (CRPT1, CRPT2, and CRT) showed no improvement in corrosion performance compared to conventional reinforcing steel. Microalloyed steel corroded at similar or even higher rates than conventional steel, and the corrosion potentials indicated that they had a similar tendency to corrode.

MMFX microcomposite steel had corrosion losses that ranged from 26 to 60% of the corrosion loss of conventional steel, while corrosion potentials indicated that they had a similar tendency to corrode.

Epoxy-coated steel had low corrosion losses based on the total area of the bar, with corrosion losses between 6% and 19% of that of uncoated conventional steel.

The 2101(2) and 2205 duplex steels evaluated in a pickled condition showed very good corrosion performance in all tests. The average corrosion losses for these steels ranged from 0.3 to 1.8% of the corrosion loss of conventional steel, and in most cases, the corrosion potentials indicated a very low tendency to corrode, even at high salt concentrations.

### 3.9.2 Corrosion Inhibitors and Low Water-Cement Ratio

The effect of using a concrete or mortar with a lower water-cement ratio and/or corrosion inhibitors was evaluated with the macrocell and bench-scale tests. Specimens were prepared with a water-cement ratio of 0.45 with or without corrosion inhibitors and with a water-cement ratio of 0.35 with and without corrosion inhibitors. The corrosion inhibitors evaluated were Rheocrete 222+ and DCI-S.

In the macrocell test, specimens with a water-cement ratio of 0.35 and no inhibitor had an average total corrosion loss equal to 60% of that of the specimens with a water-cement ratio of 0.45 and no inhibitor. The specimens with corrosion inhibitors had corrosion losses between 17% and 44% of the corrosion loss specimens without corrosion inhibitors (see Figure 3.12 and Table 3.4). The corrosion potentials of the anode, Figure 3.13, show active corrosion for all specimens. In these tests, the corrosion inhibitors and the concrete with a low water-cement ratio (0.35) provided better corrosion protection to the steel than the control specimens, which were fabricated with mortar or concrete with a water-cement ratio of 0.45 and no inhibitor. These results are consistent with the study by Trepanier et al. (2001) for specimens with a water-cement ratio of 0.50, where corrosion inhibitors delayed the initiation of corrosion and had lower corrosion rates than the control samples.

For the Southern Exposure test, specimens were prepared with normalized and Thermex-treated conventional steels. When the results obtained with these two steels are averaged for specimens without a corrosion inhibitor, at 70 weeks, the specimens with a water-cement ratio of 0.35 exhibited an average total corrosion loss equal to 7% of the corrosion loss of the control specimens (water-cement ratio of 0.45), as shown in Tables 3.5 and 3.7. Specimens with a water-cement ratio of 0.45 and corrosion inhibitors had corrosion losses equal to 7% and 68% for specimens with

Rheocrete 222+ and DCI-S, respectively, of that of the specimens with a water-cement ratio of 0.45 and no inhibitor. The specimens with a water-cement ratio of 0.35 and corrosion inhibitors had the lowest average total corrosion losses, with values of 1.3% and 4% for specimens with Rheocrete 222+ and DCI-S, respectively, of the losses exhibited by the specimens with a water-cement ratio of 0.35 and no inhibitor. The use of corrosion inhibitors and a low water-cement ratio increases the corrosion protection of the steel in the case of uncracked concrete. At week 70, the specimens with Rheocrete 222+ had approximately ¼ of the corrosion losses of specimens with DCI-S, for specimens with a water-cement ratio of 0.45, and ½ of the corrosion loss of specimens with DCI-S, for specimens with a water-cement ratio of 0.35. It is known that DCI-S works better at lower water-cement ratios (Berke et al. 1993). For the specimens with a water-cement ratio of 0.45, the average corrosion potentials, shown in Figures 3.16 and 3.22, indicated the initiation of corrosion at 5 weeks for untreated specimens, 26 weeks for specimens with Rheocrete 222+, and 30 weeks for specimens with DCI-S. These results do not agree with the study by Nmai et al. (1992), where specimens with organic inhibitors did not show signs of corrosion after 180 days, while specimens with calcium nitrite showed corrosion activity after 30 days.

In the cracked beam test, specimens were also prepared with normalized and Thermex-treated conventional steels. The results obtained with these two steels are averaged for the present discussion. In the cracked beam tests, the average corrosion losses, shown in Tables 3.10 and 3.12, for specimens with a water-cement ratio of 0.35 and no inhibitor were 59% of the corrosion loss of specimens with a water-cement ratio of 0.45 and no inhibitor. Thus, a lower-water cement ratio provided only limited additional corrosion protection when cracks provided a direct path for

the chlorides to the steel. For specimens with a water-cement ratio of 0.45, the corrosion losses were 51% and 155% for specimens with Rheocrete 222+ and DCI-S, respectively, of the corrosion loss of specimens with no inhibitors. For specimens with a water-cement ratio of 0.35, the corrosion losses were 86% and 179% for specimens with Rheocrete 222+ and DCI-S, respectively, of the corrosion loss of specimens with no inhibitors. For cracked concrete, Rheocrete 222+ provided some corrosion protection while the presence of DCI-S did not improve the corrosion protection over the steel. The lower corrosion rates obtained for specimens with a low water-cement ratio and/or Rheocrete 222+ are likely due to a reduced rate of diffusion of oxygen and water to the cathode bars because of the lower permeability of the material. Based on the average corrosion potentials, shown in Figures 3.16 and 3.19, all specimens started corroding during the first week. Again, these results differ from those of Nmai et al. (1992), where it took between 17 and 35 days for Southern Exposure specimens with calcium nitrite to start corroding, and 118 days for specimens with organic inhibitors to start corroding. Nmai et al. (1992), however, used specimens with cracks that where perpendicular, rather than on top and parallel, to the reinforcing steel, and drying of the specimens occurred at room temperature instead of at 100$^{o}$F. Cracks on top and parallel to the reinforcing steel simulate settlement cracking observed in concrete bridge decks

In the ASTM G 109 test, significant corrosion activity was observed only for specimens with a water-cement ratio of 0.45 and no inhibitor and specimens with a water-cement ratio of 0.45 and DCI-S, as shown in Figures 3.32 and 3.33. The remaining specimens had very low corrosion rates throughout the test period. The fact that lower corrosion activity was observed in the G 109 test is attributed to the lower salt concentration of the solution ponded over the specimens and to the less

aggressive ponding and drying cycle to which the specimens were subjected, compared to the other two bench-scale tests (Southern Exposure and cracked beam). The two factors reduce the rate at which chlorides penetrate into the concrete in the ASTM G 109 test, which makes this test less effective than the Southern Exposure and cracked beam tests in evaluating the behavior of the materials in a relatively short period of time.

### 3.9.3 Microalloyed Steel

Three microalloyed steels were evaluated along with Thermex-treated conventional steel. Results for these tests were previously reported by Balma et al. (2002). The bars were evaluated in a bare condition and partly embedded in mortar using the macrocell test with a 1.6 m ion NaCl and simulated concrete pore solution. The macrocell tests, summarized in Figures 3.40 to 3.45 and Tables 3.15 to 3.20, indicate no improvement in corrosion resistance for the microalloyed steels or the Thermex-treated steel, compared to conventional, normalized steel, and in some cases, these steels had higher corrosion rates than the conventional steel.

In the bench-scale tests, only one of the microalloyed steels, CRT, showed lower corrosion losses than conventional, normalized steel on the three tests. After 70 weeks, corrosion losses for CRT steel were 90%, 96% and 36% of the corrosion losses of conventional steel in the Southern Exposure, cracked beam, and G 109 tests, respectively (Tables 3.22, 3.24, and 3.26). The corrosion potentials measured in the bench-scale tests (Figures 3.48, 3.52, and 3.56) show similar behavior for the five steels, with values indicating active corrosion throughout the test period in the cracked beam test (Figure 3.32) and beginning at week 25 in the Southern Exposure test (Figure 3.30).

### 3.9.4 MMFX Microcomposite Steel

Test results for MMFX microcomposite steel and epoxy-coated steel were previously reported by Darwin et al. (2002) and Gong et al. (2002). At the time of the reports, the bench-scale tests were 23 and 40 weeks old, respectively. The present report covers the full 96-week test period.

MMFX microcomposite steel was evaluated in a bare condition using the macrocell test in simulated concrete pore solution and at NaCl ion concentrations of 1.6 and 6.04 m and with mortar-wrapped bars at the lower NaCl concentration. Some bars were sandblasted to remove the mill scale or bent to evaluate the effect of bending and the resulting residual stresses. For the bare specimens in 1.6 m ion NaCl, the sandblasted bars had similar corrosion losses to the bars that were not sandblasted (Table 3.28). The average corrosion losses for the straight No. 16 [No. 5] bars evaluated were 35% of the average corrosion loss of conventional steel. The corrosion potential of the anode bars indicated active corrosion (Figure 3.60). The MMFX steel in 6.04 m ion NaCl solution had the same corrosion loss as conventional steel after 15 weeks (Table 3.30) and the same corrosion potentials throughout the test period (Figure 3.66).

In the macrocell tests with mortar-wrapped bars, MMFX steel had an average corrosion loss equal to 25% of that of conventional steel (Table 3.32). The corrosion potentials (Figure 3.64) indicated active corrosion for MMFX steel at week 3 and for conventional steel before the end of week 1.

In the Southern Exposure tests, after 70 weeks, MMFX steel had an average corrosion loss equal to 26% of the corrosion loss of conventional steel (Table 3.34). Top mat potentials (Figure 3.74) showed active corrosion for both steels at week 70. The average corrosion potentials indicated the initiation of corrosion at week 11 for

conventional steel and week 25 for MMFX steel, indicating that MMFX steel has a higher chloride threshold. In the cracked beam test, the corrosion loss of MMFX steel was equal to 35% of that of conventional steel (Table 3.36). Both MMFX and conventional steel showed active corrosion of the top mat after the first week (Figure 3.79).

### 3.9.5 Epoxy-Coated Steel

Epoxy-coated steel was evaluated using the macrocell and bench-scale tests. Uncoated conventional steel from the same heat as the epoxy-coated steel was used in the cathode in the macrocell test and in the bottom mat of the bench-scale specimens. The coating was intentionally damaged by drilling four 3.2-mm ($^1/_8$-in.) diameter holes in the epoxy to expose the steel. Corrosion rates were calculated based on both the area of exposed steel (area of the four holes) and the total area of the bar exposed to solution.

For mortar-wrapped bars exposed to a 1.6 m ion NaCl and simulated concrete pore solution (Table 3.38) and the Southern Exposure specimens (Table 3.40), the epoxy-coated bars had a corrosion loss, based on the total area of the bars, equal to 6% of the corrosion loss of uncoated conventional steel. When the corrosion losses were calculated based on the exposed area of steel, the corrosion losses were 7 and 31 times the corrosion loss of the uncoated steel, for the macrocell and Southern Exposure tests, respectively.

For the cracked beam test, the corrosion loss of the epoxy-coated steel was 19% of the corrosion loss of the uncoated steel based on the total area of the bars and 94 times that of the uncoated steel based on the exposed area of steel (Table 3.42).

### 3.9.6 Duplex Stainless Steels

Two types of duplex steel were evaluated: 2205 (22% chromium and 5% nickel) and 2101 (21% chromium and 1% nickel). Two heats of 2101 steel were received. The steel labeled 2101(1) was defective due to a lack of boron; these bars were slightly deformed and showed small cracks on the surface. The duplex steel labeled 2101(2) steel was received as a replacement. All duplex steels were evaluated in both "as-rolled" and pickled conditions. In addition, 2101(2) steel was sandblasted to remove the mill scale. The pickled 2101(2) and 2205 [2101(2)p and 2205p] steels showed very low corrosion losses in all tests.

For bare bars exposed to a 1.6 m ion NaCl and simulated concrete pore solution in the macrocell test, 2205, 2205p, and 2101(2)p steels had corrosion losses that were less than 0.4% of the corrosion loss of conventional steel (Table 3.44). For bare bars in a 6.04 m ion NaCl solution (Table 3.46), the lowest corrosion losses were exhibited by 2205p and 2101(2)p steel, with 0.3% and 1.8%, respectively, of the corrosion loss of conventional steel. Corrosion potentials (Figures 3.96 and 3.99) indicated a very low tendency to corrode at the anode for these two steels, even at the high salt concentrations. For mortar-wrapped bars, 2205, 2205p, and 2101(2)p steels had corrosion losses equal to 0.8% of conventional steel (Table 3.48) and the corrosion potentials indicated a passive condition at the anode (Figure 3.108).

In the Southern Exposure and cracked beam tests (Tables 3.50 and 3.52, respectively), 2101(2) and 2205p steels had corrosion losses equal to 0.3% of that of conventional steel. In the Southern Exposure tests, 2205 and 2205p steel showed the lowest tendency to corrode, based on corrosion potential measurements. The average corrosion potentials (Figure 3.119) indicated that the time to corrosion initiation was 5 weeks for conventional steel and 85 weeks for 2101(2) steel, while 2205 steel

remained passive during the test period. The results for 2205 are consistent with results of Clemeña and Virmani (2002), where 2205 steel did not show signs of corrosion after 2 years of exposure. For the current study, in the cracked beam test (Figure 3.125), only 2205p remained passive throughout the test period, while the average corrosion potential of 2101(2)p became more negative after week 74.

Results for specimens with a combination of conventional and 2205 steel show that specimens with conventional steel in the top mat and 2205 steel in the bottom mat had similar corrosion rates and losses as specimens with conventional steel in the top and bottom mats. Specimens with 2205 steel in the top mat and conventional steel in the bottom mat had similar corrosion rates and losses as specimens with 2205 steel in the top and bottom mats. These results indicate mixing the steel is not a problem.

In general, for the duplex stainless steels, 2205 steel performed better than either heat of 2101 steel, when tested in the same condition (pickled or non-pickled). For bars of the same type of steel, pickled bars exhibited lower corrosion rates than the bars that were not pickled. The bars that performed best were 2205p and 2101(2)p, with the 2205p bars showing lower corrosion rates than 2101(2)p in most cases. Some of the 2101(2) pickled bars showed some corrosion activity. This could be caused by steel that is not fully pickled. In the case of 2205 steel, however, even the unpickled bars showed good corrosion protection.

### 3.9.7 Economic Analysis

The economic analysis included the calculation of the present costs of bridge decks with different corrosion protection systems as well as the ratio of premium of using duplex steel over savings in repair costs when duplex steel is used instead of

conventional uncoated or epoxy-coated steel. Decks containing epoxy-coated steel were compared with decks containing 2101 pickled or 2205 pickled steels, since these two steels showed the best corrosion performance of all materials evaluated. A 75-year economic life, was assumed for the bridge decks and the time to first repair of the bridge decks containing conventional uncoated and epoxy-coated steel was obtained from estimates by KDOT and SSDOT. The time to first repair of the duplex steels was assumed to be more than 75 years since they did not show signs of corrosion initiation. Additional repairs are performed every 25 years after the first repair. Discount rates of 2, 4, and 6% were used in the calculations.

Based on the economic analysis, the lowest cost option at discount rate of 2% or 4% is either a 216 or 230-mm bridge deck containing 2101 pickled steel, with present costs of $\$229.23/m^2$ and $\$235.95/m^2$, respectively. At a 6% discount rate, the lowest cost option is a 230-mm deck containing epoxy-coated steel, at $\$209.33/m^2$ or $\$219.91/m^2$ for 40 or 35 years for the time to first repair, respectively. At a 2% discount rate, decks containing 2101p steel had premium/savings ratios that range from 14% to 53%, while decks containing 2205p steel had premium/savings ratios that range from 32% to 79%. At a discount rate of 4%, decks containing 2101p steel had premium/savings ratios as low as 30%, but some were as high as 201%, while for decks containing 2205p steel, no option had a premium/savings ratio lower than 52%. At discount rates of 6%, the option with a premium/savings ratio lower than 50% was the 216-mm deck containing 2101p steel, when the low end of the cost of the steel was used.

The cost of a bridge deck containing 2101 pickled steel is lower than the cost of a bridge deck containing 2205 pickled steel. However, since some of the 2101(2) pickled bars showed some corrosion activity it is important to consider the fact that

the steel might not be fully pickled, which would increase the corrosion rate of the steel. In the case of 2205 steel, even the unpickled bars showed low corrosion rates, so even if they are not fully pickled they would still provide good protection against corrosion.

# CHAPTER 4

# COMPARISON BETWEEN TEST METHODS

This chapter presents a comparison between the Southern Exposure, cracked beam, and rapid macrocell tests. These tests were used to evaluate the corrosion protection systems listed in Section 2.1, and the results are discussed in the previous chapter. The corrosion protection systems include microalloyed steel, MMFX microcomposite steel, epoxy-coated steel, duplex stainless steel, corrosion inhibitors, and variations in the water-cement ratio. For the comparison, the corrosion rates and total corrosion losses for the Southern Exposure and cracked beam tests are plotted versus the same results for the rapid macrocell test to determine the degree of correlation between the tests. The results of the cracked beam test are also compared with those of the Southern Exposure test. The coefficient of variation is used to compare the variability of corrosion rates and total corrosion losses for individual tests and to compare the variability of the results for the rapid macrocell, Southern Exposure and cracked beam tests. Impedance spectroscopy analysis is performed to obtain equivalent electrical circuits to represent the Southern Exposure and rapid macrocell tests.

Total corrosion losses show good correlation between the Southern Exposure test and the rapid macrocell test in all cases, except when comparing the SE test with the rapid macrocell test for microalloyed steel. As shown in Chapter 3, microalloyed steel behaves much like conventional steel. Since the corrosion rates and losses are similar for the microalloyed and conventional steels and the scatter is relatively high, a correlation between the test methods cannot be obtained from these specimens. For the other comparisons between total corrosion losses for different tests, the

coefficients of determination $R^2$ range from 0.80 to 0.95, with the highest value of $R^2$ for comparisons between the Southern Exposure test and the macrocell test with mortar-wrapped specimens. The coefficients of determination for comparisons between corrosion rates range from 0.54 to 0.97. Since corrosion rates often vary from week to week, correlations between corrosion rates exhibit greater variation than total corrosion losses, which change gradually from week to week.

The coefficients of determination indicate good correlation between the total corrosion losses in the cracked beam tests and total corrosion losses in the macrocell tests with bare bars in 1.6 m ion NaCl, with bare bars in 6.04 m ion NaCl, and with mortar-wrapped specimens. The coefficients of determination for these comparisons range from 0.84 to 0.97, with the highest value for comparisons between the cracked beam test and macrocell tests with mortar-wrapped specimens. Correlations are poor between the cracked beam test and the rapid macrocell test with lollipop specimens for the microalloyed steels and changes in the concrete/mortar mix designs. As mentioned before, the microalloyed steels corrode at similar rates to conventional steel, making it difficult to distinguish between the steels, much less use the tests to determine the degree of correlation between the two test methods. For changes in the concrete/mortar mix designs, no correlation is expected since the cracked beam test is not sensitive to properties of the concrete.

The correlation between the Southern Exposure and cracked beam tests is good for specimens fabricated with the same concrete and different reinforcing steels, with a coefficient of determination of 0.91 for total corrosion losses. The comparisons for specimens evaluating differences in concrete properties do not show good correlation since, as explained above, the cracked beam test is not effective for evaluating the effect of changes in the concrete properties.

Comparisons between the corrosion rates and total corrosion losses based on the coefficients of variation show that total corrosion losses exhibit less scatter than corrosion rates. The coefficients of variation are similar for the rapid macrocell and bench-scale tests. Comparison of the levels of significance obtained from the Student's t-test give similar results for the rapid macrocell test when compared with the Southern Exposure and cracked beam tests.

Results from the impedance spectroscopy analysis show two equivalent circuits that provide a good fit for the measured spectrum. In both cases, resistors are used to model the solution resistance and the charge-transfer resistance at the anode and cathode. For one of the models, the double layer capacitance at the anode and cathode is modeled with capacitors, and in the other model it is modeled using constant-phase elements. One of the equivalent circuits contains Warburg impedance, which can be used to model diffusion.

Section 4.1 gives a description of linear regression analysis. Section 4.2 shows the correlation of the results of the Southern Exposure and cracked beam tests versus the macrocell test and the correlation of the results for the Southern Exposure test with those of the cracked beam test. Section 4.3 presents the analysis of the variation between the corrosion rates and total corrosion losses and between the rapid macrocell, Southern Exposure, and cracked beam tests. Section 4.4 shows the results from the impedance spectroscopy analysis and the equivalent electronic circuits obtained for the rapid macrocell and the Southern Exposure tests.

## 3.2 LINEAR REGRESSION

Regression analysis is used to determine the relationship between two or more variables. The simplest model uses linear regression, in which the relationship

between the variables is described by a straight line, $y = ax + b$, where $a$ is the slope of the regression line, $b$ is the intercept with the y-axis, and $x$ and $y$ are the variables. The approach used to find the best-fit line through data is to minimize the sum of the square of the residuals, which is given by Eq. (4.1).

$$SSR = \sum \left( y - \hat{y} \right)^2 \tag{4.1}$$

where $y$ is the observed $y$-value and $\hat{y}$ is the value calculated from the linear relationship. If this approach is used, the slope and intercept of the line are given by Eqs. (4.2) and (4.3), respectively.

$$a = \frac{\sum x_i^2 \sum y_i - \sum x_i \sum x_i y_i}{n \sum x_i^2 - \left( \sum x_i \right)^2} \tag{4.2}$$

$$b = \frac{n \sum x_i y_i - \sum x_i \sum y_i}{n \sum x_i^2 - \left( \sum x_i \right)^2} \tag{4.3}$$

where $n$ is the number of data points.

The "goodness of fit" of the linear relationship can be evaluated using different parameters. These include the linear correlation coefficient, the coefficient of determination, and the distribution of residuals.

The linear correlation coefficient $R$ is used to define the extent of the correlation between the two variables. It is defined as

$$R = \frac{n \sum x_i y_i - \sum x_i \sum y_i}{\left[ n \sum x_i^2 - \left( \sum x_i \right)^2 \right]^{1/2} \left[ n \sum y_i^2 - \left( \sum y_i \right)^2 \right]^{1/2}} \tag{4.4}$$

If the linear correlation coefficient $R$ is equal to +1 or –1, there is a perfect correlation between the variables. As the absolute value of $R$ decreases, so does the correlation between the variables.

When the number of data points $n$ is small, values of $|R|$ greater than 0.8 may be obtained even when $x$ and $y$ are totally uncorrelated. Table 4.1 gives the probability of obtaining a value of $R$ when the values of $x$ and $y$ are uncorrelated. If the probability of obtaining a given value of $R$ when the data are uncorrelated is less than 0.05, then the correlation coefficient is considered significant (Kirkup 2002).

**Table 4.1 –** Probabilities of obtaining calculated $R$ values when the $x$-$y$ data are uncorrelated (from Kirkup 2002)

| | ***R* calculated from *x*-*y* data** | | | | | | |
|---|---|---|---|---|---|---|---|
| **n** | **0.50** | **0.60** | **0.70** | **0.80** | **0.90** | **0.95** | **1.00** |
| **3** | 0.667 | 0.590 | 0.506 | 0.410 | 0.287 | 0.202 | 0.000 |
| **4** | 0.500 | 0.400 | 0.300 | 0.200 | 0.100 | 0.050 | 0.000 |
| **5** | 0.391 | 0.285 | 0.188 | 0.105 | 0.037 | 0.013 | 0.000 |
| **6** | 0.313 | 0.208 | 0.122 | 0.056 | 0.014 | 0.004 | 0.000 |
| **7** | 0.253 | 0.154 | 0.080 | 0.031 | 0.006 | 0.001 | 0.000 |
| **8** | 0.207 | 0.116 | 0.053 | 0.017 | 0.002 | <0.001 | 0.000 |
| **9** | 0.170 | 0.088 | 0.036 | 0.010 | 0.001 | <0.001 | 0.000 |
| **10** | 0.141 | 0.067 | 0.024 | 0.005 | <0.001 | <0.001 | 0.000 |

The square of the linear correlation coefficient is known as the coefficient of determination $R^2$. The value of the coefficient of determination indicates the proportion of the variability of $y$ explained by the linear relationship. For example, a value of $R^2 = 0.782$ indicates that approximately 78% of the variation of $y$ can be attributed to the linear relationship between $x$ and $y$.

The distribution of residuals is useful in determining if the linear relationship is appropriate to model the data or if another type of relationship might exist. To

obtain the distribution of residuals, the residual, $\Delta y = y - \hat{y}$ is plotted against the value of $\hat{y}$ or $x$. If only random errors exist in the measurements, the residuals will show random scatter about the $\Delta y = 0$ axis. If the residuals plot shows groupings of positive and negative residuals, as shown in Figure 4.1, a linear model is not appropriate. If the residuals plot shows a funnel shape, as shown in Figure 4.2, it indicates that the error variance is not constant and that a weighted regression should be used.

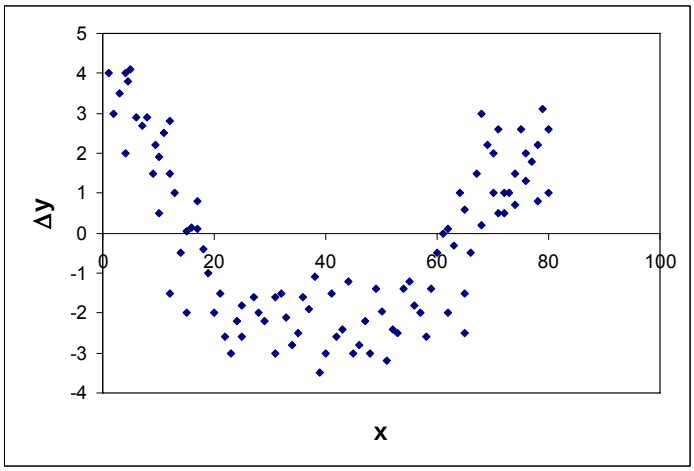


**Figure 4.1 –** Plot of residuals indicating that linear model is inappropriate for modeling the data.

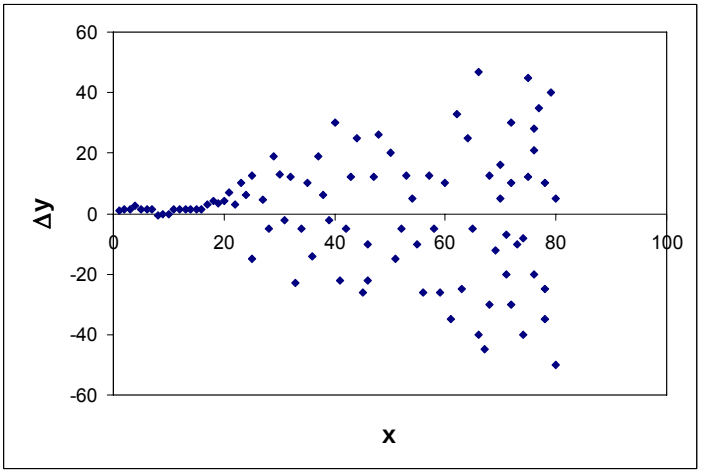


**Figure 4.2 –** Plot of residuals indicating that weighted regression should be used.

Residual plots are also used to identify data points that are outliers. If the residual is divided by the error standard deviation $\sigma_e$, the standardized residual $\Delta y/\sigma_e$ is obtained. The error standard deviation is given by

$$\sigma_e = \left[ \frac{1}{n-2} \sum (y_i - \hat{y}_i)^2 \right]^{1/2} \tag{4.5}$$

As a rule of thumb, a data point is considered to be a possible outlier if the absolute value of $\Delta y/\sigma_e$ is larger than 3 (Hayter 1996). The sum of the residuals should be equal to zero.

## 1.3. CORRELATION BETWEEN TEST METHODS

The results at week 70 for the Southern Exposure and cracked beam tests are compared with the results at week 15 of the rapid macrocell test. The results of the Southern Exposure test are also compared with the results of the cracked beam test, both at week 70. The corrosion protection systems evaluated, listed in Section 2.1 include microalloyed steel, MMFX microcomposite steel, epoxy-coated steel, duplex stainless steel, corrosion inhibitors, and variations in the water-cement ratio. For the rapid macrocell test, the samples are divided based on the type of specimen (bare, lollipop, mortar-wrapped) and the NaCl ion concentration at the anode (1.6 m, 6.04 m). The plots include error bars for each data point. The magnitude of the error bars is +/- one standard deviation of the sample to illustrate the magnitude of the scatter observed for the individual specimens. A linear regression is performed to determine if a linear relationship exists between the variables. To determine the goodness of fit, the analysis includes the coefficient of linear correlation, coefficient of linear determination, and plots showing the distribution of the standardized residuals.

Figures D.1 through D.9 in Appendix D show the distribution of the standardized residuals for the linear regressions presented in this chapter. All the plots show random scatter of the residuals, indicating that the fitted regression lines are appropriate. This section presents the results of the linear regressions between the tests rapid macrocell test and the Southern Exposure and cracked beam tests, and between the Southern Exposure and cracked beam tests.

### 4.2.1 Rapid macrocell test versus Southern Exposure test

Figures 4.3(a) and 4.3(b) show the correlation of the corrosion rates and total corrosion losses, respectively, between the Southern Exposure test and the macrocell test with bare bars in 1.6 m ion NaCl and simulated concrete pore solution. The concrete in the Southern Exposure tests had a water-cement ratio of 0.45. These tests include specimens with conventional, MMFX microcomposite, microalloyed, and duplex steel. For the corrosion rates, the linear correlation coefficient $R$ is 0.73. Based on the number of data points, 13, and the probabilities shown in Table 4.1, the correlation can be considered significant, but the coefficient of determination $R^2$, 0.54, is very low which indicates that only 54% of the variability of the Southern Exposure test results can be attributed to the linear relationship between the two tests. For the total corrosion losses, the coefficients of correlation and determination are higher, 0.93 and 0.86, respectively. Both of these values indicate a very good correlation between the corrosion losses of both tests. Due to the complexity of the corrosion process, the corrosion rates increase or decrease from week to week, so the correlation will depend mainly on the corrosion rates measured at that given week. The total corrosion losses, however, increase gradually with time, since they take into consideration the corrosion rates throughout the test period. These points, along with

the improved correlation based on total corrosion losses indicate that a comparison based on the total corrosion losses is more effective. Table E.1 shows the ratio of the corrosion rates and the ratio of the total corrosion losses between the Southern Exposure test and the macrocell test with bare bars in 1.6 m ion NaCl for 13 reinforcing steels. For the corrosion rates, out of the 13 steels, only two, 2101(1) and 2101(1)p, have ratios above 1.00, indicating that they have a higher corrosion rate in the Southern Exposure test at week 70 than in the rapid macrocell test at week 15. The remaining 11 steels had ratios below 0.32. For the total corrosion losses, four steels have a ratio above 1.00, and the remaining 9 steels have ratios below 0.81.

Figures 4.4(a) and 4.4(b) show the correlation of the corrosion rates and total corrosion losses, respectively, between the Southern Exposure test and the macrocell test with bare bars in 6.04 m ion NaCl and simulated concrete pore solution. The concrete in the Southern Exposure tests had a water-cement ratio of 0.45. These tests include specimens with conventional, MMFX microcomposite, and duplex steel. The corrosion rates and total corrosion losses, with coefficients of determination of 0.86 and 0.90, respectively show good correlation between both tests. The correlation coefficients, 0.93 and 0.95 for the corrosion rates and losses, respectively, indicate that the linear correlation between the tests is significant. Table E.2 shows the ratio of the corrosion rates and the ratio of the total corrosion losses between the Southern Exposure test and the macrocell test with bare bars in 6.04 m ion NaCl for seven reinforcing steels. For the corrosion rates, the highest ratio is 0.36, and for the total corrosion losses, the highest ratio is 0.76. Since all are lower than 1.00, this means that the corrosion rates and losses obtained in the Southern Exposure test at week 70 are always lower than the values obtained for the rapid macrocell test with bare bars in 6.04 m ion NaCl at week 15.

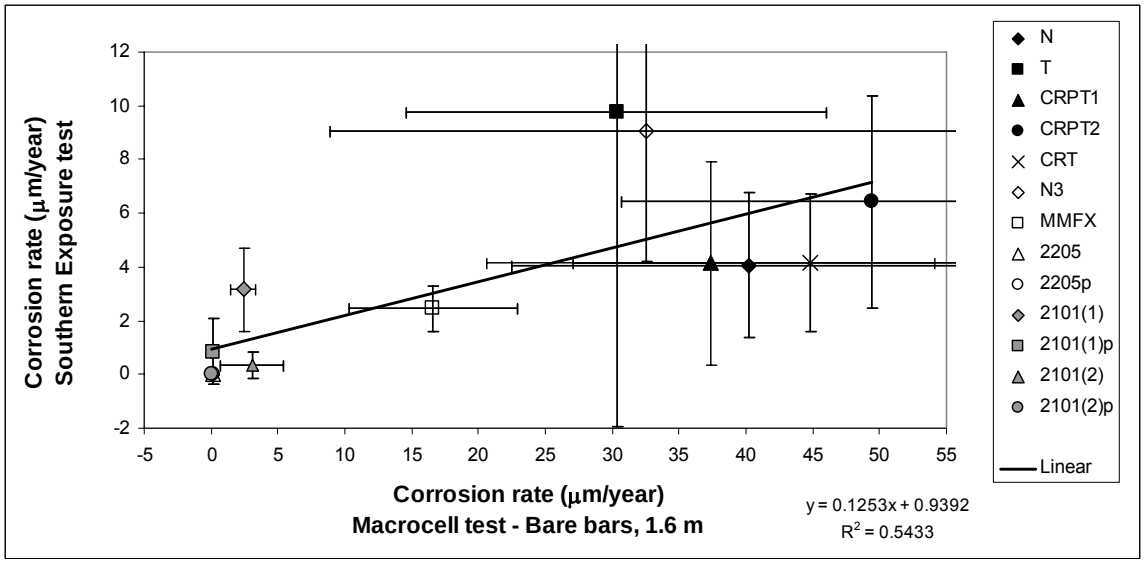


(a)

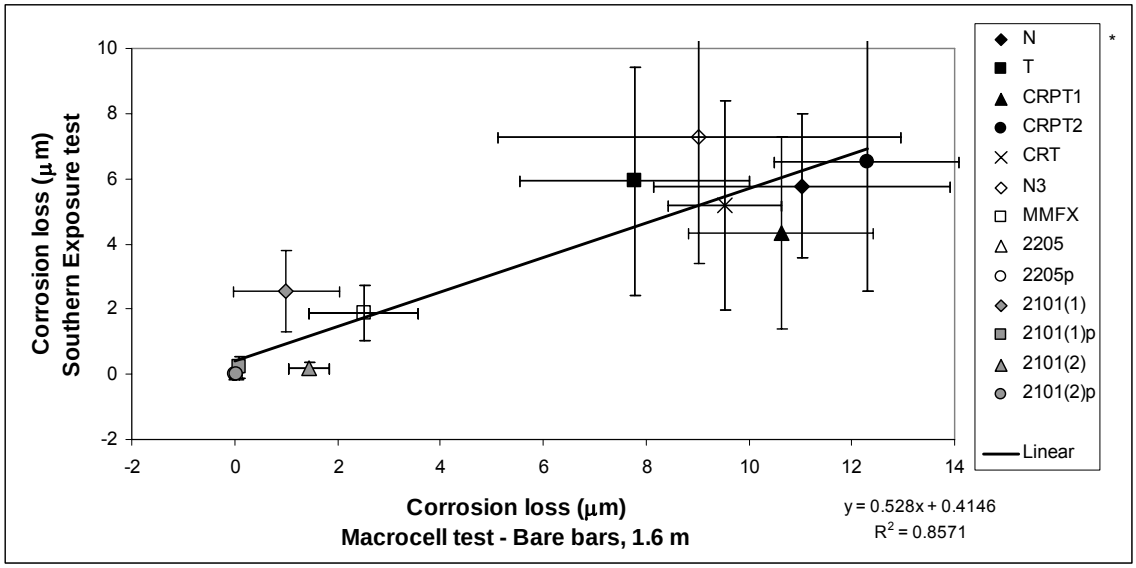


(b)

*** Steel type** → N and N3: conventional, normalized steel, T: Thermex-treated conventional steel, CRPT1: Thermex- treated microalloyed steel with a high phosphorus content (0.117%), CRPT2: Thermex-treated microalloyed steel with a high phosphorus content (0.100%), CRT: Thermex treated microalloyed steel with normal phosphorus content (0.017%), 2101(1) and 2101(2): duplex stainless steel (21% chromium, 1% nickel), 2205: duplex stainless steel (25% chromium, 5% nickel), p: pickled.

**Figure 4.3 –**Southern Exposure test (week 70) versus macrocell test with bare bars in 1.6 m ion NaCl and simulated concrete pore solution (week 15). (a) Corrosion rates and (b) total corrosion losses.

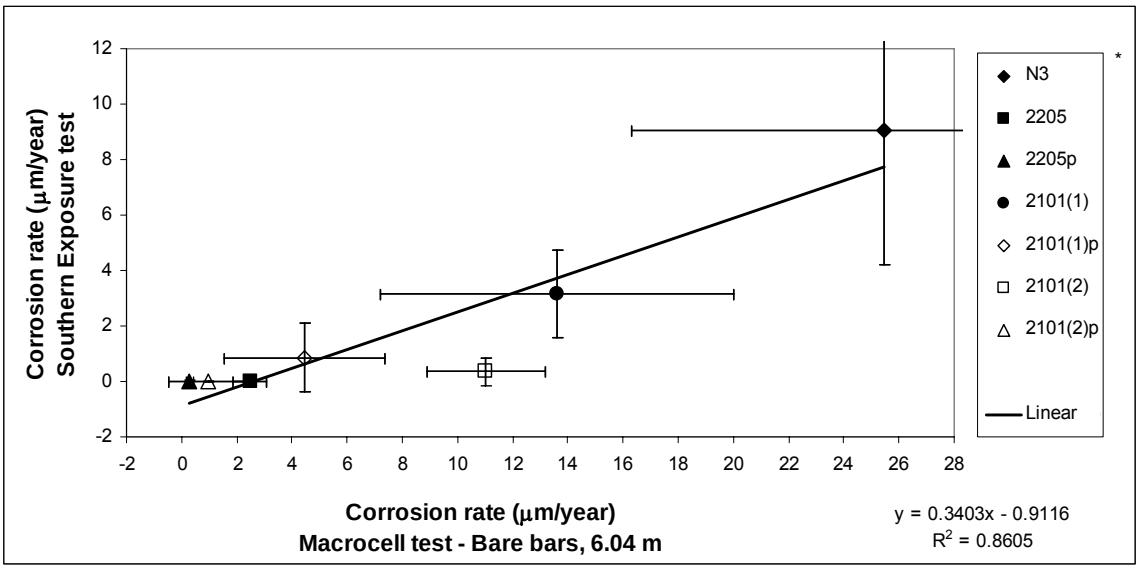


(a)

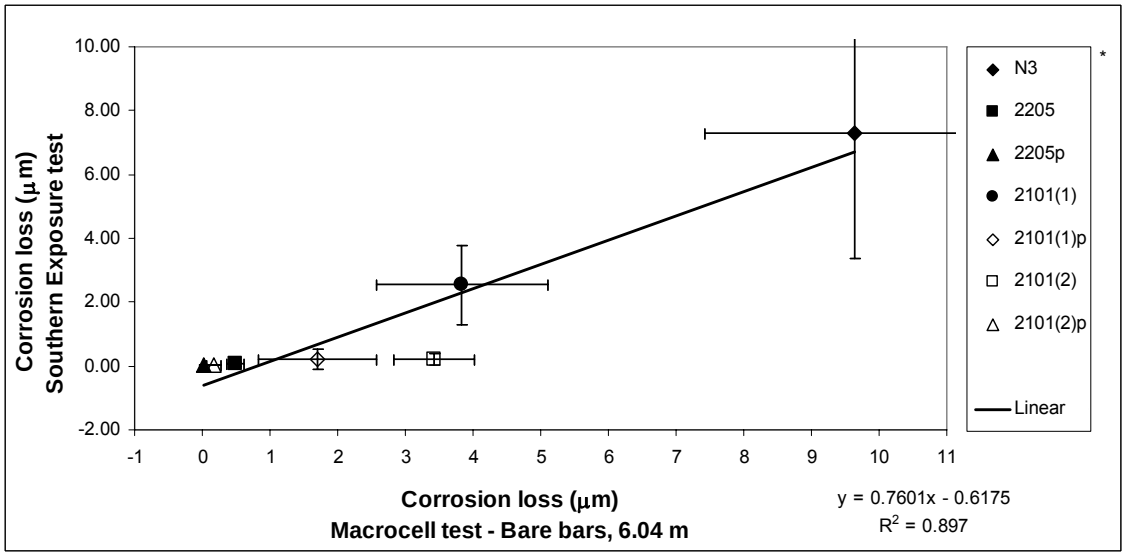


(b)

*** Steel type** → N3: conventional, normalized steel, 2101(1) and 2101(2): duplex stainless steel (21% chromium, 1% nickel), 2205: duplex stainless steel (25% chromium, 5% nickel), p: pickled.

**Figure 4.4 –**Southern Exposure test (week 70) versus macrocell test with bare bars in 6.04 m ion NaCl and simulated concrete pore solution (week 15). (a) Corrosion rates and (b) total corrosion losses.

Figures 4.5(a) and 4.5(b) show the correlation of corrosion rates and losses, respectively, between the Southern Exposure test and the macrocell test using lollipop specimens to evaluate the effects of changes in the water-cement ratio and the presence of corrosion inhibitors. All specimens were fabricated with conventional, normalized steel. The coefficients of determination were 0.97 and 0.80 for the corrosion rates and losses, respectively, indicating good correlation between the tests. The correlation coefficients 0.98 and 0.89 for the corrosion rates and losses, respectively, indicate that the linear relationships are significant. In both cases, the linear relationship is influenced by the high value of the corrosion rates and losses of specimens with a water-cement ratio of 0.45 and no inhibitor (N-45). A change in the values for these specimens might have a significant impact on the correlation. Table E.3 shows the ratio of the corrosion rates and ratio of the total corrosion losses between the Southern Exposure test and the macrocell test with lollipop specimens. The specimens include those used to compare the behavior of specimens with corrosion inhibitors and those with variations in the water-cement ratio. For the corrosion rates, out of the six sets of tests, only one, N-DC35, had higher corrosion rates for the Southern Exposure than for the rapid macrocell test. For the total corrosion losses, only one set, N-RH35, had lower total corrosion losses for the Southern Exposure test than for the rapid macrocell test.

Figures 4.6(a) and 4.6(b) show the correlation of the corrosion rates and losses, respectively, between the Southern Exposure test and the macrocell test with mortar-wrapped specimens in 1.6 m ion NaCl and simulated concrete pore solution. The concrete in the Southern Exposure specimens had a water-cement ratio of 0.45, and the mortar in the mortar-wrapped specimens had a water-cement ratio of 0.50. These tests include specimens with conventional, MMFX microcomposite, epoxy-

coated, and duplex steel. The corrosion rates and losses had coefficients of determination of 0.76 and 0.95, respectively, indicating a good correlation between the tests, especially for the corrosion losses. The correlation coefficients, 0.87 and 0.97 for the corrosion rates and losses, respectively, indicate that the linear relationships between the tests are significant. Table E.4 shows the ratio of the corrosion rates and the ratio of the total corrosion losses between the Southern Exposure test and the macrocell test with mortar-wrapped specimens for 11 sets of tests. For the corrosion rates, only one set, 2101(1)p, had higher corrosion rates for the Southern Exposure test than for the rapid macrocell test, with a ratio of 42.50. For the total corrosion losses, this same set had a ratio of 21.00. These specimens had unusually low corrosion rates in the rapid macrocell test with mortar-wrapped specimens, resulting in the high ratios. Only three sets, 2205p, 2101(2), and 2101(2)p have ratios below 1.00.

As described in the material preceding Section 4.1, the results of the Southern Exposure test versus the macrocell test for specimens with microalloyed steel show no significant relationships.

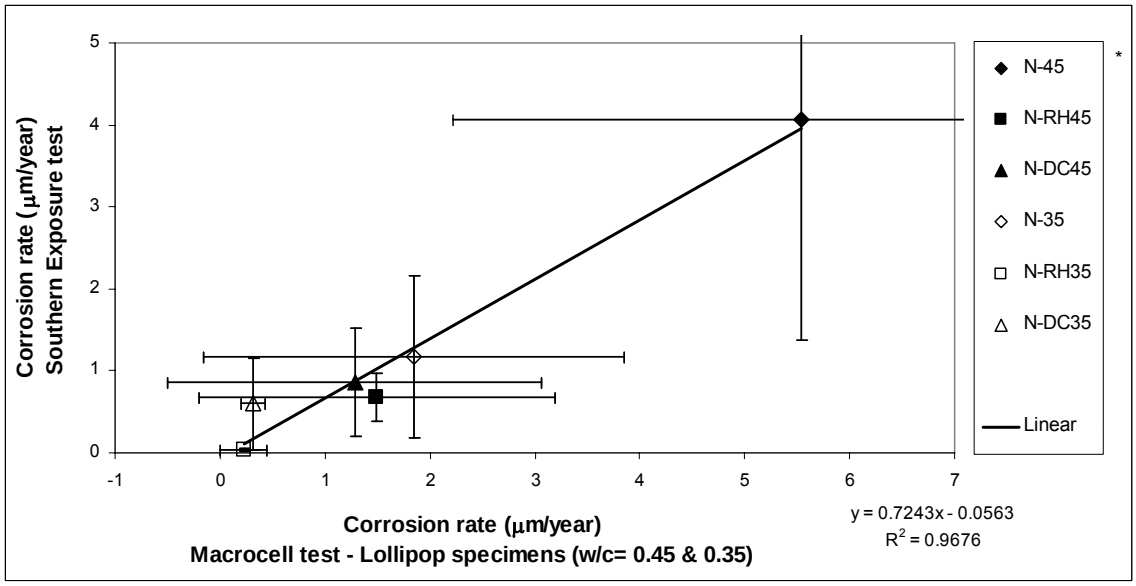


(a)

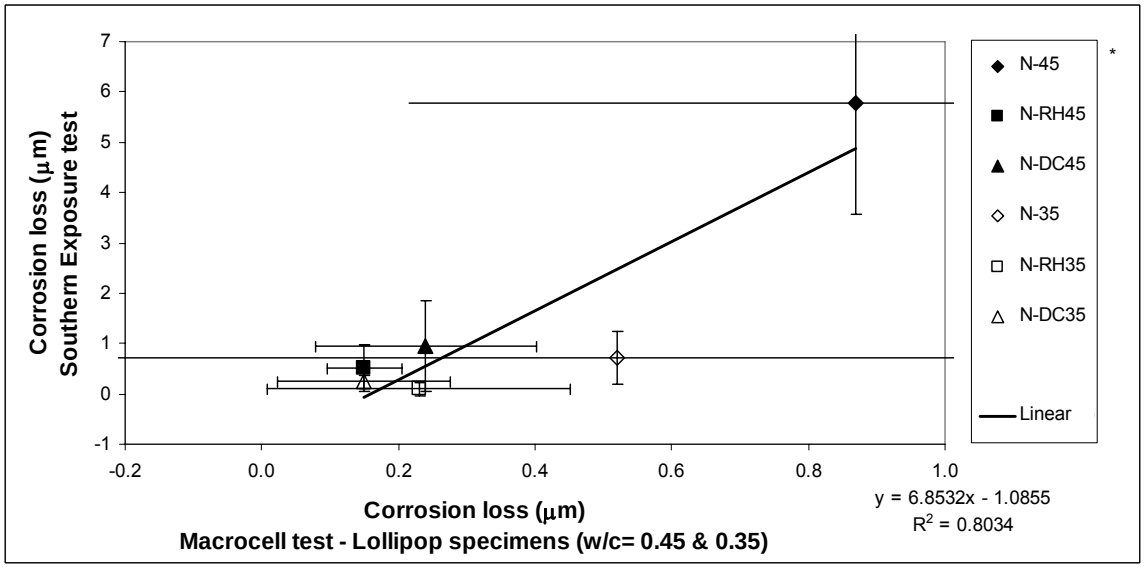


(b)

* A-B
A: steel type → N: conventional, normalized steel.
B: mix design → 45: water-cement ratio of 0.45 and no inhibitor, RH45: water-cement ratio of 0.45 and Rheocrete 222+, DC45: water-cement ratio of 0.45 and DCI-S, 35: water-cement ratio of 0.35 and no inhibitor, RH35: water-cement ratio of 0.35 and Rheocrete 222+, DC35: water-cement ratio of 0.35 and DCI-S.

**Figure 4.5 –**Southern Exposure test (week 70) versus macrocell test with lollipop specimens in 1.6 m ion NaCl and simulated concrete pore solution (week 15). (a) Corrosion rates and (b) total corrosion losses.

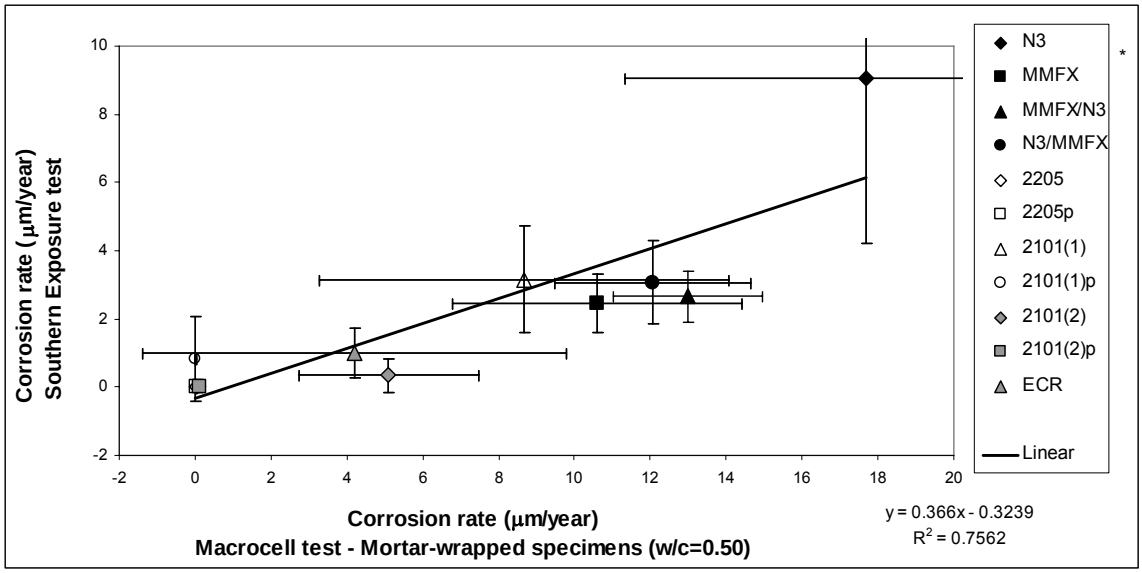


(a)

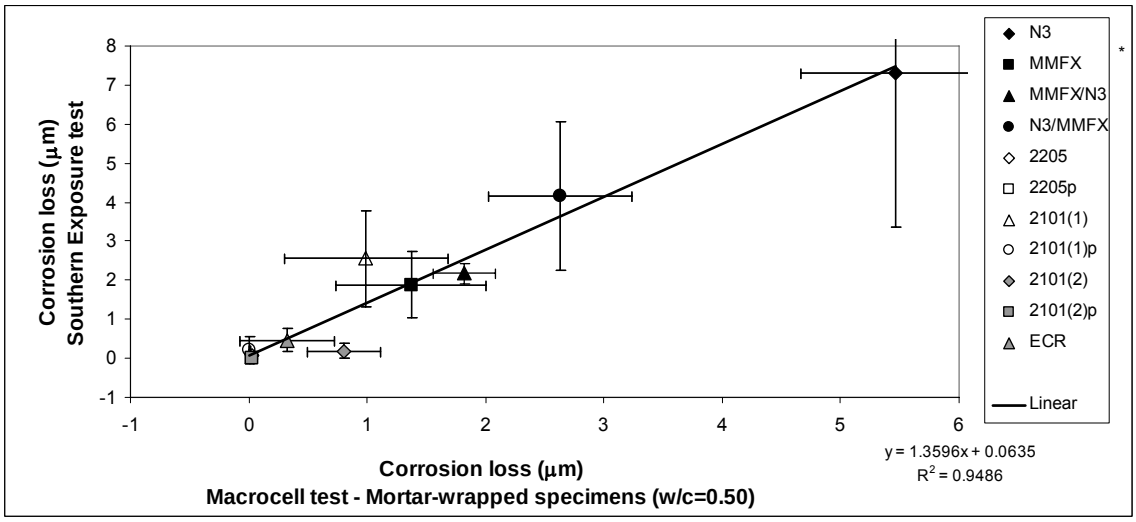


(b)

*** Steel type →** N3: conventional, normalized steel, MMFX: MMFX microcomposite steel, MMFX/N3: MMFX steel in the top mat and N3 steel in the bottom mat, N3/MMFX: N3 steel in the top mat and MMFX steel in the bottom mat, 2101(1) and 2101(2): duplex stainless steel (21% chromium, 1% nickel), 2205: duplex stainless steel (25% chromium, 5% nickel), ECR: epoxy-coated steel, p: pickled.

**Figure 4.6 –**Southern Exposure test (week 70) versus macrocell test with mortar-wrapped specimens in 1.6 m ion NaCl and simulated concrete pore solution (week 70). (a) Corrosion rates and (b) total corrosion losses.

### 4.2.2 Rapid macrocell test versus cracked beam test

Figures 4.7(a) and 4.7(b) show the correlation of the corrosion rates and total corrosion losses, respectively, between the cracked beam test and the macrocell test with bare bars in 1.6 m ion NaCl and simulated concrete pore solution. The concrete in the cracked beam specimens had a water-cement ratio of 0.45. These tests include specimens with conventional, microalloyed, MMFX microcomposite, and duplex steel. The coefficient of determination for the corrosion rates is 0.67, which indicates that 67% of the variability of the corrosion rate in the cracked beam test can be attributed to the linear relationship between the tests. The coefficient of determination for the corrosion losses is 0.84, which indicates a good correlation between the tests. The values of the correlation coefficient, 0.82 and 0.91 for the corrosion rates and losses, respectively, indicate that the linear relationship between the tests is significant. Table E.5 shows the ratio of the corrosion rates and the ratio of the total corrosion losses between the cracked beam test and the macrocell test with bare bars in 1.6 m ion NaCl for 13 reinforcing steels. For the corrosion rates, all have higher values in the rapid macrocell test than in the cracked beam test. The highest ratio is 0.89. For the total corrosion losses, five steels have higher ratios for the rapid macrocell test than for the cracked beam test.

Figures 4.8(a) and 4.8(b) show the correlation of the corrosion rates and losses, respectively, between the cracked beam test and the macrocell test with bare bars in 6.04 m ion NaCl and simulated concrete pore solution. The concrete in the cracked beam specimens had a water-cement ratio of 0.45. These tests include specimens with conventional and duplex steel. The coefficients of determination for the corrosion rates and losses are 0.76 and 0.91, respectively, indicating that a high percentage of the variation in the cracked beam results can be attributed to the

variations in the results from the macrocell test. The correlation coefficients, 0.87 and 0.95 for the corrosion rates and losses, respectively, indicate that the linear relationships are significant.

The results of the macrocell test with bare bars in 6.04 m ion NaCl were also plotted against the results at week 96 of the cracked beam test to determine if the increases in the corrosion rates of some of the duplex steels in the cracked beam test after week 70 have any effect in the correlations. The plots for the corrosion rates and total corrosion losses are shown in Figures 4.9(a) and 4.9(b), respectively. At week 96, the corrosion rates of conventional steel, N3, had dropped to a value of 1.41 μm/year, which illustrates the variation that can occur in corrosion rates with time, as mentioned in the previous section. The coefficient of determination for the corrosion rates is only 0.20, and the correlation coefficient is 0.44, which indicates that a linear relationship does not exist. For the total corrosion losses, the coefficient of determination is still high, 0.91, indicating a very good correlation between the tests.

Table E.6 shows the ratio of the corrosion rates and the ratio of the total corrosion losses between the cracked beam test at 70 weeks and the macrocell test with bare specimens in 6.04 m ion NaCl and Table E.7 shows the ratio of the corrosion rates and the ratio of the total corrosion losses between the cracked beam test at 96 weeks and the macrocell test with bare specimens in 6.04 m ion NaCl. The tests evaluate seven reinforcing steels. For the corrosion rates, in all cases the cracked beam had lower corrosion rates than the rapid macrocell test. For the corrosion losses, all steels except N3 steel had lower total corrosion losses for the cracked beam test than for the rapid macrocell test.

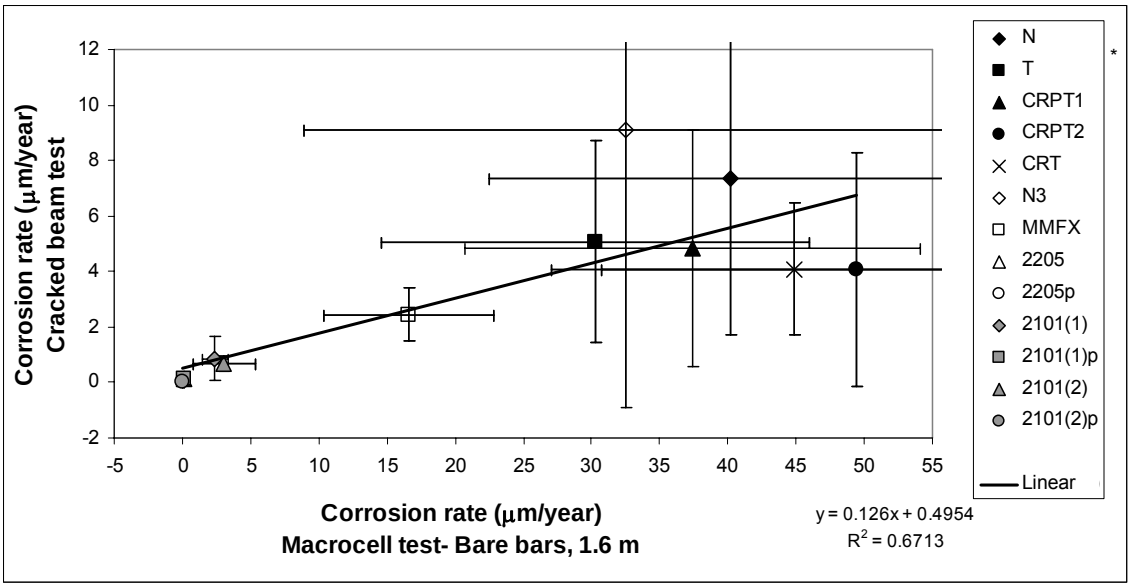


(a)

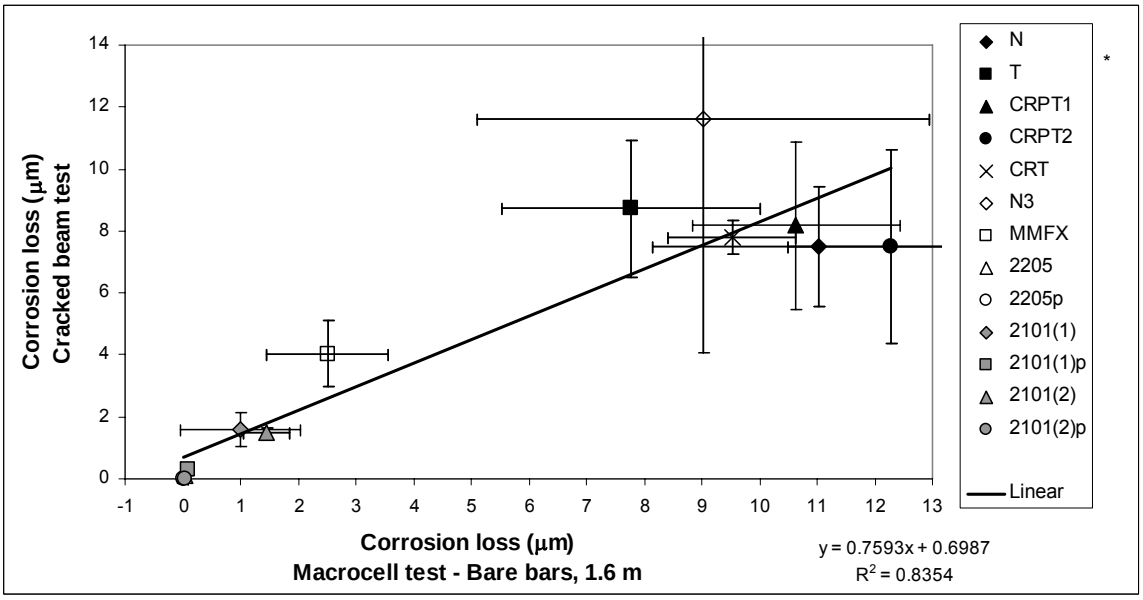


(b)

*** Steel type** → N and N3: conventional, normalized steel, T: Thermex-treated conventional steel, CRPT1: Thermex- treated microalloyed steel with a high phosphorus content (0.117%), CRPT2: Thermex-treated microalloyed steel with a high phosphorus content (0.100%), CRT: Thermex treated microalloyed steel with normal phosphorus content (0.017%), 2101(1) and 2101(2): duplex stainless steel (21% chromium, 1% nickel), 2205: duplex stainless steel (25% chromium, 5% nickel), p: pickled.

**Figure 4.7 –**Cracked beam test (week 70) versus macrocell test with bare bars in 1.6 m ion NaCl and simulated concrete pore solution (week 15). (a) Corrosion rates and (b) total corrosion losses.

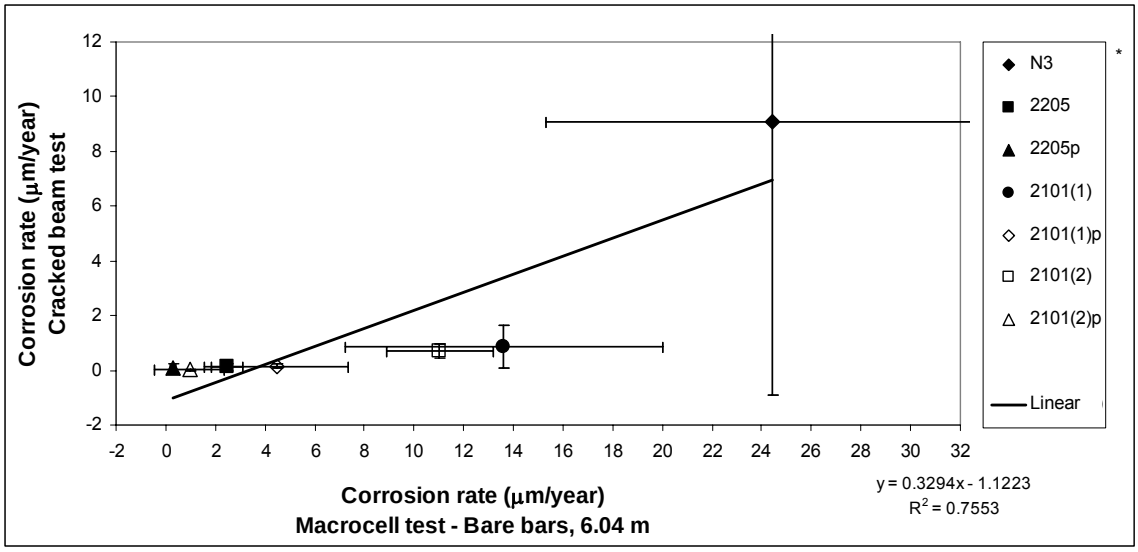


(a)

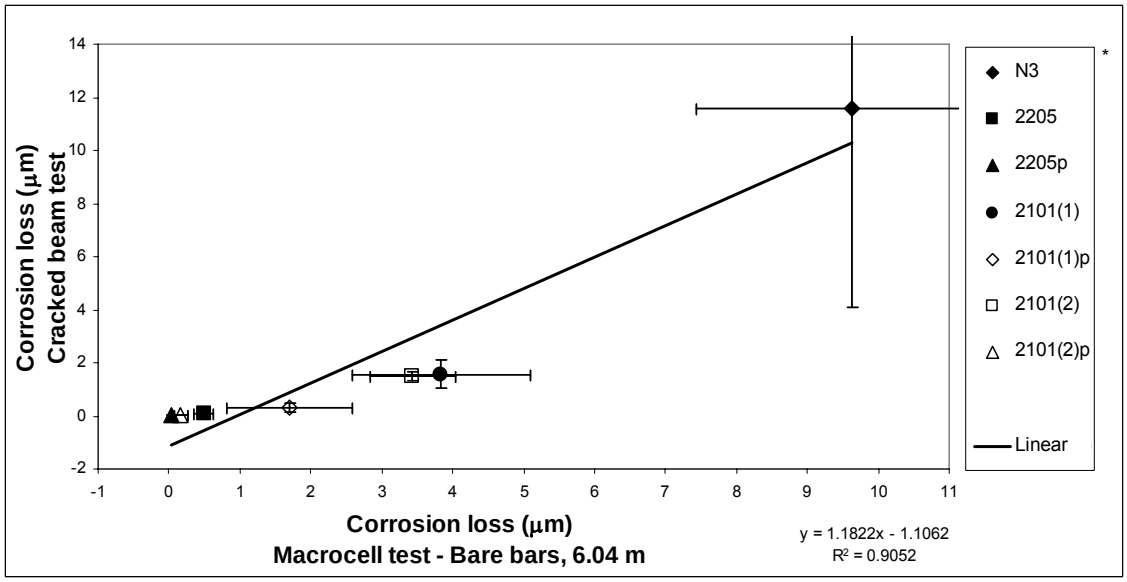


(b)

*** Steel type** → N3: conventional, normalized steel, 2101(1) and 2101(2): duplex stainless steel (21% chromium, 1% nickel), 2205: duplex stainless steel (25% chromium, 5% nickel), p: pickled.

**Figure 4.8 –**Cracked beam test (week 70) versus macrocell test with bare bars in 6.04 m ion NaCl and simulated concrete pore solution (week 15). (a) Corrosion rates and (b) total corrosion losses.

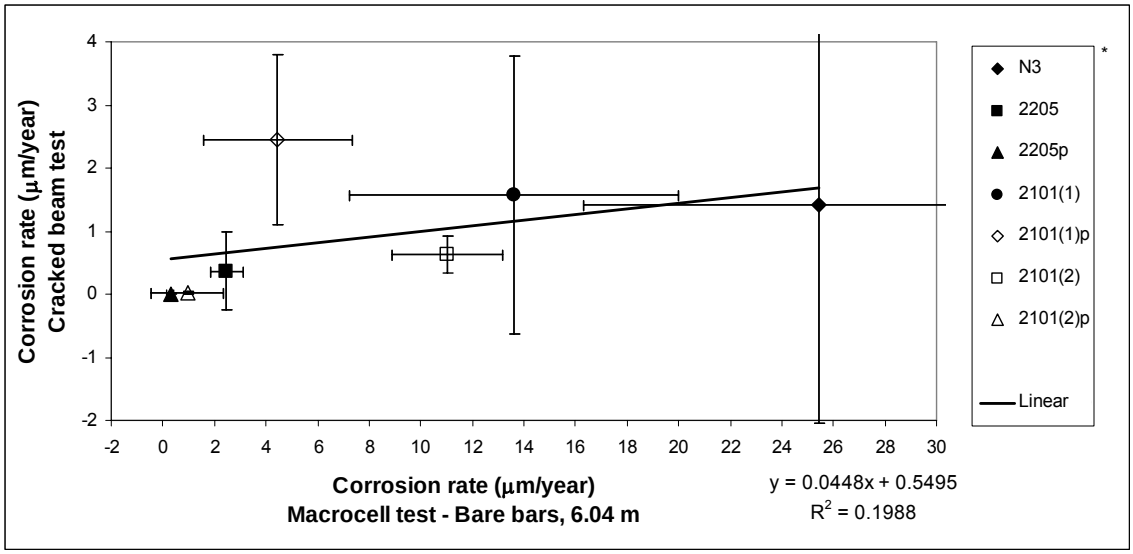


(a)

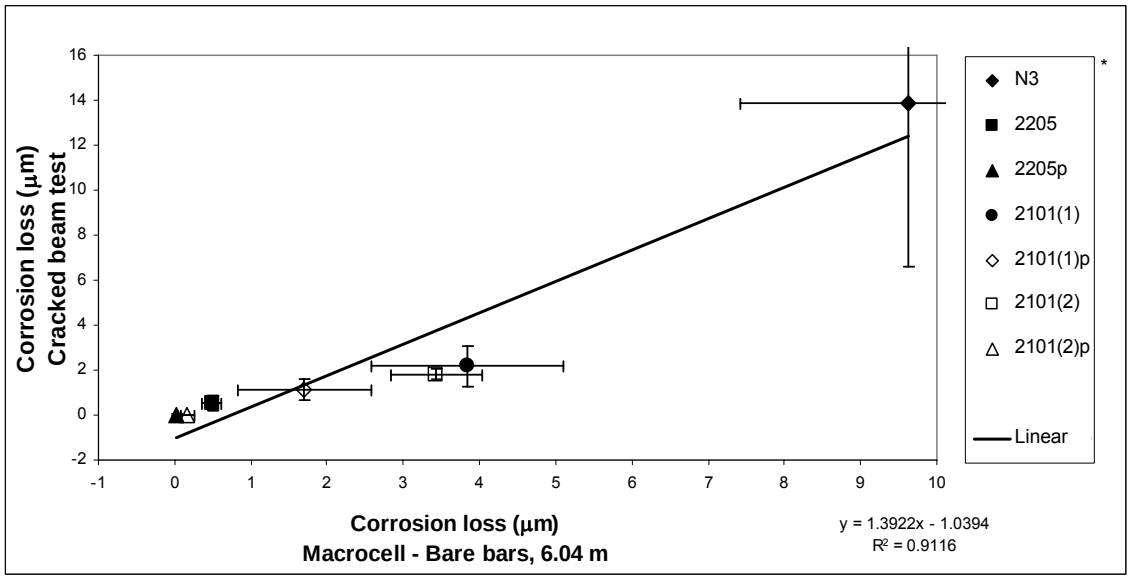


(b)

*** Steel type** → N3: conventional, normalized steel, 2101(1) and 2101(2): duplex stainless steel (21% chromium, 1% nickel), 2205: duplex stainless steel (25% chromium, 5% nickel), p: pickled.

**Figure 4.9 –**Cracked beam test (week 96) versus macrocell test with bare bars in 6.04 m ion NaCl and simulated concrete pore solution (week 15). (a) Corrosion rates and (b) total corrosion losses.

Figures 4.10(a) and 4.10(b) show the comparison of the corrosion rates and total corrosion losses, respectively, between the cracked beam test and the macrocell test with mortar-wrapped specimens in 1.6 m ion NaCl and simulated concrete pore solution. The concrete in the cracked beam specimens had a water-cement ratio of 0.45 and the mortar in the mortar-wrapped specimens had a water-cement ratio of 0.50. These tests include specimens with conventional, MMFX microcomposite, epoxy-coated, and duplex steel. The coefficients of determination are 0.77 and 0.97 for the corrosion rates and total corrosion losses, respectively, which indicate a good correlation between the results of both tests, especially for the corrosion losses. The correlation coefficients, 0.88 and 0.98 for the corrosion rates and total corrosion losses, respectively, indicate that the linear relationships are significant. Table E.8 shows the ratio of the corrosion rates and the ratio of the total corrosion losses in the cracked beam test and macrocell test with mortar-wrapped specimens for nine reinforcing steels. For the corrosion rates, out of the nine steels, three have ratios higher than 1.00, while the remaining have ratios below 0.51. For the total corrosion losses, only two steels have ratios lower than 1.00.

The corrosion rates and total corrosion losses of the cracked beam versus the macrocell test for specimens used to evaluate variations in the water-cement ratio and the presence of corrosion inhibitors show no correlation. The linear regression gives a negative slope for both the corrosion rates and total corrosion losses and coefficients of determination of 0.04 and 0.01, respectively. Due to the presence of the crack, the cracked beam specimen is not useful for evaluating changes in concrete properties, so no correlation between these tests was expected.

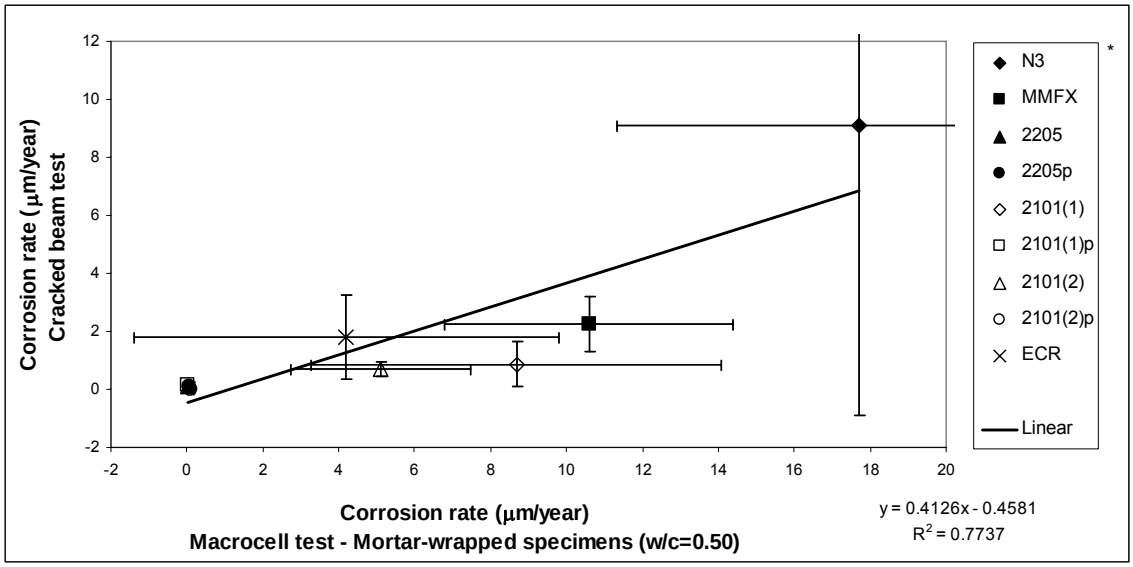


(a)

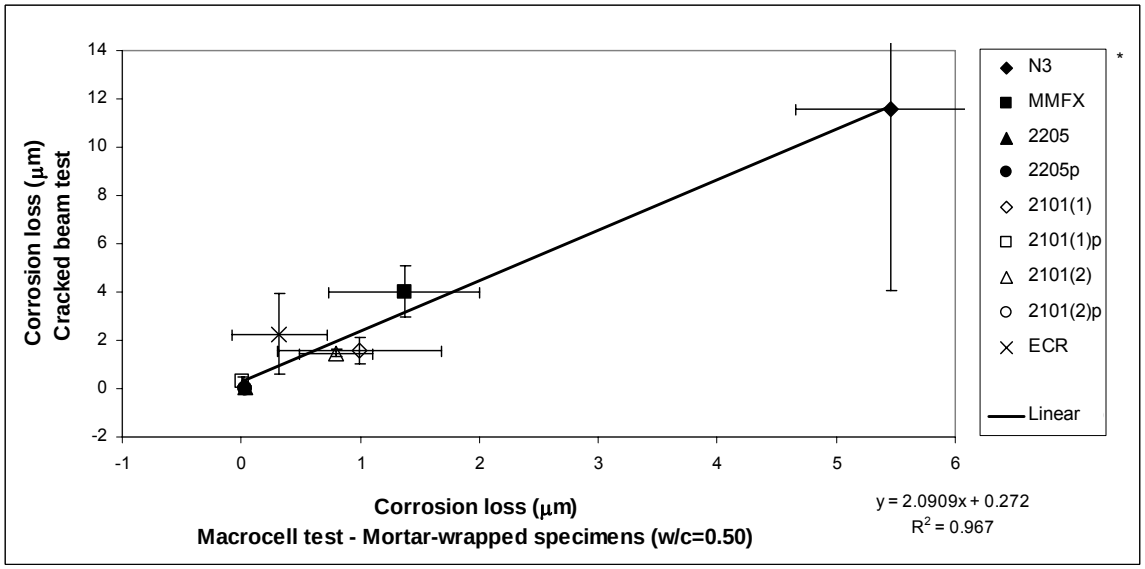


(b)

*** Seel type** → N3: conventional, normalized steel, MMFX: MMFX microcomposite steel, 2101(1) and 2101(2): duplex stainless steel (21% chromium, 1% nickel), 2205: duplex stainless steel (25% chromium, 5% nickel), ECR: epoxy-coated steel, p: pickled.

**Figure 4.10 –**Cracked beam test (week 70) versus macrocell test with mortar-wrapped specimens in 1.6 m ion NaCl and simulated concrete pore solution (week 15). (a) Corrosion rates and (b) total corrosion losses.

As discussed earlier, the results for the microalloyed steel cannot be used to determine the degree of correlation between the cracked beam and rapid macrocell tests.

### 4.2.3 Southern Exposure versus cracked beam test

Figures 4.11(a) and 4.11(b) show the correlations of the corrosion rates and total corrosion losses, respectively, between the cracked beam and Southern Exposure tests for specimens with conventional, microalloyed, MMFX microcomposite, epoxy-coated, and duplex steel. The best fit correlation between the corrosion rates of the cracked beam and Southern Exposure tests has a coefficient of determination of 0.69. The corrosion losses give a better correlation between the tests, with a coefficient of determination of 0.91, as shown in Figure 4.11(b). The corrosion rates and total corrosion losses have correlation coefficients of 0.83 and 0.95, respectively, which indicate that the linear relationships are significant. Table E.9 shows the ratio of the corrosion rates and the ratio of the total corrosion losses in the cracked beam and Southern Exposure test. Table E.9 shows the ratio of the corrosion rates and the ratio of the total corrosion losses between the Southern Exposure test and the cracked beam tests for 14 reinforcing steels. For the corrosion rates six steels had higher corrosion rates for the Southern Exposure test than for the cracked beam test, with the highest values for 2205 and 2205p. For the corrosion losses only 2101(1) steel had lower corrosion losses for the Southern Exposure test than for the cracked beam test. Ten of the steels had ratios of the total corrosion losses of the cracked beam over total corrosion losses of the Southern Exposure test that ranged from 1.00 to 1.83.

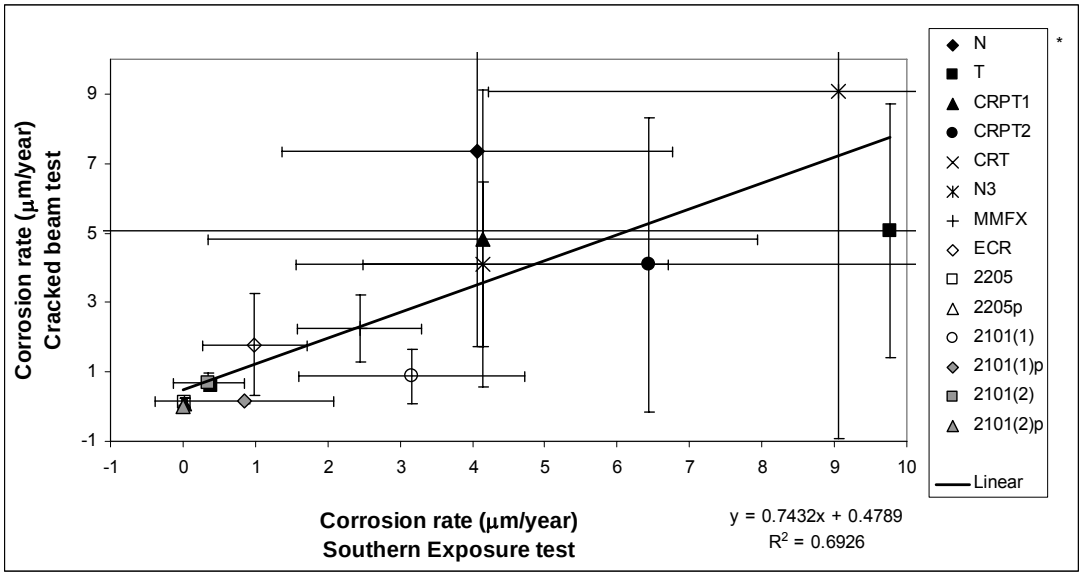


(a)

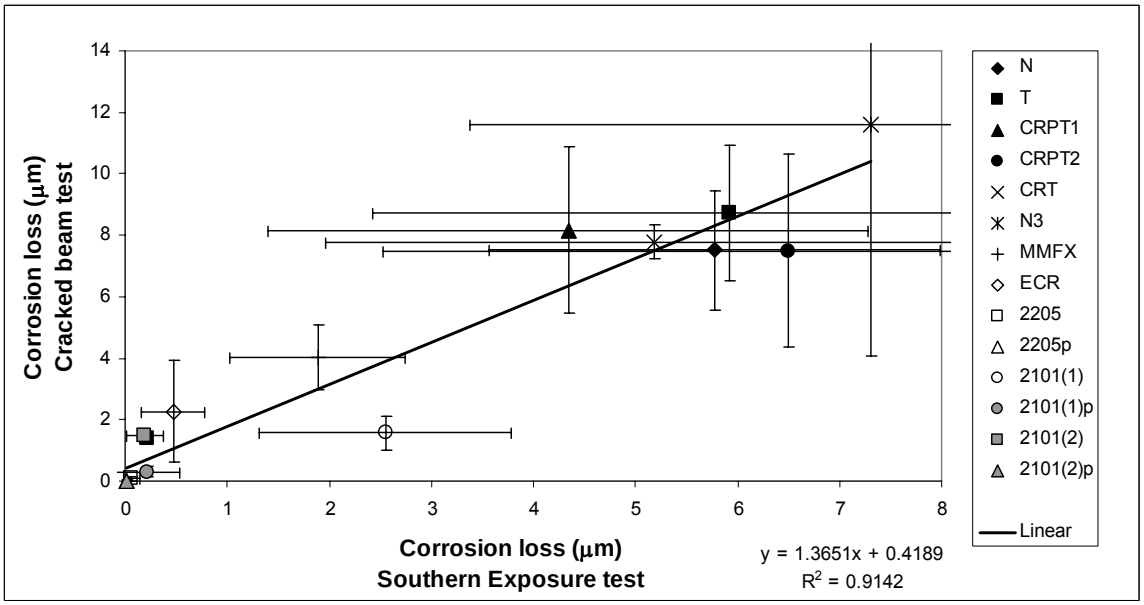


(b)

*** Steel type** → N and N3: conventional, normalized steel, T: Thermex-treated conventional steel, CRPT1: Thermex- treated microalloyed steel with a high phosphorus content (0.117%), CRPT2: Thermex-treated microalloyed steel with a high phosphorus content (0.100%), CRT: Thermex treated microalloyed steel with normal phosphorus content (0.017%), MMFX, MMFX microcomposite steel, ECR: epoxy-coated steel, 2101(1) and 2101(2): duplex stainless steel (21% chromium, 1% nickel), 2205: duplex stainless steel (25% chromium, 5% nickel), p: pickled.

**Figure 4.11 –**Cracked beam test (week 70) versus Southern Exposure test (week 70) for specimens fabricated with different reinforcing steels. (a) Corrosion rates and (b) total corrosion losses

As expected, the comparison between the cracked beam test and Southern Exposure test for specimens with variations in the water-cement ratio and with or without corrosion inhibitors does not show a good correlation. As mentioned in the previous sections, the cracked beam test is not an effective test for evaluating the effect of changes in the concrete since the crack provides direct access of the salt to the reinforcing steel.

## 4.3 COMPARISON OF THE VARIATIONS IN TEST RESULTS

The variability in results for a particular corrosion protection system and test can be evaluated using the coefficient of variation, *COV*, the ratio of the standard deviation *s* to the average $\bar{y}$.

$$COV = \frac{s}{\bar{y}} \tag{4.6}$$

The values of the coefficients of variation are calculated for the corrosion rates and total corrosion losses at week 15 for the macrocell test and week 70 for the Southern Exposure and cracked beam tests. The average corrosion rates and total corrosion losses, as well as the corresponding standard deviations, are listed in Tables 3.3 to 3.52.

Tables 4.2 to 4.6 list the coefficients of variation of the corrosion rates and total corrosion losses for the rapid macrocell, Southern Exposure, cracked beam, and ASTM G 109 tests discussed in Chapter 3. Lower coefficients of variation indicate a better reliability. The results include 125 sets of tests. Out of the 125 sets, 88 (70% of the results) had a lower coefficient of variation for the total corrosion loss than for the corresponding corrosion rate. Of the 37 sets where the corrosion rate had a lower coefficient of variation than the total corrosion loss, in 11 cases the coefficient of

variation for the corrosion rate was within 10% of the value for the total corrosion loss. The higher variation in the corrosion rates is expected since the measured values for corrosion rates can increase or decrease from one week to the next, while the corrosion losses will only increase with time and variations will average out over time.

Tables 4.7 to 4.10 compare the coefficients of variation for the corrosion rates and total corrosion losses for the rapid macrocell test with those of the Southern Exposure test, and Tables 4.11 to 4.13 show similar comparisons for the rapid macrocell and the cracked beam tests. The comparisons are made for the tests that showed a significant correlation in Section 4.2 – for example, the macrocell test with mortar-wrapped specimens versus the Southern Exposure test, shown in Figure 4.6. Out of the 66 comparisons shown in Tables 4.7 to 4.13, the macrocell test had a lower coefficient of variation than the matching bench-scale test based on the corrosion rates in 40 cases, or 60% of the time. When comparing the coefficients of variation for total corrosion losses, the macrocell test had lower variability than the bench-scale tests on 34 occasions, or 52% of the time. Overall, the tests show similar results. Both tests have similar levels of reliability in spite of the fact that the averaging of the variations, mentioned in the previous paragraph, is done over 70 weeks in the Southern Exposure test instead of only 15 weeks in the rapid macrocell test.

**Table 4.2 –** Comparison between coefficients of variation of corrosion rates and losses of specimens with corrosion inhibitors and different water-cement ratios.

| Specimen designation* | Corrosion rate | Corrosion loss |
|---|---|---|
| **"Lollipop" specimens in 1.6 m ion NaCl** | | |
| **M-N-45** | 0.60 | 0.76 |
| **M-N-RH45** | 1.13 | 0.37 |
| **M-N-DC45** | 1.39 | 0.69 |
| **M-N-35** | 1.09 | 1.55 |
| **M-N-RH35** | 0.98 | 0.98 |
| **M-N-DC35** | 0.34 | 0.85 |
| **Southern Exposure test** | | |
| **SE-N-45** | 0.66 | 0.38 |
| **SE-N-RH45** | 0.42 | 0.92 |
| **SE-N-DC45** | 0.76 | 0.96 |
| **SE-N-35** | 0.84 | 0.74 |
| **SE-N-RH35** | 0.41 | 1.29 |
| **SE-N-DC35** | 0.93 | 0.55 |
| **SE-T-45** | 1.20 | 0.59 |
| **SE-T-RH45** | 1.13 | 0.76 |
| **SE-T-DC45** | 1.23 | 0.75 |
| **SE-T-35** | 1.73 | 0.35 |
| **SE-T-RH35** | 1.33 | 0.55 |
| **SE-T-DC35** | 0.25 | 0.98 |
| **Cracked beam test** | | |
| **CB-N-45** | 0.76 | 0.26 |
| **CB-N-RH45** | 0.53 | 0.10 |
| **CB-N-DC45** | 0.52 | 0.28 |
| **CB-N-35** | 0.48 | 0.09 |
| **CB-N-RH35** | 0.72 | 0.16 |
| **CB-N-DC35** | 0.52 | 0.46 |
| **CB-T-45** | 0.72 | 0.25 |
| **CB-T-RH45** | 0.93 | 0.35 |
| **CB-T-DC45** | 0.87 | 1.25 |
| **CB-T-35** | 0.95 | 0.18 |
| **CB-T-RH35** | 0.75 | 0.64 |
| **CB-T-DC35** | 1.14 | 0.13 |
| **ASTM G 109 test** | | |
| **G-N-45** | 1.04 | 0.45 |
| **G-N-RH45** | - | 0.32 |
| **G-N-DC45** | 1.17 | 1.25 |
| **G-N-35** | 0.43 | 0.43 |
| **G-N-RH35** | 1.73 | 0.19 |
| **G-N-DC35** | 1.15 | 0.59 |
| **G-T-45** | 1.11 | 1.63 |
| **G-T-RH45** | 0.00 | 0.53 |
| **G-T-DC45** | 0.35 | 0.23 |
| **G-T-35** | 0.92 | 0.96 |
| **G-T-RH35** | 0.87 | 0.75 |
| **G-T-DC35** | - | 0.66 |

* T - A - B

**T**: test → M: macrocell test, SE: Southern Exposure test, CB: cracked beam test, G: ASTM G 109 test

**A**: steel type → N: conventional, normalized steel, T: Thermex-treated conventional steel.

**B**: mix design → 45: water-cement ratio of 0.45 and no inhibitor, RH45: water-cement ratio of 0.45 and Rheocrete 222+, DC45: water-cement ratio of 0.45 and DCI-S, 35: water-cement ratio of 0.35 and no inhibitor, RH35: water-cement ratio of 0.35 and Rheocrete 222+, DC35: water-cement ratio of 0.35 and DCI-S.

**Table 4.3 –** Comparison between coefficients of variation of corrosion rates and losses of conventional normalized, conventional Thermex-treated, and microalloyed steels.

| Specimen designation* | Corrosion rate | Corrosion loss |
|---|---|---|
| **Bare bars in 1.6 m NaCl** | | |
| **M-N** | 0.44 | 0.26 |
| **M-T** | 0.52 | 0.29 |
| **M-CRPT1** | 0.45 | 0.17 |
| **M-CRPT2** | 0.38 | 0.15 |
| **M-CRT** | 0.40 | 0.12 |
| **"Lollipop" specimens with caps in 1.6 m ion NaCl** | | |
| **M-Nc-50** | 0.60 | 0.56 |
| **M-Tc-50** | 0.44 | 0.63 |
| **M-CPRT1c-50** | 0.39 | 0.28 |
| **M-CRPT2c-50** | 0.32 | 0.34 |
| **M-CRTc-50** | 0.45 | 0.33 |
| **"Lollipop" specimens without caps in 1.6 m ion NaCl** | | |
| **M-N-50** | 0.46 | 0.40 |
| **M-T-50** | 0.43 | 0.50 |
| **M-CPRT1-50** | 0.65 | 0.61 |
| **M-CRPT2-50** | 0.47 | 0.49 |
| **M-CRT-50** | 0.50 | 0.55 |
| **Southern Exposure test** | | |
| **SE-N-45** | 0.66 | 0.38 |
| **SE-T-45** | 1.20 | 0.59 |
| **SE-CRPT1-45** | 0.92 | 0.68 |
| **SE-CRPT2-45** | 0.61 | 0.61 |
| **SE-CRT-45** | 0.62 | 0.62 |
| **SE-N/CRPT1-45** | 0.37 | 0.29 |
| **SE-CRPT1/N/45** | 0.63 | 0.48 |
| **Cracked beam test** | | |
| **CB-N-45** | 0.76 | 0.26 |
| **CB-T-45** | 0.72 | 0.25 |
| **CB-CRPT1-45** | 0.88 | 0.33 |
| **CB-CRPT2-45** | 1.03 | 0.42 |
| **CB-CRT-45** | 0.58 | 0.07 |
| **ASTM G 109 test** | | |
| **G-N-45** | 1.04 | 0.45 |
| **G-T-45** | 1.11 | 1.63 |
| **G-CRPT1-45** | 0.97 | 1.23 |
| **G-CRPT2-45** | 1.15 | 1.67 |
| **G-CRT-45** | 0.75 | 0.83 |

* T - A - B

**T**: test → M: macrocell test, SE: Southern Exposure test, CB: cracked beam test, G: ASTM G 109 test

**A**: steel type → N: conventional, normalized steel, T: Thermex-treated conventional steel, CRPT1: Thermex-treated microalloyed steel with a high phosphorus content (0.117%), CRPT2: Thermex-treated microalloyed steel with a high phosphorus content (0.100%), CRT: Thermex treated microalloyed steel with normal phosphorus content (0.017%), c: epoxy-filled caps on the end.

**B**: mix design → 50: water-cement ratio of 0.50 and no inhibitor, 45: water-cement ratio of 0.45 and no inhibitor.

**Table 4.4 –** Comparison between coefficients of variation of corrosion rates and losses of conventional and MMFX microcomposite steels.

| Specimen designation* | Corrosion rate | Corrosion loss |
|---|---|---|
| **Bare bars in 1.6 m NaCl** | | |
| **M-N3** | 0.66 | 0.43 |
| **M-MMFX(1)** | 0.55 | 0.24 |
| **M-MMFX(2)** | 0.38 | 0.42 |
| **M-MMFXs** | 0.55 | 0.21 |
| **M-MMFXb** | 0.43 | 0.32 |
| **M-MMFX#19** | 0.21 | 0.35 |
| **Bare bars in 6.04 m NaCl** | | |
| **M-N3h** | 0.41 | 0.23 |
| **M-MMFXsh** | 0.23 | 0.32 |
| **Mortar-wrapped specimens in 1.6 m NaCl** | | |
| **M-N3-50** | 0.36 | 0.15 |
| **M-MMFX-50** | 0.36 | 0.46 |
| **M-MMFX/N3-50** | 0.15 | 0.14 |
| **M-N3/MMFX-50** | 0.21 | 0.23 |
| **Southern Exposure test** | | |
| **SE-N3-45** | 0.53 | 0.54 |
| **SE-MMFX-45** | 0.35 | 0.46 |
| **SE-MMFXb-45** | 0.20 | 0.25 |
| **SE-MMFX/N3-45** | 0.28 | 0.12 |
| **SE-N3/MMFX-45** | 0.40 | 0.40 |
| **Cracked beam test** | | |
| **CB-N3-45** | 1.10 | 0.65 |
| **CB-MMFX-45** | 0.42 | 0.26 |

* T - A - B

**T**: test → M: macrocell test, SE: Southern Exposure test, CB: cracked beam test

**A**: steel type → N, and N3: conventional, normalized steel, MMFX: MMFX microcomposite steel, s: sandblasted, b: bent bars in the anode or top mat, h: 6.04 m ion concentration.

**B**: mix design → 50: water-cement ratio of 0.50 and no inhibitor, 45: water-cement ratio of 0.45 and no inhibitor.

**Table 4.5 –** Comparison between coefficients of variation for corrosion rates and losses of conventional uncoated and epoxy-coated steel

| Specimen designation* | Corrosion rate | Corrosion loss |
|---|---|---|
| **Mortar-wrapped specimens in 1.6 m NaCl** | | |
| **M-N3-50** | 0.36 | 0.15 |
| **M-ECR-50** | 1.33 | 1.26 |
| **Southern Exposure test** | | |
| **SE-N3-45** | 0.53 | 0.54 |
| **SE-ECR-45** | 0.73 | 0.66 |
| **Cracked beam test** | | |
| **CB-N3-45** | 1.10 | 0.65 |
| **CB-ECR-45** | 0.81 | 0.74 |

* T - A - B
**T**: test → M: macrocell test, SE: Southern Exposure test, CB: cracked beam test
**A**: steel type → N3: conventional, normalized steel, ECR: epoxy-coated rebar,
**B**: mix design → 50: water-cement ratio of 0.50 and no inhibitor, 45: water-cement ratio of 0.45 and no inhibitor.

**Table 4.6 –** Comparison between coefficients of variation for corrosion rates and losses of conventional and duplex stainless steels

| Specimen designation* | Corrosion rate | Corrosion loss |
|---|---|---|
| **Bare bars in 1.6 m NaCl** | | |
| **M-N3** | 0.66 | 0.43 |
| **M-2205** | 0.76 | 0.39 |
| **M-2205p** | 0.34 | 0.13 |
| **M-2101(1)** | 0.38 | 1.02 |
| **M-2101(1)p** | 1.05 | 0.71 |
| **M-2101(2)** | 0.75 | 0.28 |
| **M-2101(2)p** | 0.91 | 1.06 |
| **M-2101(2)s** | 2.00 | 1.05 |
| **Bare bars in 6.04 m NaCl** | | |
| **M-N3h** | 0.41 | 0.23 |
| **M-2205h** | 0.25 | 0.27 |
| **M-2205ph** | 0.45 | 0.49 |
| **M-2101(1)h** | 0.47 | 0.33 |
| **M-2101(1)ph** | 0.65 | 0.52 |
| **M-2101(2)h** | 0.19 | 0.18 |
| **M-2101(2)ph** | 1.47 | 0.59 |
| **M-2101(2)sh** | 0.92 | 0.89 |
| **Mortar-wrapped specimens in 1.6 m NaCl** | | |
| **M-N2-50** | 0.44 | 0.39 |
| **M-2205-50** | 0.89 | 0.26 |
| **M-2205p-50** | 1.14 | 0.38 |
| **M-2101(1)-50** | 0.62 | 0.70 |
| **M-2101(1)p-50** | 1.28 | 0.51 |
| **M-2101(2)-50** | 0.46 | 0.38 |
| **M-2101(2)p-50** | 0.68 | 0.28 |
| **Southern Exposure test** | | |
| **SE-N-45** | 0.66 | 0.38 |
| **SE-2205-45** | 1.12 | 1.38 |
| **SE-2205p-45** | 1.87 | 0.52 |
| **SE-2101(1)-45** | 0.49 | 0.49 |
| **SE-2101(1)p-45** | 1.47 | 1.58 |
| **SE-2101(2)-45** | 1.40 | 0.98 |
| **SE-2101(2)p-45** | 1.49 | 0.26 |
| **SE-N2/2205-45** | 0.42 | 0.37 |
| **SE-2205/N2-45** | 0.89 | 0.96 |
| **Cracked beam test** | | |
| **CB-N-45** | 0.76 | 0.26 |
| **CB-2205-45** | 1.25 | 0.69 |
| **CB-2205p-45** | 1.85 | 0.50 |
| **CB-2101(1)-45** | 0.89 | 0.35 |
| **CB-2101(1)p-45** | 0.50 | 0.58 |
| **CB-2101(2)-45** | 0.38 | 0.11 |
| **CB-2101(2)p-45** | 1.26 | 0.55 |

* T - A - B

**T**: test → M: macrocell test, SE: Southern Exposure test, CB: cracked beam test

**A**: steel type → N, N2, and N3: conventional, normalized steel, 2101(1) and 2101(2): duplex stainless steel (21% chromium, 1% nickel), 2205: duplex stainless steel (25% chromium, 5% nickel), p: pickled, s: sandblasted, h: 6.04 m ion concentration.

**B**: mix design → 50: water-cement ratio of 0.50 and no inhibitor, 45: water-cement ratio of 0.45 and no inhibitor.

**Table 4.7 –** Comparison between coefficients of variation of the macrocell test with bare bars in 1.6 m ion NaCl and simulated concrete pore solution and the Southern Exposure test.

| Steel type * | Corrosion rates | | Corrosion losses | |
|---|---|---|---|---|
| | Macrocell | SE | Macrocell | SE |
| **N** | 0.44 | 0.66 | 0.26 | 0.38 |
| **T** | 0.52 | 1.20 | 0.29 | 0.59 |
| **CRPT1** | 0.45 | 0.92 | 0.17 | 0.68 |
| **CRPT2** | 0.38 | 0.61 | 0.15 | 0.61 |
| **CRT** | 0.40 | 0.62 | 0.12 | 0.62 |
| **N3** | 0.66 | 0.53 | 0.43 | 0.54 |
| **MMFX** | 0.38 | 0.35 | 0.42 | 0.46 |
| **2205** | 0.76 | 1.12 | 0.39 | 1.38 |
| **2205p** | 0.34 | 1.87 | 0.13 | 0.52 |
| **2101(1)** | 0.38 | 0.49 | 1.02 | 0.49 |
| **2101(1)p** | 1.05 | 1.47 | 0.71 | 1.58 |
| **2101(2)** | 0.75 | 1.40 | 0.28 | 0.98 |
| **2101(2)p** | 0.91 | 1.49 | 1.06 | 0.26 |

*** Steel type →** N and N3: conventional, normalized steel, T: Thermex-treated conventional steel, CRPT1: Thermex- treated microalloyed steel with a high phosphorus content (0.117%), CRPT2: Thermex-treated microalloyed steel with a high phosphorus content (0.100%), CRT: Thermex treated microalloyed steel with normal phosphorus content (0.017%), MMFX: MMFX microcomposite steel, 2101(1) and 2101(2): duplex stainless steel (21% chromium, 1% nickel), 2205: duplex stainless steel (25% chromium, 5% nickel), p: pickled.

**Table 4.8 –** Comparison between coefficients of variation of the macrocell test with bare bars in 6.04 m ion NaCl and simulated concrete pore solution and the Southern Exposure test.

| Steel type * | Corrosion rates | | Corrosion losses | |
|---|---|---|---|---|
| | Macrocell | SE | Macrocell | SE |
| **N3** | 0.41 | 0.66 | 0.23 | 0.38 |
| **2205** | 0.25 | 1.12 | 0.27 | 1.38 |
| **2205p** | 0.45 | 1.87 | 0.49 | 0.52 |
| **2101(1)** | 0.47 | 0.49 | 0.33 | 0.49 |
| **2101(1)p** | 0.65 | 1.47 | 0.52 | 1.58 |
| **2101(2)** | 0.19 | 1.40 | 0.18 | 0.98 |
| **2101(2)p** | 1.47 | 1.49 | 0.59 | 0.26 |

*** Steel type →** N3: conventional, normalized steel, 2101(1) and 2101(2): duplex stainless steel (21% chromium, 1% nickel), 2205: duplex stainless steel (25% chromium, 5% nickel), p: pickled.

**Table 4.9 –** Comparison between coefficients of variation of the macrocell test with lollipop specimens in 1.6 m ion NaCl and simulated concrete pore solution and the Southern Exposure test.

| Steel type - Mix design * | Corrosion rates | | Corrosion losses | |
|---|---|---|---|---|
| | Macrocell | SE | Macrocell | SE |
| **N-45** | 0.60 | 0.66 | 0.76 | 0.38 |
| **N-RH45** | 1.13 | 0.42 | 0.37 | 0.92 |
| **N-DC45** | 1.39 | 0.76 | 0.69 | 0.96 |
| **N-35** | 1.09 | 0.84 | 1.55 | 0.74 |
| **N-RH35** | 0.98 | 0.41 | 0.98 | 1.29 |
| **N-DC35** | 0.34 | 0.93 | 0.85 | 0.55 |

* A-B
A: steel type → N: conventional, normalized steel.
B: mix design → 45: water-cement ratio of 0.45 and no inhibitor, RH45: water-cement ratio of 0.45 and Rheocrete 222+, DC45: water-cement ratio of 0.45 and DCI-S, 35: water-cement ratio of 0.35 and no inhibitor, RH35: water-cement ratio of 0.35 and Rheocrete 222+, DC35: water-cement ratio of 0.35 and DCI-S.

**Table 4.10 –** Comparison between coefficients of variation of the macrocell test with mortar-wrapped specimens in 1.6 m ion NaCl and simulated concrete pore solution and the Southern Exposure test.

| Steel type * | Corrosion rates | | Corrosion losses | |
|---|---|---|---|---|
| | Macrocell | SE | Macrocell | SE |
| **N3** | 0.36 | 0.53 | 0.15 | 0.54 |
| **MMFX** | 0.36 | 0.35 | 0.46 | 0.46 |
| **MMFX/N3** | 0.15 | 0.28 | 0.14 | 0.12 |
| **N3/MMFX** | 0.21 | 0.40 | 0.23 | 0.40 |
| **2205** | 0.89 | 1.12 | 0.26 | 1.38 |
| **2205p** | 1.14 | 1.87 | 0.38 | 0.52 |
| **2101(1)** | 0.62 | 0.49 | 0.70 | 0.49 |
| **2101(1)p** | 1.28 | 1.47 | 0.51 | 1.58 |
| **2101(2)** | 0.46 | 1.40 | 0.38 | 0.98 |
| **2101(2)p** | 0.68 | 1.49 | 0.28 | 0.26 |
| **ECR** | 1.33 | 0.73 | 1.26 | 0.66 |

*** Steel type** → N3: conventional, normalized steel, MMFX: MMFX microcomposite steel, MMFX/N3: MMFX steel in the top mat and N3 steel in the bottom mat, N3/MMFX: N3 steel in the top mat and MMFX steel in the bottom mat, 2101(1) and 2101(2): duplex stainless steel (21% chromium, 1% nickel), 2205: duplex stainless steel (25% chromium, 5% nickel), ECR: epoxy-coated steel, p: pickled.

**Table 4.11 –** Comparison between coefficients of variation of the macrocell test with bare bars in 1.6 m ion NaCl and simulated concrete pore solution and the cracked beam test.

| Steel type * | Corrosion rates | | Corrosion losses | |
|---|---|---|---|---|
| | Macrocell | CB | Macrocell | CB |
| **N** | 0.44 | 0.76 | 0.26 | 0.26 |
| **T** | 0.52 | 0.72 | 0.29 | 0.25 |
| **CRPT1** | 0.45 | 0.88 | 0.17 | 0.33 |
| **CRPT2** | 0.38 | 1.03 | 0.15 | 0.42 |
| **CRT** | 0.40 | 0.58 | 0.12 | 0.07 |
| **N3** | 0.66 | 1.10 | 0.43 | 0.65 |
| **MMFX** | 0.38 | 0.42 | 0.42 | 0.26 |
| **2205** | 0.76 | 1.25 | 0.39 | 0.69 |
| **2205p** | 0.34 | 1.85 | 0.13 | 0.50 |
| **2101(1)** | 0.38 | 0.89 | 1.02 | 0.35 |
| **2101(1)p** | 1.05 | 0.50 | 0.71 | 0.58 |
| **2101(2)** | 0.75 | 0.38 | 0.28 | 0.11 |
| **2101(2)p** | 0.91 | 1.26 | 1.06 | 0.55 |

*** Steel type →** N and N3: conventional, normalized steel, T: Thermex-treated conventional steel, CRPT1: Thermex- treated microalloyed steel with a high phosphorus content (0.117%), CRPT2: Thermex-treated microalloyed steel with a high phosphorus content (0.100%), CRT: Thermex treated microalloyed steel with normal phosphorus content (0.017%), MMFX: MMFX microcomposite steel, 2101(1) and 2101(2): duplex stainless steel (21% chromium, 1% nickel), 2205: duplex stainless steel (25% chromium, 5% nickel), p: pickled.

**Table 4.12 –** Comparison between coefficients of variation of the macrocell test with bare bars in 6.04 m ion NaCl and simulated concrete pore solution and the cracked beam test.

| Steel type * | Corrosion rates | | Corrosion losses | |
|---|---|---|---|---|
| | Macrocell | CB | Macrocell | CB |
| **N3** | 0.41 | 1.10 | 0.23 | 0.65 |
| **2205** | 0.25 | 1.25 | 0.27 | 0.69 |
| **2205p** | 0.45 | 1.85 | 0.49 | 0.50 |
| **2101(1)** | 0.47 | 0.89 | 0.33 | 0.35 |
| **2101(1)p** | 0.65 | 0.50 | 0.52 | 0.58 |
| **2101(2)** | 0.19 | 0.38 | 0.18 | 0.11 |
| **2101(2)p** | 1.47 | 1.26 | 0.59 | 0.55 |

*** Steel type →** N3: conventional, normalized steel, 2101(1) and 2101(2): duplex stainless steel (21% chromium, 1% nickel), 2205: duplex stainless steel (25% chromium, 5% nickel), p: pickled.

**Table 4.13 –** Comparison between coefficients of variation of the macrocell test with mortar-wrapped specimens in 1.6 m ion NaCl and simulated concrete pore solution and the cracked beam test.

| Steel type * | Corrosion rates | | Corrosion losses | |
|---|---|---|---|---|
| | Macrocell | CB | Macrocell | CB |
| **N3** | 0.36 | 1.10 | 0.15 | 0.65 |
| **MMFX** | 0.36 | 0.42 | 0.46 | 0.26 |
| **2205** | 0.89 | 1.25 | 0.26 | 0.69 |
| **2205p** | 1.14 | 1.85 | 0.38 | 0.50 |
| **2101(1)** | 0.62 | 0.89 | 0.70 | 0.35 |
| **2101(1)p** | 1.28 | 0.50 | 0.51 | 0.58 |
| **2101(2)** | 0.46 | 0.38 | 0.38 | 0.11 |
| **2101(2)p** | 0.68 | 1.26 | 0.28 | 0.55 |
| **ECR** | 1.33 | 0.81 | 1.26 | 0.74 |

*** Steel type** → N3: conventional, normalized steel, 2101(1) and 2101(2): duplex stainless steel (21% chromium, 1% nickel), 2205: duplex stainless steel (25% chromium, 5% nickel), p: pickled.

The results of the Student's t-test were discussed in Chapter 3, and the results are shown in Tables C.1 to C.14. Tables 4.14 to 4.17 compare the levels of significance obtained for the corrosion rates and total corrosion losses for the rapid macrocell, Southern Exposure and cracked beam test. These tables include 45 comparisons made between the macrocell and Southern Exposure tests. Out of these 45 comparisons, for the corrosion rates, in 23 cases the macrocell test and the Southern Exposure test have the same level of significance, and in 4 cases the level of significance for the SE test was 0.05, while for the macrocell test it was 0.02. For the corrosion losses, in 25 cases these two tests have the same level of significance, and in 4 cases the level of significance for the SE test was 0.05, while for the macrocell test it was 0.02

Tables 4.14 to 4.17 include 40 comparisons between the macrocell and cracked beam test. Out of these 40 comparisons, for the corrosion rate, in 14 cases the macrocell test and the cracked beam test had the same level of significance, and in 16 cases the level of significance for the CB test is 0.05, while for the macrocell test it is 0.02. For the total corrosion losses, in 28 cases these two tests had the same level of significance, and in 1 case the level of significance for the CB test is 0.05, while for the macrocell test it is 0.02

The results from the comparisons of the levels of significance obtained for the corrosion rates and total corrosion losses in the rapid macrocell, Southern Exposure, and cracked beam tests show that the rapid macrocell test yields results that are comparable to those obtained from the Southern Exposure and cracked beam test. At the same time, the rapid macrocell test exhibits similar reliability than the bench-scale tests.

**Table 4.14 –** Comparison of the levels of significance obtained from the Student's t-test for the rapid macrocell test with bare bars in 1.6 m ion NaCl and simulated concrete pore solution and the Southern Exposure and cracked beam tests.

Corrosion rates

| Type of steel * | | Macrocell | SE | CB |
|---|---|---|---|---|
| N | N3 | - | 0.10 | - |
| N | T | - | - | - |
| N | CRPT1 | - | - | - |
| N | CRPT2 | - | - | - |
| N | CRT | - | - | - |
| N3 | MMFX | 0.20 | 0.05 | 0.20 |
| N3 | 2205 | 0.02 | 0.02 | 0.05 |
| N3 | 2205p | 0.02 | 0.02 | 0.05 |
| N3 | 2101(1) | 0.02 | - | 0.05 |
| N3 | 2101(1)p | 0.02 | 0.05 | 0.05 |
| N3 | 2101(2) | 0.02 | 0.05 | 0.05 |
| N3 | 2101(2)p | 0.02 | 0.02 | 0.05 |
| 2205 | 2205p | - | - | - |
| 2101(1) | 2101(1)p | 0.02 | 0.20 | - |
| 2101(2) | 2101(2)p | 0.05 | 0.20 | 0.02 |
| 2101(2)p | 2205p | 0.05 | - | - |

Corrosion losses

| Type of steel * | | Macrocell | SE | CB |
|---|---|---|---|---|
| N | N3 | - | - | - |
| N | T | 0.10 | - | - |
| N | CRPT1 | - | - | - |
| N | CRPT2 | - | - | - |
| N | CRT | - | - | - |
| N3 | MMFX | 0.02 | 0.05 | 0.10 |
| N3 | 2205 | 0.02 | 0.02 | 0.02 |
| N3 | 2205p | 0.02 | 0.02 | 0.02 |
| N3 | 2101(1) | 0.02 | 0.05 | 0.02 |
| N3 | 2101(1)p | 0.02 | 0.02 | 0.02 |
| N3 | 2101(2) | 0.02 | 0.02 | 0.02 |
| N3 | 2101(2)p | 0.02 | 0.02 | 0.02 |
| 2205 | 2205p | 0.20 | - | 0.10 |
| 2101(1) | 2101(1)p | 0.20 | 0.10 | 0.10 |
| 2101(2) | 2101(2)p | 0.02 | 0.10 | 0.02 |
| 2101(2)p | 2205p | - | - | - |

*** Steel type** → N and N3: conventional, normalized steel, T: Thermex-treated conventional steel, CRPT1: Thermex- treated microalloyed steel with a high phosphorus content (0.117%), CRPT2: Thermex-treated microalloyed steel with a high phosphorus content (0.100%), CRT: Thermex treated microalloyed steel with normal phosphorus content (0.017%), 2101(1) and 2101(2): duplex stainless steel (21% chromium, 1% nickel), 2205: duplex stainless steel (25% chromium, 5% nickel), p: pickled.

**Table 4.15 –** Comparison of the levels of significance obtained from the Student's t-test for the rapid macrocell test with bare bars in 6.04 m ion NaCl and simulated concrete pore solution and the Southern Exposure and cracked beam tests.

Corrosion rates

| Type of steel * | | Macrocell | SE | CB |
|---|---|---|---|---|
| N3 | 2205 | 0.02 | 0.02 | 0.05 |
| N3 | 2205p | 0.02 | 0.02 | 0.05 |
| N3 | 2101(1) | 0.10 | - | 0.05 |
| N3 | 2101(1)p | 0.02 | 0.05 | 0.05 |
| N3 | 2101(2) | 0.05 | 0.05 | 0.05 |
| N3 | 2101(2)p | 0.02 | 0.02 | 0.05 |
| 2205 | 2205p | 0.02 | - | - |
| 2101(1) | 2101(1)p | 0.05 | 0.20 | - |
| 2101(2) | 2101(2)p | 0.02 | 0.20 | 0.02 |
| 2101(2)p | 2205p | - | - | - |

Corrosion losses

| Type of steel * | | Macrocell | SE | CB |
|---|---|---|---|---|
| N3 | 2205 | 0.02 | 0.02 | 0.02 |
| N3 | 2205p | 0.02 | 0.02 | 0.02 |
| N3 | 2101(1) | 0.02 | 0.05 | 0.02 |
| N3 | 2101(1)p | 0.02 | 0.02 | 0.02 |
| N3 | 2101(2) | 0.02 | 0.02 | 0.02 |
| N3 | 2101(2)p | 0.02 | 0.02 | 0.02 |
| 2205 | 2205p | 0.02 | - | 0.10 |
| 2101(1) | 2101(1)p | 0.02 | 0.10 | 0.10 |
| 2101(2) | 2101(2)p | 0.02 | 0.10 | 0.02 |
| 2101(2)p | 2205p | 0.02 | - | - |

*** Steel type** → N3: conventional, normalized steel, 2101(1) and 2101(2): duplex stainless steel (21% chromium, 1% nickel), 2205: duplex stainless steel (25% chromium, 5% nickel), p: pickled.

**Table 4.16 –** Comparison of the levels of significance obtained from the Student's t-test for the rapid macrocell test with lollipop specimens and the Southern Exposure test.

Corrosion rates

| Type of steel - Mix design * | | Macrocell | SE |
|---|---|---|---|
| N-45 | N-RH45 | 0.10 | 0.05 |
| N-45 | N-DC45 | 0.05 | 0.05 |
| N-45 | N-35 | 0.10 | 0.10 |
| N-35 | N-RH35 | 0.20 | 0.20 |
| N-35 | N-DC35 | 0.20 | - |

Corrosion losses

| Type of steel - Mix design * | | Macrocell | SE |
|---|---|---|---|
| N-45 | N-RH45 | 0.10 | 0.02 |
| N-45 | N-DC45 | 0.20 | 0.02 |
| N-45 | N-35 | - | 0.02 |
| N-35 | N-RH35 | - | 0.20 |
| N-35 | N-DC35 | - | - |

* A-B
A: steel type → N: conventional, normalized steel.
B: mix design → 45: water-cement ratio of 0.45 and no inhibitor, RH45: water-cement ratio of 0.45 and Rheocrete 222+, DC45: water-cement ratio of 0.45 and DCI-S, 35: water-cement ratio of 0.35 and no inhibitor, RH35: water-cement ratio of 0.35 and Rheocrete 222+, DC35: water-cement ratio of 0.35 and DCI-S.

**Table 4.17 –** Comparison of the levels of significance obtained from the Student's t-test for the rapid macrocell test with bare bars in 1.6 m ion NaCl and simulated concrete pore solution and the Southern Exposure and cracked beam tests.

Corrosion rates

| Type of steel * | | Macrocell | SE | CB |
|---|---|---|---|---|
| N3 | MMFX | 0.05 | 0.05 | 0.20 |
| N3 | N3/MMFX | 0.20 | 0.05 | N/A |
| MMFX | MMFX/N3 | - | - | N/A |
| N3 | 2205 | 0.02 | 0.02 | 0.05 |
| N3 | 2205p | 0.02 | 0.02 | 0.05 |
| N3 | 2101(1) | 0.05 | - | 0.05 |
| N3 | 2101(1)p | 0.02 | 0.05 | 0.05 |
| N3 | 2101(2) | 0.02 | 0.05 | 0.05 |
| N3 | 2101(2)p | 0.02 | 0.02 | 0.05 |
| N3 | ECR | 0.02 | 0.02 | 0.20 |
| 2205 | 2205p | - | - | - |
| 2101(1) | 2101(1)p | 0.05 | 0.20 | - |
| 2101(2) | 2101(2)p | 0.02 | 0.20 | 0.02 |
| 2101(2)p | 2205p | - | - | - |

Corrosion losses

| Type of steel * | | Macrocell | SE | CB |
|---|---|---|---|---|
| N3 | MMFX | 0.02 | 0.05 | 0.10 |
| N3 | N3/MMFX | 0.02 | - | N/A |
| MMFX | MMFX/N3 | 0.20 | - | N/A |
| N3 | 2205 | 0.02 | 0.02 | 0.02 |
| N3 | 2205p | 0.02 | 0.02 | 0.02 |
| N3 | 2101(1) | 0.02 | 0.05 | 0.02 |
| N3 | 2101(1)p | 0.02 | 0.02 | 0.02 |
| N3 | 2101(2) | 0.02 | 0.02 | 0.02 |
| N3 | 2101(2)p | 0.02 | 0.02 | 0.02 |
| N3 | ECR | 0.02 | 0.02 | 0.05 |
| 2205 | 2205p | - | - | 0.10 |
| 2101(1) | 2101(1)p | 0.10 | 0.10 | 0.10 |
| 2101(2) | 2101(2)p | 0.02 | 0.10 | 0.02 |
| 2101(2)p | 2205p | - | - | - |

*** Steel type →** N3: conventional, normalized steel, MMFX: MMFX microcomposite steel, MMFX/N3: MMFX steel in the top mat and N3 steel in the bottom mat, N3/MMFX: N3 steel in the top mat and MMFX steel in the bottom mat, 2101(1) and 2101(2): duplex stainless steel (21% chromium, 1% nickel), 2205: duplex stainless steel (25% chromium, 5% nickel), ECR: epoxy-coated steel, p: pickled.

## 4.3 ELECTROCHEMICAL IMPEDANCE SPECTROSCOPY

In electrochemical impedance spectroscopy (EIS) tests, a small-amplitude alternating potential is applied to an electrochemical cell over a range of frequencies and the current through the cell is measured. The impedance, or resistance to current flow, is measured. Any electrochemical cell can be modeled with an equivalent circuit consisting of a combination of resistors, capacitors, and inductors. The analysis of the electrochemical impedance data is performed to find an equivalent circuit that fits the measured data. EIS is explained in more detail in Section 1.3.4.

Electrochemical impedance measurements were performed on the Southern Exposure and rapid macrocell tests, as described in Section 2.4. The specimen used for the rapid macrocell test was a mortar-wrapped specimen with conventional, normalized steel, in 1.6 m ion NaCl and simulated concrete pore solution. The mortar had a water-cement ratio of 0.50. The Southern Exposure test had conventional, normalized steel and the concrete had a water-cement ratio of 0.45. The analysis of the impedance spectrum was performed to determine the equivalent circuit that provides the best fit between the model's spectrum and the measured spectrum. Results of the impedance modulus and the phase angle versus log frequency, Bode plots, for the macrocell and Southern Exposure tests are shown in Figures 4.12(a) and 4.12(b), respectively.

The equivalent circuits shown in Figures 4.13 to 4.15 were used to model the measured spectrums shown in Figure 4.12. The selection of the equivalent circuits is based on previous research on steel-concrete systems, as described in Section 1.3.4.2. In all cases, a resistor $R_s$ is used to model the resistance of the solution and salt bridge in the rapid macrocell test and the concrete and pore solution in the Southern Exposure test, and resistors $R_a$ and $R_c$ are used to model the charge-transfer resistance

at the anode (top mat in the SE test) and cathode (bottom mat in the SE test), respectively. Capacitors $C_a$ and $C_c$ are used to model the double-layer capacitance at the anode and cathode, respectively. Variables $A$ and $n$ are used to define the constant-phase elements used to model the non-ideal behavior of the capacitors, with subscripts $c$ and $a$ used for the cathode and anode, respectively. A Warburg impedance, shown in Figure 4.15, is used to model diffusion, and the Warburg coefficient is represented by $\sigma$.

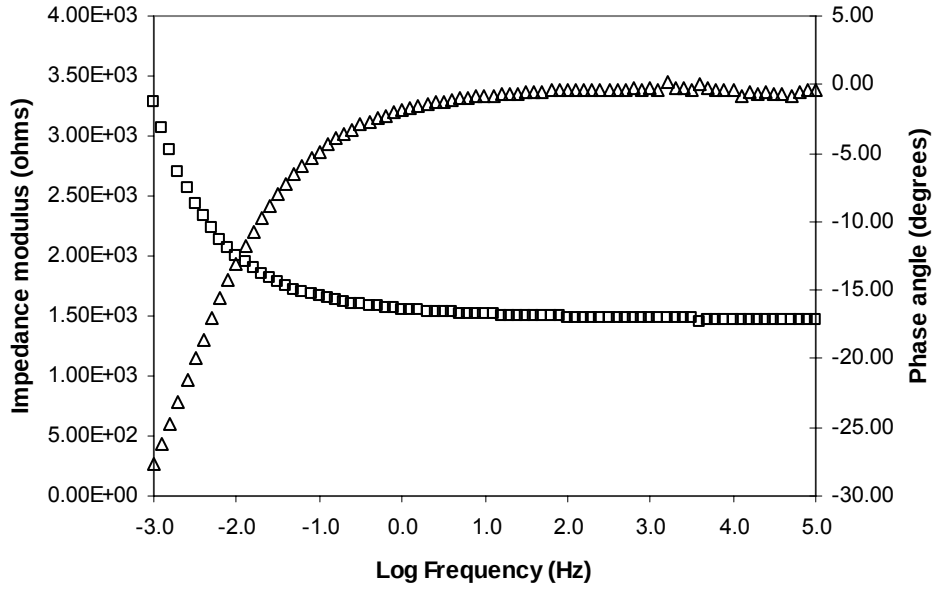


(a) Rapid macrocell test

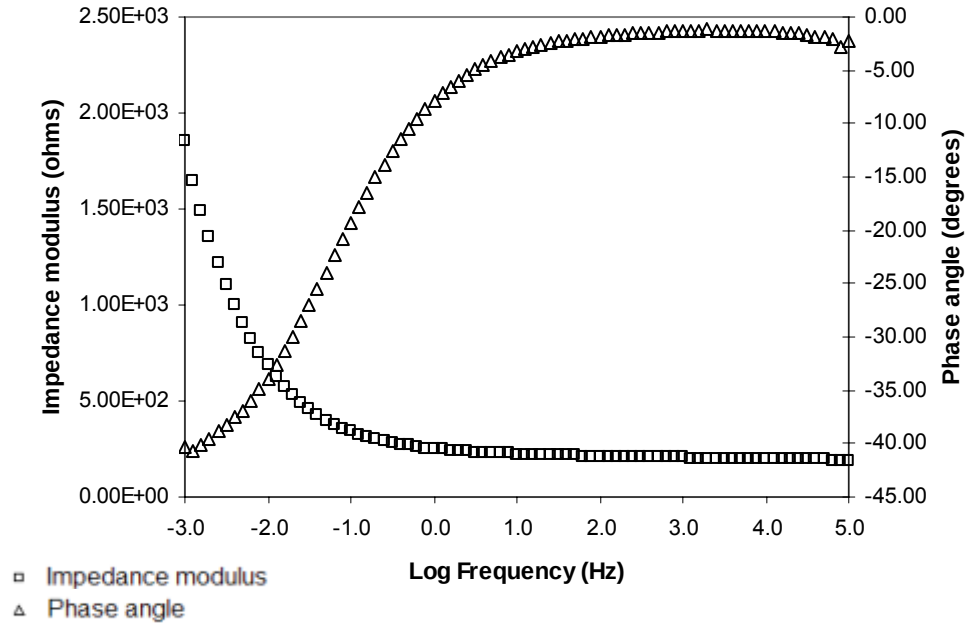


(b) Southern Exposure test

**Figure 4.12 –** Bode plots of measured impedance spectrum for (a) rapid macrocell test and (b) Southern Exposure test.

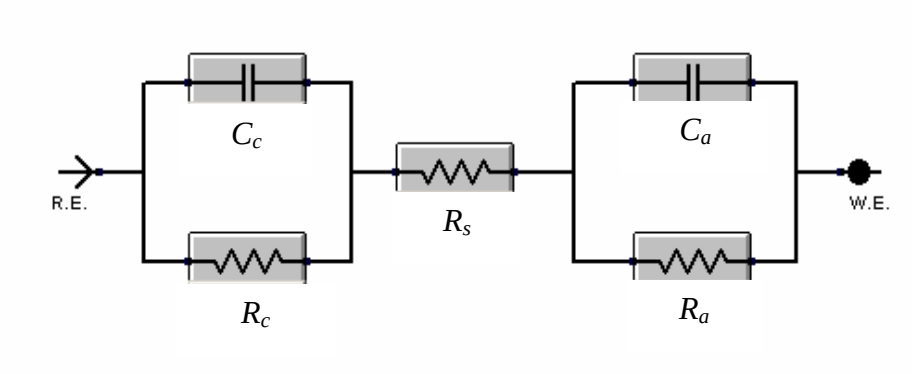


**Figure 4.13 –** Equivalent circuit #1

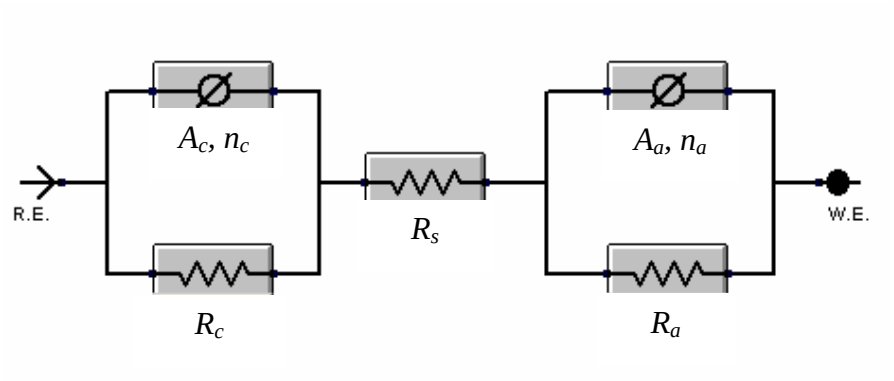


**Figure 4.14 –** Equivalent circuit #2

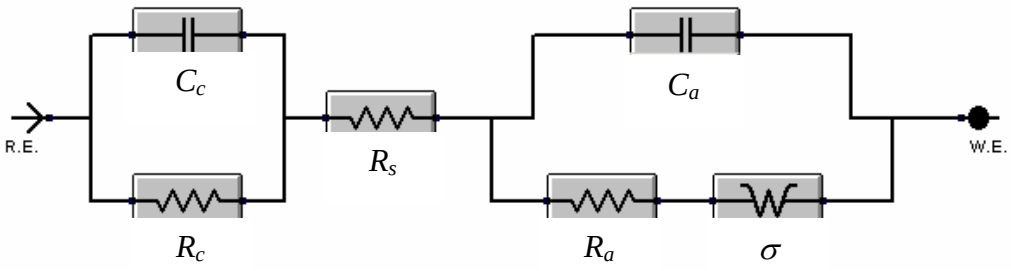


**Figure 4.15–** Equivalent circuit #3

Equivalent circuit #1, shown in Figure 4.13, is based on the basic Randles circuit described in Section 1.3.4.2. For this circuit, a capacitor and a resistor in parallel are used to model the anode and the cathode in the macrocell test, and the top and bottom mat of the Southern Exposure test. As shown in Figure 4.16, this circuit does not provide a good fit, since the continuous line representing the spectrum for the equivalent circuit does not match the measured spectrum for the system, and in fact, exhibits anomalous, non-monotonic behavior.

For equivalent circuit #2, shown in Figure 4.14, the capacitors in equivalent circuit #1 are replaced with constant-phase elements, which, as explained in Section 1.3.4.2, represent non-ideal capacitors. The Bode plots for this circuit are shown in Figure 4.17(a) and 4.17(b) for the macrocell and Southern Exposure test, respectively. This equivalent circuit provides a very good fit since the spectrums for the circuit closely match the measured spectrums. The values for the electrical circuit elements for this model are summarized in Table 4.18.

**Table 4.18 –** Value of electrical circuit elements for Equivalent Circuit #2

| Variable | Macrocell | Southern Exposure |
|---|---|---|
| $R_s$ (ohms) | 1473 | 117 |
| $R_a$ (ohms) | 4773 | 17400 |
| $R_c$ (ohms) | 8055 | 241 |
| $A_a$ (ohms/s$^n$) | 179 | 110 |
| $n_a$ | 0.37 | 0.55 |
| $A_c$ (ohms/s$^n$) | 27 | 203 |
| $n_c$ | 0.78 | 0.05 |

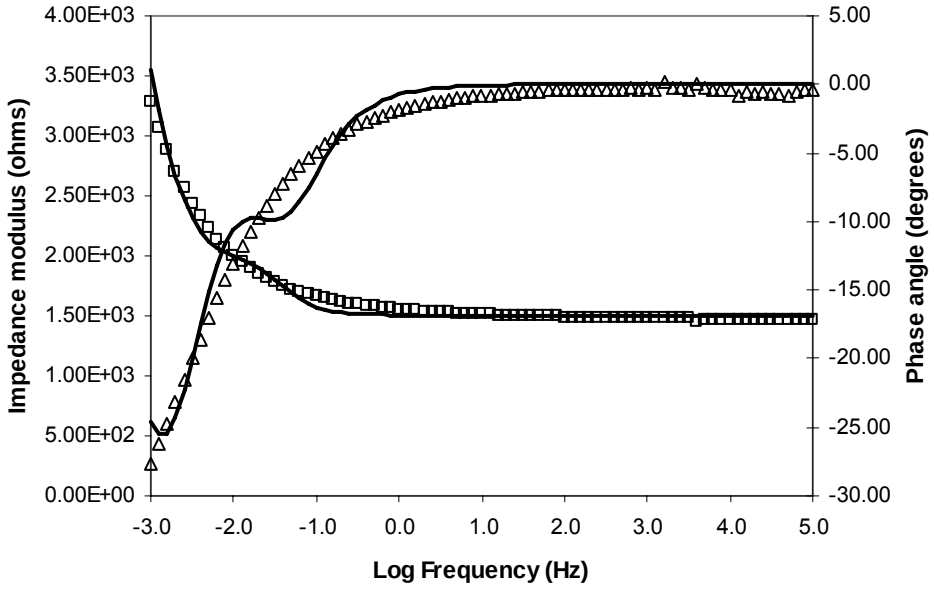


(a) Rapid macrocell test

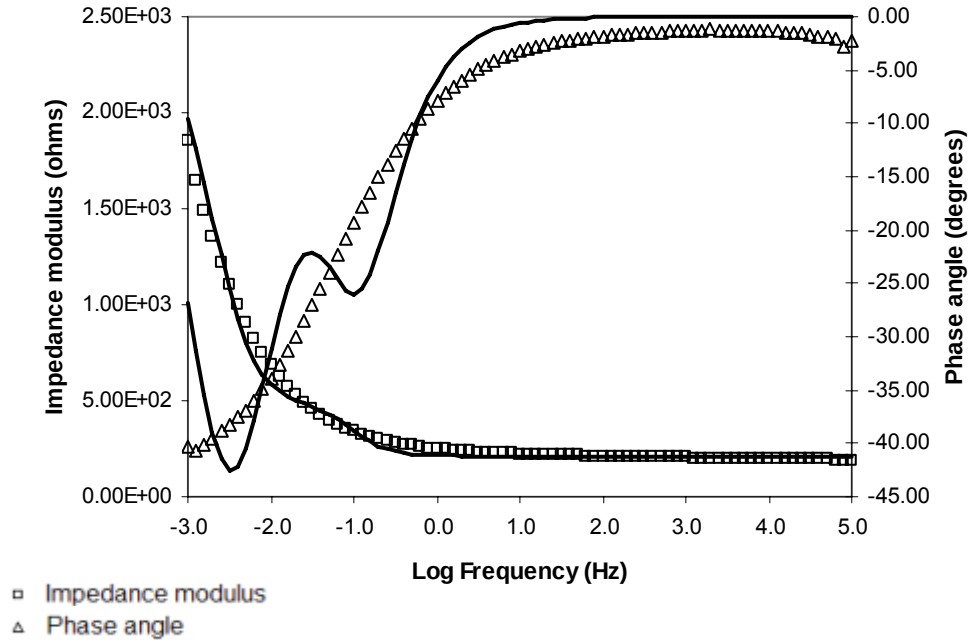


(b) Southern Exposure test

**Figure 4.16 –** Bode plots for equivalent circuit #1 for (a) rapid macrocell test and (b) Southern Exposure test.

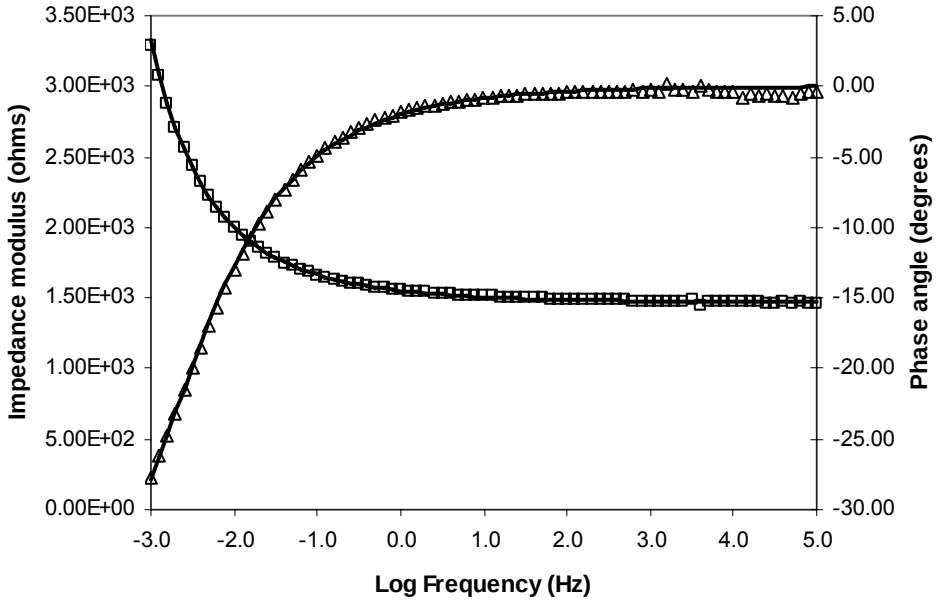


(a) Rapid macrocell test

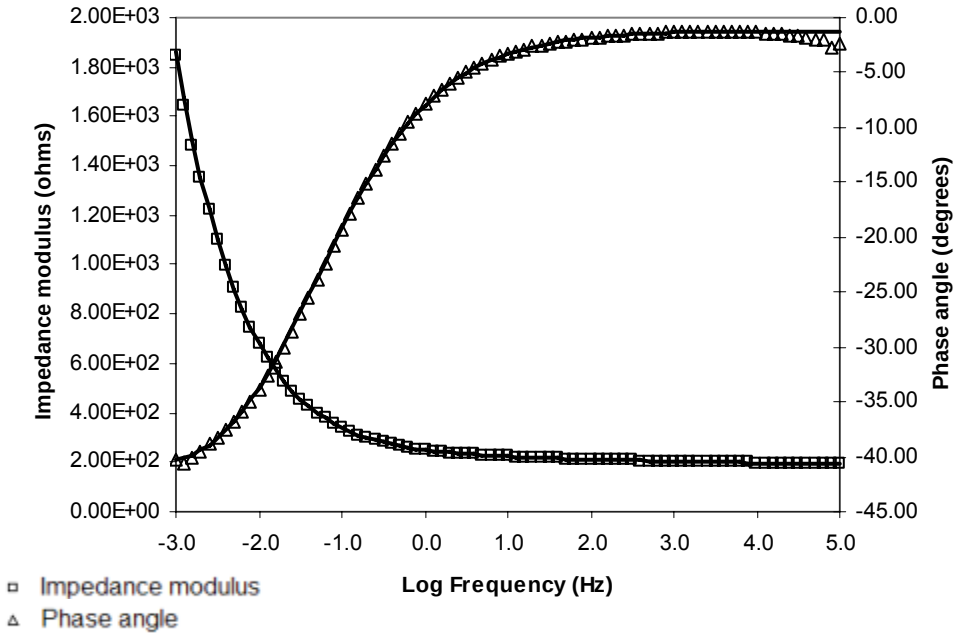


(b) Southern Exposure test

**Figure 4.17 –** Bode plots for equivalent circuit #2 for (a) rapid macrocell test and (b) Southern Exposure test.

For equivalent circuit #3, shown in Figure 4.15, equivalent circuit #1 is modified by adding a Warburg impedance in series with the resistor at the anode or top mat, $R_a$. The Warburg impedance is used to model diffusion. A very good fit is obtained for this model, as shown in Figure 4.18. The values for the electrical circuit elements for this model are summarized in Table 4.19.

**Table 4.19 –** Value of electrical circuit elements for Equivalent Circuit #3

| Variable | Macrocell | Southern Exposure |
|---|---|---|
| $R_s$ (ohms) | 1454 | 185 |
| $R_a$ (ohms) | 25 | 10 |
| $R_c$ (ohms) | 25 | 14 |
| $C_a$ (F) | 2.20E-07 | 2.07E-07 |
| $C_c$ (F) | 5.80E-05 | 1.71E-05 |
| $\sigma$ (ohms-s$^{-1/2}$) | 115 | 92 |

The circuits used in this section to model the tests differ from circuits used by other researchers (see Section 1.4.3) in that they do not require more than one combination of capacitor and resistor to model each of the electrodes (i.e. anode, cathode, top mat, bottom mat). The addition of more elements to the circuits should improve the fit, but additional elements are not needed to represent the laboratory models used in this study.

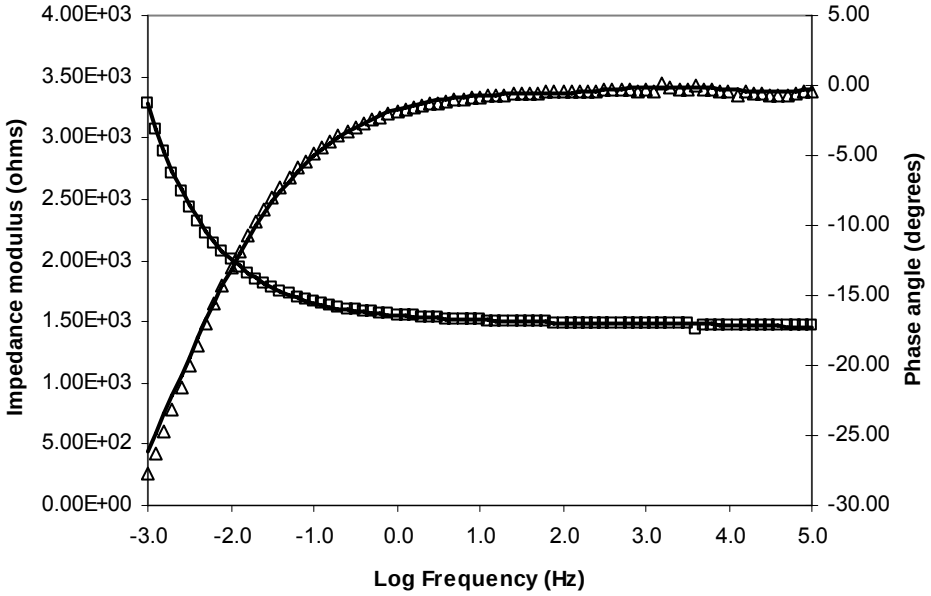


(a) Rapid macrocell test

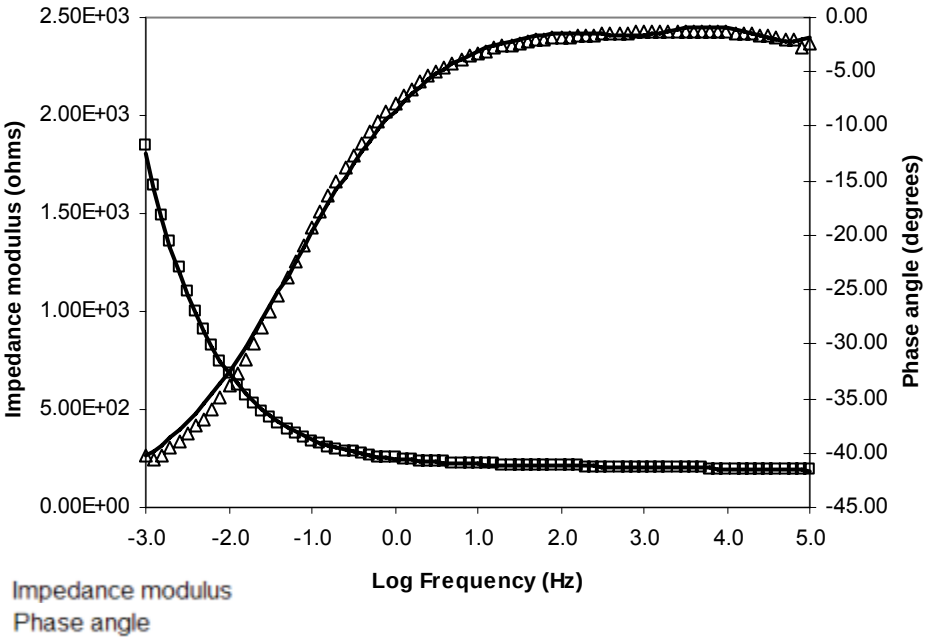


(b) Southern Exposure test

**Figure 4.18 –** Bode plots for equivalent circuit #3 for (a) rapid macrocell test and (b) Southern Exposure test.

# CHAPTER 5

# CONCLUSIONS AND RECOMMENDATIONS

## 5.1 SUMMARY

This report presents the results of the evaluation of corrosion protection systems for reinforcing steel in concrete and the laboratory methods used to evaluate these systems. The corrosion protection systems evaluated include:

- Two corrosion inhibitors, one with calcium nitrite (DCI-S) and one organic inhibitor (Rheocrete 222+)
- Concrete with a low water-cement ratio
- Three microalloyed steels
  - Microalloyed steel with a high phosphorus content, 0.117%, Thermex-treated (CRPT1)
  - Microalloyed steel with a high phosphorus content, 0.100%, Thermex-treated (CRPT2)
  - Microalloyed steel with a normal phosphorus content, 0.017%, Thermex-treated (CRT)
- One conventional steel, Thermex-treated (T)
- MMFX microcomposite steel
- Epoxy-coated steel (ECR) with intentionally damaged coating
- Two duplex stainless steels, 2101 and 2205, which were tested in two conditions: (i) "as-rolled", and (ii) pickled, to remove the mill scale.
- Three heats of conventional hot-rolled steel, N, N2, and N3, were used to cast control specimens.

Two heats of 2101 duplex steel were tested. The duplex stainless steel labeled 2101(1) lacked boron; as a result, the bars were slightly deformed and showed small cracks on the surface. Tests on 2101(1) steel were continued, although the duplex steel labeled 2101(2) steel was received as a substitute. Both, 2101(1) and 2101(2) were evaluated in both the "as-rolled" and pickled condition.

The rapid macrocell test with bare bars and with bars embedded in mortar, and three bench-scale tests, the Southern Exposure (SE), cracked beam (CB), and ASTM G 109 tests, were used to evaluate the corrosion protection systems. The Student's t-test was used to determine if there is a significant difference in the mean corrosion rates and losses for the different corrosion protection systems. An economic analysis was performed to determine the most cost effective corrosion protection systems.

A comparison between the results of the rapid macrocell, Southern Exposure, and cracked beam tests was performed. For the comparison, the corrosion rates and total corrosion losses for the Southern Exposure and the cracked beam tests were compared with the same results for the rapid macrocell tests to determine the degree of correlation between the tests. The results of the cracked beam test were also compared with those of the Southern Exposure test. The coefficient of variation was used to compare the variability in the corrosion rates and the total corrosion losses for the different tests. Impedance spectroscopy analysis was performed to obtain equivalent electrical circuits to represent the Southern Exposure and the rapid macrocell test.

## 5.2 CONCLUSIONS

The following conclusions are based in the results and observations presented in this report.

### 5.2.1 Evaluation of Corrosion Protection Systems

1. In mortar or concrete with a low water-cement ratio, corrosion losses are lower than observed at higher water-cement ratios for either cracked or uncracked mortar or concrete. In cracked concrete, a lower-water cement ratio provides only limited additional corrosion protection when cracks provide a direct path for the chlorides to the steel.
2. In uncracked mortar or concrete (rapid macrocell and Southern Exposure test) containing corrosion inhibitors, corrosion losses are lower than observed at the same water-cement ratio but with no inhibitor.
3. For concrete with cracks above and parallel to the reinforcing steel (cracked beam test), the use of a low-water-cement ratio or an organic inhibitor like Rheocrete 222+ improves the corrosion protection of the steel due to the lower permeability of the concrete, which reduces the rate of diffusion of oxygen and water to the cathode. For cracked concrete, DCI-S does not improve the corrosion protection of the steel.
4. Lower corrosion activity is observed in the ASTM G 109 tests than observed in the Southern Exposure and cracked beam tests. The lower corrosion rates and losses are attributed to the lower salt concentration of the solution ponded over the specimens and to the less aggressive ponding and drying cycle to which the specimens are subjected. The two factors reduce the rate at which chlorides penetrate into the concrete in the ASTM G 109 test, making this test less effective

than the Southern Exposure or cracked beam test for evaluating the behavior of the materials in a relatively short period of time.

5. Microalloyed steel and conventional Thermex-treated steel show no improvement in corrosion resistance when compared to conventional normalized steel.
6. MMFX microcomposite steel exhibits corrosion losses between 26 and 60% of the losses of conventional steel. Based on corrosion potentials, the two steels have a similar tendency to corrode.
7. MMFX steel has a higher chloride corrosion threshold than conventional steel. Based on the average corrosion potentials in the Southern Exposure test, corrosion initiated at week 11 for conventional steel and week 25 for MMFX steel
8. Epoxy-coated steel exhibits low corrosion losses based on the total area of the bar, with corrosion losses between 6% and 19% of that of uncoated conventional steel. The bars were intentionally damaged by drilling four 3.2-mm ($^1/_8$-in.) diameter holes in the coating. The specimens had uncoated conventional steel at the cathode for the rapid macrocell test and bottom mat for the Southern Exposure and cracked beam tests.
9. Pickled 2101(2) and 2205 duplex steels exhibit very good corrosion performance. The average corrosion losses for these steels ranged from 0.3% to 1.8% of the corrosion loss for conventional steel, and in most cases, the corrosion potentials indicated a very low tendency to corrode, even when exposed to high salt concentrations.
10. 2205 steel performs better than 2101 steel when tested in the same condition (pickled or non-pickled).
11. For bars of the same type of steel, pickled bars exhibit lower corrosion rates than the bars that are not pickled.

12. Combining conventional and 2205 steel does not increase the rate of corrosion for either material.
13. In the tests, some of the 2101(2) pickled bars showed some corrosion activity. This could have been a result of steel that had not been fully pickled. In the case of 2205 steel, however, even the unpickled bars showed good corrosion behavior.
14. Decks containing pickled 2101 or 2205 steel are more cost effective than decks containing epoxy-coated or uncoated conventional steel. Based on the present cost at a 2% discount rate, the cost of decks containing pickled 2101 or 2205 steel is between 56 and 91% of the cost of decks containing epoxy-coated steel and between 38 and 67% of the cost of decks containing uncoated conventional steel. Based on the ratio of the premium for using duplex steel over the savings in repair costs when duplex steel is used instead of epoxy-coated steel, at a discount rate of 2%, the premium/savings ratios range from 11% to 83%.
15. The present cost of a bridge deck containing 2101 pickled steel ranges between 82 and 85% of the cost of a bridge deck containing 2205 pickled steel. However, since some of the 2101(2) pickled bars showed some corrosion activity, it is important to consider the fact that incomplete pickling might be a problem. In the case of 2205 steel, even the unpickled bars show low corrosion rates. Therefore, even if 2205 steel is not fully pickled, it should still provide good protection against corrosion.

### 5.2.2 Comparison Between Test Methods

1. Total corrosion losses show good correlation between the Southern Exposure test and the rapid macrocell test in all cases, except when comparing the Southern Exposure test with the rapid macrocell test with microalloyed steel, since the

microalloyed steels corrode at similar rates as conventional steel, making it difficult to distinguish between the steels.

2. Since corrosion rates often vary from week to week, correlations between corrosion rates exhibit greater variation than total corrosion losses, which change gradually from week to week.
3. The coefficients of determination indicate a good correlation between the total corrosion losses in the macrocell tests with bare bars in 1.6 m ion NaCl, with bare bars in 6.04 m ion NaCl, and with mortar-wrapped specimens and the total corrosion losses in the cracked beam tests.
4. The correlation between the Southern Exposure and cracked beam tests is good for specimens fabricated with the same concrete when used to evaluate different reinforcing steels.
5. Comparisons between the corrosion rates and total corrosion losses based on the coefficients of variation show that the corrosion losses have less scatter than the corrosion rates.
6. The coefficients of variation show similar reliability for the rapid macrocell test than for the Southern Exposure or cracked beam test.
7. Comparison of the levels of significance obtained from the Student's t-test give similar results for the rapid macrocell test when compared with the Southern Exposure and cracked beam test.
8. The rapid macrocell and Southern Exposure tests can each be represented by the same equivalent electrical circuits, although with different values for the electrical components.

## 5.3 RECOMMENDATIONS

Pickled 2101 and 2205 duplex stainless steels in a pickled condition are recommended for use in reinforced concrete bridge decks. Both showed average total corrosion losses that ranged from 0.3 to 1.8% of the corrosion loss of conventional steel. Pickled 2101 and 2205 duplex stainless steels had corrosion potentials that indicated that the steels had a low probability of corroding even at high salt concentrations. Epoxy-coated steel also showed good corrosion behavior, with average total corrosion losses that ranged from 6 to 19% of that of uncoated conventional steel for tests using uncoated steel at the cathode.

A lower water-cement ratio or corrosion inhibitors should not be used as the sole corrosion protection system for concrete subjected to chlorides. The reason is that, while concrete with a low water-cement ratio or a corrosion inhibitor provides good protection in uncracked concrete, it provides only limited additional corrosion protection in cracked concrete. Lower corrosion rates are obtained for cracked concrete at low water-cement ratios compared to high water-cement ratios due to the reduced rate of diffusion of oxygen and water to the cathode bars because of the lower permeability provided by the lower w/c ratio material. This reduction, however, is not adequate by itself. Rheocrete 222+ also reduces the rate of corrosion in cracked concrete since it also reduces the permeability of the concrete. DCI-S does not improve the corrosion protection of steel in cracked concrete.

Based on the economic analysis, decks containing 2101 pickled steel are less expensive than decks containing 2205 pickled steel, but some of the 2101 pickled bars showed signs of corrosion, which is an indication that they might not be fully pickled. 2101 steel without pickling had total corrosion losses that ranged between 3 and 36% of the corrosion loss of conventional steel, while 2205 steel without pickling

had total corrosion losses that ranged between 1.0 and 5.1% of the corrosion loss of conventional steel, which shows that even if the steel is not fully pickled, 2205 steel offers some protection.

The rapid macrocell test with bare or mortar-wrapped specimens can be used to evaluate the corrosion performance of reinforcing steels. The rapid macrocell test with mortar-wrapped specimens can be used to evaluate the effect of concrete properties on the corrosion protection of steel. The cracked beam test should not be used to evaluate the effect of concrete properties on the corrosion protection of steel. The rapid macrocell tests showed good correlation with the Southern Exposure and cracked beam tests, and had similar variability in the results. Overall, the rapid macrocell and bench-scale tests produce similar results.

## 5.4 FUTURE WORK

The following research will complement the findings presented in this report.

1. Obtain corrosion rate and corrosion potential measurements on bridge decks. These measurements can be compared to measurements obtained in laboratory specimens with the same corrosion protection systems as used in the bridge decks to determine a correlation between the values obtained in the laboratory and real structures.
2. Obtain chloride corrosion thresholds for different reinforcing steels to determine the time for corrosion initiation for different reinforcing steels. This information will help determine the time to first repair more accurately.
3. Evaluate multiple corrosion protection systems for reinforcing steel in concrete to determine if a combination of corrosion protection systems lengthens the time to first repair.

## REFERENCES


Amleh, L. and Mirza, S. (1999). "Corrosion Influence on Bond Between Steel and Concrete," *ACI Structural Journal*, Vol. 96, No. 3, pp. 415-423.

ASTM C 192/C 192M-00 (2002). "Practice for Making and Curing Concrete Test Specimens in the Laboratory," *2002 Annual Book of ASTM Standards*, Vol. 04.04, American Society for Testing and Materials, West Conshohocken, PA.

ASTM C 305-99, (2002). "Standard Practice for Mechanical Mixing of Hydraulic Cement Pastes and Mortars of Plastic Consistency," *2002 Annual Book of ASTM Standards*, Vol. 04.01, American Society for Testing and Materials, West Conshohocken, PA.

ASTM C 778-00, (2002). "Standard Specification for Standard Sand," *2002 Annual Book of ASTM Standards*, Vol. 04.01, American Society for Testing and Materials, West Conshohocken, PA.

ASTM C 876-91 (2002). "Standard Test Method for Half-Cell Potentials of Uncoated Reinforcing Steel in Concrete," *2002 Annual Book of ASTM Standards*, Vol. 03.02, American Society for Testing and Materials, West Conshohocken, PA.

ASTM G 109-92a (1999). "Standard Test Method for Determining the Effects of Chemical Admixtures on the Corrosion of Embedded Steel Reinforcement in Concrete Exposed to Chloride Environments," *1999 ASTM Annual Book of ASTM Standards*, Vol. 04.02, American Society for Testing and Materials, West Conshohocken, PA.

Balma, J., Darwin, D., Browning, J. P., and Locke, C. E. (2002). "Evaluation of the Corrosion Resistance of Microalloyed Reinforcing Steel," *SM Report* No. 71, The University of Kansas Center for Research, Inc., Lawrence, KS, 171 pp.

Berke, N. S. and Rosenberg, A. (1989). "Technical Review of Calcium Nitrite Corrosion Inhibitor in Concrete," *Transportation Research Record* No. 1211, pp. 18-27.

Berke, N. S., Dallaire, M. P., Kicks, M. C., and Hoopes, R. J. (1993). "Corrosion of Steel in Cracked Concrete," *Corrosion Engineering*, Vol. 49, No. 11, pp. 934-943.

Clemeña, G. G. and Virmani, Y. P. (2002). "Testing of Selected Metallic Reinforcing Bars for Extending the Service Life of Future Concrete Bridges: Testing in Outdoor Concrete Blocks", Virginia Transportation Research Council, *VTRC 03-R6*, December 2002, 24 pp.

Clemeña, G. G. (2003). "Investigation of the Resistance of Several New Metallic Reinforcing Bars to Chloride-Induced Corrosion in Concrete," Virginia Transportation Research Council, *VTRC 04-R7*, December 2003, 24 pp.

Darwin, D. (1995). "Corrosion-Resistant Reinforcing Steel," *SL Report* 95-2, The University of Kansas Center for Research, Inc., Lawrence, KS, 22 pp.

Darwin, D. and Hadge-Ghaffari, H. (1990). "Effects of PE-217 on Steel-Concrete Bond Strength," *Report*, University of Kansas, Lawrence, KS, 10 pp.

Darwin, D., Locke, Browning, J.P, Nguyen, T.V., Carl E., Jr., (2002). "Mechanical and Corrosion Properties of a High-Strength, High Chromium Reinforcing Steel for Concrete," *SM Report* No. 66, The University of Kansas Center for Research, Inc., Lawrence, KS, 142 pp.

Feliú, V., González, J. A., Andrade, C., and Feliú, S. (1998). "Equivalent Circuit for Modeling the Steel-Concrete Interface. I. Experimental Evidence and Theoretical Predictions," *Corrosion Science*, Vol. 40, No. 6, pp. 975-993.

Gamry (1999), *Electrochemical Measurement System Software Installation Manuals, Revision 3.1*, Gamry Instruments Inc.

Gong, L., Darwin, D., Browning, J. P., and Locke, C. E. (2002). "Evaluation of Mechanical and Corrosion Properties of MMFX Reinforcing Steel in Concrete," *SM Report* No. 70, The University of Kansas Center for Research, Inc, Lawrence, KS, 112 pp.

Hausmann, D. A. (1965). "Steel Corrosion in Concrete," *Materials Protection*, Vol. 6, November 1967, pp. 19-23.

Hansson, C. M., Mammolitu, L., and Hope, B. B. (1998). "Corrosion Inhibitors in Concrete – Part 1: The Principles," *Cement and Concrete Research,* Vol. 28, No. 2, Elsevier Science Ltd., pp 1775-1781.

Hayter, A. J. (1996). *Probability and Statistics for Engineers and Scientists*, PWS Publishing Company, Boston, MA, 948 pp.

Hope, B. B., Page, J. A., and Ip, A. K. C. (1986). "Corrosion Rates of Steel in Concrete," *Cement and Concrete Research*, Vol. 16, No. 5, pp. 771-786.

John, D. G., Searson, P. C., and Dawson, J. L. (1981), "Use of AC Impedance Technique in Studies on Steel in Concrete in Immersed Conditions," *British Corrosion Journal*, Vol. 16, No. 2, pp. 102-106.

Jones, D.A. (1996). *Principles and Prevention of Corrosion*, Macmillan Publishing Company, New York, NY, 572 pp.

Kahrs, J., Darwin, D., and Locke, C. E., (2001). "Evaluation of Corrosion Resistance of Type 304 Stainless Steel Clad Reinforcing Bars," *SM Report* No. 65, The University of Kansas Center for Research, Inc., Lawrence, KS, 76 pp.

Kayyali, O. A. and Haque M. N. (1995), "The $Cl^-/OH^-$ Ratio in Chloride-Contaminated Concrete – A Most Important Criterion," *Magazine of Concrete Research*, Vol. 47, No. 172, pp. 235-242.

Kepler, J., Darwin, D., Locke, C.E., Jr. (2000). "Evaluation of Corrosion Protection Methods for Reinforced Concrete Highway Structures," *SM Report* No. 58, The University of Kansas Center for Research, Inc., Lawrence, KS, 219 pp.

Kirkup, Les (2002). *Data Analysis with Excel: An Introduction for Physical Scientists*, Cambridge University Press, Cambridge, United Kingdom, 446 pp.

Lorentz, T. E., French, C. W., and Leon, R. T. (1992). "Corrosion of Coated and Uncoated Reinforcing Steel in Concrete," *Structural Engineering Report* No. 92-03, University of Minnesota Center of Transportation Studies, 1992, 204 pp.

Martinez, S. L., Darwin, D., McCabe, S. L., and Locke, Carl E., Jr. (1990). "Rapid Test for Corrosion Effects of Deicing Chemicals in Reinforced Concrete," *SL Report* 90-4, The University of Kansas Center for Research, Inc., Lawrence, KS, 61 pp.

McDonald, D. B., Pfeifer, D. W., and Sherman, M. R. (1998). "Corrosion Evaluation of Epoxy-Coated, Metallic-Clad and Solid Metallic Reinforcing Bars in Concrete," *Publication* No. FHWA-RD-98-153, Federal Highway Administration, McLean, VA, 127 pp.

Miller, G. and Darwin, D. (2000). "Performance and Constructability of Silica Fume Bridge Deck Overlays," *SM Report* No. 57, The University of Kansas Center for Research, Inc., Lawrence, KS, 423 pp.

Nmai, C. K, Farrington, S. A., Bobrowski, G. (1992). "Organic-Based Corrosion-Inhibiting Admixture for Reinforced Concrete," *Concrete International*, Vol. 14, No. 4, pp. 45-51.

Nmai, C. K., Bury, Mark, A., and Farzam, H. (1994). "Corrosion Evaluation of a Sodium Thiocyanate-Based Admixture," *Concrete International*, Vol. 16, No. 4, pp. 22-25.

Pfeifer, D. W., and Scali, M. J. (1981). "Concrete Sealers for Protection of Bridge Structures," *National Cooperative Highway Research Board Program Report 244*, Transportation Research Board, National Research Council, Washington, D.C., 138 pp.

Pfeifer, D. W. (2000), "High Performance Concrete and Reinforcing Steel with a 100-Year Service Life," *PCI Journal*, Vol. 45, No. 3, pp. 46-54.

Roberge, P. R. (2000). *Handbook of Corrosion Engineering*, McGraw Hill Companies, New York, 1139 pp.

Sagues, A., Powers, R., and Zayed, A. (1990). "Marine Environment Corrosion of Epoxy-Coated Reinforcing Steel," *Corrosion of Reinforcement in Concrete*, C. Page, K. Treadaway, and P. Bamforth, Editors, Elsevier Applied Science, London-New York, 1990, pp. 539-549.

Schmitt, T. R. and Darwin, D. (1995). "Cracking in Concrete Bridge Decks," *SM Report* No. 39, The University of Kansas Center for Research, Lawrence, KS, 151 pp.

Schmitt, T. R., and Darwin, D. (1999). "Effect of Material Properties on Cracking in Bridge Decks," *Journal of Bridge Engineering*, Vol. 4, No. 1, pp. 8-13.

Schwensen, S. M., Darwin, D., and Locke, C. E., Jr. (1995). "Rapid Evaluation of Corrosion-Resistant Concrete Reinforcing Steel in the Presence of Deicers," SL *Report* 95-6, The University of Kansas Center for Research, Inc., Lawrence, KS, 90 pp.

Senecal, M. R., Darwin, D., and Locke, C. E., Jr. (1995). "Evaluation of Corrosion-Resistant Steel Reinforcing Bars," *SM Report* No. 40, The University of Kansas Center for Research, Inc., Lawrence, KS, 142 pp.

Sherman, M. R., McDonald, D. B., Pfeifer, D. W. (1996). "Durability Aspects of Precast Prestressed Concrete Part 2: Chloride Permeability Study," *PCI Journal*, Vol. 41, No. 4, pp. 76-95.

Smith, F. N. and Tullman, M. (1999). "Using Stainless Steel as Long-Lasting Rebar Material," *Materials Performance*, Vol. 38, No. 5, pp. 72-76.

Smith, J. L., Darwin, D., and Locke, C. E., Jr. (1995). "Corrosion-Resistant Steel Reinforcing Bars Initial Tests," *SL Report* 95-1, The University of Kansas Center for Research, Inc., Lawrence, KS, 43 pp.

Srinivasan, S., Venkatachan, G., Rengaswamy, N. S., and Balakrishnan, K. (1987). "Application of Impedance Technique to Study the Corrosion Behavior of Steel in Concrete," *Key Engineering Materials*, Vol. 20-28, Pt. 1-4, pp. 1525-1531

Stern, M., and Geary, A. L. (1957). "Electrochemical Polarization. I. A Theoretical Analysis of the Shape of Polarization Curves," *Journal of the Electrochemical Society*, Vol. 104, No. 1, pp. 56-63.

Tata Iron and Steel Co. (1991). "Development of New Corrosion Resistant Steel (CRS) Reinforcing Bars at Tata Steel," *Report*, Tata Iron and Steel Co., Jamshedpur, India, 32 pp.

Trejo, D. (2002). "Evaluation of the Critical Chloride Threshold and Corrosion Rate for Different Steel Reinforcement Types," Texas Engineering Experimental Station *Interim Report*, July 2002, 38 pp.

Trepanier S. M., Hope, B.B., and Hansson, C. M. (2001). "Corrosion inhibitors in concrete – Part III: Effect on Time to Chloride-Induced Corrosion Initiation and Subsequent Corrosion Rates of Steel in Mortar," *Cement and Concrete Research*, Vol. 31, No. 5, Elsevier Science, Ltd., pp. 713-718.

Vincent, J. F. and Rolf, P. R. (1994). "Repairs to Paulina Street Parking Structure," *Concrete International*, Vol.16, No.3, pp. 39-41.

Uhlig, Herbert H. and Revie, Winston R. (1985). *Corrosion and Corrosion Control. An Introduction to Corrosion Science and Engineering,* John Wiley & Sons, Inc., New York, 441 pp.

Weil, T. G (1988). "Addressing Parking Garage Corrosion with Silica Fume," *Transportation Research Record*, No. 1204, pp. 8-10.

Wenger, F., Zhang, J., Galland, J., and Lemoine, L. (1987). "Corrosion of Steel in Concrete Studied by Electrochemical Impedance Measurements: Application to the Monitoring of Concrete Structures," *Key Engineering Materials*, Vol. 20-28, Pt. 1-4, pp. 1539-1546.

Yonezawa, T., Ashworth, V., and Procter, R. P. M. (1988). "Study of the Pore Solution Composition and Chloride Effects in the Corrosion of Steel in Concrete," *Corrosion*, Vol. 44, No. 7, pp. 489-499.

Yunovich, M., Thompson, N. G., Balvanyos, T., and Lave, L. (2002). "Highway Bridges," Appendix D, *Corrosion Cost and Preventive Strategies in the United States*, by G. H. Koch, M. PO., H. Broongers, N. G. Thompson, Y. P. Virmani, and J. H. Payer, Report No. FHWA-RD-01-156, Federal Highway Administration, McLean, VA, Mar. 2002, 773 pp.

# APPENDIX A

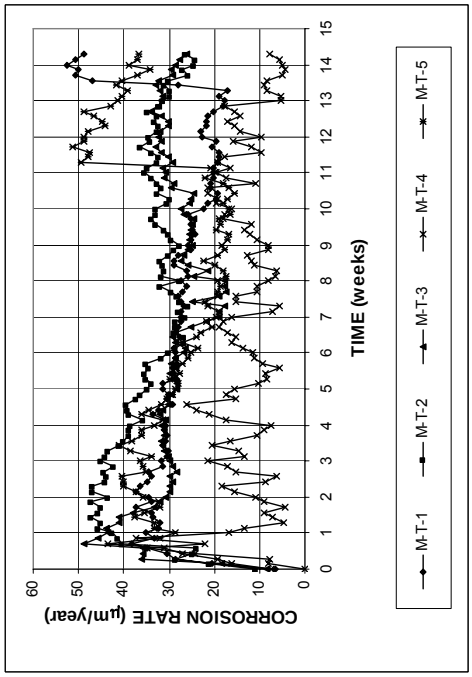


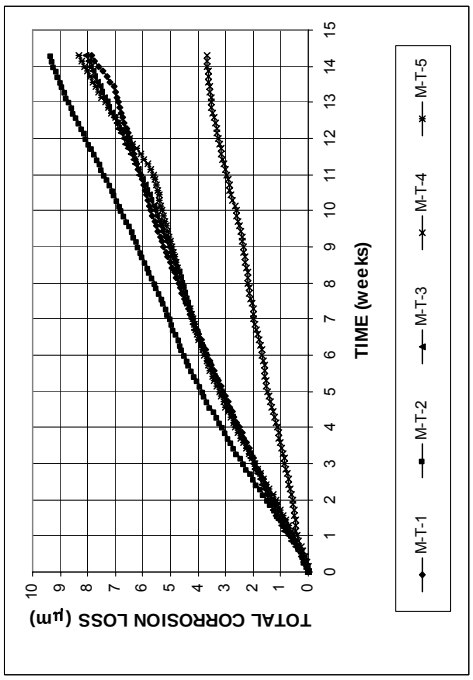


**Figure A.1** - (a) Corrosion rates and (b) total corrosion losses as measured in the rapid macrocell test for bare conventional normalized steel (N) in 1.6 m ion NaCl and simulated concrete pore solution.







**Figure A.2** - (a) Corrosion rates and (b) total corrosion losses as measured in the rapid macrocell test for bare conventional Thermex-treated steel (T) in 1.6 m ion NaCl and simulated concrete pore solution.

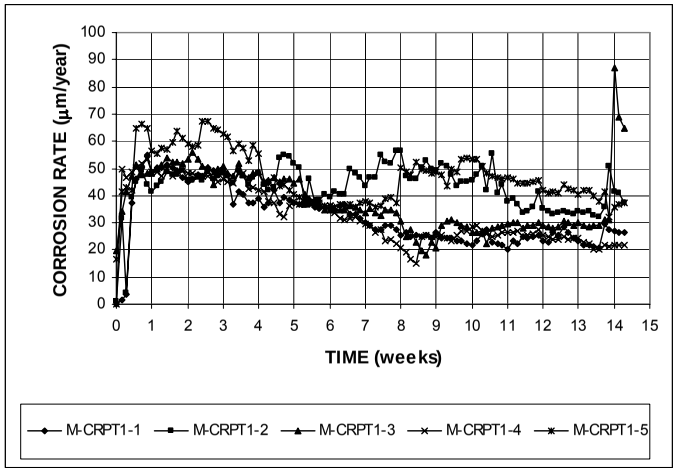


(a)

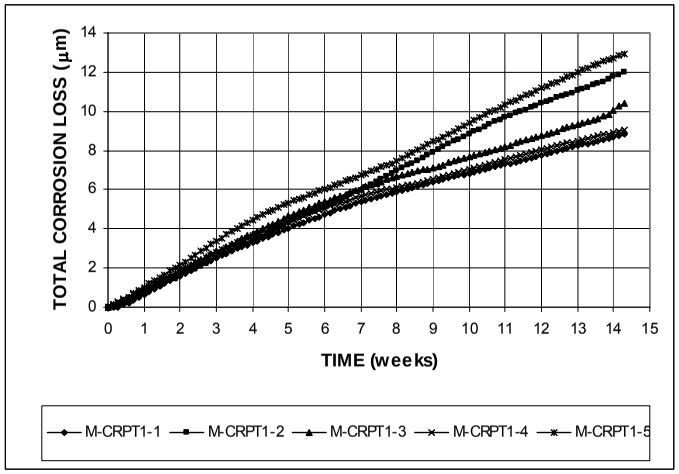


(b)

**Figure A.3 -** (a) Corrosion rates and (b) total corrosion losses as measured in the rapid macrocell test for bare microalloyed steel with high phosphorus content, 0.117%, Thermex-treated (CRPT1) in 1.6 m ion NaCl and simulated concrete pore solution.

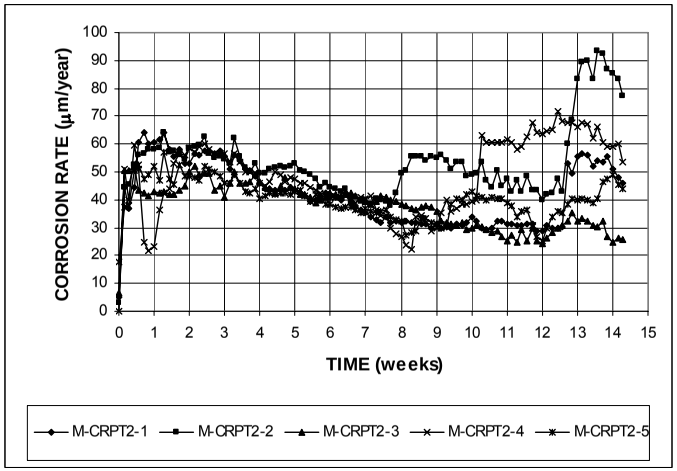


(a)

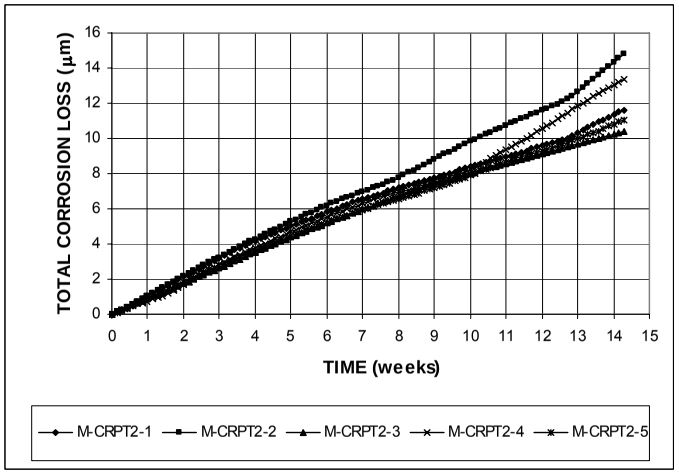


(b)

**Figure A.4 -** (a) Corrosion rates and (b) total corrosion losses as measured in the rapid macrocell test for bare microalloyed steel with high phosphorus content, 0.100%, Thermex-treated (CRPT2) in 1.6 m ion NaCl and simulated concrete pore solution.

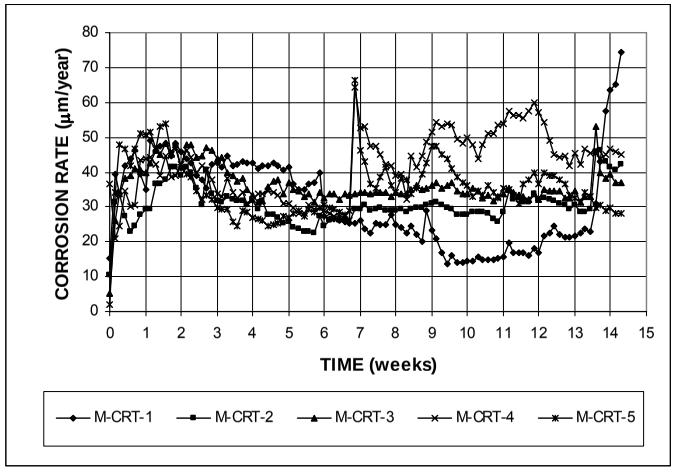


(a)

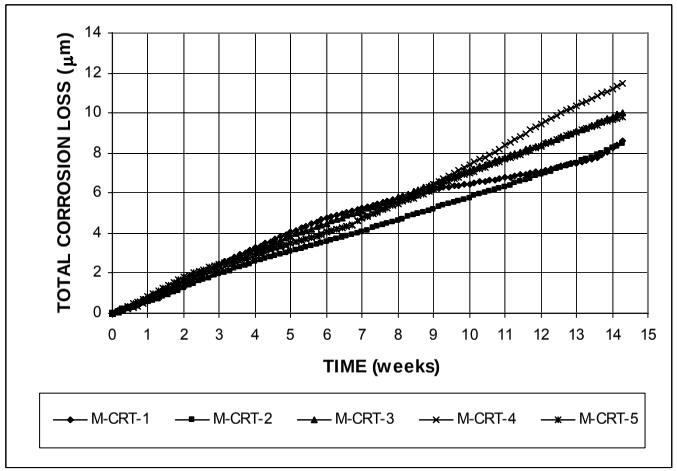


(b)

**Figure A.5 -** (a) Corrosion rates and (b) total corrosion losses as measured in the rapid macrocell test for bare microalloyed steel with normal phosphorus content, 0.017%, Thermex-treated (CRT) in 1.6 m ion NaCl and simulated concrete pore solution.

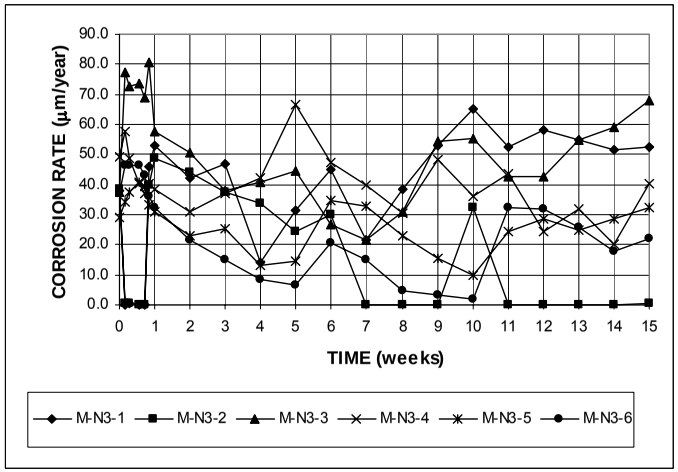


(a)

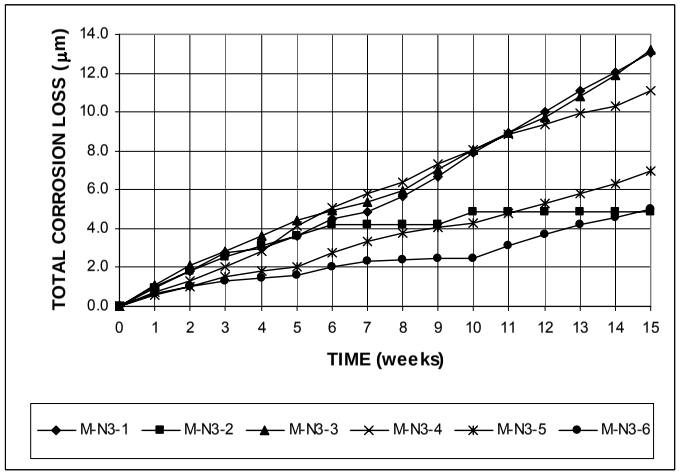


(b)

**Figure A.6 -** (a) Corrosion rates and (b) total corrosion losses as measured in the rapid macrocell test for bare conventional normalized steel (N3) in 1.6 m ion NaCl and simulated concrete pore solution.

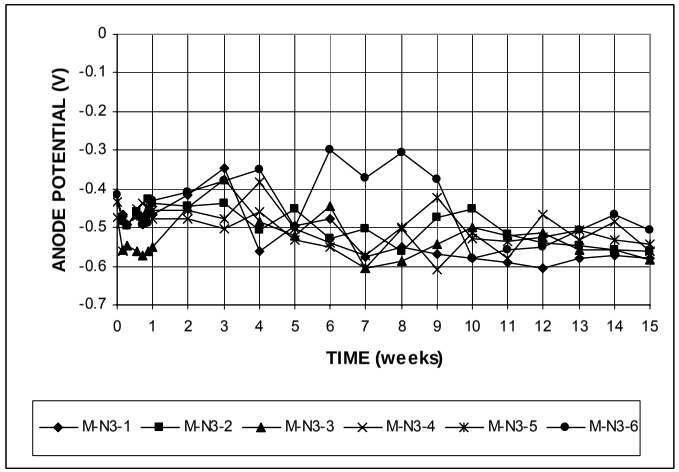


(a)

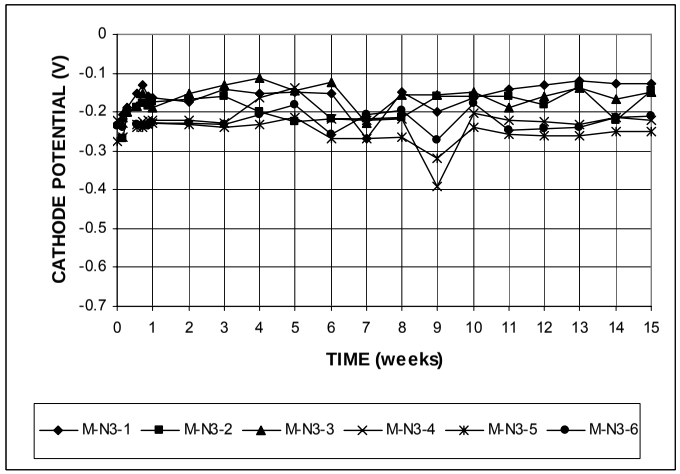


(b)

**Figure A.7 -** (a) Anode corrosion potentials and (b) cathode corrosion potentials with respect to saturated calomel electrode as measured in the rapid macrocell test for bare conventional normalized steel (N3) in 1.6 m ion NaCl and simulated concrete pore solution.

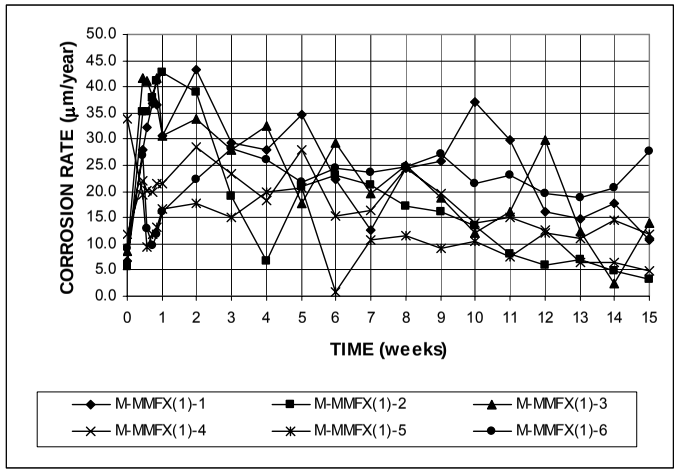


(a)

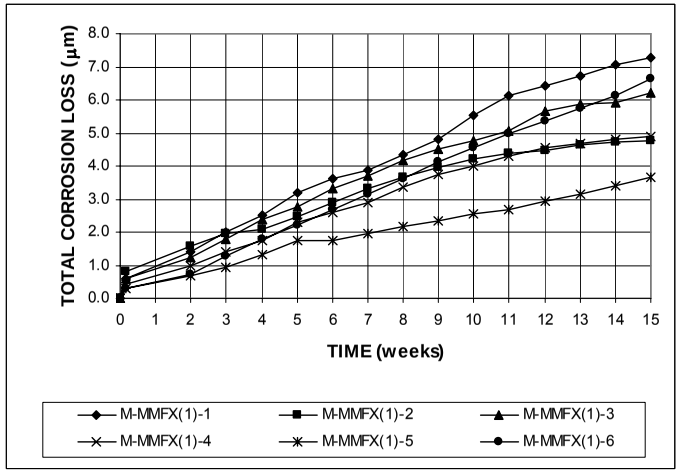


(b)

**Figure A.8 -** (a) Corrosion rates and (b) total corrosion losses as measured in the rapid macrocell test for bare MMFX microcomposite steel [MMFX(1)] in 1.6 m ion NaCl and simulated concrete pore solution.

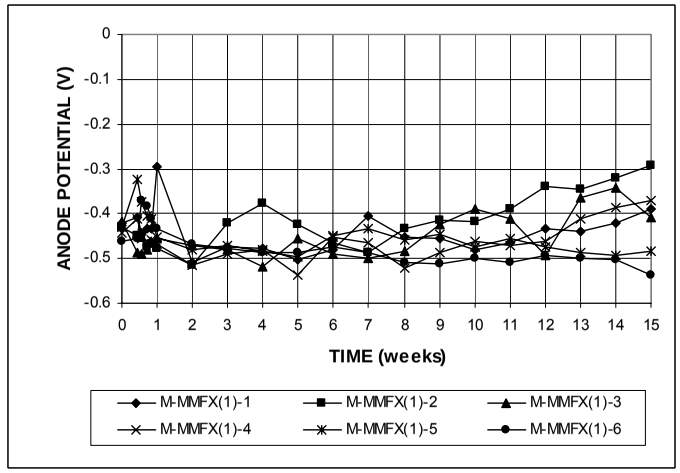


(a)

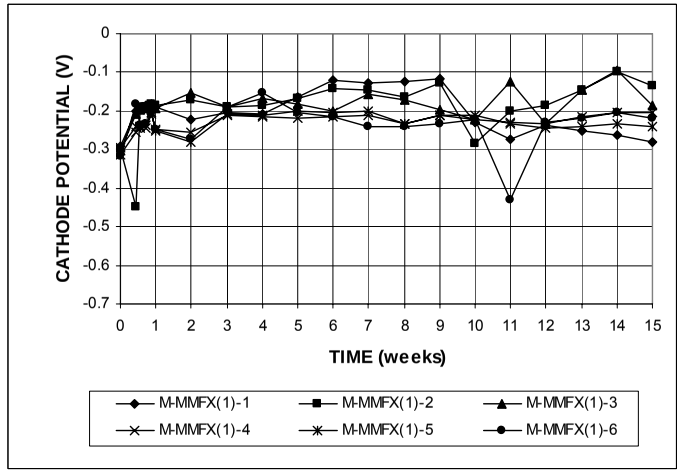


(b)

**Figure A.9 -** (a) Anode corrosion potentials and (b) cathode corrosion potentials with respect to saturated calomel electrode as measured in the rapid macrocell test for bare MMFX microcomposite steel [MMFX(1)] in 1.6 m ion NaCl and simulated concrete pore solution.

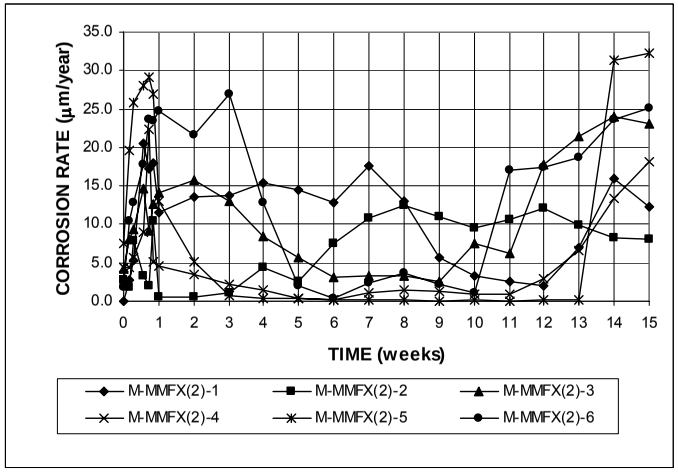


(a)

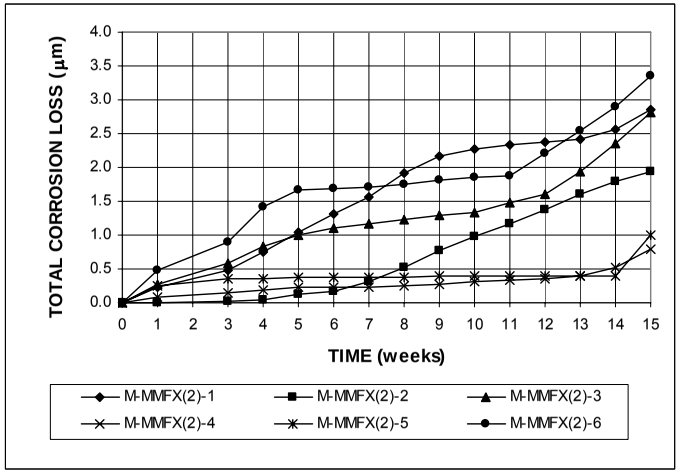


(b)

**Figure A.10 -** (a) Corrosion rates and (b) total corrosion losses as measured in the rapid macrocell test for bare MMFX microomposite steel [MMFX(2)] in 1.6 m ion NaCl and simulated concrete pore solution.

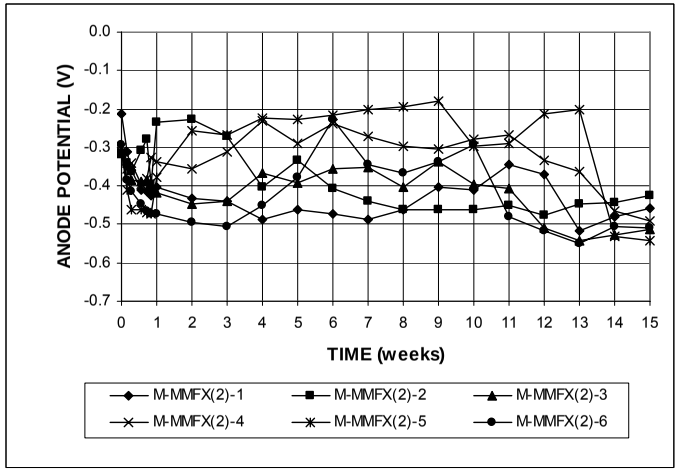


(a)

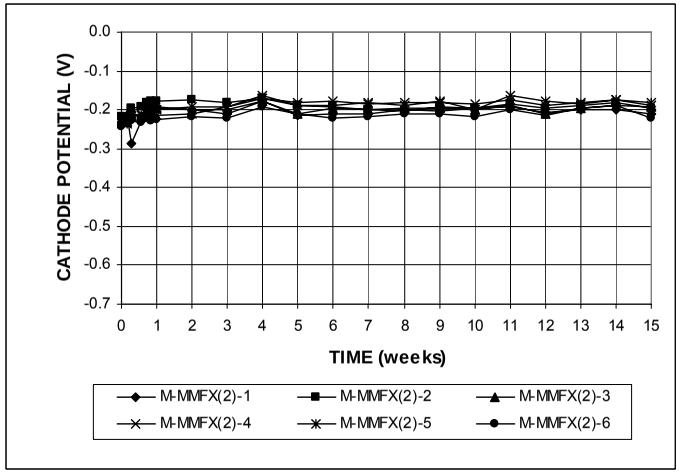


(b)

**Figure A.11 -** (a) Anode corrosion potentials and (b) cathode corrosion potentials with respect to saturated calomel electrode as measured in the rapid macrocell test for bare MMFX microcomposite steel [MMFX(2)] in 1.6 m ion NaCl and simulated concrete pore solution.

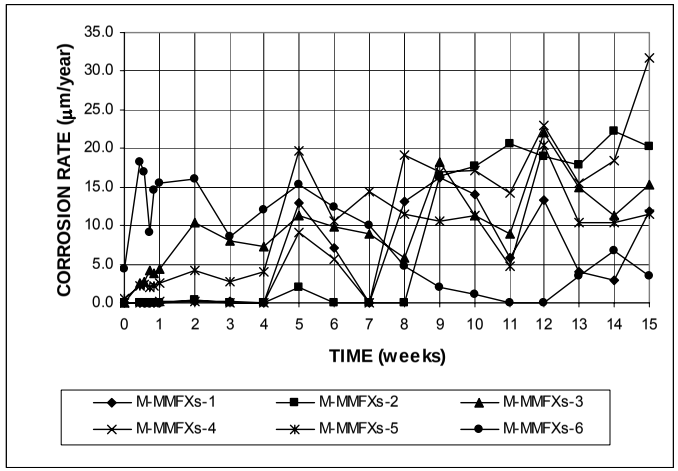


(a)

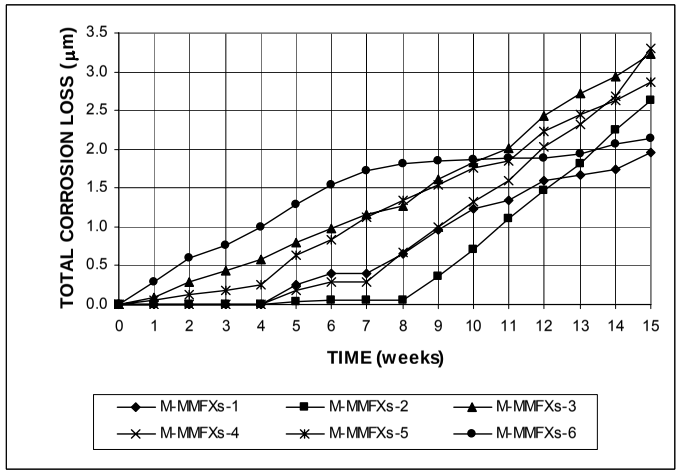


(b)

**Figure A.12 -** (a) Corrosion rates and (b) total corrosion losses as measured in the rapid macrocell test for bare, sandblasted MMFX microcomposite steel in 1.6 m ion NaCl and simulated concrete pore solution.

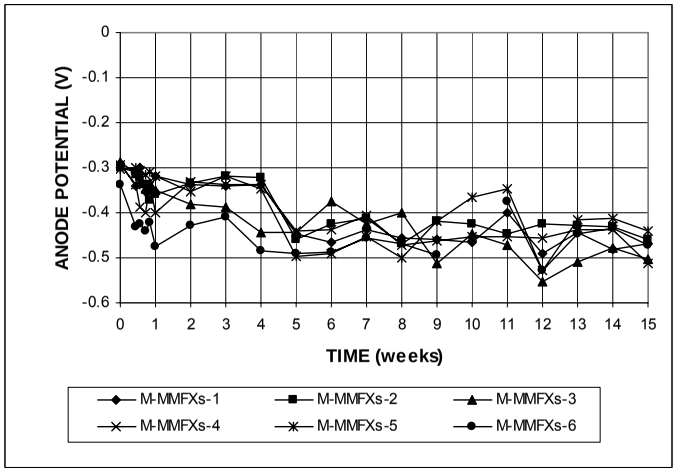


(a)

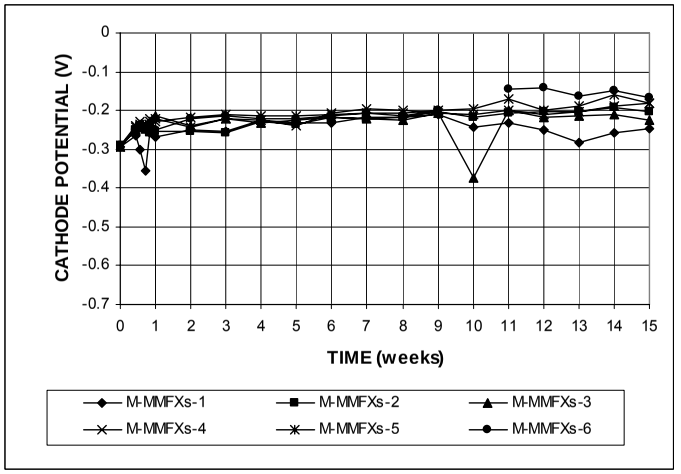


(b)

**Figure A.13 -** (a) Anode corrosion potentials and (b) cathode corrosion potentials with respect to saturated calomel electrode as measured in the rapid macrocell test for bare, sandblasted MMFX microcomposite steel in 1.6 m ion NaCl and simulated concrete pore solution.

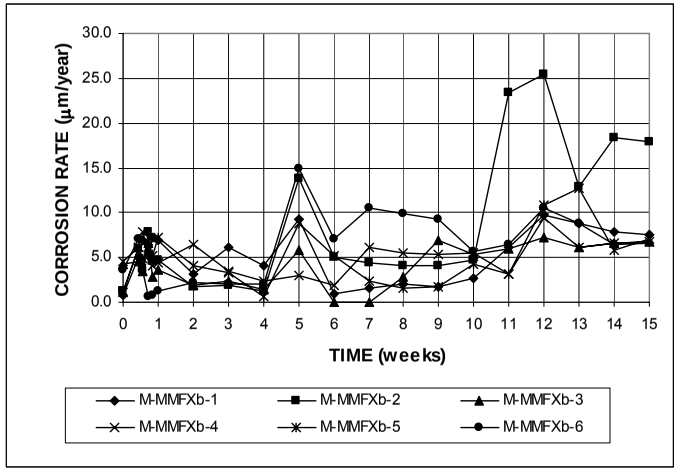


(a)

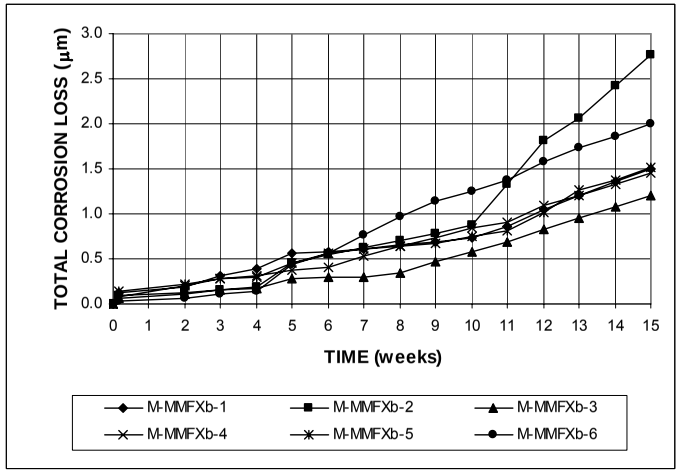


(b)

**Figure A.14 -** (a) Corrosion rates and (b) total corrosion losses as measured in the rapid macrocell test for bare MMFX microcomposite steel in 1.6 m ion NaCl and simulated concrete pore solution with bent bars in the anode.

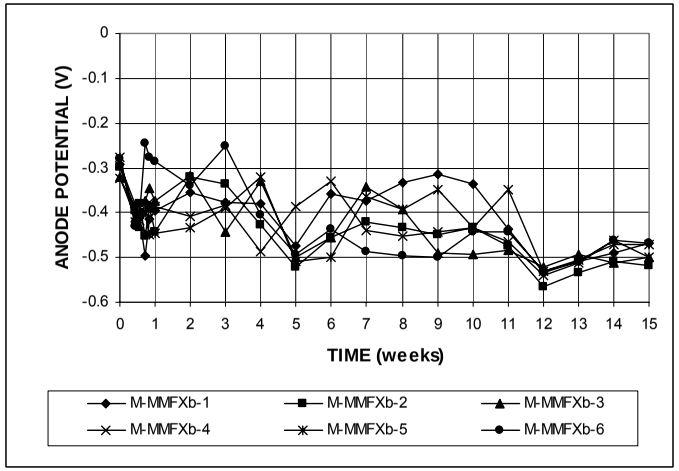


(a)

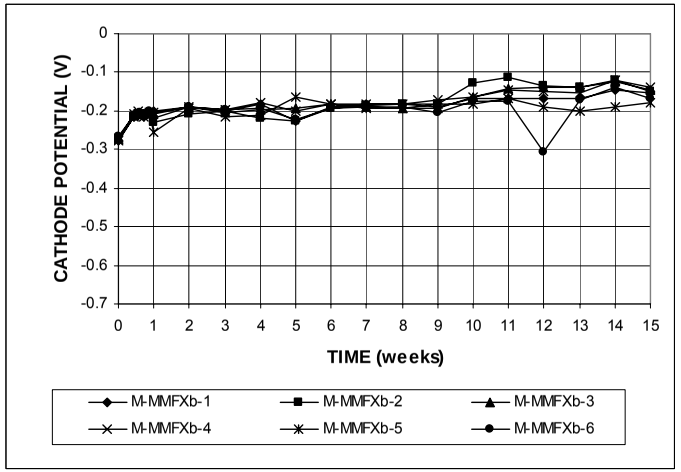


(b)

**Figure A.15 -** (a) Anode corrosion potentials and (b) cathode corrosion potentials with respect to saturated calomel electrode as measured in the rapid macrocell test for bare MMFX microcomposite steel in 1.6 m ion NaCl and simulated concrete pore solution with bent bars in the anode.

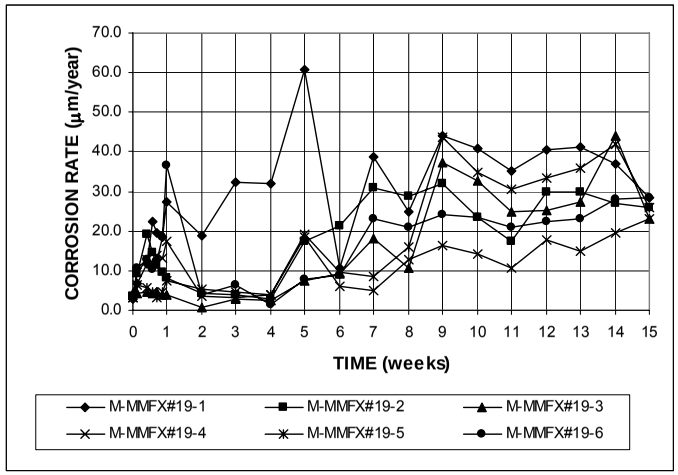


(a)

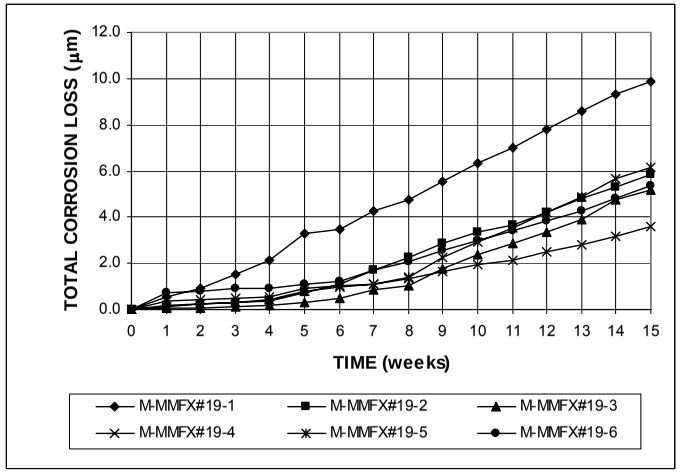


(b)

**Figure A.16 -** (a) Corrosion rates and (b) total corrosion losses as measured in the rapid macrocell test for No. 19 bare MMFX microcomposite steel in 1.6 m ion NaCl and simulated concrete pore solution.

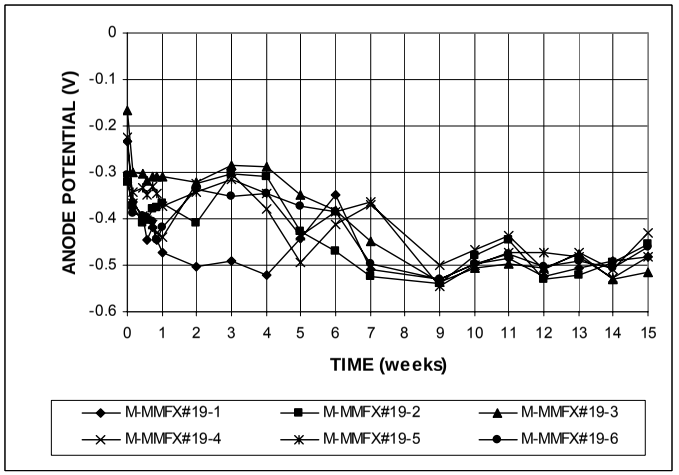


(a)

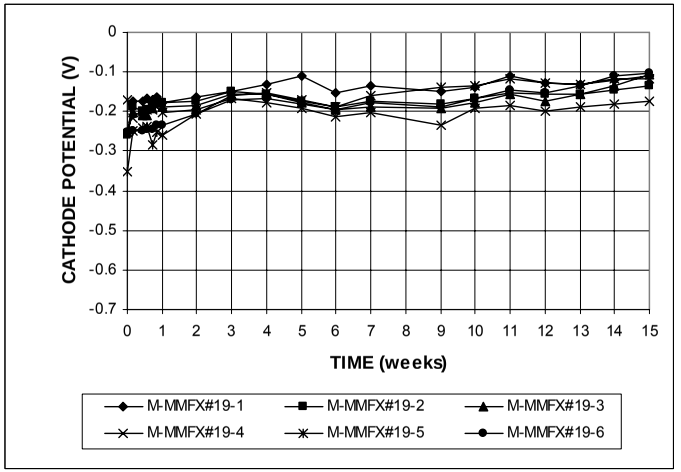


(b)

**Figure A.17 -** (a) Anode corrosion potentials and (b) cathode corrosion potentials with respect to saturated calomel electrode as measured in the rapid macrocell test for No. 19 bare MMFX microcomposite steel in 1.6 m ion NaCl and simulated concrete pore solution.

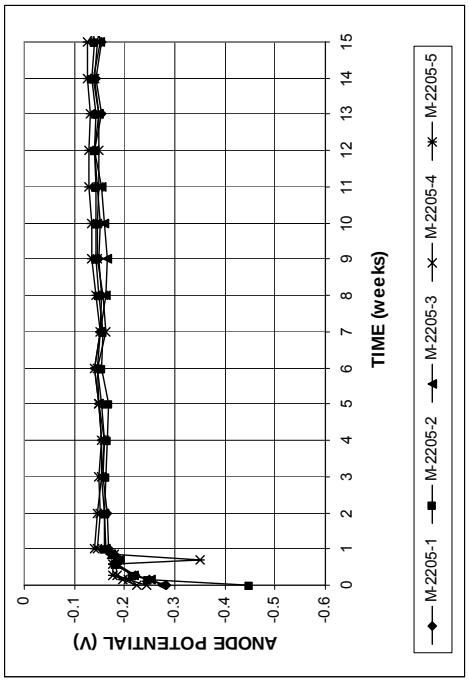


(a)

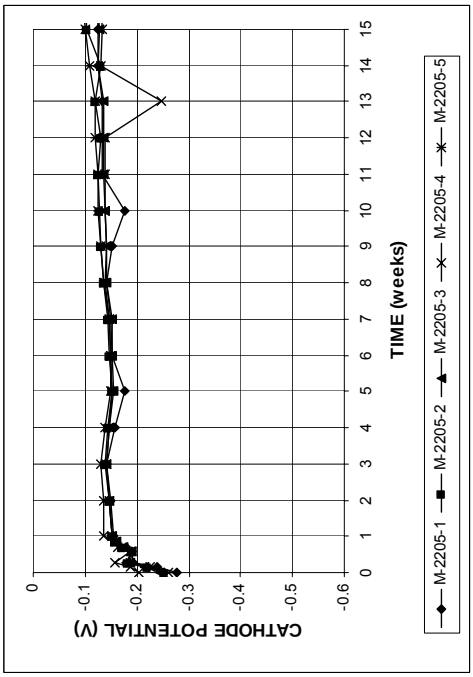


(b)

**Figure A.19 -** (a) Anode corrosion potentials and (b) cathode corrosion potentials with respect to saturated calomel electrode as measured in the rapid macrocell test for bare 2205 duplex steel in 1.6 m ion NaCl and simulated concrete pore solution.

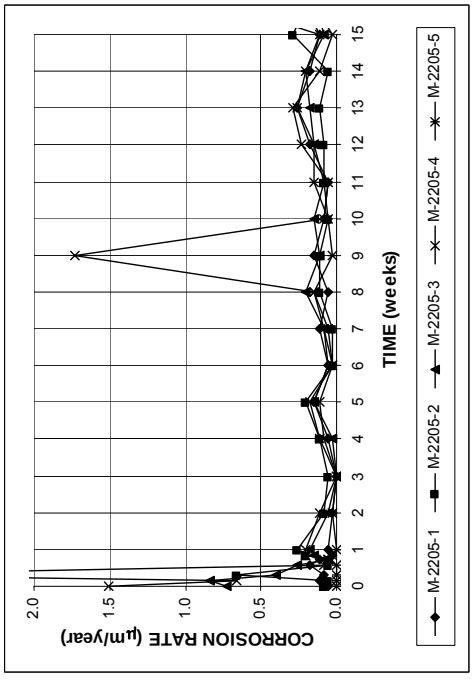


(a)

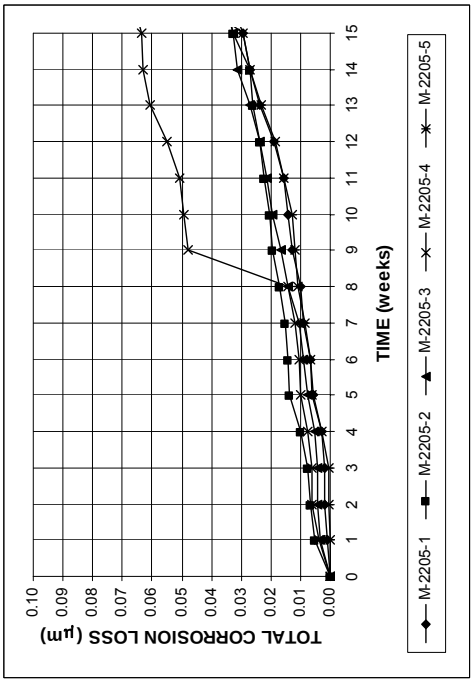


(b)

**Figure A.18 -** (a) Corrosion rates and (b) total corrosion losses as measured in the rapid macrocell test for bare 2205 duplex steel in 1.6 m ion NaCl and simulated concrete pore solution.

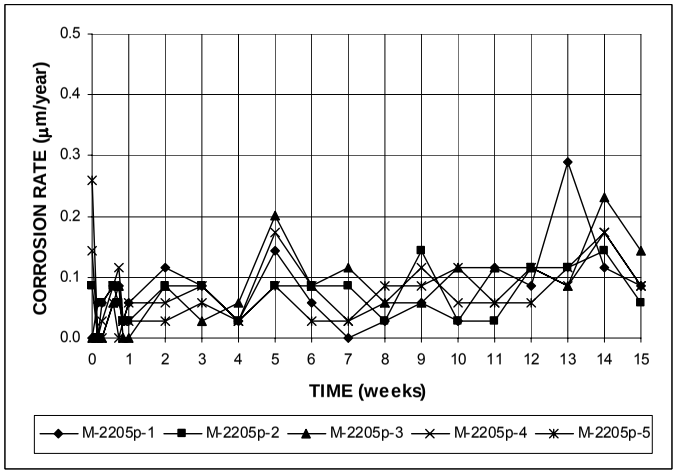


(a)

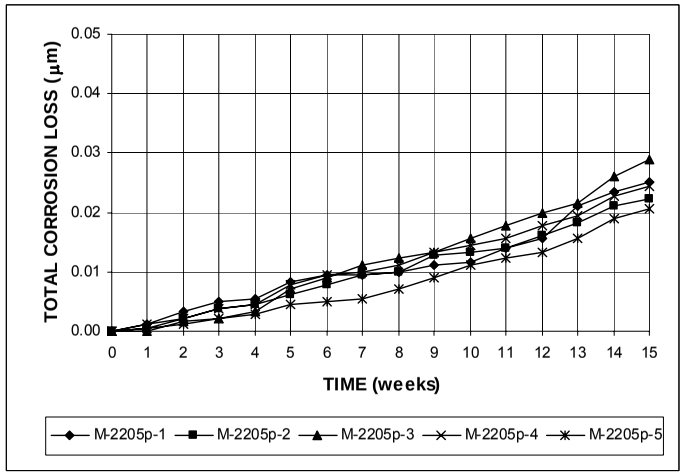


(b)

**Figure A.20 -** (a) Corrosion rates and (b) total corrosion losses as measured in the rapid macrocell test for bare 2205 pickled duplex steel in 1.6 m ion NaCl and simulated concrete pore solution.

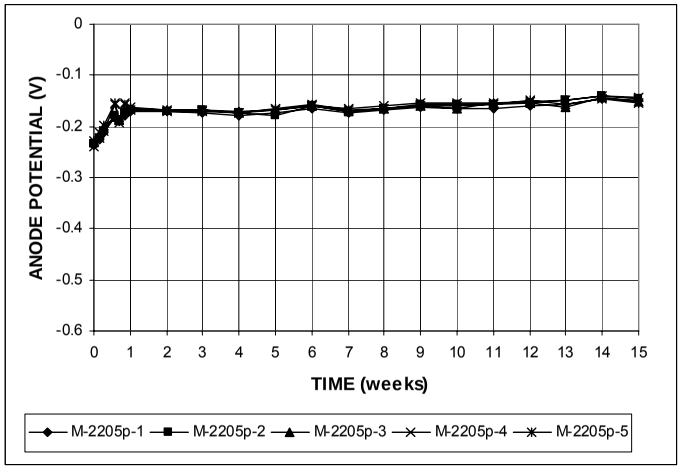


(a)

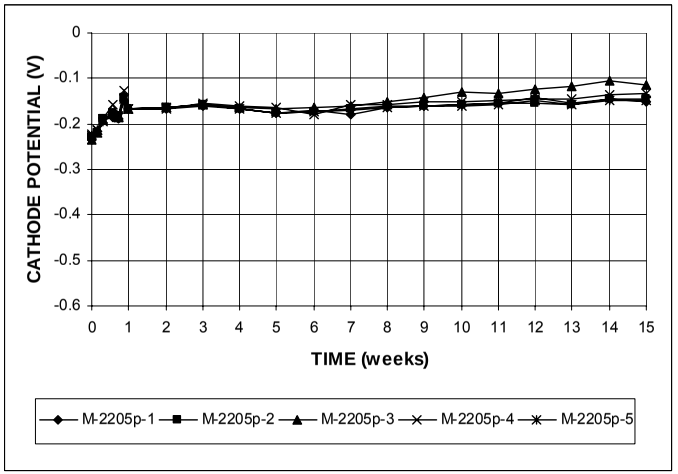


(b)

**Figure A.21 -** (a) Anode corrosion potentials and (b) cathode corrosion potentials with respect to saturated calomel electrode as measured in the rapid macrocell test for bare 2205 pickled duplex steel in 1.6 m ion NaCl and simulated concrete pore solution.

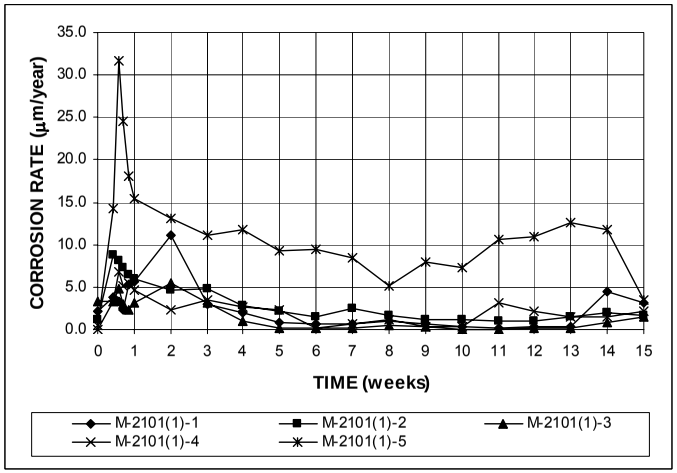


(a)

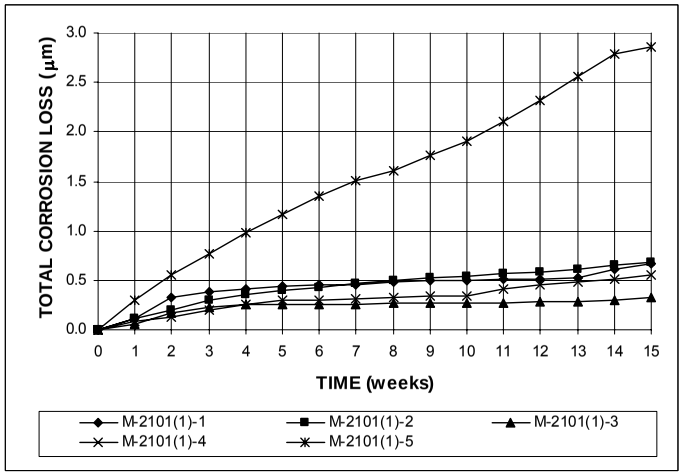


(b)

**Figure A.22 -** (a) Corrosion rates and (b) total corrosion losses as measured in the rapid macrocell test for bare 2101(1) duplex steel in 1.6 m ion NaCl and simulated concrete pore solution.

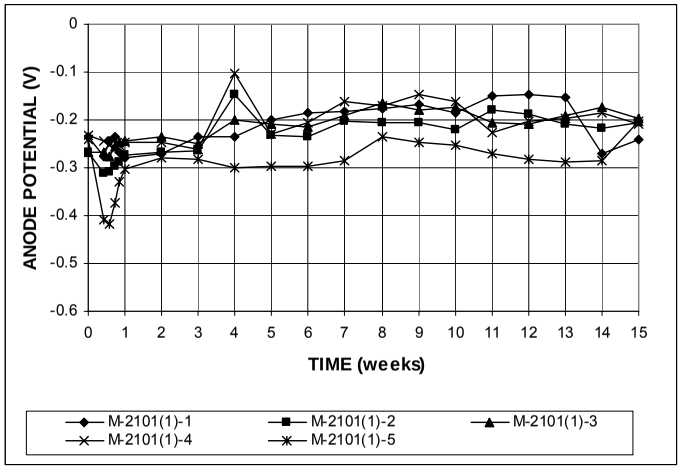


(a)

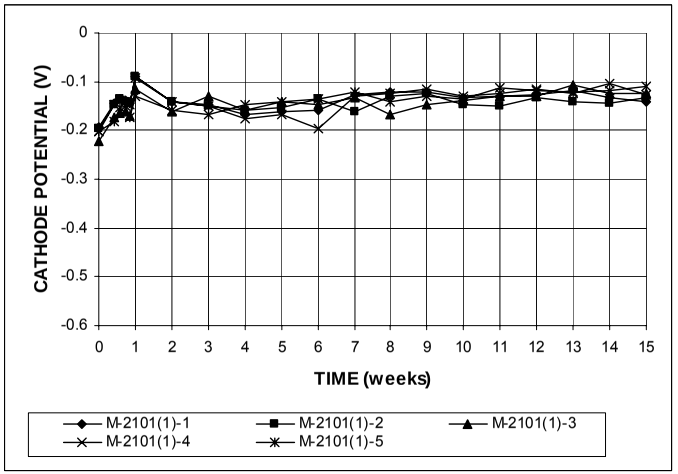


(b)

**Figure A.23 -** (a) Anode corrosion potentials and (b) cathode corrosion potentials with respect to saturated calomel electrode as measured in the rapid macrocell test for bare 2101(1) duplex steel in 1.6 m ion NaCl and simulated concrete pore solution.

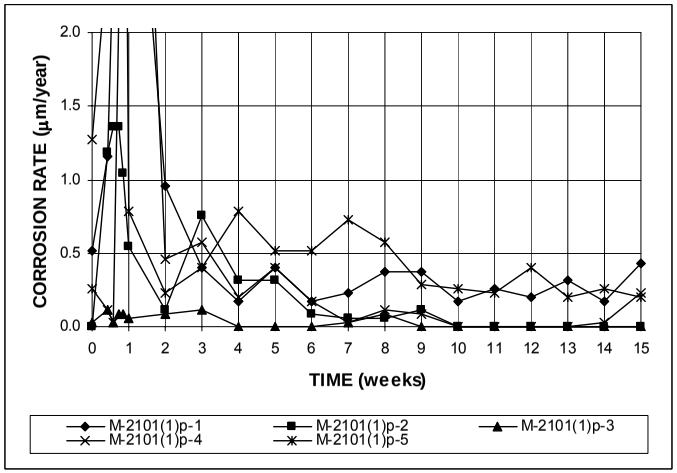


(a)

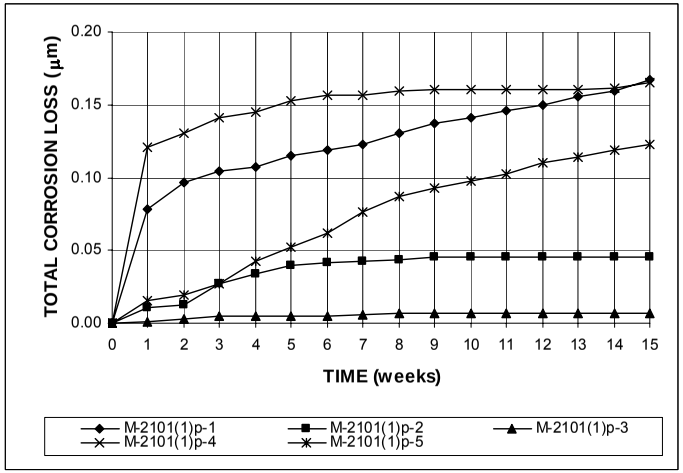


(b)

**Figure A.24 -** (a) Corrosion rates and (b) total corrosion losses as measured in the rapid macrocell test for bare 2101(1) pickled duplex steel in 1.6 m ion NaCl and simulated concrete pore solution.

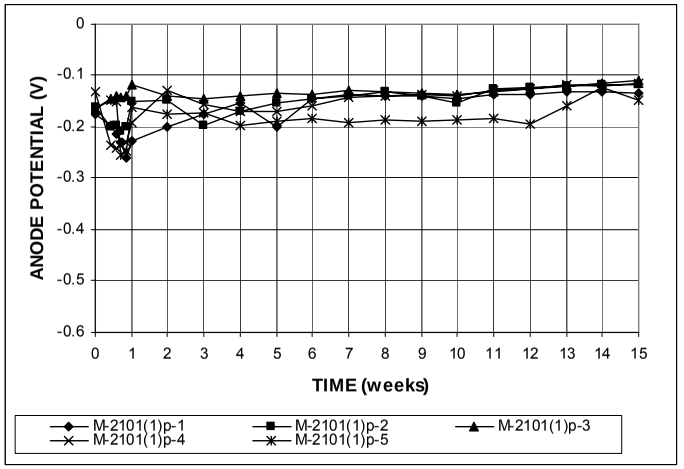


(a)

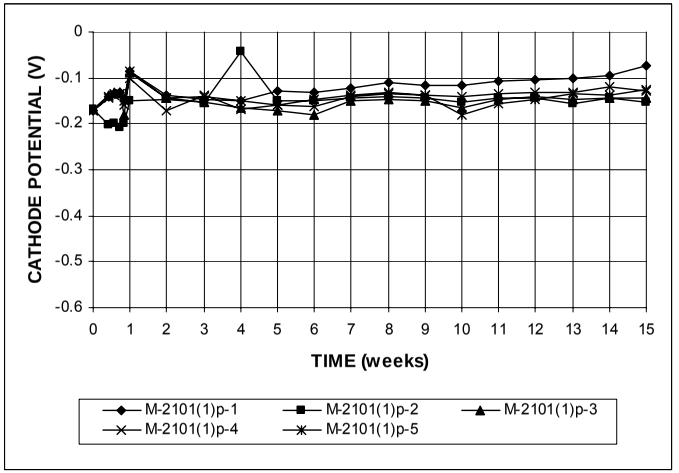


(b)

**Figure A.25 -** (a) Anode corrosion potentials and (b) cathode corrosion potentials with respect to saturated calomel electrode as measured in the rapid macrocell test for bare 2101(1) pickled duplex steel in 1.6 m ion NaCl and simulated concrete pore solution.

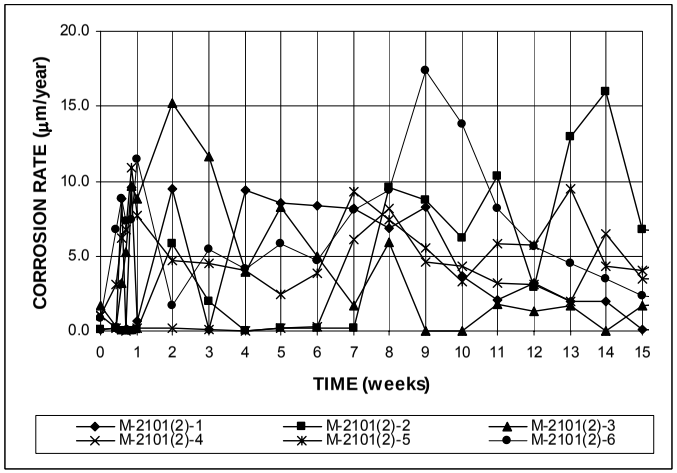


(a)

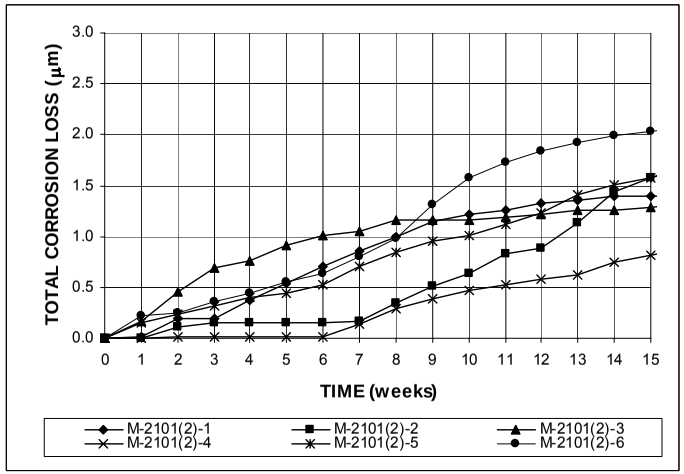


(b)

**Figure A.26 -** (a) Corrosion rates and (b) total corrosion losses as measured in the rapid macrocell test for bare 2101(2) duplex steel in 1.6 m ion NaCl and simulated concrete pore solution.

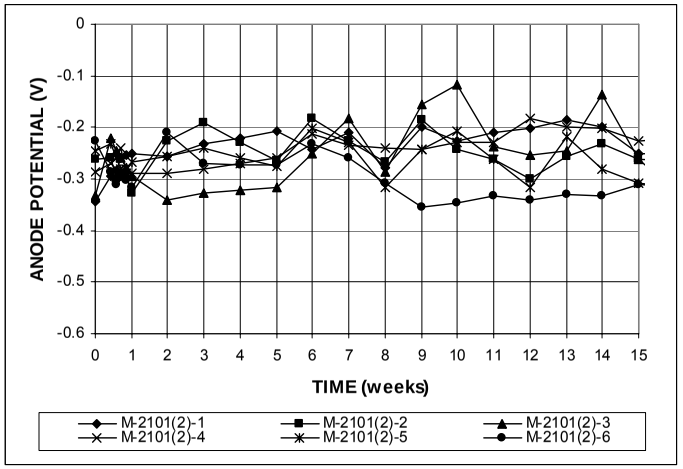


(a)

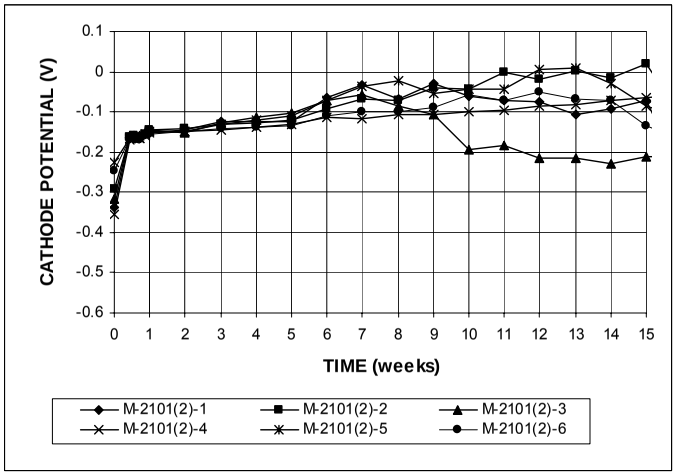


(b)

**Figure A.27 -** (a) Anode corrosion potentials and (b) cathode corrosion potentials with respect to saturated calomel electrode as measured in the rapid macrocell test for bare 2101(2) duplex steel in 1.6 m ion NaCl and simulated concrete pore solution.

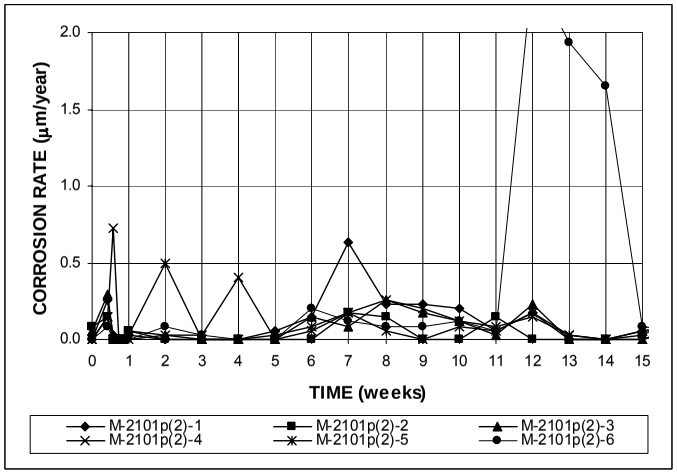


(a)

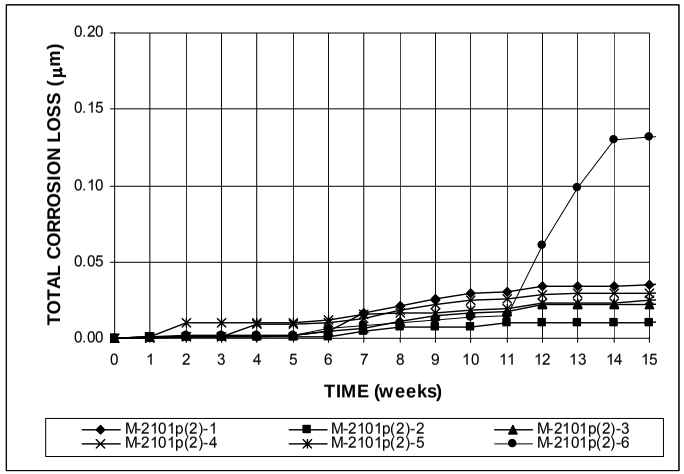


(b)

**Figure A.28 -** (a) Corrosion rates and (b) total corrosion losses as measured in the rapid macrocell test for bare 2101(2) pickled duplex steel in 1.6 m ion NaCl and simulated concrete pore solution.

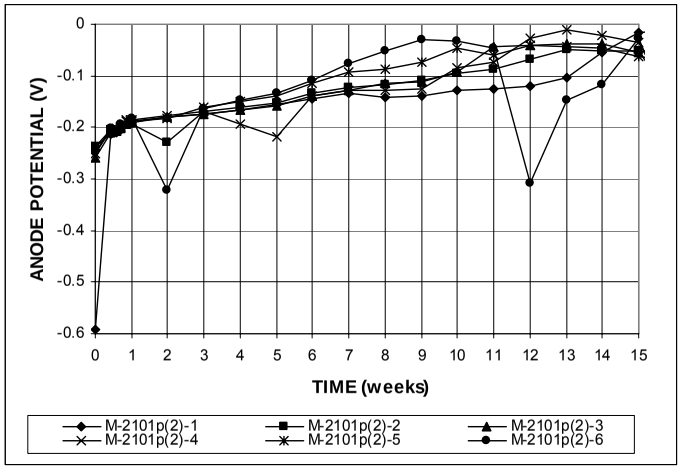


(a)

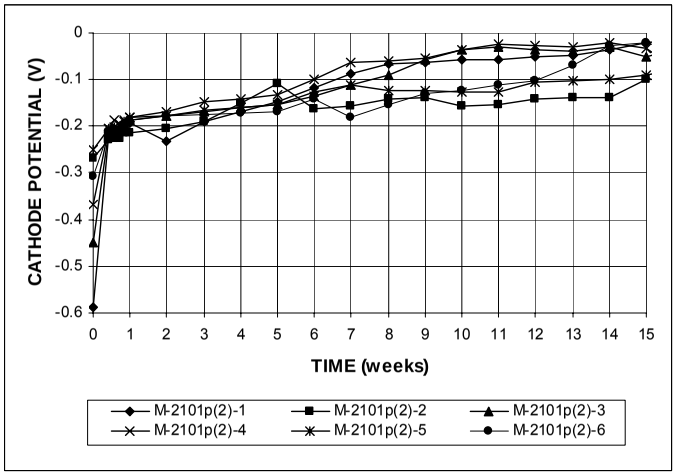


(b)

**Figure A.29 -** (a) Anode corrosion potentials and (b) cathode corrosion potentials with respect to saturated calomel electrode as measured in the rapid macrocell test for bare 2101(2) pickled duplex steel in 1.6 m ion NaCl and simulated concrete pore solution.

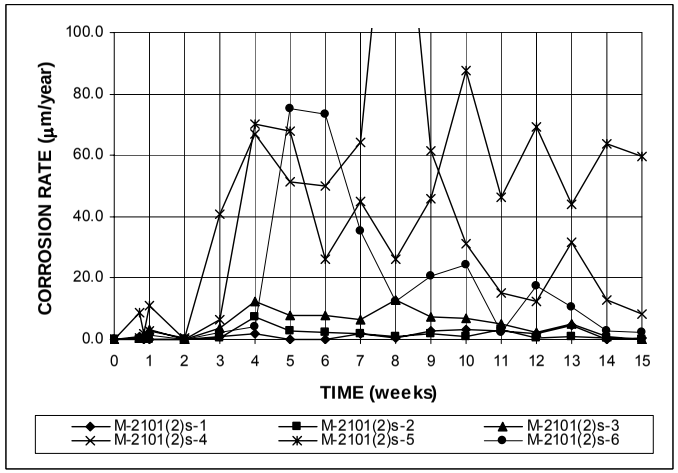


(a)

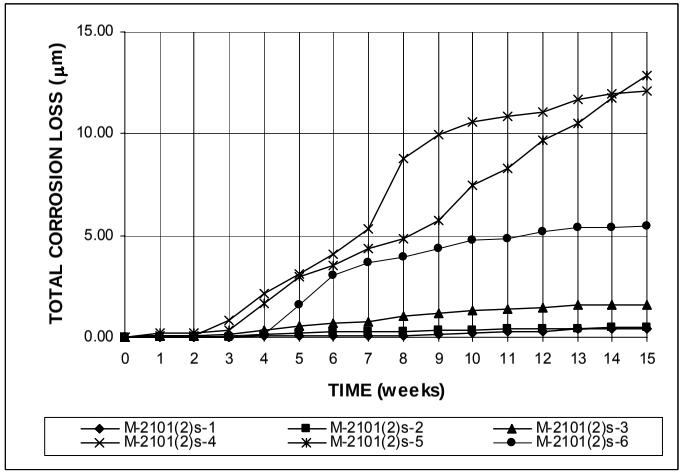


(b)

**Figure A.30 -** (a) Corrosion rates and (b) total corrosion losses as measured in the rapid macrocell test for bare, sandblasted 2101(2) duplex steel in 1.6 m ion NaCl and simulated concrete pore solution.

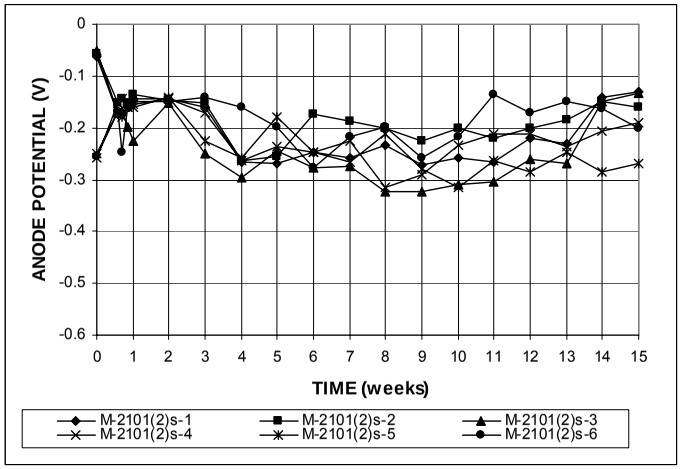


(a)

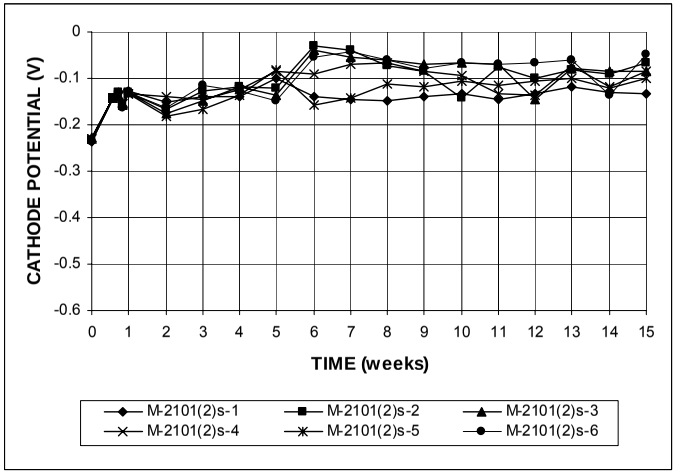


(b)

**Figure A.31 -** (a) Anode corrosion potentials and (b) cathode corrosion potentials with respect to saturated calomel electrode as measured in the rapid macrocell test for bare, sandblasted 2101(2) duplex steel in 1.6 m ion NaCl and simulated concrete pore solution.

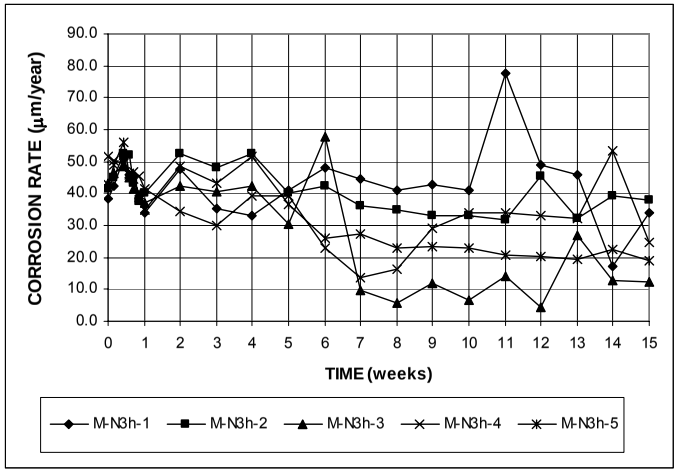


(a)

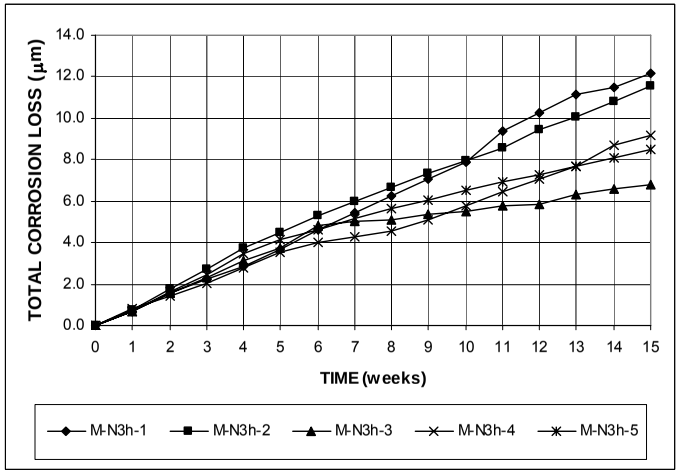


(b)

**Figure A.32 -** (a) Corrosion rates and (b) total corrosion losses as measured in the rapid macrocell test for bare conventional normalized steel (N3) in 6.04 m ion NaCl and simulated concrete pore solution.

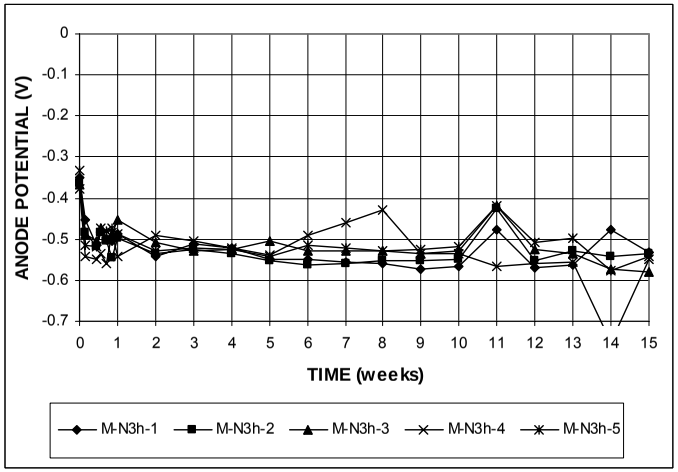


(a)

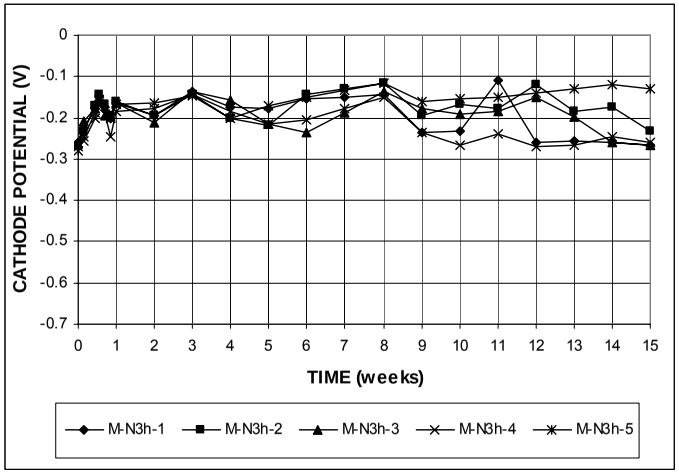


(b)

**Figure A.33 -** (a) Anode corrosion potentials and (b) cathode corrosion potentials with respect to saturated calomel electrode as measured in the rapid macrocell test for bare conventional normalized steel (N3) in 6.04 m ion NaCl and simulated concrete pore solution.

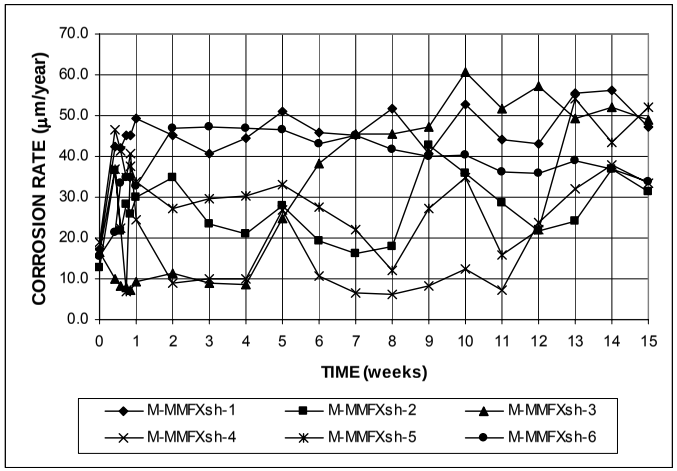


(a)

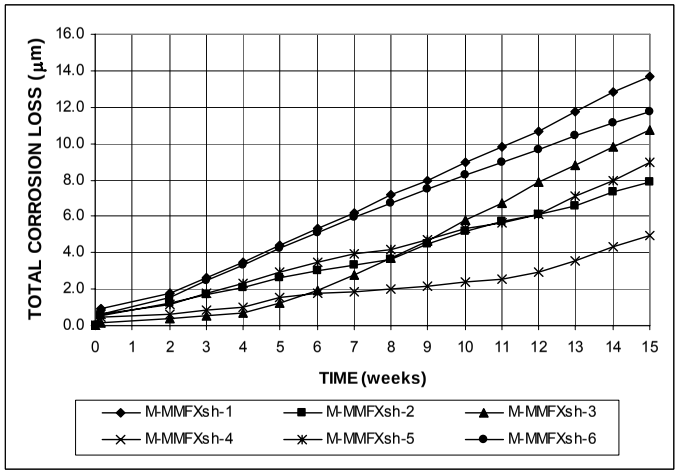


(b)

**Figure A.34 -** (a) Corrosion rates and (b) total corrosion losses as measured in the rapid macrocell test for bare MMFX microomposite sandblasted steel in 6.04 m NaCl and simulated concrete pore solution.

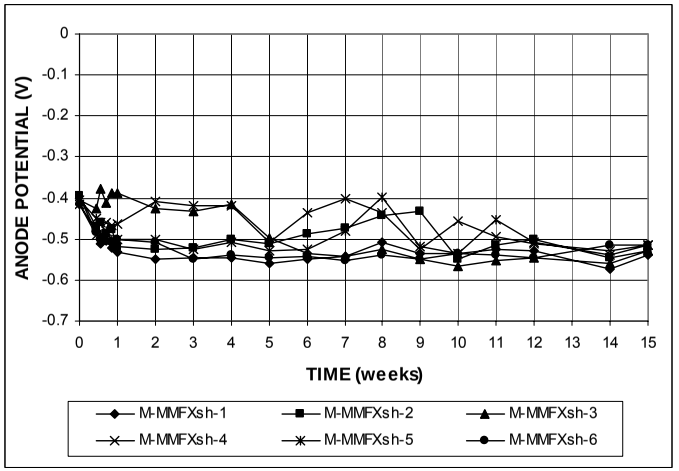


(a)

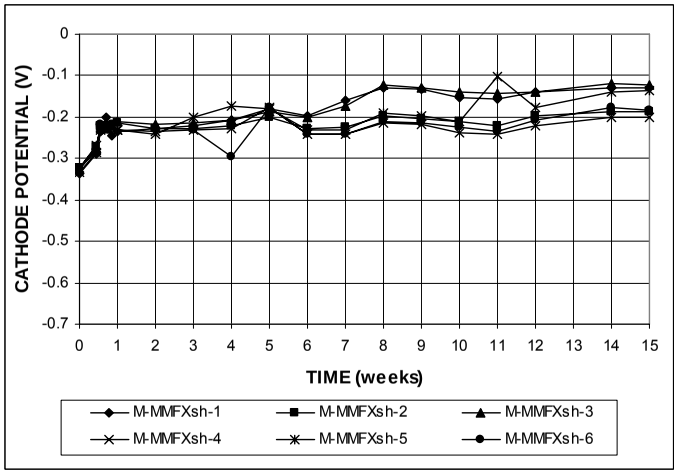


(b)

**Figure A.35 -** (a) Anode corrosion potentials and (b) cathode corrosion potentials with respect to saturated calomel electrode as measured in the rapid macrocell test for bare MMFX microcomposite sandblasted steel in 6.04 m ion NaCl and simulated concrete pore

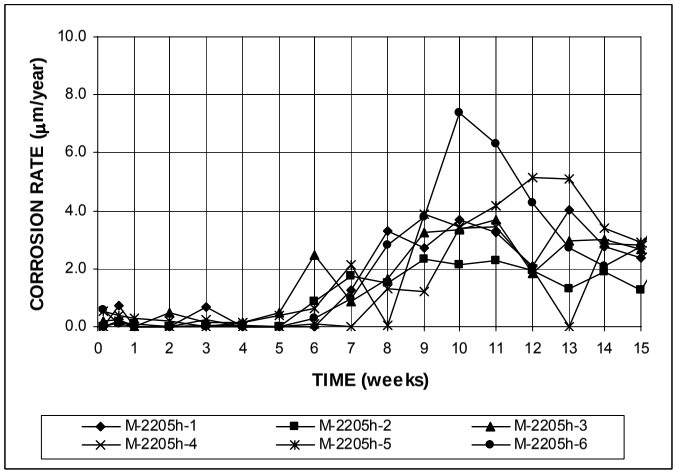


(a)

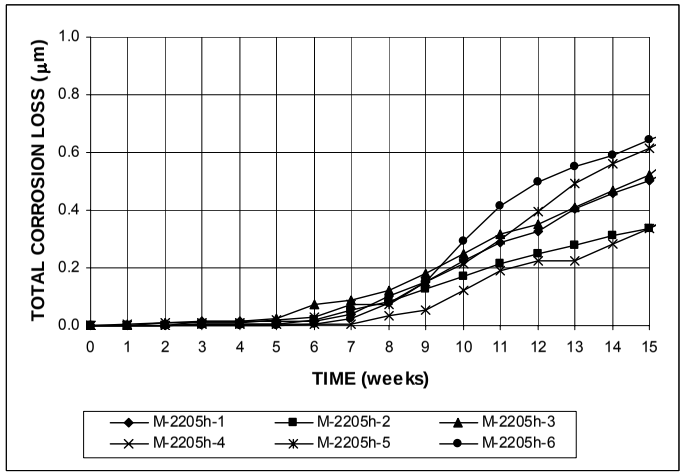


(b)

**Figure A.36 -** (a) Corrosion rates and (b) total corrosion losses as measured in the rapid macrocell test for bare 2205 duplex steel in 6.04 m ion NaCl and simulated concrete pore solution.

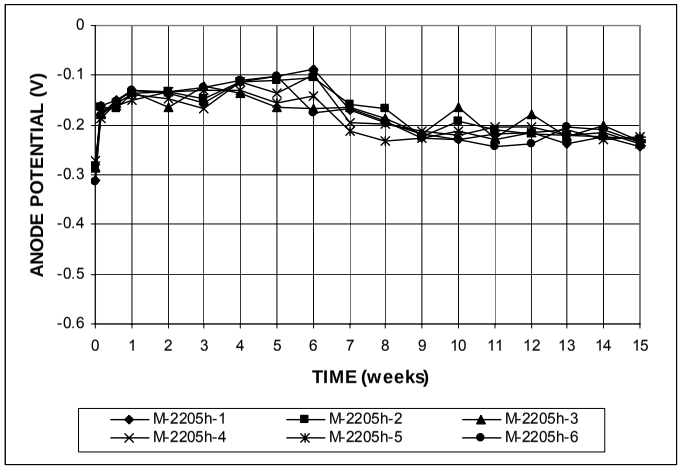


(a)

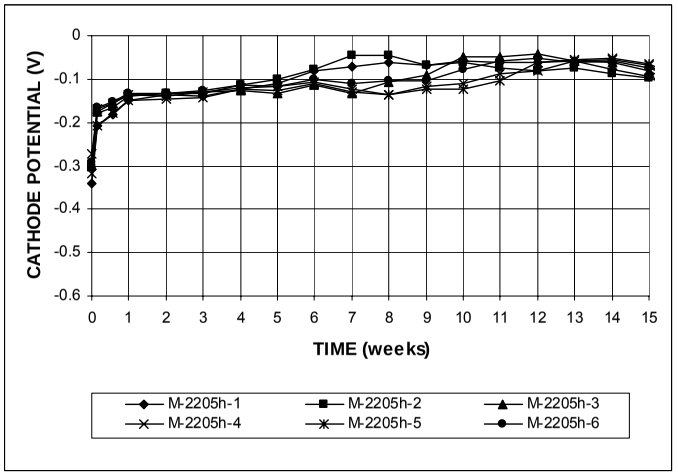


(b)

**Figure A.37 -** (a) Anode corrosion potentials and (b) cathode corrosion potentials with respect to saturated calomel electrode as measured in the rapid macrocell test for bare 2205 duplex steel in 6.04 m ion NaCl and simulated concrete pore solution.

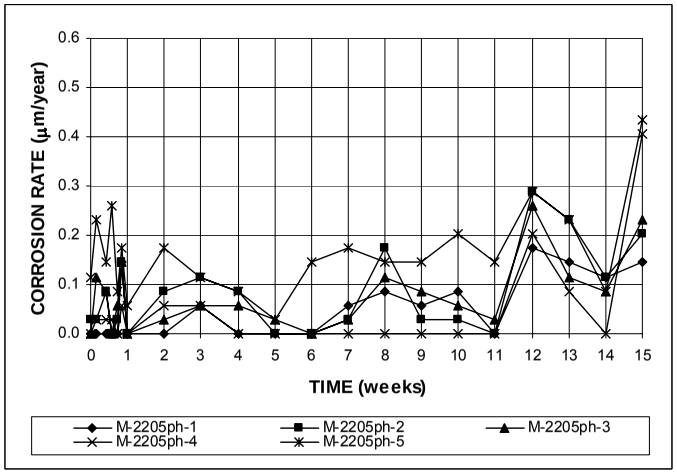


(a)

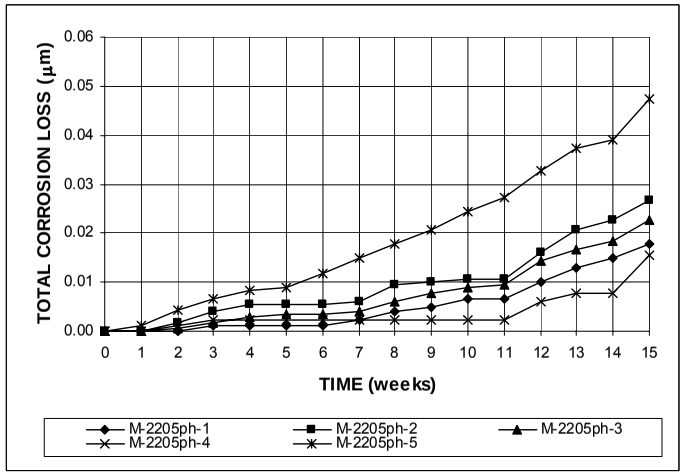


(b)

**Figure A.38 -** (a) Corrosion rates and (b) total corrosion losses as measured in the rapid macrocell test for bare 2205 pickled duplex steel in 6.04 m ion NaCl and simulated concrete pore solution.

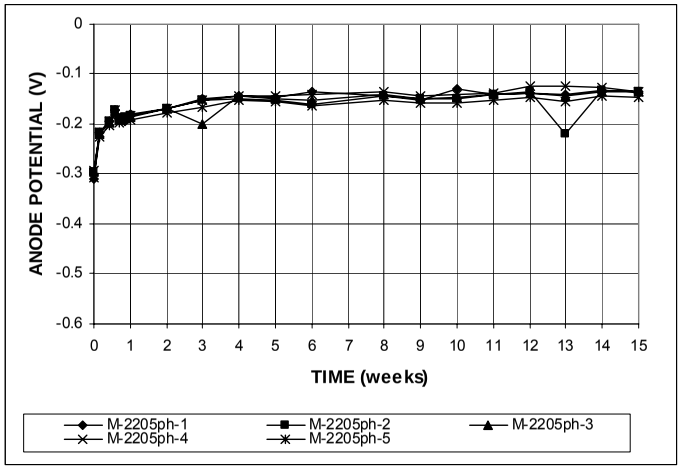


(a)

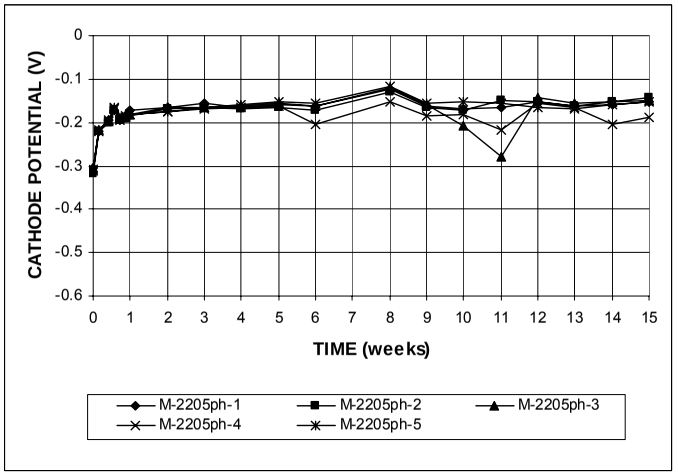


(b)

**Figure A.39 -** (a) Anode corrosion potentials and (b) cathode corrosion potentials with respect to saturated calomel electrode as measured in the rapid macrocell test for bare 2205 pickled duplex steel in 6.04 m ion NaCl and simulated concrete pore solution.

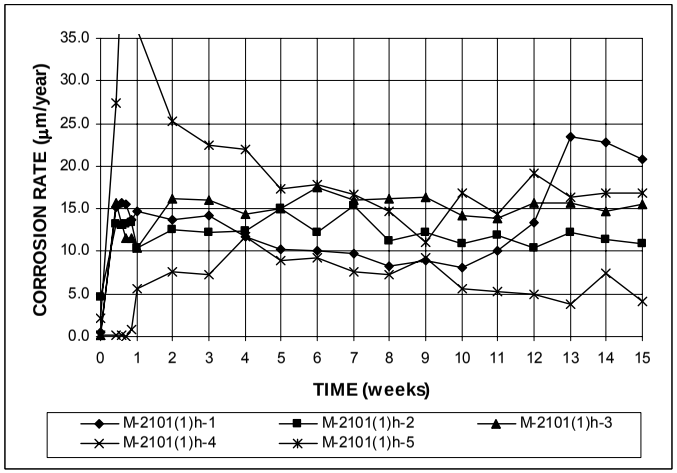


(a)

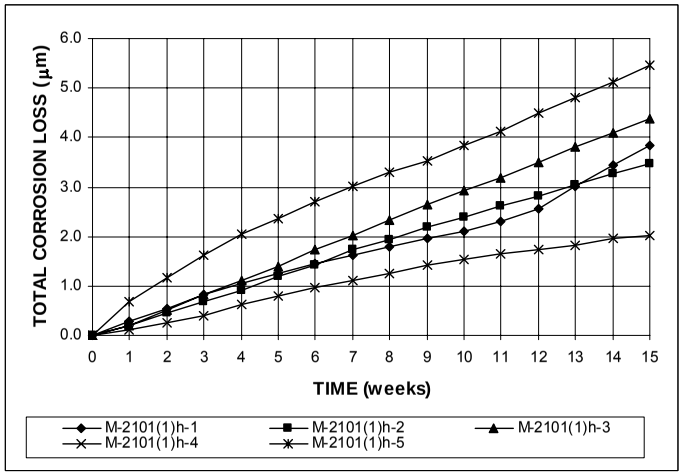


(b)

**Figure A.40 -** (a) Corrosion rates and (b) total corrosion losses as measured in the rapid macrocell test for bare 2101(1) duplex steel in 6.04 m ion NaCl and simulated concrete pore solution.

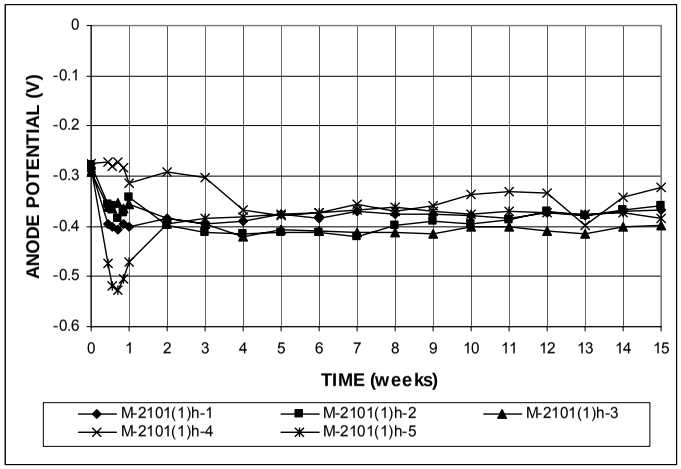


(a)

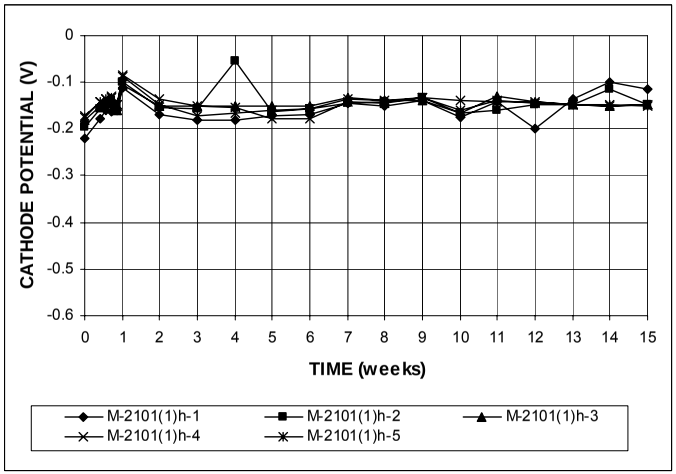


(b)

**Figure A.41 -** (a) Anode corrosion potentials and (b) cathode corrosion potentials with respect to saturated calomel electrode as measured in the rapid macrocell test for bare 2101(1) duplex steel in 6.04 m ion NaCl and simulated concrete pore solution.

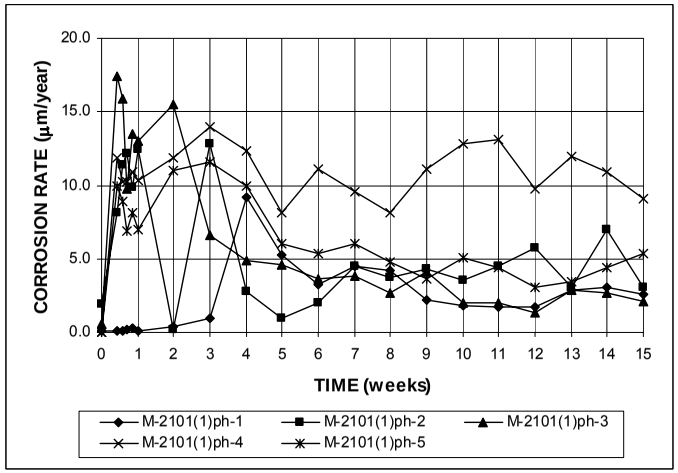


(a)

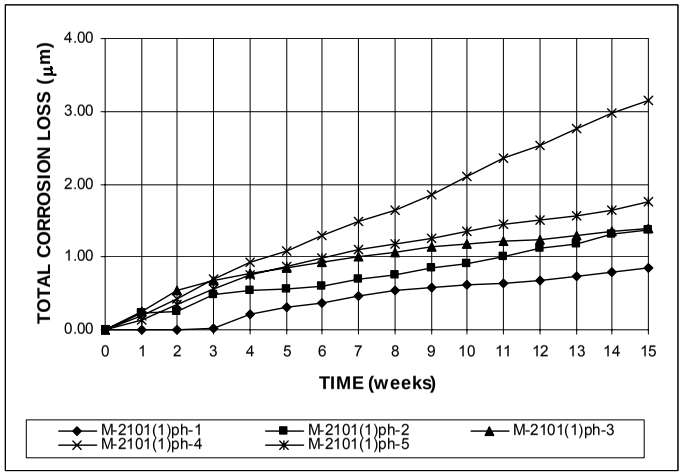


(b)

**Figure A.42 -** (a) Corrosion rates and (b) total corrosion losses as measured in the rapid macrocell test for bare 2101(1) pickled duplex steel in 6.04 m ion NaCl and simulated concrete pore solution.

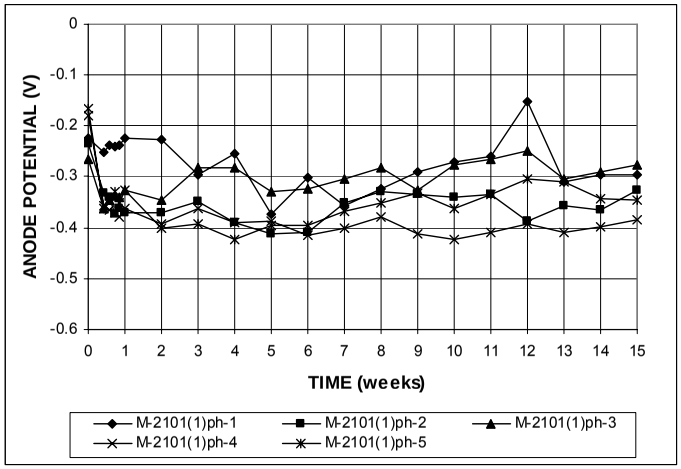


(a)

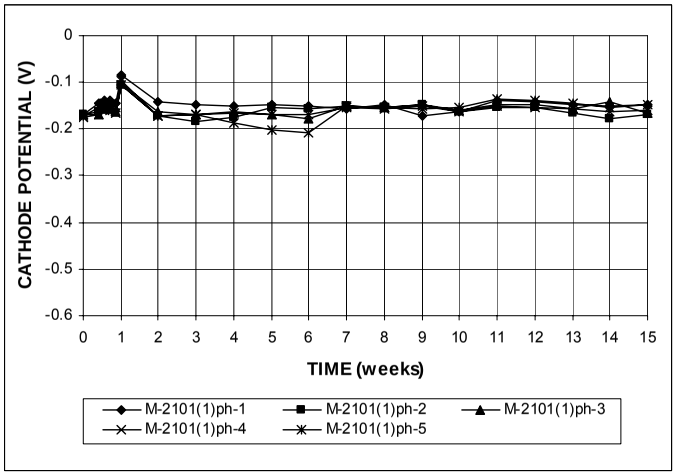


(b)

**Figure A.43 -** (a) Anode corrosion potentials and (b) cathode corrosion potentials with respect to saturated calomel electrode as measured in the rapid macrocell test for bare 2101(1) pickled duplex steel in 6.04 m ion NaCl and simulated concrete pore solution.

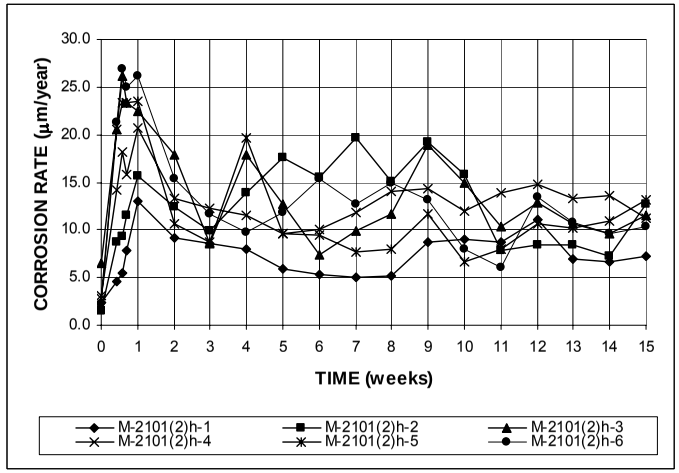


(a)

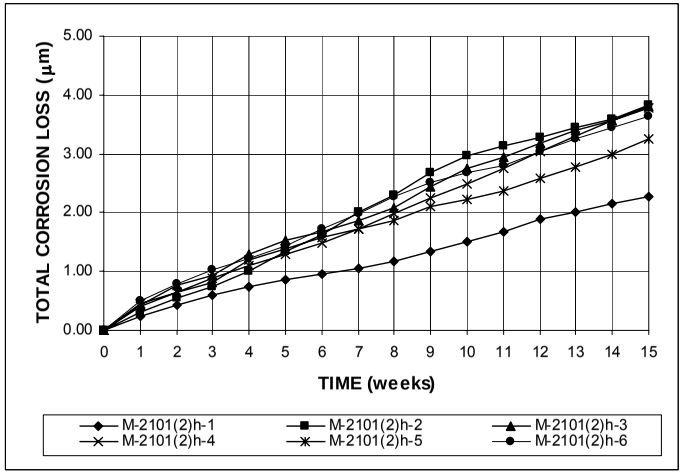


(b)

**Figure A.44 -** (a) Corrosion rates and (b) total corrosion losses as measured in the rapid macrocell test for bare 2101(2) duplex steel in 6.04 m ion NaCl and simulated concrete pore solution.

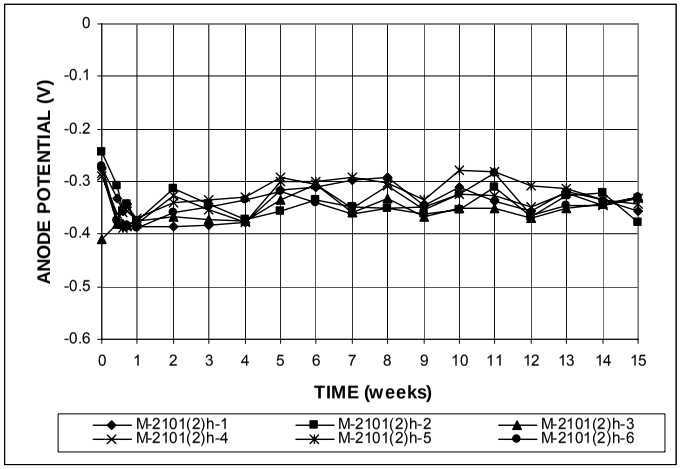


(a)

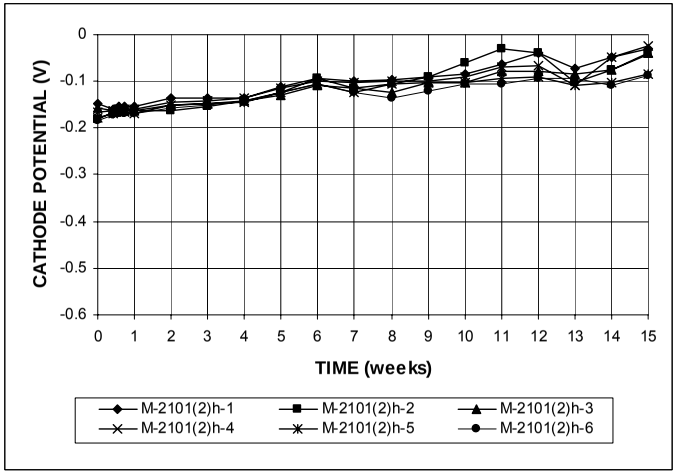


(b)

**Figure A.45 -** (a) Anode corrosion potentials and (b) cathode corrosion potentials with respect to saturated calomel electrode as measured in the rapid macrocell test for bare 2101(2) duplex steel in 6.04 m ion NaCl and simulated concrete pore solution.

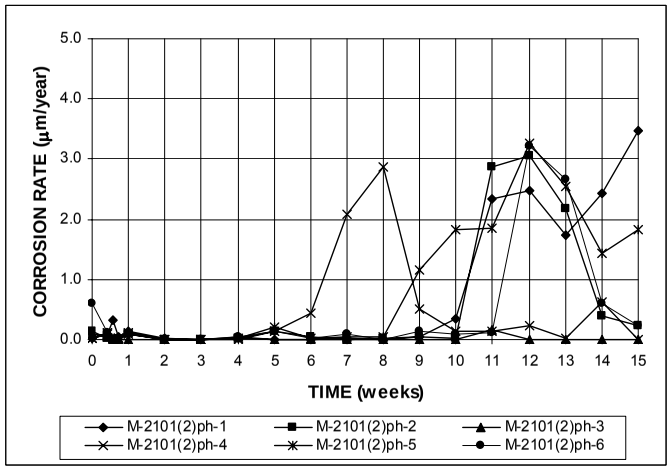


(a)

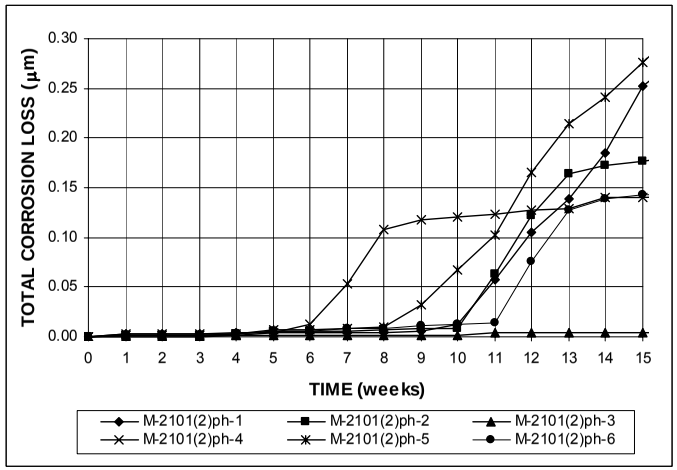


(b)

**Figure A.46** - (a) Corrosion rates and (b) total corrosion losses as measured in the rapid macrocell test for bare 2101(2) pickled duplex steel in 6.04 m ion NaCl and simulated concrete pore solution.

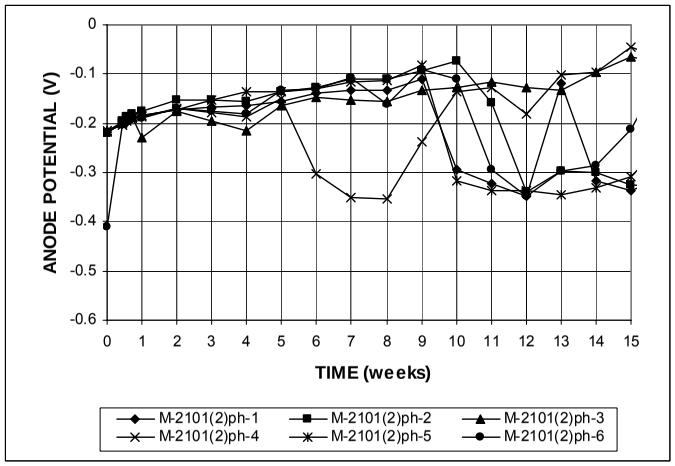


(a)

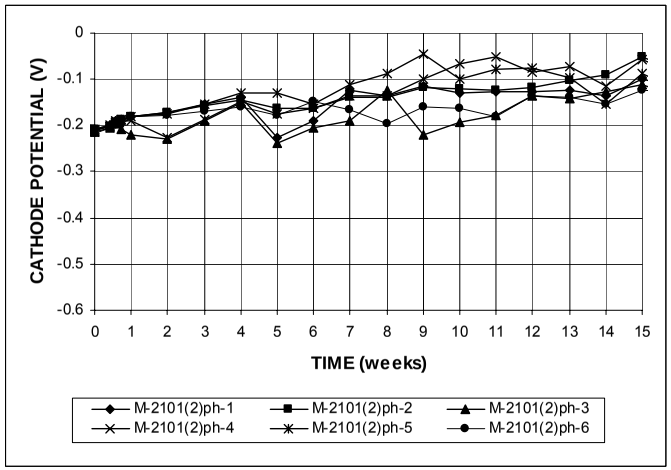


(b)

**Figure A.47** - (a) Anode corrosion potentials and (b) cathode corrosion potentials with respect to saturated calomel electrode as measured in the rapid macrocell test for bare 2101(2) pickled duplex steel in 6.04 m ion NaCl and simulated concrete pore solution.

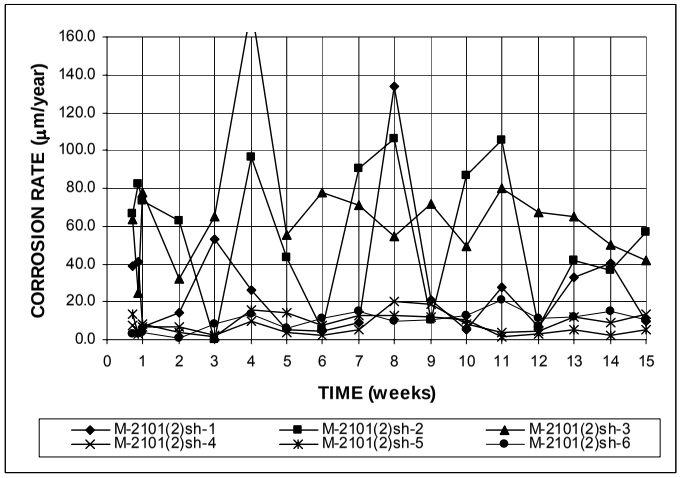


(a)

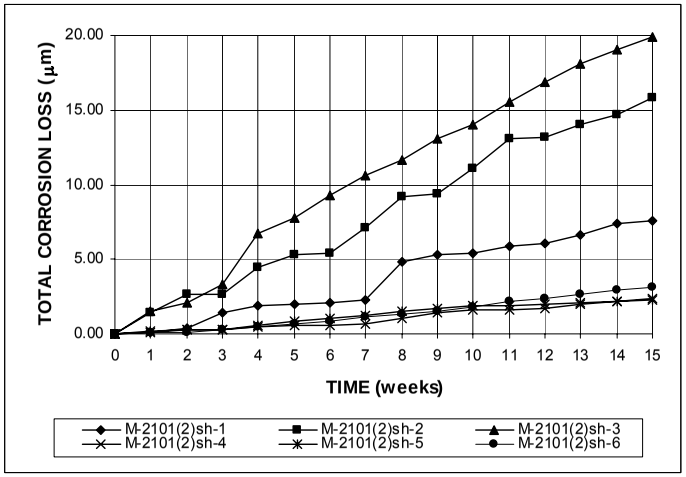


(b)

**Figure A.48 -** (a) Corrosion rates and (b) total corrosion losses as measured in the rapid macrocell test for bare, sandblasted 2101(2) duplex steel in 6.04 m ion NaCl and simulated concrete pore solution.

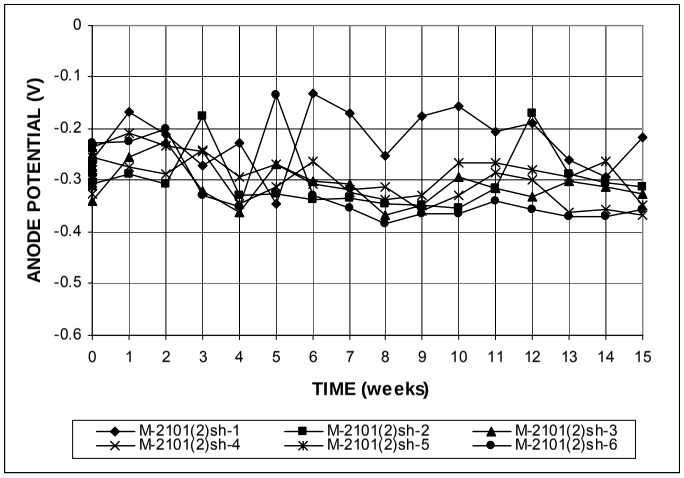


(a)

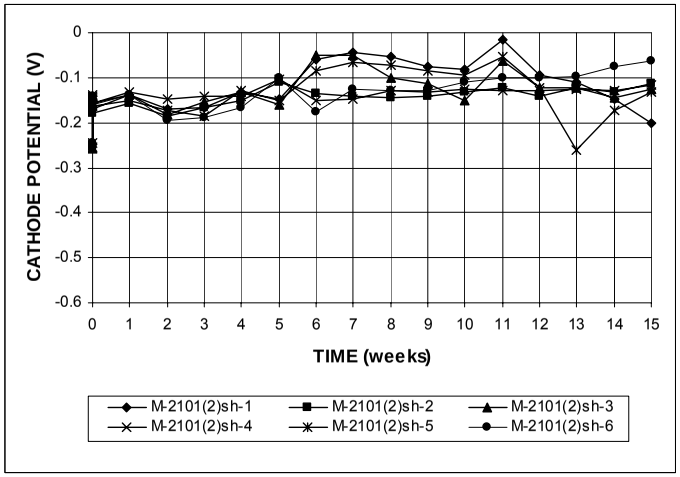


(b)

**Figure A.49 -** (a) Anode corrosion potentials and (b) cathode corrosion potentials with respect to saturated calomel electrode as measured in the rapid macrocell test for bare, sandblasted 2101(2) duplex steel in 6.04 m ion NaCl and simulated concrete pore solution.

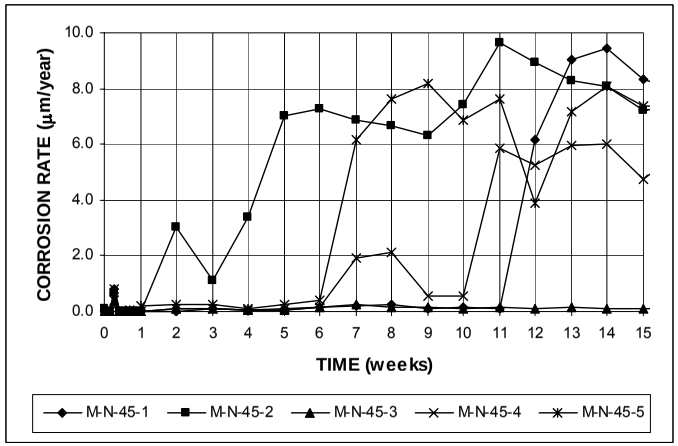


(a)

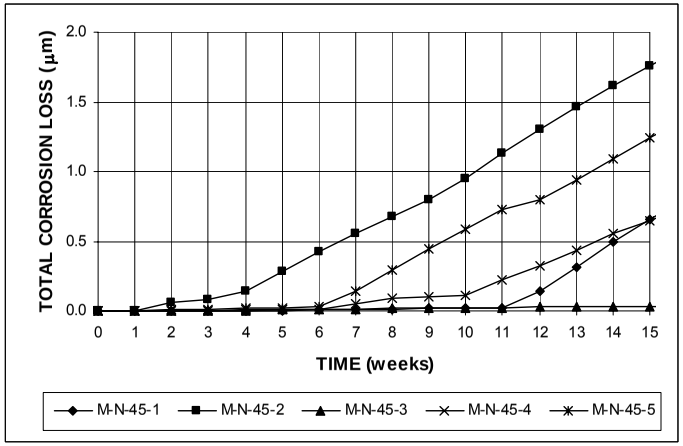


(b)

**Figure A.50 -** (a) Corrosion rates and (b) total corrosion losses as measured in the rapid macrocell test for lollipop specimens with a water-cement ratio of 0.45, no inhibitor, and conventional normalized steel (N) in 1.6 m ion NaCl and simulated concrete pore solution.

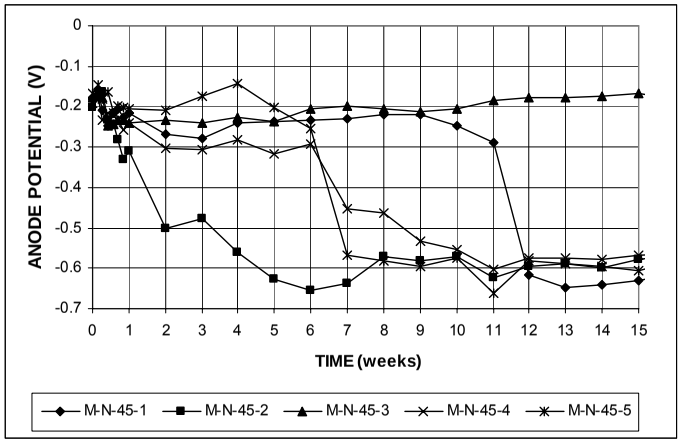


(a)

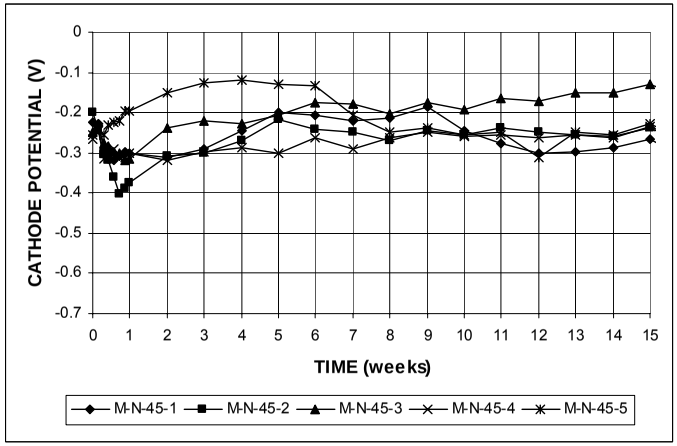


(b)

**Figure A.51 -** (a) Anode corrosion potentials and (b) cathode corrosion potentials with respect to saturated calomel electrode as measured in the rapid macrocell test for lollipop specimens with a water-cement ratio of 0.45, no inhibitor, and conventional normalized steel (N) in 1.6 m ion NaCl and simulated concrete pore solution.

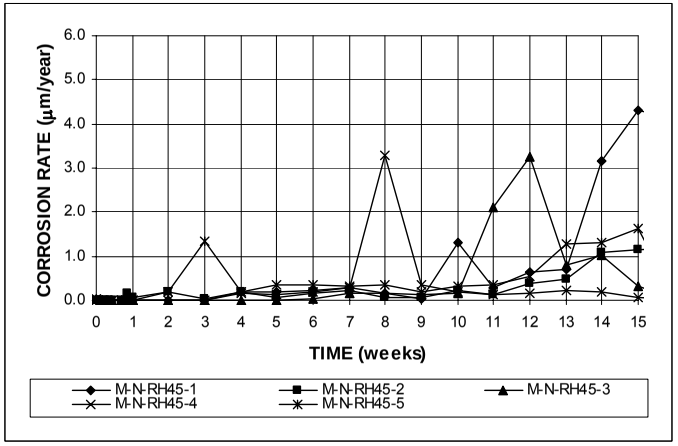


(a)

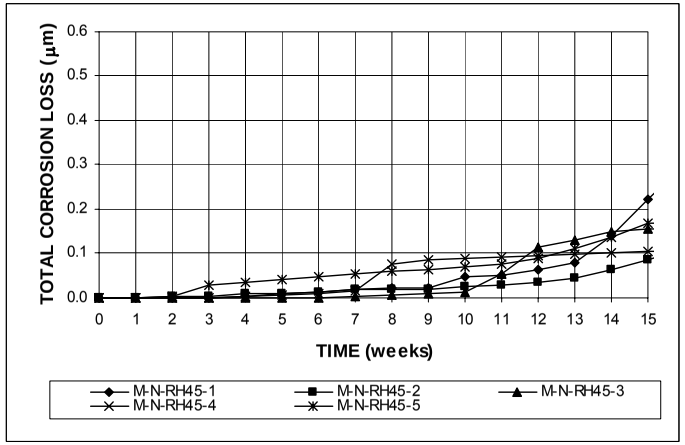


(b)

**Figure A.52 -** (a) Corrosion rates and (b) total corrosion losses as measured in the rapid macrocell test for lollipop specimens with a water-cement ratio of 0.45, Rheocrete 222+, and conventional normalized steel (N) in 1.6 m ion NaCl and simulated concrete pore solution.

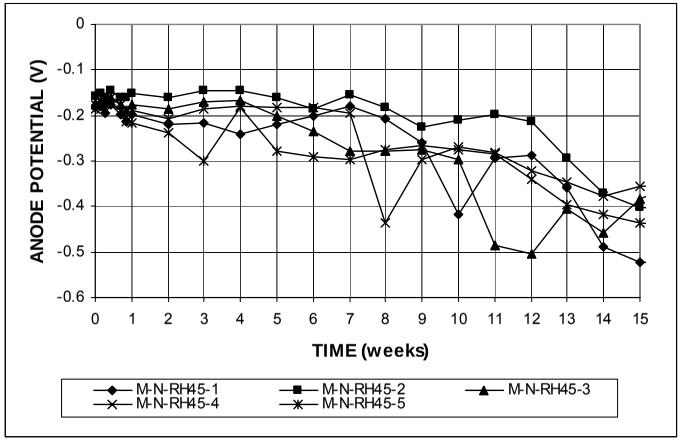


(a)

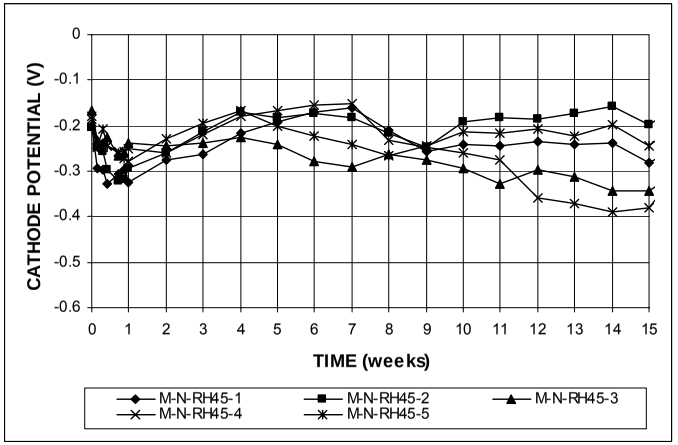


(b)

**Figure A.53 -** (a) Anode corrosion potentials and (b) cathode corrosion potentials with respect to saturated calomel electrode as measured in the rapid macrocell test for lollipop specimens with a water-cement ratio of 0.45, Rheocrete 222+, and conventional normalized steel (N) in 1.6 m ion NaCl and simulated concrete pore solution.

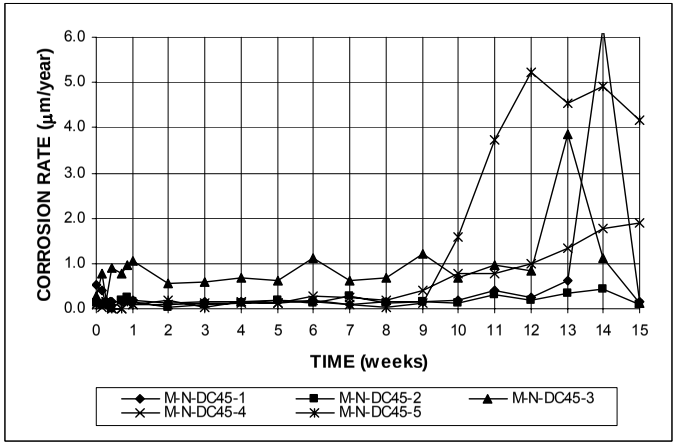


(a)

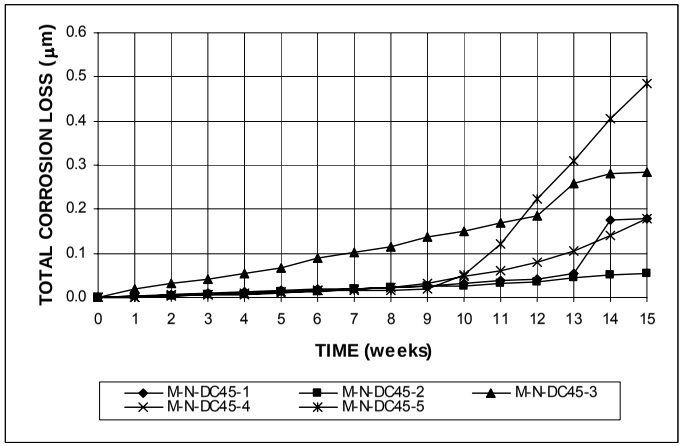


(b)

**Figure A.54 -** (a) Corrosion rates and (b) total corrosion losses as measured in the rapid macrocell test for lollipop specimens with a water-cement ratio of 0.45, DCI-S, and conventional normalized steel (N) in 1.6 m ion NaCl and simulated concrete pore solution.

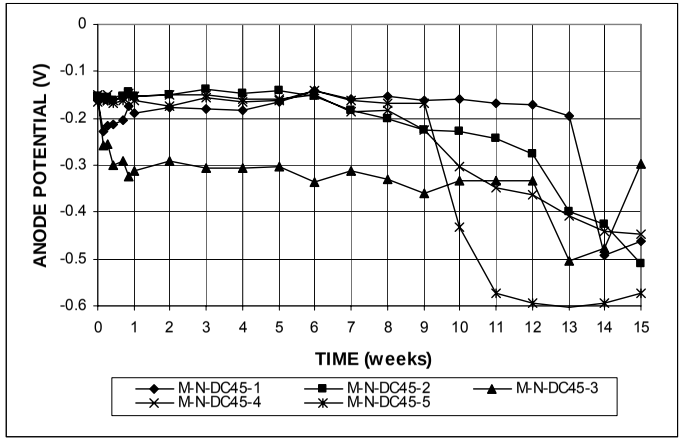


(a)

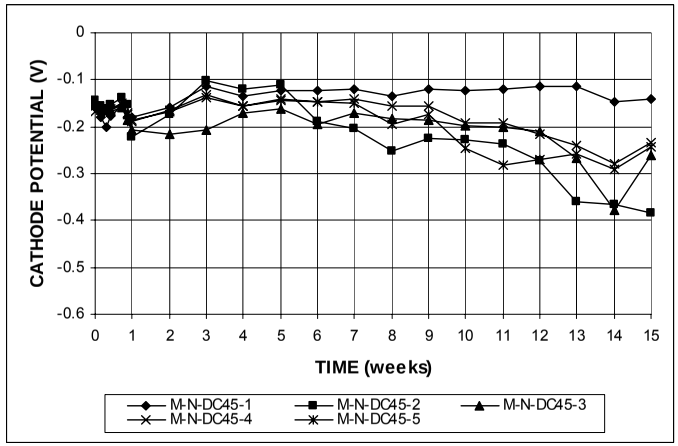


(b)

**Figure A.55 -** (a) Anode corrosion potentials and (b) cathode corrosion potentials with respect to saturated calomel electrode as measured in the rapid macrocell test for lollipop specimens with a water-cement ratio of 0.45, DCI-S, and conventional normalized steel (N) in 1.6 m ion NaCl and simulated concrete pore solution.

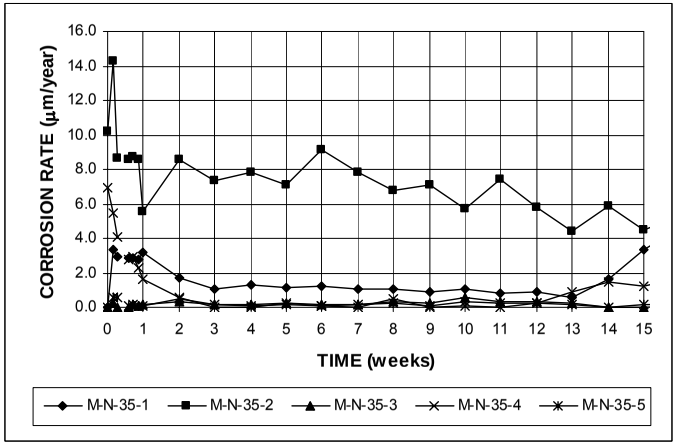


(a)

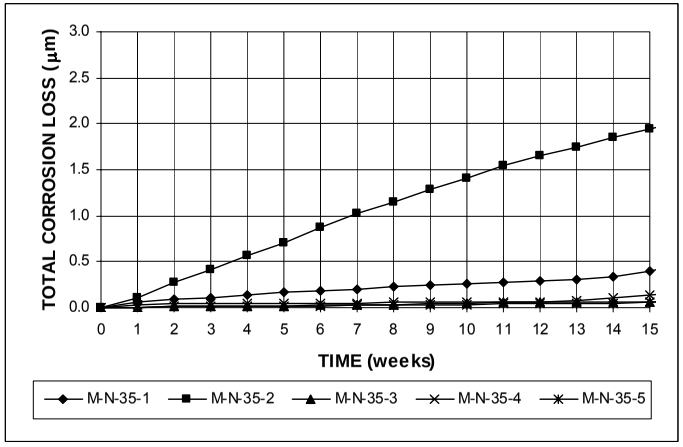


(b)

**Figure A.56 -** (a) Corrosion rates and (b) total corrosion losses as measured in the rapid macrocell test for lollipop specimens with a water-cement ratio of 0.35, no inhibitor, and conventional normalized steel (N) in 1.6 m ion NaCl and simulated concrete pore solution.

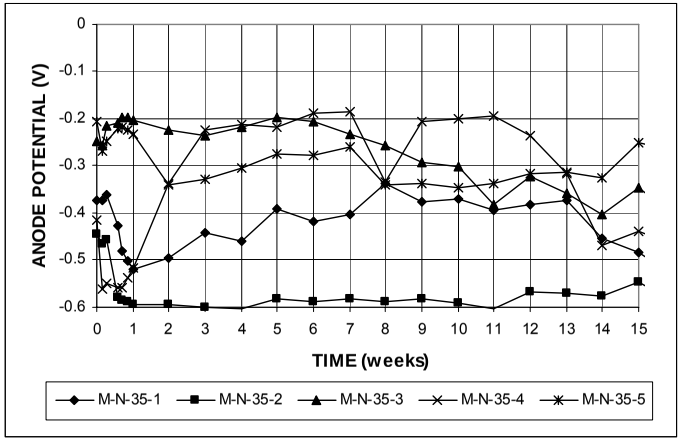


(a)

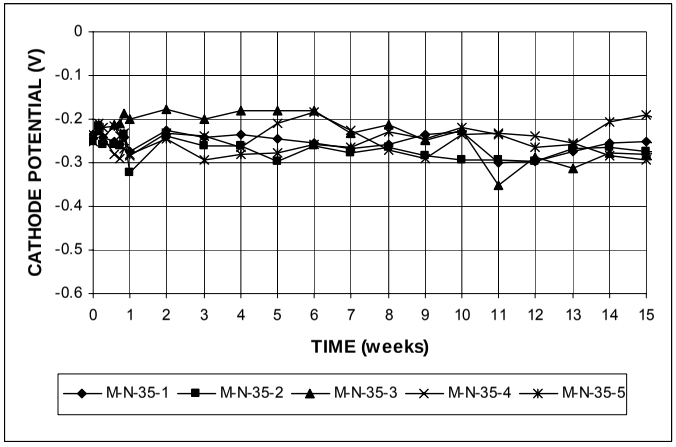


(b)

**Figure A.57 -** (a) Anode corrosion potentials and (b) cathode corrosion potentials with respect to saturated calomel electrode as measured in the rapid macrocell test for lollipop specimens with a water-cement ratio of 0.35, no inhibitor, and conventional normalized steel (N) in 1.6 m ion NaCl and simulated concrete pore solution.

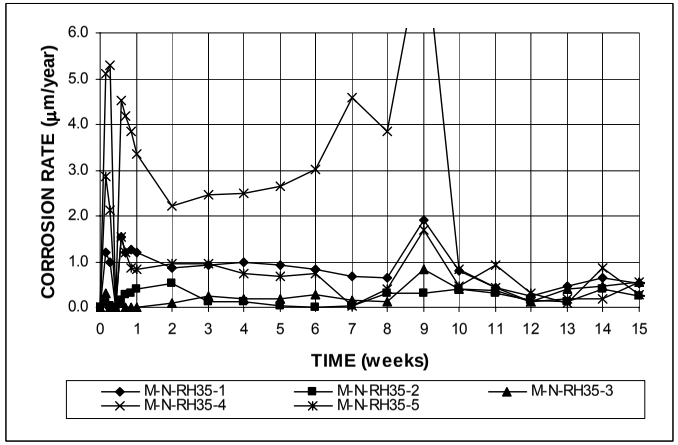


(a)

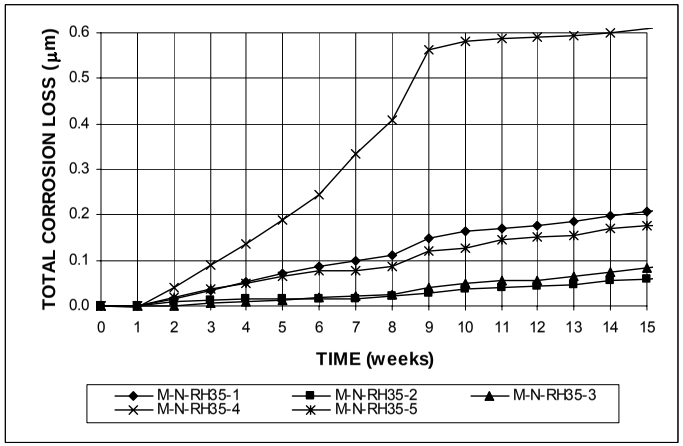


(b)

**Figure A.58 -** (a) Corrosion rates and (b) total corrosion losses as measured in the rapid macrocell test for lollipop specimens with a water-cement ratio of 0.35, Rheocrete 222+, and conventional normalized steel (N) in 1.6 m ion NaCl and simulated concrete pore solution.

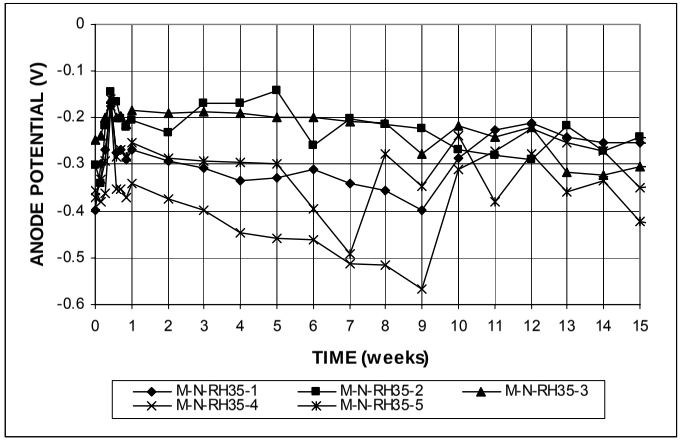


(a)

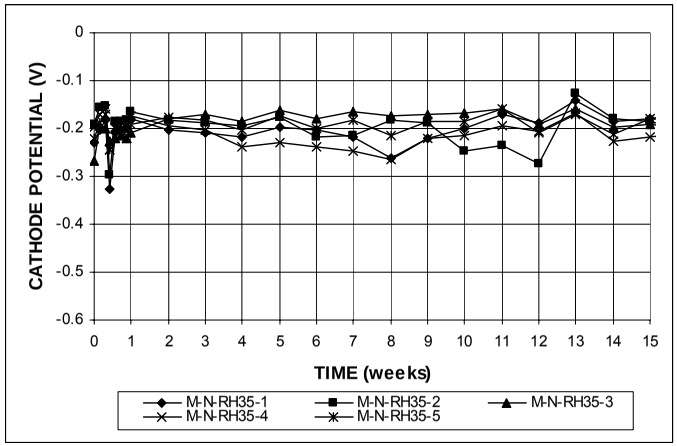


(b)

**Figure A.59 -** (a) Anode corrosion potentials and (b) cathode corrosion potentials with respect to saturated calomel electrode as measured in the rapid macrocell test for lollipop specimens with a water-cement ratio of 0.35, Rheocrete 222+, and conventional normalized steel (N) in 1.6 m ion NaCl and simulated concrete pore solution.

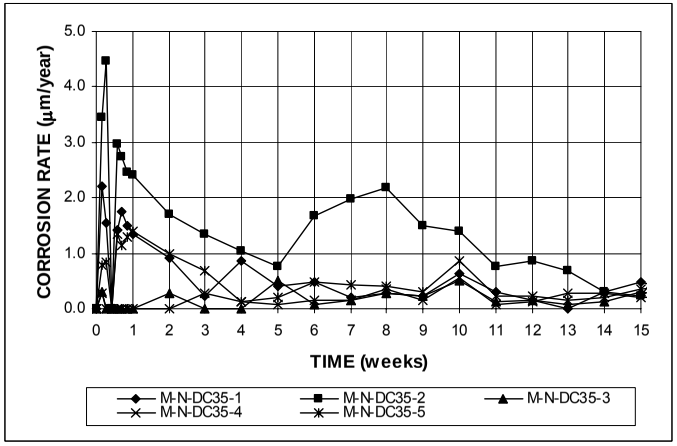


(a)

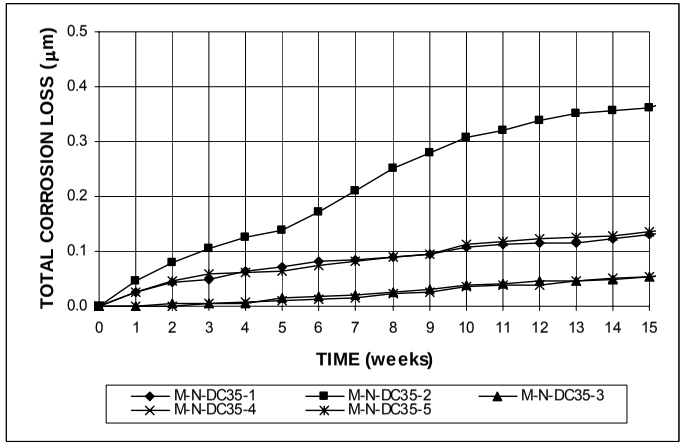


(b)

**Figure A.60 -** (a) Corrosion rates and (b) total corrosion losses as measured in the rapid macrocell test for lollipop specimens with a water-cement ratio of 0.35, DCI-S, and conventional normalized steel (N) in 1.6 m ion NaCl and simulated concrete pore solution.

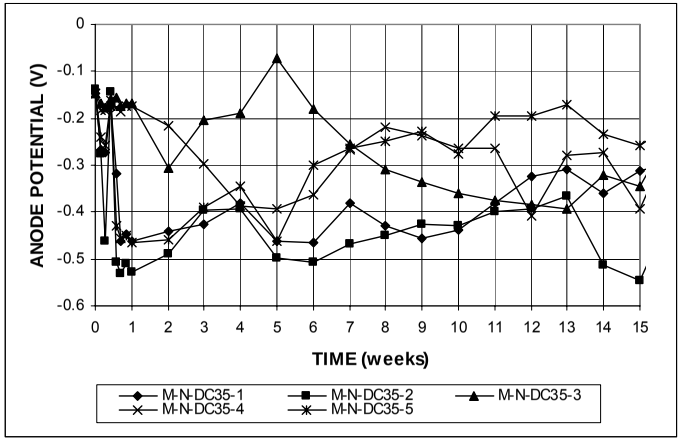


(a)

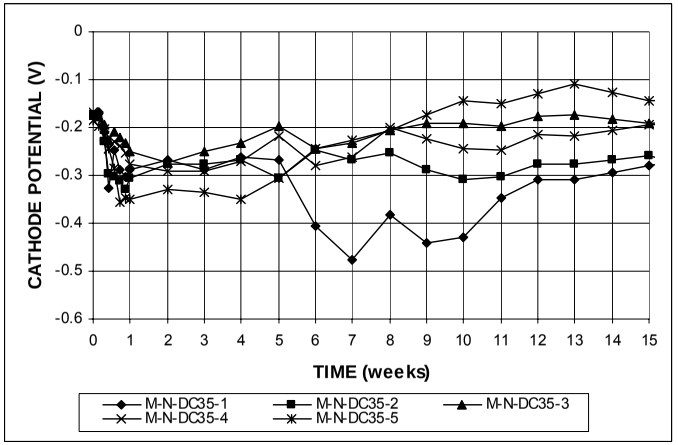


(b)

**Figure A.61 -** (a) Anode corrosion potentials and (b) cathode corrosion potentials with respect to saturated calomel electrode as measured in the rapid macrocell test for lollipop specimens with a water-cement ratio of 0.35, DCI-S, and conventional normalized steel (N) in 1.6 m ion NaCl and simulated concrete pore solution.

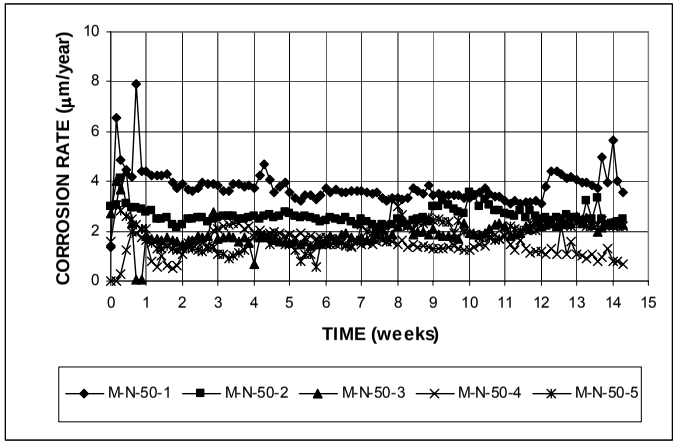


(a)

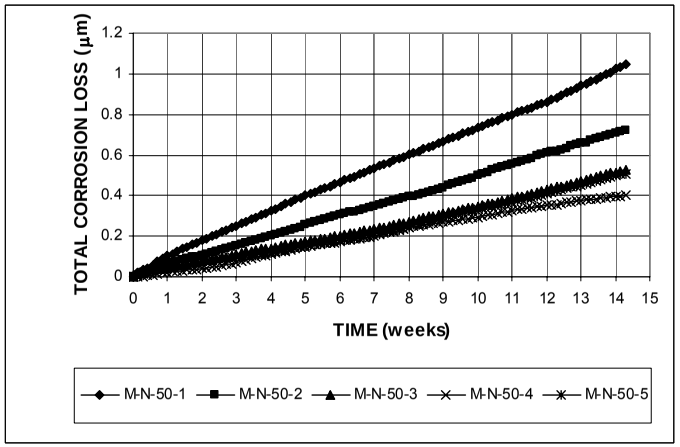


(b)

**Figure A.62 -** (a) Corrosion rates and (b) total corrosion losses as measured in the rapid macrocell test for lollipop specimens with conventional normalized steel (N) in 1.6 m ion NaCl and simulated concrete pore solution.

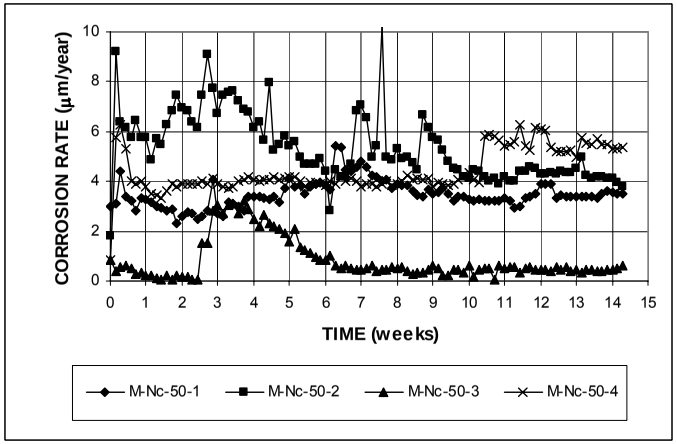


(a)

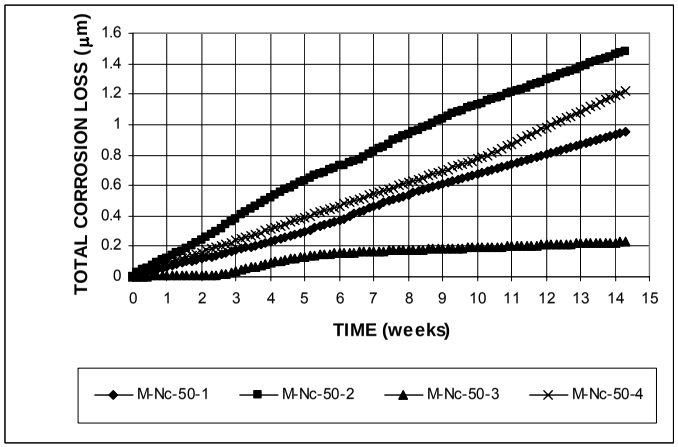


(b)

**Figure A.63 -** (a) Corrosion rates and (b) total corrosion losses as measured in the rapid macrocell test for lollipop specimens with conventional normalized steel (N) with epoxy-filled caps on the ends, in 1.6 m ion NaCl and simulated concrete pore solution.

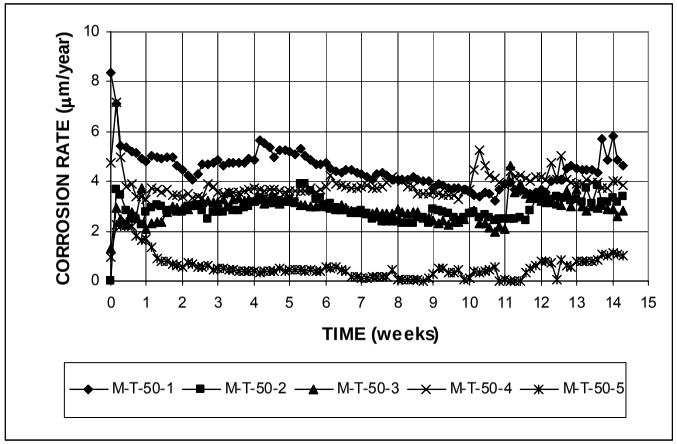


(a)

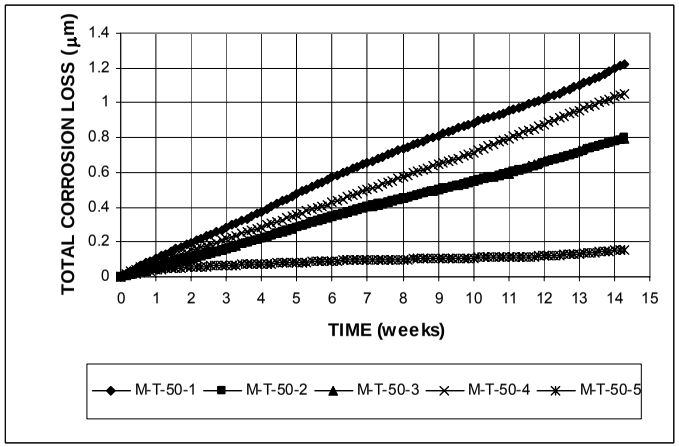


(b)

**Figure A.64 -** (a) Corrosion rates and (b) total corrosion losses as measured in the rapid macrocell test for lollipop specimens with conventional Thermex-treated steel (T) in 1.6 m ion NaCl and simulated concrete pore solution.

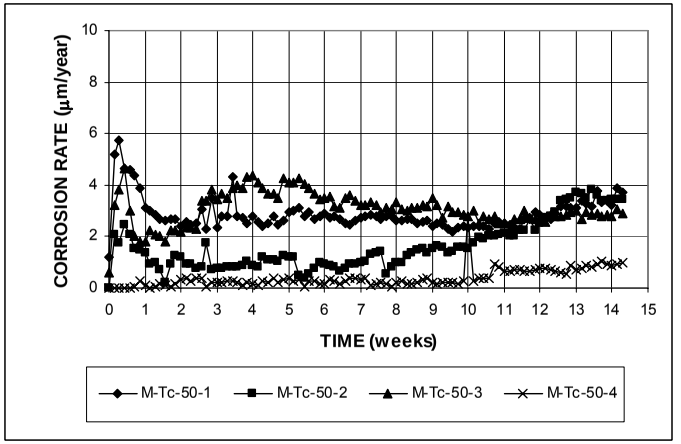


(a)

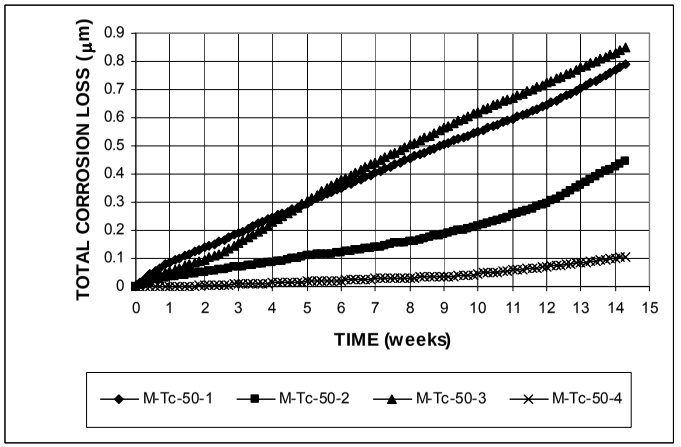


(b)

**Figure A.65 -** (a) Corrosion rates and (b) total corrosion losses as measured in the rapid macrocell test for lollipop specimens with conventional Thermex-treated steel (T) with epoxy-filled caps on the ends, in 1.6 m ion NaCl and simulated concrete pore solution.

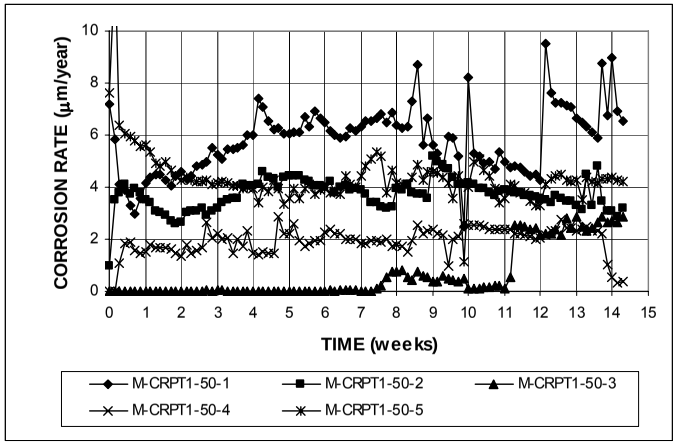


(a)

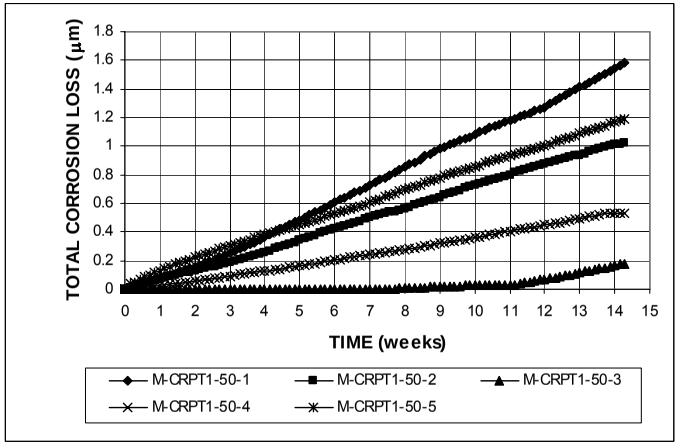


(b)

**Figure A.66 -** (a) Corrosion rates and (b) total corrosion losses as measured in the rapid macrocell test for lollipop specimens with microalloyed steel with a high phosphorus content, 0.117%, Thermex-treated (CRPT1) in 1.6 m ion NaCl and simulated concrete pore solution.

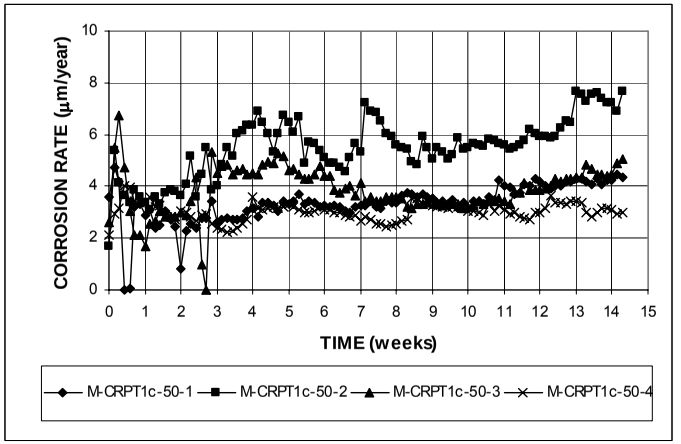


(a)

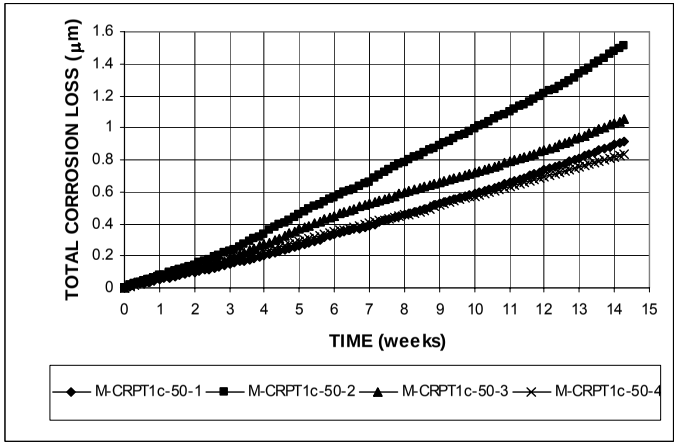


(b)

**Figure A.67 -** (a) Corrosion rates and (b) total corrosion losses as measured in the rapid macrocell test for lollipop specimens with microalloyed steel with a high phosphorus content, 0.117%, Thermex-treated (CRPT1) with epoxy-filed caps on the ends, in 1.6 m ion NaCl and simulated l concrete pore solution.

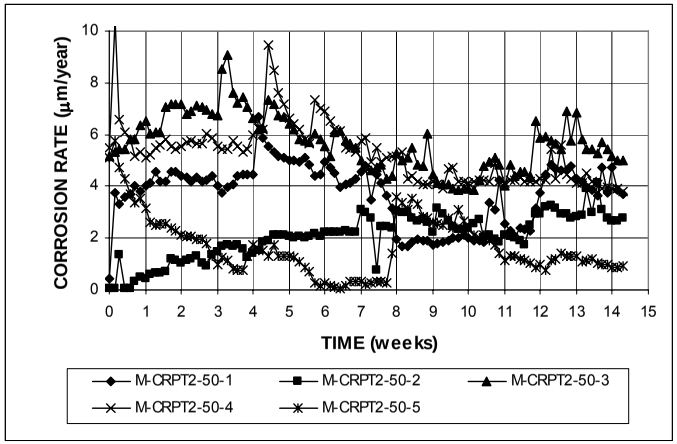


(a)

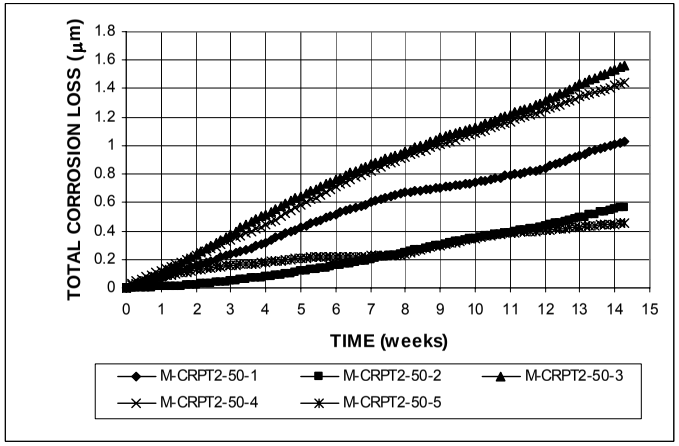


(b)

**Figure A.68 -** (a) Corrosion rates and (b) total corrosion losses as measured in the rapid macrocell test for lollipop specimens with microalloyed steel with a high phosphorus content, 0.100%, Thermex-treated (CRPT2) in 1.6 m ion NaCl and simulated concrete pore solution.

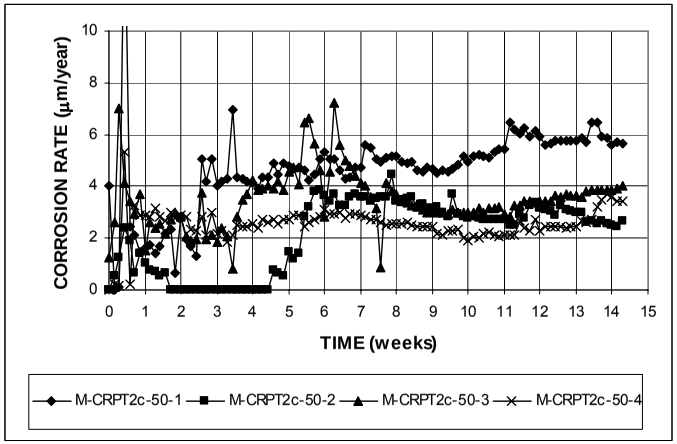


(a)

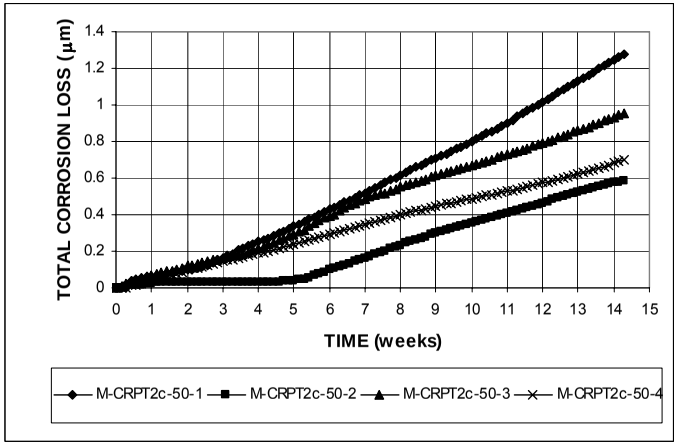


(b)

**Figure A.69 -** (a) Corrosion rates and (b) total corrosion losses as measured in the rapid macrocell test for lollipop specimens with microalloyed steel with a high phosphorus content, 0.100%, Thermex-treated (CRPT2) with epoxy-filled caps on the ends, in 1.6 m ion NaCl and simulated concrete pore solution.

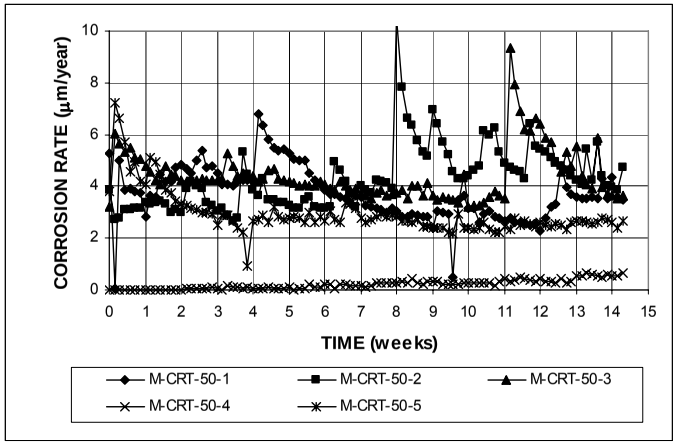


(a)

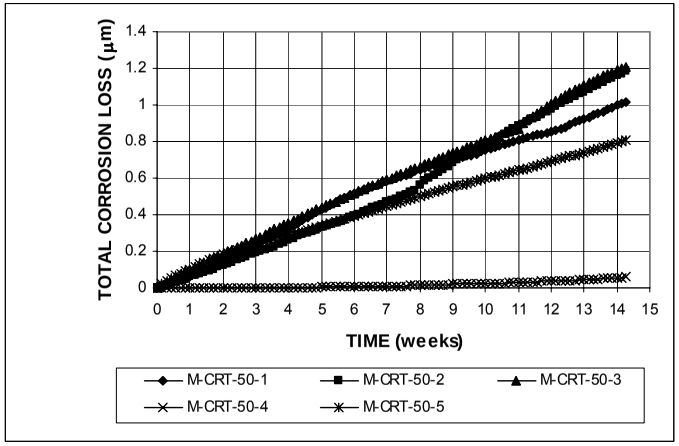


(b)

**Figure A.70 -** (a) Corrosion rates and (b) total corrosion losses as measured in the rapid macrocell test for lollipop specimens with microalloyed steel with a normal phosphorus content, 0.017%, Thermex-treated (CRT) in 1.6 m ion NaCl and simulated concrete pore solution.

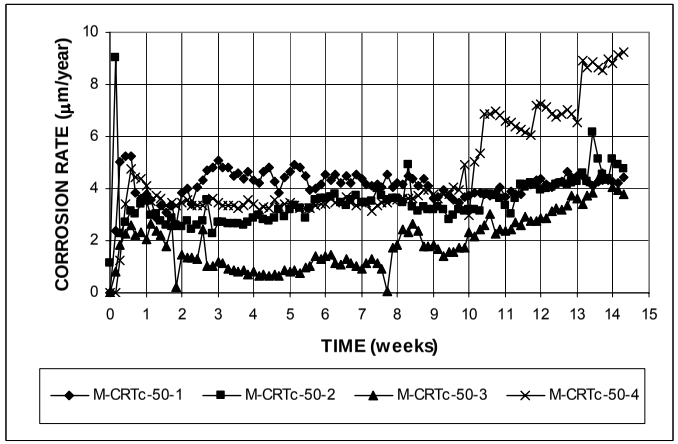


(a)

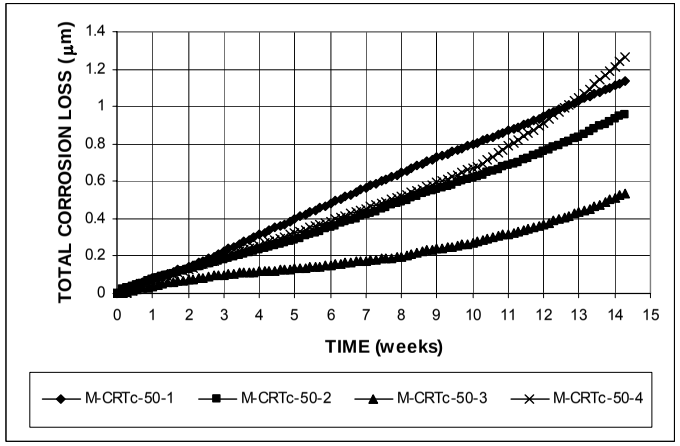


(b)

**Figure A.71 -** (a) Corrosion rates and (b) total corrosion losses as measured in the rapid macrocell test for lollipop specimens with microalloyed steel with a normal phosphorus content, 0.017%, Thermex-treated (CRT) with epoxy-filled caps on the ends, in 1.6 m ion NaCl and simulated concrete pore solution.

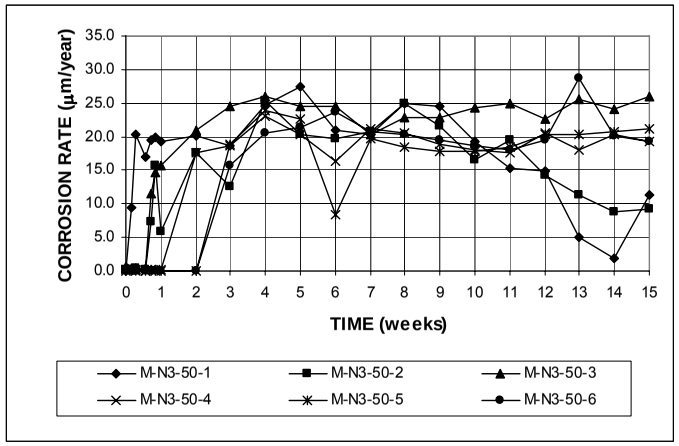


(a)

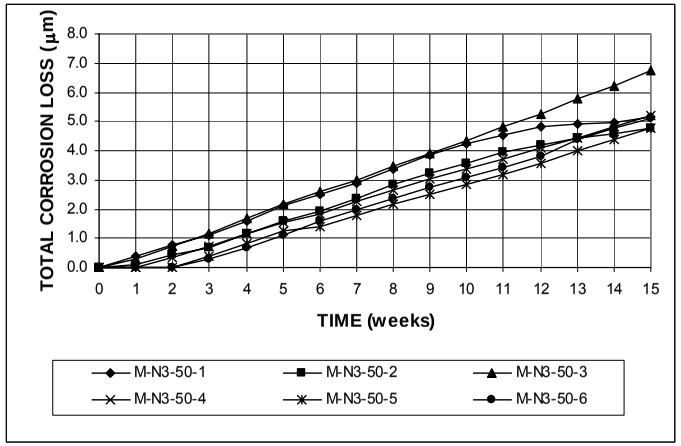


(b)

**Figure A.72 -** (a) Corrosion rates and (b) total corrosion losses as measured in the rapid macrocell test for mortar-wrapped specimens with conventional normalized steel (N3) in 1.6 m ion NaCl and simulated concrete pore solution.

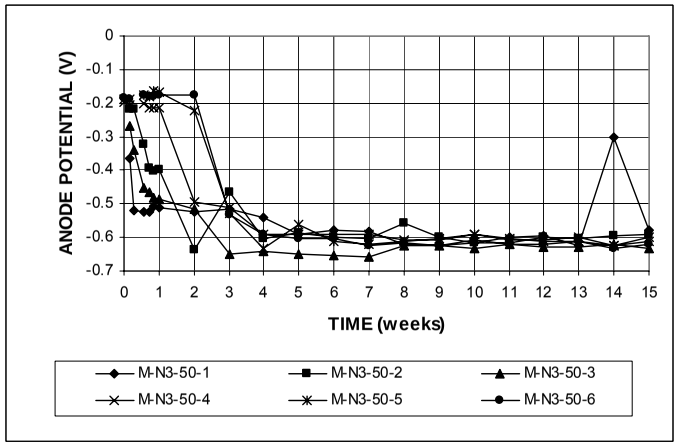


(a)

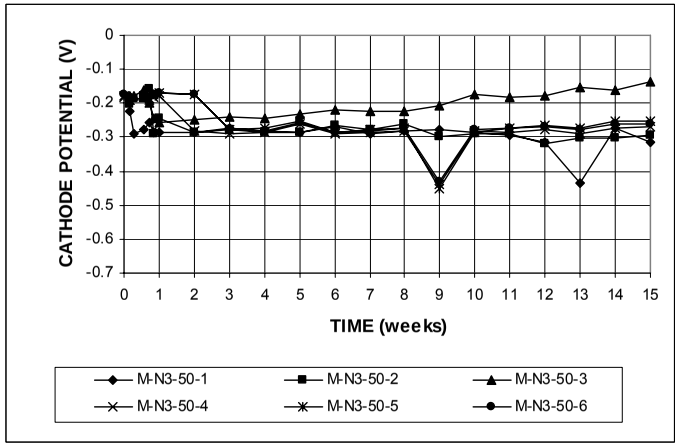


(b)

**Figure A.73 -** (a) Anode corrosion potentials and (b) cathode corrosion potentials with respect to saturated calomel electrode as measured in the rapid macrocell test for mortar-wrapped specimens with conventional normalized steel (N3) in 1.6 m ion NaCl and simulated concrete pore solution.

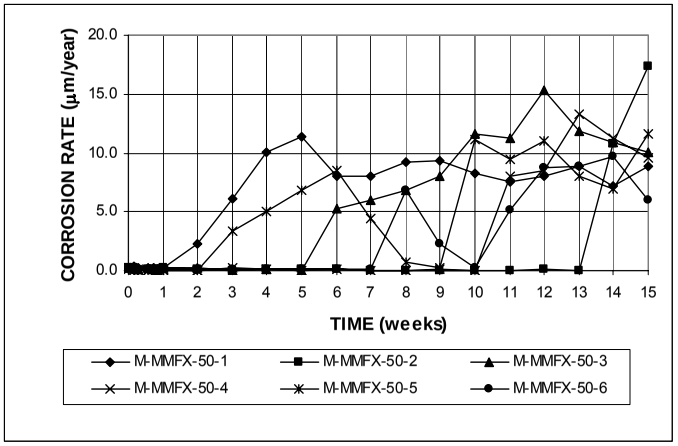


(a)

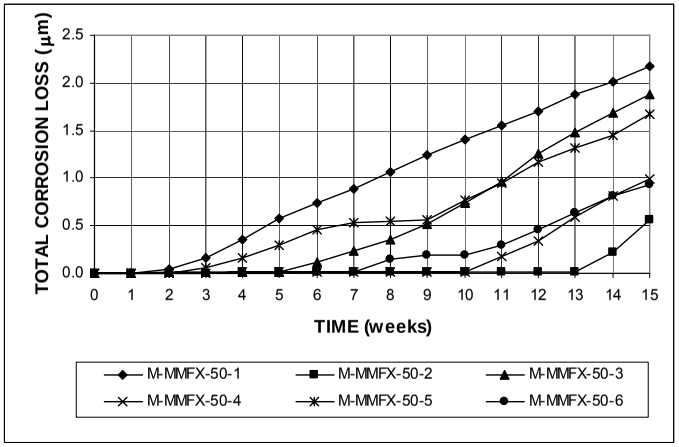


(b)

**Figure A.74 -** (a) Corrosion rates and (b) total corrosion losses as measured in the rapid macrocell test for mortar-wrapped specimens with MMFX microcomposite steel in 1.6 m ion NaCl and simulated concrete pore solution.

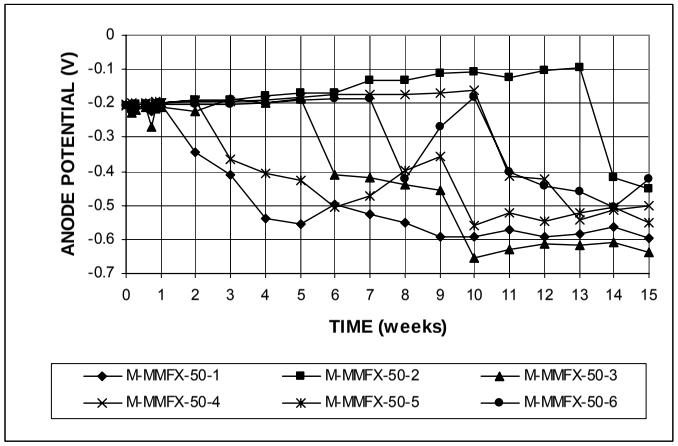


(a)

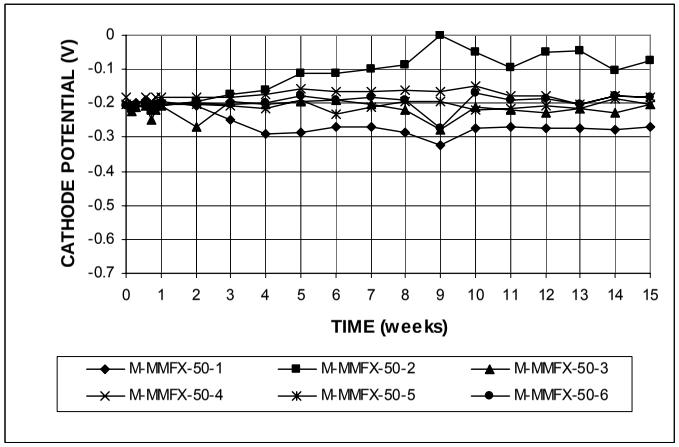


(b)

**Figure A.75 -** (a) Anode corrosion potentials and (b) cathode corrosion potentials with respect to saturated calomel electrode as measured in the rapid macrocell test for mortar-wrapped specimens with MMFX microcomposite steel in 1.6 m ion NaCl and simulated concrete pore solution.

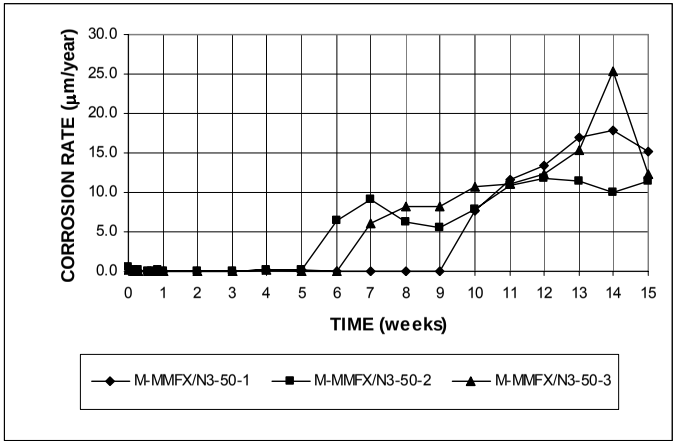


(a)

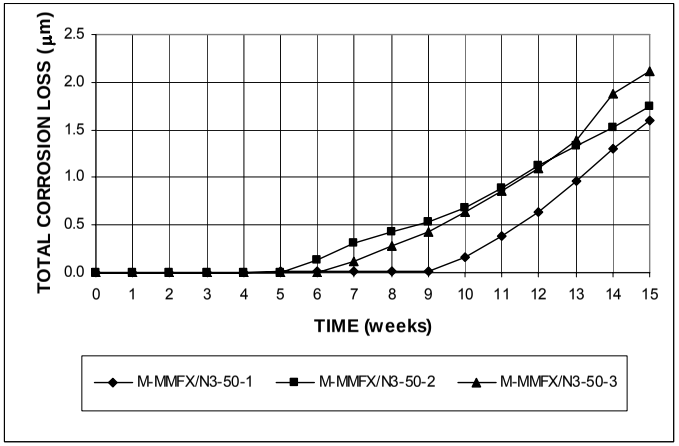


(b)

**Figure A.76 -** (a) Corrosion rates and (b) total corrosion losses as measured in the rapid macrocell test for mortar-wrapped specimens with MMFX microcomposite steel in 1.6 m ion NaCl and simulated concrete pore solution in the anode and N3 steel in simulated concrete pore solution in the cathode.

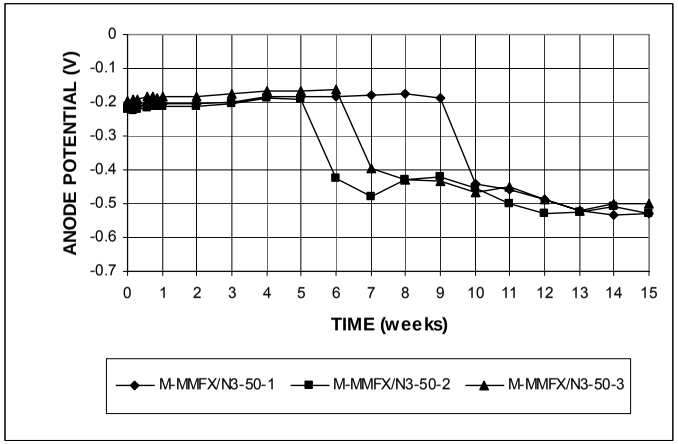


(a)

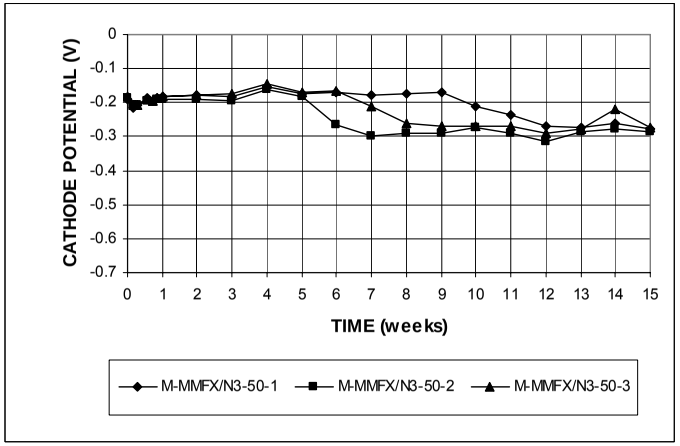


(b)

**Figure A.77 -** (a) Anode corrosion potentials and (b) cathode corrosion potentials as measured in the rapid macrocell test for mortar-wrapped specimens with MMFX microcomposite steel in 1.6 m ion NaCl and simulated concrete pore solution in the anode and N3 steel in simulated concrete pore solution in the cathode.

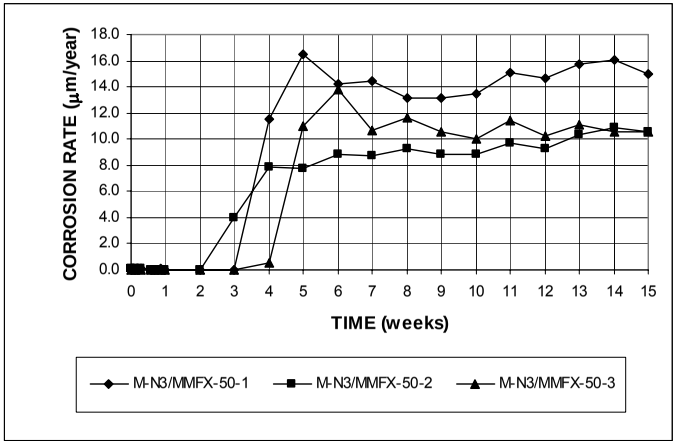


(a)

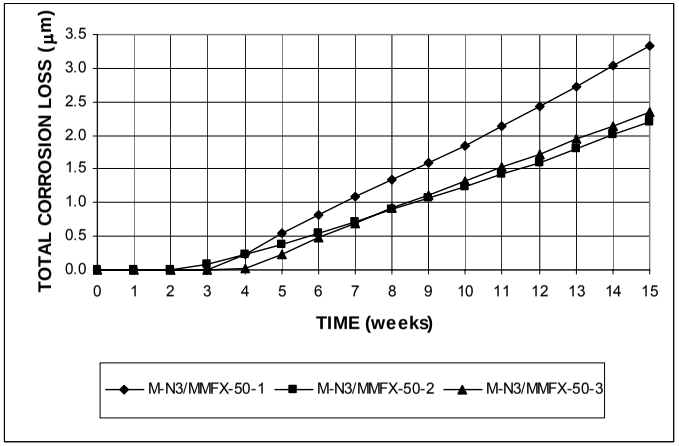


(b)

**Figure A.78 -** (a) Corrosion rates and (b) total corrosion losses as measured in the rapid macrocell test for mortar-wrapped specimens with N3 steel in 1.6 m ion NaCl and simulated concrete pore solution in the anode and MMFX microcomposite steel in simulated concrete pore solution in the cathode.

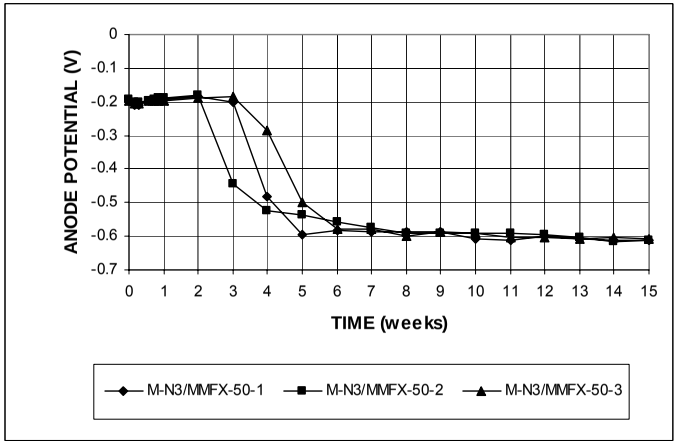


(a)

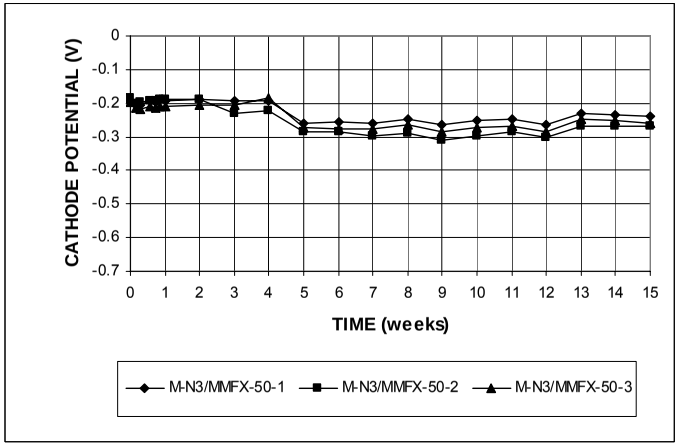


(b)

**Figure A.79 -** (a) Anode corrosion potentials and (b) cathode corrosion potentials with respect to saturated calomel electrode as measured in the rapid macrocell test for mortar-wrapped specimens with N3 steel in 1.6 m ion NaCl and simulated concrete pore solution in the anode and MMFX microcoposite steel in simulated concrete pore solution in the cathode.

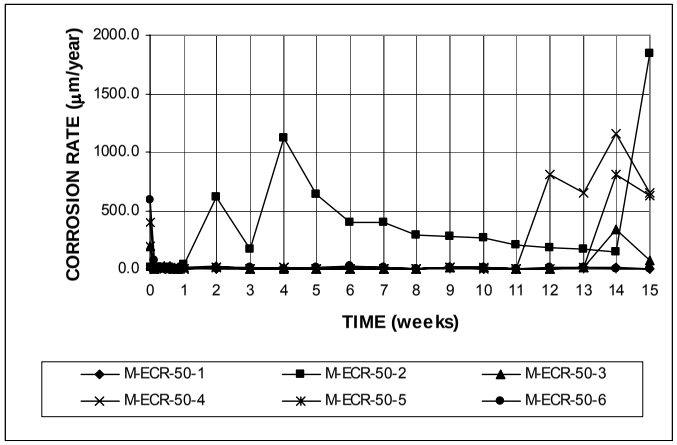


(a)

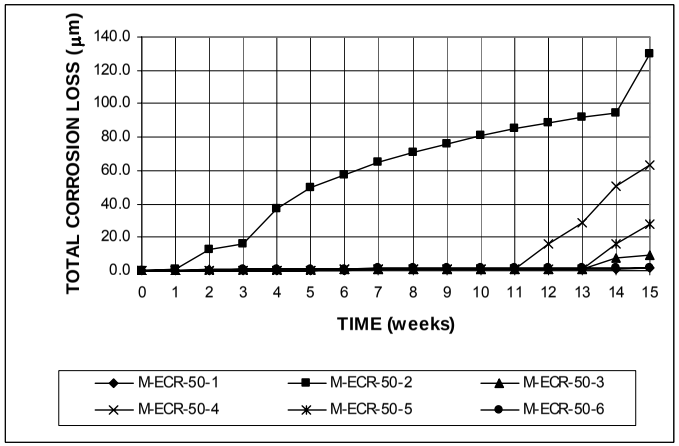


(b)

**Figure A.80 -** (a) Corrosion rates and (b) total corrosion losses based on the exposed area of steel (four $^{1}/_{8}$-in. diameter holes), as measured in the rapid macrocell test for mortar-wrapped specimens with epoxy-coated steel in 1.6 m ion NaCl and simulated concrete pore solution.

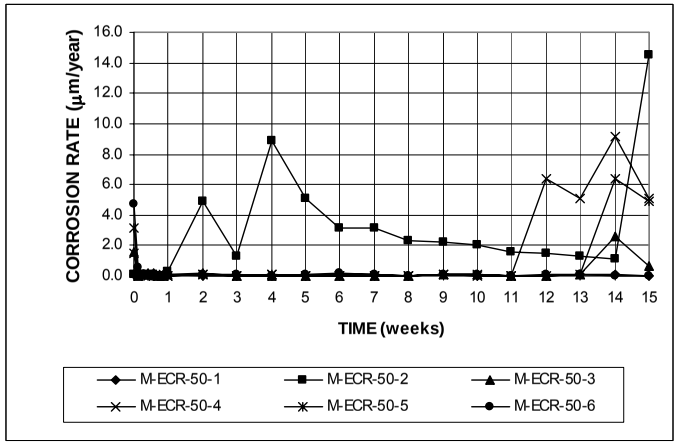


(a)

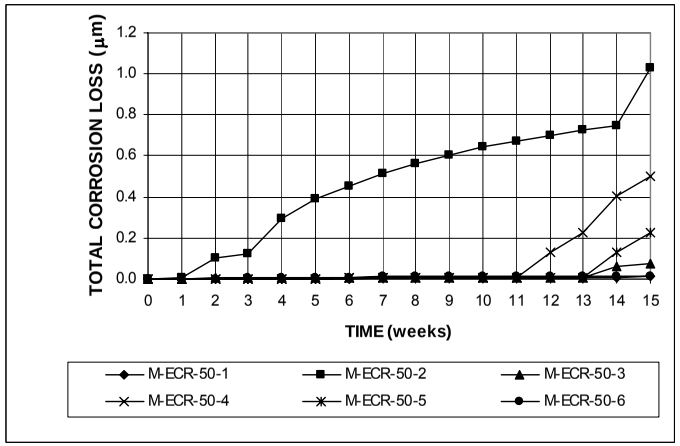


(b)

**Figure A.81 -** (a) Corrosion rates and (b) total corrosion losses based on the total area of the bar, as measured in the rapid macrocell test for mortar-wrapped specimens with epoxy-coated steel in 1.6 m ion NaCl and simulated concrete pore solution.

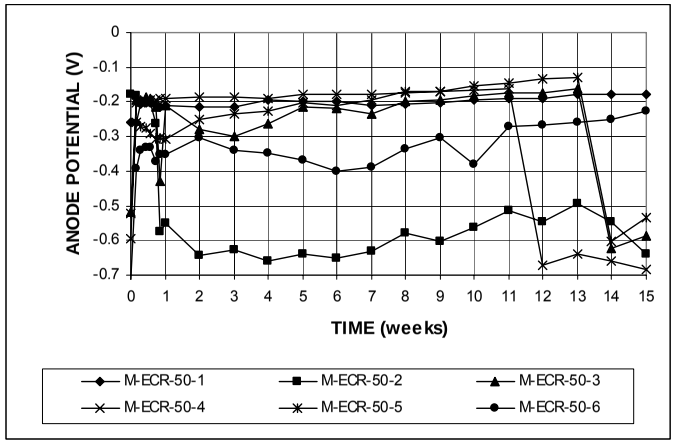


(a)

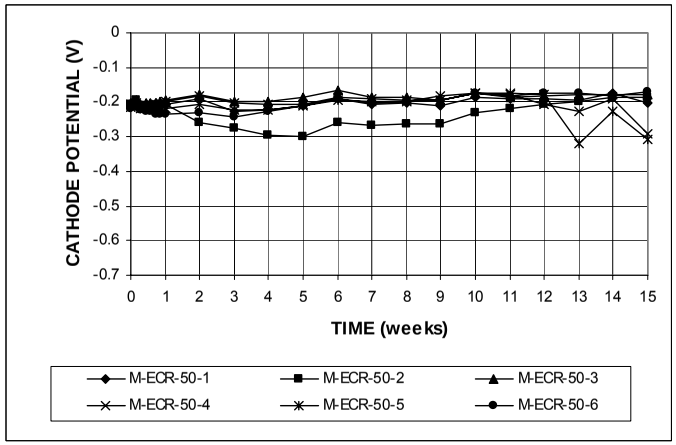


(b)

**Figure A.82 -** (a) Anode corrosion potentials and (b) cathode corrosion potentials with respect to saturated calomel electrode as measured in the rapid macrocell test for mortar-wrapped specimens with epoxy-coated steel in 1.6 m ion NaCl and simulated concrete pore solution.

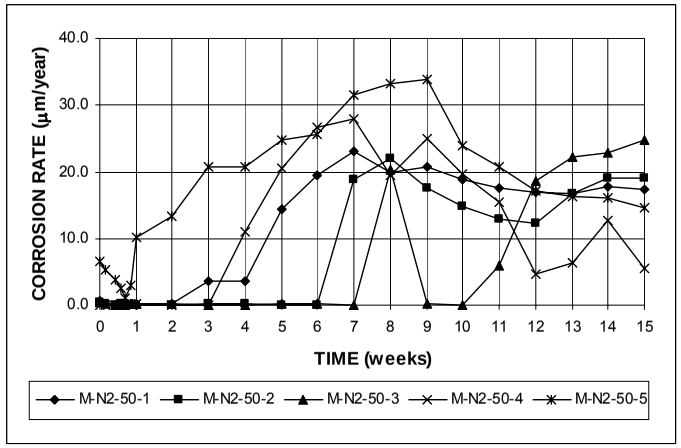


(a)

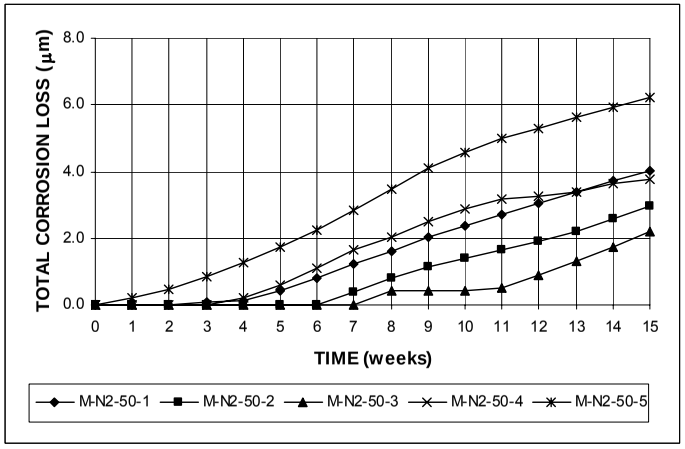


(b)

**Figure A.83 -** (a) Corrosion rates and (b) total corrosion losses as measured in the rapid macrocell test for mortar-wrapped specimens with conventional normalized steel (N2) in 1.6 m ion NaCl and simulated concrete pore solution.

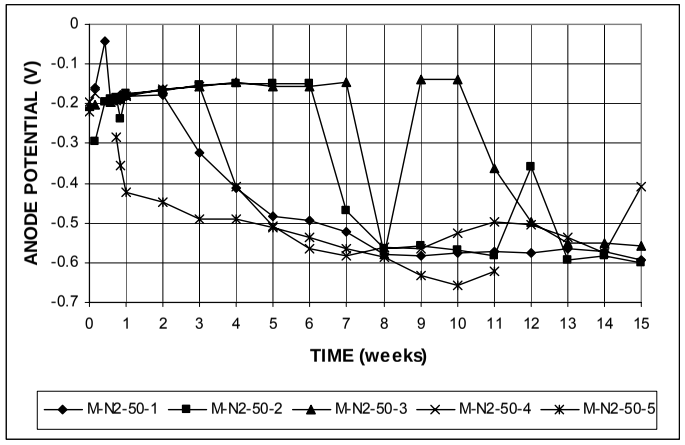


(a)

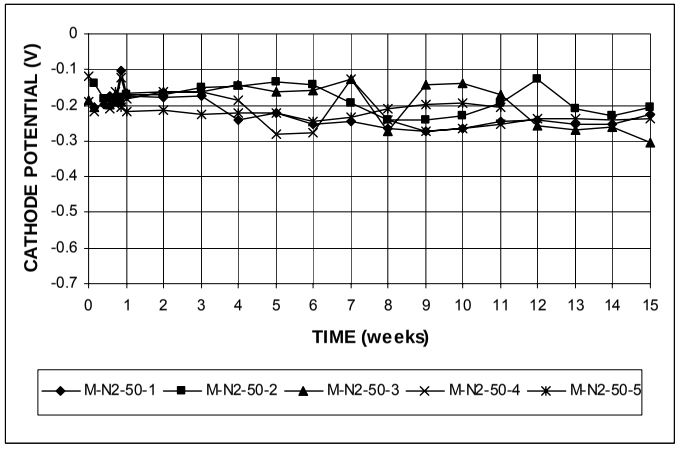


(b)

**Figure A.84 -** (a) Anode corrosion potentials and (b) cathode corrosion potentials with respect to saturated calomel electrode as measured in the rapid macrocell test for mortar-wrapped specimens with conventional normalized steel (N2) in 1.6 m ion NaCl and simulated concrete pore solution.

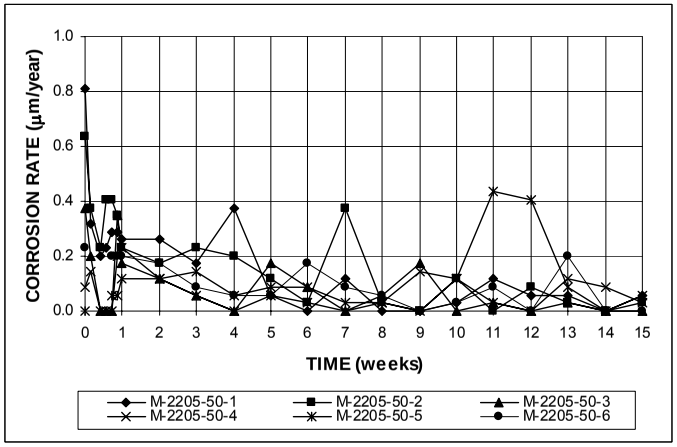


(a)

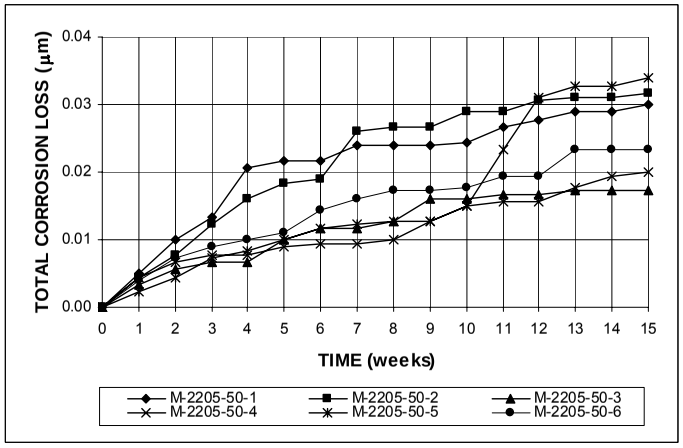


(b)

**Figure A.85 -** (a) Corrosion rates and (b) total corrosion losses as measured in the rapid macrocell test for mortar-wrapped specimens with 2205 duplex steel in 1.6 m ion NaCl and simulated concrete pore solution.

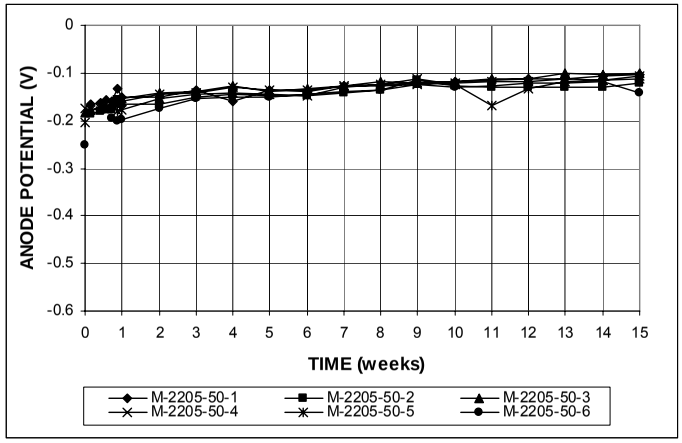


(a)

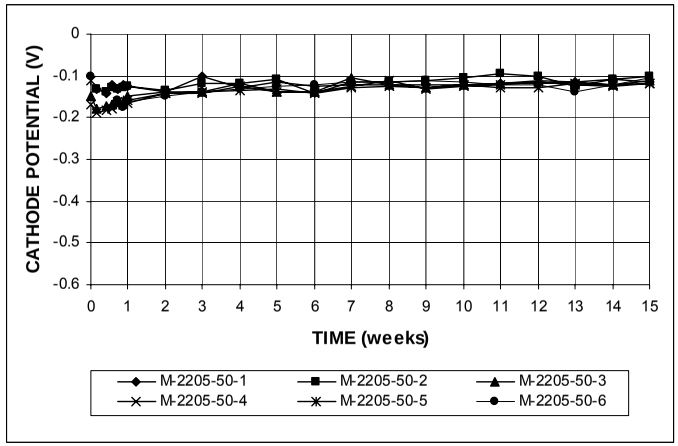


(b)

**Figure A.86 -** (a) Anode corrosion potentials and (b) cathode corrosion potentials with respect to saturated calomel electrode as measured in the rapid macrocell test for mortar-wrapped specimens with 2205 duplex steel in 1.6 m ion NaCl and simulated concrete pore solution.

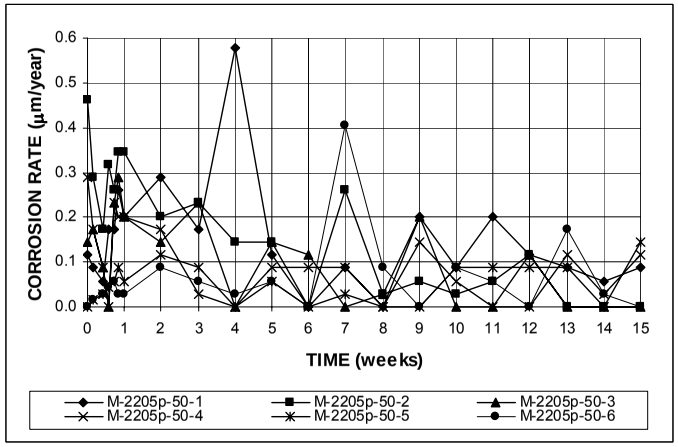


(a)

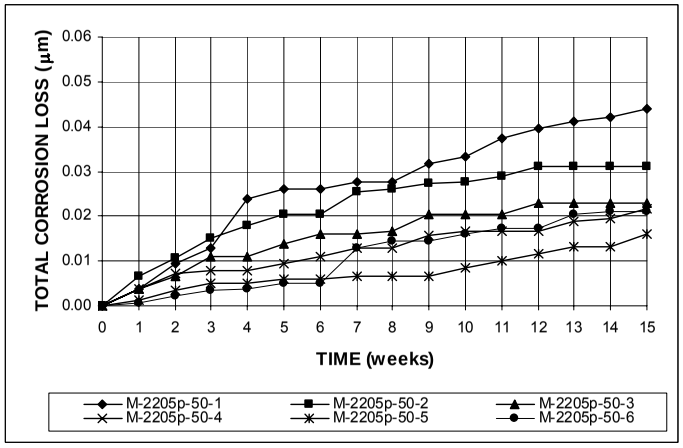


(b)

**Figure A.87 -** (a) Corrosion rates and (b) total corrosion losses as measured in the rapid macrocell test for mortar-wrapped specimens with 2205 pickled duplex steel in 1.6 m ion NaCl and simulated concrete pore solution.

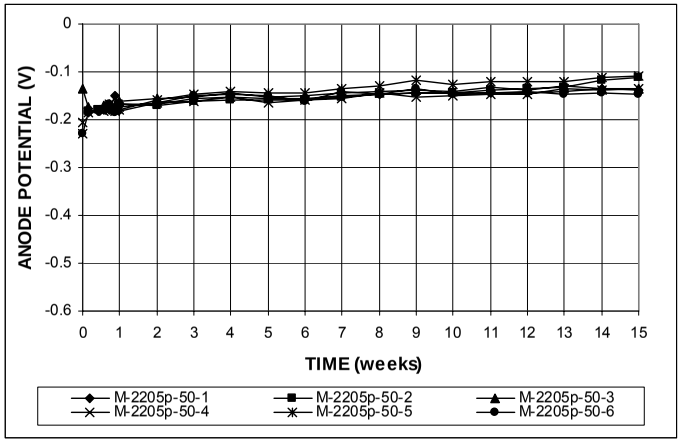


(a)

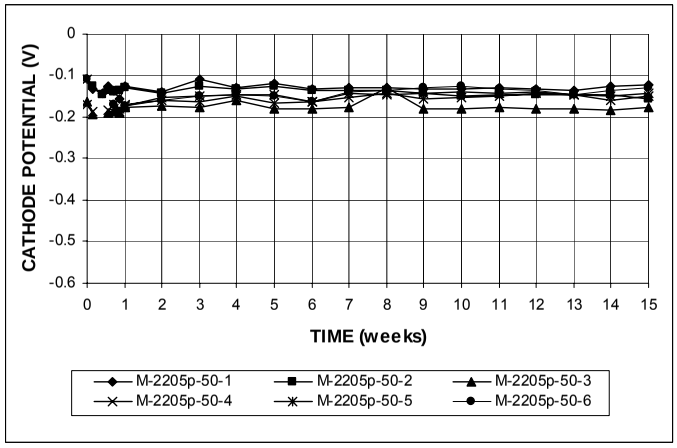


(b)

**Figure A.88 -** (a) Anode corrosion potentials and (b) cathode corrosion potentials with respect to saturated calomel electrode as measured in the rapid macrocell test for mortar-wrapped specimens with 2205 pickled duplex steel in 1.6 m ion NaCl and simulated concrete pore solution.

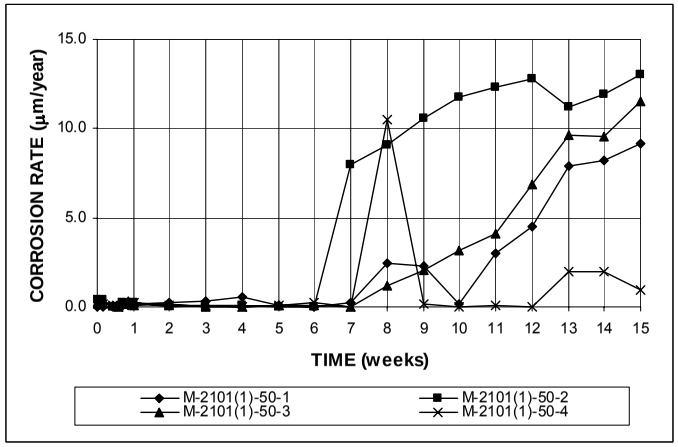


(a)

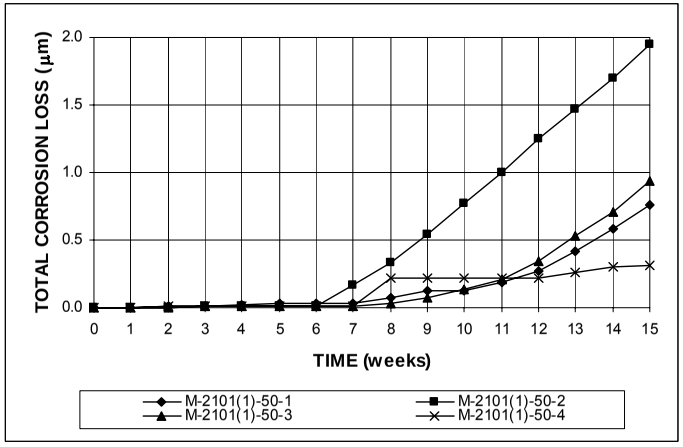


(b)

**Figure A.89 -** (a) Corrosion rates and (b) total corrosion losses as measured in the rapid macrocell test for mortar-wrapped specimens with 2101(1) duplex steel in 1.6 m ion NaCl and simulated concrete pore solution.

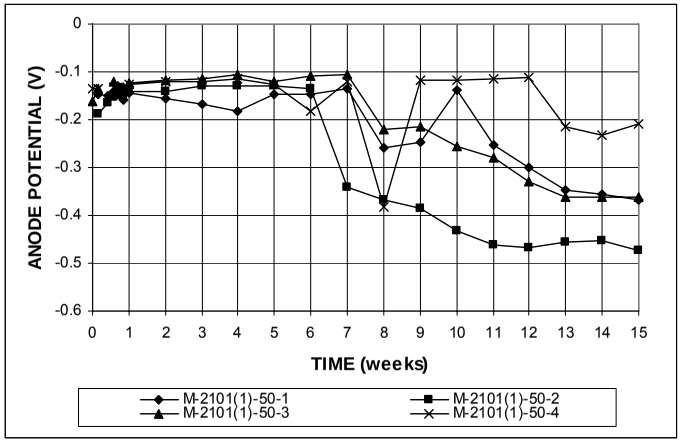


(a)

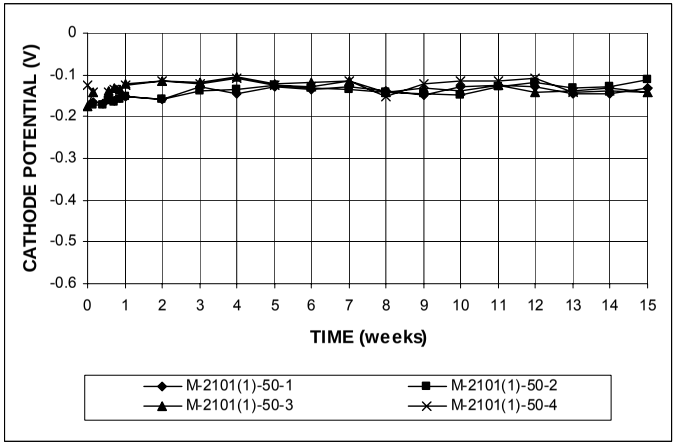


(b)

**Figure A.90 -** (a) Anode corrosion potentials and (b) cathode corrosion potentials with respect to saturated calomel electrode as measured in the rapid macrocell test for mortar-wrapped specimens with 2101(1) duplex steel in 1.6 m ion NaCl and simulated concrete pore solution.

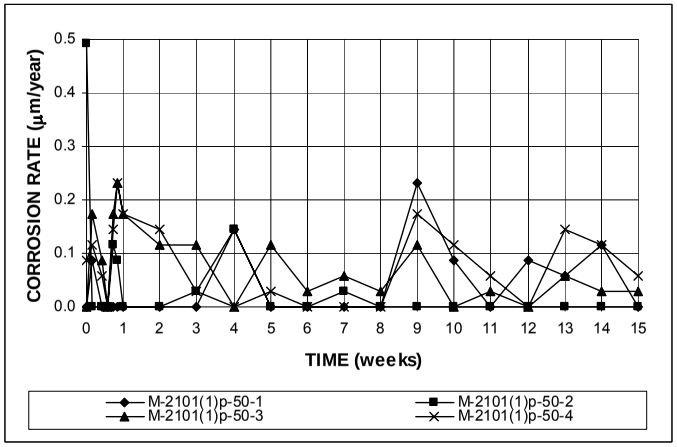


(a)

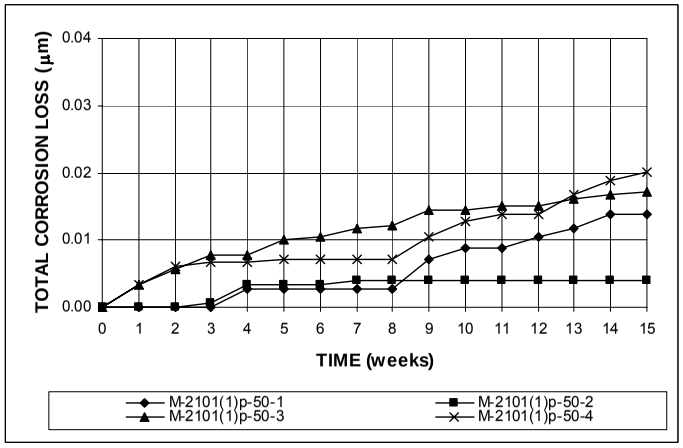


(b)

**Figure A.91 -** (a) Corrosion rates and (b) total corrosion losses as measured in the rapid macrocell test for mortar-wrapped specimens with 2101(1) pickled duplex steel in 1.6 m ion NaCl and simulated concrete pore solution.

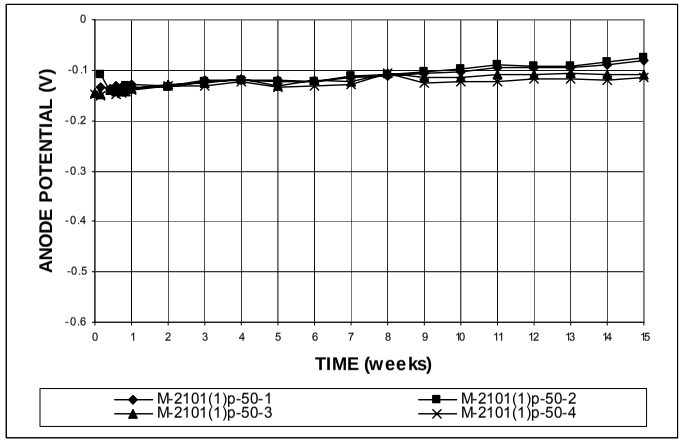


(a)

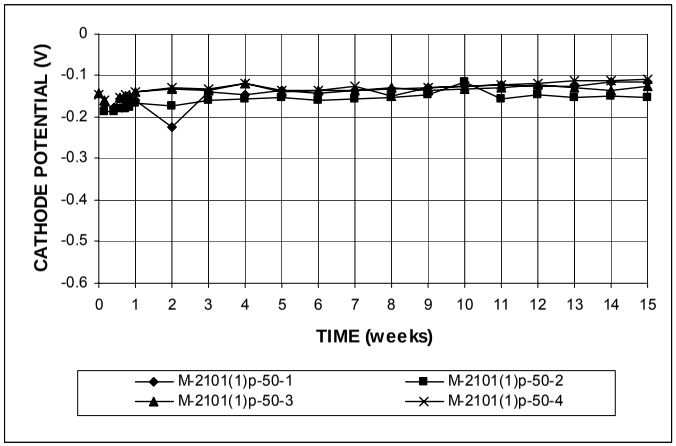


(b)

**Figure A.92 -** (a) Anode corrosion potentials and (b) cathode corrosion potentials with respect to saturated calomel electrode as measured in the rapid macrocell test for mortar-wrapped specimens with 2101(1) pickled duplex steel in 1.6 m ion NaCl and simulated concrete pore solution.

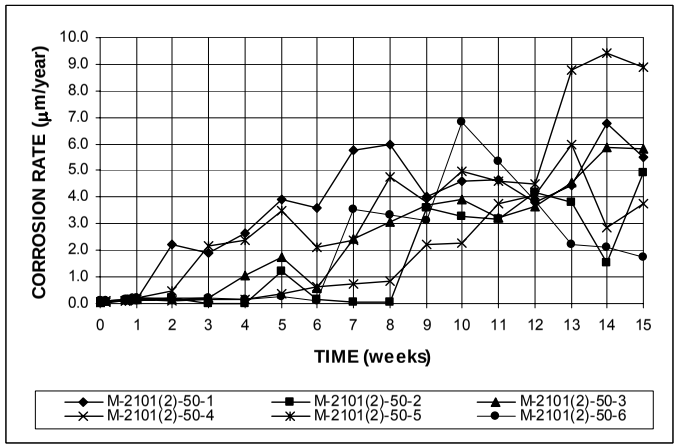


(a)

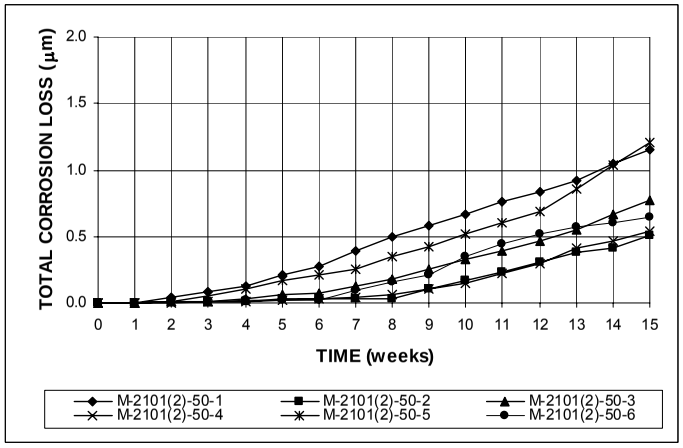


(b)

**Figure A.93 -** (a) Corrosion rates and (b) total corrosion losses as measured in the rapid macrocell test for mortar-wrapped specimens with 2101(2) duplex steel in 1.6 m ion NaCl and simulated concrete pore solution.

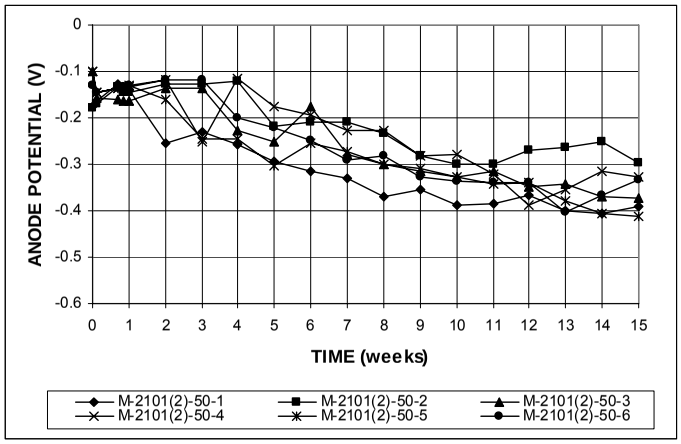


(a)

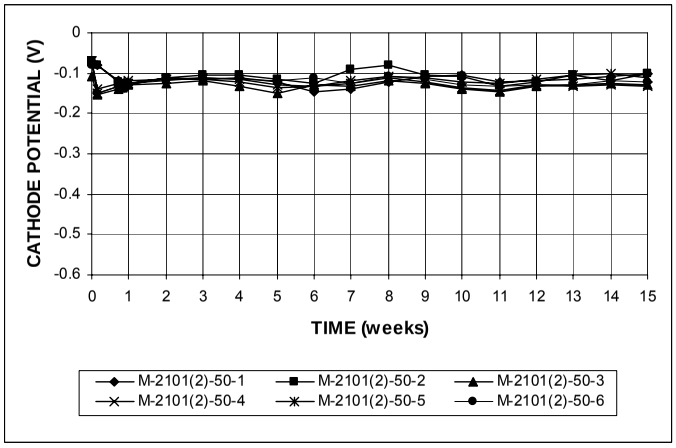


(b)

**Figure A.94 -** (a) Anode corrosion potentials and (b) cathode corrosion potentials with respect to saturated calomel electrode as measured in the rapid macrocell test for mortar-wrapped specimens with 2101(2) duplex steel in 1.6 m ion NaCl and simulated concrete pore solution.

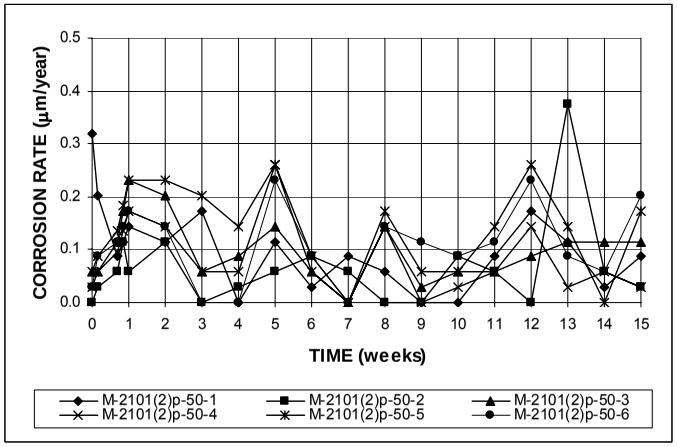


(a)

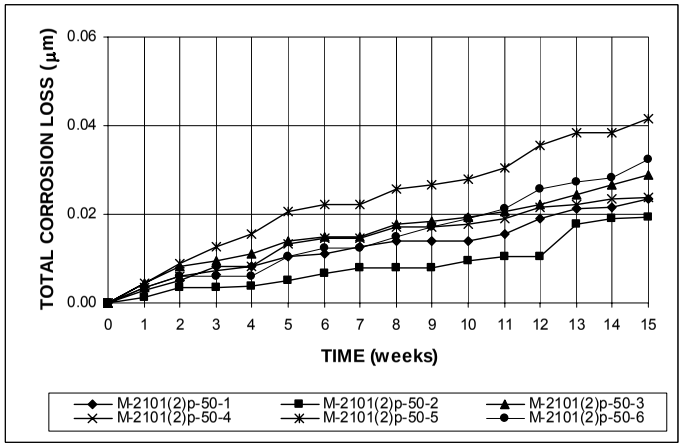


(b)

**Figure A.95 -** (a) Corrosion rates and (b) total corrosion losses as measured in the rapid macrocell test for mortar-wrapped specimens with 2101(2) pickled duplex steel in 1.6 m ion NaCl and simulated concrete pore solution.

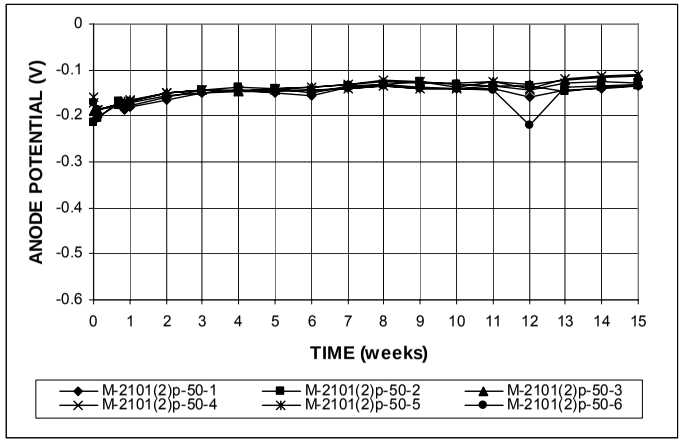


(a)

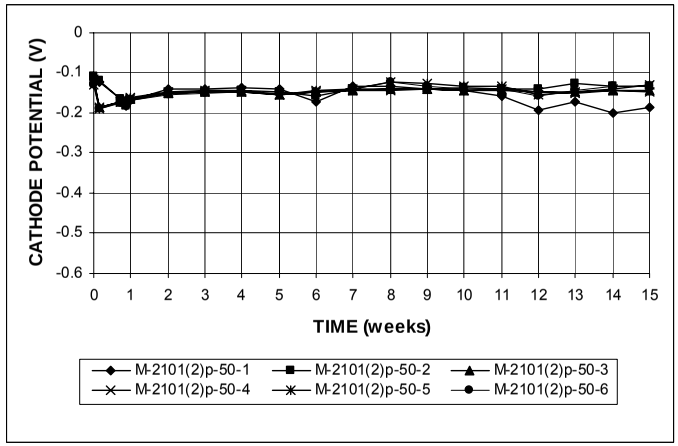


(b)

**Figure A.96 -** (a) Anode corrosion potentials and (b) cathode corrosion potentials with respect to saturated calomel electrode as measured in the rapid macrocell test for mortar-wrapped specimens with 2101(2) pickled duplex steel in 1.6 m ion NaCl and simulated concrete pore solution.

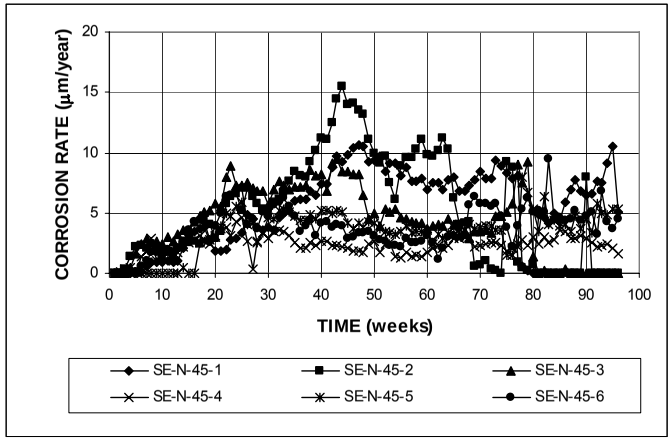


(a)

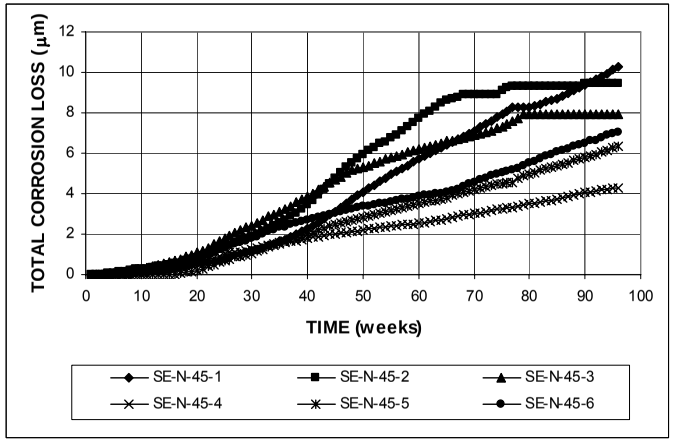


(b)

**Figure A.97 -** (a) Corrosion rates and (b) total corrosion losses as measured in the Southern Exposure test for specimens with conventional normalized steel (N).

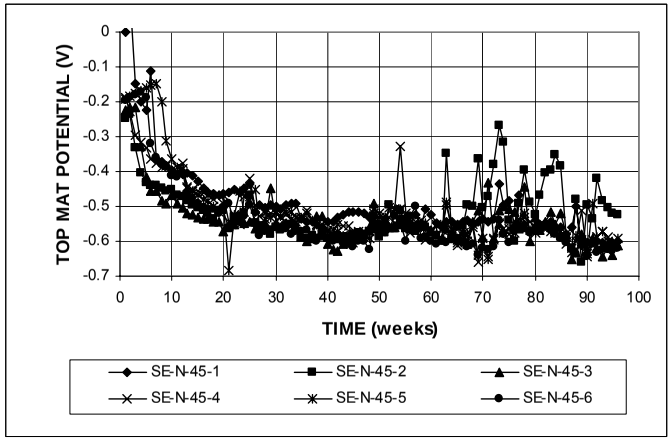


(a)

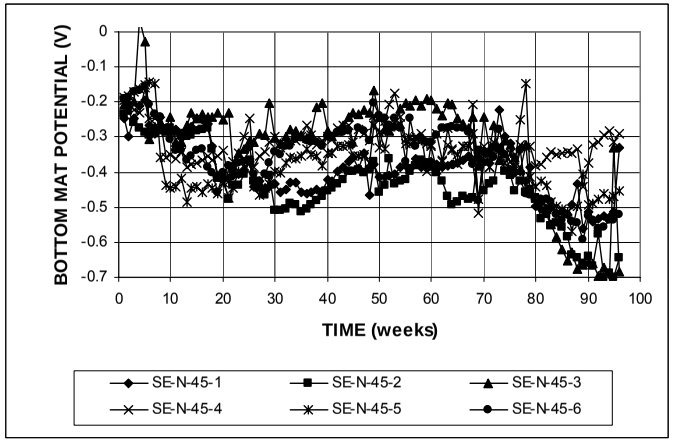


(b)

**Figure A.98 -** (a) Top mat corrosion potentials and (b) bottom mat corrosion potentials, with respect to copper-copper sulfate electrode as measured in the Southern Exposure test for specimens with conventional normalized steel (N).

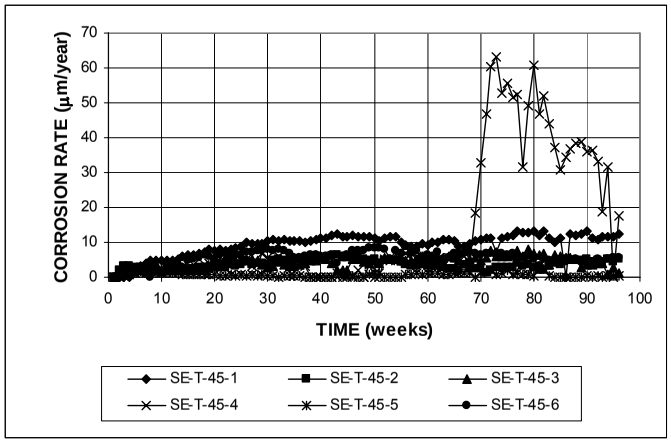


(a)

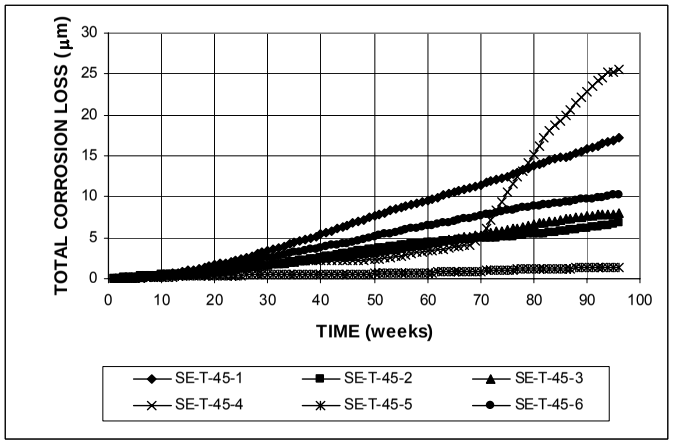


(b)

**Figure A.99 -** (a) Corrosion rates and (b) total corrosion losses as measured in the Southern Exposure test for specimens with conventional Thermex-treated steel (T).

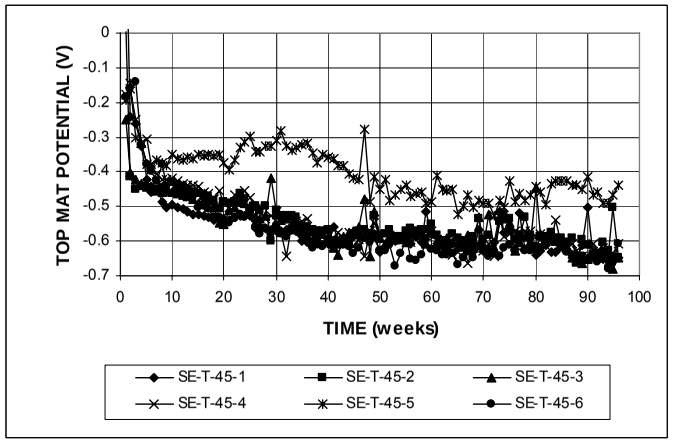


(a)

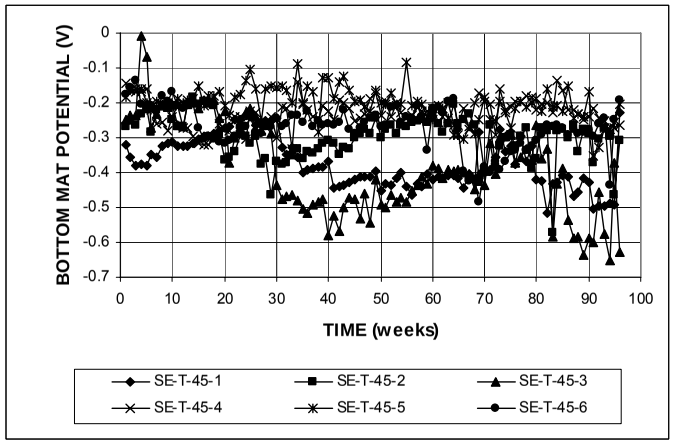


(b)

**Figure A.100 -** (a) Top mat corrosion potentials and (b) bottom mat corrosion potentials, with respect to copper-copper sulfate electrode as measured in the Southern Exposure test for specimens with conventional Thermex-treated steel (T).

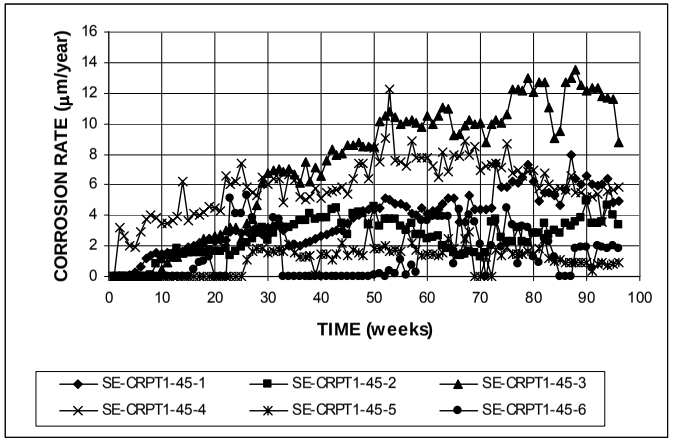


(a)

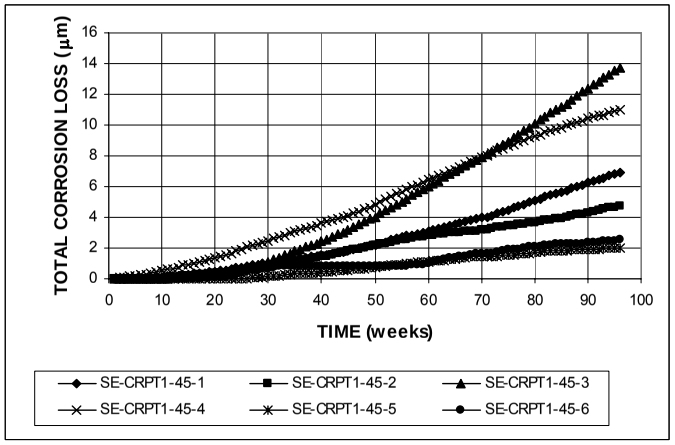


(b)

**Figure A.101** - (a) Corrosion rates and (b) total corrosion losses as measured in the Southern Exposure test for specimens with microalloyed steel with a high phosphorus content, 0.117%, Thermex-treated (CRPT1).

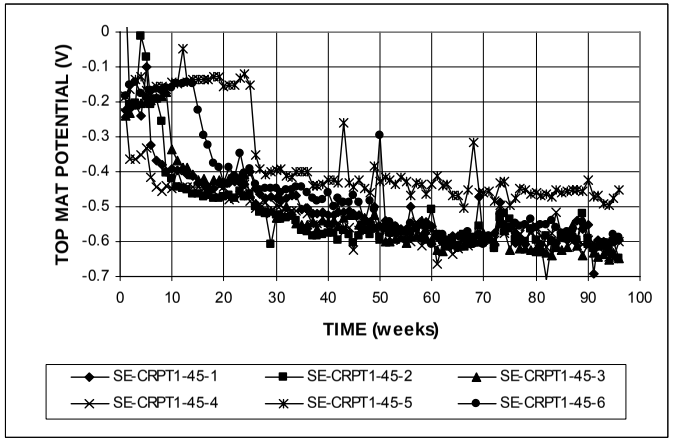


(a)

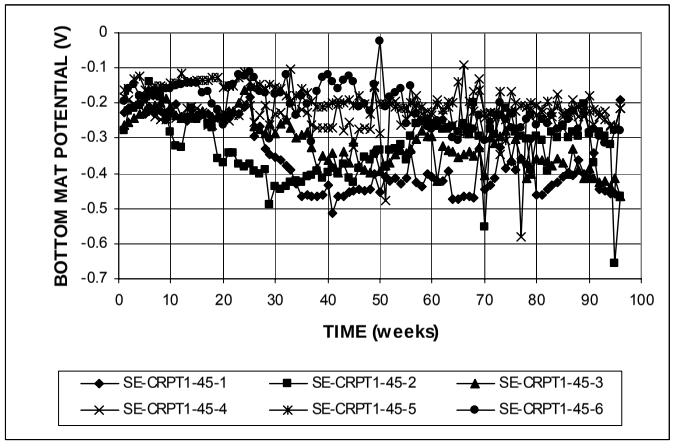


(b)

**Figure A.102** - (a) Top mat corrosion potentials and (b) bottom mat corrosion potentials, with respect to copper-copper sulfate electrode as measured in the Southern Exposure test for specimens with microalloyed steel with a high phosphorus content, 0.117%, Thermex-treated (CRPT1).

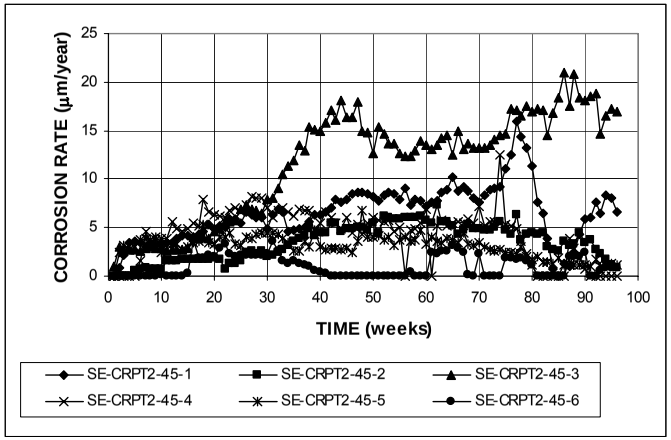


(a)

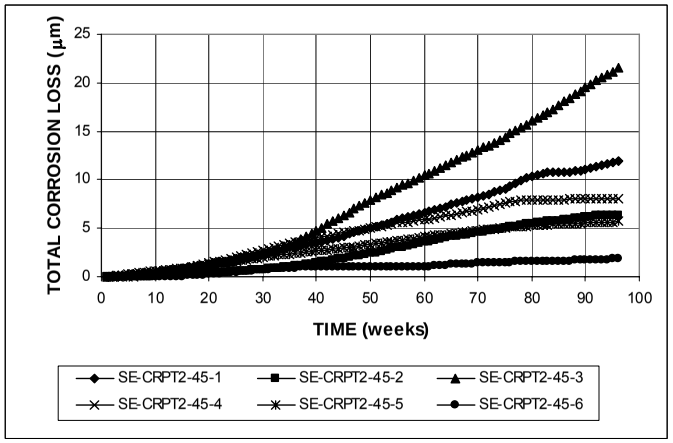


(b)

**Figure A.103 -** (a) Corrosion rates and (b) total corrosion losses as measured in the Southern Exposure test for specimens with microalloyed steel with a high phosphorus content, 0.100%, Thermex-treated (CRPT2).

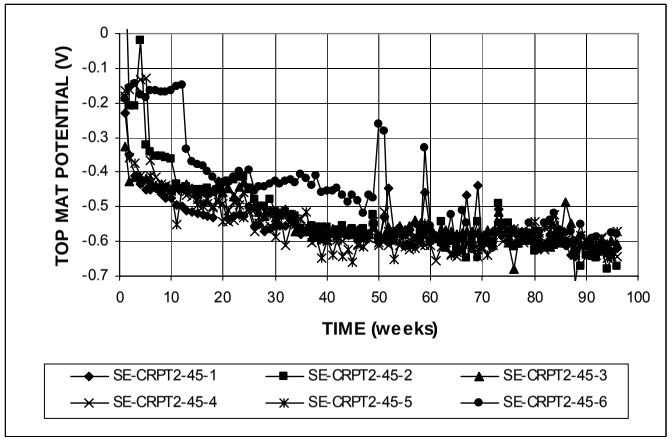


(a)

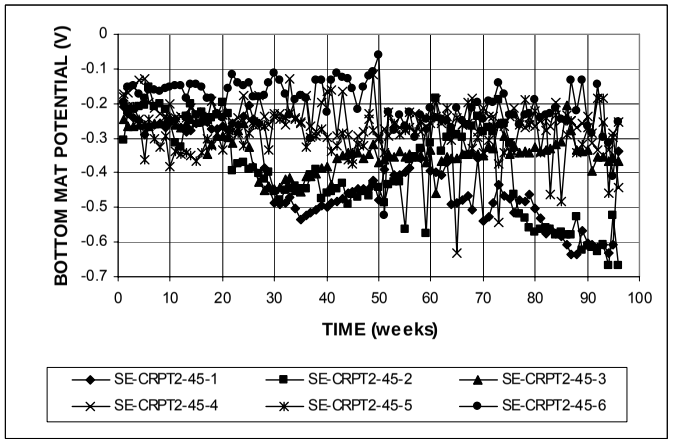


(b)

**Figure A.104 -** (a) Top mat corrosion potentials and (b) bottom mat corrosion potentials, with respect to copper-copper sulfate electrode as measured in the Southern Exposure test for specimens with microalloyed steel with a high phosphorus content, 0.100%, Thermex-treated (CRPT2).

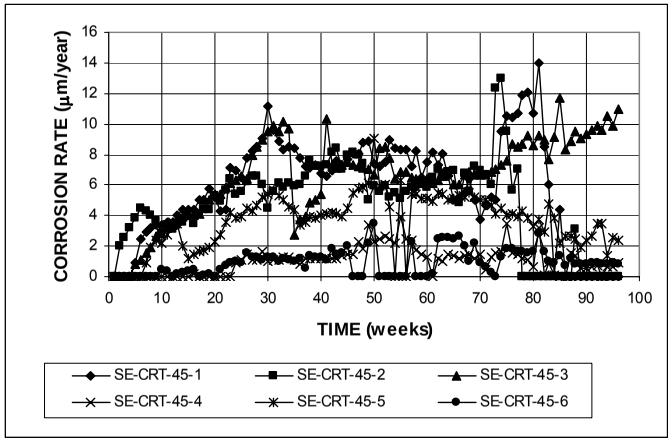


(a)

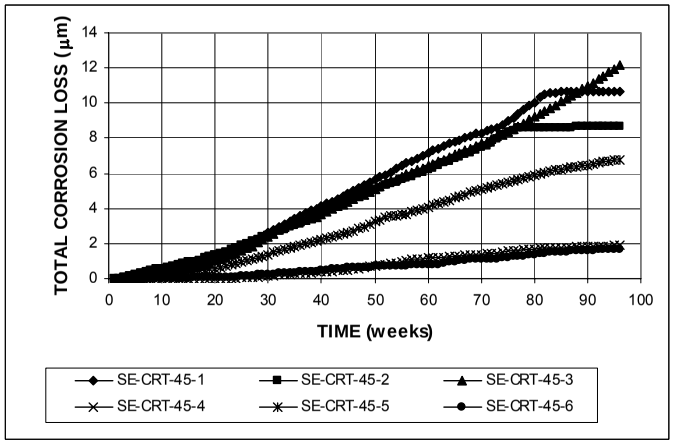


(b)

**Figure A.105 -** (a) Corrosion rates and (b) total corrosion losses as measured in the Southern Exposure test for specimens with microalloyed steel with normal phosphorus content, 0.017%, Thermex-treated (CRT).

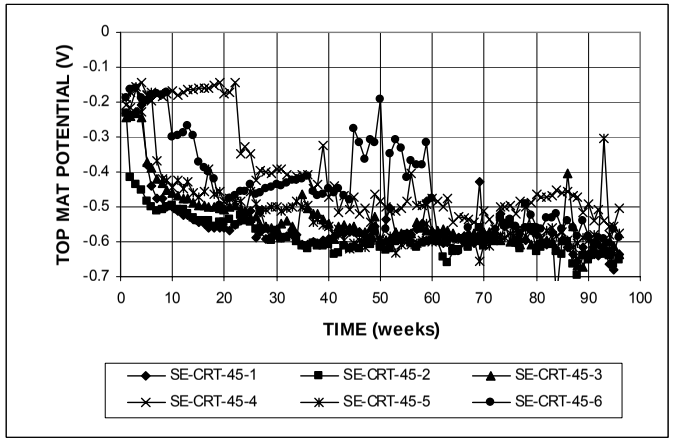


(a)

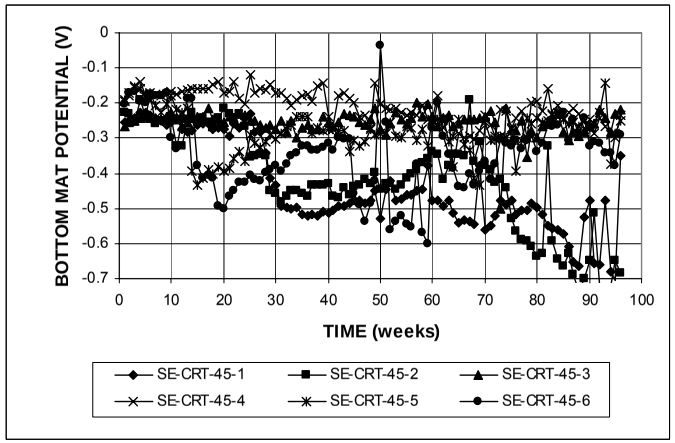


(b)

**Figure A.106 -** (a) Top mat corrosion potentials and (b) bottom mat corrosion potentials, with respect to copper-copper sulfate electrode as measured in the Southern Exposure test for specimens with microalloyed steel with normal phosphorus content, 0.017%, Thermex-treated (CRT).

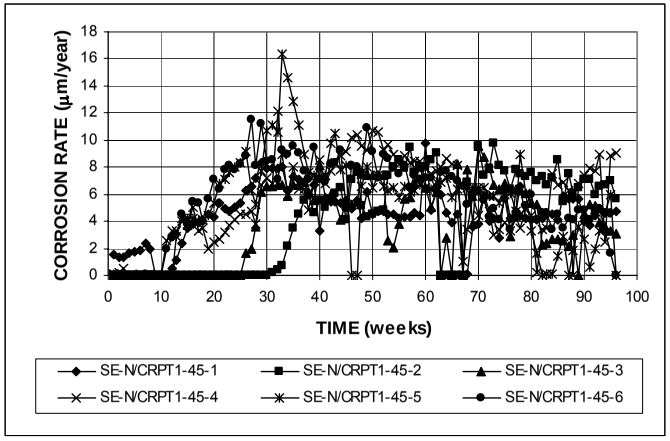


(a)

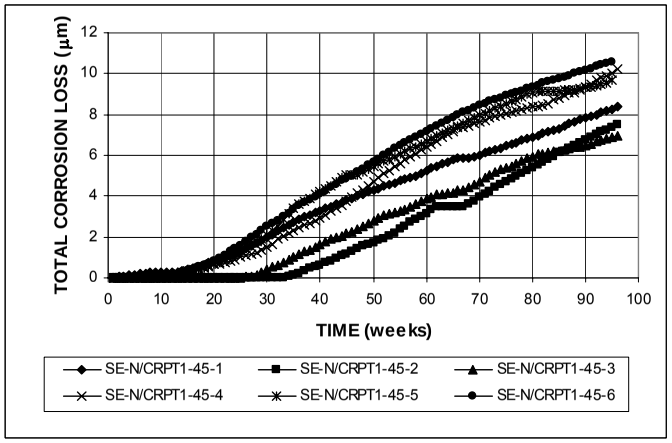


(b)

**Figure A.107 -** (a) Corrosion rates and (b) total corrosion losses as measured in the Southern Exposure test for specimens with conventional normalized steel (N) in the top mat and microalloyed steel with a high phosphorus content, 0.117%, Thermex-treated (CRPT1) in the bottom mat.

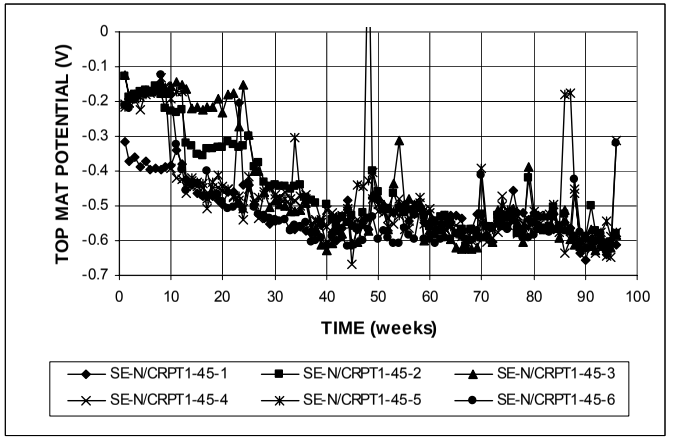


(a)

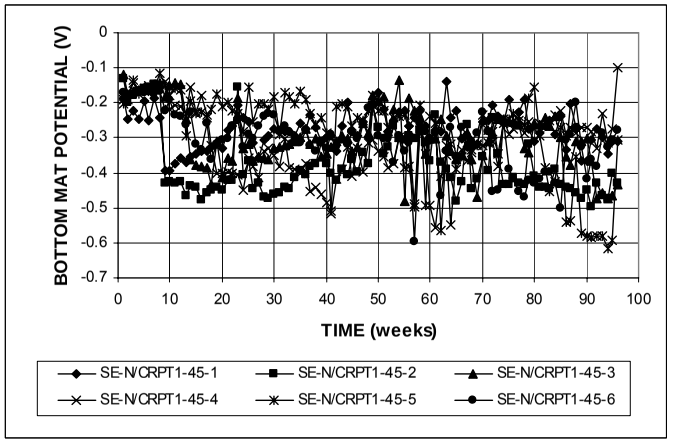


(b)

**Figure A.108 -** (a) Top mat corrosion potentials and (b) bottom mat corrosion potentials, with respect to copper-copper sulfate electrode as measured in the Southern Exposure test for specimens with conventional normalized steel (N) in the top mat and microalloyed steel with a high phosphorus content, 0.117%, Thermex-treated (CRPT1) in the bottom mat.

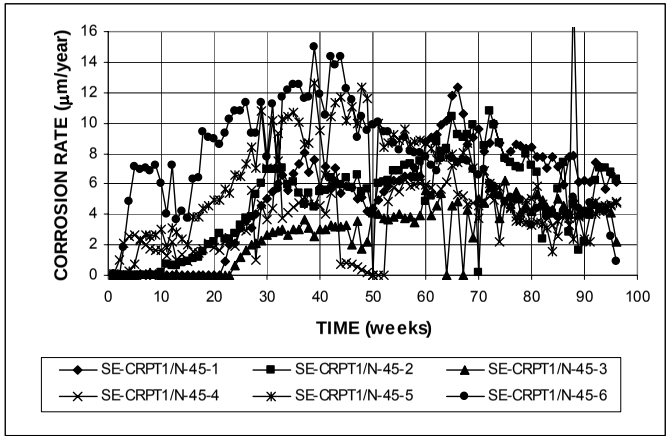


(a)

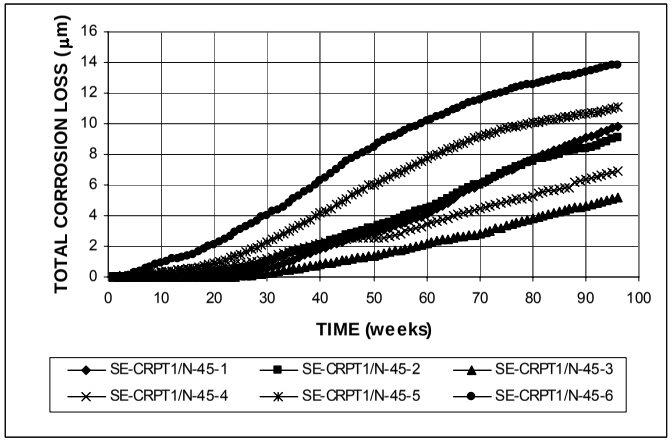


(b)

**Figure A.109 -** (a) Corrosion rates and (b) total corrosion losses as measured in the Southern Exposure test for specimens with microalloyed steel with a high phosphorus content, 0.117%, Thermex-treated (CRPT1) in the top mat and conventional normalized steel (N) in the bottom mat.

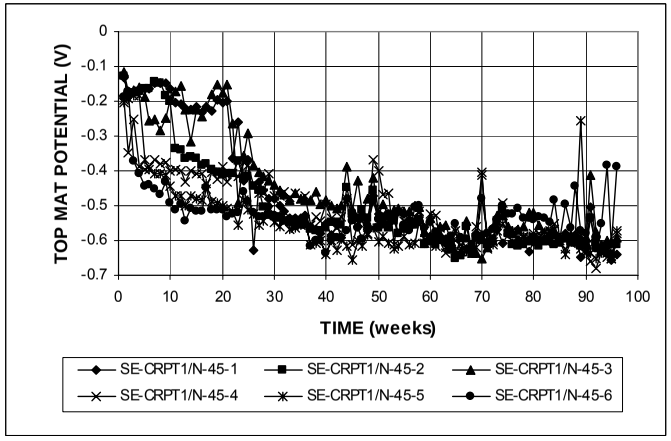


(a)

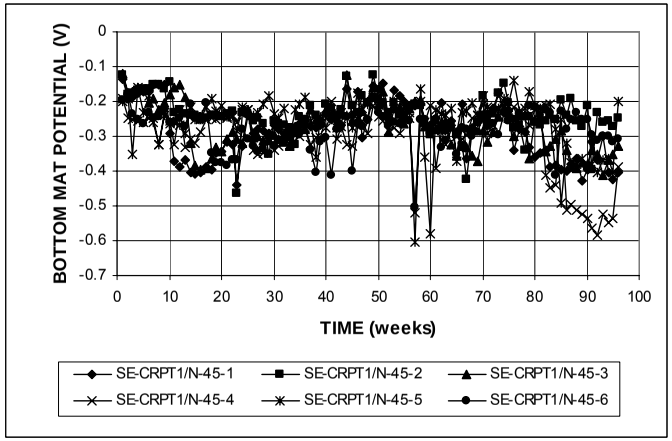


(b)

**Figure A.110 -** (a) Top mat corrosion potentials and (b) bottom mat corrosion potentials, with respect to copper-copper sulfate electrode as measured in the Southern Exposure test for specimens with microalloyed steel with a high phosphorus content, 0.117%, Thermex-treated (CRPT1) in the top mat and conventional normalized steel (N) in the bottom mat.

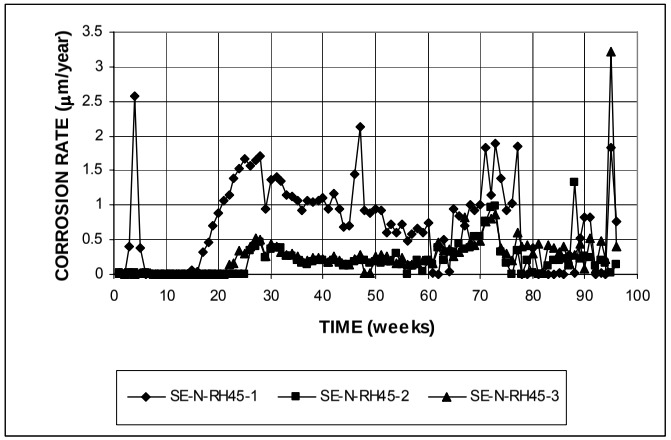


(a)

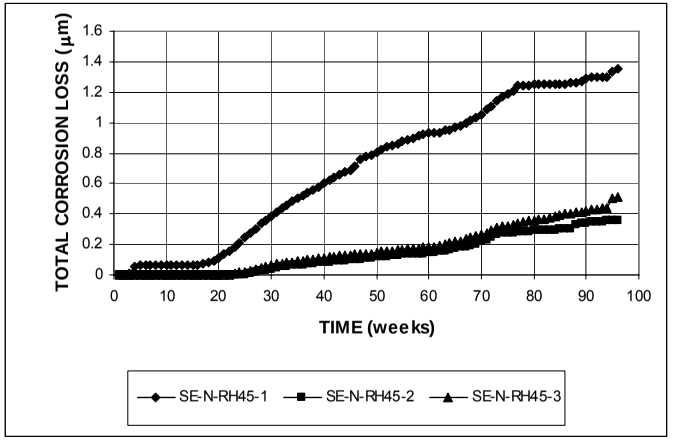


(b)

**Figure A.111 -** (a) Corrosion rates and (b) total corrosion losses as measured in the Southern Exposure test for specimens with conventional normalized steel (N), a water-cement ratio of 0.45, and Rheocrete 222+.

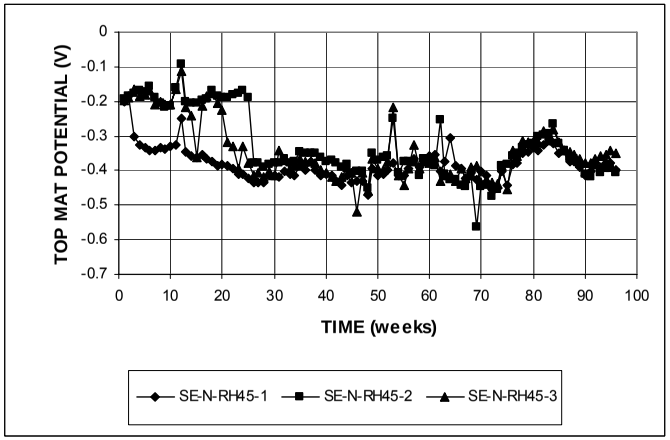


(a)

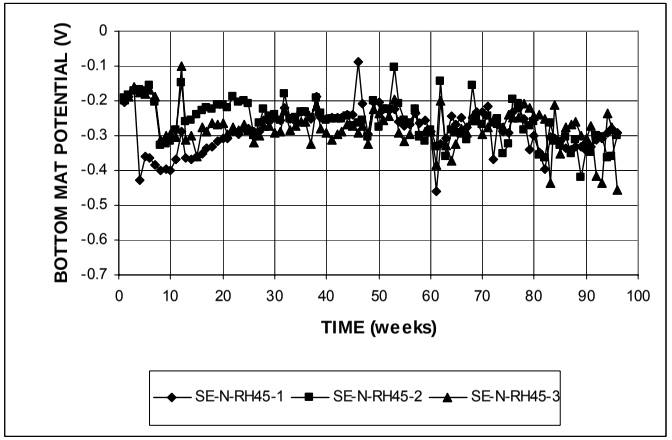


(b)

**Figure A.112 -** (a) Top mat corrosion potentials and (b) bottom mat corrosion potentials, with respect to copper-copper sulfate electrode as measured in the Southern Exposure test for specimens with conventional normalized steel (N), a water-cement ratio of 0.45, and Rheocrete 222+.

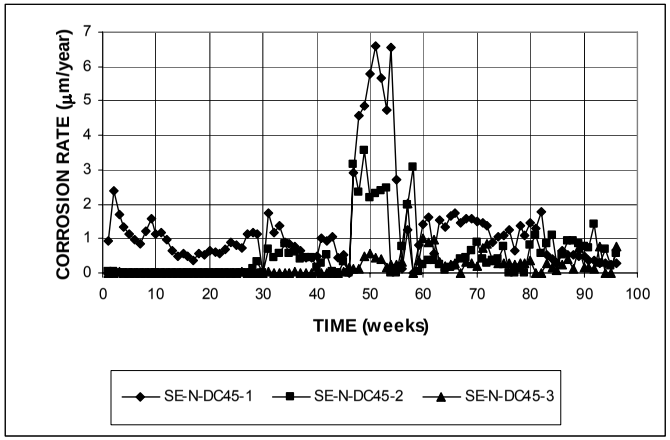


(a)

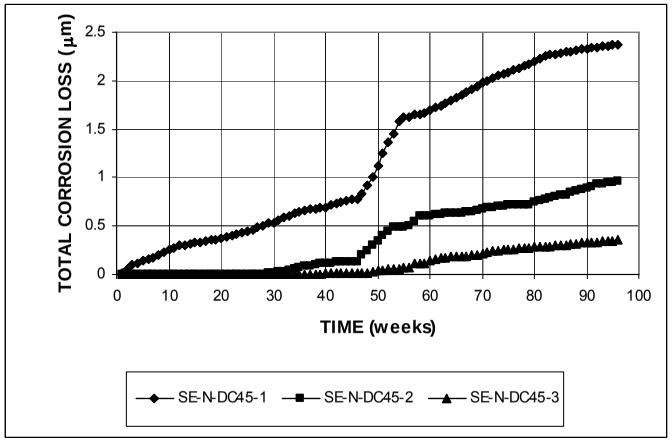


(b)

**Figure A.113 -** (a) Corrosion rates and (b) total corrosion losses as measured in the Southern Exposure test for specimens with conventional normalized steel (N), a water-cement ratio of 0.45, and DCI-S.

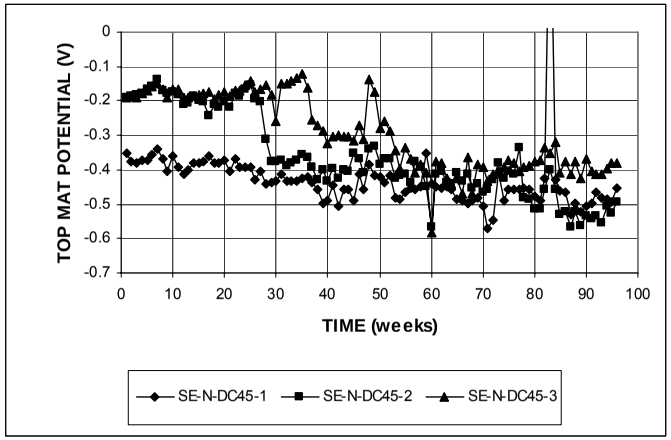


(a)

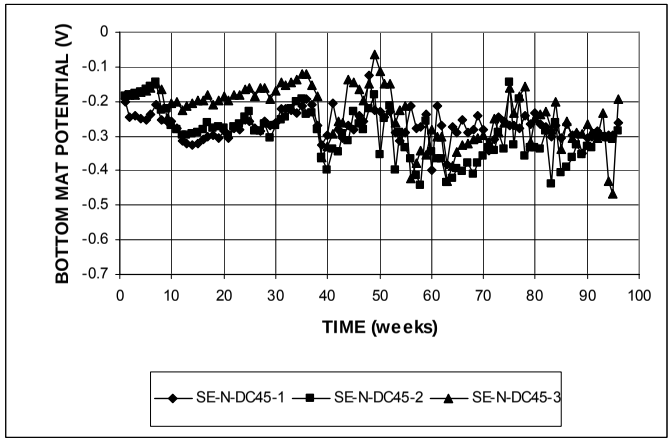


(b)

**Figure A.114 -** (a) Top mat corrosion potentials and (b) bottom mat corrosion potentials, with respect to copper-copper sulfate electrode as measured in the Southern Exposure test for specimens with conventional normalized steel (N), a water-cement ratio of 0.45, and DCI-S.

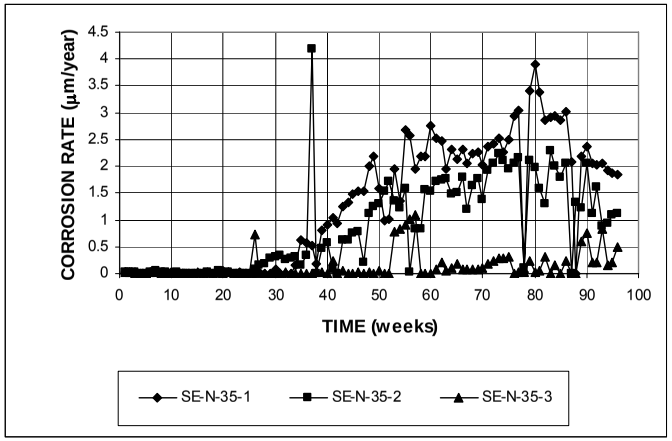


(a)

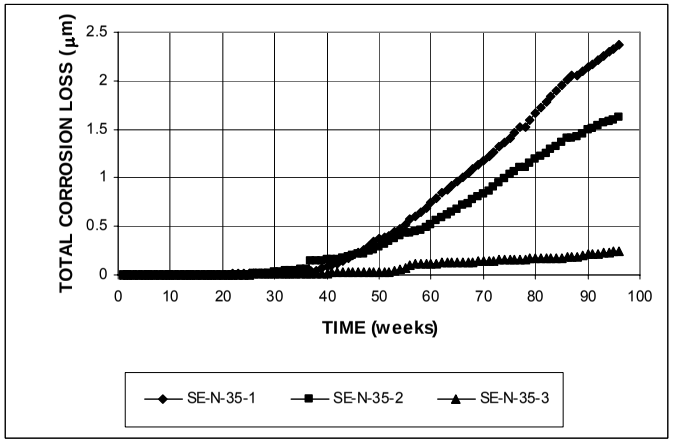


(b)

**Figure A.115 -** (a) Corrosion rates and (b) total corrosion losses as measured in the Southern Exposure test for specimens with conventional normalized steel (N), a water-cement ratio of 0.35, and no inhibitor.

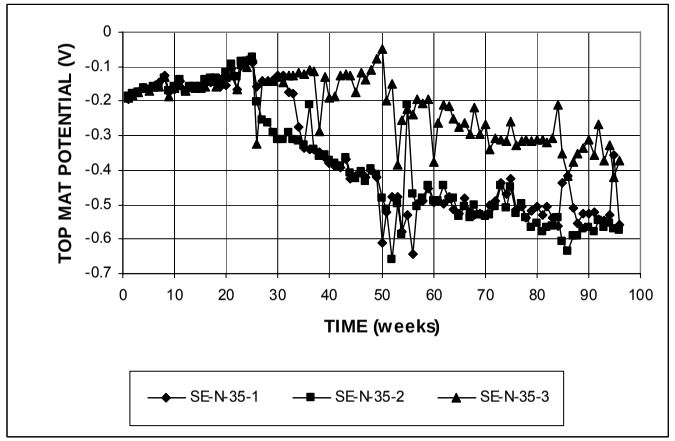


(a)

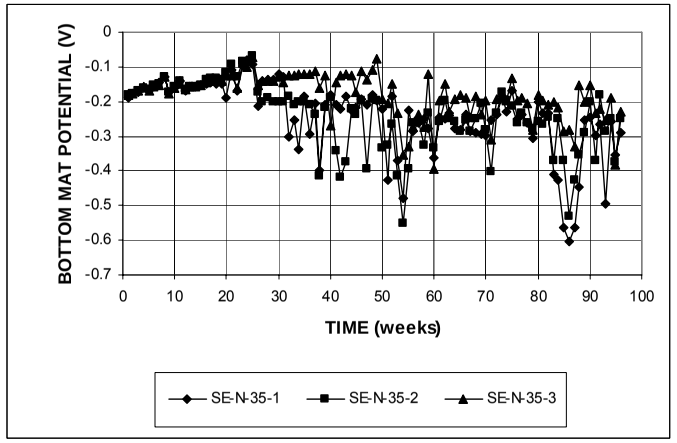


(b)

**Figure A.116 -** (a) Top mat corrosion potentials and (b) bottom mat corrosion potentials, with respect to copper-copper sulfate electrode as measured in the Southern Exposure test for specimens with conventional normalized steel (N), a water-cement ratio of 0.35, and no inhibitor.

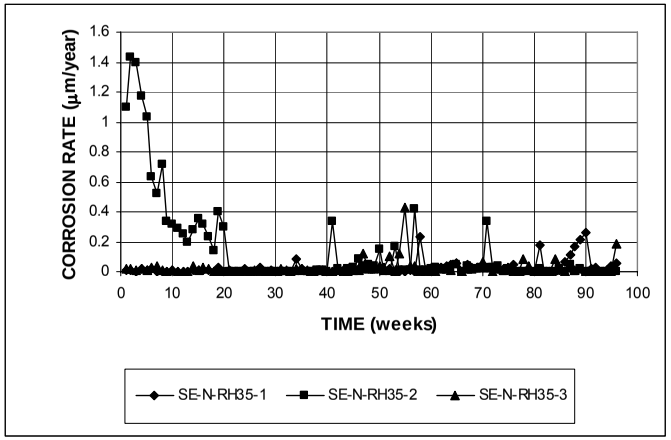


(a)

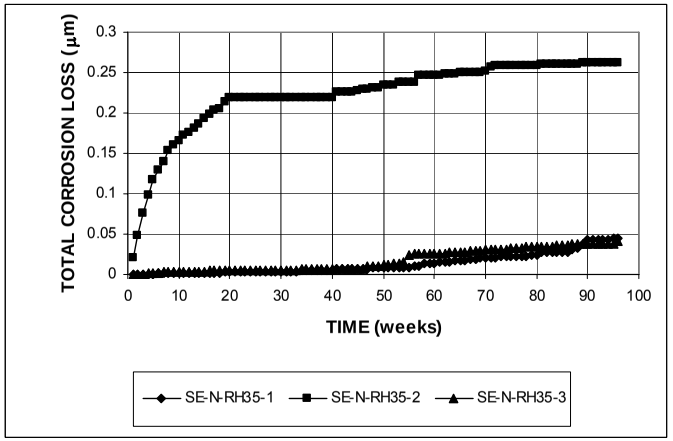


(b)

**Figure A.117 -** (a) Corrosion rates and (b) total corrosion losses as measured in the Southern Exposure test for specimens with conventional normalized steel (N), a water-cement ratio of 0.35, and Rheocrete 222+.

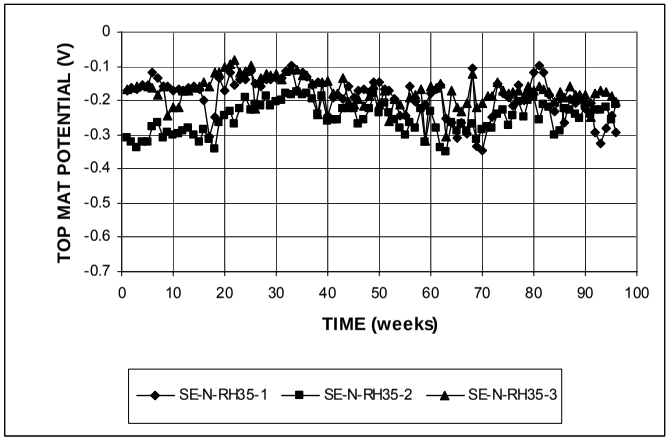


(a)

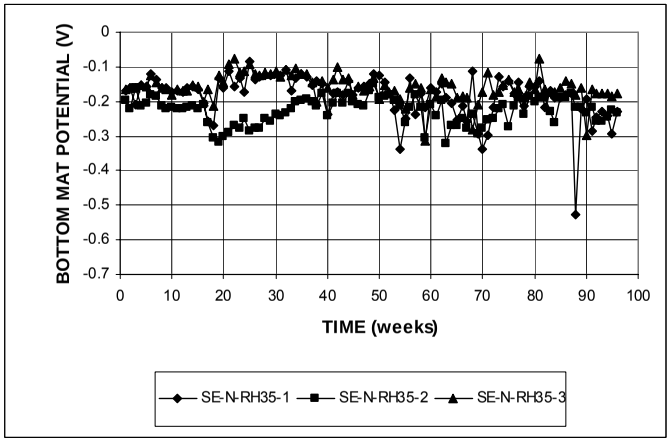


(b)

**Figure A.118 -** (a) Top mat corrosion potentials and (b) bottom mat corrosion potentials, with respect to copper-copper sulfate electrode as measured in the Southern Exposure test for specimens with conventional normalized steel (N), a water-cement ratio of 0.35, and Rheocrete 222+.

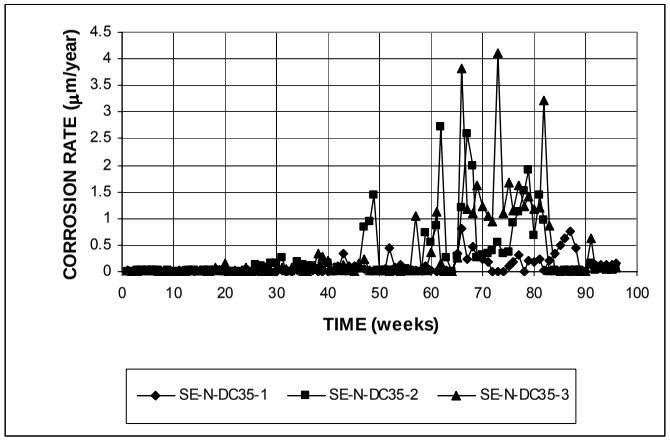


(a)

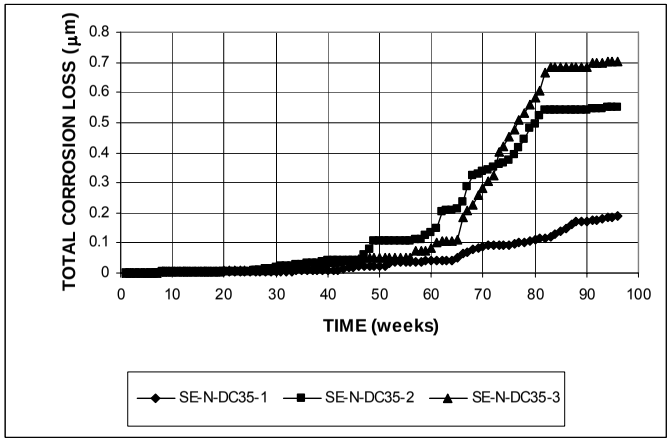


(b)

**Figure A.119 -** (a) Corrosion rates and (b) total corrosion losses as measured in the Southern Exposure test for specimens with conventional normalized steel (N), a water-cement ratio of 0.35, and DCI-S.

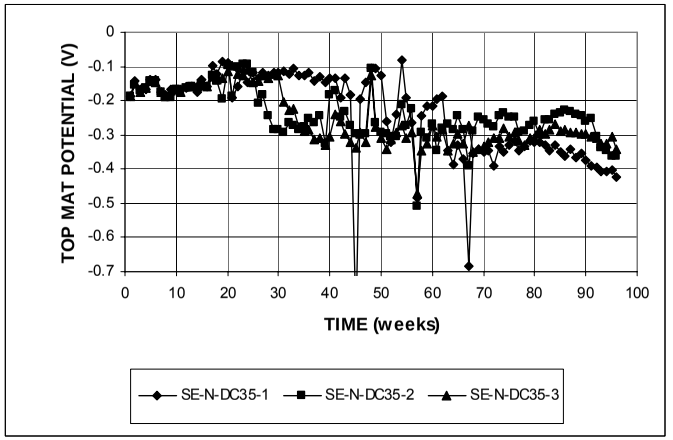


(a)

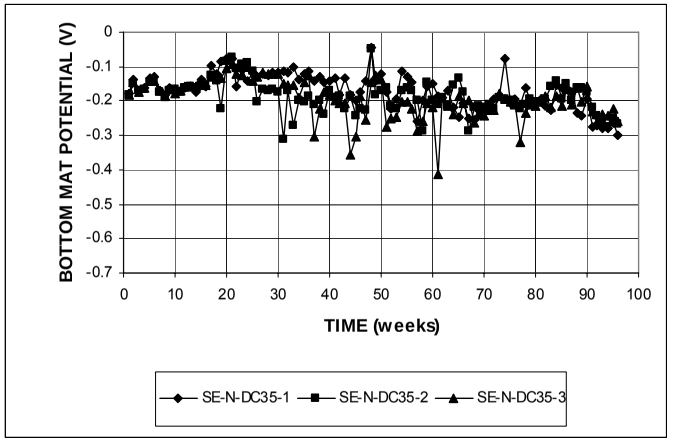


(b)

**Figure A.120 -** (a) Top mat corrosion potentials and (b) bottom mat corrosion potentials, with respect to copper-copper sulfate electrode as measured in the Southern Exposure test for specimens with conventional normalized steel (N), a water-cement ratio of 0.35, and DCI-S.

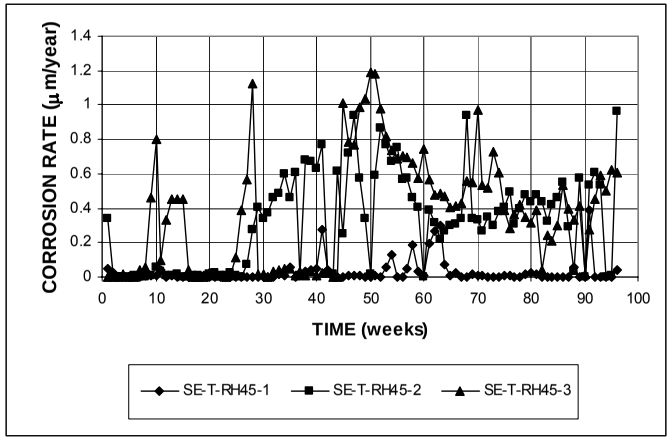


(a)

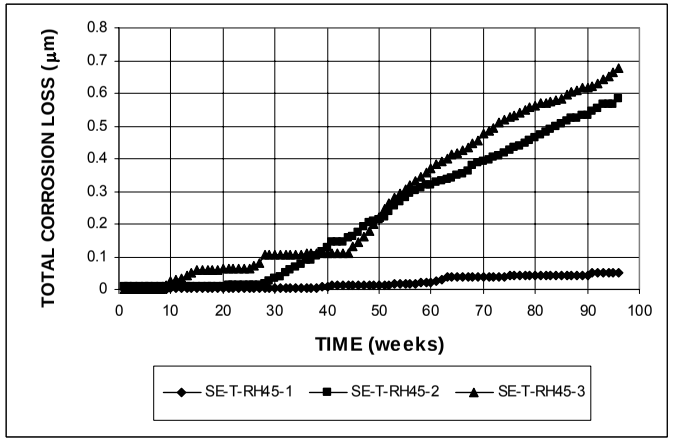


(b)

**Figure A.121 -** (a) Corrosion rates and (b) total corrosion losses as measured in the Southern Exposure test for specimens with conventional Thermex-treated steel (T), a water-cement ratio of 0.45, and Rheocrete 222+.

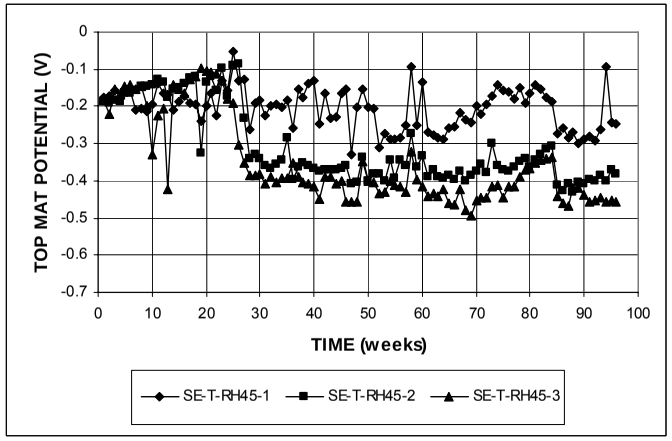


(a)

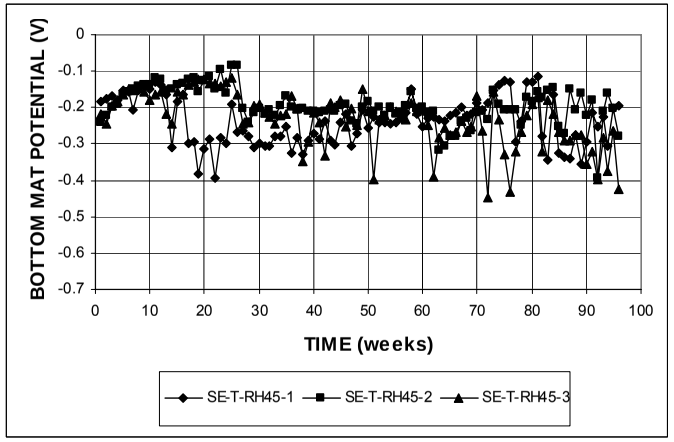


(b)

**Figure A.122 -** (a) Top mat corrosion potentials and (b) bottom mat corrosion potentials, with respect to copper-copper sulfate electrode as measured in the Southern Exposure test for specimens with conventional Thermex-treated steel (T), a water-cement ratio of 0.45, and Rheocrete 222+.

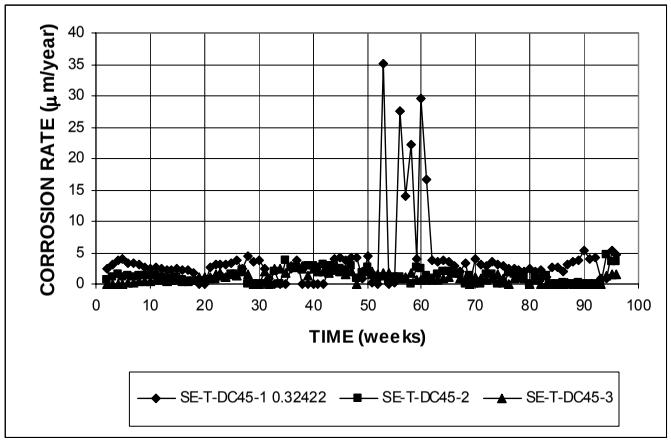


(a)

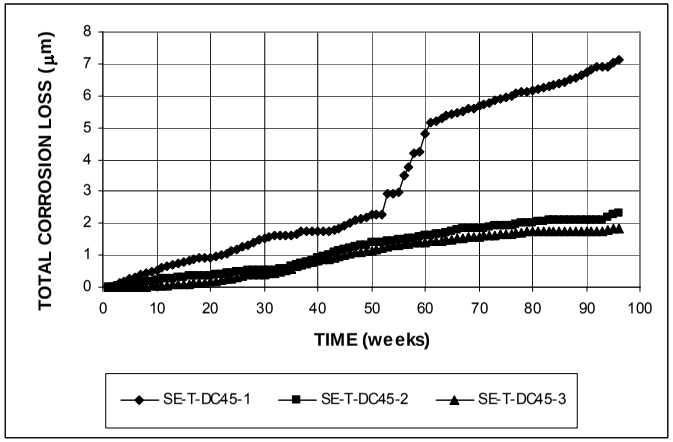


(b)

**Figure A.123 -** (a) Corrosion rates and (b) total corrosion losses as measured in the Southern Exposure test for specimens with conventional Thermex-treated steel (T), a water-cement ratio of 0.45, and DCI-S.

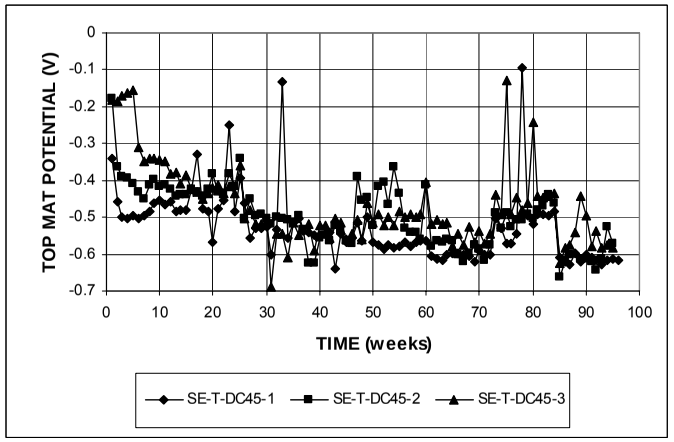


(a)

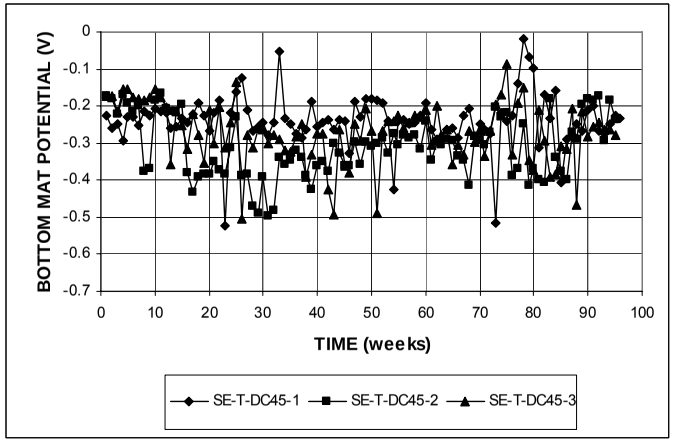


(b)

**Figure A.124 -** (a) Top mat corrosion potentials and (b) bottom mat corrosion potentials, with respect to copper-copper sulfate electrode as measured in the Southern Exposure test for specimens with conventional Thermex-treated steel (T), a water-cement ratio of 0.45, and DCI-S.

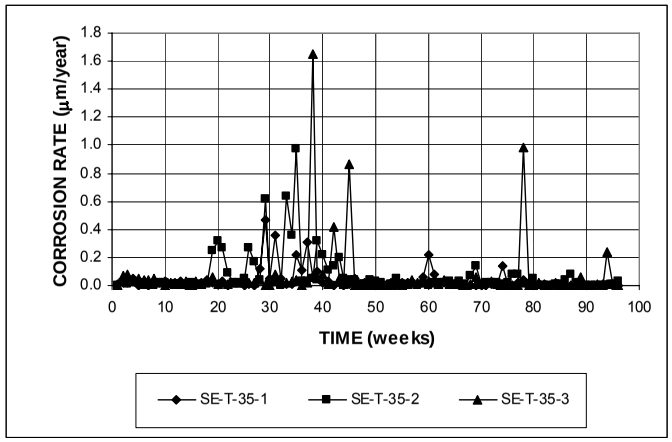


(a)

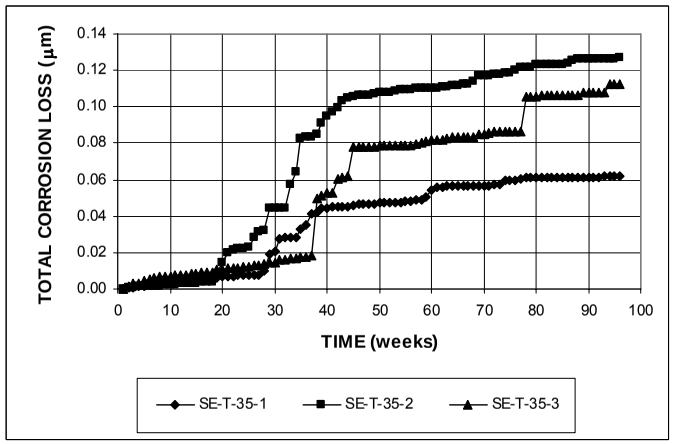


(b)

**Figure A.125 -** (a) Corrosion rates and (b) total corrosion losses as measured in the Southern Exposure test for specimens with conventional Thermex-treated steel (T), a water-cement ratio of 0.35, and no inhibitor.

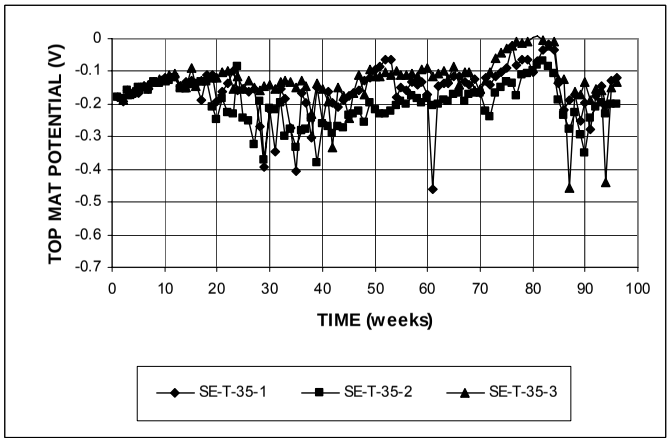


(a)

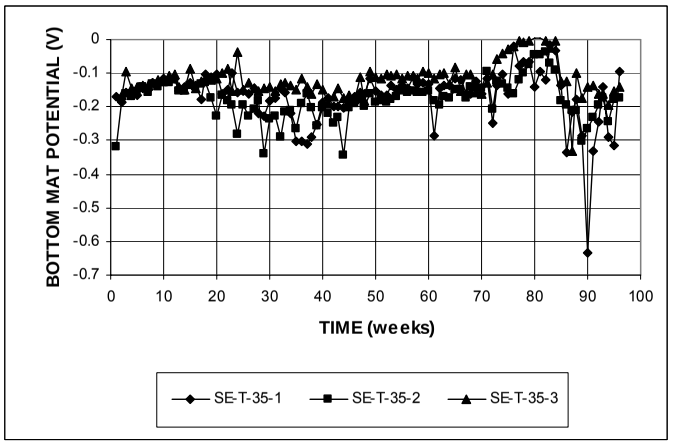


(b)

**Figure A.126 -** (a) Top mat corrosion potentials and (b) bottom mat corrosion potentials, with respect to copper-copper sulfate electrode as measured in the Southern Exposure test for specimens with conventional Thermex-treated steel (T), a water-cement ratio of 0.35, and no inhibitor.

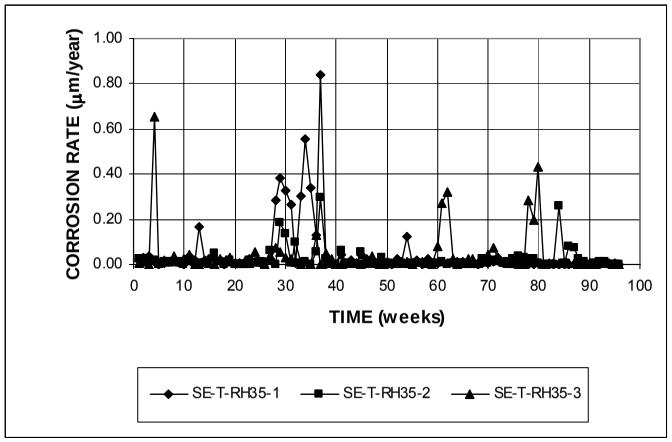


(a)

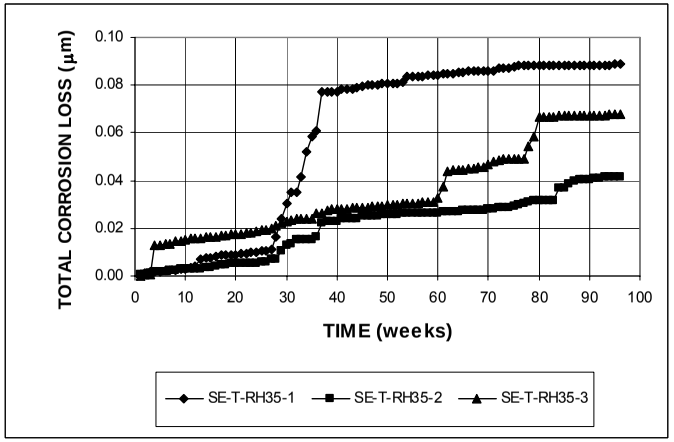


(b)

**Figure A.127 -** (a) Corrosion rates and (b) total corrosion losses as measured in the Southern Exposure test for specimens with conventional Thermex-treated steel (T), a water-cement ratio of 0.35, and Rheocrete 222+.

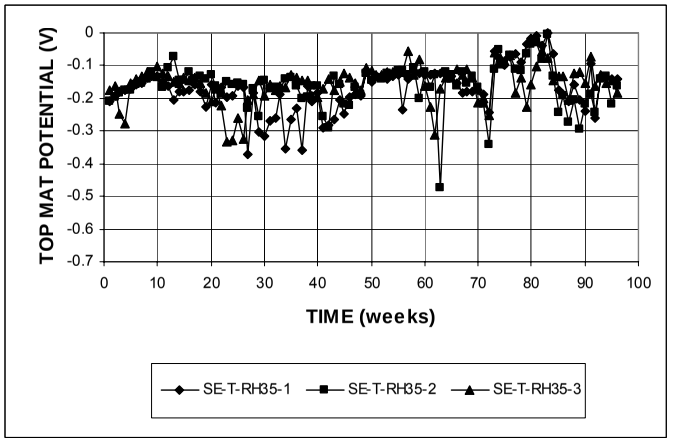


(a)

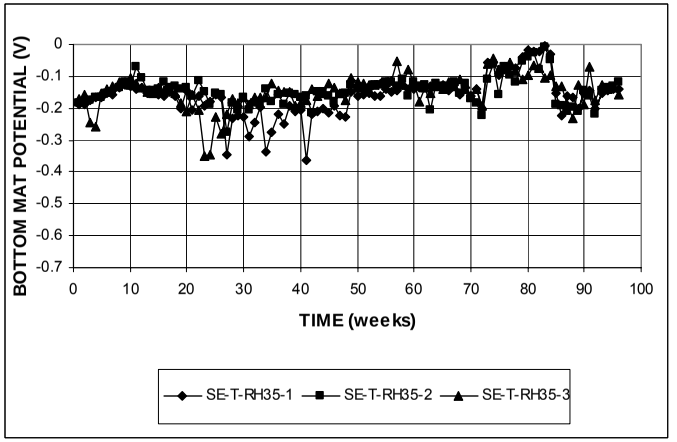


(b)

**Figure A.128 -** (a) Top mat corrosion potentials and (b) bottom mat corrosion potentials, with respect to copper-copper sulfate electrode as measured in the Southern Exposure test for specimens with conventional Thermex-treated steel (T), a water-cement ratio of 0.35, and Rheocrete 222+.

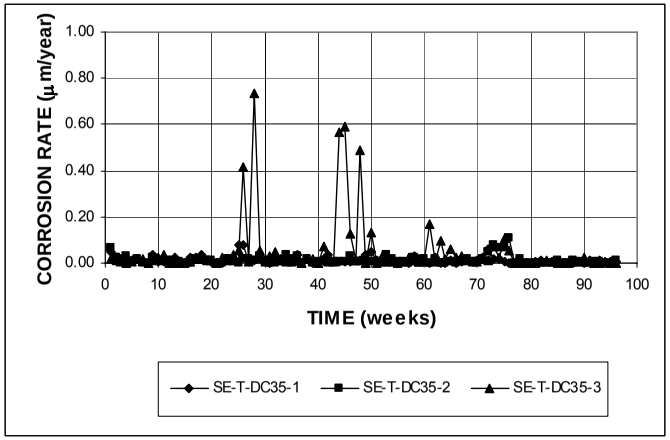


(a)

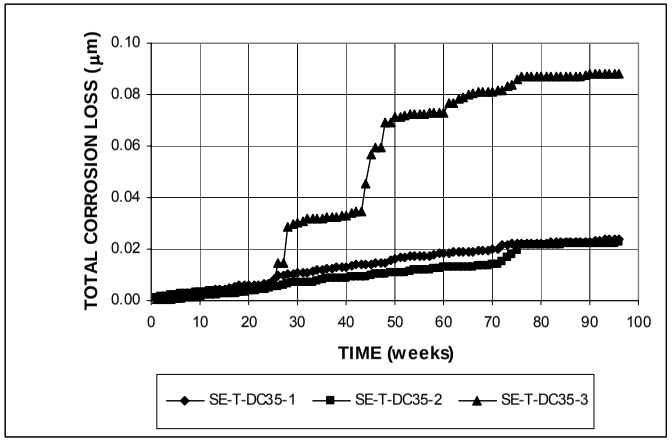


(b)

**Figure A.129 -** (a) Corrosion rates and (b) total corrosion losses as measured in the Southern Exposure test for specimens with conventional Thermex-treated steel (T), a water-cement ratio of 0.35, and DCI-S.

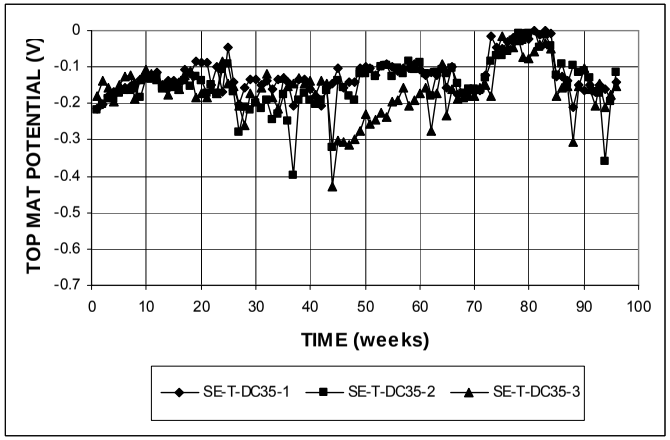


(a)

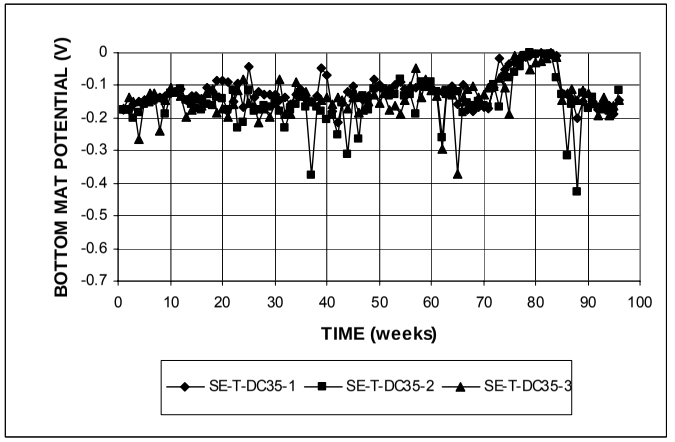


(b)

**Figure A.130 -** (a) Top mat corrosion potentials and (b) bottom mat corrosion potentials, with respect to copper-copper sulfate electrode as measured in the Southern Exposure test for specimens with conventional Thermex-treated steel (T), a water-cement ratio of 0.35, and DCI-S.

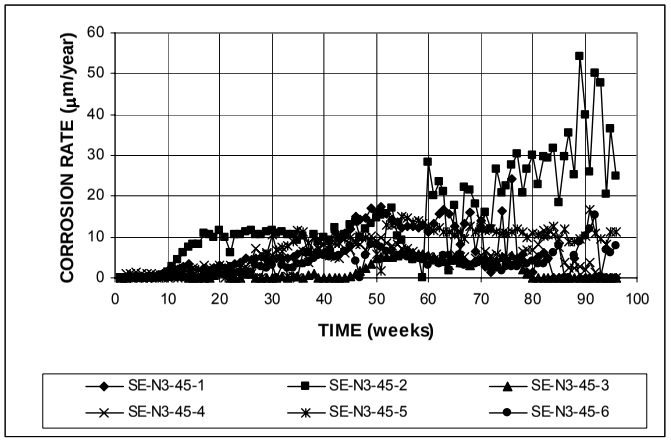


(a)

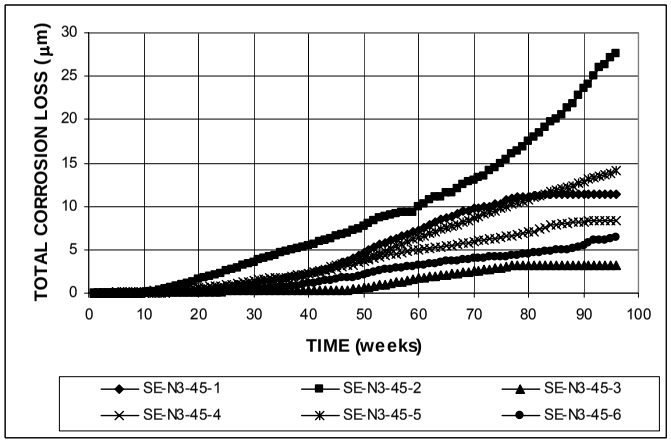


(b)

**Figure A.131 -** (a) Corrosion rates and (b) total corrosion losses as measured in the Southern Exposure test for specimens with conventional normalized steel (N3).

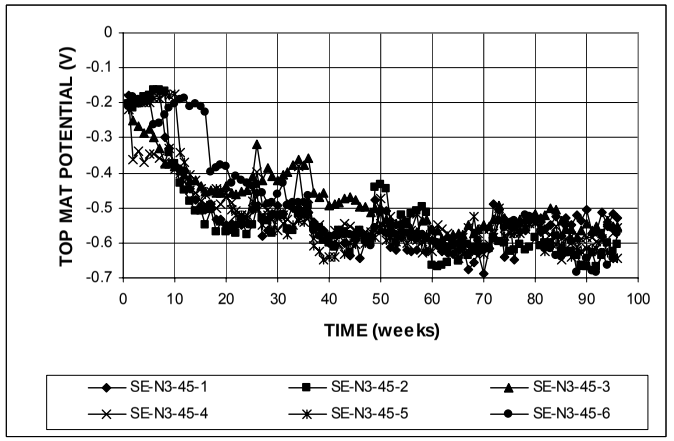


(a)

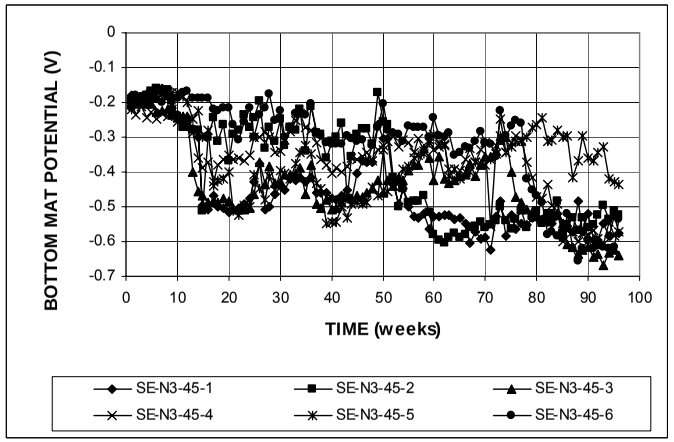


(b)

**Figure A.132 -** (a) Top mat corrosion potentials and (b) bottom mat corrosion potentials, with respect to copper-copper sulfate electrode as measured in the Southern Exposure test for specimens with conventional normalized steel (N3).

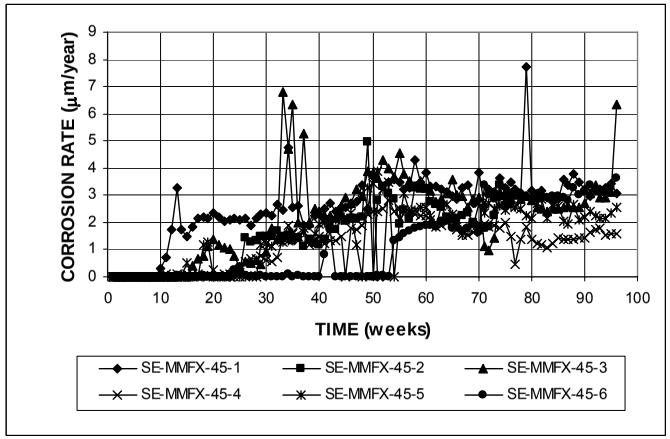


(a)

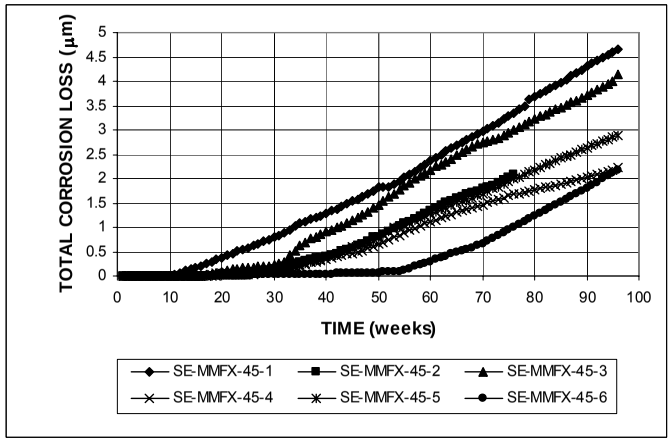


(b)

**Figure A.133 -** (a) Corrosion rates and (b) total corrosion losses as measured in the Southern Exposure test for specimens with MMFX microcomposite steel.

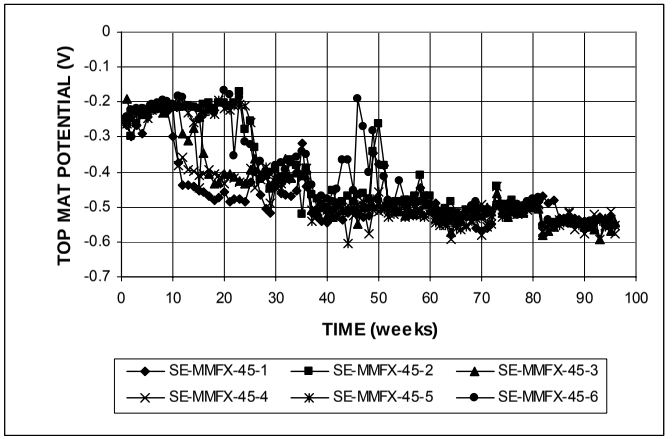


(a)

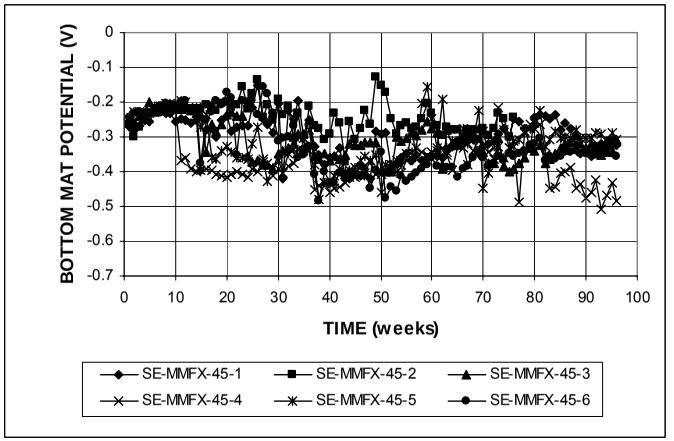


(b)

**Figure A.134 -** (a) Top mat corrosion potentials and (b) bottom mat corrosion potentials, with respect to copper-copper sulfate electrode as measured in the Southern Exposure test for specimens with MMFX microcomposite steel.

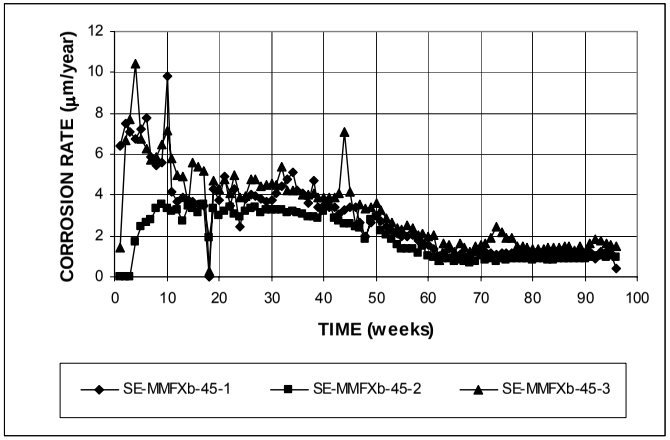


(a)

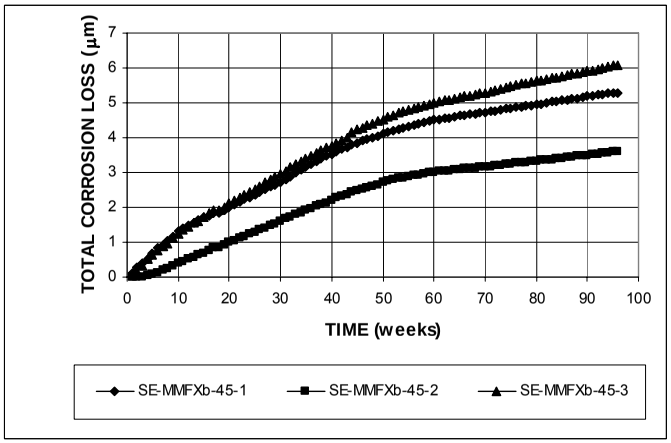


(b)

**Figure A.135 -** (a) Corrosion rates and (b) total corrosion losses as measured in the Southern Exposure test for specimens with MMFX microcomposite steel with bent bars in the top mat.

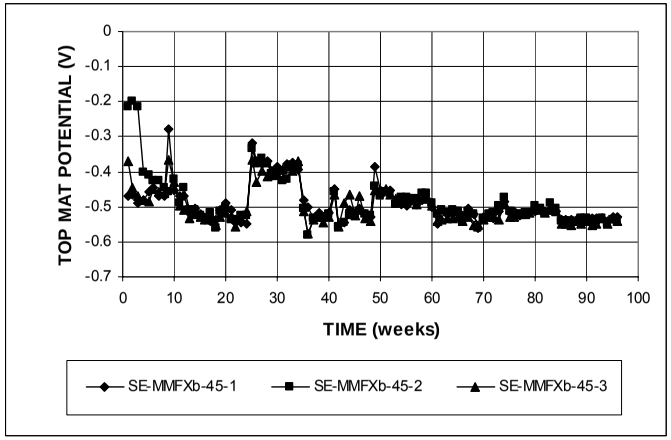


(a)

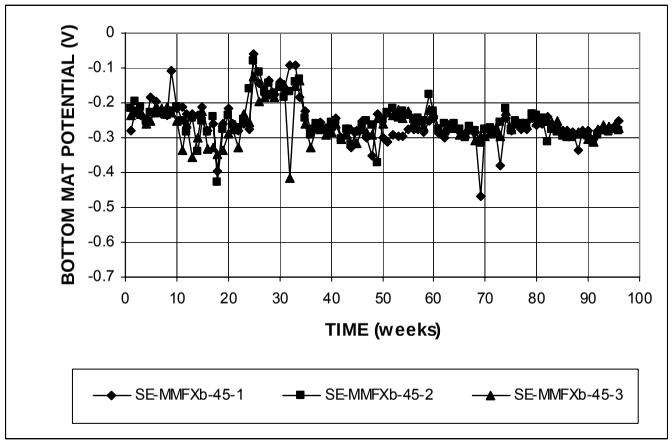


(b)

**Figure A.136 -** (a) Top mat corrosion potentials and (b) bottom mat corrosion potentials, with respect to copper-copper sulfate electrode as measured in the Southern Exposure test for specimens with MMFX microcomposite steel with bent bars in the top mat.

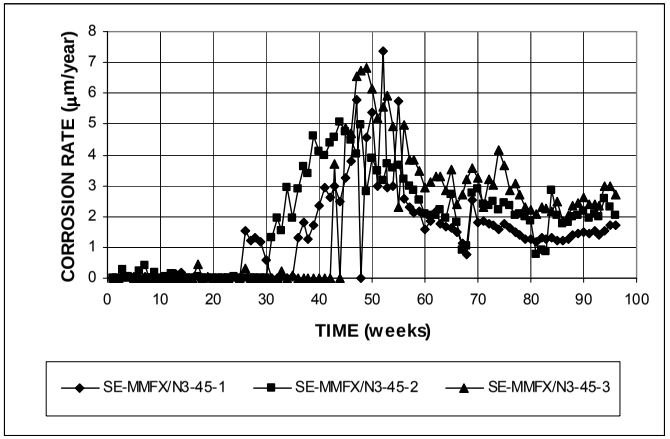


(a)

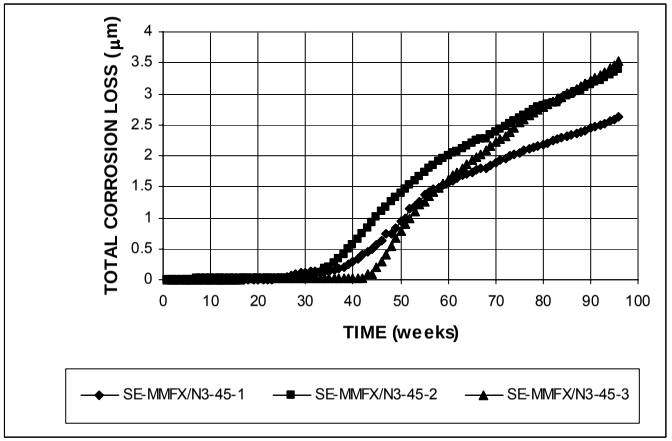


(b)

**Figure A.137 -** (a) Corrosion rates and (b) total corrosion losses as measured in the Southern Exposure test for specimens with MMFX microcomposite steel in the top mat and conventional normalized steel (N3) in the bottom mat.

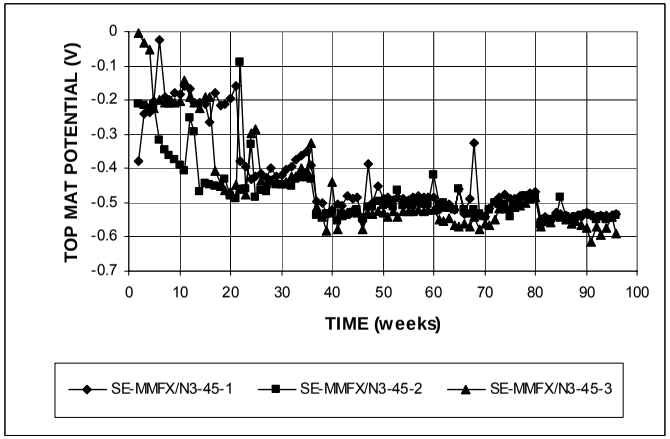


(a)

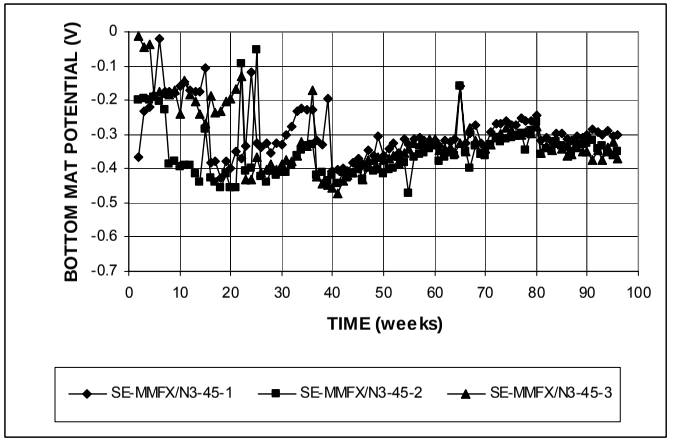


(b)

**Figure A.138 -** (a) Top mat corrosion potentials and (b) bottom mat corrosion potentials, with respect to copper-copper sulfate electrode as measured in the Southern Exposure test for specimens with MMFX microcomposite steel. in the top mat and conventional normalized steel (N3) in the bottom mat.

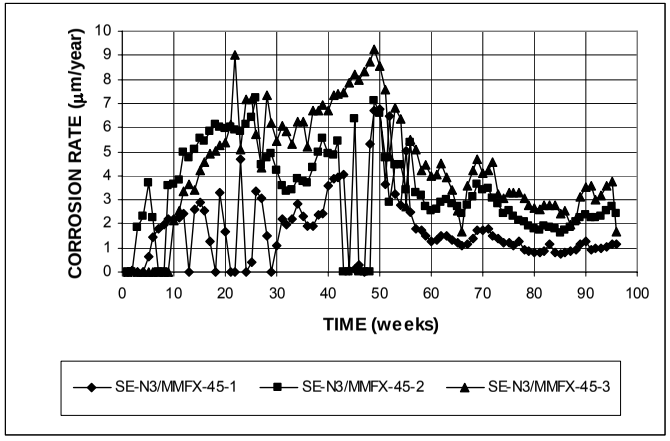


(a)

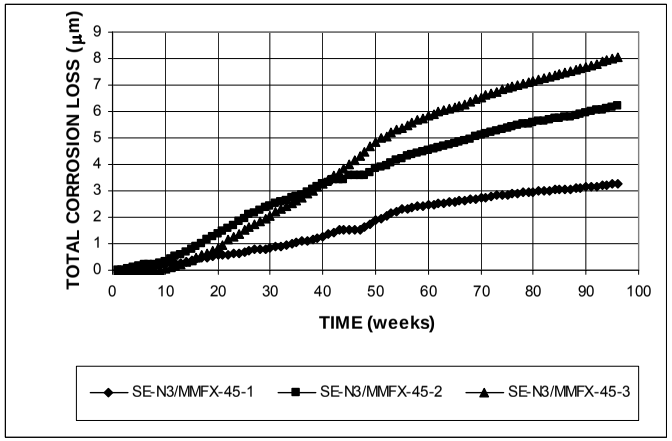


(b)

**Figure A.139 -** (a) Corrosion rates and (b) total corrosion losses as measured in the Southern Exposure test for specimens with conventional normalized steel (N3) in the top mat and MMFX microcomposite steel in the bottom mat.

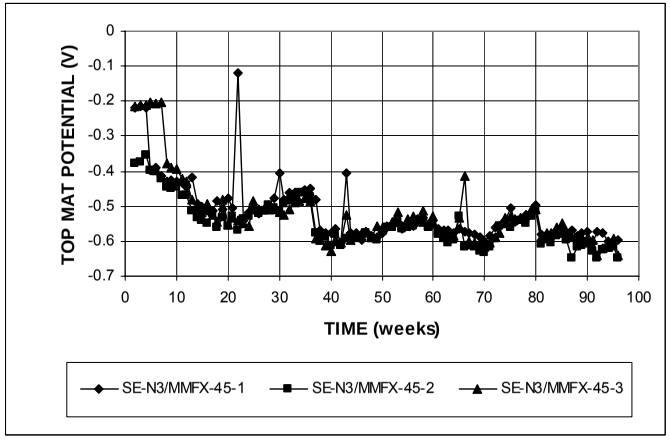


(a)

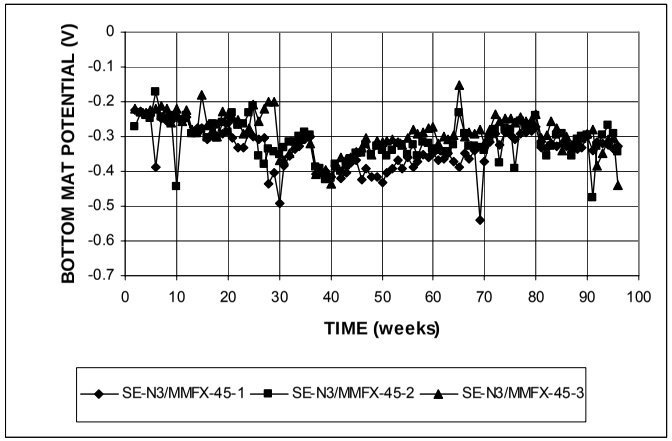


(b)

**Figure A.140 -** (a) Top mat corrosion potentials and (b) bottom mat corrosion potentials, with respect to copper-copper sulfate electrode as measured in the Southern Exposure test for specimens with conventional normalized steel (N3) in the top mat and MMFX microcomposite steel in the bottom mat.

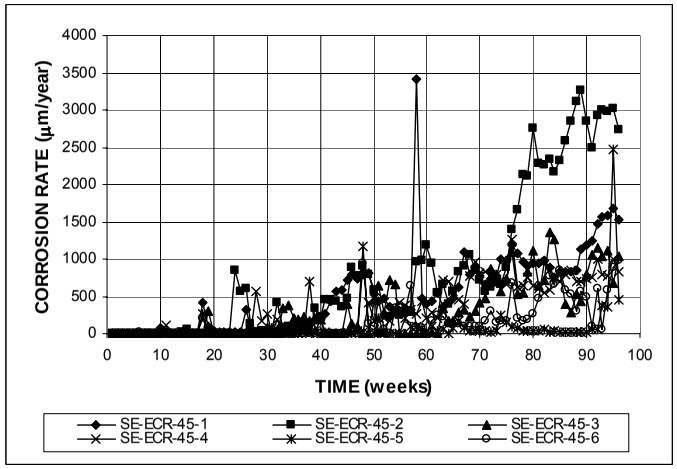


(a)

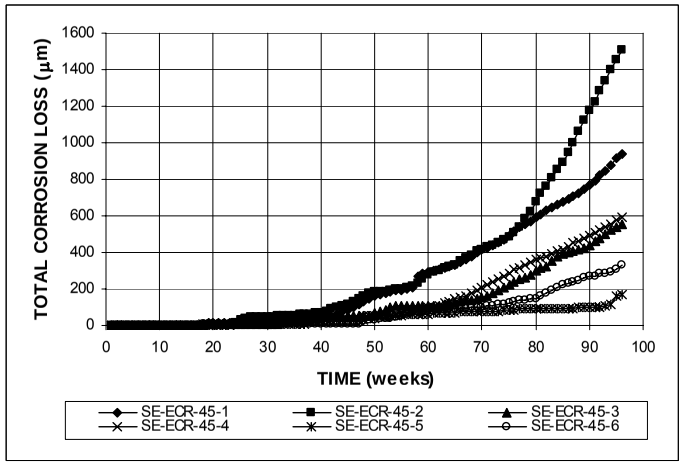


(b)

**Figure A.141 -** (a) Corrosion rates and (b) total corrosion losses exposed area of the bar (four $^{1}/_{8}$-in. diameter holes) as measured in the Southern Exposure test for specimens with epoxy-coated steel.

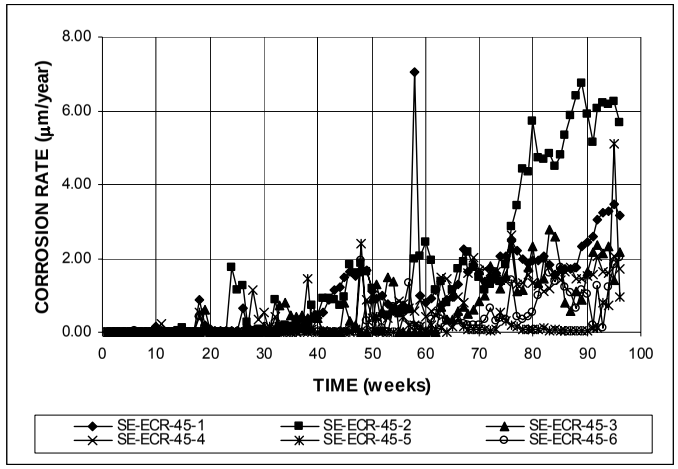


(a)

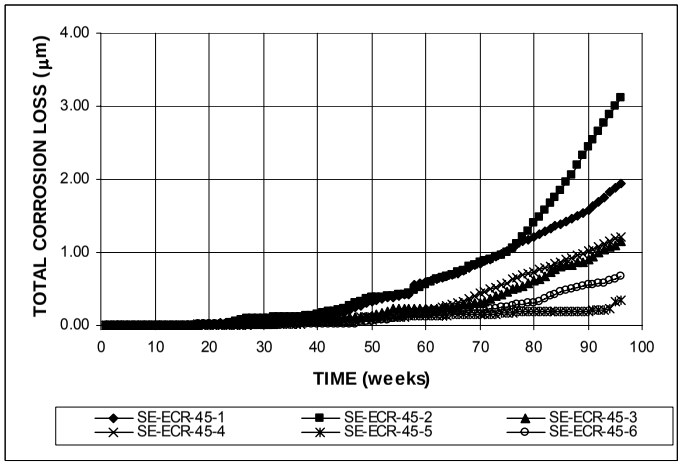


(b)

**Figure A.142 -** (a) Corrosion rates and (b) total corrosion losses total area of the bar as measured in the Southern Exposure test for specimens with epoxy-coated steel.

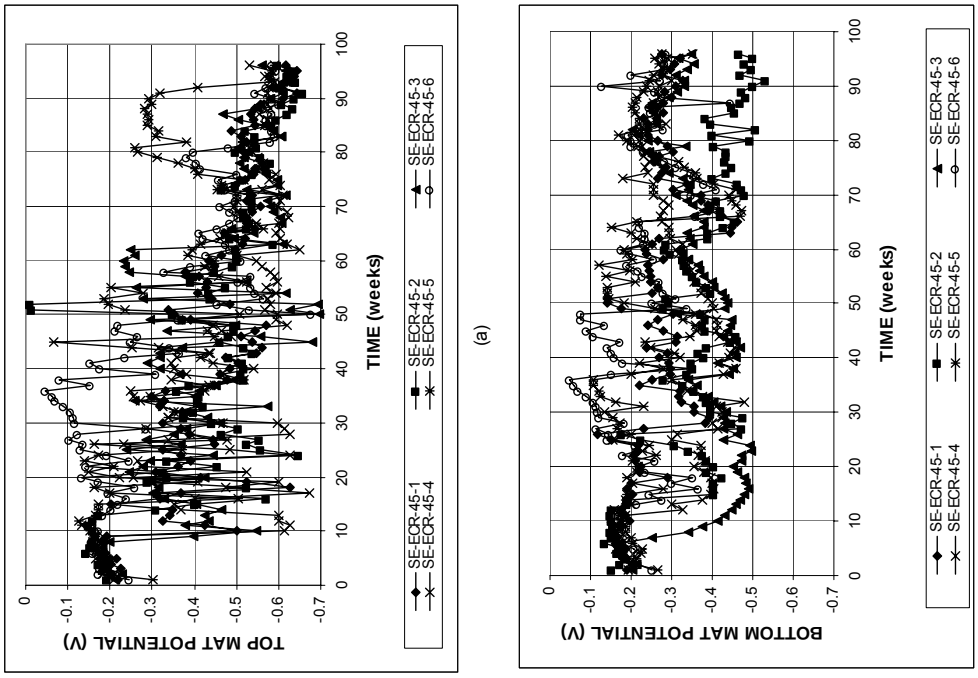


**Figure A.143** - (a) Top mat corrosion potentials and (b) bottom mat corrosion potentials with respect to copper-copper sulfate electrode as measured in the Southern Exposure test for specimens with epoxy-coated steel.

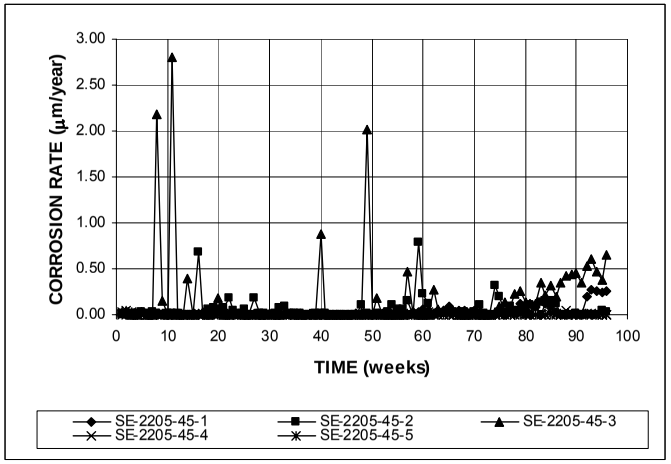


(a)

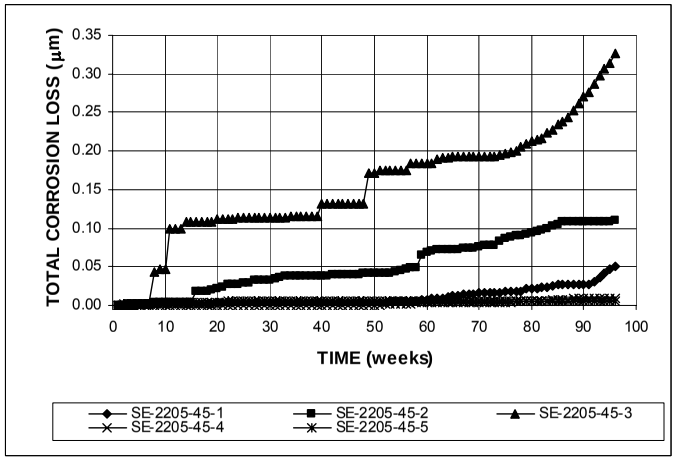


(b)

**Figure A.144 -** (a) Corrosion rates and (b) total corrosion losses as measured in the Southern Exposure test for specimens with 2205 duplex steel.

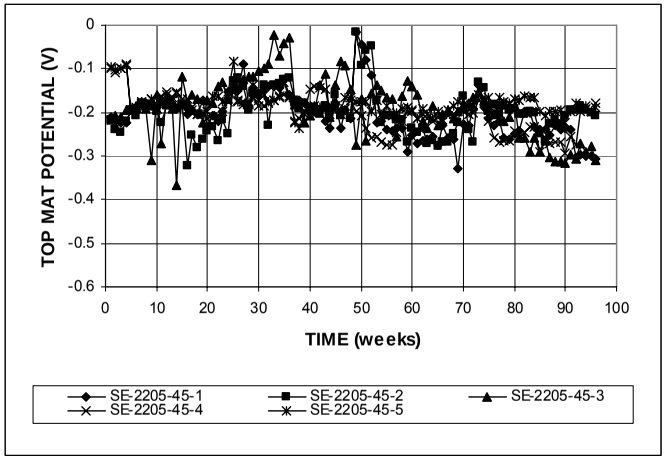


(a)

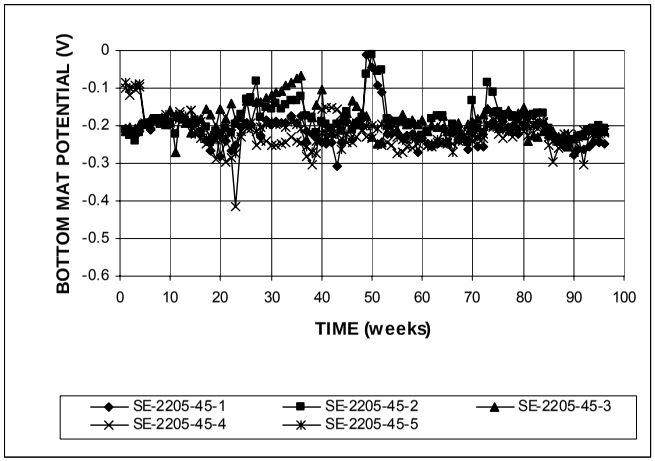


(b)

**Figure A.145 -** (a) Top mat corrosion potentials and (b) bottom mat corrosion potentials, with respect to copper-copper sulfâte electrode as measured in the Southern Exposure test for specimens with 2205 duplex steel.

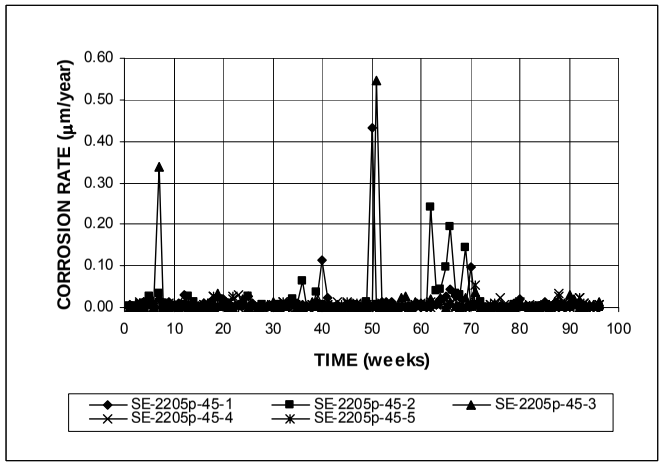


(a)

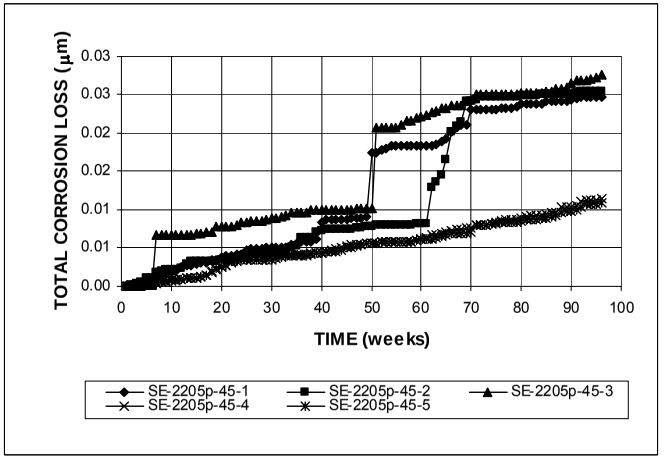


(b)

**Figure A.146** - (a) Corrosion rates and (b) total corrosion losses as measured in the Southern Exposure test for specimens with 2205 pickled duplex steel.

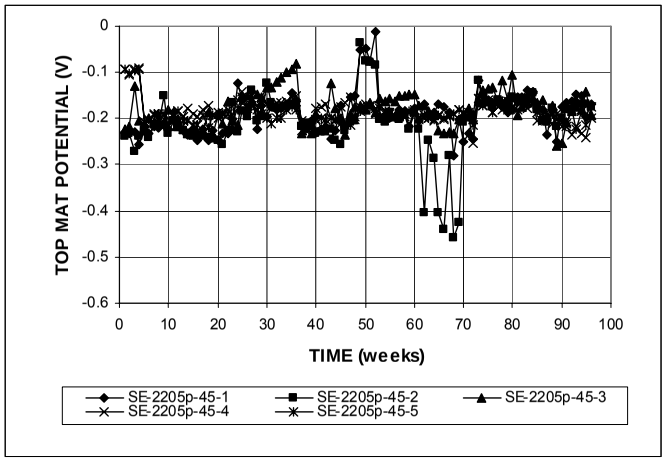


(a)

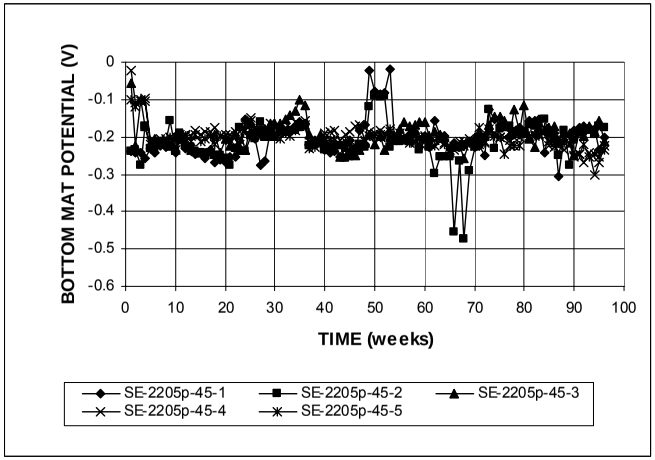


(b)

**Figure A.147** - (a) Top mat corrosion potentials and (b) bottom mat corrosion potentials, with respect to copper-copper sulfate electrode as measured in the Southern Exposure test for specimens with 2205 pickled duplex steel.

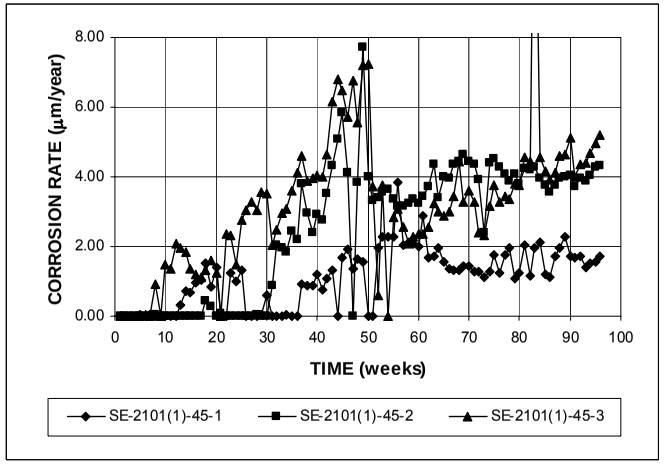


(a)

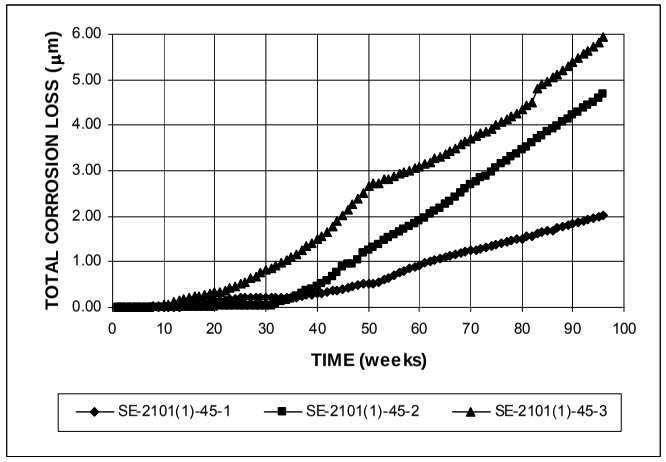


(b)

**Figure A.148 -** (a) Corrosion rates and (b) total corrosion losses as measured in the Southern Exposure test for specimens with 2101(1) duplex steel.

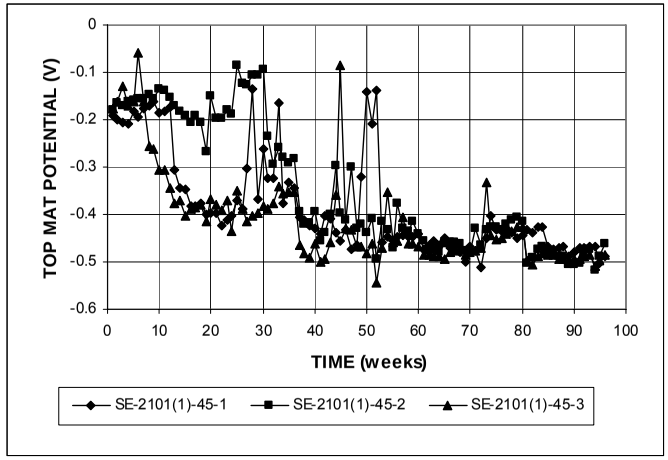


(a)

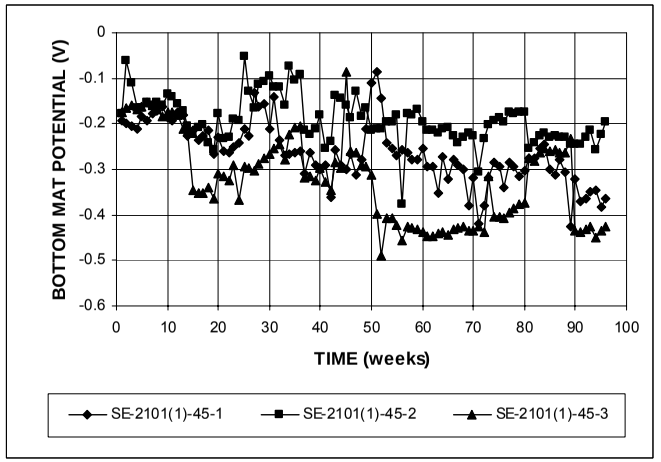


(b)

**Figure A.149 -** (a) Top mat corrosion potentials and (b) bottom mat corrosion potentials, with respect to copper-copper sulfate electrode as measured in the Southern Exposure test for specimens with 2101(1) duplex steel.

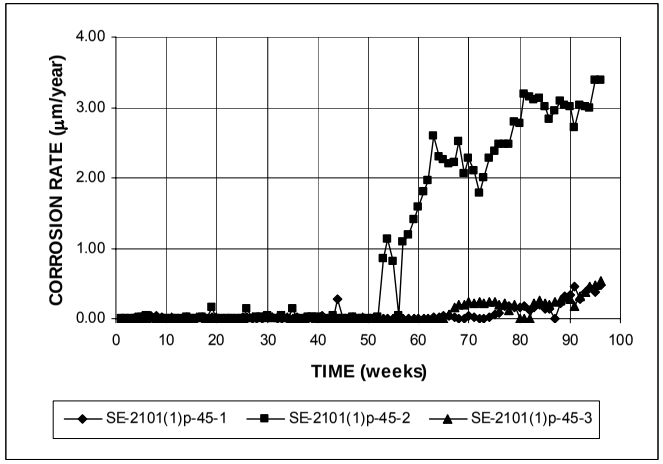


(a)

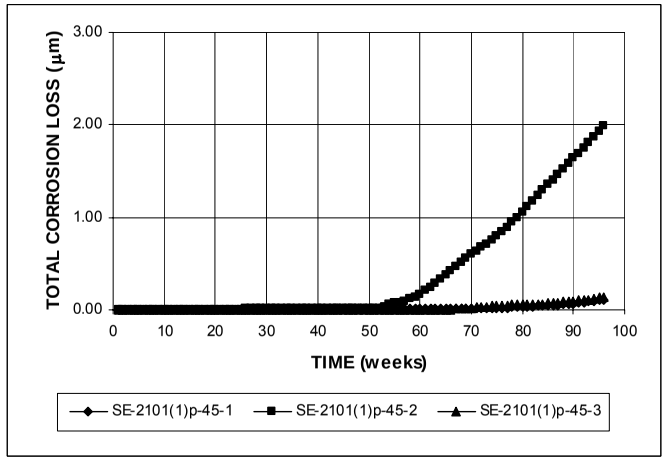


(b)

**Figure A.150 -** (a) Corrosion rates and (b) total corrosion losses as measured in the Southern Exposure test for specimens with 2101(1) pickled duplex steel.

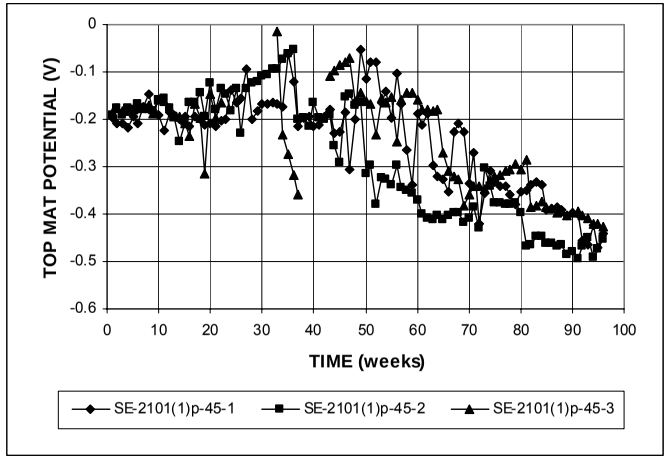


(a)

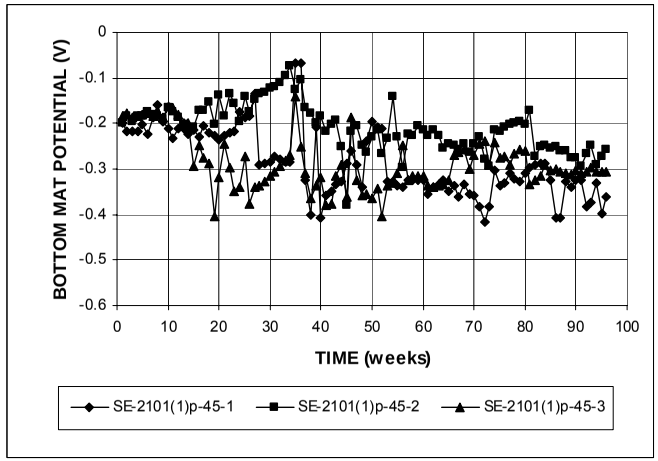


(b)

**Figure A.151 -** (a) Top mat corrosion potentials and (b) bottom mat corrosion potentials, with respect to copper-copper sulfate electrode as measured in the Southern Exposure test for specimens with 2101(1) pickled duplex steel.

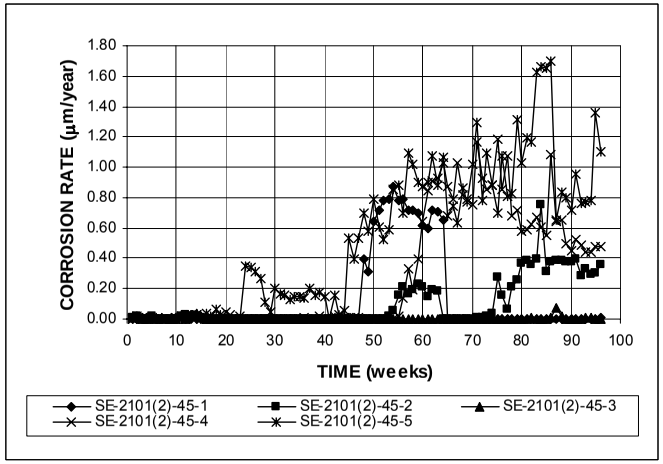


(a)

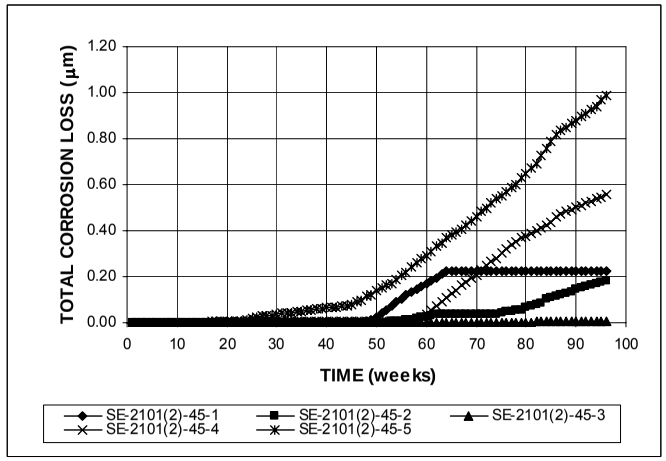


(b)

**Figure A.152 -** (a) Corrosion rates and (b) total corrosion losses as measured in the Southern Exposure test for specimens with 2101(2) duplex steel.

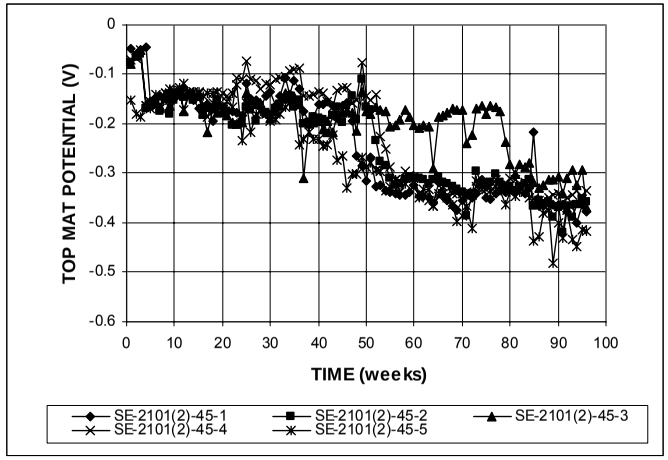


(a)

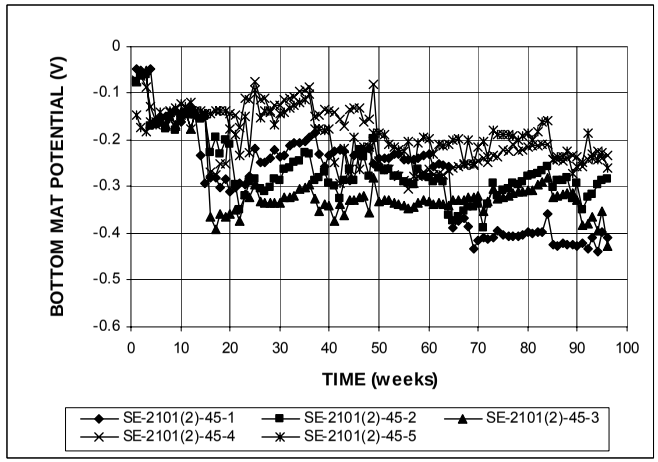


(b)

**Figure A.153 -** (a) Top mat corrosion potentials and (b) bottom mat corrosion potentials, with respect to copper-copper sulfate electrode as measured in the Southern Exposure test for specimens with 2101(2) duplex steel.

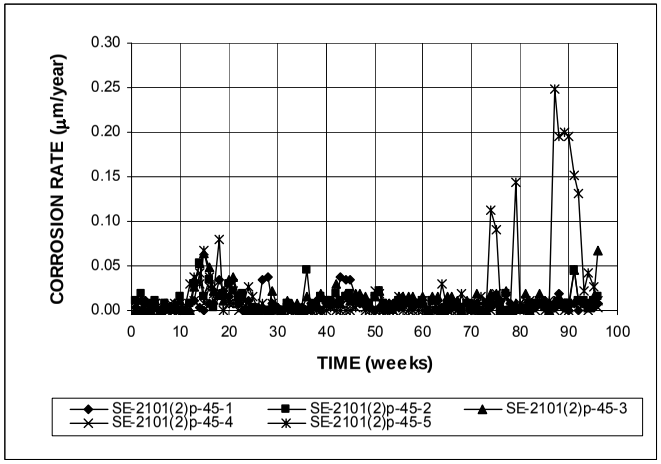


(a)

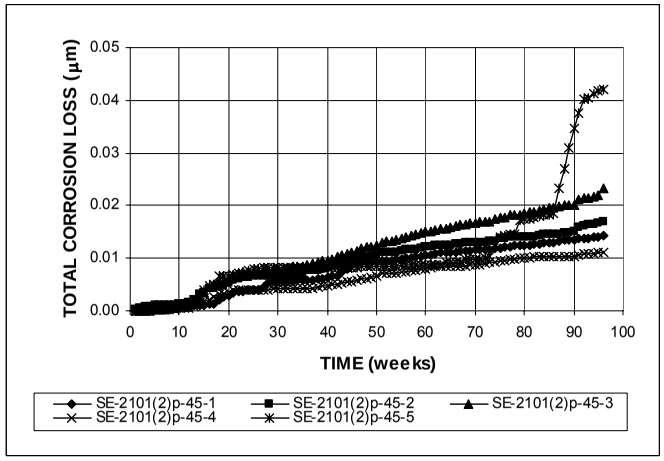


(b)

**Figure A.154 -** (a) Corrosion rates and (b) total corrosion losses as measured in the Southern Exposure test for specimens with 2101(2) pickled duplex steel.

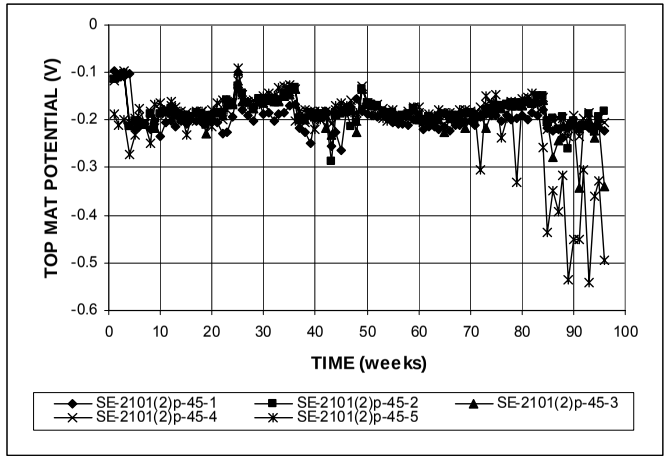


(a)

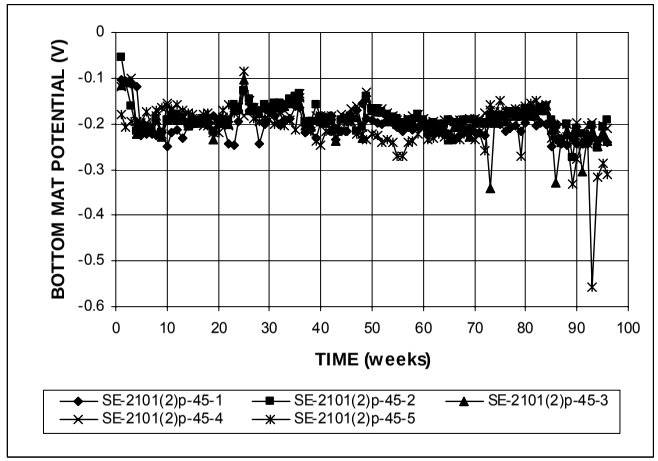


(b)

**Figure A.155 -** (a) Top mat corrosion potentials and (b) bottom mat corrosion potentials, with respect to copper-copper sulfate electrode as measured in the Southern Exposure test for specimens with 2101(2) pickled duplex steel.

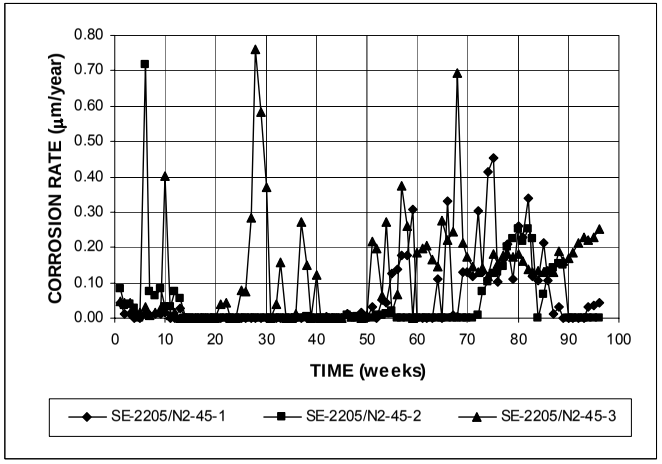


(a)

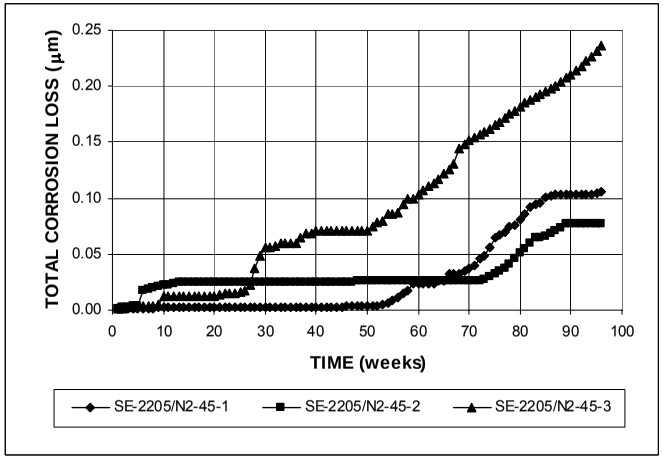


(b)

**Figure A.156 -** (a) Corrosion rates and (b) total corrosion losses as measured in the Southern Exposure test for specimens with 2205 duplex steel in the top mat and conventional normalized steel (N2) in the bottom mat.

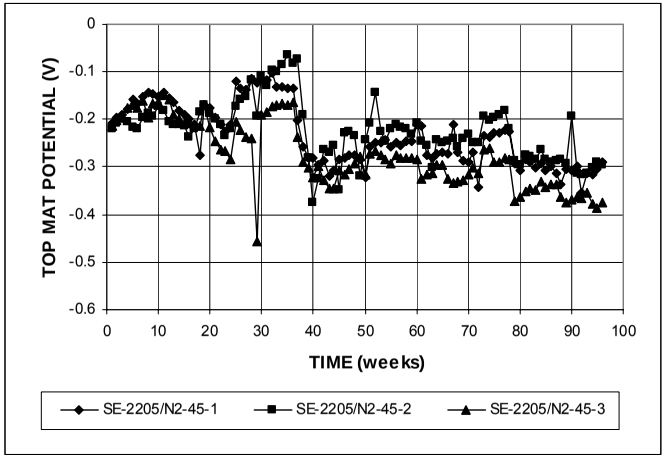


(a)

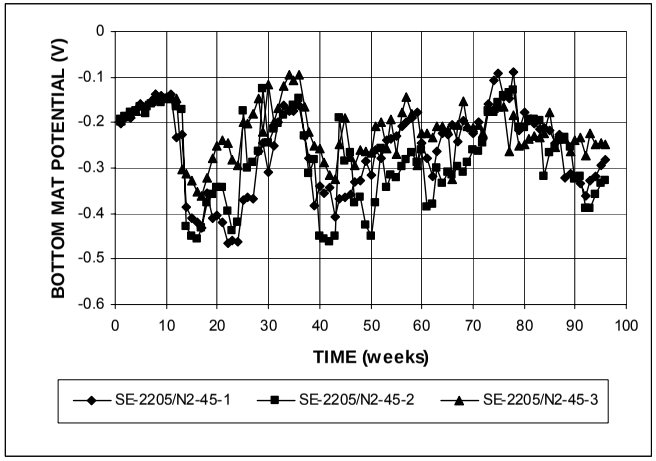


(b)

**Figure A.157 -** (a) Top mat corrosion potentials and (b) bottom mat corrosion potentials, with respect to copper-copper sulfate electrode as measured in the Southern Exposure test for specimens with 2205 duplex steel in the top mat and conventional normalized steel (N2) in the bottom mat.

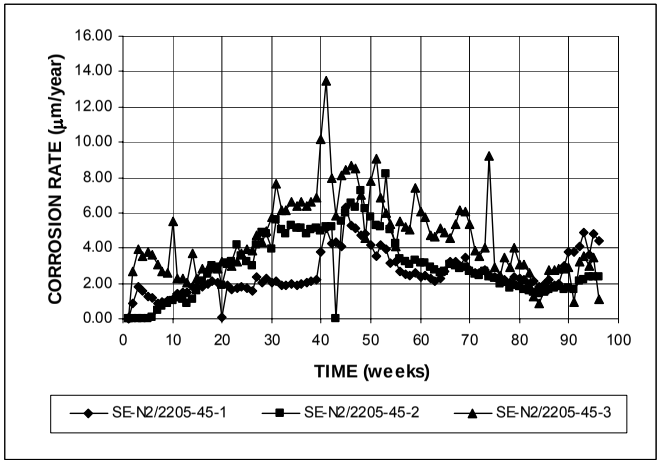


(a)

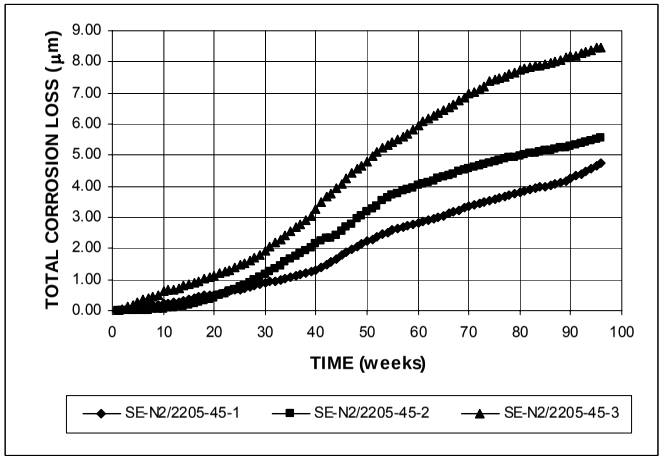


(b)

**Figure A.158 -** (a) Corrosion rates and (b) total corrosion losses as measured in the Southern Exposure test for specimens with conventional normalized steel (N2) in the top mat and 2205 duplex steel in the bottom mat.

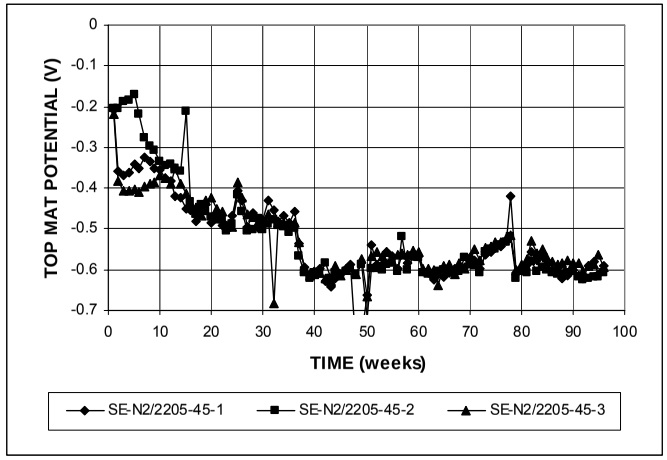


(a)

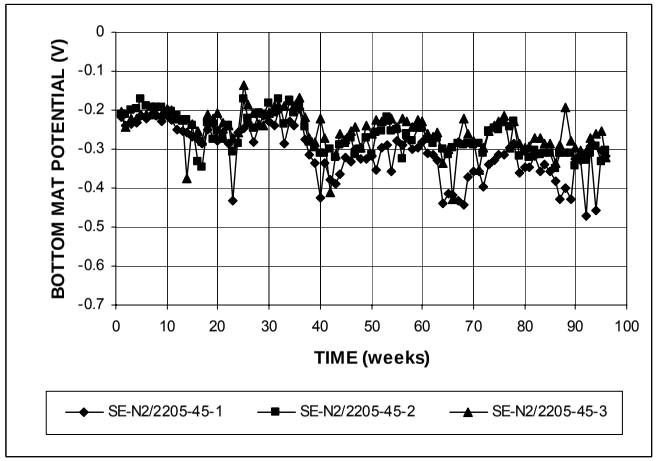


(b)

**Figure A.159 -** (a) Top mat corrosion potentials and (b) bottom mat corrosion potentials, with respect to copper-copper sulfate electrode as measured in the Southern Exposure test for specimens with conventional normalized steel in the top mat and 2205 duplex steel in the bottom mat.

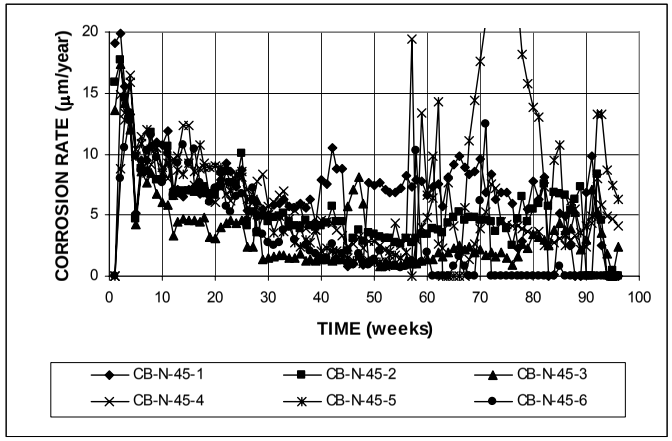


(a)

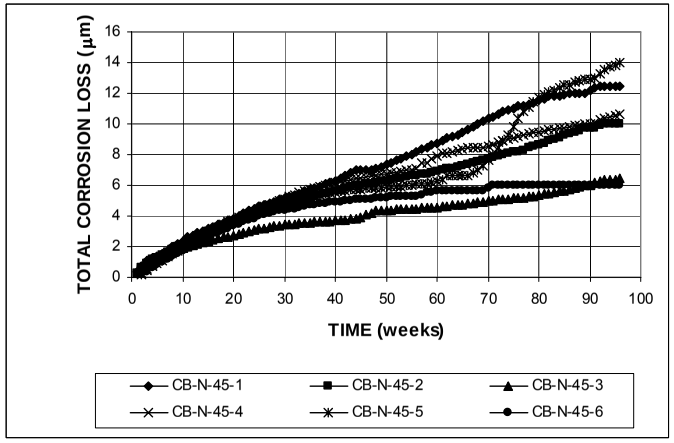


(b)

**Figure A.160 -** (a) Corrosion rates and (b) total corrosion losses as measured in the cracked beam test for specimens with conventional normalized steel (N).

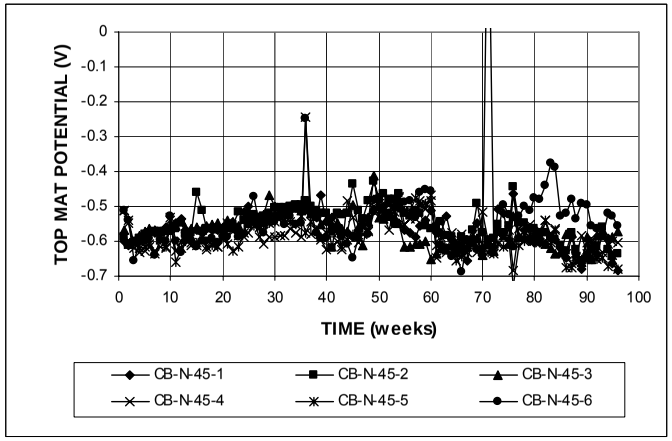


(a)

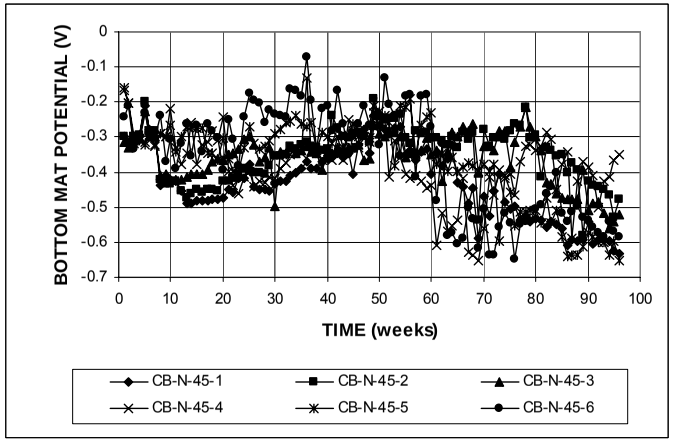


(b)

**Figure A.161 -** (a) Top mat corrosion potentials and (b) bottom mat corrosion potentials, with respect to copper-copper sulfate electrode as measured in the cracked beam test for specimens with conventional normalized steel (N).

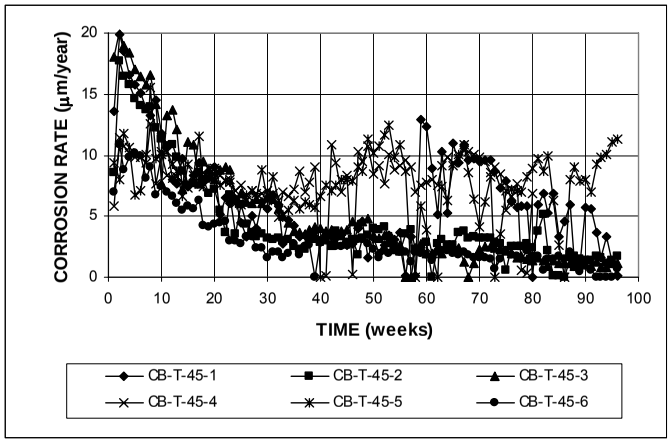


(a)

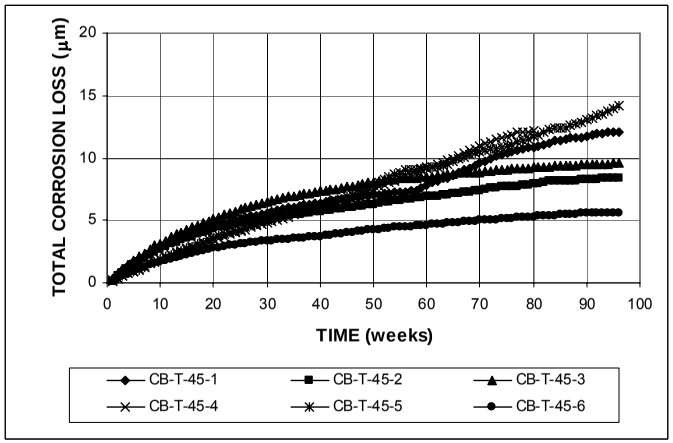


(b)

**Figure A.162 -** (a) Corrosion rates and (b) total corrosion losses as measured in the cracked beam test for specimens with conventional Thermex-treated steel (T).

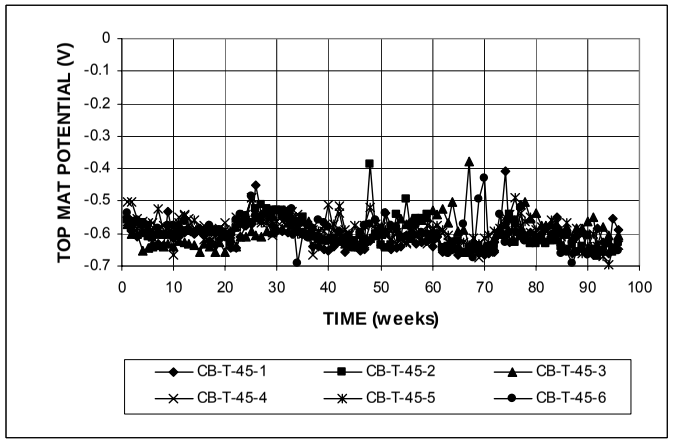


(a)

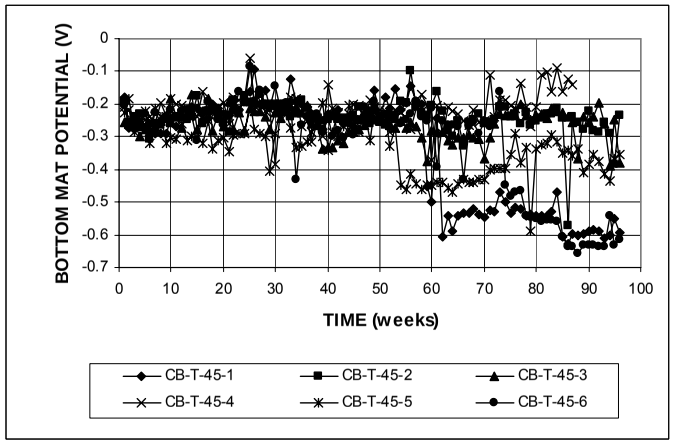


(b)

**Figure A.163 -** (a) Top mat corrosion potentials and (b) bottom mat corrosion potentials, with respect to copper-copper sulfate electrodeas measured in the cracked beam test for specimens with conventional Thermex-treated steel (T).

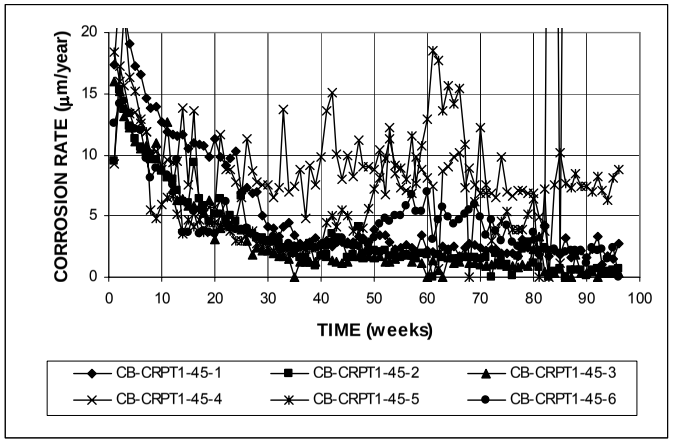


(a)

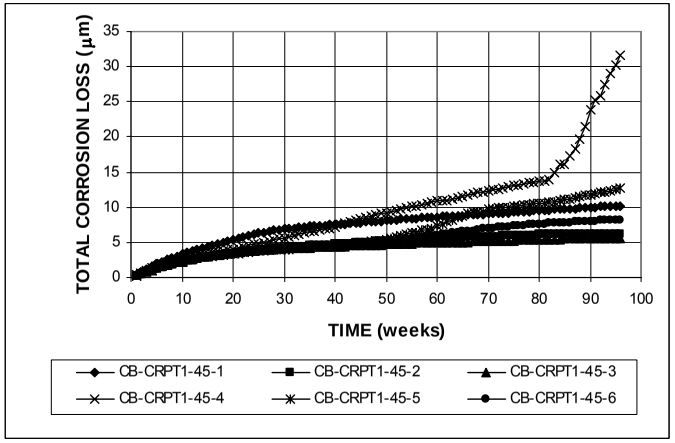


(b)

**Figure A.164 -** (a) Corrosion rates and (b) total corrosion losses as measured in the cracked beam test for specimens with microalloyed steel with a high phosphorus content, 0.117%, Thermex-treated (CRPT1).

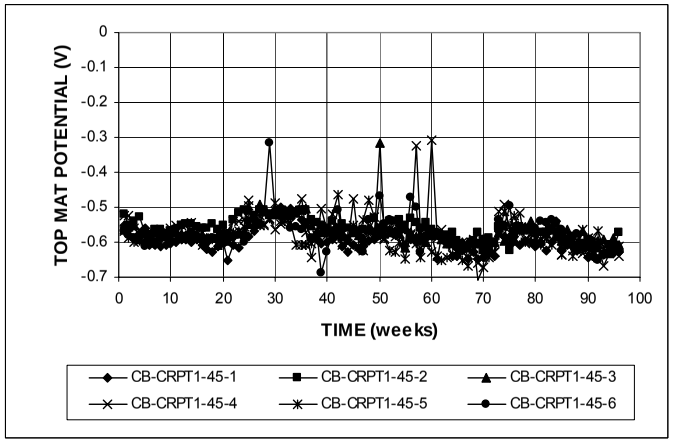


(a)

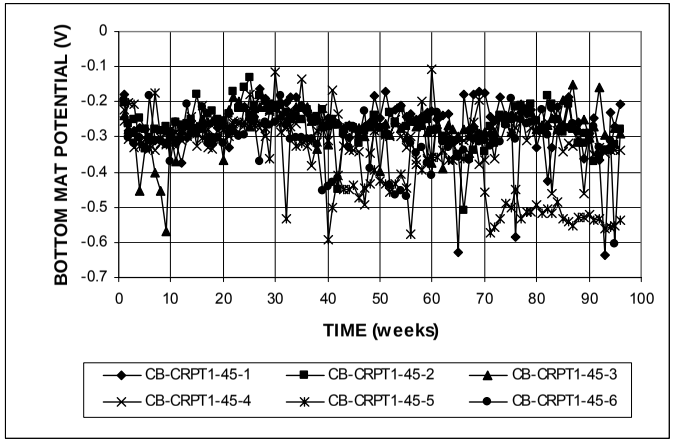


(b)

**Figure A.165 -** (a) Top mat corrosion potentials and (b) bottom mat corrosion potentials, with respect to copper-copper sulfate electrode as measured in the cracked beam test for specimens with microalloyed steel with a high phosphorus content, 0.117%, Thermex-treated (CRPT1).

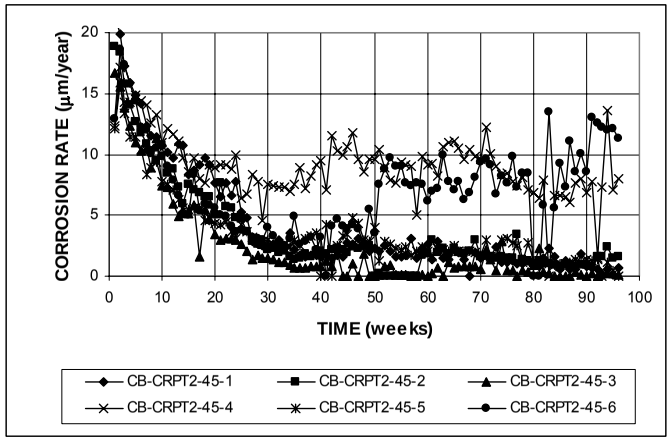


(a)

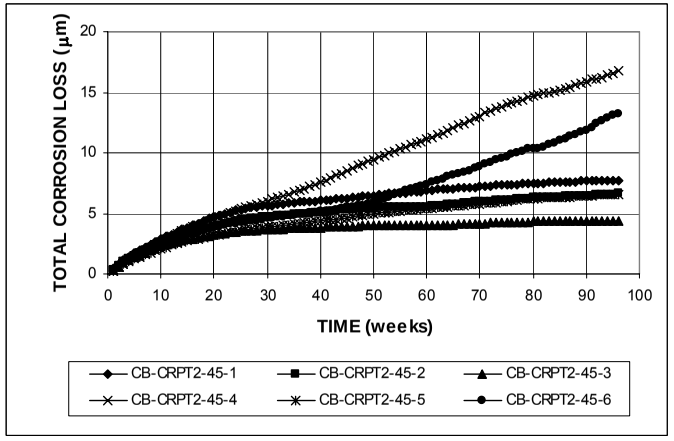


(b)

**Figure A.166 -** (a) Corrosion rates and (b) total corrosion losses as measured in the cracked beam test for specimens with microalloyed steel with a high phosphorus content, 0.100%, Thermex-treated (CRPT2).

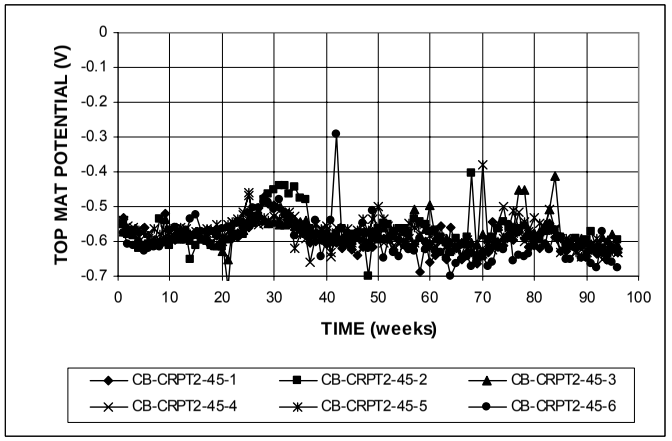


(a)

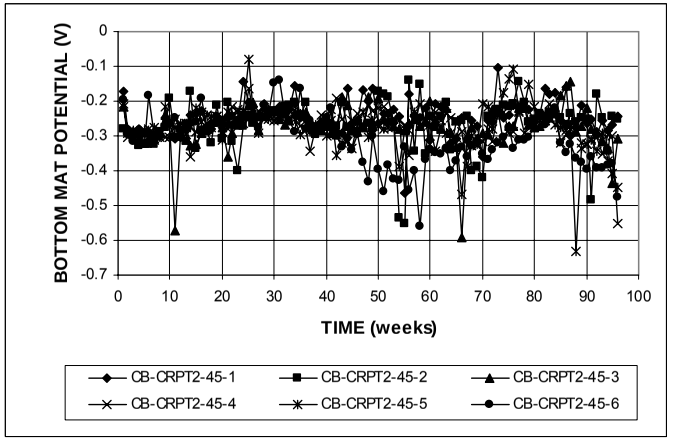


(b)

**Figure A.167 -** (a) Top mat corrosion potentials and (b) bottom mat corrosion potentials, with respect to copper-copper sulfate electrode as measured in the cracked beam test for specimens with microalloyed steel with a high phosphorus content, 0.100%, Thermex-treated (CRPT2).

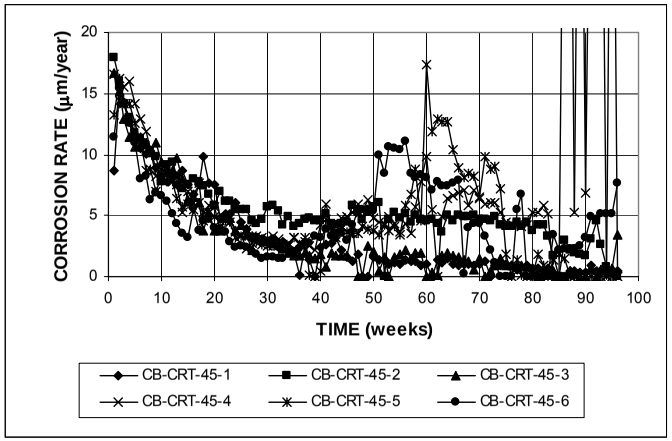


(a)

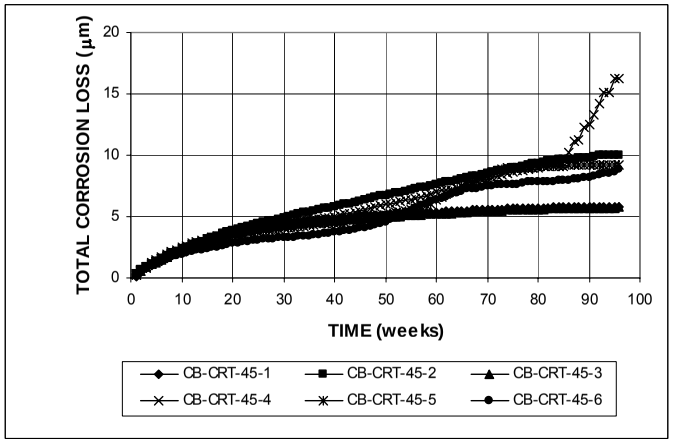


(b)

**Figure A.168** - (a) Corrosion rates and (b) total corrosion losses as measured in the cracked beam test for specimens with microalloyed steel with normal phosphorus content, 0.017%, Thermex-treated (CRT).

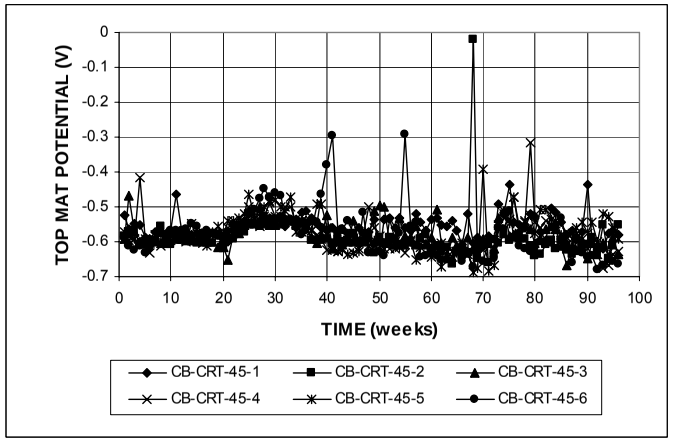


(a)

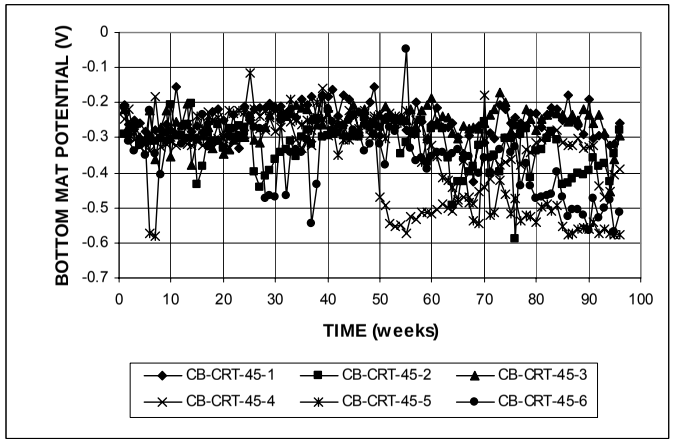


(b)

**Figure A.169** - (a) Top mat corrosion potentials and (b) bottom mat corrosion potentials, with respect to copper-copper sulfate electrode as measured in the cracked beam test for specimens with microalloyed steel with normal phosphorus content, 0.017%, Thermex-treated (CRT).

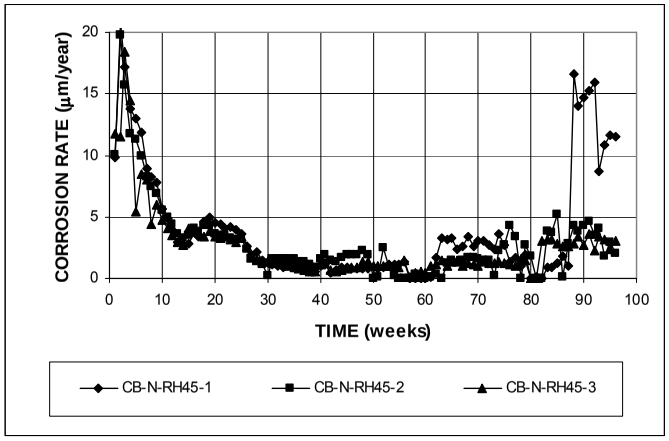


(a)

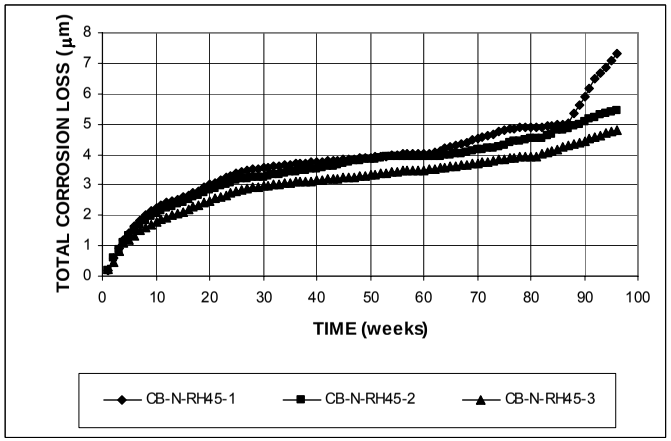


(b)

**Figure A.170 -** (a) Corrosion rates and (b) total corrosion losses as measured in the cracked beam test for specimens with conventional normalized steel (N), a water-cement ratio of 0.45, and Rheocrete 222+.

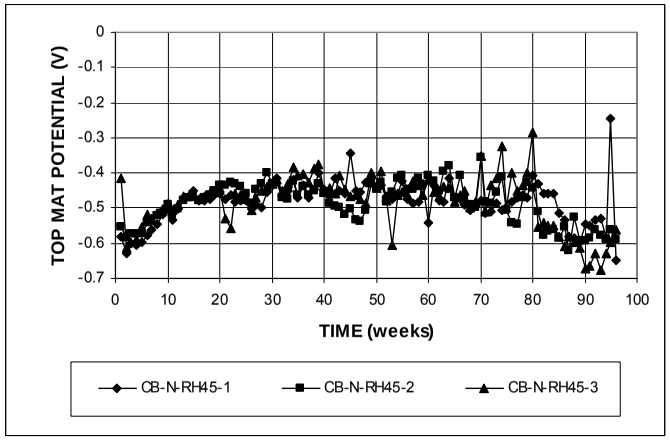


(a)

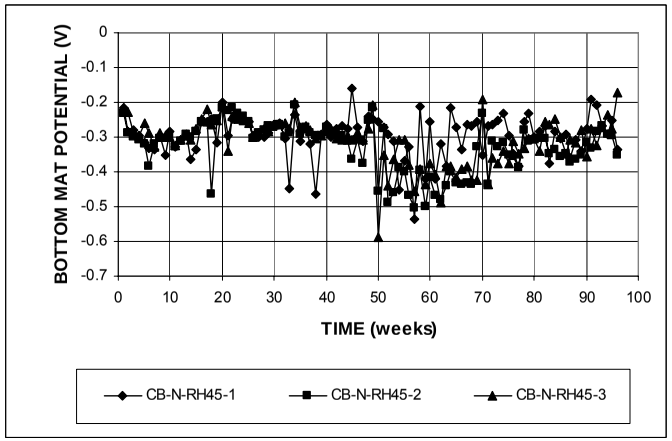


(b)

**Figure A.171 -** (a) Top mat corrosion potentials and (b) bottom mat corrosion potentials, with respect to copper-copper sulfate electrode as measured in the cracked beam test for specimens with conventional normalized steel (N), a water-cement ratio of 0.45, and Rheocrete 222+.

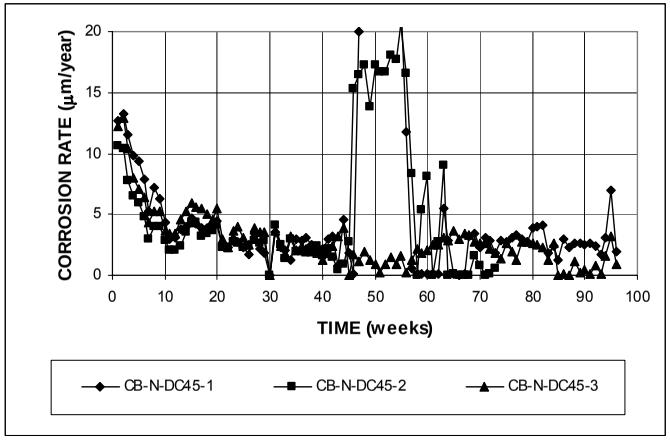


(a)

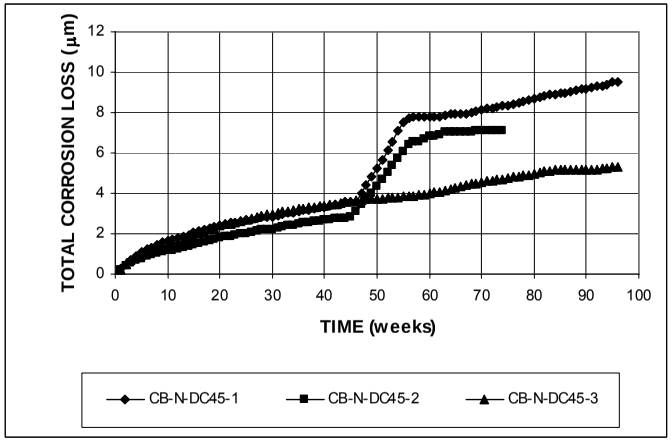


(b)

**Figure A.172 -** (a) Corrosion rates and (b) total corrosion losses as measured in the cracked beam test for specimens with conventional normalized steel (N), a water-cement ratio of 0.45, and DCI-S.

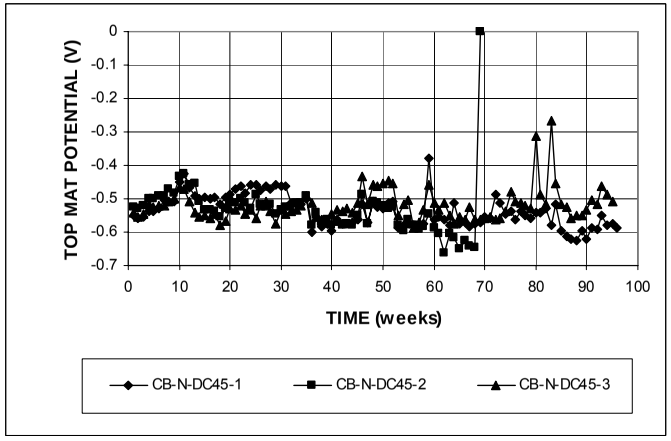


(a)

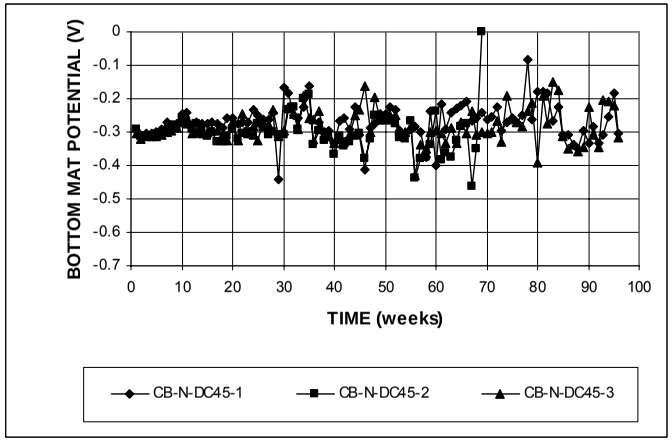


(b)

**Figure A.173 -** (a) Top mat corrosion potentials and (b) bottom mat corrosion potentials, with respect to copper-copper sulfate electrode as measured in the cracked beam test for specimens with conventional normalized steel (N), a water-cement ratio of 0.45, and DCI-S.

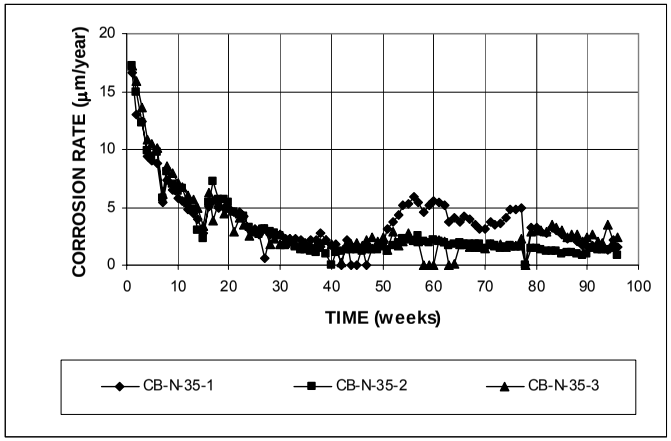


(a)

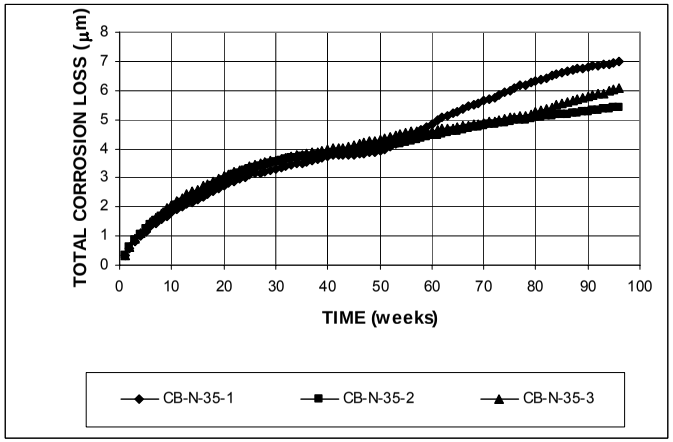


(b)

**Figure A.174 -** (a) Corrosion rates and (b) total corrosion losses as measured in the cracked beam test for specimens with conventional normalized steel (N), a water-cement ratio of 0.35, and no inhibitor.

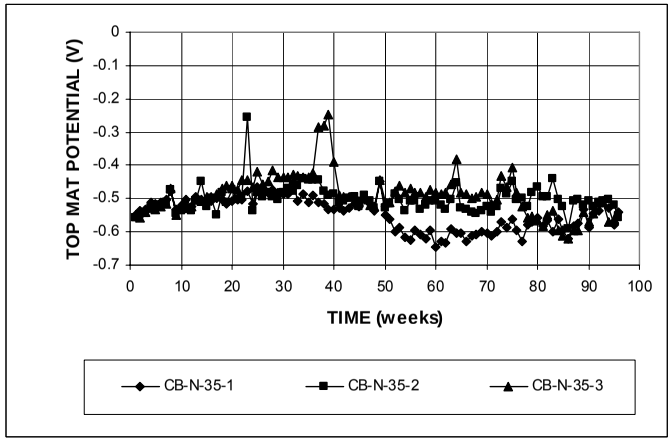


(a)

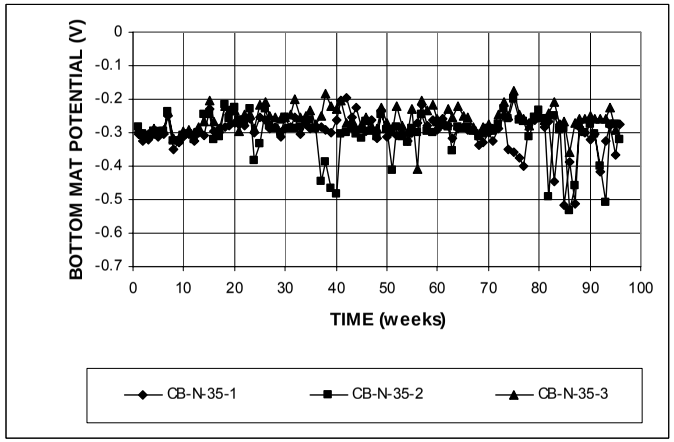


(b)

**Figure A.175 -** (a) Top mat corrosion potentials and (b) bottom mat corrosion potentials, with respect to copper-copper sulfate electrode as measured in the cracked beam test for specimens with conventional normalized steel (N), a water-cement ratio of 0.35, and no inhibitor.

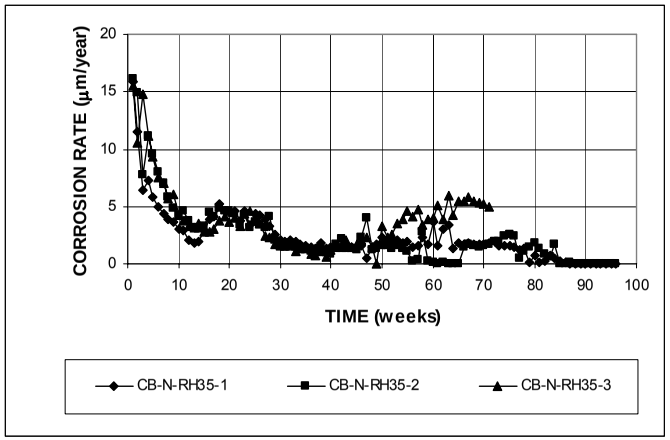


(a)

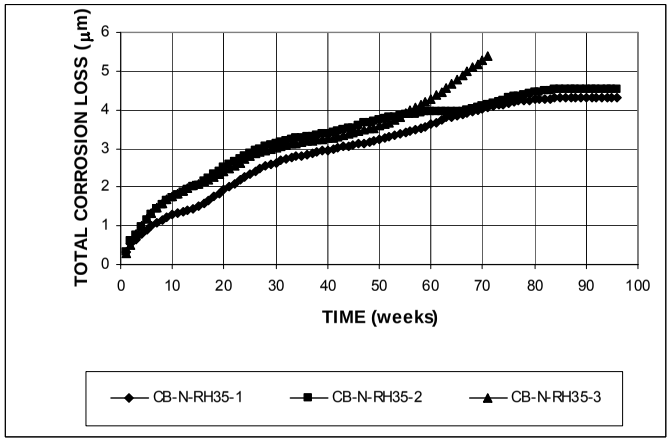


(b)

**Figure A.176 -** (a) Corrosion rates and (b) total corrosion losses as measured in the cracked beam test for specimens with conventional normalized steel (N), a water-cement ratio of 0.35, and Rheocrete 222+.

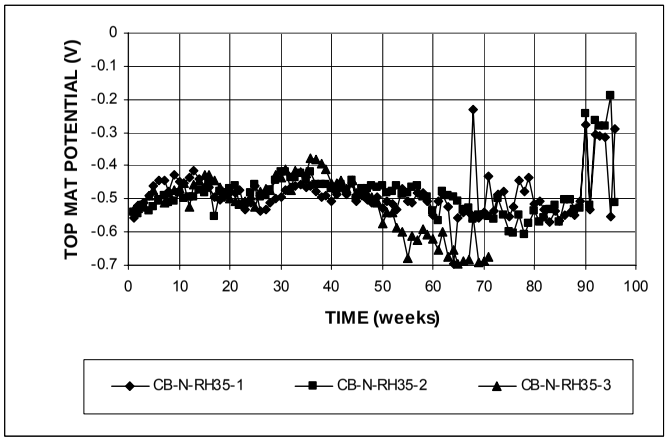


(a)

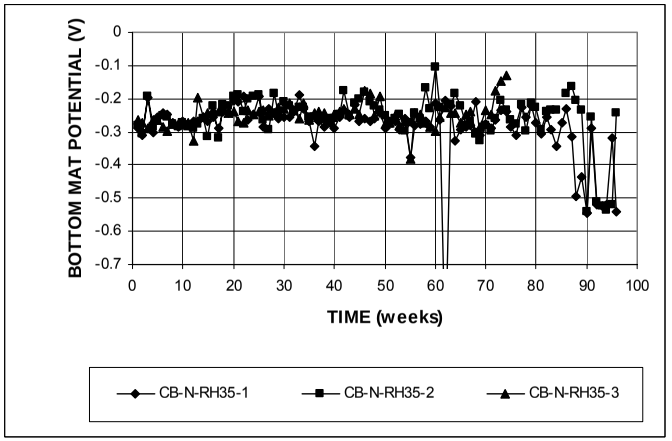


(b)

**Figure A.177 -** (a) Top mat corrosion potentials and (b) bottom mat corrosion potentials, with respect to copper-copper sulfate electrode as measured in the cracked beam test for specimens with conventional normalized steel (N), a water-cement ratio of 0.35, and Rheocrete 222+.

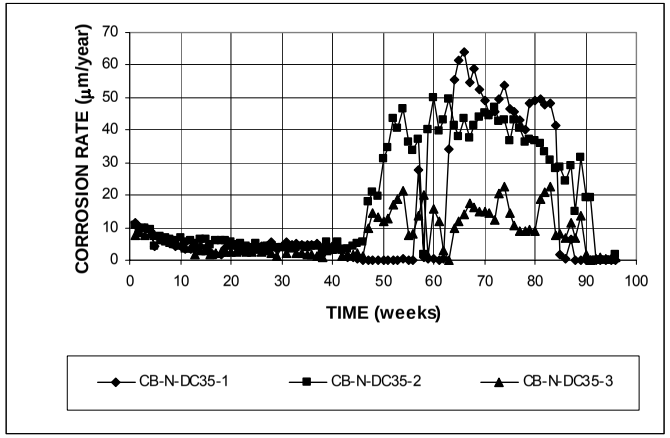


(a)

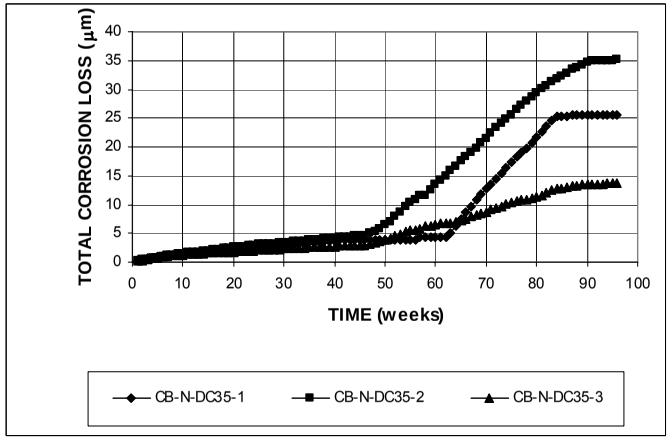


(b)

**Figure A.178 -** (a) Corrosion rates and (b) total corrosion losses as measured in the cracked beam test for specimens with conventional normalized steel (N), a water-cement ratio of 0.35, and DCI-S.

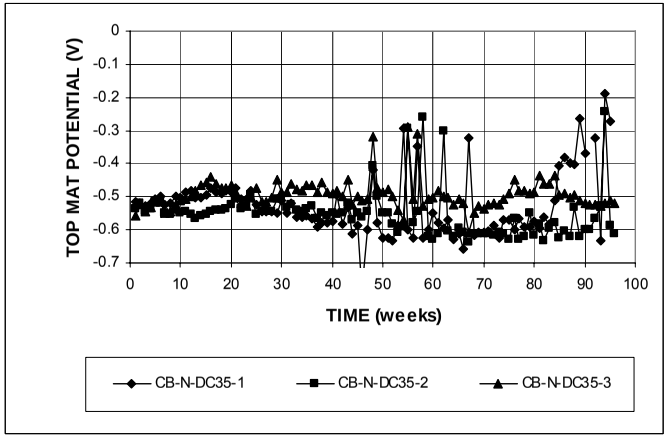


(a)

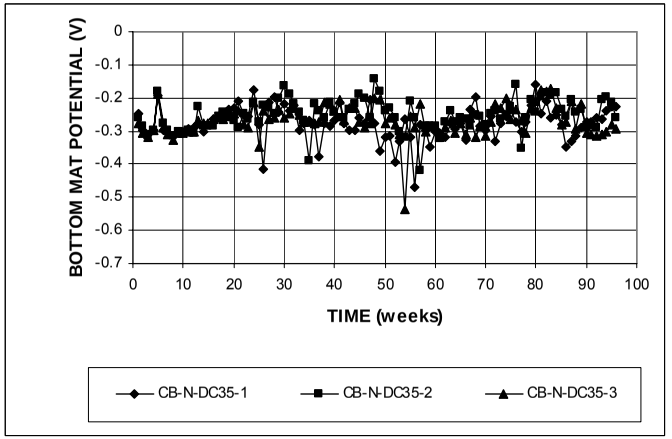


(b)

**Figure A.179 -** (a) Top mat corrosion potentials and (b) bottom mat corrosion potentials, with respect to copper-copper sulfate electrode as measured in the cracked beam test for specimens with conventional normalized steel (N), a water-cement ratio of 0.35, and DCI-S.

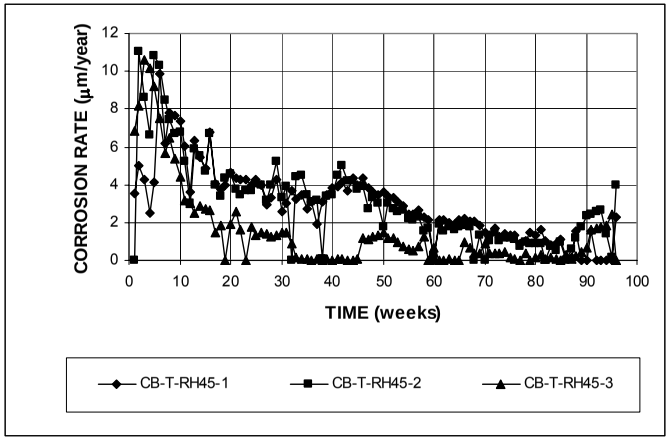


(a)

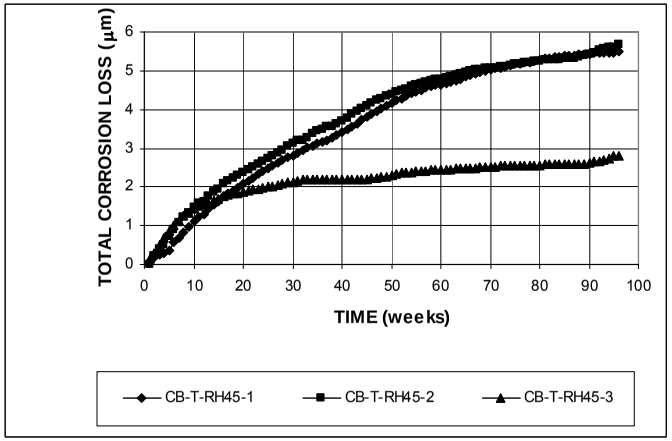


(b)

**Figure A.180 -** (a) Corrosion rates and (b) total corrosion losses as measured in the cracked beam test for specimens with conventional Thermex-treated steel (T), a water-cement ratio of 0.45, and Rheocrete 222+.

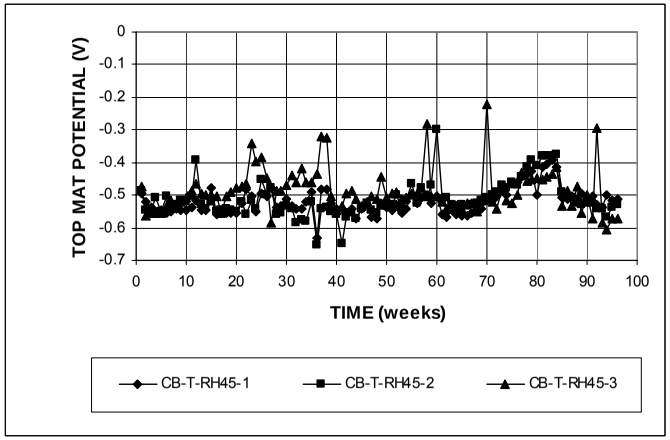


(a)

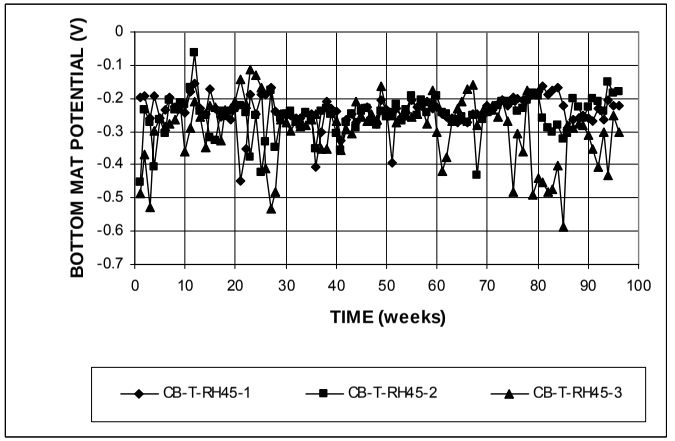


(b)

**Figure A.181 -** (a) Top mat corrosion potentials and (b) bottom mat corrosion potentials, with respect to copper-copper sulfate electrode as measured in the cracked beam test for specimens with conventional Thermex-treated steel (T), a water-cement ratio of 0.45, and Rheocrete 222+.

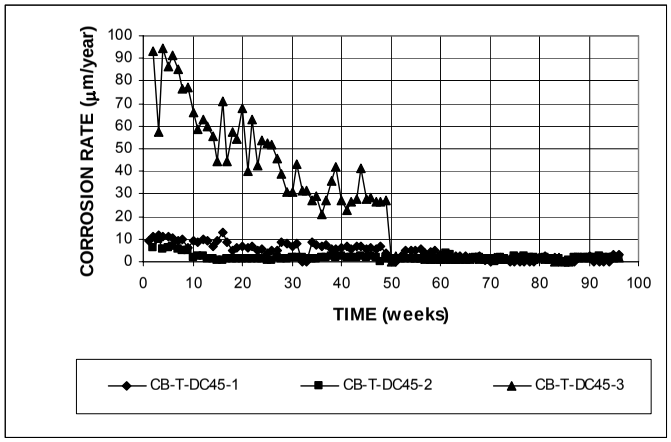


(a)

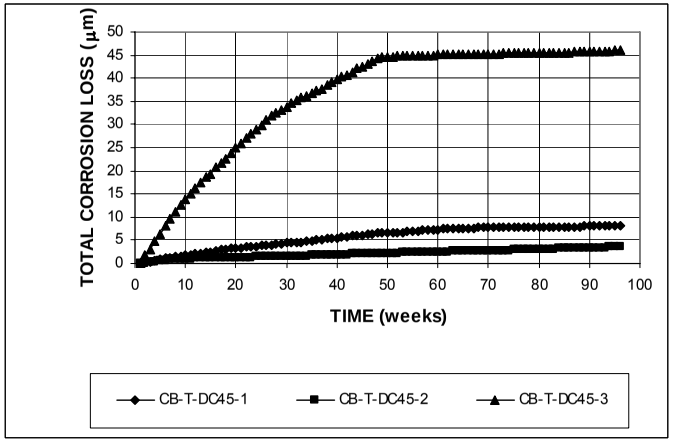


(b)

**Figure A.182 -** (a) Corrosion rates and (b) total corrosion losses as measured in the cracked beam test for specimens with conventional Thermex-treated steel (T), a water-cement ratio of 0.45, and DCI-S.

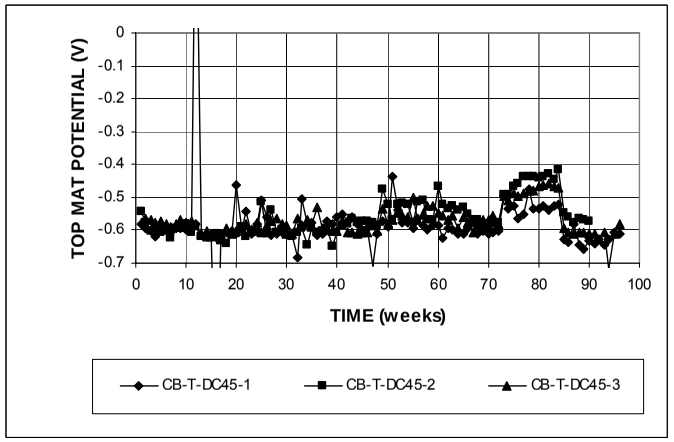


(a)

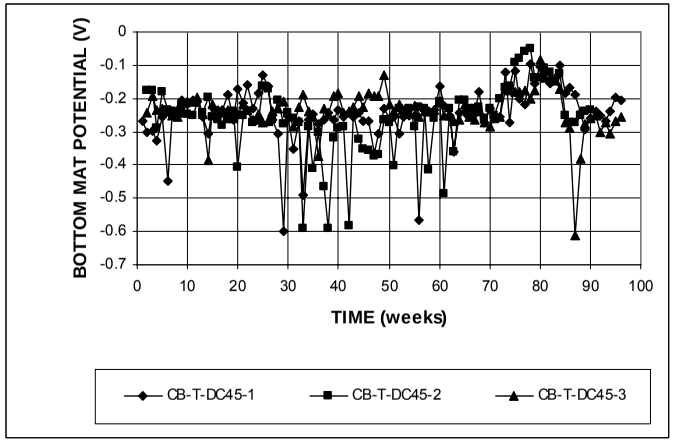


(b)

**Figure A.183 -** (a) Top mat corrosion potentials and (b) bottom mat corrosion potentials, with respect to copper-copper sulfate electrode as measured in the cracked beam test for specimens with conventional Thermex-treated steel (T), a water-cement ratio of 0.45, and DCI-S.

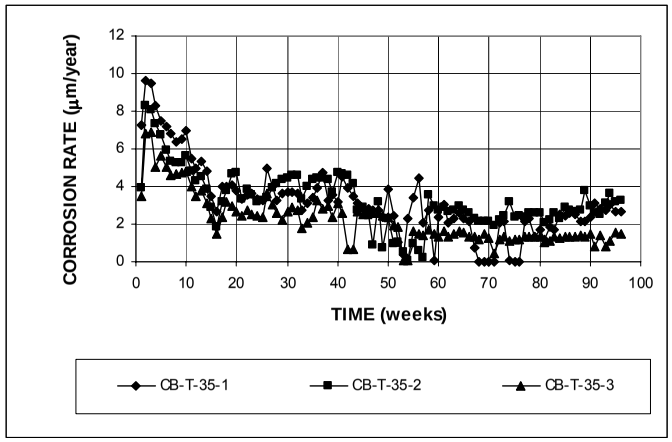


(a)

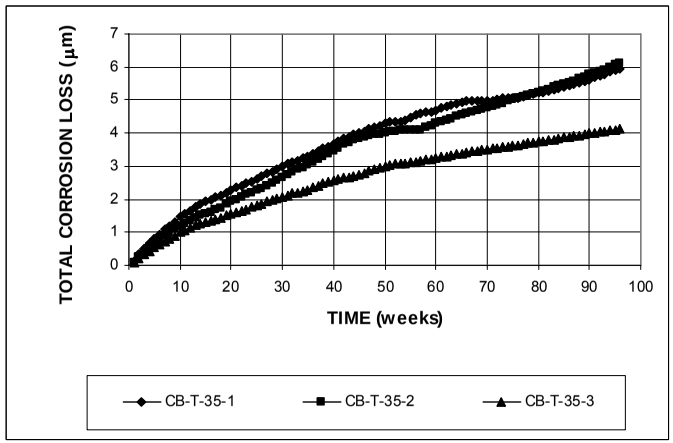


(b)

**Figure A.184 -** (a) Corrosion rates and (b) total corrosion losses as measured in the cracked beam test for specimens with conventional Thermex-treated steel (T), a water-cement ratio of 0.35, and no inhibitor.

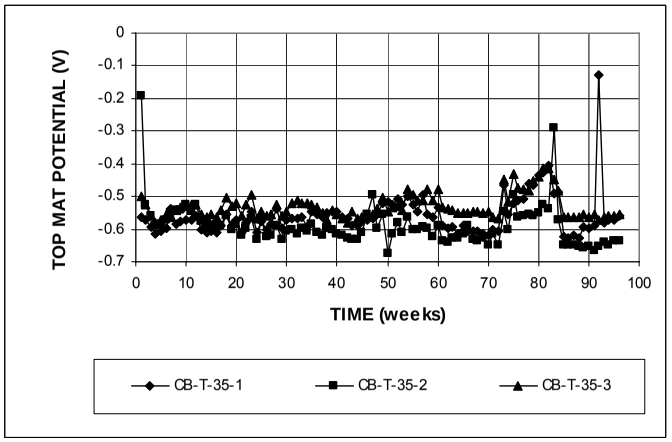


(a)

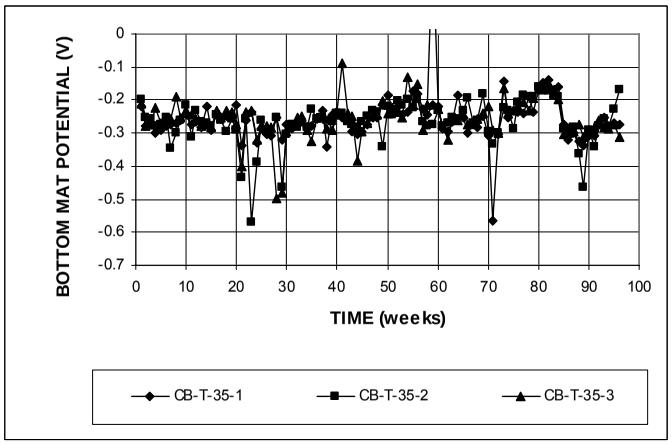


(b)

**Figure A.185 -** (a) Top mat corrosion potentials and (b) bottom mat corrosion potentials, with respect to copper-copper sulfate electrode as measured in the cracked beam test for specimens with conventional Thermex-treated steel (T), a water-cement ratio of 0.35, and no inhibitor.

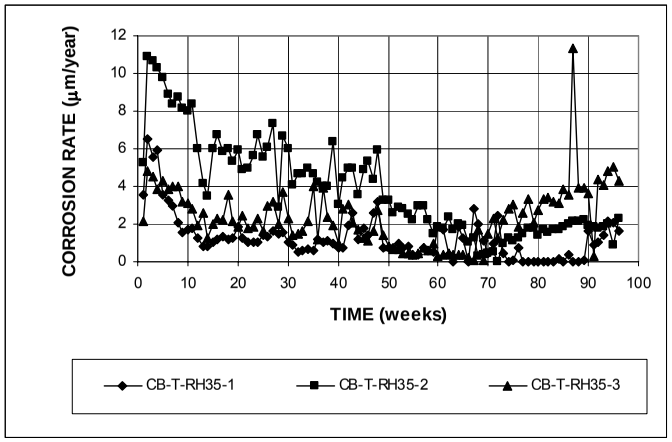


(a)

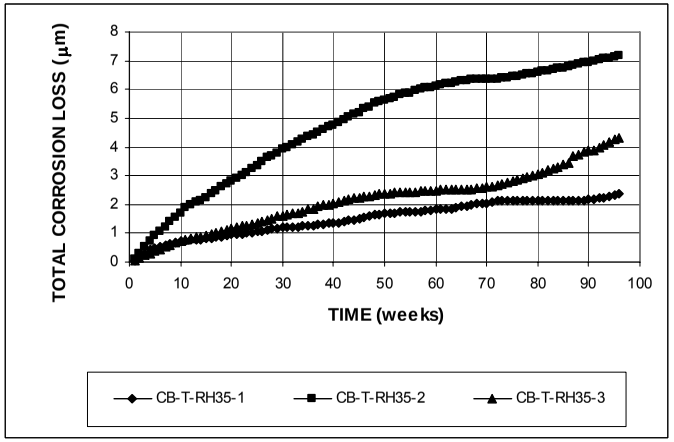


(b)

**Figure A.186 -** (a) Corrosion rates and (b) total corrosion losses as measured in the cracked beam test for specimens with conventional Thermex-treated steel (T), a water-cement ratio of 0.35, and Rheocrete 222+.

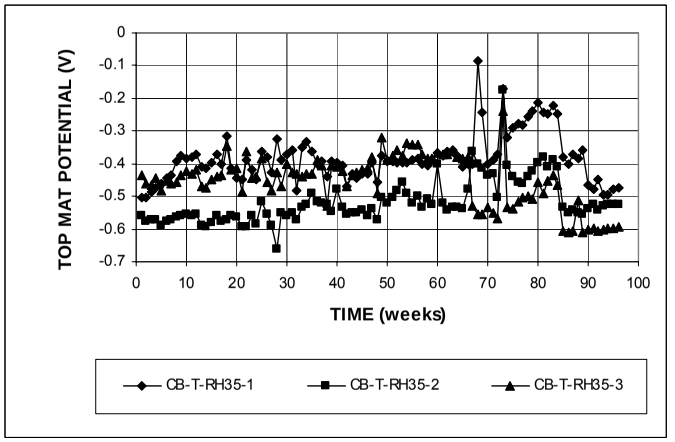


(a)

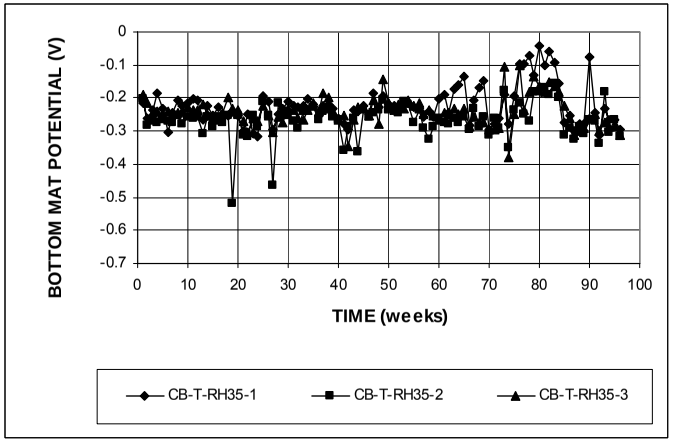


(b)

**Figure A.187 -** (a) Top mat corrosion potentials and (b) bottom mat corrosion potentials, with respect to copper-copper sulfate electrode as measured in the cracked beam test for specimens with conventional Thermex-treated steel (T), a water-cement ratio of 0.35, and Rheocrete 222+.

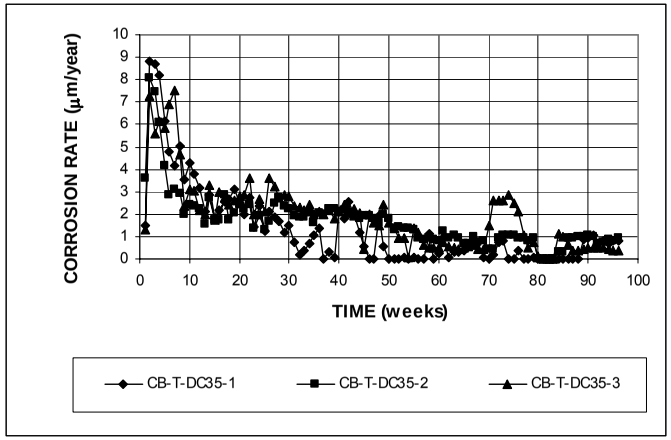


(a)

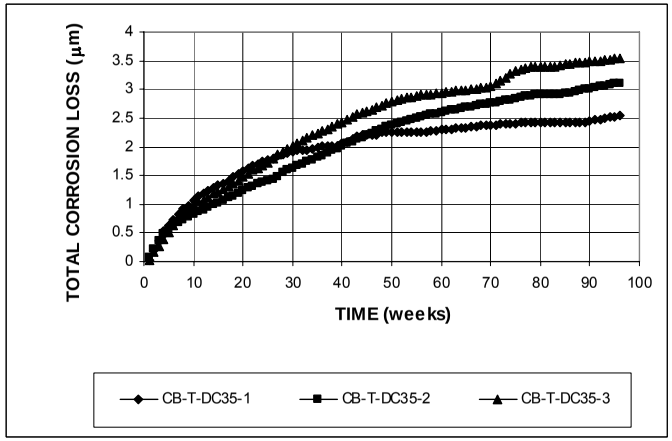


(b)

**Figure A.188 -** (a) Corrosion rates and (b) total corrosion losses as measured in the cracked beam test for specimens with conventional Thermex-treated steel (T), a water-cement ratio of 0.35, and DCI-S.

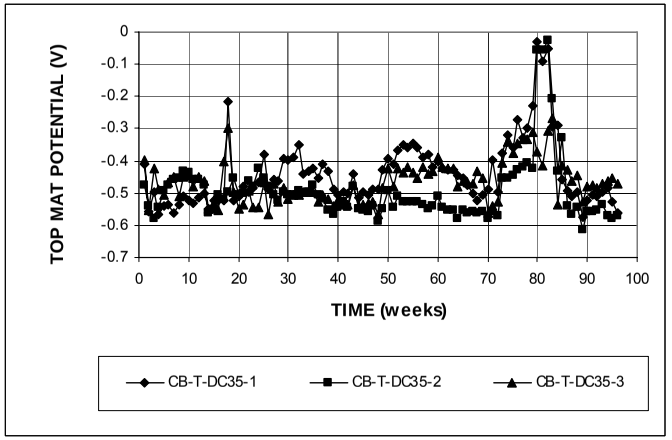


(a)

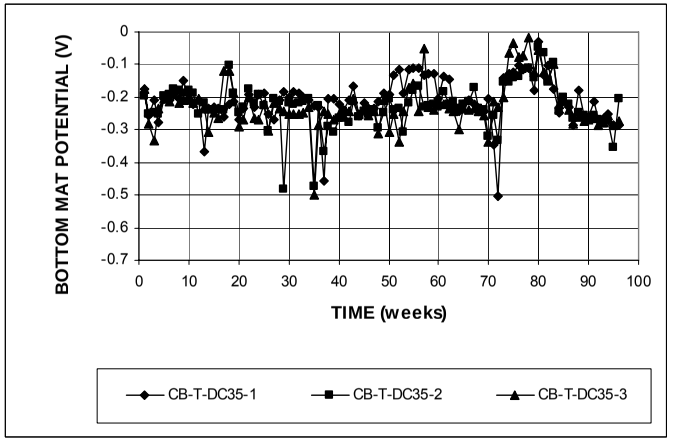


(b)

**Figure A.189 -** (a) Top mat corrosion potentials and (b) bottom mat corrosion potentials, with respect to copper-copper sulfate electrode as measured in the cracked beam test for specimens with conventional Thermex-treated steel (T), a water-cement ratio of 0.35, and DCI-S.

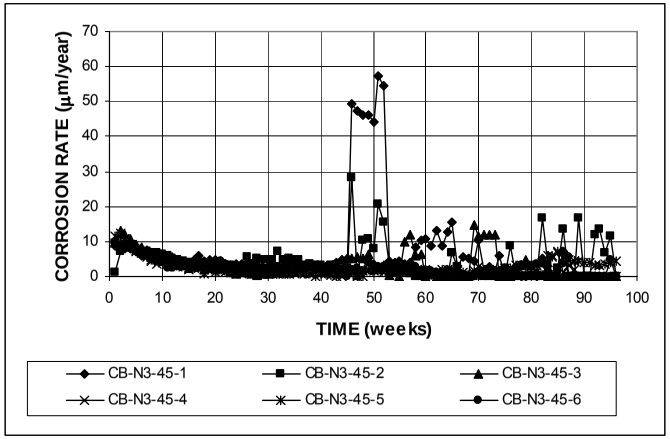


(a)

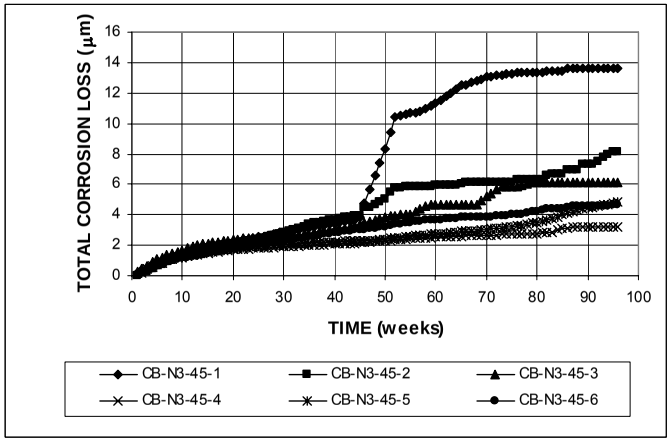


(b)

**Figure A.190 -** (a) Corrosion rates and (b) total corrosion losses as measured in the cracked beam test for specimens with conventional normalized steel (N3).

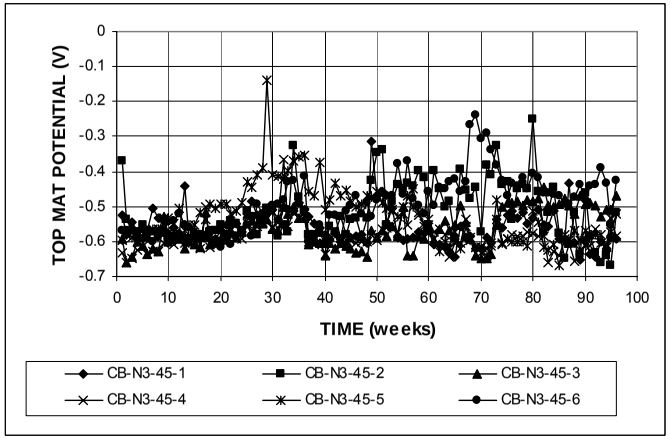


(a)

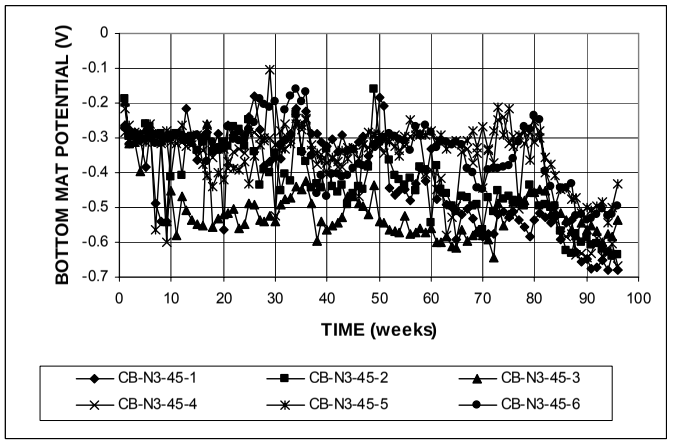


(b)

**Figure A.191 -** (a) Top mat corrosion potentials and (b) bottom mat corrosion potentials, with respect to copper-copper sulfate electrode as measured in the cracked beam test for specimens with conventional normalized steel (N3).

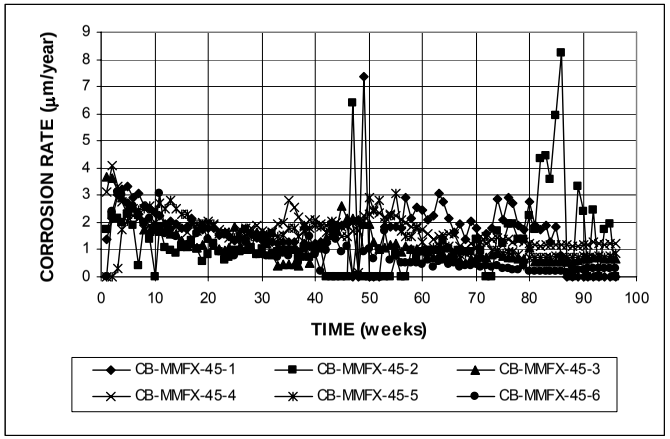


(a)

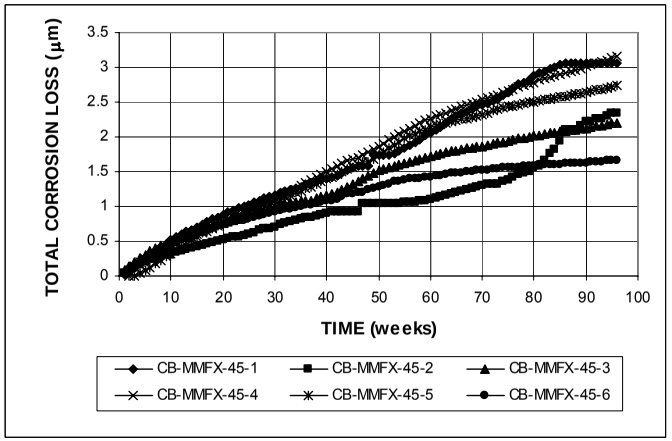


(b)

**Figure A.192 -** (a) Corrosion rates and (b) total corrosion losses as measured in the cracked beam test for specimens with MMFX microcomposite steel.

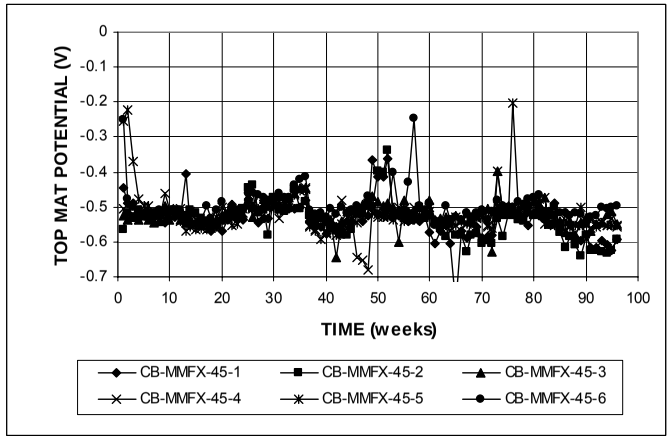


(a)

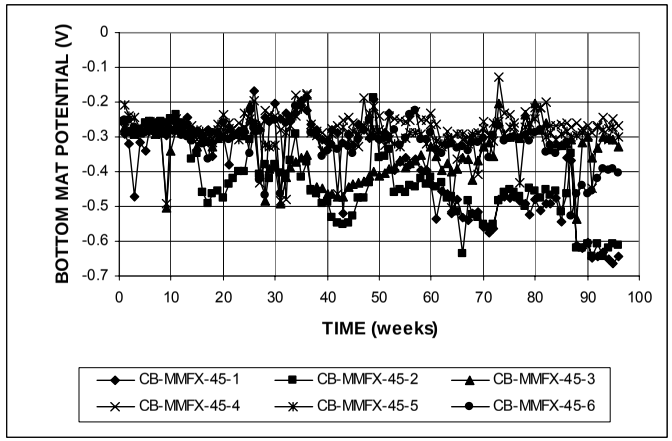


(b)

**Figure A.193 -** (a) Top mat corrosion potentials and (b) bottom mat corrosion potentials, with respect to copper-copper sulfate electrode as measured in the cracked beam test for specimens with MMFX microcomposite steel.

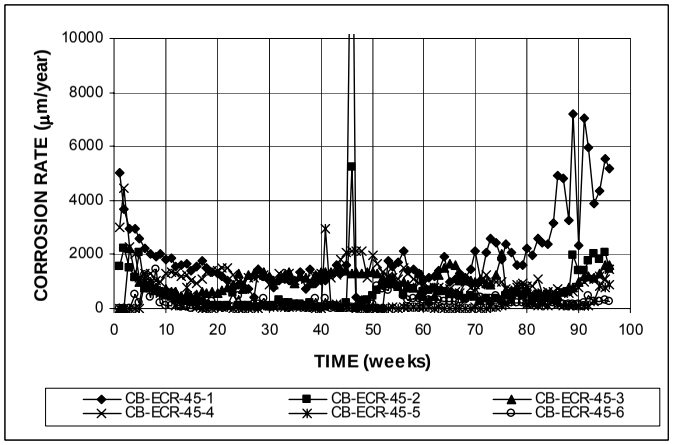


(a)

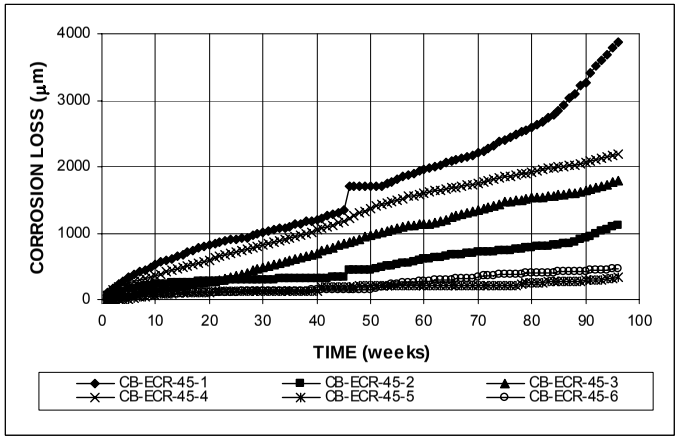


(b)

**Figure A.194 -** (a) Corrosion rates and (b) total corrosion losses based on the exposed area of the bar (fpur 1/8-in. diamater holes) as measured in the cracked beam test for specimens with epoxy-coated steel.

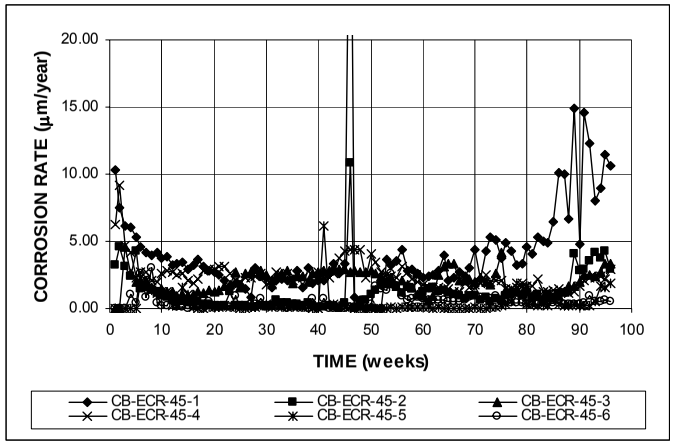


(a)

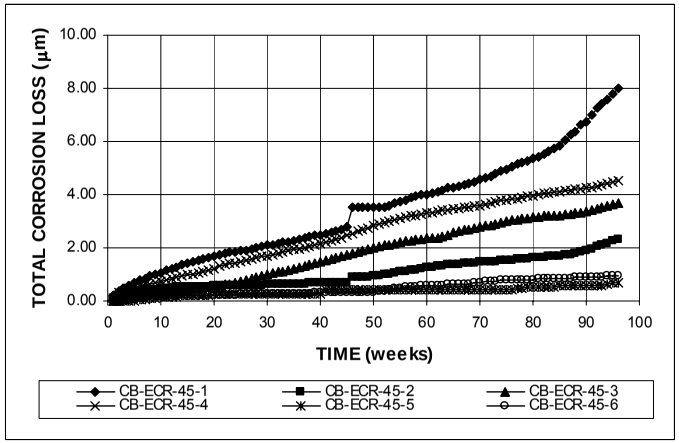


(b)

**Figure A.195 -** (a) Corrosion rates and (b) total corrosion losses based on the total area of the bar, as measured in the cracked beam test for specimens with epoxy-coated steel.

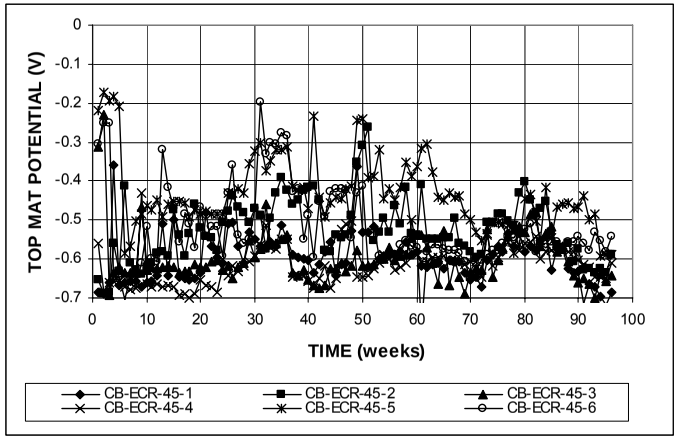


(a)

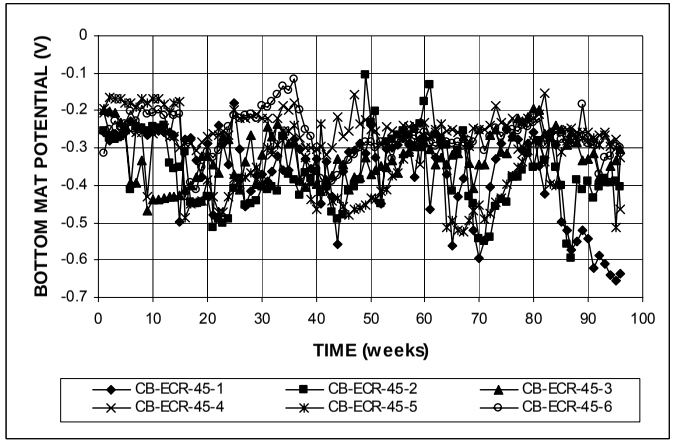


(b)

**Figure A.196 -** (a) Top mat corrosion potentials and (b) bottom mat corrosion potentials, with respect to copper-copper sulfate electrode as measured in the cracked beam test for specimens epoxy-coated steel.

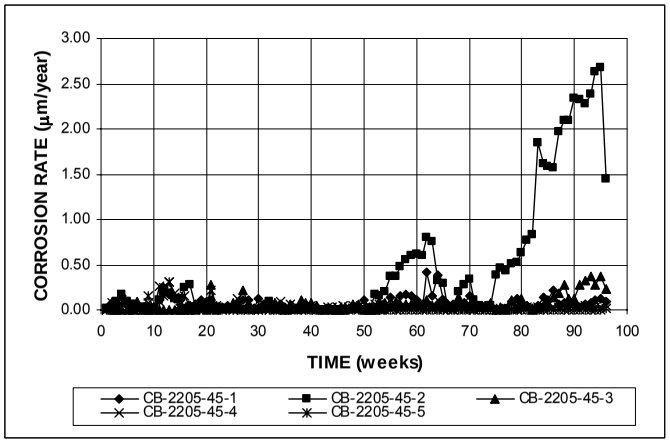


(a)

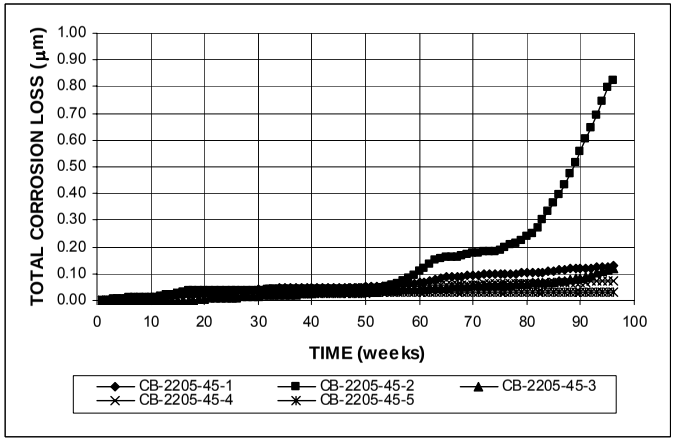


(b)

**Figure A.197 -** (a) Corrosion rates and (b) total corrosion losses as measured in the cracked beam test for specimens with 2205 duplex steel.

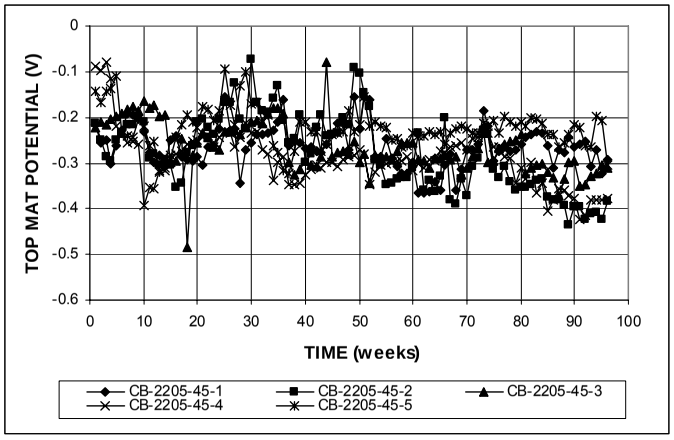


(a)

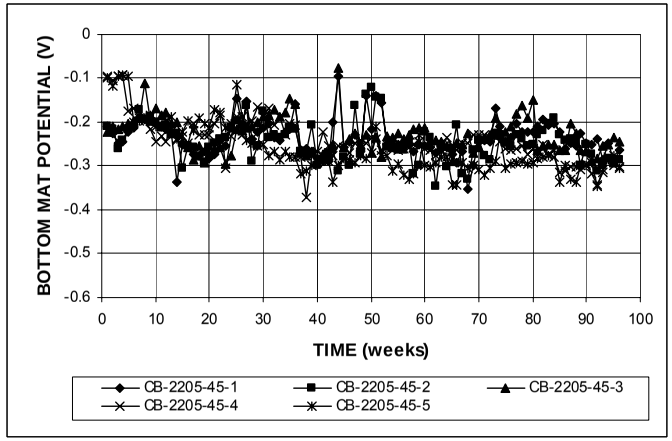


(b)

**Figure A.198 -** (a) Top mat corrosion potentials and (b) bottom mat corrosion potentials, with respect to copper-copper sulfate electrode as measured in the cracked beam test for specimens with 2205 duplex steel.

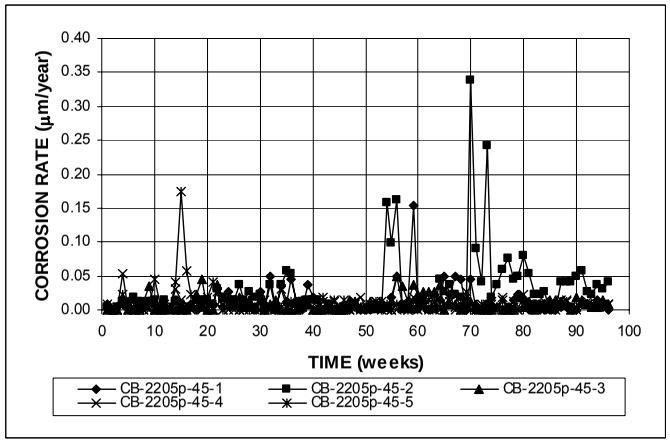


(a)

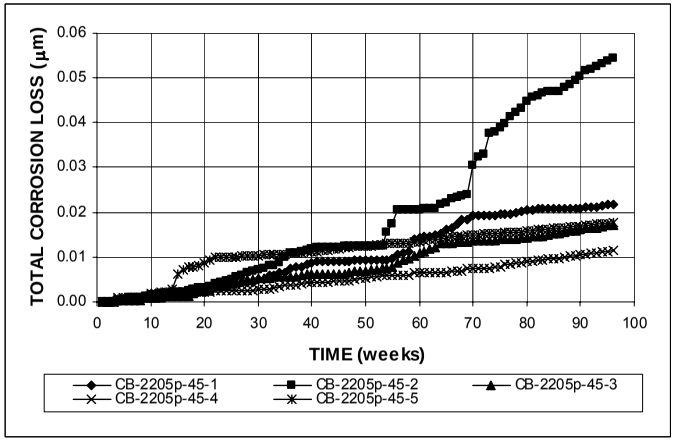


(b)

**Figure A.199 -** (a) Corrosion rates and (b) total corrosion losses as measured in the cracked beam test for specimens with 2205 pickled duplex steel.

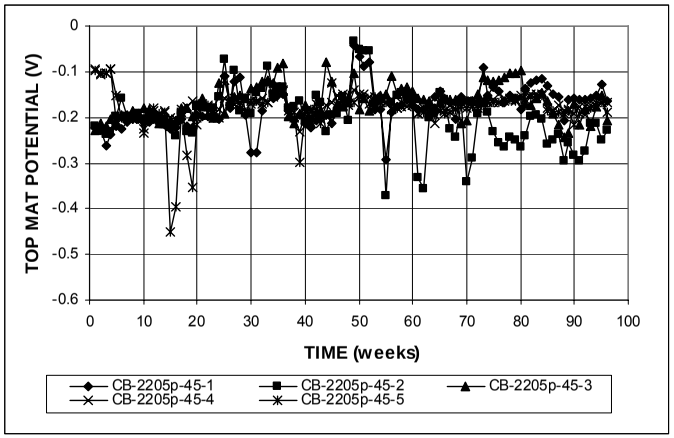


(a)

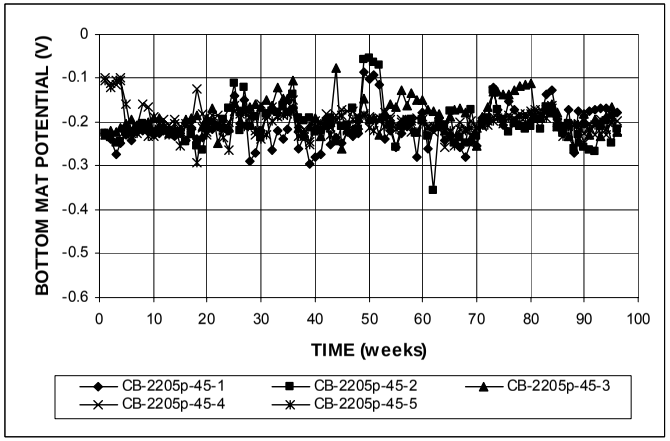


(b)

**Figure A.200 -** (a) Top mat corrosion potentials and (b) bottom mat corrosion potentials, with respect to copper-copper sulfate electrode as measured in the cracked beam test for specimens with 2205 pickled duplex steel.

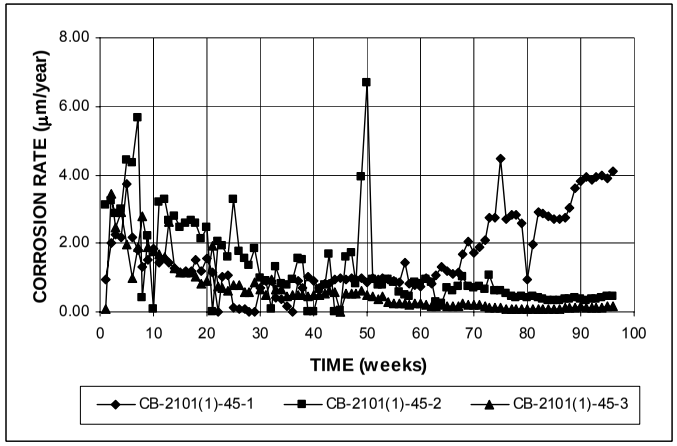


(a)

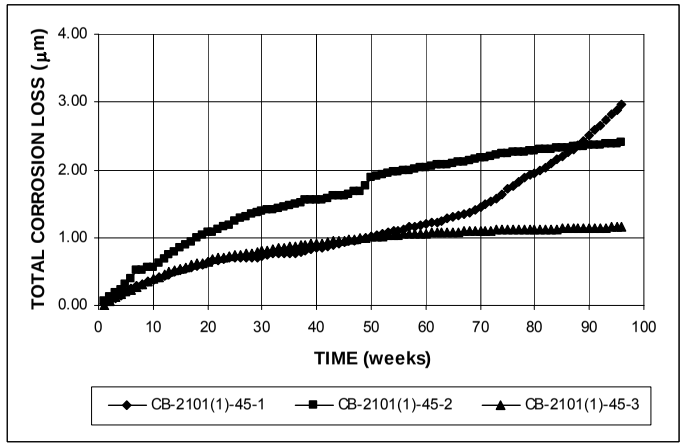


(b)

**Figure A.201 -** (a) Corrosion rates and (b) total corrosion losses as measured in the cracked beam test for specimens with 2101(1) duplex steel.

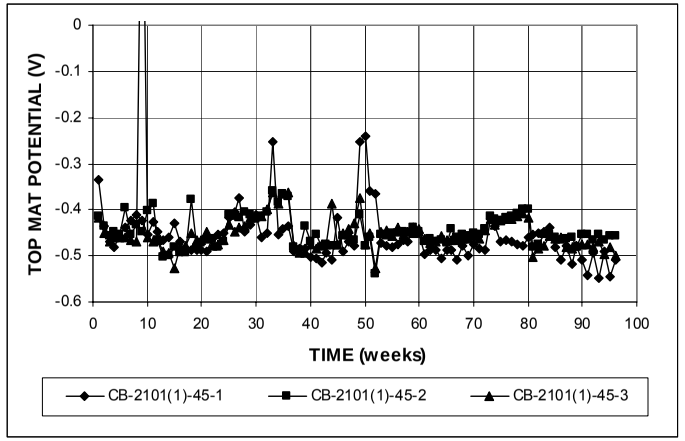


(a)

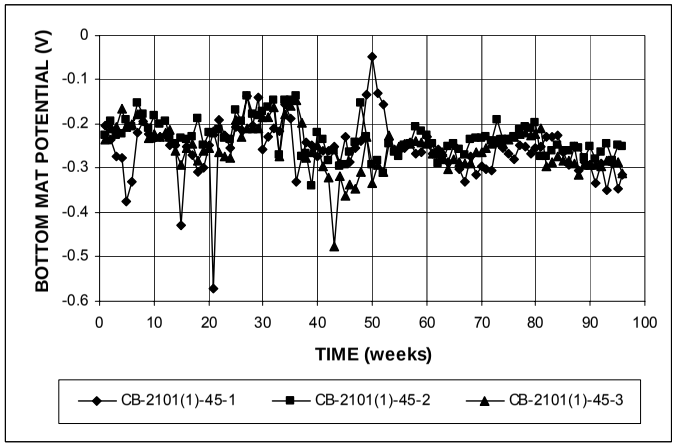


(b)

**Figure A.202 -** (a) Top mat corrosion potentials and (b) bottom mat corrosion potentials, with respect to copper-copper sulfate electrode as measured in the cracked beam test for specimens with 2101(1) duplex steel.

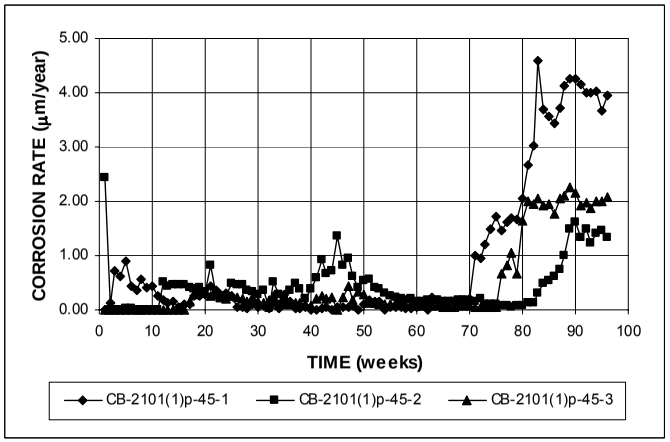


(a)

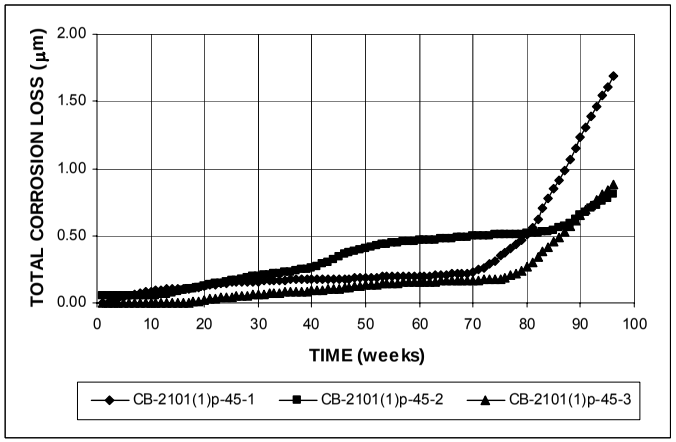


(b)

**Figure A.203 -** (a) Corrosion rates and (b) total corrosion losses as measured in the cracked beam test for specimens with 2101(1) pickled duplex steel.

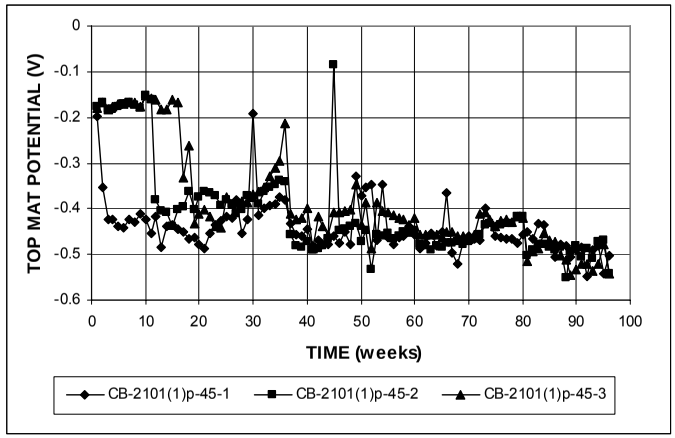


(a)

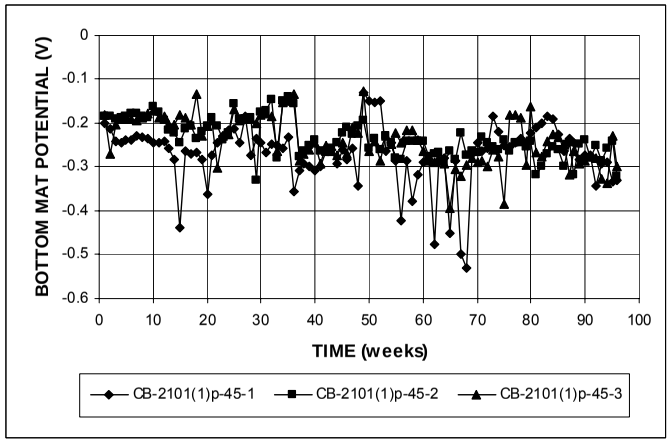


(b)

**Figure A.204 -** (a) Top mat corrosion potentials and (b) bottom mat corrosion potentials, with respect to copper-copper sulfate electrode as measured in the cracked beam test for specimens with 2101(1) pickled duplex steel.

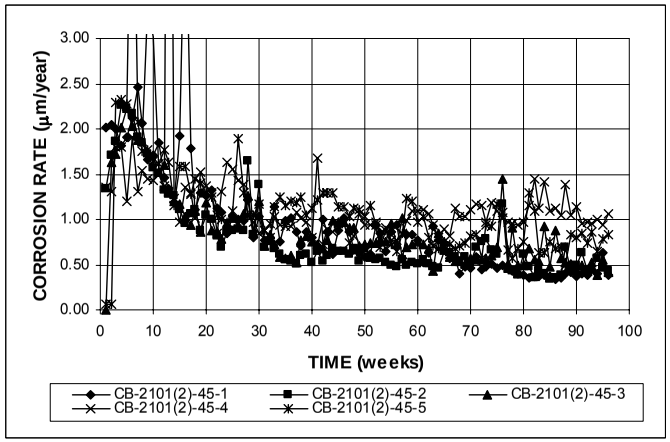


(a)

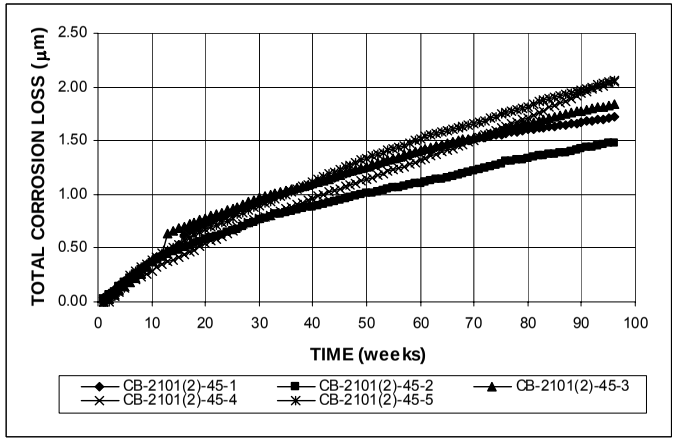


(b)

**Figure A.205 -** (a) Corrosion rates and (b) total corrosion losses as measured in the cracked beam test for specimens with 2101(2) duplex steel.

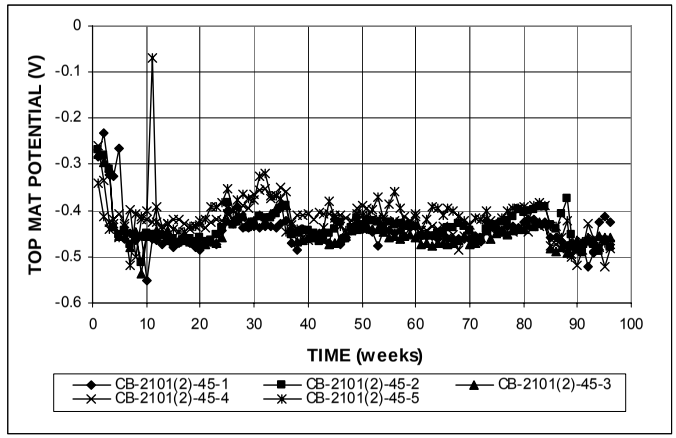


(a)

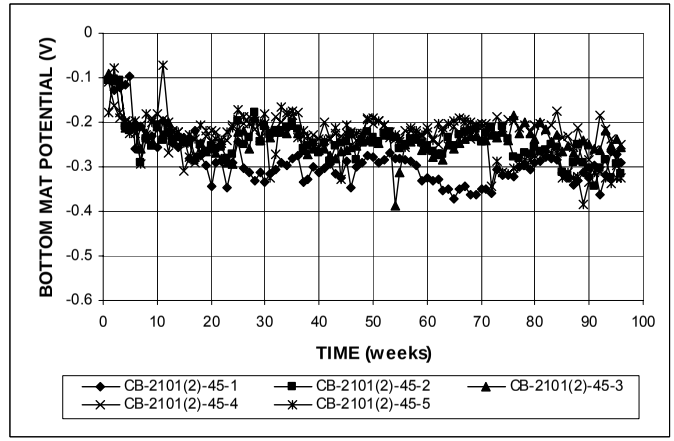


(b)

**Figure A.206 -** (a) Top mat corrosion potentials and (b) bottom mat corrosion potentials, with respect to copper-copper sulfate electrode as measured in the cracked beam test for specimens with 2101(2) duplex steel.

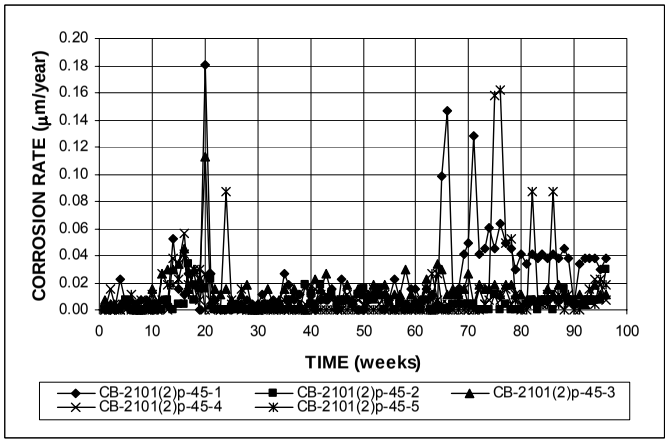


(a)

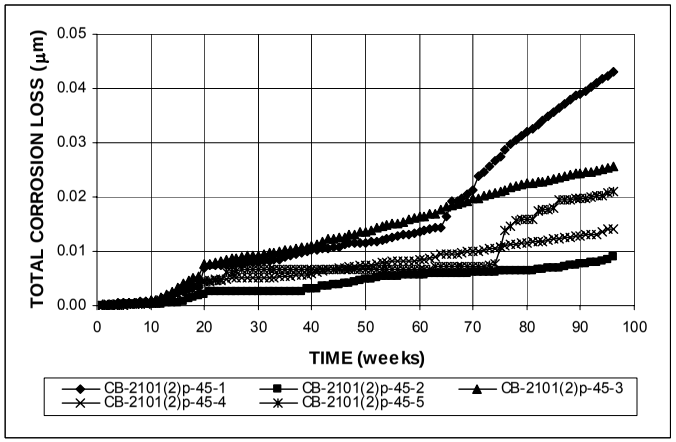


(b)

**Figure A.207** - (a) Corrosion rates and (b) total corrosion losses as measured in the cracked beam test for specimens with 2101(2) pickled duplex steel.

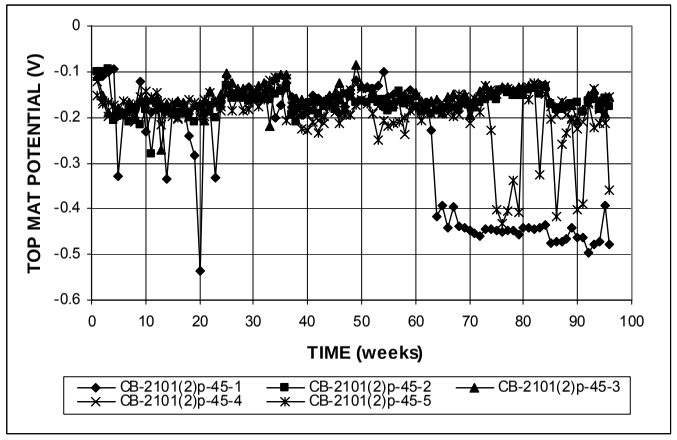


(a)

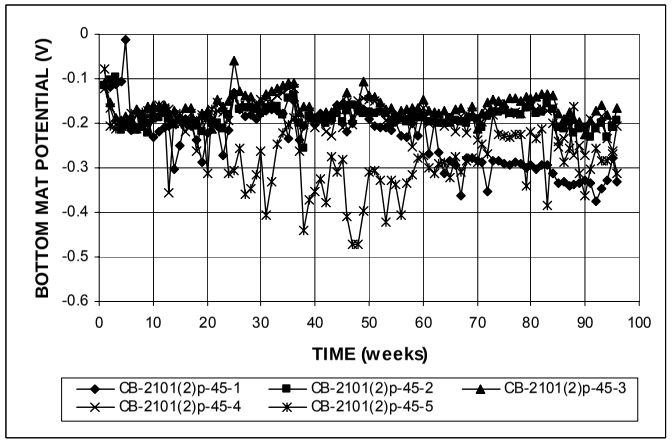


(b)

**Figure A.208** - (a) Top mat corrosion potentials and (b) bottom mat corrosion potentials, with respect to copper-copper sulfate electrode as measured in the cracked beam test for specimens with 2101(2) pickled duplex steel.

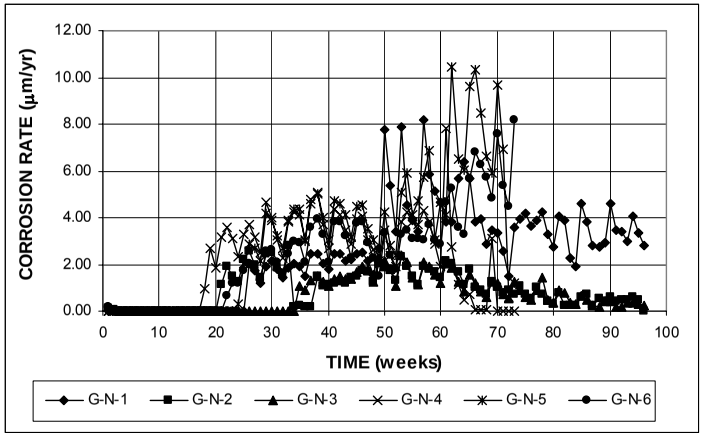


(a)

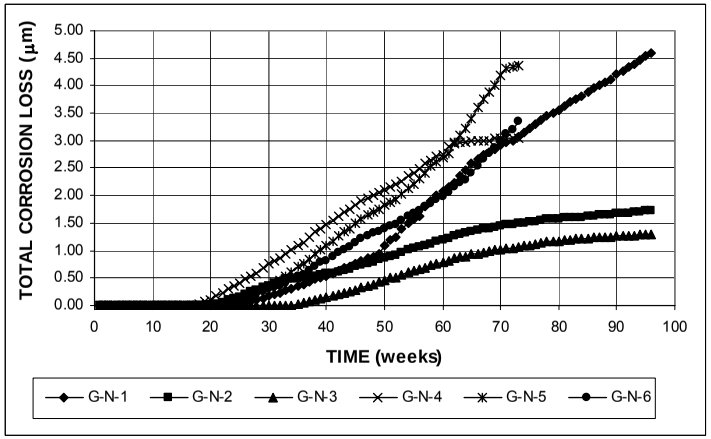


(b)

**Figure A.209 -** (a) Corrosion rates and (b) total corrosion losses as measured in the ASTM G 109 test for specimens with conventional normalized steel (N).

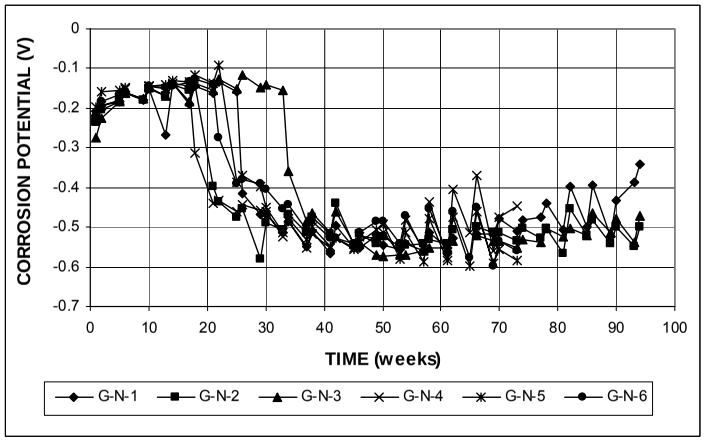


(a)

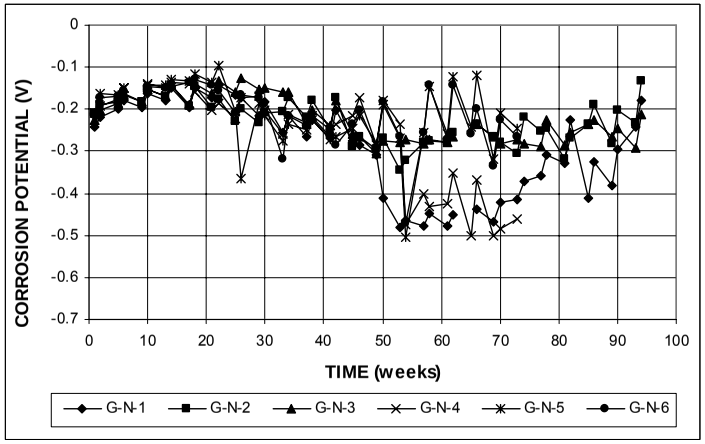


(b)

**Figure A.210 -** (a) Top mat corrosion potentials and (b) bottom mat corrosion potentials, with respect to copper-copper sulfate electrode as measured in the ASTM G 109 test for specimens with conventional normalized steel (N).

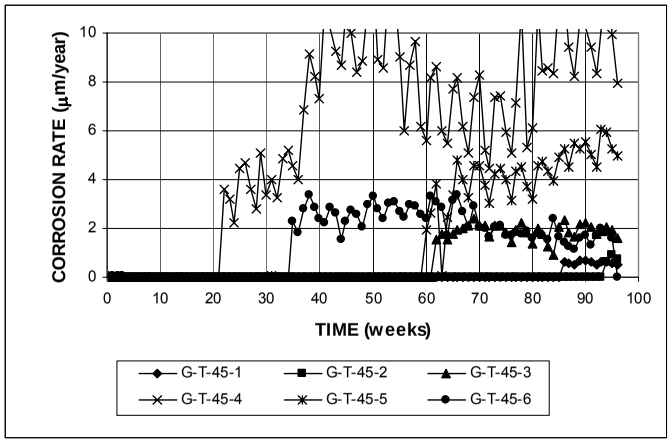


(a)

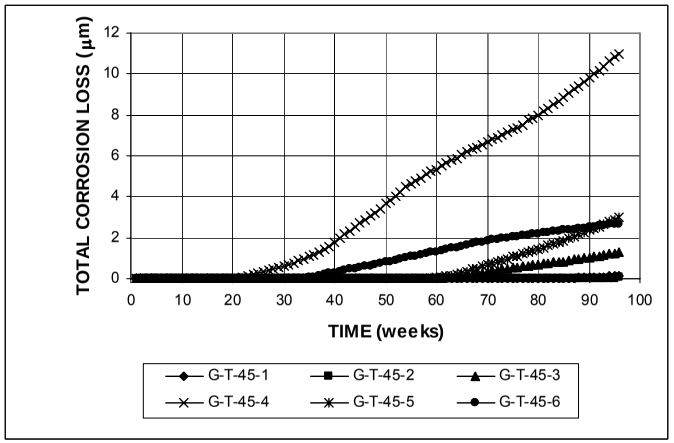


(b)

**Figure A.211 -** (a) Corrosion rates and (b) total corrosion losses as measured in the ASTM G 109 test for specimens with conventional Thermex-treated steel (T).

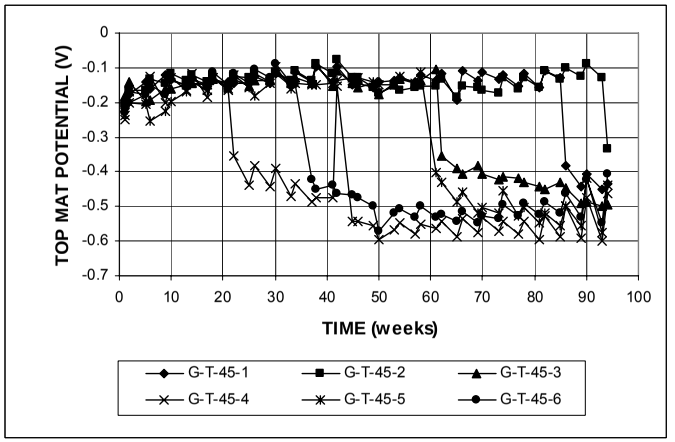


(a)

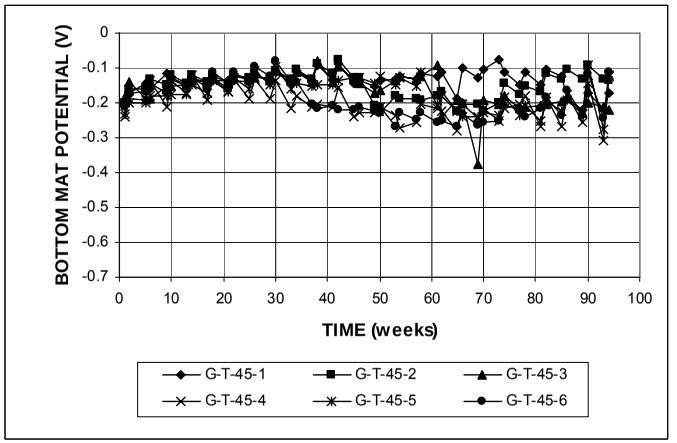


(b)

**Figure A.212 -** (a) Top mat corrosion potentials and (b) bottom mat corrosion potentials, with respect to copper-copper sulfate electrode as measured in the ASTM G 109 test for specimens with conventional Thermex-treated steel (T).

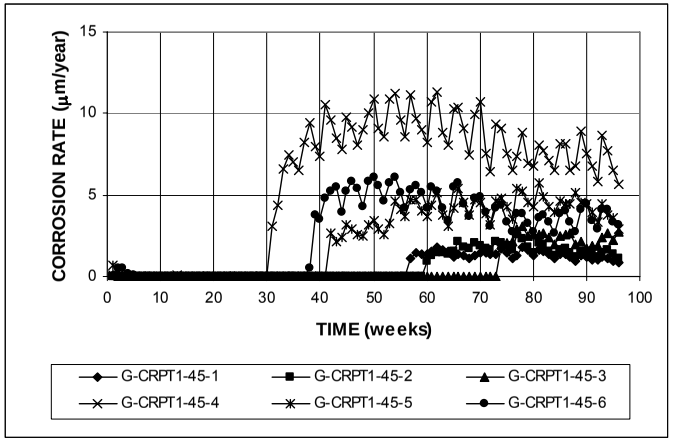


(a)

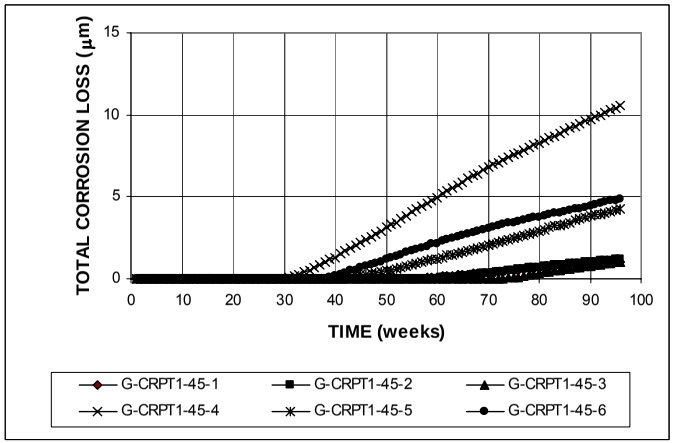


(b)

**Figure A.213 -** (a) Corrosion rates and (b) total corrosion losses as measured in the ASTM G 109 test for specimens with microalloyed steel with a high phosphorus content, 0.117%, Thermex-treated (CRPT1).

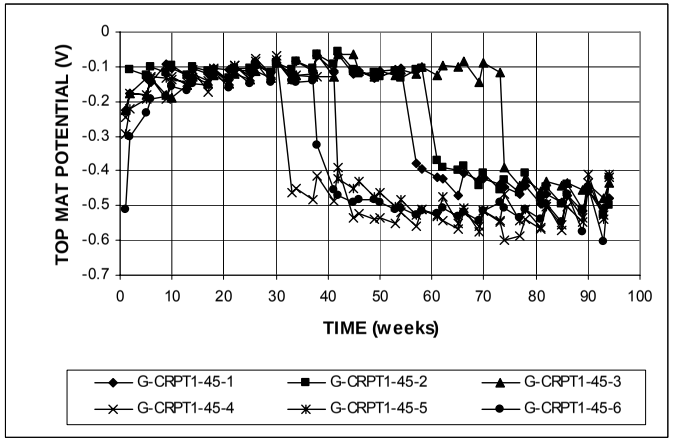


(a)

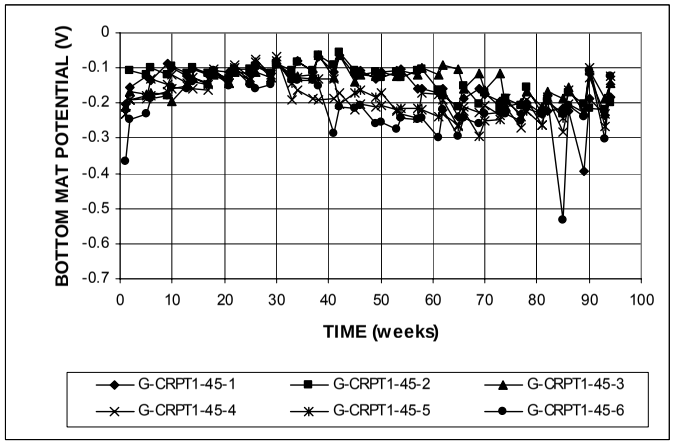


(b)

**Figure A.214 -** (a) Top mat corrosion potentials and (b) bottom mat corrosion potentials, with respect to copper-copper sulfate electrode as measured in the ASTM G 109 test for specimens with microalloyed steel with a high phosphorus content, 0.117%, Thermex-treated (CRPT1).

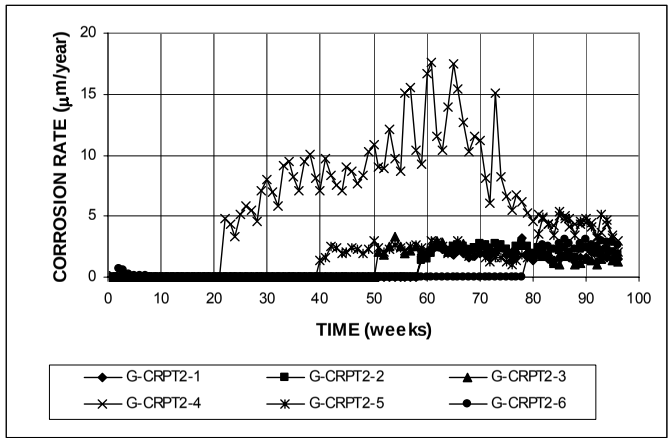


(a)

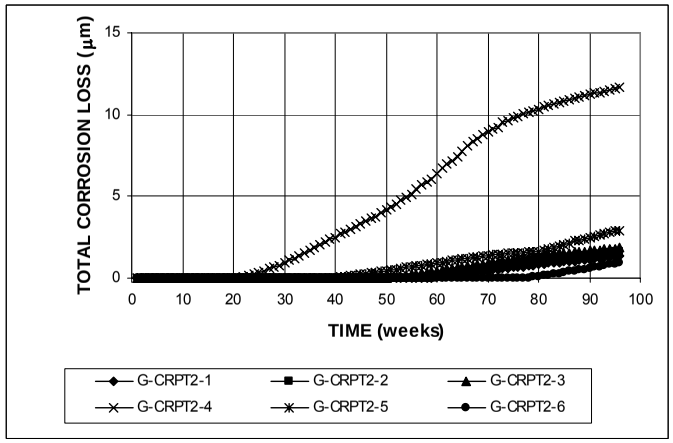


(b)

**Figure A.215 -** (a) Corrosion rates and (b) total corrosion losses as measured in the ASTM G 109 test for specimens with microalloyed steel with a high phosphorus content, 0.100%, Thermex-treated (CRPT2).

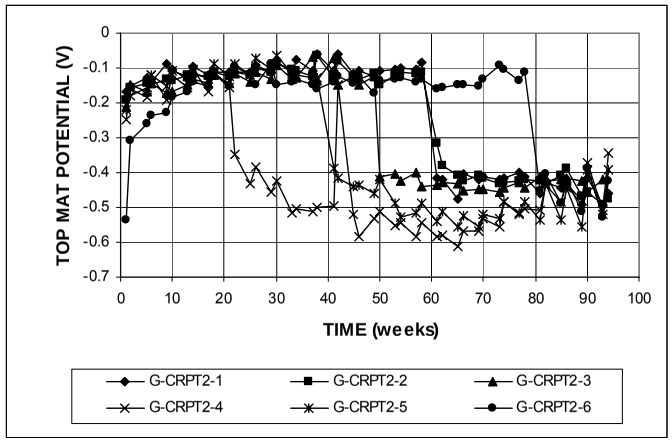


(a)

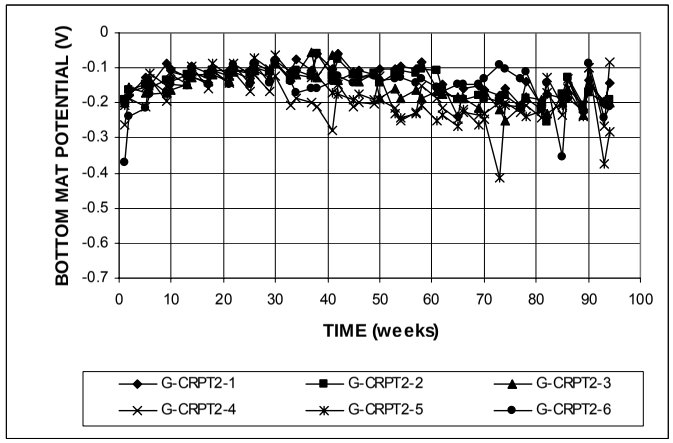


(b)

**Figure A.216 -** (a) Top mat corrosion potentials and (b) bottom mat corrosion potentials, with respect to copper-copper sulfate electrode as measured in the ASTM G 109 test for specimens with microalloyed steel with a high phosphorus content, 0.100%, Thermex-treated (CRPT2).

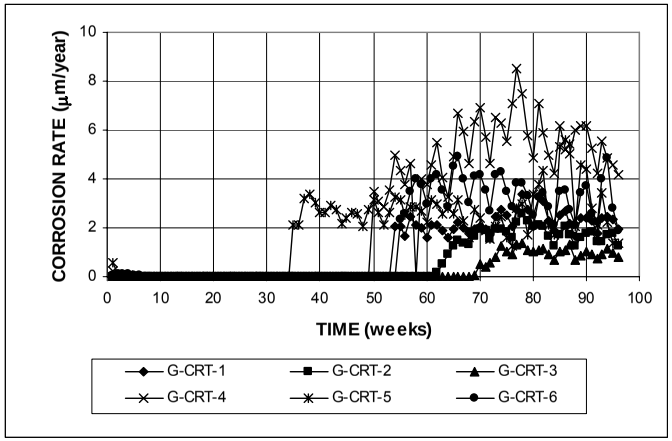


(a)

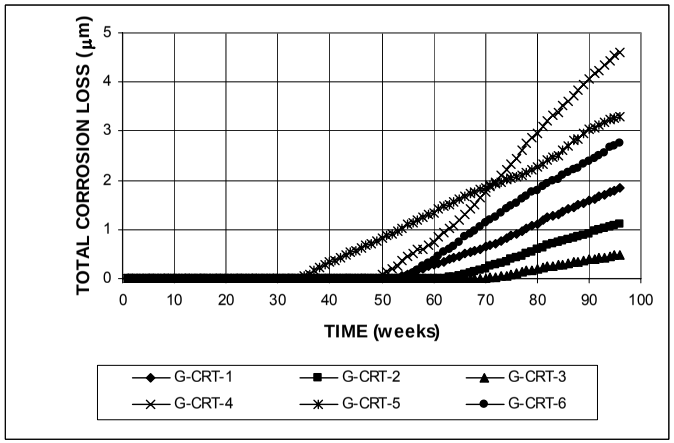


(b)

**Figure A.217 -** (a) Corrosion rates and (b) total corrosion losses as measured in the ASTM G 109 test for specimens with microalloyed steel with normal phosphorus content, 0.017%, Thermex-treated (CRT).

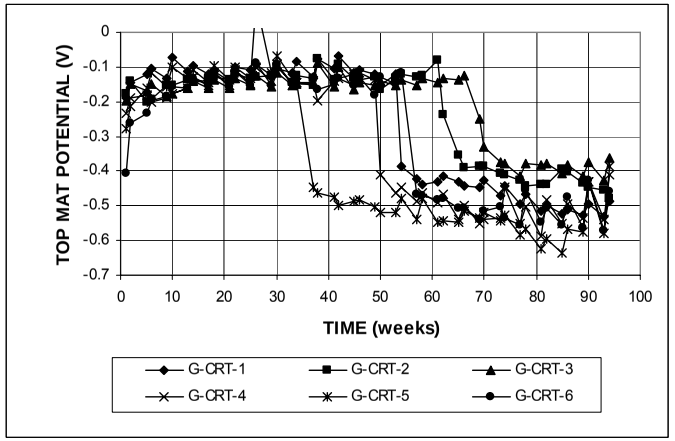


(a)

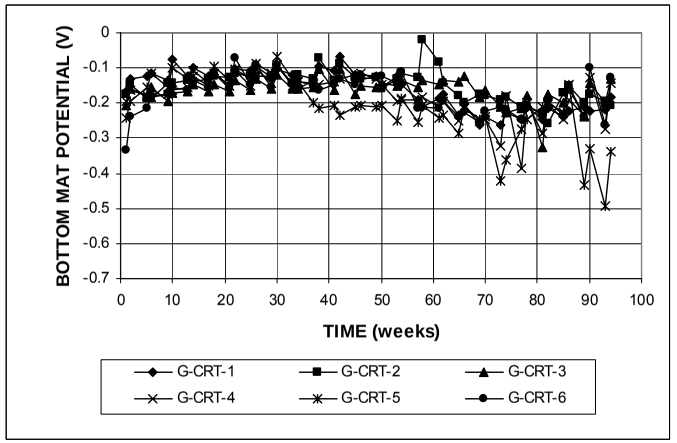


(b)

**Figure A.218 -** (a) Top mat corrosion potentials and (b) bottom mat corrosion potentials, with respect to copper-copper sulfate electrode as measured in the ASTM G 109 test for specimens with microalloyed steel with normal phosphorus content, 0.017%, Thermex-treated (CRT).

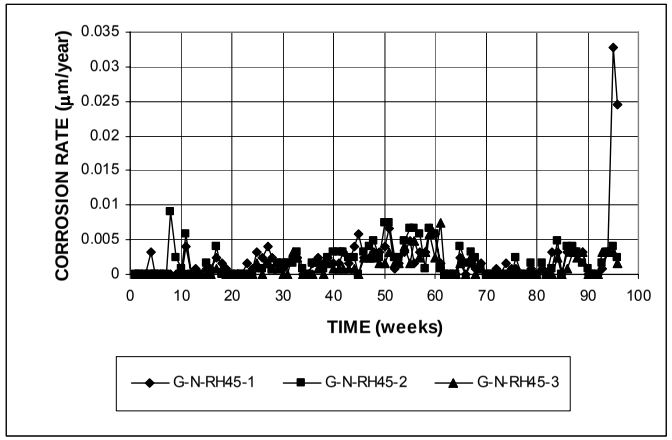


(a)

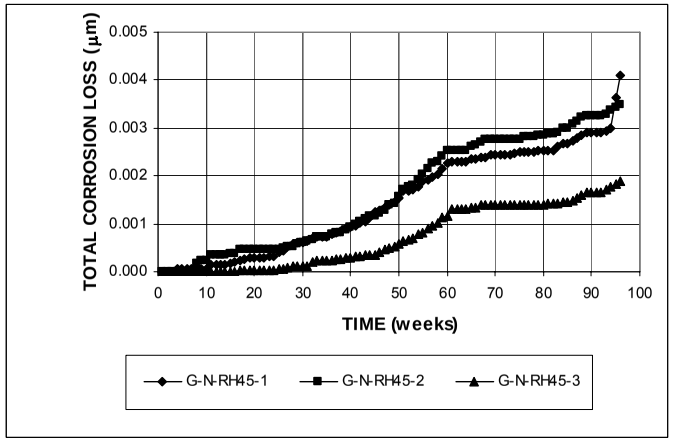


(b)

**Figure A.219 -** (a) Corrosion rates and (b) total corrosion losses as measured in the ASTM G 109 test for specimens with conventional normalized steel (N), a water-cement ratio of 0.45, and Rheocrete 222+.

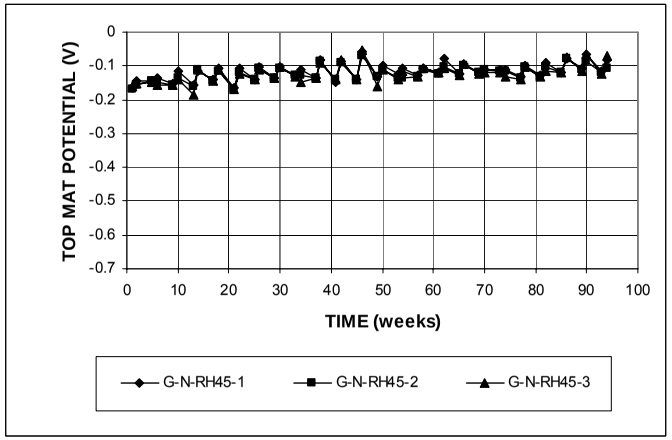


(a)

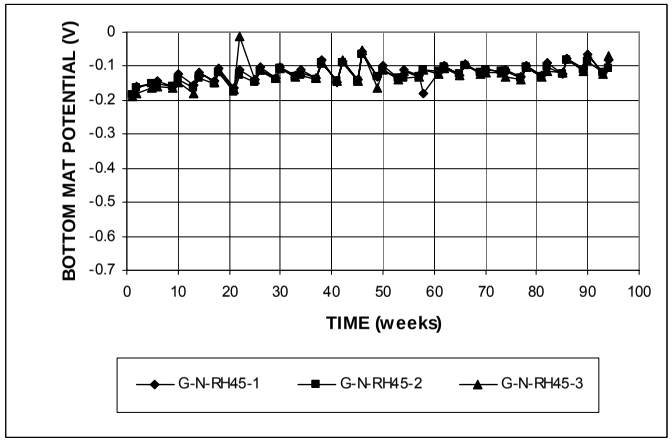


(b)

**Figure A.220 -** (a) Top mat corrosion potentials and (b) bottom mat corrosion potentials, with respect to copper-copper sulfate electrode as measured in the ASTM G 109 test for specimens with conventional normalized steel (N), a water-cement ratio of 0.45, and Rheocrete 222+.

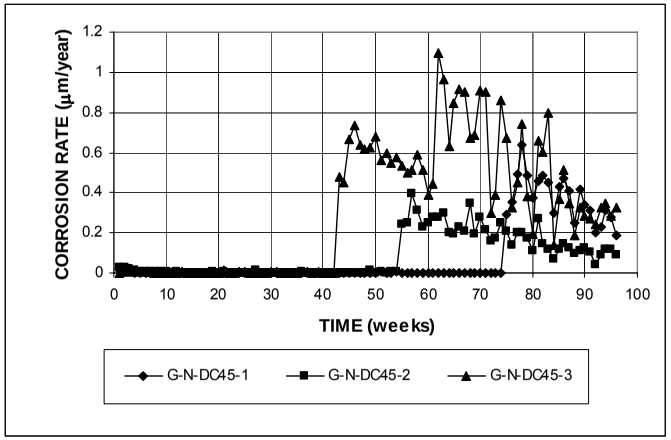


(a)

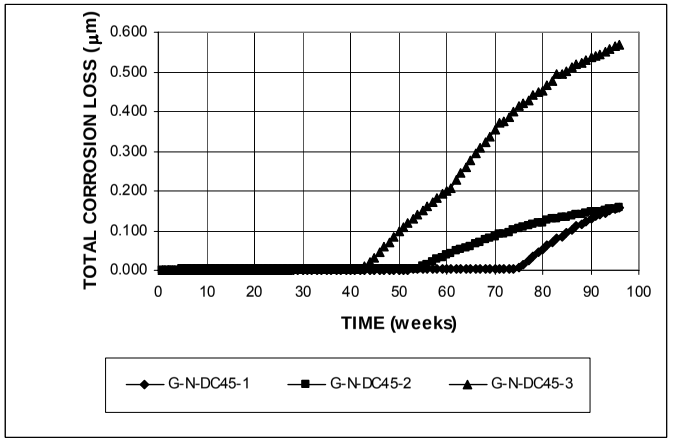


(b)

**Figure A.221 -** (a) Corrosion rates and (b) total corrosion losses as measured in the ASTM G 109 test for specimens with conventional normalized steel (N), a water-cement ratio of 0.45, and DCI-S.

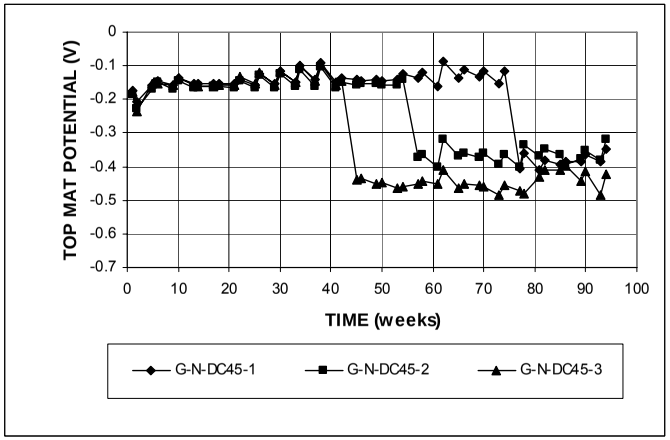


(a)

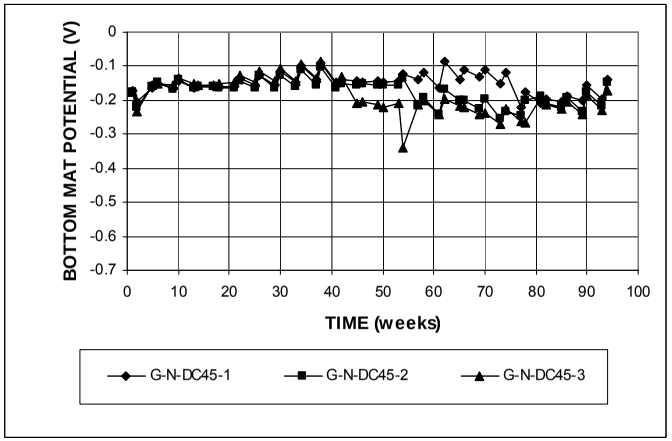


(b)

**Figure A.222 -** (a) Top mat corrosion potentials and (b) bottom mat corrosion potentials, with respect to copper-copper sulfate electrode as measured in the ASTM G 109 test for specimens with conventional normalized steel (N), a water-cement ratio of 0.45, and DCI-S.

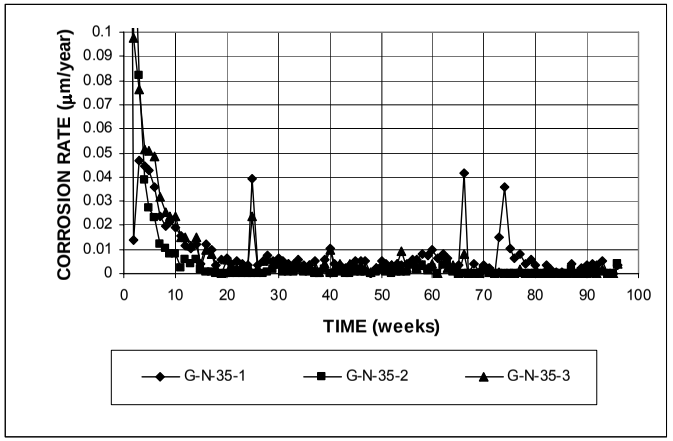


(a)

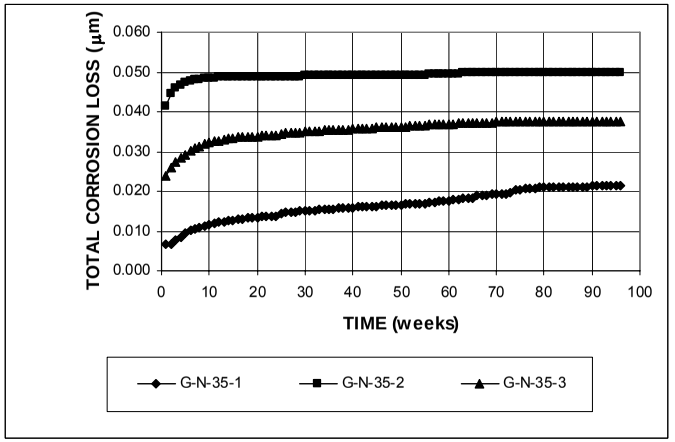


(b)

**Figure A.223 -** (a) Corrosion rates and (b) total corrosion losses as measured in the ASTM G 109 test for specimens with conventional normalized steel (N), a water-cement ratio of 0.35, and no inhibitor.

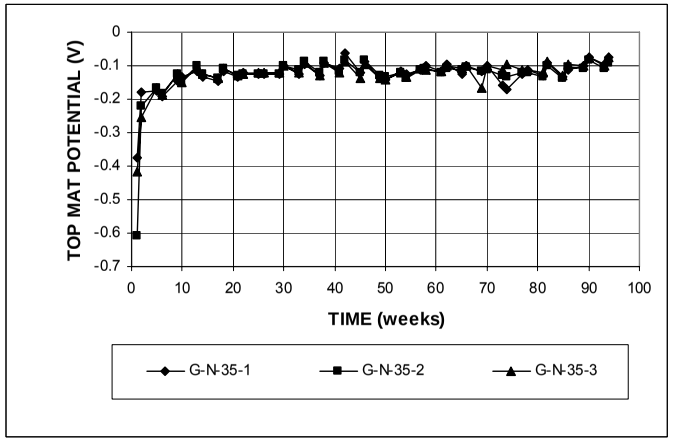


(a)

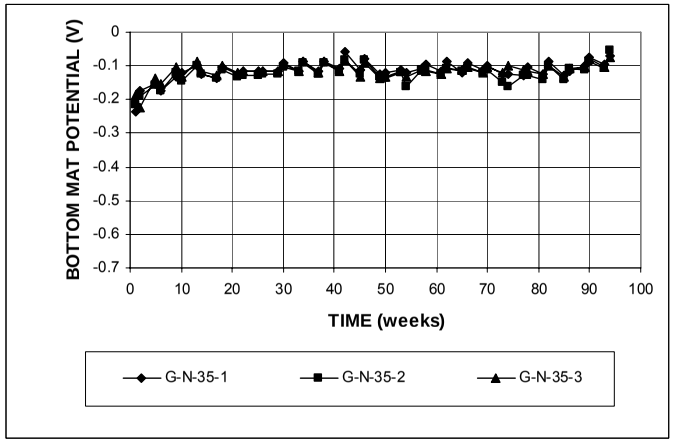


(b)

**Figure A.224 -** (a) Top mat corrosion potentials and (b) bottom mat corrosion potentials, with respect to copper-copper sulfate electrode as measured in the ASTM G 109 test for specimens with conventional normalized steel (N), a water-cement ratio of 0.35, and no inhibitor.

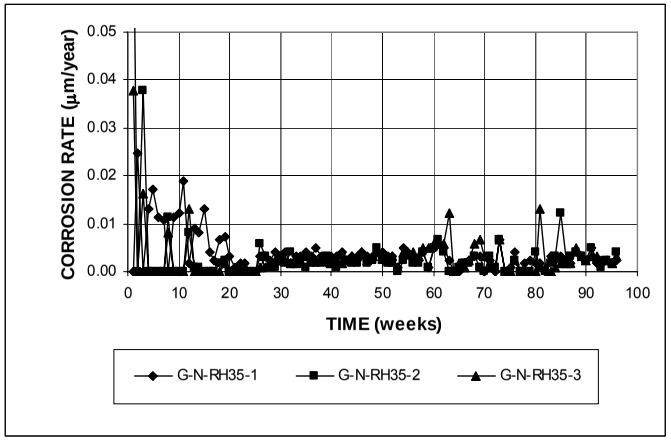


(a)

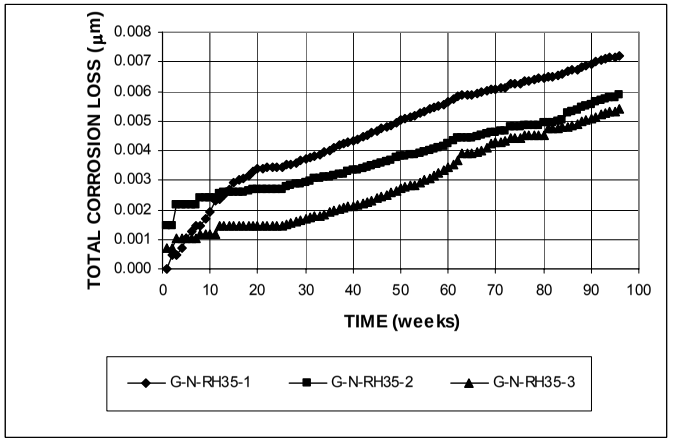


(b)

**Figure A.225 -** (a) Corrosion rates and (b) total corrosion losses as measured in the ASTM G 109 test for specimens with conventional normalized steel (N), a water-cement ratio of 0.35, and Rheocrete 222+.

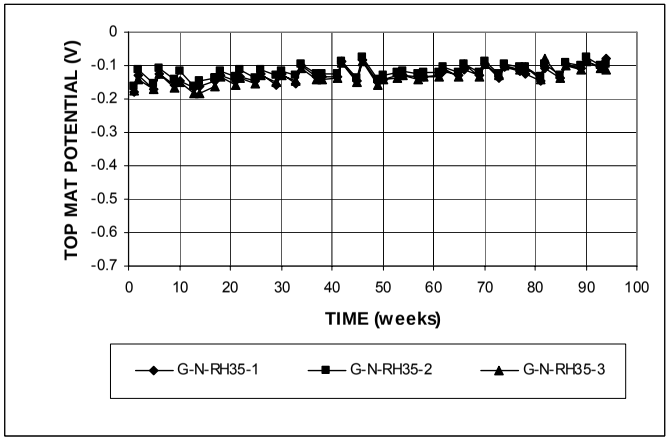


(a)

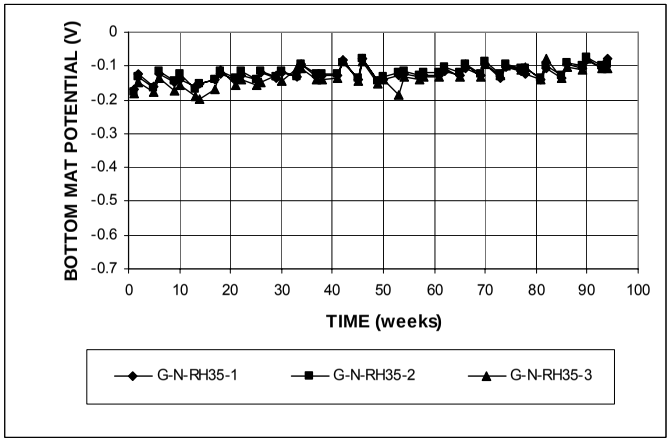


(b)

**Figure A.226 -** (a) Top mat corrosion potentials and (b) bottom mat corrosion potentials, with respect to copper-copper sulfate electrode as measured in the ASTM G 109 test for specimens with conventional normalized steel (N), a water-cement ratio of 0.35, and Rheocrete 222+.

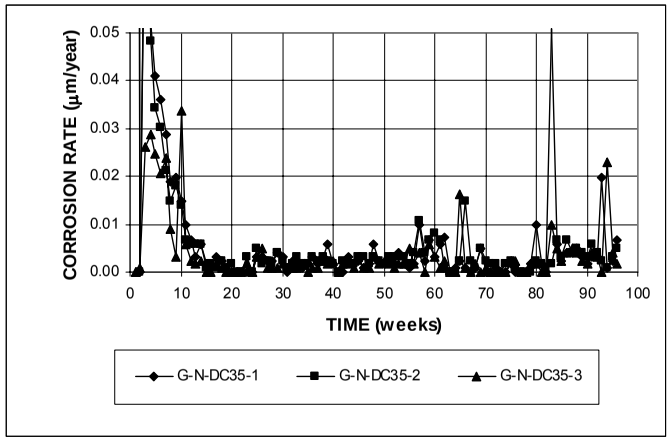


(a)

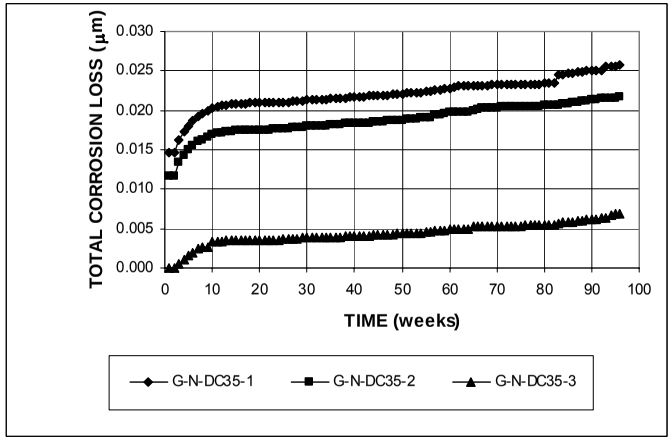


(b)

**Figure A.227 -** (a) Corrosion rates and (b) total corrosion losses as measured in the ASTM G 109 test for specimens with conventional normalized steel (N), a water-cement ratio of 0.35, and DCI-S.

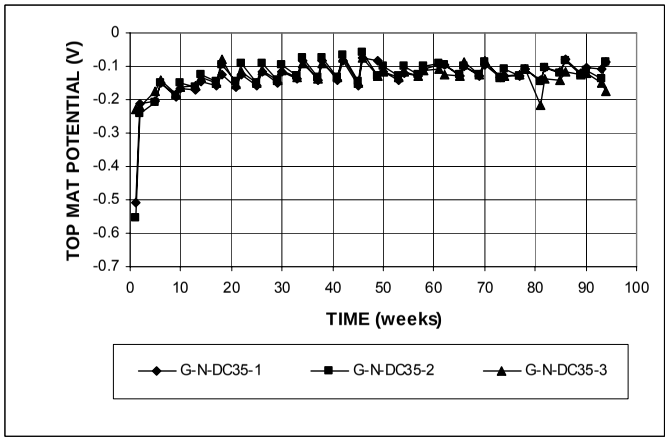


(a)

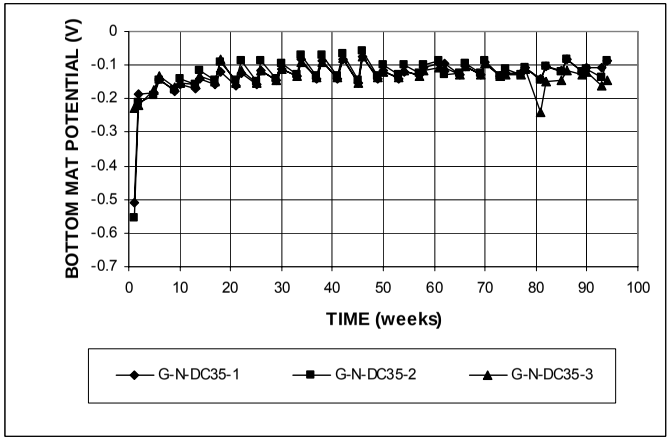


(b)

**Figure A.228 -** (a) Top mat corrosion potentials and (b) bottom mat corrosion potentials, with respect to copper-copper sulfate electrode as measured in the ASTM G 109 test for specimens with conventional normalized steel (N), a water-cement ratio of 0.35, and DCI-S.

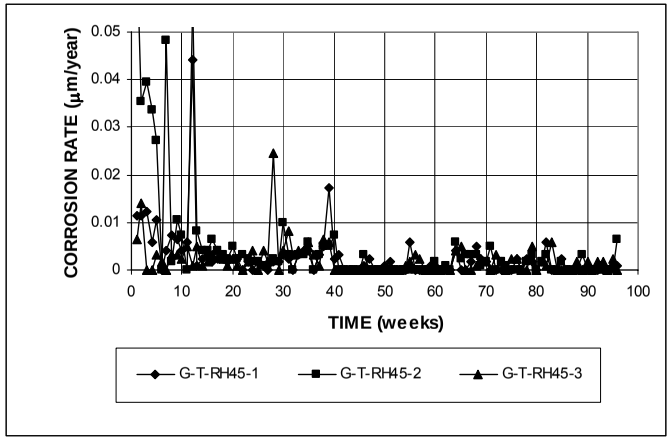


(a)

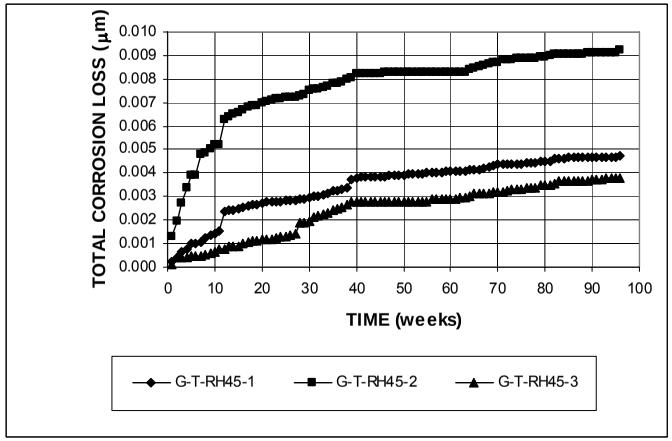


(b)

**Figure A.229 -** (a) Corrosion rates and (b) total corrosion losses as measured in the ASTM G 109 test for specimens with conventional Thermex-treated steel (T), a water-cement ratio of 0.45, and Rheocrete 222+.

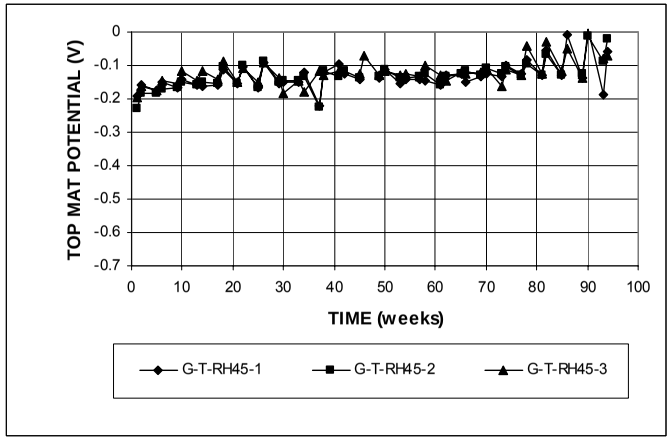


(a)

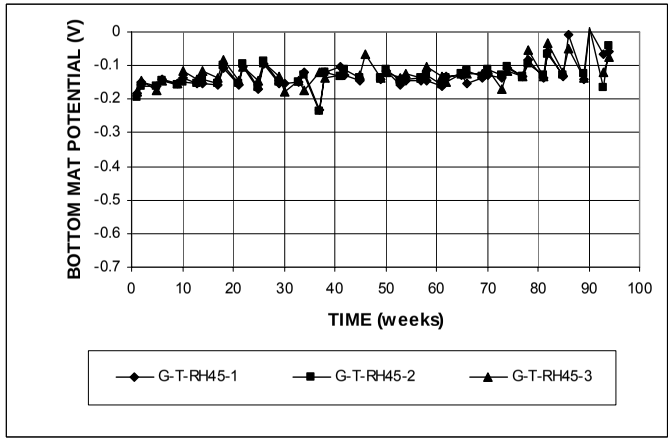


(b)

**Figure A.230 -** (a) Top mat corrosion potentials and (b) bottom mat corrosion potentials, with respect to copper-copper sulfate electrode as measured in the ASTM G 109 test for specimens with conventional Thermex-treated steel (T), a water-cement ratio of 0.45, and Rheocrete 222+.

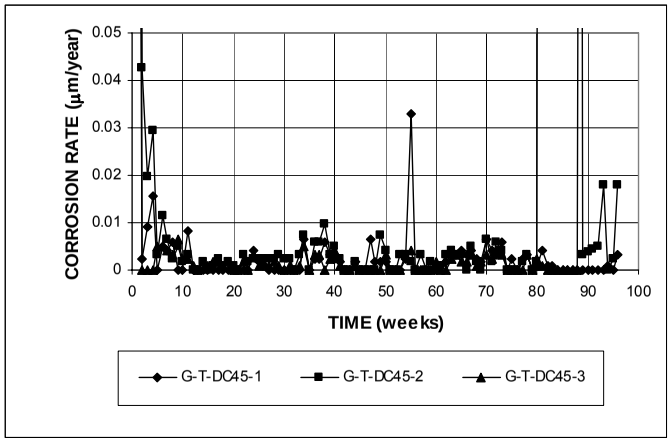


(a)

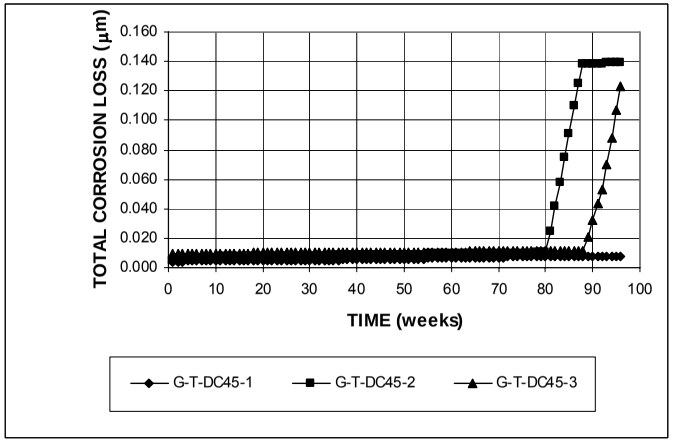


(b)

**Figure A.231 -** (a) Corrosion rates and (b) total corrosion losses as measured in the ASTM G 109 test for specimens with conventional Thermex-treated steel (T), a water-cement ratio of 0.45, and DCI-S.

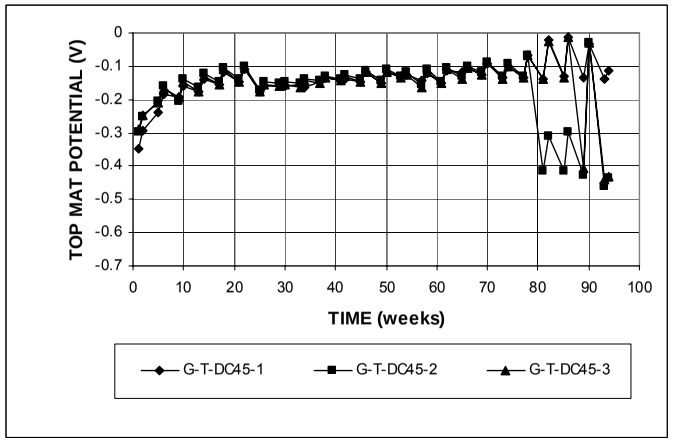


(a)

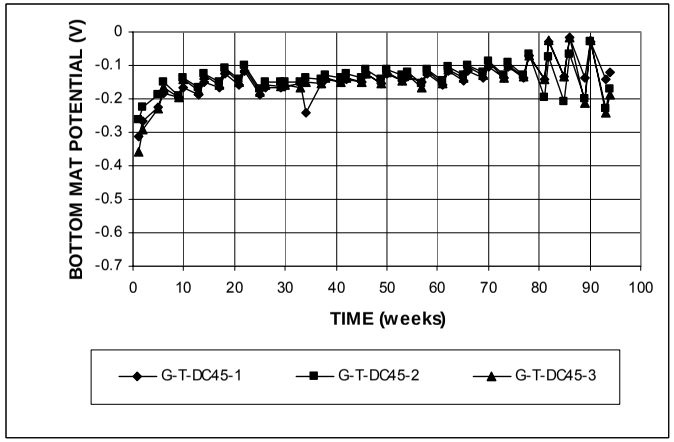


(b)

**Figure A.232 -** (a) Top mat corrosion potentials and (b) bottom mat corrosion potentials, with respect to copper-copper sulfate electrode as measured in the ASTM G 109 test for specimens with conventional Thermex-treated steel (T), a water-cement ratio of 0.45, and DCI-S.

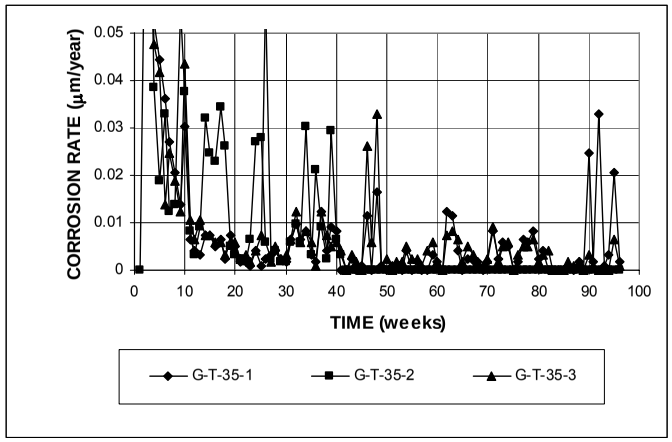


(a)

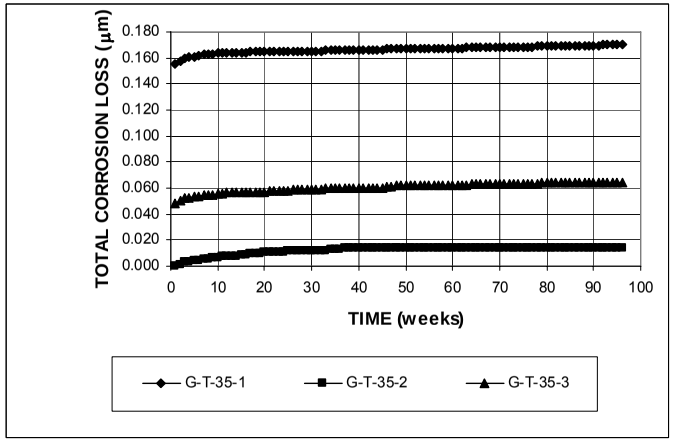


(b)

**Figure A.233 -** (a) Corrosion rates and (b) total corrosion losses as measured in the ASTM G 109 test for specimens with conventional Thermex-treated steel (T), a water-cement ratio of 0.35, and no inhibitor.

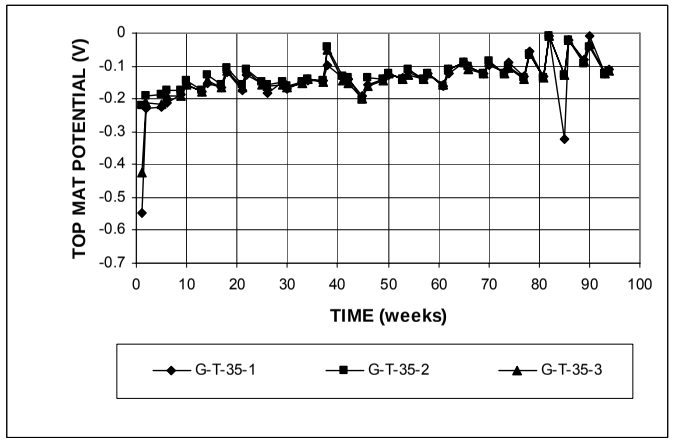


(a)

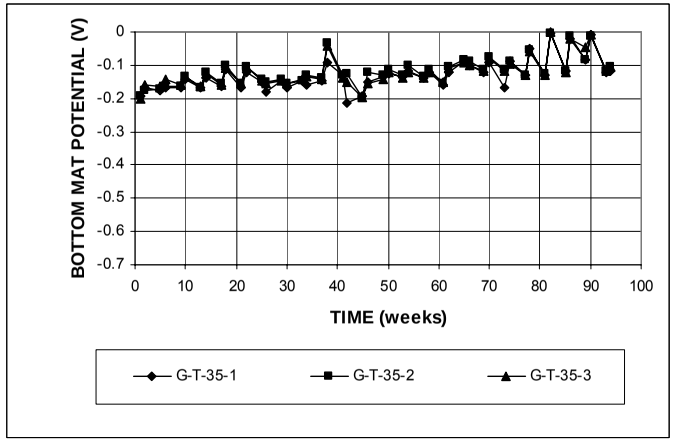


(b)

**Figure A.234 -** (a) Top mat corrosion potentials and (b) bottom mat corrosion potentials, with respect to copper-copper sulfate electrode as measured in the ASTM G 109 test for specimens with conventional Thermex-treated steel (T), a water-cement ratio of 0.35, and no inhibitor.

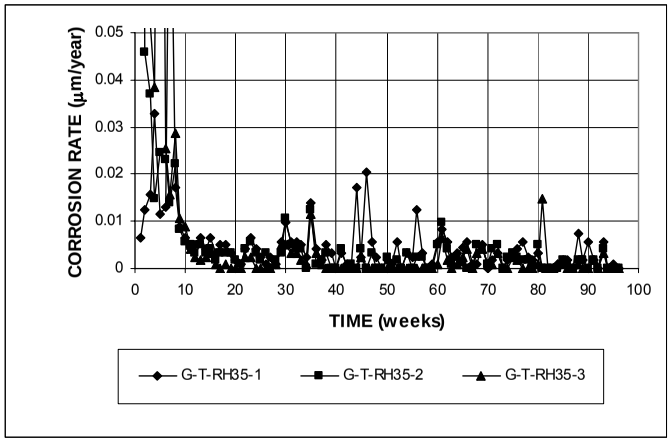


(a)

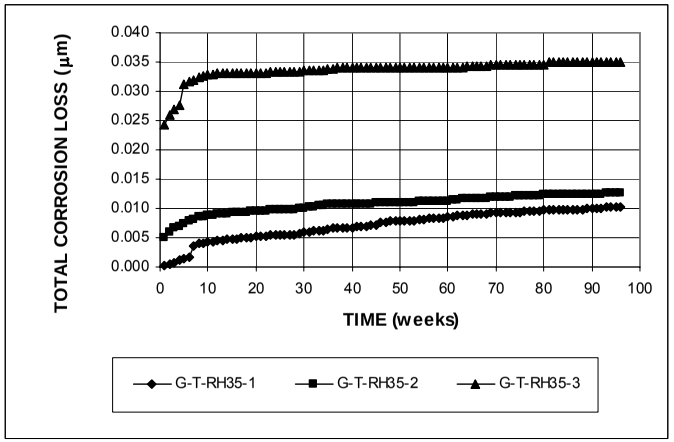


(b)

**Figure A.235 -** (a) Corrosion rates and (b) total corrosion losses as measured in the ASTM G 109 test for specimens with conventional Thermex-treated steel (T), a water-cement ratio of 0.35, and Rheocrete 222+.

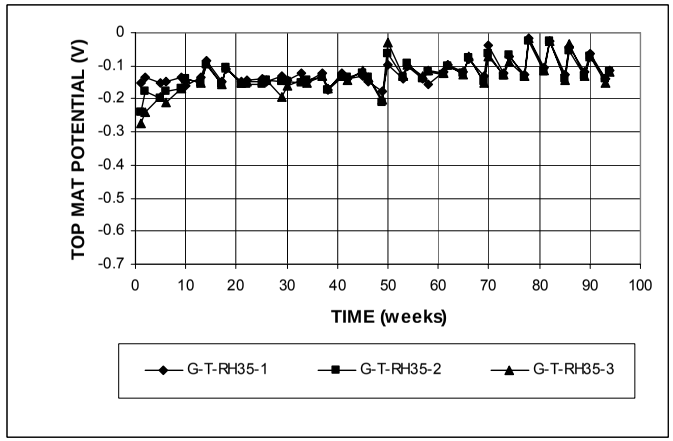


(a)

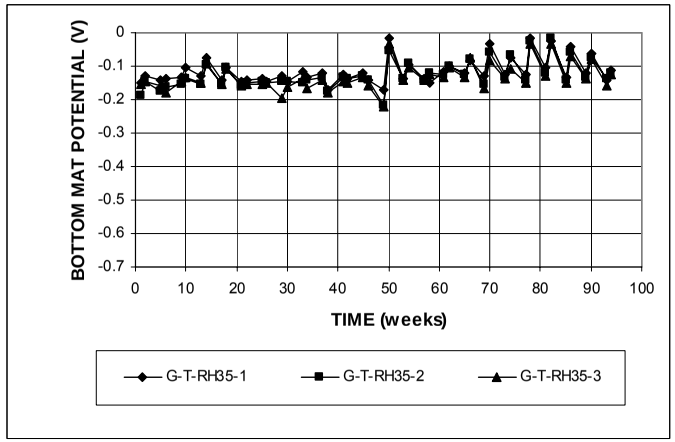


(b)

**Figure A.236 -** (a) Top mat corrosion potentials and (b) bottom mat corrosion potentials, with respect to copper-copper sulfate electrode as measured in the ASTM G 109 test for specimens with conventional Thermex-treated steel (T), a water-cement ratio of 0.35, and Rheocrete 222+.

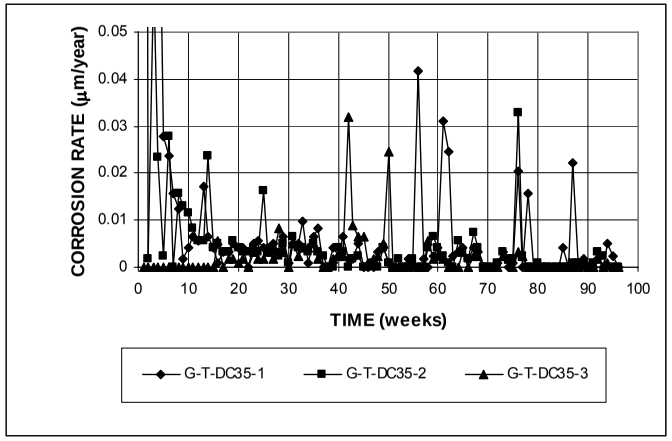


(a)

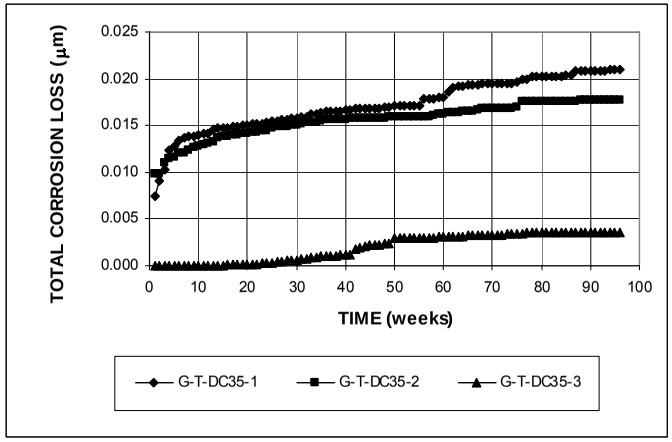


(b)

**Figure A.237 -** (a) Corrosion rates and (b) total corrosion losses as measured in the ASTM G 109 test for specimens with conventional Thermex-treated steel (T), a water-cement ratio of 0.35, and DCI-S.

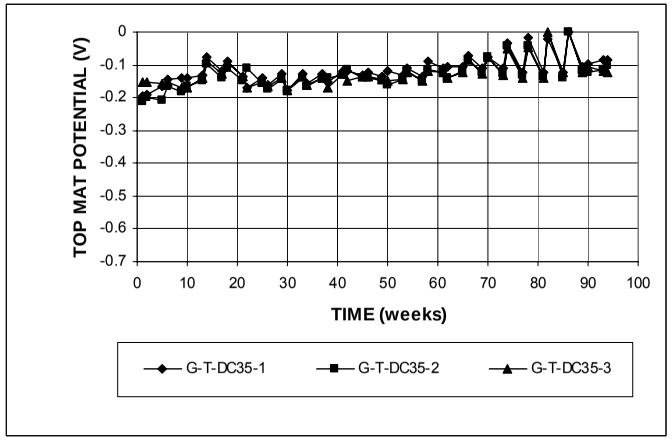


(a)

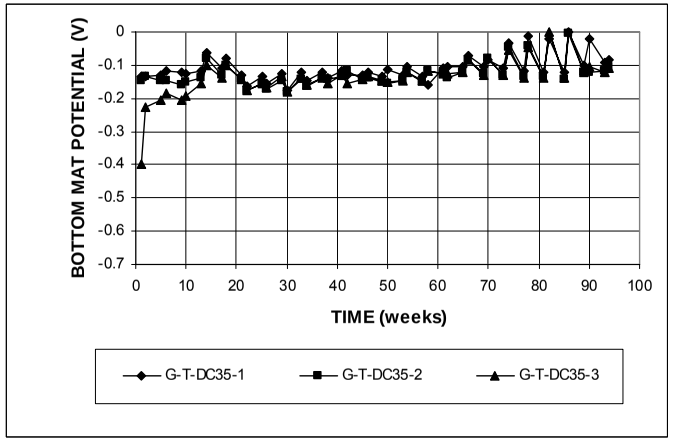


(b)

**Figure A.238 -** (a) Top mat corrosion potentials and (b) bottom mat corrosion potentials, with respect to copper-copper sulfate electrode as measured in the ASTM G 109 test for specimens with conventional Thermex-treated steel (T), a water-cement ratio of 0.35, and DCI-S.

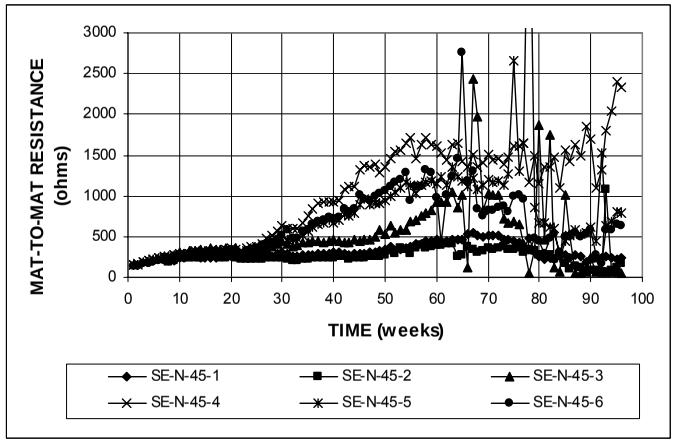


**Figure B.1** - Mat-to-mat resistances as measured in the Southern Exposure test for specimens with conventional normalized steel (N).

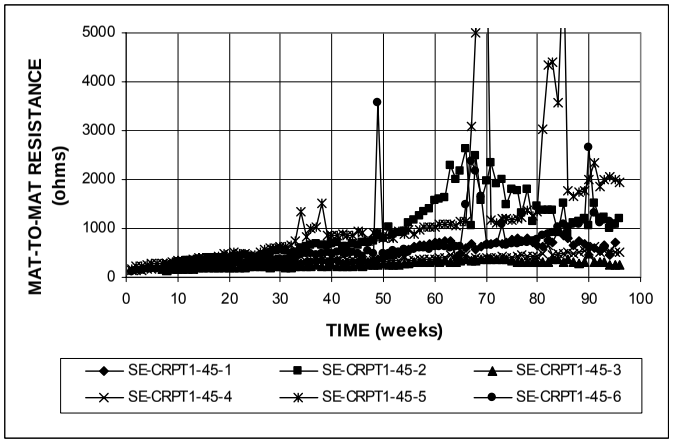


**Figure B.3** - Mat-to-mat resistances as measured in the Southern Exposure test for specimens with microalloyed steel with high phosphorus content, 0.117%, Thermex-treated (CRPT1)

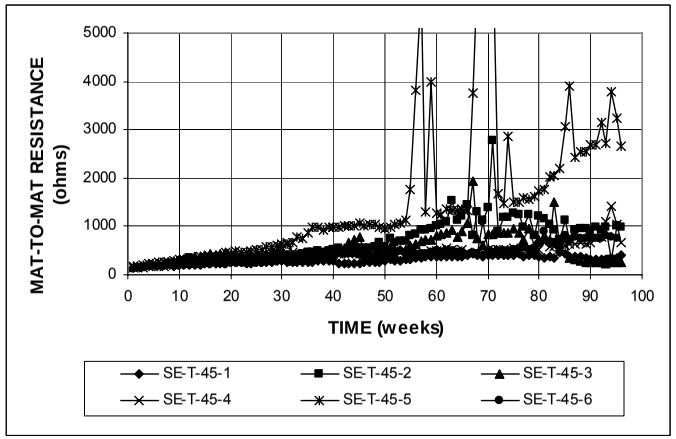


**Figure B.2** - Mat-to-mat resistances as measured in the Southern Exposure test for specimens with conventional Thermex-treated steel (T).

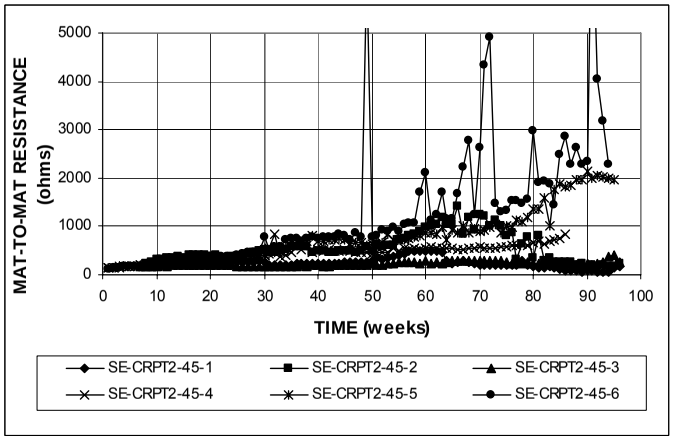


**Figure B.4** - Mat-to-mat resistances as measured in the Southern Exposure test for specimens with microalloyed steel with high phosphorus content, 0.100%, Thermex-treated (CRPT1)

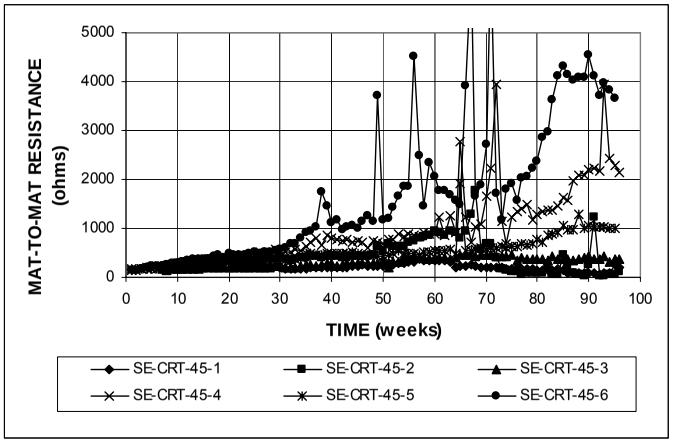


**Figure B.5 -** Mat-to-mat resistances as measured in the Southern Exposure test for specimens with microalloyed steel with normal phosphorus content, 0.017%, Thermex-treated (CRPT1)

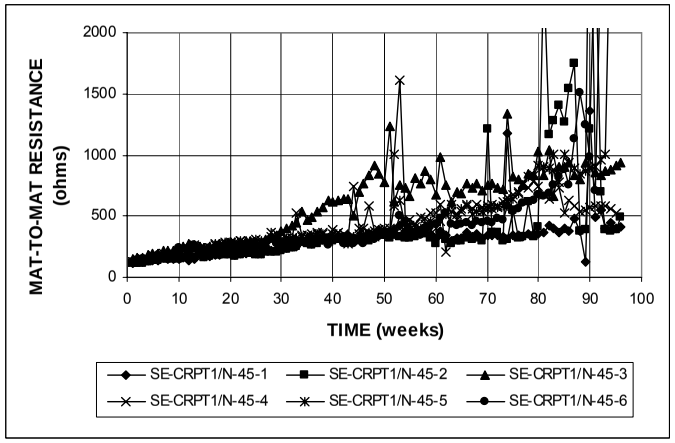


**Figure B.7 -** Mat-to-mat resistances as measured in the Southern Exposure test for specimens with microalloyed steel with high phosphorus content, 0.117%, Thermex--treated (CRPT1) in the top mat and conventional normalized steel (N) in the bottom mat.

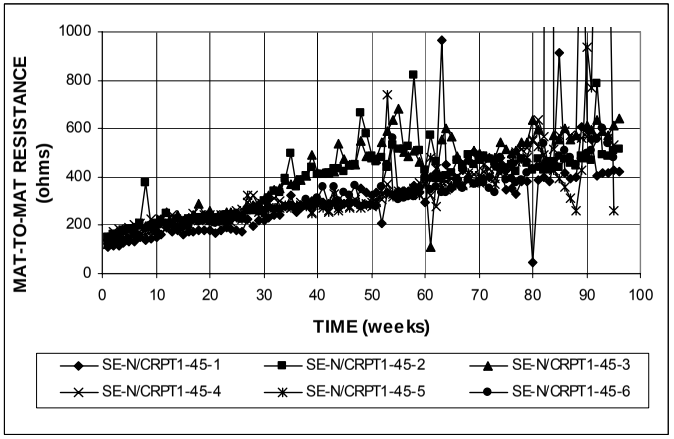


**Figure B.6 -** Mat-to-mat resistances as measured in the Southern Exposure test for specimens with conventional normalized steel (N) in the top mat and microalloyed steel with high phosphorus content, 0.117%, Thermex-treated (CRPT1) in the bottom mat.

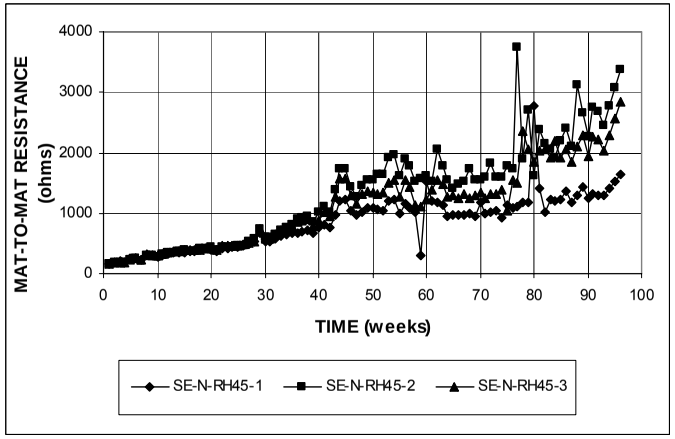


**Figure B.8 -** Mat-to-mat resistances as measured in the Southern Exposure test for specimens with conventional normalized steel (N), a water-cement ratio of 0.45, and Rheocrete 222+.

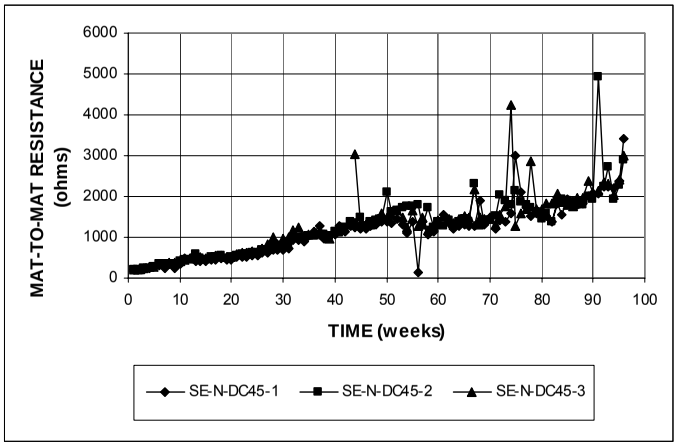


**Figure B.9** - Mat-to-mat resistances as measured in the Southern Exposure test for specimens with conventional normalized steel (N), a water-cement ratio of 0.45, and DCI-S.

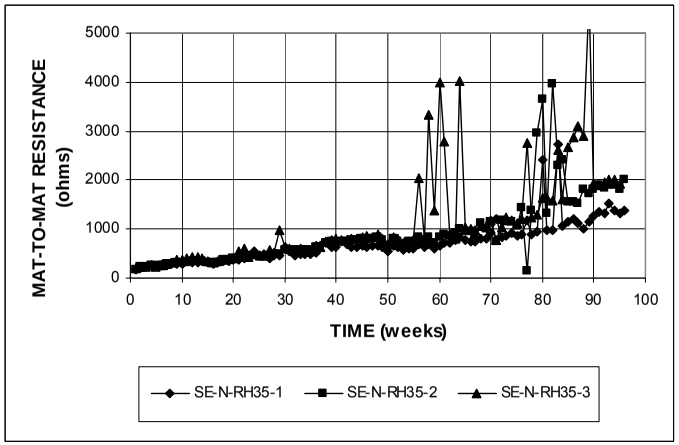


**Figure B.11** - Mat-to-mat resistances as measured in the Southern Exposure test for specimens with conventional normalized steel (N), a water-cement ratio of 0.35, and Rheocrete 222+.

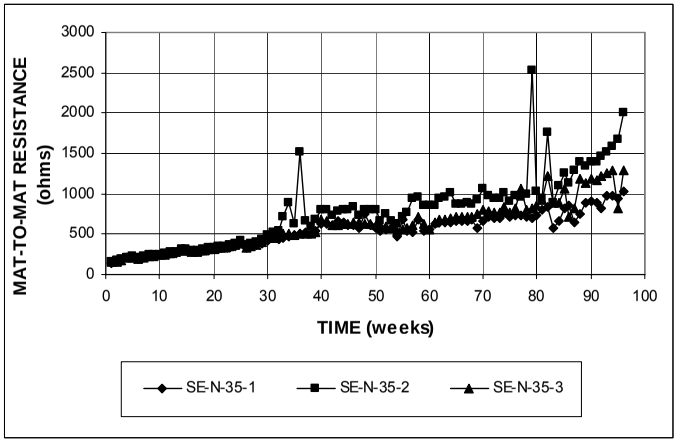


**Figure B.10** - Mat-to-mat resistances as measured in the Southern Exposure test for specimens with conventional normalized steel (N), a water-cement ratio of 0.35, and no inhibitor.

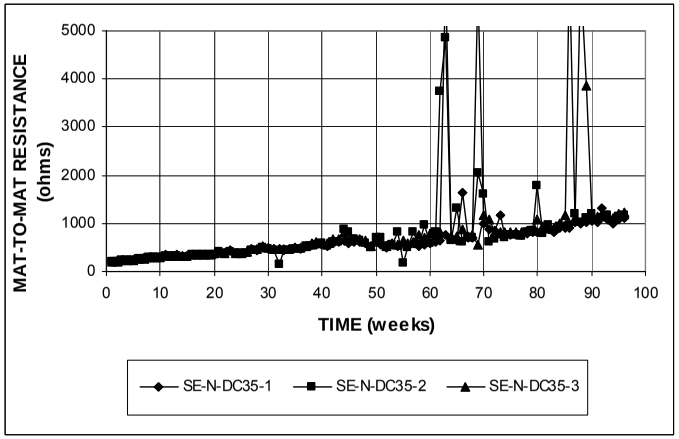


**Figure B.12** - Mat-to-mat resistances as measured in the Southern Exposure test for specimens with conventional normalized steel (N), a water-cement ratio of 0.35, and DCI-S.

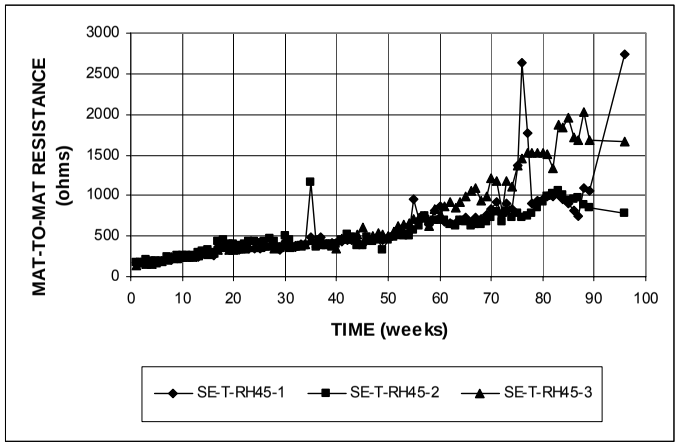


**Figure B.13** - Mat-to-mat resistances as measured in the Southern Exposure test for specimens with conventional Thermex-treated steel (N), a water-cement ratio of 0.45, and Rheocrete 222+.

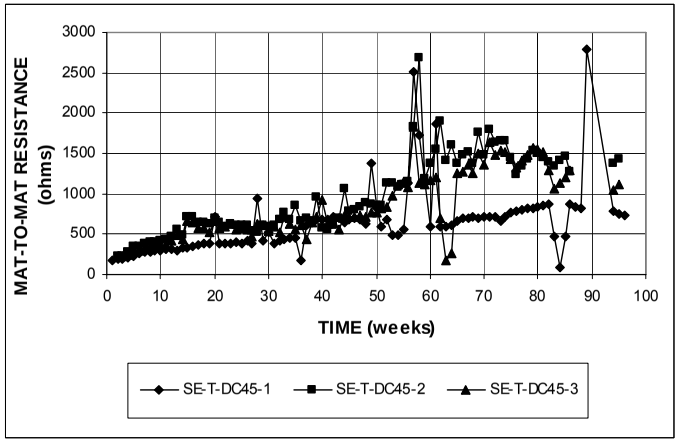


**Figure B.14** - Mat-to-mat resistances as measured in the Southern Exposure test for specimens with conventional Thermex-treated steel (N), a water-cement ratio of 0.45, and DCI-S.

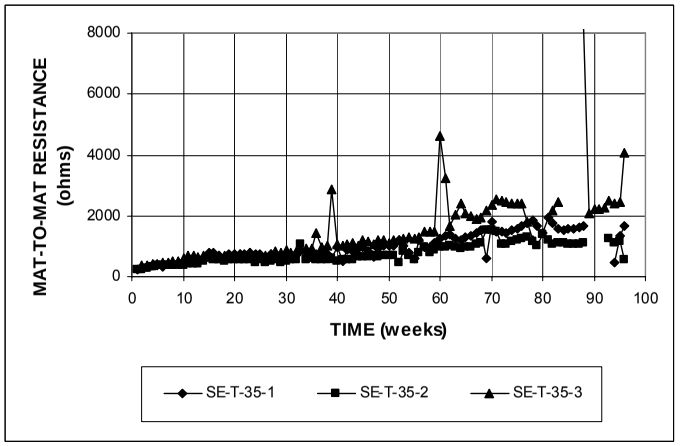


**Figure B.15** - Mat-to-mat resistances as measured in the Southern Exposure test for specimens with conventional Thermex-treated steel (N), a water-cement ratio of 0.35, and no inhibitor.

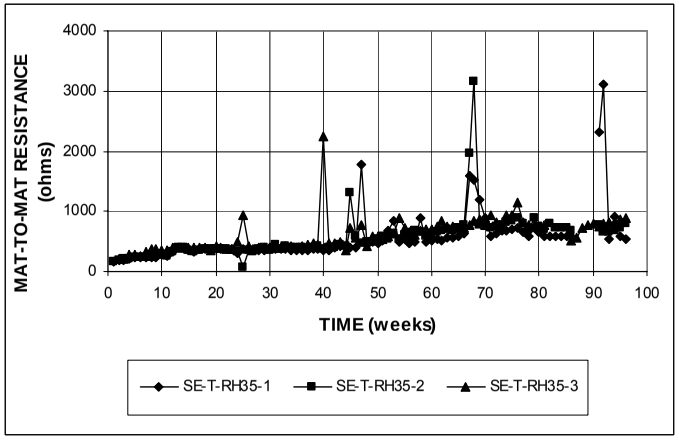


**Figure B.16** - Mat-to-mat resistances as measured in the Southern Exposure test for specimens with conventional Thermex-treated steel (N), a water-cement ratio of 0.35, and Rheocrete 222+.

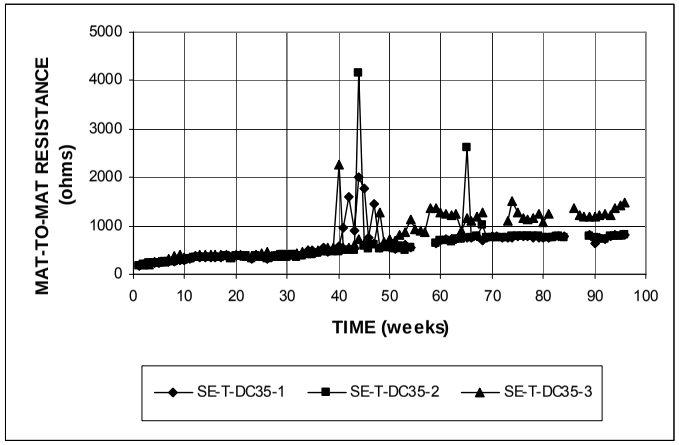


**Figure B.17** - Mat-to-mat resistances as measured in the Southern Exposure test for specimens with conventional Thermex-treated steel (N), a water-cement ratio of 0.35, and DCI-S.

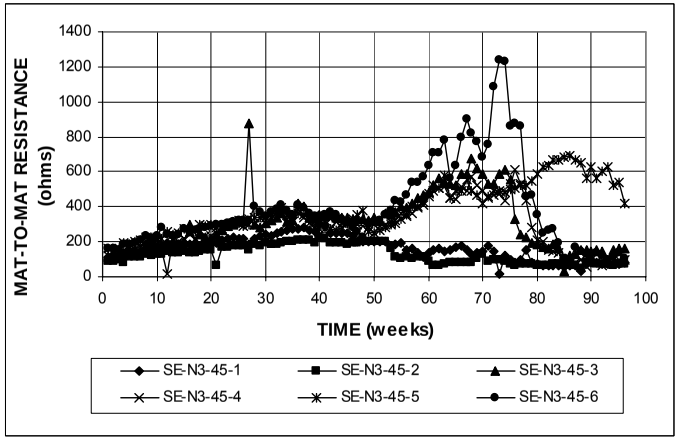


**Figure B.18** - Mat-to-mat resistances as measured in the Southern Exposure test for specimens with conventional normalized steel (N3).

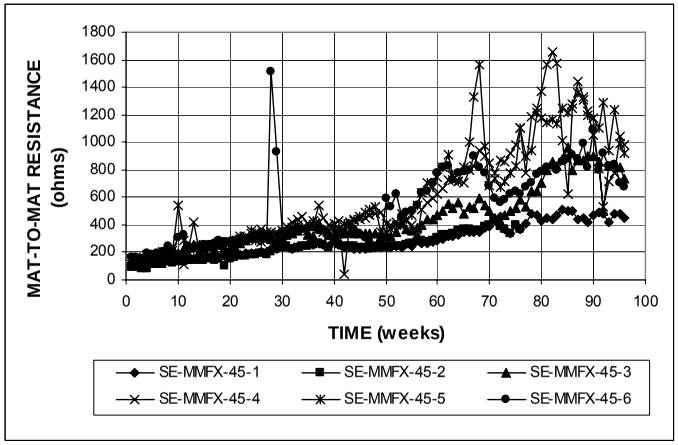


**Figure B.19** - Mat-to-mat resistances as measured in the Southern Exposure test for specimens with MMFX microcomposite steel.

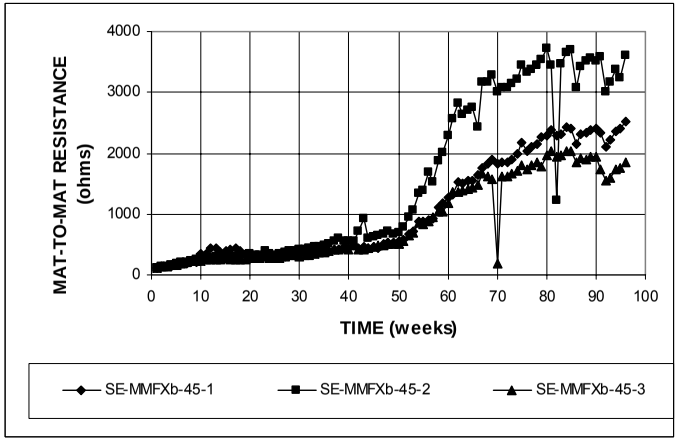


**Figure B.20** - Mat-to-mat resistances as measured in the Southern Exposure test for specimens with MMFX microcomposite steel, with bent bars in the top mat.

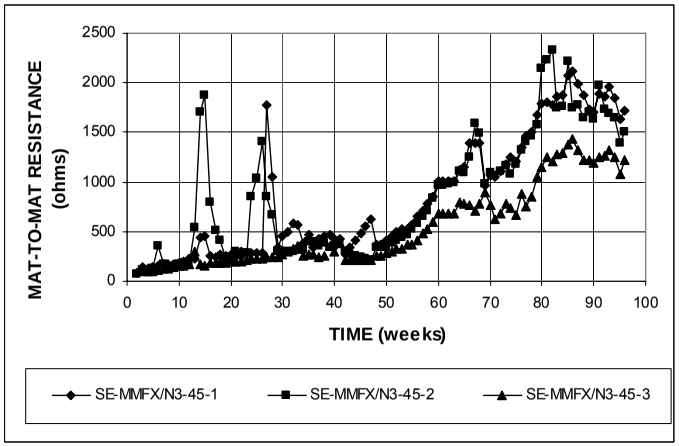


**Figure B.21 -** Mat-to-mat resistances as measured in the Southern Exposure test for specimens with MMFX microcomposite steel in the top mat and conventional normalized steel (N3) in the bottom mat.

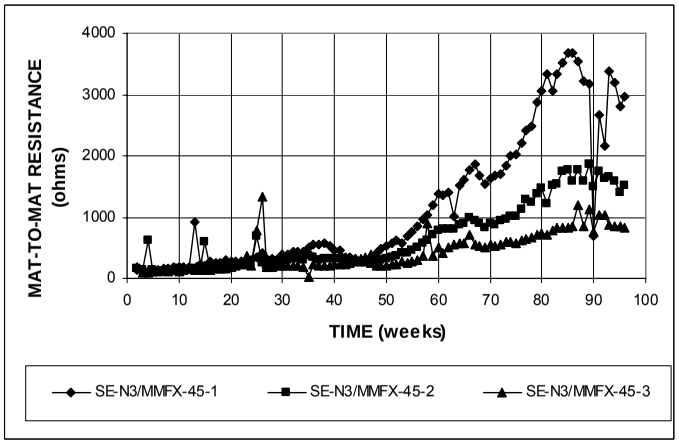


**Figure B.22 -** Mat-to-mat resistances as measured in the Southern Exposure test for specimens with conventional normalized steel (N3) in the top mat and MMFX microcomposite steel in the bottom mat.

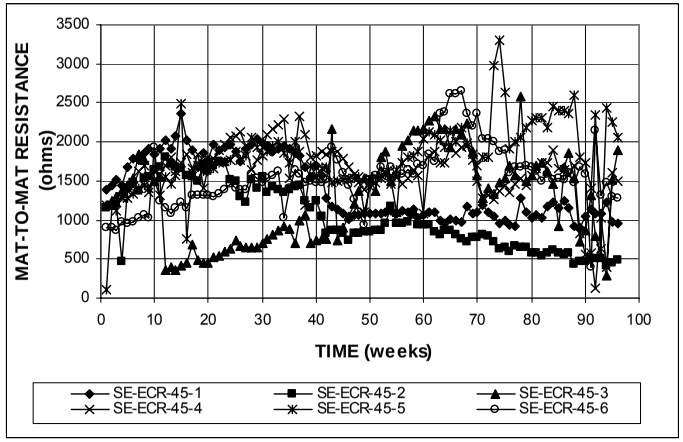


**Figure B.23 -** Mat-to-mat resistances as measured in the Southern Exposure test for specimens with epoxy-coated steel.

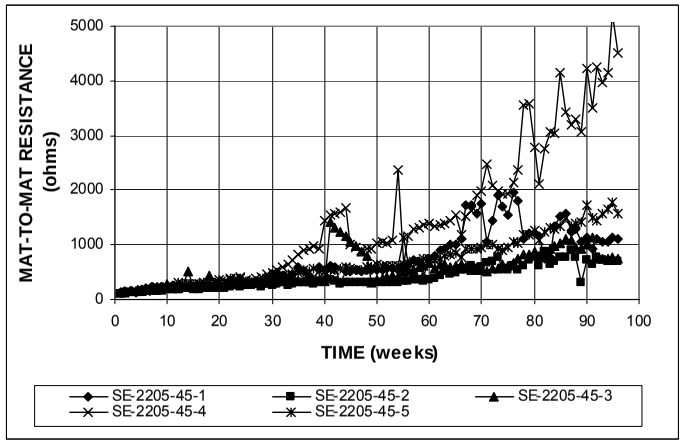


**Figure B.24 -** Mat-to-mat resistances as measured in the Southern Exposure test for specimens with 2205 duplex steel.

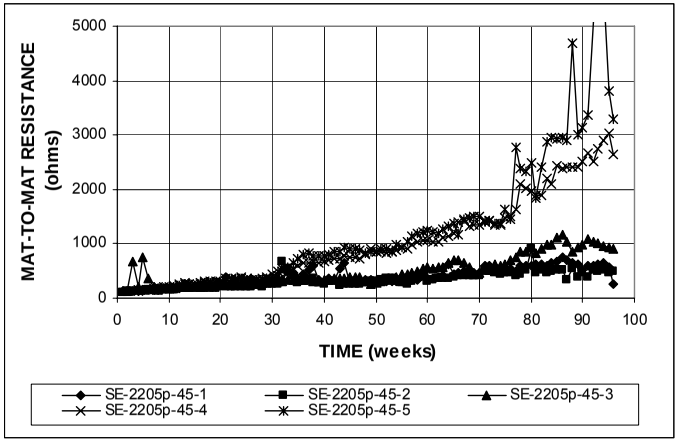


**Figure B.25** - Mat-to-mat resistances as measured in the Southern Exposure test for specimens with 2205 pickled duplex steel.

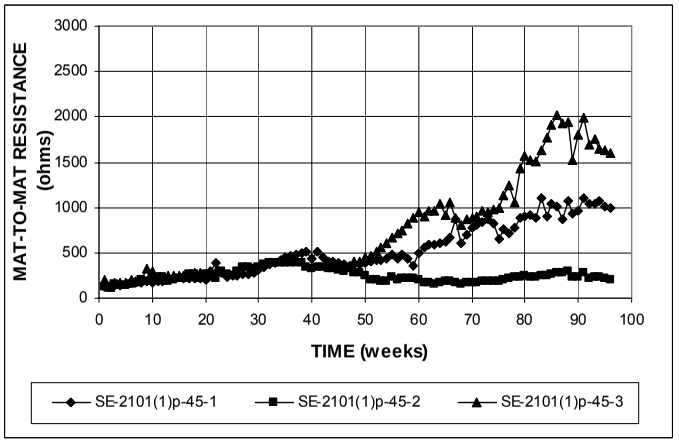


**Figure B.27** - Mat-to-mat resistances as measured in the Southern Exposure test for specimens with 2101(1) pickled duplex steel.

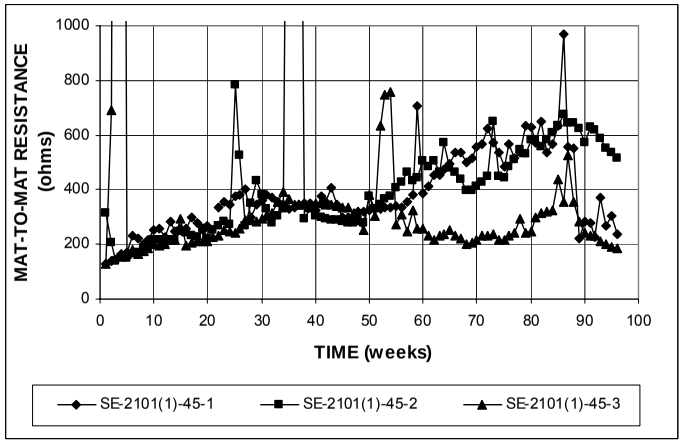


**Figure B.26** - Mat-to-mat resistances as measured in the Southern Exposure test for specimens with 2101(1) duplex steel.

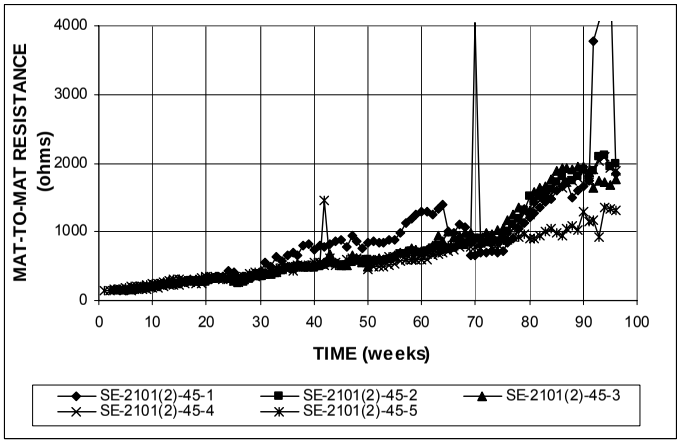


**Figure B.28** - Mat-to-mat resistances as measured in the Southern Exposure test for specimens with 2101(2) duplex steel.

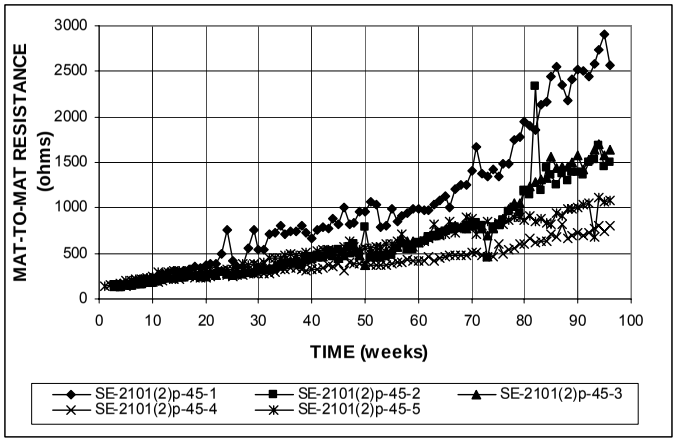


**Figure B.29** - Mat-to-mat resistances as measured in the Southern Exposure test for specimens with 2101(2) pickled duplex steel.

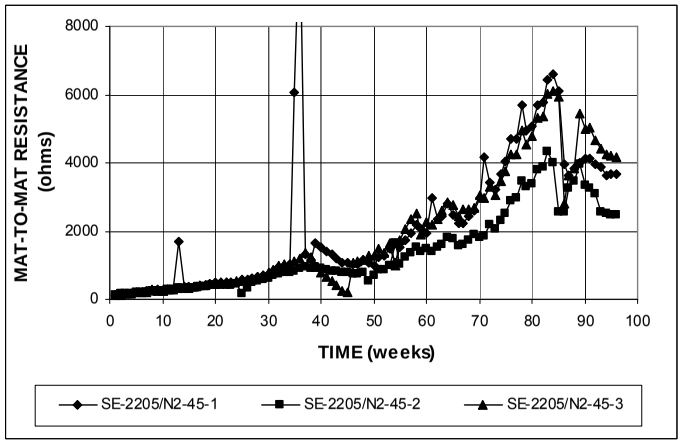


**Figure B.30** - Mat-to-mat resistances as measured in the Southern Exposure test for specimens with 2205 duplex steel in the top mat and conventional normalized steel (N2) in the bottom mat.

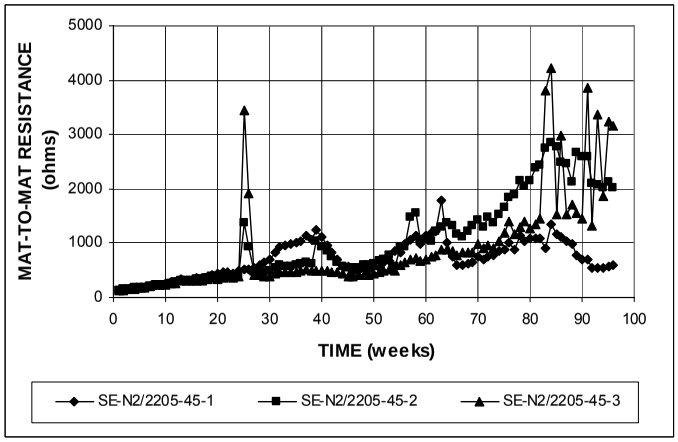


**Figure B.31** - Mat-to-mat resistances as measured in the Southern Exposure test for specimens with conventional normalized steel (N2) in the top mat and 2205 duplex steel in the bottom mat.

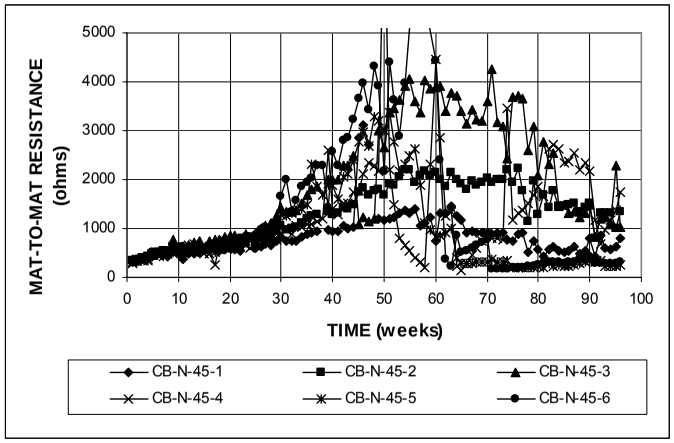


**Figure B.32 -** Mat-to-mat resistances as measured in the cracked beam test for specimens with conventional normalized steel (N).

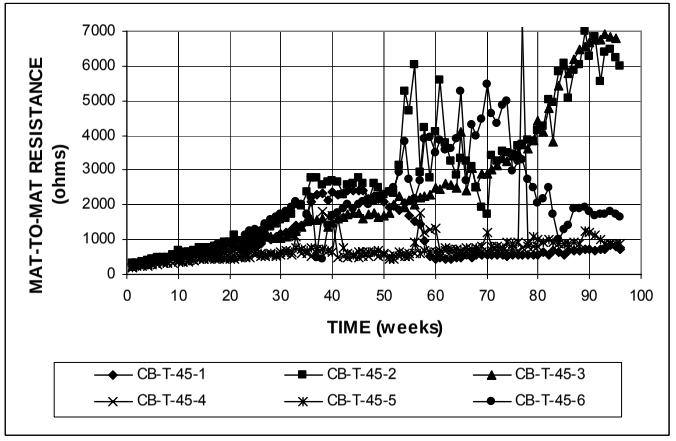


**Figure B.33 -** Mat-to-mat resistances as measured in the cracked beam test for specimens with conventional Thermex-treated steel (T).

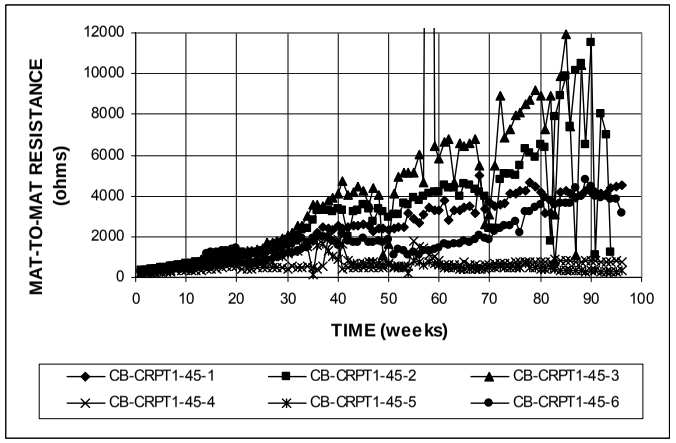


**Figure B.34 -** Mat-to-mat resistances as measured in the cracked beam test for specimens with microalloyed steel with high phosphorus content, 0.117%, Thermex-treated (CRPT1)

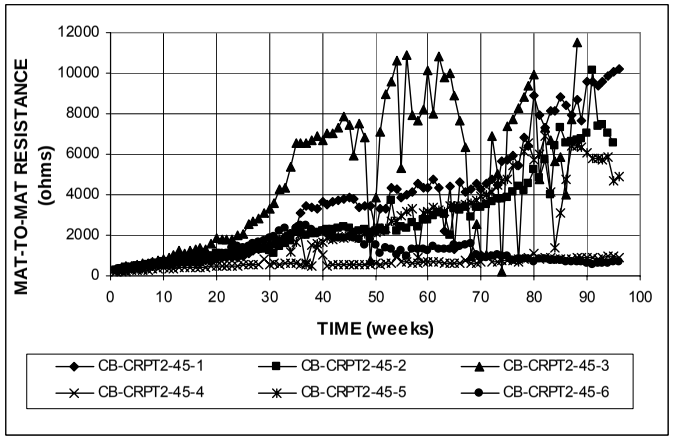


**Figure B.35 -** Mat-to-mat resistances as measured in the cracked beam test for specimens with microalloyed steel with high phosphorus content, 0.100%, Thermex-treated (CRPT1)

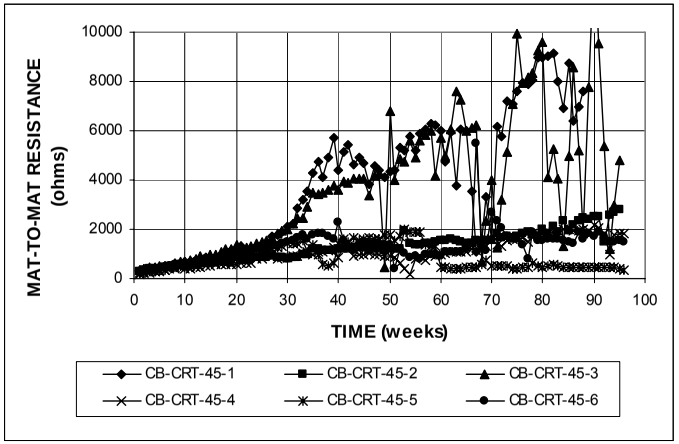


**Figure B.36** - Mat-to-mat resistances as measured in the cracked beam test for specimens with microalloyed steel with normal phosphorus content, 0.017%, Thermex-treated (CRPT1)

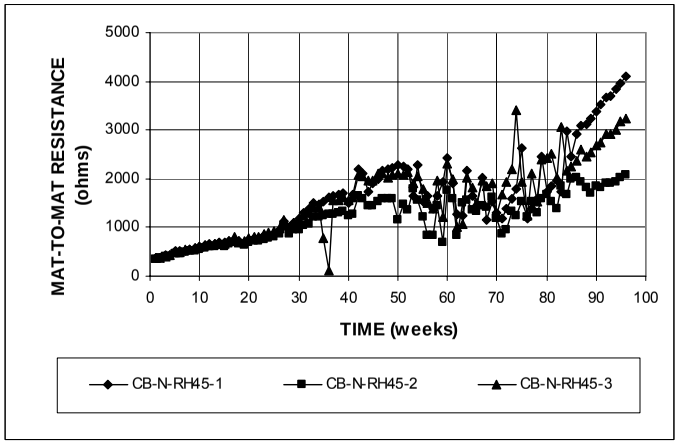


**Figure B.37** - Mat-to-mat resistances as measured in the cracked beam test for specimens with conventional normalized steel (N), a water-cement ratio of 0.45, and Rheocrete 222+.

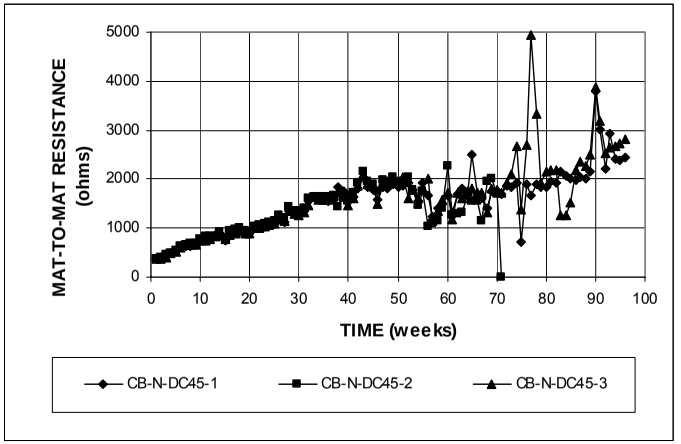


**Figure B.38** - Mat-to-mat resistances as measured in the cracked beam for specimens with conventional normalized steel (N), a water-cement ratio of 0.45, and DCI-S.

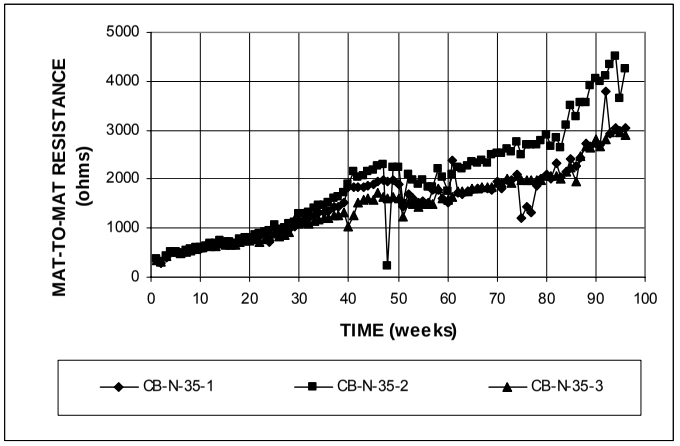


**Figure B.39** - Mat-to-mat resistances as measured in the cracked beam test for specimens with conventional normalized steel (N), a water-cement ratio of 0.35, and no inhibitor.

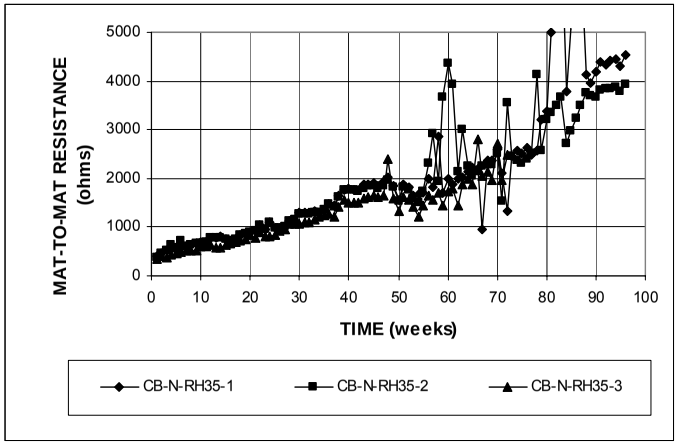


**Figure B.40**- Mat-to-mat resistances as measured in the cracked beam test for specimens with conventional normalized steel (N), a water-cement ratio of 0.35, and Rheocrete 222+.

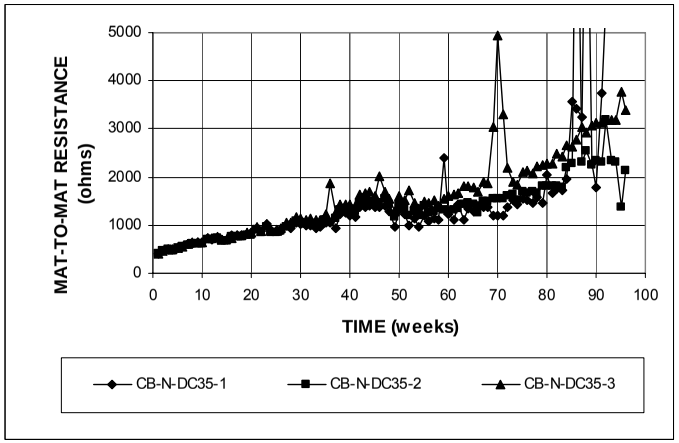


**Figure B.41** - Mat-to-mat resistances as measured in the Scracked beam test for specimens with conventional normalized steel (N), a water-cement ratio of 0.35, and DCI-S.

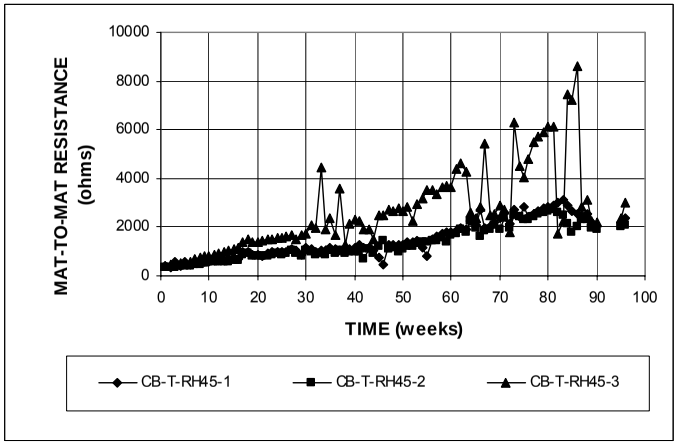


**Figure B.42** - Mat-to-mat resistances as measured in the cracked beam test for specimens with conventional Thermex-treated steel (N), a water-cement ratio of 0.45, and Rheocrete 222+.

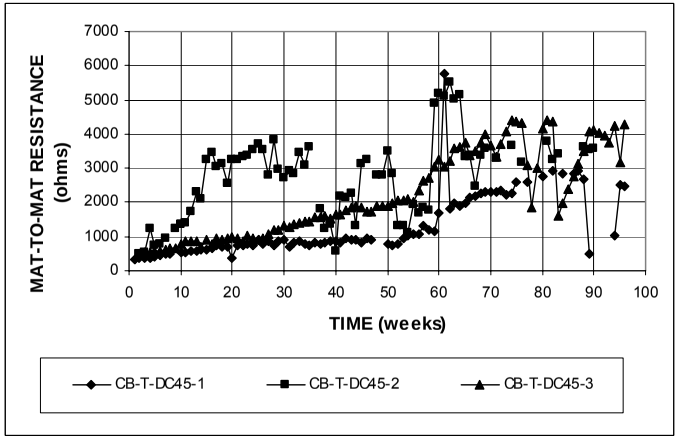


**Figure B.43** - Mat-to-mat resistances as measured in the cracked beam test for specimens with conventional Thermex-treated steel (N), a water-cement ratio of 0.45, and DCI-S.

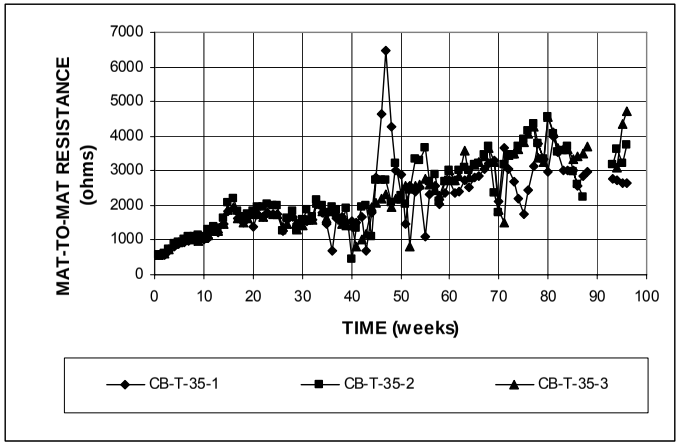


**Figure B.44 -** Mat-to-mat resistances as measured in the cracked beam test for specimens with conventional Thermex-treated steel (N), a water-cement ratio of 0.35, and no inhibitor.

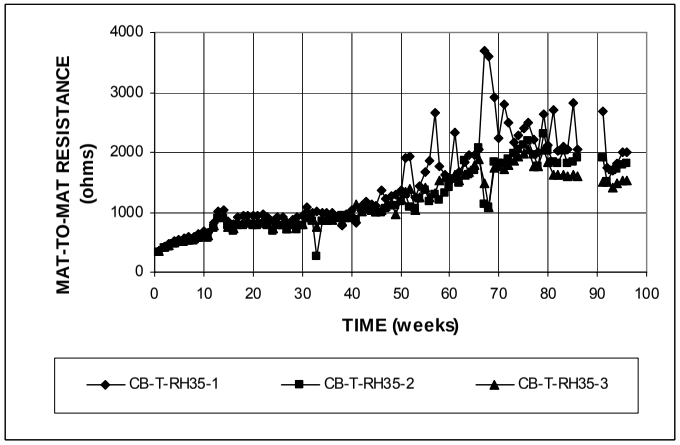


**Figure B.45 -** Mat-to-mat resistances as measured in the cracked beam test for specimens with conventional Thermex-treated steel (N), a water-cement ratio of 0.35, and Rheocrete 222+.

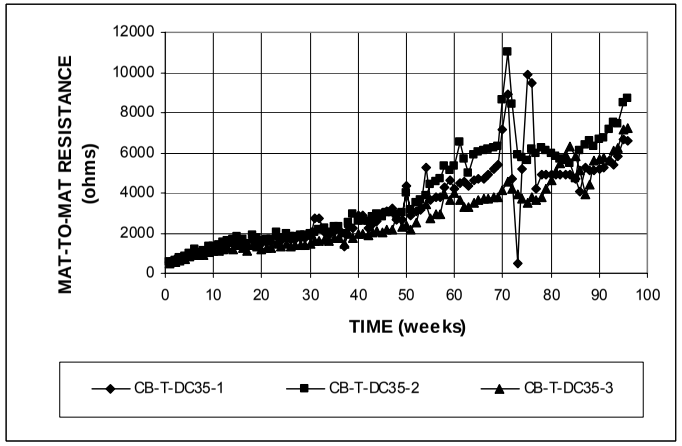


**Figure B.46 -** Mat-to-mat resistances as measured in the cracked beam test for specimens with conventional Thermex-treated steel (N), a water-cement ratio of 0.35, and DCI-S.

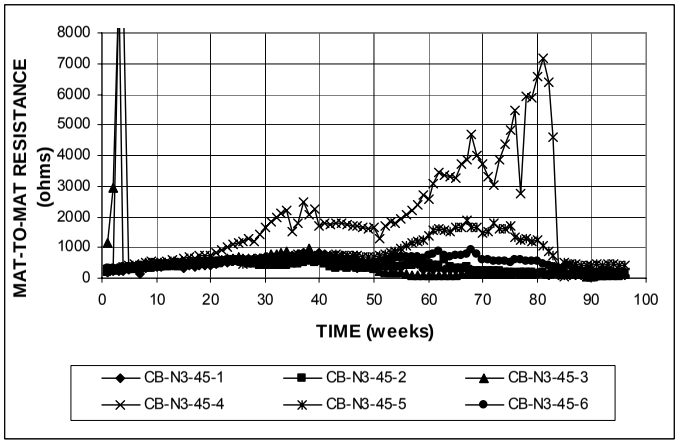


**Figure B.47 -** Mat-to-mat resistances as measured in the cracked beam test for specimens with conventional normalized steel (N3).

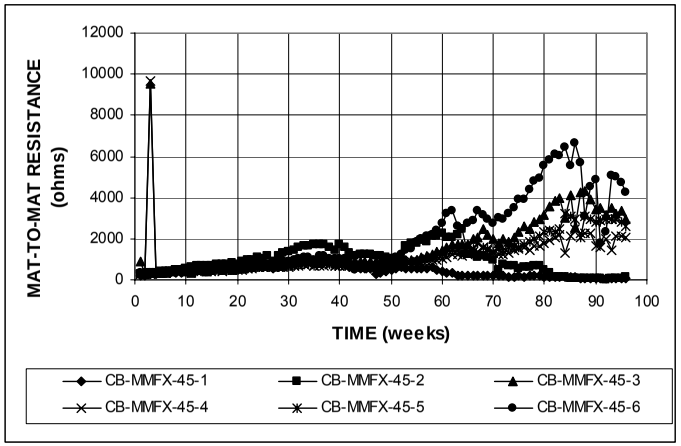


**Figure B.48** - Mat-to-mat resistances as measured in the cracked beam test for specimens with MMFX microcomposite steel.

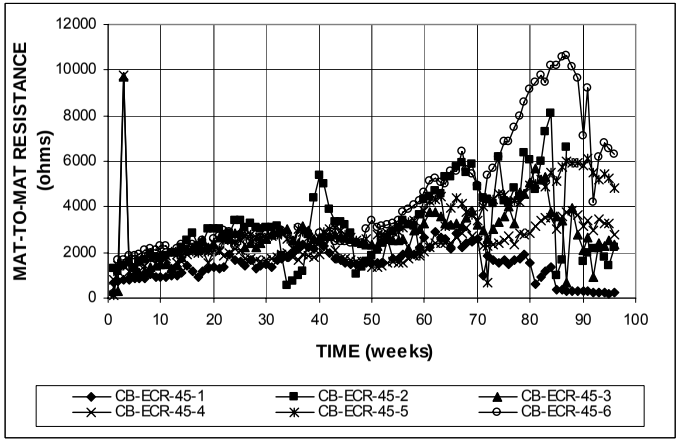


**Figure B.49** - Mat-to-mat resistances as measured in the cracked beam test for specimens with epoxy-coated steel.

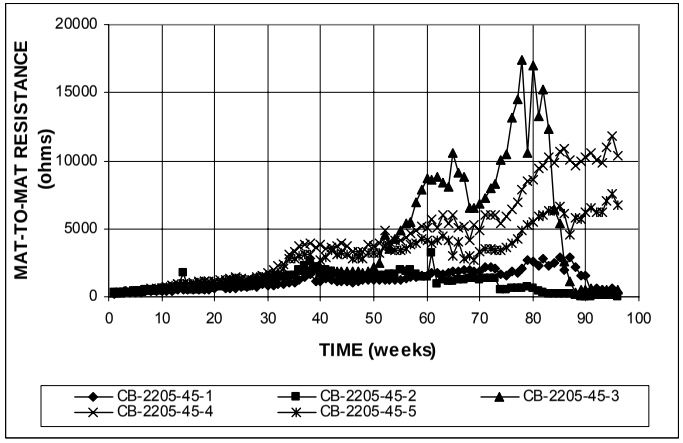


**Figure B.50** - Mat-to-mat resistances as measured in the cracked beam test for specimens with 2205 duplex steel.

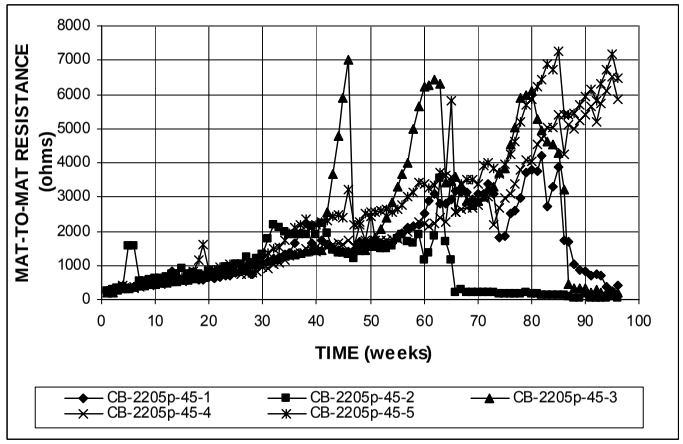


**Figure B.51** - Mat-to-mat resistances as measured in the cracked beam test for specimens with 2205 pickled duplex steel.

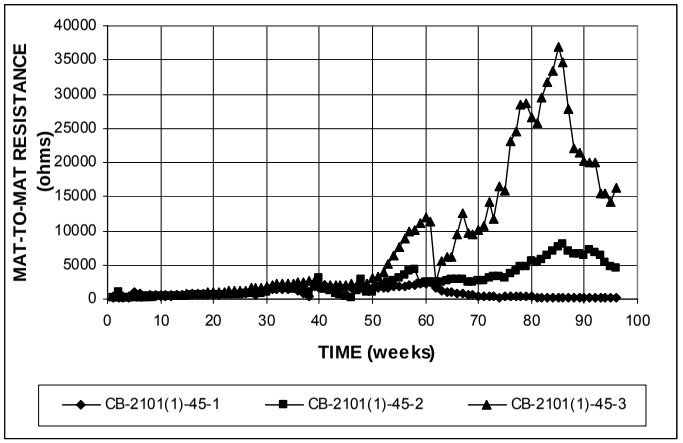


**Figure B.52** - Mat-to-mat resistances as measured in the cracked beam test for specimens with 2101(1) duplex steel.

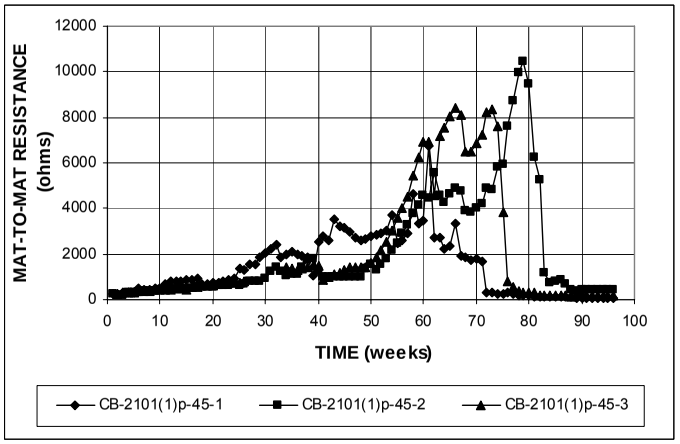


**Figure B.53** - Mat-to-mat resistances as measured in the cracked beam test for specimens with 2101(1) pickled duplex steel.

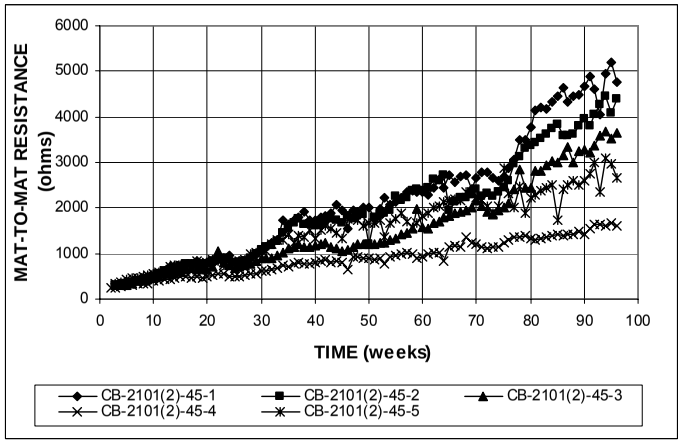


**Figure B.54** - Mat-to-mat resistances as measured in the cracked beam test for specimens with 2101(2) duplex steel.

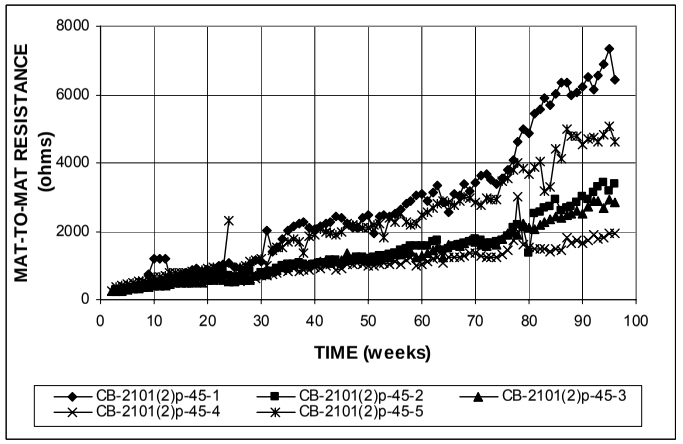


**Figure B.55** - Mat-to-mat resistances as measured in the cracked beam test for specimens with 2101(2) pickled duplex steel.

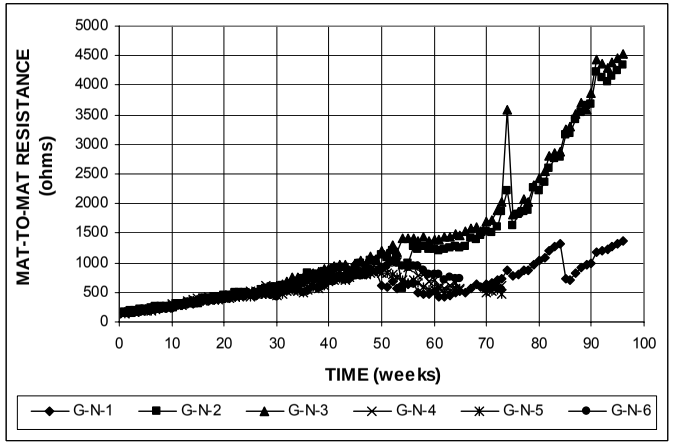


**Figure B.56 -** Mat-to-mat resistances as measured in the ASTM G 109 test for specimens with conventional normalized steel (N).

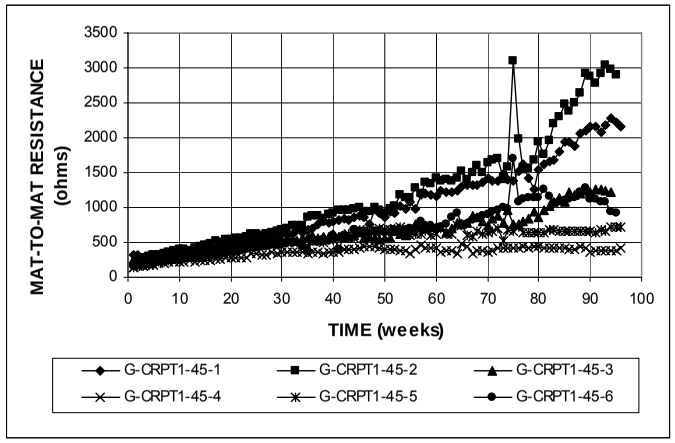


**Figure B.58 -** Mat-to-mat resistances as measured in the ASTM G 109 test for specimens with microalloyed steel with high phosphorus content, 0.117%, Thermex-treated (CRPT1)

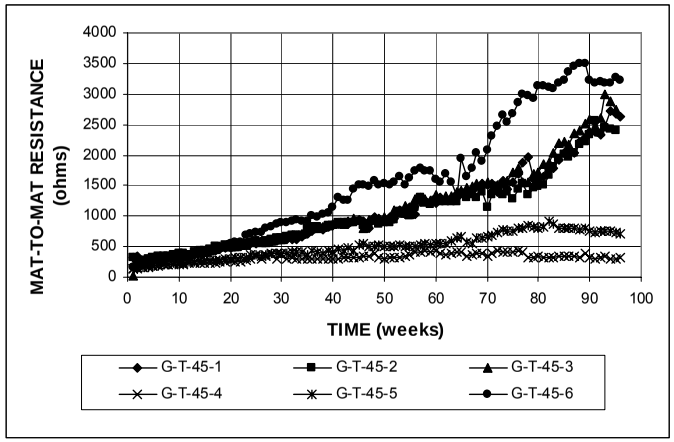


**Figure B.57 -** Mat-to-mat resistances as measured in the ASTM G 109 test for specimens with conventional Thermex-treated steel (T).

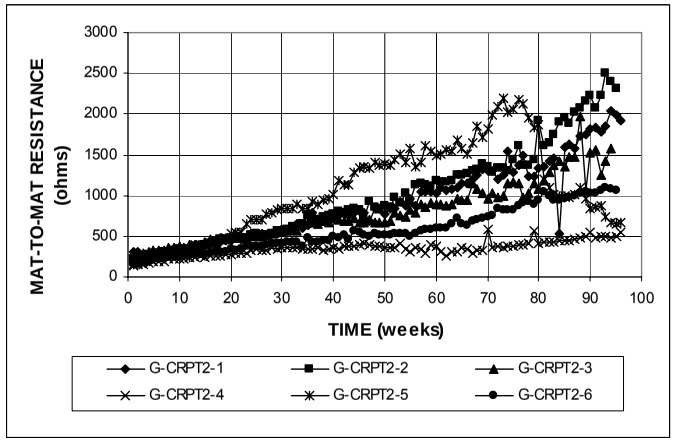


**Figure B.59 -** Mat-to-mat resistances as measured in the ASTM G 109 test for specimens with microalloyed steel with high phosphorus content, 0.100%, Thermex-treated (CRPT1)

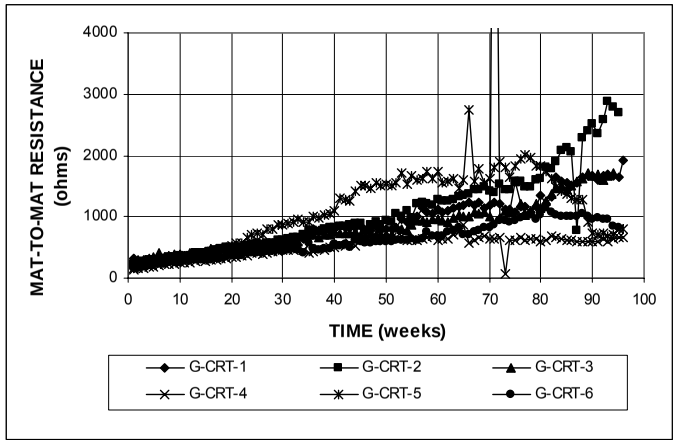


**Figure B.60 -** Mat-to-mat resistances as measured in the ASTM G 109 test for specimens with microalloyed steel with normal phosphorus content, 0.017%, Thermex-treated (CRPT1)

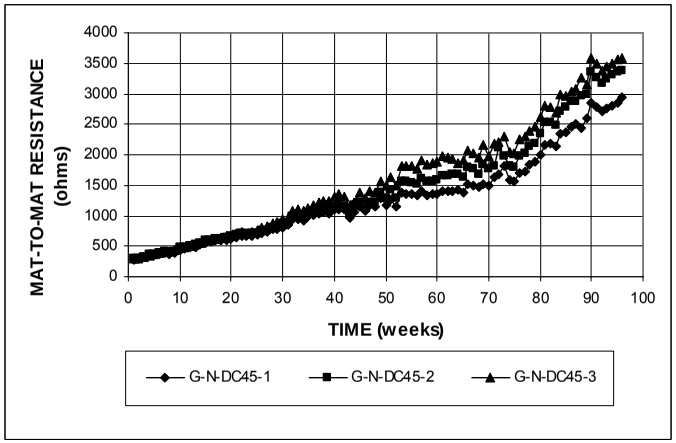


**Figure B.62 -** Mat-to-mat resistances as measured in the ASTM G 109 test for specimens with conventional normalized steel (N), a water-cement ratio of 0.45, and DCI-S.

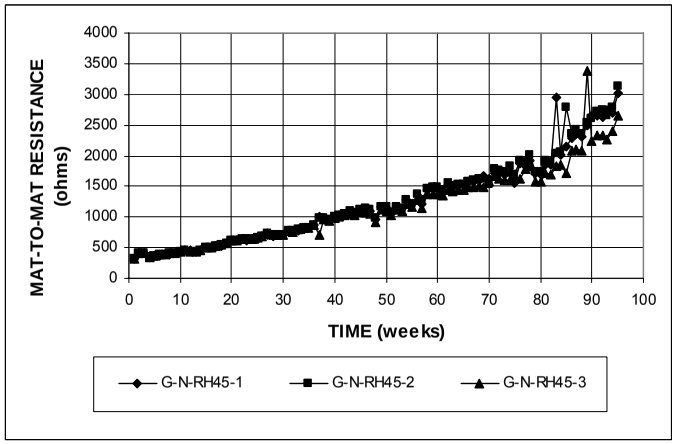


**Figure B.61 -** Mat-to-mat resistances as measured in the ASTM G 109 test for specimens with conventional normalized steel (N), a water-cement ratio of 0.45, and Rheocrete 222+.

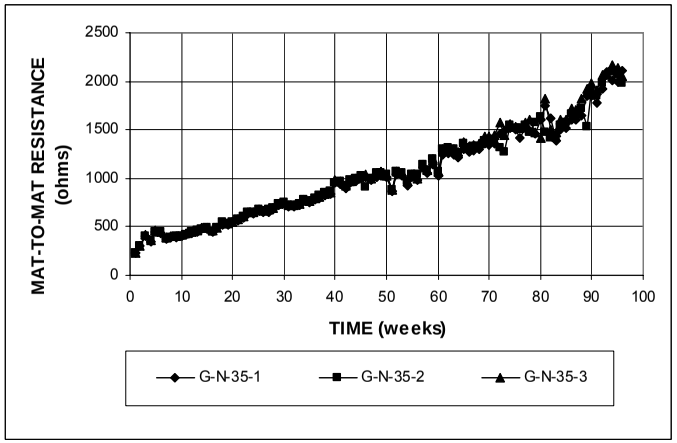


**Figure B.63 -** Mat-to-mat resistances as measured in the ASTM G 109 test for specimens with conventional normalized steel (N), a water-cement ratio of 0.35, and no inhibitor.

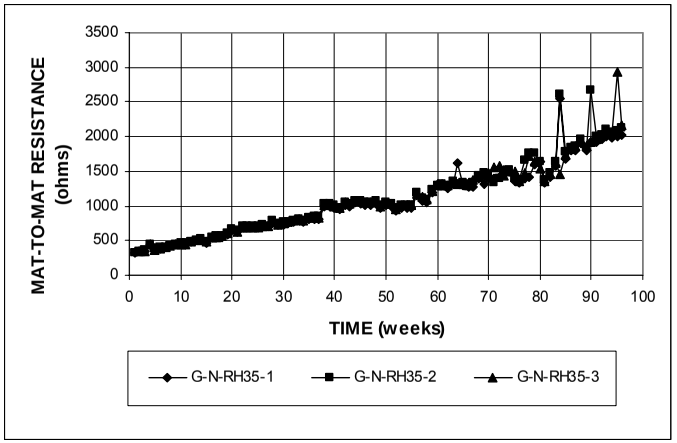


**Figure B.64** - Mat-to-mat resistances as measured in the ASTM G 109 test for specimens with conventional normalized steel (N), a water-cement ratio of 0.35, and Rheocrete 222+.

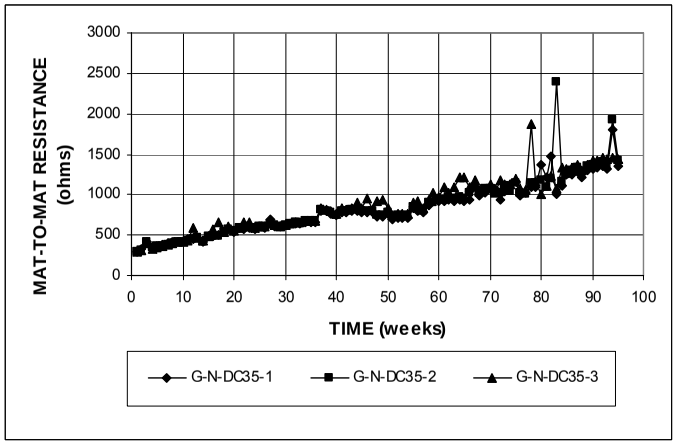


**Figure B.65** - Mat-to-mat resistances as measured in the ASTM G 109 test for specimens with conventional normalized steel (N), a water-cement ratio of 0.35, and DCI-S.

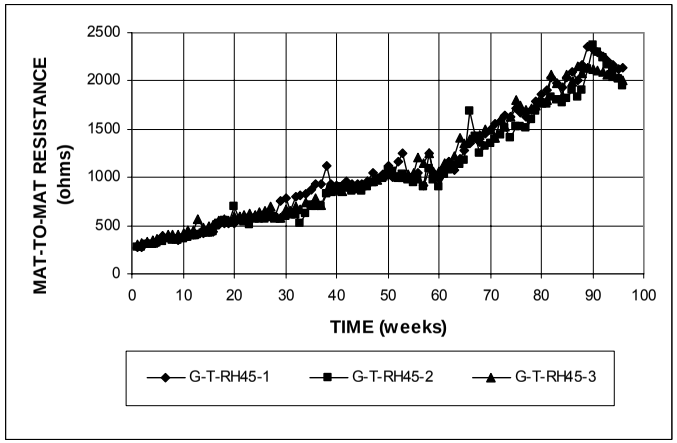


**Figure B.66** - Mat-to-mat resistances as measured in the ASTM G 109 test for specimens with conventional Thermex-treated steel (N), a water-cement ratio of 0.45, and Rheocrete 222+.

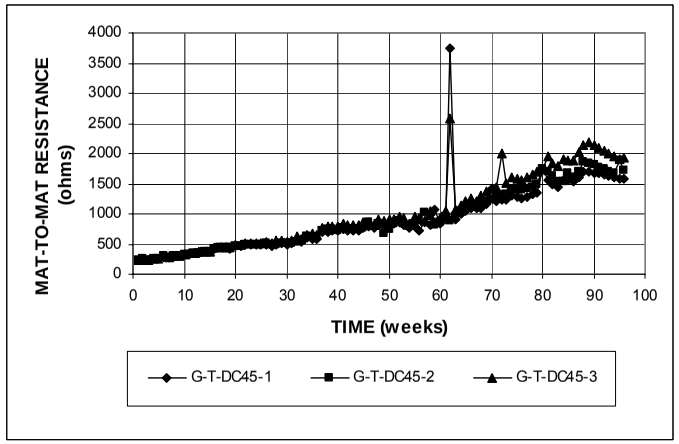


**Figure B.67** - Mat-to-mat resistances as measured in the ASTM G 109 test for specimens with conventional Thermex-treated steel (N), a water-cement ratio of 0.45, and DCI-S.

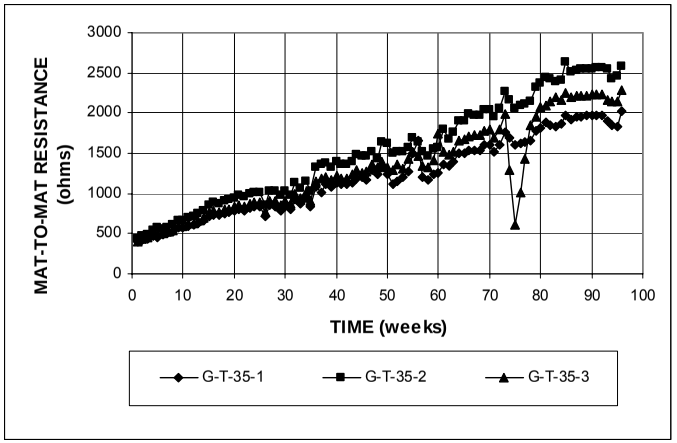


**Figure B.68** - Mat-to-mat resistances as measured in the ASTM G 109 test for specimens with conventional Thermex-treated steel (N), a water-cement ratio of 0.35, and no inhibitor.

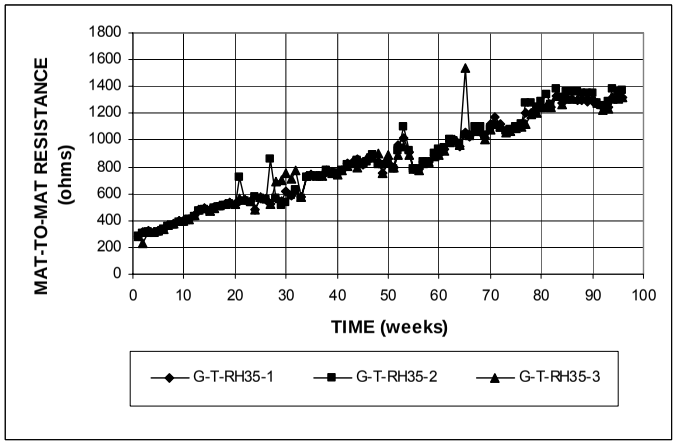


**Figure B.69** - Mat-to-mat resistances as measured in the ASTM G 109 test for specimens with conventional Thermex-treated steel (N), a water-cement ratio of 0.35, and Rheocrete 222+.

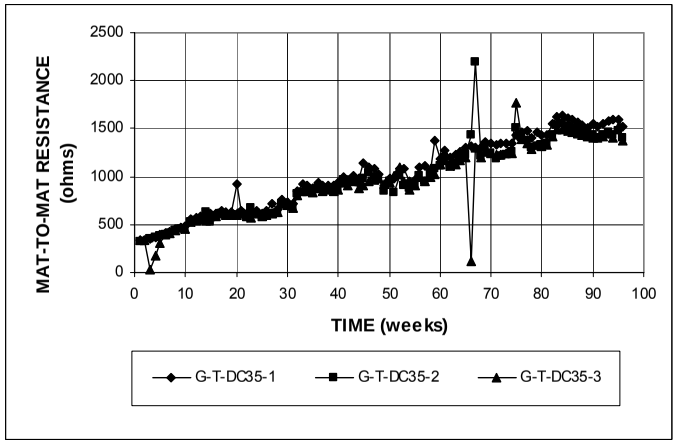


**Figure B.70** - Mat-to-mat resistances as measured in the ASTM G 109 test for specimens with conventional Thermex-treated steel (N), a water-cement ratio of 0.35, and DCI-S.

# APPENDIX C

**Table C.1 –** Student's t-test for comparing the mean corrosion rates of specimens with different conventional steels.

| Specimens * | | $t_{stat}$ | $t_{crit}$ X%: | 80% | 90% | 95% | 98% |
|---|---|---|---|---|---|---|---|
| | | | α: | 0.20 | 0.10 | 0.05 | 0.02 |
| Macrocell test with bare specimens | | | | | | | |
| M-N | M-N3 | 0.347 | | 1.383 N | 1.833 N | 2.262 N | 2.821 N |
| Macrocell test with mortar specimens | | | | | | | |
| M-N-50 | M-N3-50 | -5.861 | | 1.476 Y | 2.015 Y | 2.571 Y | 3.365 Y |
| M-N-50 | M-N2-50 | -4.382 | | 1.533 Y | 2.132 Y | 2.776 Y | 3.747 Y |
| M-N3-50 | M-N2-50 | 0.346 | | 1.397 N | 1.860 N | 2.306 N | 2.896 N |
| Southern Exposure test | | | | | | | |
| SE-N-45 | SE-N3-45 | -2.202 | | 1.397 Y | 1.860 Y | 2.306 N | 2.896 N |
| Cracked beam test | | | | | | | |
| CB-N-45 | CB-N3-45 | -0.373 | | 1.397 N | 1.860 N | 2.306 N | 2.896 N |

$t_{stat}$: t-test statistic, $t_{crit}$: value of t calculated from Student's t-distribution, α: level of significance, X%: confidence level, Y: statistically significant difference, i.e. null hypothesis rejected, N: not statistically significant difference, i.e. null hypothesis rejected.

* T - A - B

**T**: test → M: macrocell test, SE: Southern Exposure test, CB: cracked beam test

**A**: steel type → N, N2, and N3: conventional, normalized steel.

**B**: mix design → 50: water-cement ratio of 0.50 and no inhibitor, 45: water-cement ratio of 0.45 and no inhibitor.

**Table C.2 –** Student's t-test for comparing the mean corrosion losses of specimens with different conventional steels.

| Specimens * | | $t_{stat}$ | $t_{crit}$ X%: | 80% | 90% | 95% | 98% |
|---|---|---|---|---|---|---|---|
| | | | α: | 0.20 | 0.10 | 0.05 | 0.02 |
| Macrocell test with bare specimens | | | | | | | |
| M-N | M-N3 | 0.980 | | 1.383 N | 1.833 N | 2.262 N | 2.821 N |
| Macrocell test with mortar specimens | | | | | | | |
| M-N-50 | M-N3-50 | -13.932 | | 1.440 Y | 1.943 Y | 2.447 Y | 3.143 Y |
| M-N-50 | M-N2-50 | -4.676 | | 1.533 Y | 2.132 Y | 2.776 Y | 3.747 Y |
| M-N3-50 | M-N2-50 | 2.168 | | 1.440 Y | 1.943 Y | 2.447 N | 3.143 N |
| Southern Exposure test | | | | | | | |
| SE-N-45 | SE-N3-45 | -0.827 | | 1.397 N | 1.860 N | 2.306 N | 2.896 N |
| Cracked beam test | | | | | | | |
| CB-N-45 | CB-N3-45 | -1.291 | | 1.440 N | 1.943 N | 2.447 N | 3.143 N |

$t_{stat}$: t-test statistic, $t_{crit}$: value of t calculated from Student's t-distribution, α: level of significance, X%: confidence level, Y: statistically significant difference, i.e. null hypothesis rejected, N: not statistically significant difference, i.e. null hypothesis rejected.

* T - A - B

**T**: test → M: macrocell test, SE: Southern Exposure test, CB: cracked beam test

**A**: steel type → N, N2, and N3: conventional, normalized steel.

**B**: mix design → 50: water-cement ratio of 0.50 and no inhibitor, 45: water-cement ratio of 0.45 and no inhibitor.

**Table C.3 –** Student's t-test for comparing the mean corrosion rates of specimens with corrosion inhibitors and different water-cement ratios.

| Specimens * | | $t_{stat}$ | $t_{crit}$ X%: | 80% | 90% | 95% | 98% |
|---|---|---|---|---|---|---|---|
| | | | α: | 0.20 | 0.10 | 0.05 | 0.02 |
| Macrocell test with lollipop specimens | | | | | | | |
| M-N-45 | M-N-RH45 | 2.424 | | 1.440 Y | 1.943 Y | 2.447 N | 3.143 N |
| M-N-45 | M-N-DC45 | 2.525 | | 1.440 Y | 1.943 Y | 2.447 Y | 3.143 N |
| M-N-45 | M-N-35 | 2.129 | | 1.415 Y | 1.895 Y | 2.365 N | 2.998 N |
| M-N-35 | M-N-RH35 | 1.792 | | 1.533 Y | 2.132 N | 2.776 N | 3.747 N |
| M-N-35 | M-N-DC35 | 1.700 | | 1.533 Y | 2.132 N | 2.776 N | 3.747 N |
| Southern Exposure test | | | | | | | |
| SE-N-45 | SE-N-RH45 | 3.050 | | 1.476 Y | 2.015 Y | 2.571 Y | 3.365 N |
| SE-N-45 | SE-N-DC45 | 2.756 | | 1.440 Y | 1.943 Y | 2.447 Y | 3.143 N |
| SE-N-45 | SE-N-35 | 2.343 | | 1.415 Y | 1.895 Y | 2.365 N | 2.998 N |
| SE-N-35 | SE-N-RH35 | 1.973 | | 1.886 Y | 2.920 N | 4.303 N | 6.965 N |
| SE-N-35 | SE-N-DC35 | 0.873 | | 1.638 N | 2.353 N | 3.182 N | 4.541 N |
| SE-T-45 | SE-T-RH45 | 1.952 | | 1.476 Y | 2.015 N | 2.571 N | 3.365 N |
| SE-T-45 | SE-T-DC45 | 1.644 | | 1.440 Y | 1.943 N | 2.447 N | 3.143 N |
| SE-T-45 | SE-T-35 | 2.045 | | 1.476 Y | 2.015 Y | 2.571 N | 3.365 N |
| SE-T-35 | SE-T-RH35 | -0.600 | | 1.638 N | 2.353 N | 3.182 N | 4.541 N |
| SE-T-35 | SE-T-DC35 | -0.164 | | 1.886 N | 2.920 N | 4.303 N | 6.965 N |
| Cracked beam test | | | | | | | |
| CB-N-45 | CB-N-RH45 | 2.309 | | 1.440 Y | 1.943 Y | 2.447 N | 3.143 N |
| CB-N-45 | CB-N-DC45 | 2.296 | | 1.440 Y | 1.943 Y | 2.447 N | 3.143 N |
| CB-N-45 | CB-N-35 | 2.274 | | 1.440 Y | 1.943 Y | 2.447 N | 3.143 N |
| CB-N-35 | CB-N-RH35 | -0.650 | | 1.638 N | 2.353 N | 3.182 N | 4.541 N |
| CB-N-35 | CB-N-DC35 | -3.168 | | 1.886 Y | 2.920 Y | 4.303 N | 6.965 N |
| CB-T-45 | CB-T-RH45 | 2.764 | | 1.440 Y | 1.943 Y | 2.447 Y | 3.143 N |
| CB-T-45 | CB-T-DC45 | 2.748 | | 1.440 Y | 1.943 Y | 2.447 Y | 3.143 N |
| CB-T-45 | CB-T-35 | 2.444 | | 1.440 Y | 1.943 Y | 2.447 N | 3.143 N |
| CB-T-35 | CB-T-RH35 | 2.799 | | 1.638 Y | 2.353 Y | 3.182 N | 4.541 N |
| CB-T-35 | CB-T-DC35 | 2.834 | | 1.533 Y | 2.132 Y | 2.776 Y | 3.747 N |
| ASTM G 109 test | | | | | | | |
| G-N-45 | G-N-RH45 | 2.362 | | 1.476 Y | 2.015 Y | 2.571 N | 3.365 N |
| G-N-45 | G-N-DC45 | 2.089 | | 1.476 Y | 2.015 Y | 2.571 N | 3.365 N |
| G-N-45 | G-N-35 | 2.361 | | 1.476 Y | 2.015 Y | 2.571 N | 3.365 N |
| G-N-35 | G-N-RH35 | 0.894 | | 1.638 N | 2.353 N | 3.182 N | 4.541 N |
| G-N-35 | G-N-DC35 | 1.206 | | 1.533 N | 2.132 N | 2.776 N | 3.747 N |
| G-T-45 | G-T-RH45 | 2.203 | | 1.476 Y | 2.015 Y | 2.571 N | 3.365 N |
| G-T-45 | G-T-DC45 | 2.200 | | 1.476 Y | 2.015 Y | 2.571 N | 3.365 N |
| G-T-45 | G-T-35 | 2.203 | | 1.476 Y | 2.015 Y | 2.571 N | 3.365 N |
| G-T-35 | G-T-RH35 | 1.061 | | 1.638 N | 2.353 N | 3.182 N | 4.541 N |
| G-T-35 | G-T-DC35 | 1.890 | | 1.886 Y | 2.920 N | 4.303 N | 6.965 N |

$t_{stat}$: t-test statistic, $t_{crit}$: value of t calculated from Student's t-distribution, □: level of significance, X%: confidence level, Y: statistically significant difference, i.e. null hypothesis rejected, N: not statistically significant difference, i.e. null hypothesis rejected.

* T - A - B

**T**: test → M: macrocell test, SE: Southern Exposure test, CB: cracked beam test, G: ASTM G 109 test

**A**: steel type → N: conventional, normalized steel, T: Thermex-treated conventional steel.

**B**: mix design → 45: water-cement ratio of 0.45 and no inhibitor, RH45: water-cement ratio of 0.45 and Rheocrete 222+, DC45: water-cement ratio of 0.45 and DCI-S, 35: water-cement ratio of 0.35 and no inhibitor, RH35: water-cement ratio of 0.35 and Rheocrete 222+, DC35: water-cement ratio of 0.35 and DCI-S.

**Table C.4 –** Student's t-test for comparing the mean corrosion losses of specimens with corrosion inhibitors and different water-cement ratios.

| Specimens * | | $t_{stat}$ | $t_{crit}$ X%: | 80% | 90% | 95% | 98% |
|---|---|---|---|---|---|---|---|
| | | | α: | 0.20 | 0.10 | 0.05 | 0.02 |
| Macrocell test with lollipop specimens | | | | | | | |
| M-N-45 | M-N-RH45 | 2.442 | | 1.533 Y | 2.132 Y | 2.776 N | 3.747 N |
| M-N-45 | M-N-DC45 | 2.089 | | 1.533 Y | 2.132 N | 2.776 N | 3.747 N |
| M-N-45 | M-N-35 | 0.741 | | 1.397 N | 1.860 N | 2.306 N | 2.896 N |
| M-N-35 | M-N-RH35 | 0.785 | | 1.476 N | 2.015 N | 2.571 N | 3.365 N |
| M-N-35 | M-N-DC35 | 1.023 | | 1.533 N | 2.132 N | 2.776 N | 3.747 N |
| Southern Exposure test | | | | | | | |
| SE-N-45 | SE-N-RH45 | 5.600 | | 1.440 Y | 1.943 Y | 2.447 Y | 3.143 Y |
| SE-N-45 | SE-N-DC45 | 4.620 | | 1.415 Y | 1.895 Y | 2.365 Y | 2.998 Y |
| SE-N-45 | SE-N-35 | 5.324 | | 1.440 Y | 1.943 Y | 2.447 Y | 3.143 Y |
| SE-N-35 | SE-N-RH35 | 1.955 | | 1.886 Y | 2.920 N | 4.303 N | 6.965 N |
| SE-N-35 | SE-N-DC35 | 1.524 | | 1.886 N | 2.920 N | 4.303 N | 6.965 N |
| SE-T-45 | SE-T-RH45 | 3.923 | | 1.476 Y | 2.015 Y | 2.571 Y | 3.365 Y |
| SE-T-45 | SE-T-DC45 | 1.488 | | 1.440 Y | 1.943 N | 2.447 N | 3.143 N |
| SE-T-45 | SE-T-35 | 4.091 | | 1.476 Y | 2.015 Y | 2.571 Y | 3.365 Y |
| SE-T-35 | SE-T-RH35 | 1.348 | | 1.533 N | 2.132 N | 2.776 N | 3.747 N |
| SE-T-35 | SE-T-DC35 | 1.733 | | 1.533 Y | 2.132 N | 2.776 N | 3.747 N |
| Cracked beam test | | | | | | | |
| CB-N-45 | CB-N-RH45 | 4.110 | | 1.440 Y | 1.943 Y | 2.447 Y | 3.143 Y |
| CB-N-45 | CB-N-DC45 | 0.693 | | 1.533 N | 2.132 N | 2.776 N | 3.747 N |
| CB-N-45 | CB-N-35 | 2.886 | | 1.440 Y | 1.943 Y | 2.447 Y | 3.143 N |
| CB-N-35 | CB-N-RH35 | 1.292 | | 1.638 N | 2.353 N | 3.182 N | 4.541 N |
| CB-N-35 | CB-N-DC35 | -2.447 | | 1.886 Y | 2.920 N | 4.303 N | 6.965 N |
| CB-T-45 | CB-T-RH45 | 3.669 | | 1.440 Y | 1.943 Y | 2.447 Y | 3.143 Y |
| CB-T-45 | CB-T-DC45 | -0.733 | | 1.886 N | 2.920 N | 4.303 N | 6.965 N |
| CB-T-45 | CB-T-35 | 4.238 | | 1.415 Y | 1.895 Y | 2.365 Y | 2.998 Y |
| CB-T-35 | CB-T-RH35 | 0.528 | | 1.886 N | 2.920 N | 4.303 N | 6.965 N |
| CB-T-35 | CB-T-DC35 | 3.389 | | 1.638 Y | 2.353 Y | 3.182 Y | 4.541 N |
| ASTM G 109 test | | | | | | | |
| G-N-45 | G-N-RH45 | 5.467 | | 1.476 Y | 2.015 Y | 2.571 Y | 3.365 Y |
| G-N-45 | G-N-DC45 | 5.039 | | 1.476 Y | 2.015 Y | 2.571 Y | 3.365 Y |
| G-N-45 | G-N-35 | 5.396 | | 1.476 Y | 2.015 Y | 2.571 Y | 3.365 Y |
| G-N-35 | G-N-RH35 | 3.426 | | 1.886 Y | 2.920 Y | 4.303 N | 6.965 N |
| G-N-35 | G-N-DC35 | 1.828 | | 1.638 Y | 2.353 N | 3.182 N | 4.541 N |
| G-T-45 | G-T-RH45 | 1.502 | | 1.476 Y | 2.015 N | 2.571 N | 3.365 N |
| G-T-45 | G-T-DC45 | 1.498 | | 1.476 Y | 2.015 N | 2.571 N | 3.365 N |
| G-T-45 | G-T-35 | 1.429 | | 1.476 N | 2.015 N | 2.571 N | 3.365 N |
| G-T-35 | G-T-RH35 | 1.373 | | 1.886 N | 2.920 N | 4.303 N | 6.965 N |
| G-T-35 | G-T-DC35 | 1.502 | | 1.886 N | 2.920 N | 4.303 N | 6.965 N |

$t_{stat}$: t-test statistic, $t_{crit}$: value of t calculated from Student's t-distribution, α: level of significance, X%: confidence level, Y: statistically significant difference, i.e. null hypothesis rejected, N: not statistically significant difference, i.e. null hypothesis rejected.

* T - A - B

**T**: test → M: macrocell test, SE: Southern Exposure test, CB: cracked beam test, G: ASTM G 109 test.

**A**: steel type → N: conventional, normalized steel, T: Thermex-treated conventional steel.

**B**: mix design → 45: water-cement ratio of 0.45 and no inhibitor, RH45: water-cement ratio of 0.45 and Rheocrete 222+, DC45: water-cement ratio of 0.45 and DCI-S, 35: water-cement ratio of 0.35 and no inhibitor, RH35: water-cement ratio of 0.35 and Rheocrete 222+, DC35: water-cement ratio of 0.35 and DCI-S.

**Table C.5 –** Student's t-test for comparing the mean corrosion rates of conventional normalized, conventional Thermex-treated, and microalloyed steels.

| Specimens * | | $t_{stat}$ | $t_{crit}$ | | | |
|---|---|---|---|---|---|---|
| | | **X%:** | **80%** | **90%** | **95%** | **98%** |
| | | **α:** | **0.20** | **0.10** | **0.05** | **0.02** |
| Macrocell test with bare specimens | | | | | | |
| M-N | M-T | 0.935 | 1.397 N | 1.860 N | 2.306 N | 2.896 N |
| M-N | M-CRPT1 | 0.256 | 1.397 N | 1.860 N | 2.306 N | 2.896 N |
| M-N | M-CRPT2 | -0.800 | 1.397 N | 1.860 N | 2.306 N | 2.896 N |
| M-N | M-CRT | -0.413 | 1.397 N | 1.860 N | 2.306 N | 2.896 N |
| Macrocell test with lollipop specimens | | | | | | |
| M-Nc-50 | M-Tc-50 | 0.483 | 1.476 N | 2.015 N | 2.571 N | 3.365 N |
| M-Nc-50 | M-CRPT1c-50 | -1.220 | 1.440 N | 1.943 N | 2.447 N | 3.143 N |
| M-Nc-50 | M-CRPT2c-50 | -0.529 | 1.476 N | 2.015 N | 2.571 N | 3.365 N |
| M-Nc-50 | M-CRTc-50 | -1.415 | 1.440 N | 1.943 N | 2.447 N | 3.143 N |
| M-N-50 | M-T-50 | -1.178 | 1.415 N | 1.895 N | 2.365 N | 2.998 N |
| M-N-50 | M-CRPT1-50 | -1.074 | 1.440 N | 1.943 N | 2.447 N | 3.143 N |
| M-N-50 | M-CRPT2-50 | -1.199 | 1.415 N | 1.895 N | 2.365 N | 2.998 N |
| M-N-50 | M-CRT-50 | -0.945 | 1.415 N | 1.895 N | 2.365 N | 2.998 N |
| Southern Exposure test | | | | | | |
| SE-N-45 | SE-T-45 | -1.162 | 1.440 N | 1.943 N | 2.447 N | 3.143 N |
| SE-N-45 | SE-CRPT1-45 | -0.034 | 1.383 N | 1.833 N | 2.262 N | 2.821 N |
| SE-N-45 | SE-CRPT2-45 | -1.211 | 1.383 N | 1.833 N | 2.262 N | 2.821 N |
| SE-N-45 | SE-CRT-45 | -0.044 | 1.372 N | 1.812 N | 2.228 N | 2.764 N |
| SE-N-45 | SE-N/CRPT1-45 | -1.725 | 1.372 Y | 1.812 N | 2.228 N | 2.764 N |
| SE-CRPT1-45 | SE-CRPT1/N-45 | -0.408 | 1.372 N | 1.812 N | 2.228 N | 2.764 N |
| Cracked beam test | | | | | | |
| CB-N-45 | CB-T-45 | 0.831 | 1.383 N | 1.833 N | 2.262 N | 2.821 N |
| CB-N-45 | CB-CRPT1-45 | 0.873 | 1.383 N | 1.833 N | 2.262 N | 2.821 N |
| CB-N-45 | CB-CRPT2-45 | 1.138 | 1.383 N | 1.833 N | 2.262 N | 2.821 N |
| CB-N-45 | CB-CRT-45 | 1.313 | 1.415 N | 1.895 N | 2.365 N | 2.998 N |
| ASTM G 109 test | | | | | | |
| G-N-45 | G-T-45 | 0.464 | 1.372 N | 1.812 N | 2.228 N | 2.764 N |
| G-N-45 | G-CRPT1-45 | -0.050 | 1.372 N | 1.812 N | 2.228 N | 2.764 N |
| G-N-45 | G-CRPT2-45 | 0.177 | 1.372 N | 1.812 N | 2.228 N | 2.764 N |
| G-N-45 | G-CRT-45 | 0.432 | 1.397 N | 1.860 N | 2.306 N | 2.896 N |

$t_{stat}$: t-test statistic, $t_{crit}$: value of t calculated from Student's t-distribution, α: level of significance, X%: confidence level, Y: statistically significant difference, i.e. null hypothesis rejected, N: not statistically significant difference, i.e. null hypothesis rejected.

* T - A - B

**T**: test → M: macrocell test, SE: Southern Exposure test, CB: cracked beam test, G: ASTM G 109 test

**A**: steel type → N: conventional, normalized steel, T: Thermex-treated conventional steel, CRPT1: Thermex-treated microalloyed steel with a high phosphorus content (0.117%), CRPT2: Thermex-treated microalloyed steel with a high phosphorus content (0.100%), CRT: Thermex treated microalloyed steel with normal phosphorus content (0.017%), c: epoxy-filled caps on the end.

**B**: mix design → 50: water-cement ratio of 0.50 and no inhibitor, 45: water-cement ratio of 0.45 and no inhibitor.

**Table C.6 –** Student's t-test for comparing the mean corrosion losses of conventional normalized, conventional Thermex-treated, and microalloyed steels.

| Specimens * | | $t_{stat}$ | $t_{crit}$ | | | |
|---|---|---|---|---|---|---|
| | | **X%:** | **80%** | **90%** | **95%** | **98%** |
| | | **α:** | **0.20** | **0.10** | **0.05** | **0.02** |
| Macrocell test with bare specimens | | | | | | |
| M-N | M-T | 2.000 | 1.397 Y | 1.860 Y | 2.306 N | 2.896 N |
| M-N | M-CRPT1 | 0.260 | 1.415 N | 1.895 N | 2.365 N | 2.998 N |
| M-N | M-CRPT2 | -0.820 | 1.415 N | 1.895 N | 2.365 N | 2.998 N |
| M-N | M-CRT | 1.080 | 1.476 N | 2.015 N | 2.571 N | 3.365 N |
| Macrocell test with lollipop specimens | | | | | | |
| M-Nc-50 | M-Tc-50 | 1.321 | 1.476 N | 2.015 N | 2.571 N | 3.365 N |
| M-Nc-50 | M-CRPT1c-50 | -0.351 | 1.476 N | 2.015 N | 2.571 N | 3.365 N |
| M-Nc-50 | M-CRPT2c-50 | 0.296 | 1.476 N | 2.015 N | 2.571 N | 3.365 N |
| M-Nc-50 | M-CRTc-50 | -0.027 | 1.476 N | 2.015 N | 2.571 N | 3.365 N |
| M-N-50 | M-T-50 | -0.780 | 1.415 N | 1.895 N | 2.365 N | 2.998 N |
| M-N-50 | M-CRPT1-50 | -0.972 | 1.440 N | 1.943 N | 2.447 N | 3.143 N |
| M-N-50 | M-CRPT2-50 | -1.481 | 1.440 Y | 1.943 N | 2.447 N | 3.143 N |
| M-N-50 | M-CRT-50 | -0.889 | 1.440 N | 1.943 N | 2.447 N | 3.143 N |
| Southern Exposure test | | | | | | |
| SE-N-45 | SE-T-45 | -0.081 | 1.397 N | 1.860 N | 2.306 N | 2.896 N |
| SE-N-45 | SE-CRPT1-45 | 0.962 | 1.383 N | 1.833 N | 2.262 N | 2.821 N |
| SE-N-45 | SE-CRPT2-45 | -0.386 | 1.397 N | 1.860 N | 2.306 N | 2.896 N |
| SE-N-45 | SE-CRT-45 | 0.380 | 1.383 N | 1.833 N | 2.262 N | 2.821 N |
| SE-N-45 | SE-N/CRPT1-45 | -0.561 | 1.372 N | 1.812 N | 2.228 N | 2.764 N |
| SE-CRPT1-45 | SE-CRPT1/N-45 | -1.325 | 1.372 N | 1.812 N | 2.228 N | 2.764 N |
| Cracked beam test | | | | | | |
| CB-N-45 | CB-T-45 | -1.009 | 1.372 N | 1.812 N | 2.228 N | 2.764 N |
| CB-N-45 | CB-CRPT1-45 | -0.489 | 1.383 N | 1.833 N | 2.262 N | 2.821 N |
| CB-N-45 | CB-CRPT2-45 | -0.003 | 1.397 N | 1.860 N | 2.306 N | 2.896 N |
| CB-N-45 | CB-CRT-45 | -0.349 | 1.440 N | 1.943 N | 2.447 N | 3.143 N |
| ASTM G 109 test | | | | | | |
| G-N-45 | G-T-45 | 0.869 | 1.415 N | 1.895 N | 2.365 N | 2.998 N |
| G-N-45 | G-CRPT1-45 | 0.421 | 1.415 N | 1.895 N | 2.365 N | 2.998 N |
| G-N-45 | G-CRPT2-45 | 0.379 | 1.440 N | 1.943 N | 2.447 N | 3.143 N |
| G-N-45 | G-CRT-45 | 2.911 | 1.383 Y | 1.833 Y | 2.262 Y | 2.821 Y |

$t_{stat}$: t-test statistic, $t_{crit}$: value of t calculated from Student's t-distribution, α: level of significance, X%: confidence level, Y: statistically significant difference, i.e. null hypothesis rejected, N: not statistically significant difference, i.e. null hypothesis rejected.

* T - A - B

**T**: test → M: macrocell test, SE: Southern Exposure test, CB: cracked beam test, G: ASTM G 109 test.

**A**: steel type → N: conventional, normalized steel, T: Thermex-treated conventional steel, CRPT1: Thermex-treated microalloyed steel with a high phosphorus content (0.117%), CRPT2: Thermex-treated microalloyed steel with a high phosphorus content (0.100%), CRT: Thermex treated microalloyed steel with normal phosphorus content (0.017%), c: epoxy-filled caps on the end.

**B**: mix design → 50: water-cement ratio of 0.50 and no inhibitor, 45: water-cement ratio of 0.45 and no inhibitor.

**Table C.7 –** Student's t-test for comparing the mean corrosion rates of conventional and MMFX microcomposite steels.

| Specimens * | | $t_{stat}$ | $t_{crit}$ | | | |
|---|---|---|---|---|---|---|
| | | **X%:** | **80%** | **90%** | **95%** | **98%** |
| | | **α:** | **0.20** | **0.10** | **0.05** | **0.02** |
| Macrocell test with bare specimens in 1.6 m ion NaCl | | | | | | |
| M-N3 | M-MMFX(1) | 2.425 | 1.440 Y | 1.943 Y | 2.447 N | 3.143 N |
| M-N3 | M-MMFX(2) | 1.933 | 1.440 Y | 1.943 N | 2.447 N | 3.143 N |
| M-MMFX(1) | M-MMFX(2) | -1.352 | 1.372 N | 1.812 N | 2.228 N | 2.764 N |
| M-MMFX(2) | M-MMFXs | 0.957 | 1.372 N | 1.812 N | 2.228 N | 2.764 N |
| M-MMFX(2) | M-MMFXb | 2.595 | 1.397 Y | 1.860 Y | 2.306 Y | 2.896 N |
| M-MMFX(2) | M-MMFX#19 | -3.532 | 1.372 Y | 1.812 Y | 2.228 Y | 2.764 Y |
| Macrocell test with bare specimens in 6.04 m ion NaCl | | | | | | |
| M-N3h | M-MMFXsh | -2.783 | 1.397 Y | 1.860 Y | 2.306 Y | 2.896 N |
| Macrocell test with mortar-wrapped specimens | | | | | | |
| M-N3-50 | M-MMFX-50 | 2.349 | 1.397 Y | 1.860 Y | 2.306 Y | 2.896 N |
| M-N3-50 | M-N3/MMFX-50 | 1.888 | 1.415 Y | 1.895 N | 2.365 N | 2.998 N |
| M-MMFX-50 | M-MMFX/N3-50 | -1.236 | 1.415 N | 1.895 N | 2.365 N | 2.998 N |
| Southern Exposure test | | | | | | |
| SE-N3-45 | SE-MMFX-45 | 3.297 | 1.476 Y | 2.015 Y | 2.571 Y | 3.365 N |
| SE-N3-45 | SE-N3/MMFX-45 | 2.850 | 1.440 Y | 1.943 Y | 2.447 Y | 3.143 N |
| SE-MMFX-45 | SE-MMFX/N3-45 | -0.375 | 1.476 N | 2.015 N | 2.571 N | 3.365 N |
| SE-MMFX-45 | SE-MMFXb-45 | 2.891 | 1.415 Y | 1.895 Y | 2.365 Y | 2.998 N |
| Cracked beam test | | | | | | |
| CB-N3-45 | CB-MMFX-45 | 1.668 | 1.476 Y | 2.015 N | 2.571 N | 3.365 N |

$t_{stat}$: t-test statistic, $t_{crit}$: value of t calculated from Student's t-distribution, α: level of significance, X%: confidence level, Y: statistically significant difference, i.e. null hypothesis rejected, N: not statistically significant difference, i.e. null hypothesis rejected.

* T - A - B

**T**: test → M: macrocell test, SE: Southern Exposure test, CB: cracked beam test

**A**: steel type → N, and N3: conventional, normalized steel, MMFX: MMFX microcomposite steel, s: sandblasted, b: bent bars in the anode or top mat, h: 6.04 m ion concentration.

**B**: mix design → 50: water-cement ratio of 0.50 and no inhibitor, 45: water-cement ratio of 0.45 and no inhibitor.

**Table C.8 –** Student's t-test for comparing the mean corrosion losses of conventional and MMFX microcomposite steels.

| Specimens * | | $t_{stat}$ | $t_{crit}$ X%: | 80% | 90% | 95% | 98% |
|---|---|---|---|---|---|---|---|
| | | | α: | 0.20 | 0.10 | 0.05 | 0.02 |
| Macrocell test with bare specimens in 1.6 m ion NaCl | | | | | | | |
| M-N3 | M-MMFX(1) | 2.050 | | 1.440 Y | 1.943 Y | 2.447 N | 3.143 N |
| M-N3 | M-MMFX(2) | 3.950 | | 1.440 Y | 1.943 Y | 2.447 Y | 3.143 Y |
| M-MMFX(1) | M-MMFX(2) | 4.370 | | 1.383 Y | 1.833 Y | 2.262 Y | 2.821 Y |
| M-MMFX(2) | M-MMFXs | -0.370 | | 1.397 N | 1.860 N | 2.306 N | 2.896 N |
| M-MMFX(2) | M-MMFXb | 1.580 | | 1.397 Y | 1.860 N | 2.306 N | 2.896 N |
| M-MMFX(2) | M-MMFX#19 | -3.660 | | 1.415 Y | 1.895 Y | 2.365 Y | 2.998 Y |
| Macrocell test with bare specimens in 6.04 m ion NaCl | | | | | | | |
| M-N3h | M-MMFXsh | -0.030 | | 1.383 N | 1.833 N | 2.262 N | 2.821 N |
| Macrocell test with mortar-wrapped specimens | | | | | | | |
| M-N3-50 | M-MMFX-50 | 9.807 | | 1.372 Y | 1.812 Y | 2.228 Y | 2.764 Y |
| M-N3-50 | M-N3/MMFX-50 | 5.900 | | 1.476 Y | 2.015 Y | 2.571 Y | 3.365 Y |
| M-MMFX-50 | M-MMFX/N3-50 | -1.498 | | 1.415 Y | 1.895 N | 2.365 N | 2.998 N |
| Southern Exposure test | | | | | | | |
| SE-N3-45 | SE-MMFX-45 | 3.301 | | 1.476 Y | 2.015 Y | 2.571 Y | 3.365 N |
| SE-N3-45 | SE-N3/MMFX-45 | 1.305 | | 1.415 N | 1.895 N | 2.365 N | 2.998 N |
| SE-MMFX-45 | SE-MMFX/N3-45 | -0.733 | | 1.415 N | 1.895 N | 2.365 N | 2.998 N |
| SE-MMFX-45 | SE-MMFXb-45 | -3.600 | | 1.638 Y | 2.353 Y | 3.182 Y | 4.541 N |
| Cracked beam test | | | | | | | |
| CB-N3-45 | CB-MMFX-45 | 2.441 | | 1.476 Y | 2.015 Y | 2.571 N | 3.365 N |

$t_{stat}$: t-test statistic, $t_{crit}$: value of t calculated from Student's t-distribution, α: level of significance, X%: confidence level, Y: statistically significant difference, i.e. null hypothesis rejected, N: not statistically significant difference, i.e. null hypothesis rejected.

* T - A - B

**T**: test → M: macrocell test, SE: Southern Exposure test, CB: cracked beam test

**A**: steel type → N, and N3: conventional, normalized steel, MMFX: MMFX microcomposite steel, s: sandblasted, b: bent bars in the anode or top mat, h: 6.04 m ion concentration.

**B**: mix design → 50: water-cement ratio of 0.50 and no inhibitor, 45: water-cement ratio of 0.45 and no inhibitor.

**Table C.9 –** Student's t-test for comparing mean corrosion rates of conventional uncoated and epoxy-coated steel.

| Specimens * | | $t_{stat}$ | $t_{crit}$ | | | |
|---|---|---|---|---|---|---|
| | | | X%: | 80% | 90% | 95% | 98% |
| | | | α: | 0.20 | 0.10 | 0.05 | 0.02 |
| Macrocell test with mortar-wrapped specimens | | | | | | | |
| M-N3-50 | M-ECR-50[2] | 3.190 | | 1.372 Y | 1.812 Y | 2.228 Y | 2.764 Y |
| Southern Exposure test | | | | | | | |
| SE-N3-45 | SE-ECR-45[2] | 4.043 | | 1.476 Y | 2.015 Y | 2.571 Y | 3.365 Y |
| Cracked beam test | | | | | | | |
| CB-N3-45 | CB-ECR-45[2] | 1.767 | | 1.476 Y | 2.015 N | 2.571 N | 3.365 N |

$t_{stat}$: t-test statistic, $t_{crit}$: value of t calculated from Student's t-distribution, α: level of significance, X%: confidence level, Y: statistically significant difference, i.e. null hypothesis rejected, N: not statistically significant difference, i.e. null hypothesis rejected.

* T - A - B
**T**: test → M: macrocell test, SE: Southern Exposure test, CB: cracked beam test
**A**: steel type → N3: conventional, normalized steel, ECR: epoxy-coated rebar,
**B**: mix design → 50: water-cement ratio of 0.50 and no inhibitor, 45: water-cement ratio of 0.45 and no inhibitor.

[2] Corrosion rate based on total area of bar exposed to solution

**Table C.10 –** Student's t-test for comparing mean corrosion losses of conventional uncoated and epoxy-coated steel.

| Specimens * | | $t_{stat}$ | $t_{crit}$ | | | |
|---|---|---|---|---|---|---|
| | | | X%: | 80% | 90% | 95% | 98% |
| | | | α: | 0.20 | 0.10 | 0.05 | 0.02 |
| Macrocell test with mortar-wrapped specimens | | | | | | | |
| M-N3-50 | M-ECR-50[2] | 13.140 | | 1.397 Y | 1.860 Y | 2.306 Y | 2.896 Y |
| Southern Exposure test | | | | | | | |
| SE-N3-45 | SE-ECR-45[2] | 4.252 | | 1.476 Y | 2.015 Y | 2.571 Y | 3.365 Y |
| Cracked beam test | | | | | | | |
| CB-N3-45 | CB-ECR-45[2] | 2.968 | | 1.476 Y | 2.015 Y | 2.571 Y | 3.365 N |

$t_{stat}$: t-test statistic, $t_{crit}$: value of t calculated from Student's t-distribution, α: level of significance, X%: confidence level, Y: statistically significant difference, i.e. null hypothesis rejected, N: not statistically significant difference, i.e. null hypothesis rejected.

* T - A - B
**T**: test → M: macrocell test, SE: Southern Exposure test, CB: cracked beam test
**A**: steel type → N3: conventional, normalized steel, ECR: epoxy-coated rebar,
**B**: mix design → 50: water-cement ratio of 0.50 and no inhibitor, 45: water-cement ratio of 0.45 and no inhibitor.

[2] Corrosion loss based on total area of bar exposed to solution

**Table C.11 –** Student's t-test for comparing the mean corrosion rates of conventional and duplex stainless steels.

| Specimens * | | $t_{stat}$ | $t_{crit}$ X%: | 80% | 90% | 95% | 98% |
|---|---|---|---|---|---|---|---|
| | | | α: | 0.20 | 0.10 | 0.05 | 0.02 |
| Macrocell test with bare specimens in 1.6 m ion NaCl | | | | | | | |
| M-N3 | M-2205 | 3.710 | | 1.476 Y | 2.015 Y | 2.571 Y | 3.365 Y |
| M-N3 | M-2205p | 3.714 | | 1.476 Y | 2.015 Y | 2.571 Y | 3.365 Y |
| M-N3 | M-2101(1) | 3.472 | | 1.476 Y | 2.015 Y | 2.571 Y | 3.365 Y |
| M-N3 | M-2101(1)p | 3.706 | | 1.476 Y | 2.015 Y | 2.571 Y | 3.365 Y |
| M-N3 | M-2101(2) | 3.391 | | 1.476 Y | 2.015 Y | 2.571 Y | 3.365 Y |
| M-N3 | M-2101(2)p | 3.720 | | 1.476 Y | 2.015 Y | 2.571 Y | 3.365 Y |
| M-N3 | M-2101(2)s | 1.771 | | 1.372 Y | 1.812 N | 2.228 N | 2.764 N |
| Macrocell test with bare specimens in 6.04 m ion NaCl | | | | | | | |
| M-N3h | M-2205h | 4.878 | | 1.533 Y | 2.132 Y | 2.776 Y | 3.747 Y |
| M-N3h | M-2205ph | 5.350 | | 1.533 Y | 2.132 Y | 2.776 Y | 3.747 Y |
| M-N3h | M-2101(1)h | 2.152 | | 1.415 Y | 1.895 Y | 2.365 N | 2.998 N |
| M-N3h | M-2101(1)ph | 4.302 | | 1.476 Y | 2.015 Y | 2.571 Y | 3.365 Y |
| M-N3h | M-2101(2)h | 3.013 | | 1.533 Y | 2.132 Y | 2.776 Y | 3.747 N |
| M-N3h | M-2101(2)ph | 5.168 | | 1.533 Y | 2.132 Y | 2.776 Y | 3.747 Y |
| M-N3h | M-2101(2)sh | 0.269 | | 1.397 N | 1.860 N | 2.306 N | 2.896 N |
| Macrocell test with mortar-wrapped specimens | | | | | | | |
| M-N2-50 | M-2205-50 | 5.129 | | 1.533 Y | 2.132 Y | 2.776 Y | 3.747 Y |
| M-N2-50 | M-2205p-50 | 5.119 | | 1.533 Y | 2.132 Y | 2.776 Y | 3.747 Y |
| M-N2-50 | M-2101(1)-50 | 1.827 | | 1.415 Y | 1.895 N | 2.365 N | 2.998 N |
| M-N2-50 | M-2101(1)p-50 | 5.131 | | 1.533 Y | 2.132 Y | 2.776 Y | 3.747 Y |
| M-N2-50 | M-2101(2)-50 | 3.374 | | 1.476 Y | 2.015 Y | 2.571 Y | 3.365 Y |
| M-N2-50 | M-2101(2)p-50 | 5.104 | | 1.533 Y | 2.132 Y | 2.776 Y | 3.747 Y |
| Southern Exposure test | | | | | | | |
| SE-N-45 | SE-2205-45 | 3.684 | | 1.476 Y | 2.015 Y | 2.571 Y | 3.365 Y |
| SE-N-45 | SE-2205p-45 | 3.679 | | 1.476 Y | 2.015 Y | 2.571 Y | 3.365 Y |
| SE-N-45 | SE-2101(1)-45 | 0.642 | | 1.415 N | 1.895 N | 2.365 N | 2.998 N |
| SE-N-45 | SE-2101(1)p-45 | 2.458 | | 1.415 Y | 1.895 Y | 2.365 Y | 2.998 N |
| SE-N-45 | SE-2101(2)-45 | 3.312 | | 1.476 Y | 2.015 Y | 2.571 Y | 3.365 N |
| SE-N-45 | SE-2101(2)p-45 | 3.698 | | 1.476 Y | 2.015 Y | 2.571 Y | 3.365 Y |
| SE-N-45 | SE-N/2205-45 | 0.316 | | 1.415 N | 1.895 N | 2.365 N | 2.998 N |
| SE-2205-45 | SE-2205/N-45 | -1.577 | | 1.886 N | 2.920 N | 4.303 N | 6.965 N |
| Cracked beam test | | | | | | | |
| CB-N-45 | CB-2205-45 | 3.156 | | 1.476 Y | 2.015 Y | 2.571 Y | 3.365 N |
| CB-N-45 | CB-2205p-45 | 3.171 | | 1.476 Y | 2.015 Y | 2.571 Y | 3.365 N |
| CB-N-45 | CB-2101(1)-45 | 2.776 | | 1.476 Y | 2.015 Y | 2.571 Y | 3.365 N |
| CB-N-45 | CB-2101(1)p-45 | 3.141 | | 1.476 Y | 2.015 Y | 2.571 Y | 3.365 N |
| CB-N-45 | CB-2101(2)-45 | 2.899 | | 1.476 Y | 2.015 Y | 2.571 Y | 3.365 N |
| CB-N-45 | CB-2101(2)p-45 | 3.199 | | 1.476 Y | 2.015 Y | 2.571 Y | 3.365 N |

$t_{stat}$: t-test statistic, $t_{crit}$: value of t calculated from Student's t-distribution, α: level of significance, X%: confidence level, Y: statistically significant difference, i.e. null hypothesis rejected, N: not statistically significant difference, i.e. null hypothesis rejected.

* T - A - B

**T**: test → M: macrocell test, SE: Southern Exposure test, CB: cracked beam test

**A**: steel type → N, N2, and N3: conventional, normalized steel, 2101(1) and 2101(2): duplex stainless steel (21% chromium, 1% nickel), 2205: duplex stainless steel (25% chromium, 5% nickel), p: pickled, s: sandblasted, h: 6.04 m ion concentration.

**B**: mix design → 50: water-cement ratio of 0.50 and no inhibitor, 45: water-cement ratio of 0.45 and no inhibitor.

**Table C.12 –** Student's t-test for comparing mean corrosion rates of pickled and non-pickled duplex steels.

| Specimens * | | $t_{stat}$ | $t_{crit}$ | | | |
|---|---|---|---|---|---|---|
| | | **X%:** | **80%** | **90%** | **95%** | **98%** |
| | | **α:** | **0.20** | **0.10** | **0.05** | **0.02** |
| Macrocell test with bare specimens in 1.6 m ion NaCl | | | | | | |
| M-2205 | M-2205p | 0.759 | 1.476 N | 2.0150 N | 2.571 N | 3.365 N |
| M-2101(1) | M-2101(1)p | 5.395 | 1.533 Y | 2.1318 Y | 2.776 Y | 3.747 Y |
| M-2101(2) | M-2101(2)p | 3.204 | 1.476 Y | 2.0150 Y | 2.571 Y | 3.365 N |
| M-2205p | M-2101(2)p | 2.682 | 1.383 Y | 1.8331 Y | 2.262 Y | 2.821 N |
| Macrocell test with bare specimens in 6.04 m ion NaCl | | | | | | |
| M-2205h | M-2205ph | 8.343 | 1.476 Y | 2.0150 Y | 2.571 Y | 3.365 Y |
| M-2101(1)h | M-2101(1)ph | 2.913 | 1.440 Y | 1.9432 Y | 2.447 Y | 3.143 N |
| M-2101(2)h | M-2101(2)ph | 9.650 | 1.383 Y | 1.8331 Y | 2.262 Y | 2.821 Y |
| M-2205ph | M-2101(2)ph | -1.168 | 1.476 N | 2.0150 N | 2.571 N | 3.365 N |
| Macrocell test with mortar-wrapped specimens | | | | | | |
| M-2205-50 | M-2205p-50 | 0.175 | 1.415 N | 1.8946 N | 2.365 N | 2.998 N |
| M-2101(1)-50 | M-2101(1)p-50 | 3.207 | 1.638 Y | 2.3534 Y | 3.182 Y | 4.541 N |
| M-2101(2)-50 | M-2101(2)p-50 | 5.182 | 1.476 Y | 2.0150 Y | 2.571 Y | 3.365 Y |
| M-2205p-50 | M-2101(2)p-50 | -1.206 | 1.372 N | 1.8125 N | 2.228 N | 2.764 N |
| Southern Exposure test | | | | | | |
| SE-2205-45 | SE-2205p-45 | -0.216 | 1.440 N | 1.9432 N | 2.447 N | 3.143 N |
| SE-2101(1)-45 | SE-2101(1)p-45 | 2.011 | 1.533 Y | 2.1318 N | 2.776 N | 3.747 N |
| SE-2101(2)-45 | SE-2101(2)p-45 | 1.592 | 1.533 Y | 2.1318 N | 2.776 N | 3.747 N |
| SE-2205p-45 | SE-2101(2)p-45 | 1.074 | 1.533 N | 2.1318 N | 2.776 N | 3.747 N |
| Cracked beam test | | | | | | |
| CB-2205-45 | CB-2205p-45 | 0.365 | 1.397 N | 1.8595 N | 2.306 N | 2.896 N |
| CB-2101(1)-45 | CB-2101(1)p-45 | 1.600 | 1.886 N | 2.9200 N | 4.303 N | 6.965 N |
| CB-2101(2)-45 | CB-2101(2)p-45 | 5.697 | 1.533 Y | 2.1318 Y | 2.776 Y | 3.747 Y |
| CB-2205p-45 | CB-2101(2)p-45 | 0.945 | 1.533 N | 2.1318 N | 2.776 N | 3.747 N |

$t_{stat}$: t-test statistic, $t_{crit}$: value of t calculated from Student's t-distribution, α: level of significance, X%: confidence level, Y: statistically significant difference, i.e. null hypothesis rejected, N: not statistically significant difference, i.e. null hypothesis rejected.

* T - A - B

**T**: test → M: macrocell test, SE: Southern Exposure test, CB: cracked beam test

**A**: steel type → 2101(1) and 2101(2): duplex stainless steel (21% chromium, 1% nickel), 2205: duplex stainless steel (25% chromium, 5% nickel), p: pickled, s: sandblasted, h: 6.04 m ion concentration.

**B**: mix design → 50: water-cement ratio of 0.50 and no inhibitor, 45: water-cement ratio of 0.45 and no inhibitor.

**Table C.13 –** Student's t-test for comparing the mean corrosion losses of conventional and duplex stainless steels.

| Specimens * | | $t_{stat}$ | $t_{crit}$ X%: | 80% | 90% | 95% | 98% |
|---|---|---|---|---|---|---|---|
| | | | α: | 0.20 | 0.10 | 0.05 | 0.02 |
| Macrocell test with bare specimens in 1.6 m ion NaCl | | | | | | | |
| M-N3 | M-2205 | 5.640 | | 1.476 Y | 2.015 Y | 2.571 Y | 3.365 Y |
| M-N3 | M-2205p | 5.640 | | 1.476 Y | 2.015 Y | 2.571 Y | 3.365 Y |
| M-N3 | M-2101(1) | 482.000 | | 1.440 Y | 1.943 Y | 2.447 Y | 3.143 Y |
| M-N3 | M-2101(1)p | 5.590 | | 1.476 Y | 2.015 Y | 2.571 Y | 3.365 Y |
| M-N3 | M-2101(2) | 4.730 | | 1.476 Y | 2.015 Y | 2.571 Y | 3.365 Y |
| M-N3 | M-2101(2)p | 5.630 | | 1.476 Y | 2.015 Y | 2.571 Y | 3.365 Y |
| M-N3 | M-2101(2)s | 1.250 | | 1.383 N | 1.833 N | 2.262 N | 2.821 N |
| Macrocell test with bare specimens in 6.04 m ion NaCl | | | | | | | |
| M-N3h | M-2205h | 9.270 | | 1.533 Y | 2.132 Y | 2.776 Y | 3.747 Y |
| M-N3h | M-2205ph | 9.760 | | 1.533 Y | 2.132 Y | 2.776 Y | 3.747 Y |
| M-N3h | M-2101(1)h | 5.110 | | 1.440 Y | 1.943 Y | 2.447 Y | 3.143 Y |
| M-N3h | M-2101(1)ph | 7.490 | | 1.476 Y | 2.015 Y | 2.571 Y | 3.365 Y |
| M-N3h | M-2101(2)h | 6.120 | | 1.533 Y | 2.132 Y | 2.776 Y | 3.747 Y |
| M-N3h | M-2101(2)ph | 9.610 | | 1.533 Y | 2.132 Y | 2.776 Y | 3.747 Y |
| M-N3h | M-2101(2)sh | 0.350 | | 1.440 N | 1.943 N | 2.447 N | 3.143 N |
| Macrocell test with mortar-wrapped specimens | | | | | | | |
| M-N2-50 | M-2205-50 | 5.653 | | 1.533 Y | 2.132 Y | 2.776 Y | 3.747 Y |
| M-N2-50 | M-2205p-50 | 5.653 | | 1.533 Y | 2.132 Y | 2.776 Y | 3.747 Y |
| M-N2-50 | M-2101(1)-50 | 3.762 | | 1.440 Y | 1.943 Y | 2.447 Y | 3.143 Y |
| M-N2-50 | M-2101(1)p-50 | 5.671 | | 1.533 Y | 2.132 Y | 2.776 Y | 3.747 Y |
| M-N2-50 | M-2101(2)-50 | 4.422 | | 1.533 Y | 2.132 Y | 2.776 Y | 3.747 Y |
| M-N2-50 | M-2101(2)p-50 | 5.650 | | 1.533 Y | 2.132 Y | 2.776 Y | 3.747 Y |
| Southern Exposure test | | | | | | | |
| SE-N-45 | SE-2205-45 | 6.343 | | 1.476 Y | 2.015 Y | 2.571 Y | 3.365 Y |
| SE-N-45 | SE-2205p-45 | 6.394 | | 1.476 Y | 2.015 Y | 2.571 Y | 3.365 Y |
| SE-N-45 | SE-2101(1)-45 | 2.808 | | 1.415 Y | 1.895 Y | 2.365 Y | 2.998 N |
| SE-N-45 | SE-2101(1)p-45 | 6.041 | | 1.476 Y | 2.015 Y | 2.571 Y | 3.365 Y |
| SE-N-45 | SE-2101(2)-45 | 6.182 | | 1.476 Y | 2.015 Y | 2.571 Y | 3.365 Y |
| SE-N-45 | SE-2101(2)p-45 | 6.400 | | 1.476 Y | 2.015 Y | 2.571 Y | 3.365 Y |
| SE-N-45 | SE-N/2205-45 | 0.588 | | 1.476 N | 2.015 N | 2.571 N | 3.365 N |
| SE-2205-45 | SE-2205/N-45 | -0.024 | | 1.476 N | 2.015 N | 2.571 N | 3.365 N |
| Cracked beam test | | | | | | | |
| CB-N-45 | CB-2205-45 | 9.394 | | 1.476 Y | 2.015 Y | 2.571 Y | 3.365 Y |
| CB-N-45 | CB-2205p-45 | 9.482 | | 1.476 Y | 2.015 Y | 2.571 Y | 3.365 Y |
| CB-N-45 | CB-2101(1)-45 | 6.979 | | 1.440 Y | 1.943 Y | 2.447 Y | 3.143 Y |
| CB-N-45 | CB-2101(1)p-45 | 9.057 | | 1.476 Y | 2.015 Y | 2.571 Y | 3.365 Y |
| CB-N-45 | CB-2101(2)-45 | 7.591 | | 1.476 Y | 2.015 Y | 2.571 Y | 3.365 Y |
| CB-N-45 | CB-2101(2)p-45 | 9.488 | | 1.476 Y | 2.015 Y | 2.571 Y | 3.365 Y |

$t_{stat}$: t-test statistic, $t_{crit}$: value of t calculated from Student's t-distribution, α: level of significance, X%: confidence level, Y: statistically significant difference, i.e. null hypothesis rejected, N: not statistically significant difference, i.e. null hypothesis rejected.

* T - A - B

**T**: test → M: macrocell test, SE: Southern Exposure test, CB: cracked beam test

**A**: steel type → N, N2, and N3: conventional, normalized steel, 2101(1) and 2101(2): duplex stainless steel (21% chromium, 1% nickel), 2205: duplex stainless steel (25% chromium, 5% nickel), p: pickled, s: sandblasted, h: 6.04 m ion concentration.

**B**: mix design → 50: water-cement ratio of 0.50 and no inhibitor, 45: water-cement ratio of 0.45 and no inhibitor.

**Table C.14 –** Student's t-test for comparing mean corrosion losses of pickled and non-pickled duplex steels.

| Specimens * | | $t_{stat}$ | $t_{crit}$ X%: | 80% | 90% | 95% | 98% |
|---|---|---|---|---|---|---|---|
| | | | α: | 0.20 | 0.10 | 0.05 | 0.02 |
| Macrocell test with bare specimens in 1.6 m ion NaCl | | | | | | | |
| M-2205 | M-2205p | 2.010 | | 1.533 Y | 2.132 N | 2.776 N | 3.747 N |
| M-2101(1) | M-2101(1)p | 1.960 | | 1.533 Y | 2.132 N | 2.776 N | 3.747 N |
| M-2101(2) | M-2101(2)p | 8.480 | | 1.476 Y | 2.015 Y | 2.571 Y | 3.365 Y |
| M-2205p | M-2101(2)p | -0.980 | | 1.476 N | 2.015 N | 2.571 N | 3.365 N |
| Macrocell test with bare specimens in 6.04 m ion NaCl | | | | | | | |
| M-2205h | M-2205ph | 8.570 | | 1.476 Y | 2.015 Y | 2.571 Y | 3.365 Y |
| M-2101(1)h | M-2101(1)ph | 3.120 | | 1.415 Y | 1.895 Y | 2.365 Y | 2.998 Y |
| M-2101(2)h | M-2101(2)ph | 13.110 | | 1.476 Y | 2.015 Y | 2.571 Y | 3.365 Y |
| M-2205ph | M-2101(2)ph | -3.490 | | 1.476 Y | 2.015 Y | 2.571 Y | 3.365 Y |
| Macrocell test with mortar-wrapped specimens | | | | | | | |
| M-2205-50 | M-2205p-50 | -0.019 | | 1.383 N | 1.833 N | 2.262 N | 2.821 N |
| M-2101(1)-50 | M-2101(1)p-50 | 2.828 | | 1.638 Y | 2.353 Y | 3.182 N | 4.541 N |
| M-2101(2)-50 | M-2101(2)p-50 | 6.169 | | 1.476 Y | 2.015 Y | 2.571 Y | 3.365 Y |
| M-2205p-50 | M-2101(2)p-50 | -0.409 | | 1.372 N | 1.812 N | 2.228 N | 2.764 N |
| Southern Exposure test | | | | | | | |
| SE-2205-45 | SE-2205p-45 | 1.138 | | 1.533 N | 2.132 N | 2.776 N | 3.747 N |
| SE-2101(1)-45 | SE-2101(1)p-45 | 3.147 | | 1.886 Y | 2.920 Y | 4.303 N | 6.965 N |
| SE-2101(2)-45 | SE-2101(2)p-45 | 2.138 | | 1.533 Y | 2.132 Y | 2.776 N | 3.747 N |
| SE-2205p-45 | SE-2101(2)p-45 | 1.243 | | 1.476 N | 2.015 N | 2.571 N | 3.365 N |
| Cracked beam test | | | | | | | |
| CB-2205-45 | CB-2205p-45 | 2.533 | | 1.533 Y | 2.132 Y | 2.776 N | 3.747 N |
| CB-2101(1)-45 | CB-2101(1)p-45 | 3.869 | | 1.886 Y | 2.920 Y | 4.303 N | 6.965 N |
| CB-2101(2)-45 | CB-2101(2)p-45 | 19.964 | | 1.533 Y | 2.132 Y | 2.776 Y | 3.747 Y |
| CB-2205p-45 | CB-2101(2)p-45 | 0.847 | | 1.397 N | 1.860 N | 2.306 N | 2.896 N |

$t_{stat}$: t-test statistic, $t_{crit}$: value of t calculated from Student's t-distribution, α: level of significance, X%: confidence level, Y: statistically significant difference, i.e. null hypothesis rejected, N: not statistically significant difference, i.e. null hypothesis rejected.

* T - A - B

**T**: test → M: macrocell test, SE: Southern Exposure test, CB: cracked beam test

**A**: steel type → 2101(1) and 2101(2): duplex stainless steel (21% chromium, 1% nickel), 2205: duplex stainless steel (25% chromium, 5% nickel), p: pickled, s: sandblasted, h: 6.04 m ion concentration.

**B**: mix design → 50: water-cement ratio of 0.50 and no inhibitor, 45: water-cement ratio of 0.45 and no inhibitor.

# APPENDIX D

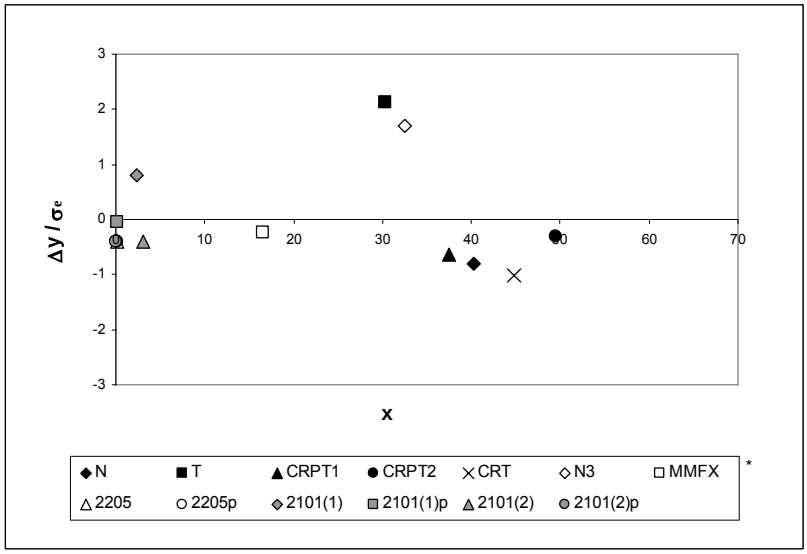


(a) Corrosion rates

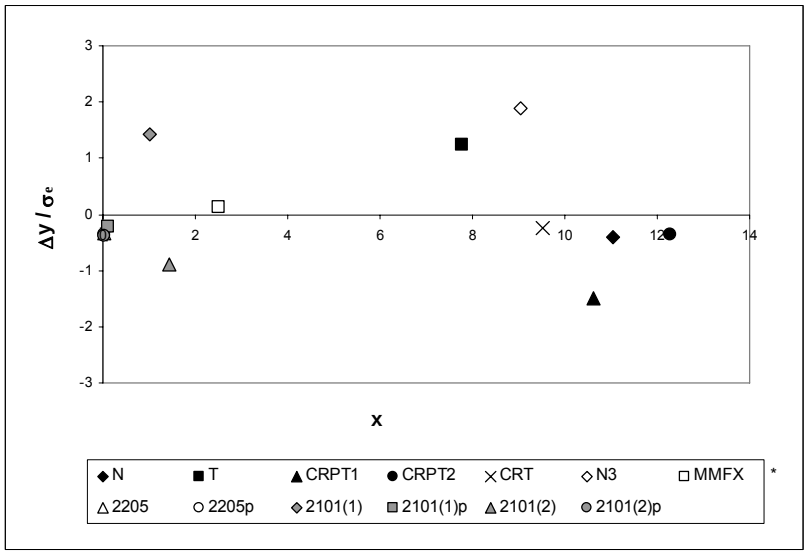


(b) Total corrosion losses

*** Steel type** → N and N3: conventional, normalized steel, T: Thermex-treated conventional steel, CRPT1: Thermex- treated microalloyed steel with a high phosphorus content (0.117%), CRPT2: Thermex-treated microalloyed steel with a high phosphorus content (0.100%), CRT: Thermex treated microalloyed steel with normal phosphorus content (0.017%), 2101(1) and 2101(2): duplex stainless steel (21% chromium, 1% nickel), 2205: duplex stainless steel (25% chromium, 5% nickel), p: pickled.

**Figure D.1 –** Distribution of standardized residuals for Southern Exposure test versus rapid macrocell test with bare bars in 1.6 m ion NaCl and simulated concrete pore solution. (a) Corrosion rates and (b) total corrosion losses.

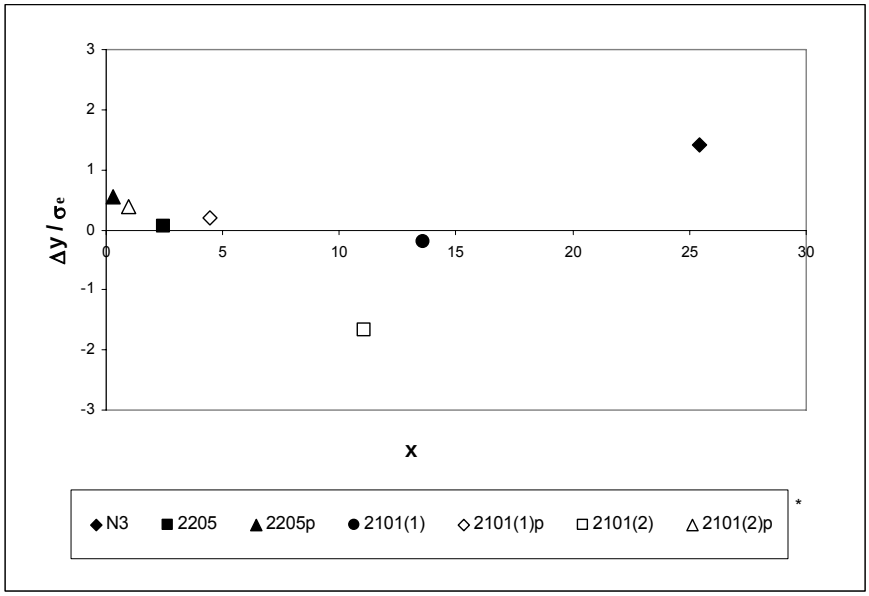


(a) Corrosion rates

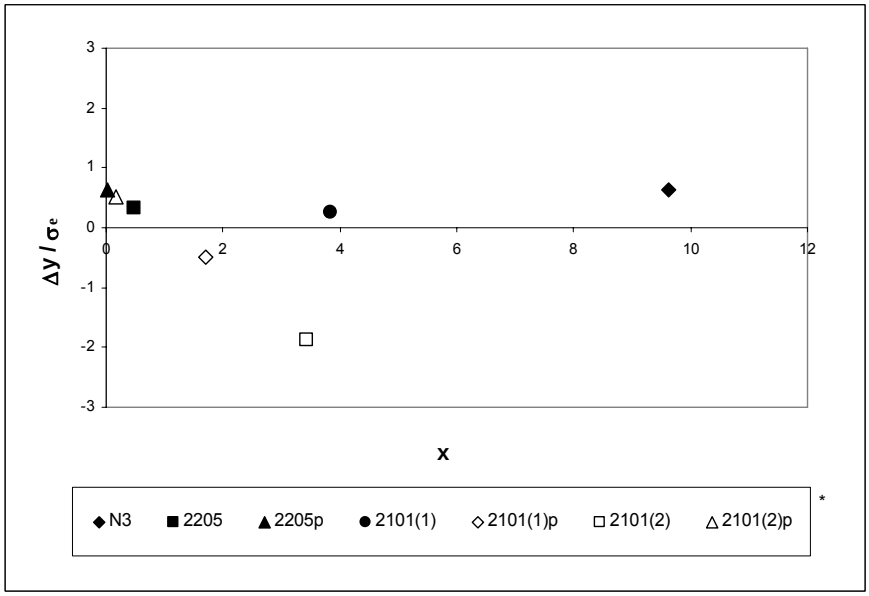


(b) Total corrosion losses

*** Steel type** → N3: conventional, normalized steel, 2101(1) and 2101(2): duplex stainless steel (21% chromium, 1% nickel), 2205: duplex stainless steel (25% chromium, 5% nickel), p: pickled.

**Figure D.2 –** Distribution of standardized residuals for Southern Exposure test versus rapid macrocell test with bare bars in 6.04 m ion NaCl and simulated concrete pore solution. (a) Corrosion rates and (b) total corrosion losses.

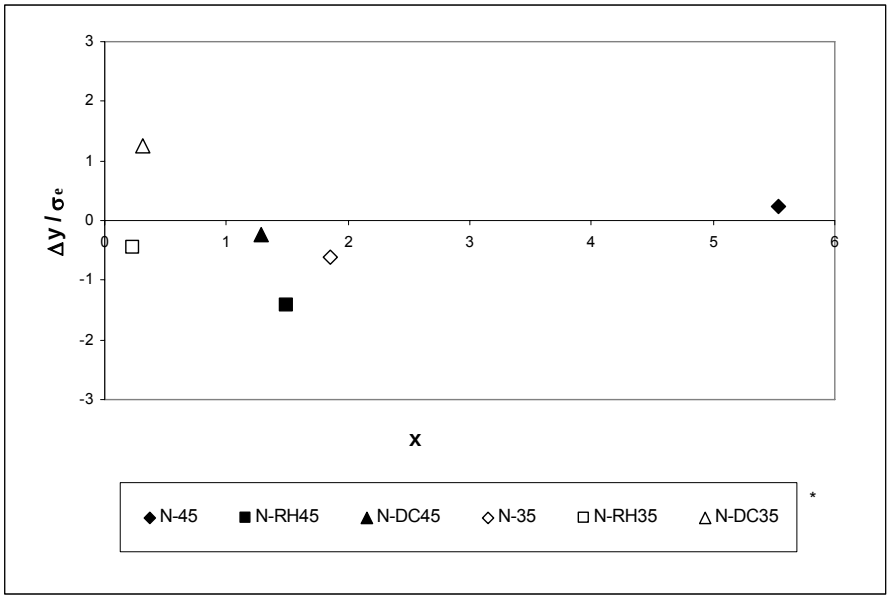


(a) Corrosion rates

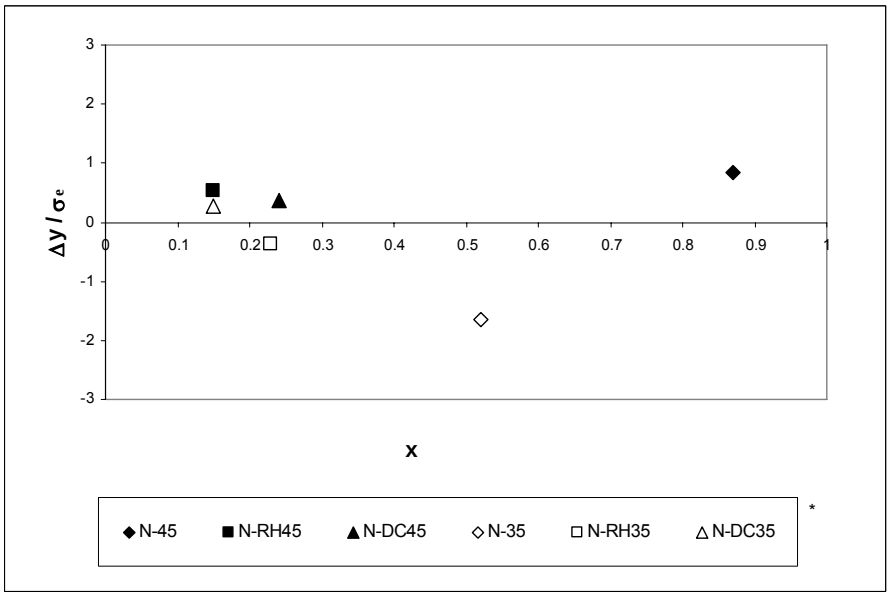


(b) Total corrosion losses

* A-B
A: steel type → N: conventional, normalized steel.
B: mix design → 45: water-cement ratio of 0.45 and no inhibitor, RH45: water-cement ratio of 0.45 and Rheocrete 222+, DC45: water-cement ratio of 0.45 and DCI-S, 35: water-cement ratio of 0.35 and no inhibitor, RH35: water-cement ratio of 0.35 and Rheocrete 222+, DC35: water-cement ratio of 0.35 and DCI-S.

**Figure D.3 –** Distribution of standardized residuals for Southern Exposure test versus rapid macrocell test with lollipop specimens in 1.6 m ion NaCl and simulated concrete pore solution. (a) Corrosion rates, (b) total corrosion losses.

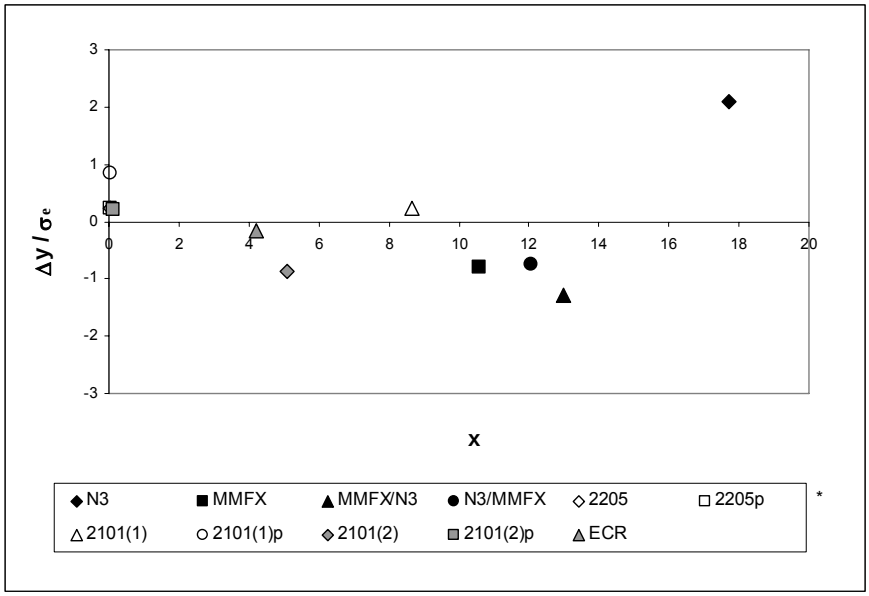


(a) Corrosion rates

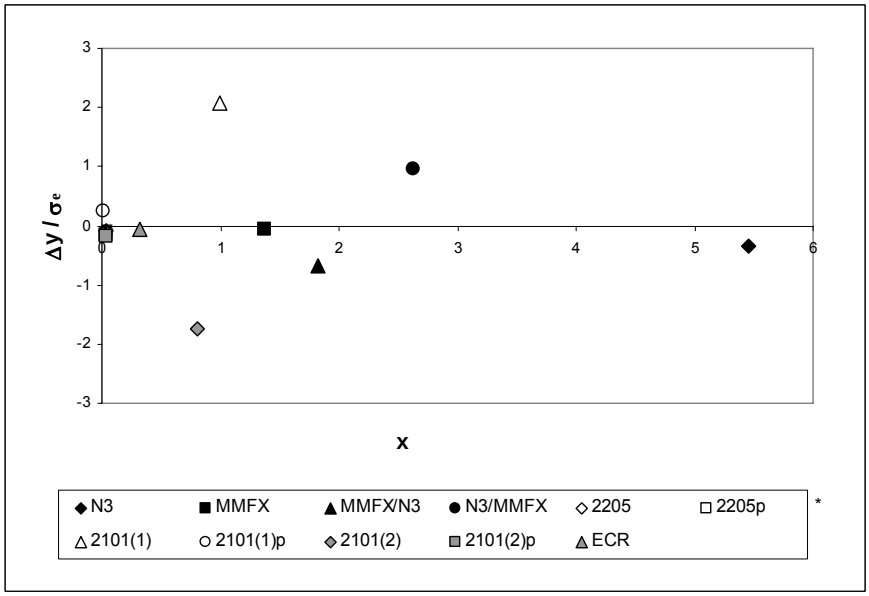


(b) Total corrosion losses

*** Steel type →** N3: conventional, normalized steel, MMFX: MMFX microcomposite steel, MMFX/N3: MMFX steel in the top mat and N3 steel in the bottom mat, N3/MMFX: N3 steel in the top mat and MMFX steel in the bottom mat, 2101(1) and 2101(2): duplex stainless steel (21% chromium, 1% nickel), 2205: duplex stainless steel (25% chromium, 5% nickel), ECR: epoxy-coated steel, p: pickled.

**Figure D.4 –** Distribution of standardized residuals for Southern Exposure test versus rapid macrocell test with mortar-wrapped specimens in 1.6 m ion NaCl and simulated concrete pore solution. (a) Corrosion rates, (b) total corrosion losses.

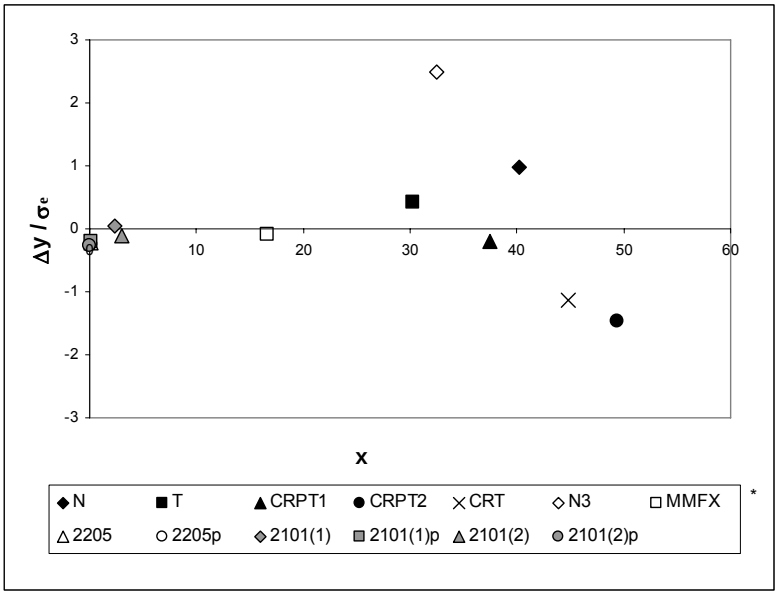


(a) Corrosion rates

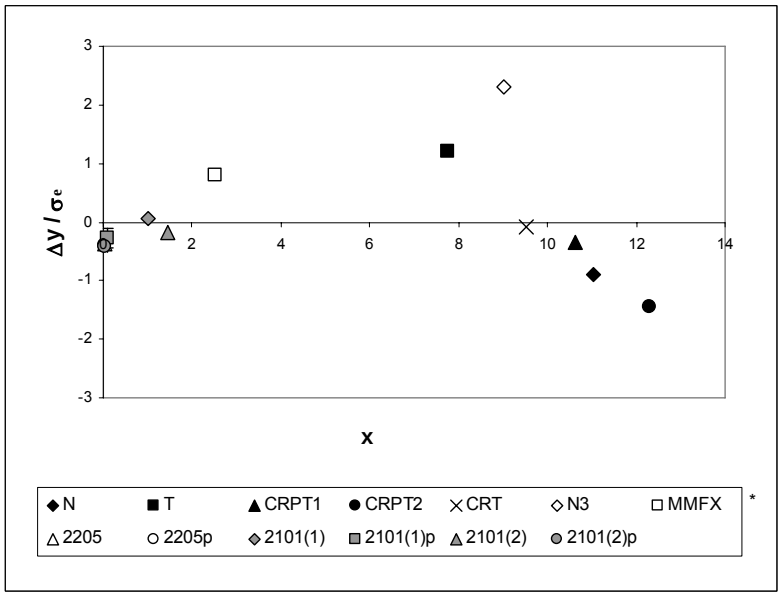


(b) Total corrosion losses

*** Steel type** → N and N3: conventional, normalized steel, T: Thermex-treated conventional steel, CRPT1: Thermex- treated microalloyed steel with a high phosphorus content (0.117%), CRPT2: Thermex-treated microalloyed steel with a high phosphorus content (0.100%), CRT: Thermex treated microalloyed steel with normal phosphorus content (0.017%), 2101(1) and 2101(2): duplex stainless steel (21% chromium, 1% nickel), 2205: duplex stainless steel (25% chromium, 5% nickel), p: pickled.

**Figure D.5 –** Distribution of standardized residuals for cracked beam test versus rapid macrocell test with bare bars in 1.6 m ion NaCl and simulated concrete pore solution. (a) Corrosion rates and (b) total corrosion losses.

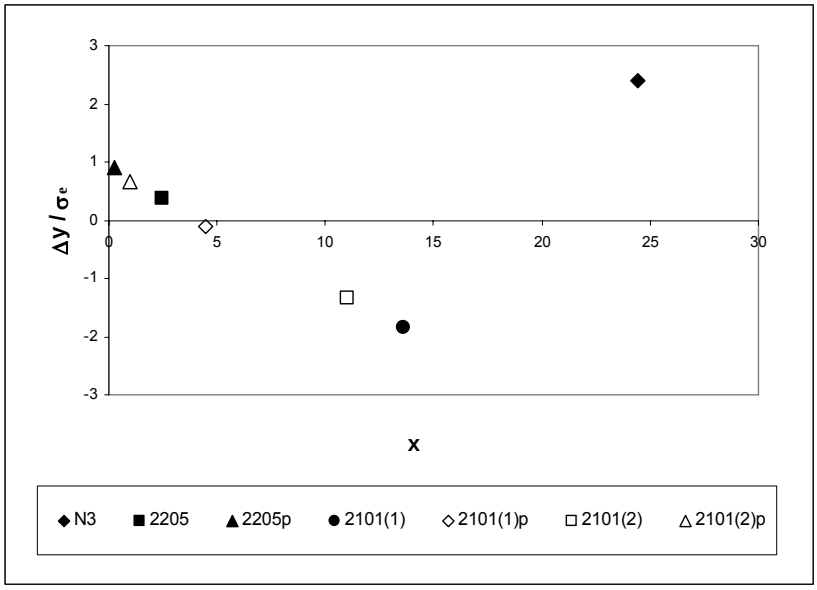


(a) Corrosion rates

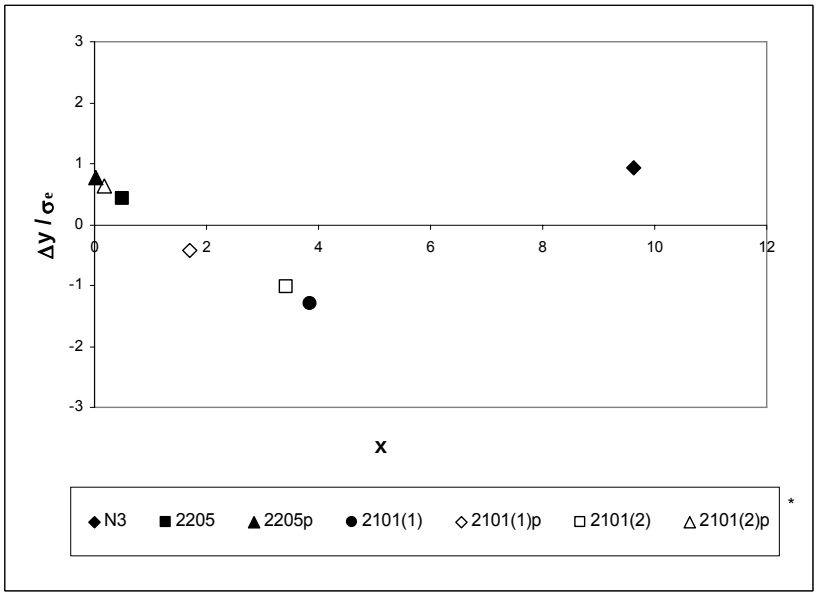


(b) Total corrosion losses

*** Steel type** → N3: conventional, normalized steel, 2101(1) and 2101(2): duplex stainless steel (21% chromium, 1% nickel), 2205: duplex stainless steel (25% chromium, 5% nickel), p: pickled.

**Figure D.6 –** Distribution of standardized residuals for cracked beam test versus rapid macrocell test with bare bars in 6.04 m ion NaCl and simulated concrete pore solution. (a) Corrosion rates and (b) total corrosion losses. (Results of cracked beam at week 70)

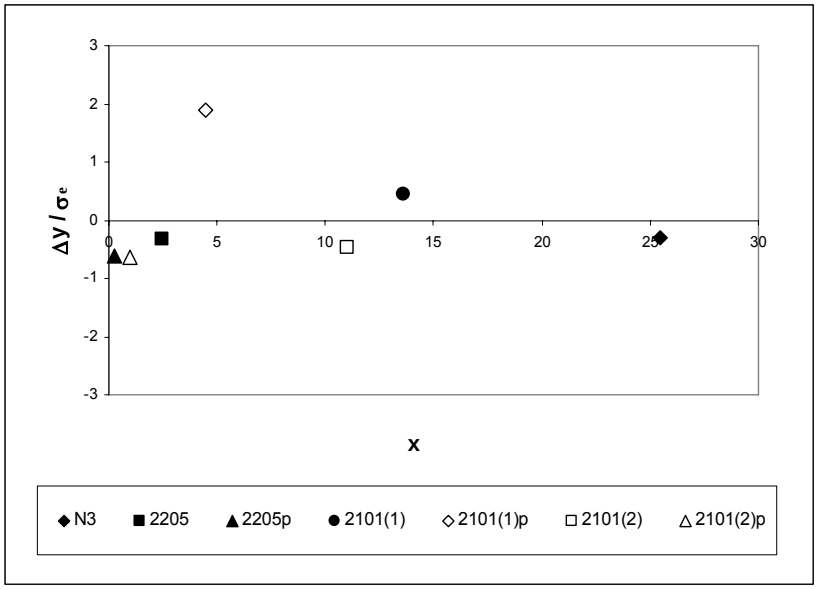


(a) Corrosion rates

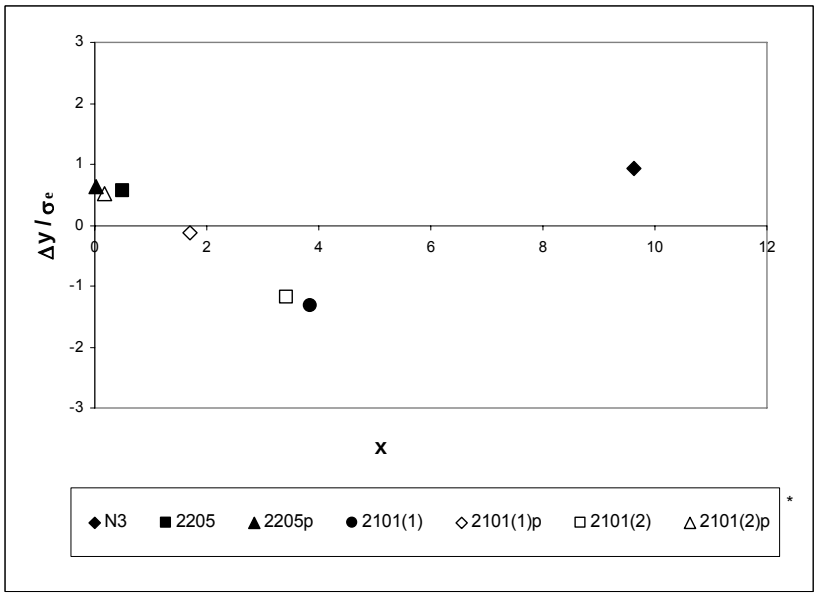


(b) Total corrosion losses

*** Steel type** → N3: conventional, normalized steel, 2101(1) and 2101(2): duplex stainless steel (21% chromium, 1% nickel), 2205: duplex stainless steel (25% chromium, 5% nickel), p: pickled.

**Figure D.7 –** Distribution of standardized residuals for cracked beam test versus rapid macrocell test with bare bars in 6.04 m ion NaCl and simulated concrete pore solution. (a) Corrosion rates and (b) total corrosion losses. (Results of cracked beam at week 96).

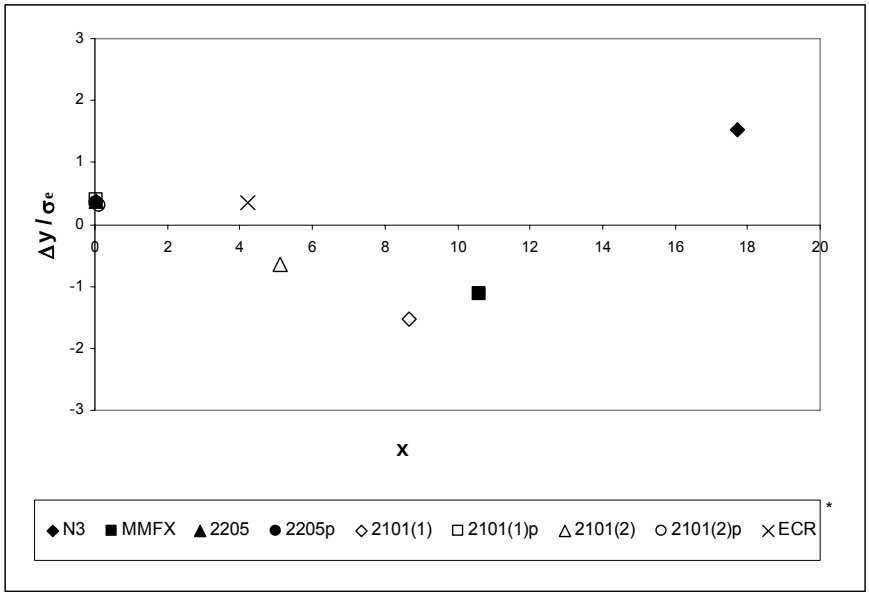


(a) Corrosion rates

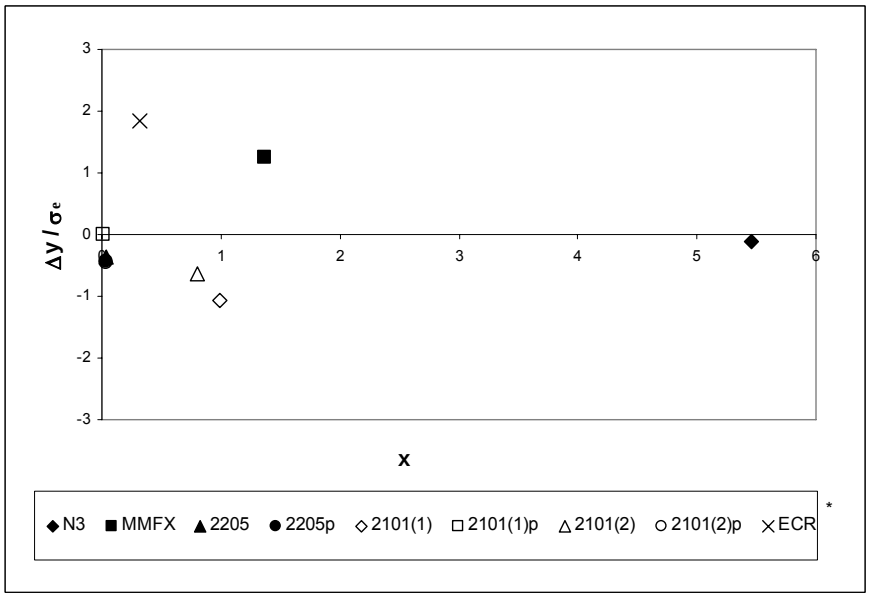


(b) Total corrosion losses

*** Seel type** → N3: conventional, normalized steel, MMFX: MMFX microcomposite steel, 2101(1) and 2101(2): duplex stainless steel (21% chromium, 1% nickel), 2205: duplex stainless steel (25% chromium, 5% nickel), ECR: epoxy-coated steel, p: pickled.

**Figure D.8 –** Distribution of standardized residuals for cracked beam test versus rapid macrocell test with mortar-wrapped specimens in 1.6 m ion NaCl and simulated concrete pore solution. (a) Corrosion rates, (b) total corrosion losses.

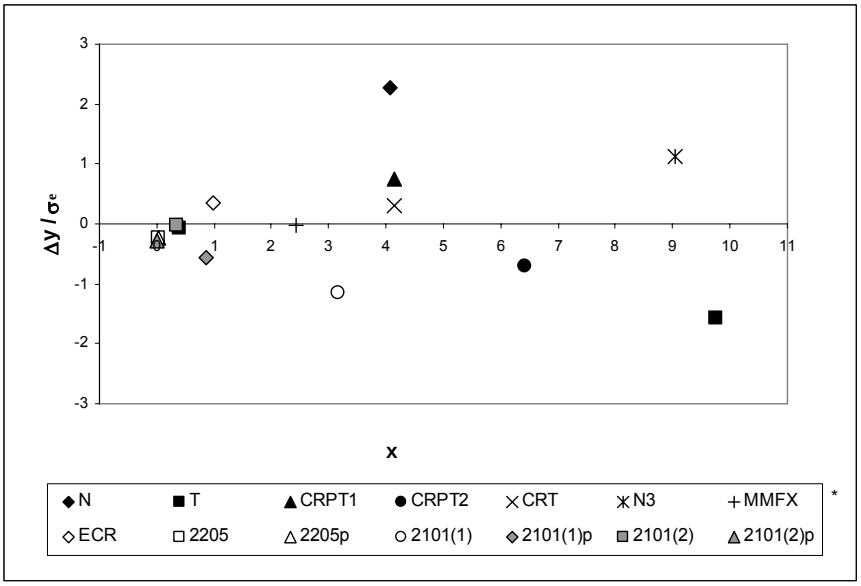


(a) Corrosion rates

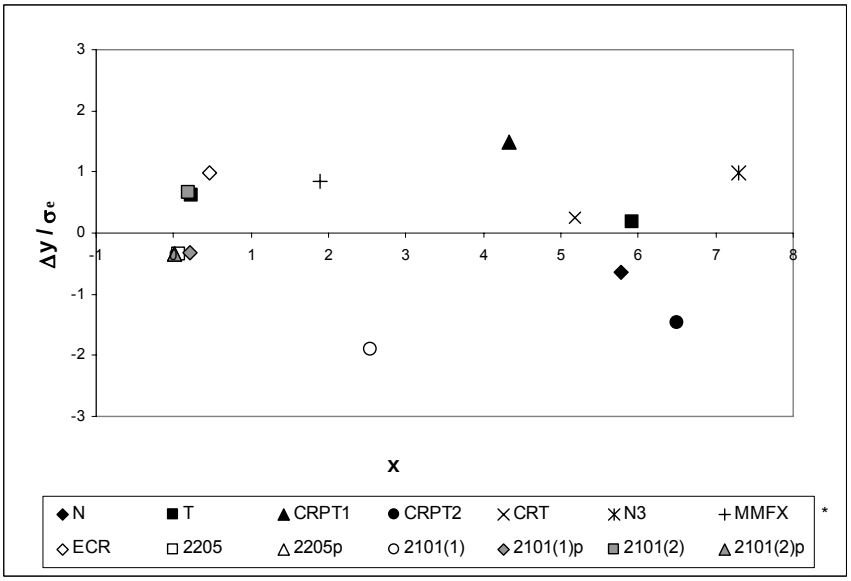


(b) Total corrosion losses

*** Steel type** → N and N3: conventional, normalized steel, T: Thermex-treated conventional steel, CRPT1: Thermex- treated microalloyed steel with a high phosphorus content (0.117%), CRPT2: Thermex-treated microalloyed steel with a high phosphorus content (0.100%), CRT: Thermex treated microalloyed steel with normal phosphorus content (0.017%), MMFX, MMFX microcomposite steel, ECR: epoxy-coated steel, 2101(1) and 2101(2): duplex stainless steel (21% chromium, 1% nickel), 2205: duplex stainless steel (25% chromium, 5% nickel), p: pickled.

**Figure D.9 –** Distribution of standardized residuals for cracked beam test versus Southern Exposure test for specimens with different reinforcing steel. (a) Corrosion rates, (b) total corrosion losses.

# APPENDIX E

**Table E.1 –** Ratio of corrosion rates and total corrosion losses between the Southern Exposure test and the rapid macrocell test with bare bars in 1.6 m ion NaCl and simulated concrete pore solution.

| Steel type * | Corrosion rates | | | Total corrosion losses | | |
|---|---|---|---|---|---|---|
| | Macrocell 1.6 m | Southern Exposure | Ratio SE/macrocell | Macrocell 1.6 m | Southern Exposure | Ratio SE/macrocell |
| **N** | 40.21 | 4.07 | 0.10 | 11.03 | 5.78 | 0.52 |
| **T** | 30.32 | 9.76 | 0.32 | 7.77 | 5.92 | 0.76 |
| **CRPT1** | 37.42 | 4.14 | 0.11 | 10.63 | 4.34 | 0.41 |
| **CRPT2** | 49.43 | 6.43 | 0.13 | 12.29 | 6.50 | 0.53 |
| **CRT** | 44.84 | 4.14 | 0.09 | 9.53 | 5.18 | 0.54 |
| **N3** | 35.88 | 9.05 | 0.25 | 9.03 | 7.30 | 0.81 |
| **MMFX** | 16.61 | 2.44 | 0.15 | 2.51 | 1.89 | 0.75 |
| **2205** | 0.13 | 0.02 | 0.15 | 0.04 | 0.06 | 1.50 |
| **2205p** | 0.09 | 0.02 | 0.22 | 0.02 | 0.02 | 1.00 |
| **2101(1)** | 2.39 | 3.16 | 1.32 | 1.01 | 2.55 | 2.52 |
| **2101(1)p** | 0.17 | 0.85 | 5.00 | 0.10 | 0.21 | 2.10 |
| **2101(2)** | 3.05 | 0.35 | 0.11 | 1.45 | 0.19 | 0.13 |
| **2101(2)p** | 0.04 | 0.00 | 0.00 | 0.04 | 0.01 | 0.25 |

- **Steel type** → N and N3: conventional, normalized steel, T: Thermex-treated conventional steel, CRPT1: Thermex-treated microalloyed steel with a high phosphorus content (0.117%), CRPT2: Thermex-treated microalloyed steel with a high phosphorus content (0.100%), CRT: Thermex treated microalloyed steel with normal phosphorus content (0.017%), 2101(1) and 2101(2): duplex stainless steel (21% chromium, 1% nickel), 2205: duplex stainless steel (25% chromium, 5% nickel), p: pickled.

**Table E.2 –** Ratio of corrosion rates and total corrosion losses between the Southern Exposure test and the rapid macrocell test with bare bars in 6.04 m ion NaCl and simulated concrete pore solution.

| Steel type * | Corrosion rates | | | Total corrosion losses | | |
|---|---|---|---|---|---|---|
| | Macrocell 6.04 m | Southern Exposure | Ratio SE/macrocell | Macrocell 6.04 m | Southern Exposure | Ratio SE/macrocell |
| **N3** | 25.46 | 9.05 | 0.36 | 9.63 | 7.30 | 0.76 |
| **2205** | 2.47 | 0.02 | 0.01 | 0.49 | 0.06 | 0.12 |
| **2205p** | 0.28 | 0.02 | 0.07 | 0.03 | 0.02 | 0.67 |
| **2101(1)** | 13.61 | 3.16 | 0.23 | 3.84 | 2.55 | 0.66 |
| **2101(1)p** | 4.46 | 0.85 | 0.19 | 1.70 | 0.21 | 0.12 |
| **2101(2)** | 11.04 | 0.35 | 0.03 | 3.43 | 0.19 | 0.06 |
| **2101(2)p** | 0.96 | 0.00 | 0.00 | 0.17 | 0.01 | 0.06 |

*** Steel type** → N3: conventional, normalized steel, 2101(1) and 2101(2): duplex stainless steel (21% chromium, 1% nickel), 2205: duplex stainless steel (25% chromium, 5% nickel), p: pickled.

**Table E.3 –** Ratio of corrosion rates and total corrosion losses between the Southern Exposure test and the rapid macrocell test with lollipop specimens in 1.6 m ion NaCl and simulated concrete pore solution.

| Specimen designation * | Corrosion rates | | | Total corrosion losses | | |
|---|---|---|---|---|---|---|
| | Macrocell lollipop | Southern Exposure | Ratio SE/macrocell | Macrocell lollipop | Southern Exposure | Ratio SE/macrocell |
| **N-45** | 5.54 | 4.07 | 0.73 | 0.87 | 5.78 | 6.64 |
| **N-RH45** | 1.50 | 0.68 | 0.45 | 0.15 | 0.51 | 3.40 |
| **N-DC45** | 1.28 | 0.86 | 0.67 | 0.24 | 0.95 | 3.96 |
| **N-35** | 1.85 | 1.17 | 0.63 | 0.52 | 0.71 | 1.37 |
| **N-RH35** | 0.23 | 0.04 | 0.17 | 0.23 | 0.10 | 0.43 |
| **N-DC35** | 0.32 | 0.60 | 1.88 | 0.15 | 0.24 | 1.60 |

* A-B

A: steel type → N: conventional, normalized steel.

B: mix design → 45: water-cement ratio of 0.45 and no inhibitor, RH45: water-cement ratio of 0.45 and Rheocrete 222+, DC45: water-cement ratio of 0.45 and DCI-S, 35: water-cement ratio of 0.35 and no inhibitor, RH35: water-cement ratio of 0.35 and Rheocrete 222+, DC35: water-cement ratio of 0.35 and DCI-S.

**Table E.4 –** Ratio of corrosion rates and total corrosion losses between the Southern Exposure test and the rapid macrocell test with mortar-wrapped specimens in 1.6 m ion NaCl and simulated concrete pore solution.

| Steel type * | Corrosion rates | | | Total corrosion losses | | |
|---|---|---|---|---|---|---|
| | Macrocell mortar-wrapped | Southern Exposure | Ratio SE/macrocell | Macrocell mortar-wrapped | Southern Exposure | Ratio SE/macrocell |
| **N3** | 17.70 | 9.05 | 0.51 | 5.46 | 7.30 | 1.34 |
| **MMFX** | 10.59 | 2.44 | 0.23 | 1.37 | 1.89 | 1.38 |
| **MMFX/N3** | 12.98 | 2.65 | 0.20 | 1.82 | 2.17 | 1.19 |
| **N3/MMFX** | 12.05 | 3.07 | 0.25 | 2.63 | 4.77 | 1.81 |
| **2205** | 0.03 | 0.02 | 0.67 | 0.03 | 0.06 | 2.00 |
| **2205p** | 0.06 | 0.02 | 0.33 | 0.03 | 0.02 | 0.67 |
| **2101(1)** | 8.68 | 3.16 | 0.36 | 0.99 | 2.55 | 2.58 |
| **2101(1)p** | 0.02 | 0.85 | 42.50 | 0.01 | 0.21 | 21.00 |
| **2101(2)** | 5.11 | 0.35 | 0.07 | 0.80 | 0.19 | 0.24 |
| **2101(2)p** | 0.11 | 0.00 | 0.00 | 0.03 | 0.01 | 0.33 |
| **ECR** | 4.20 | 0.99 | 0.24 | 0.32 | 0.47 | 1.47 |

*** Steel type →** N3: conventional, normalized steel, MMFX: MMFX microcomposite steel, MMFX/N3: MMFX steel in the top mat and N3 steel in the bottom mat, N3/MMFX: N3 steel in the top mat and MMFX steel in the bottom mat, 2101(1) and 2101(2): duplex stainless steel (21% chromium, 1% nickel), 2205: duplex stainless steel (25% chromium, 5% nickel), ECR: epoxy-coated steel, p: pickled.

**Table E.5 –** Ratio of corrosion rates and total corrosion losses between the cracked beam test and the rapid macrocell test with bare bars in 1.6 m ion NaCl and simulated concrete pore solution.

| Steel type * | Corrosion rates | | | Total corrosion losses | | |
|---|---|---|---|---|---|---|
| | Macrocell 1.6 m | Cracked beam | Ratio CB/macrocell | Macrocell 1.6 m | Cracked beam | Ratio CB/macrocell |
| **N** | 40.21 | 7.34 | 0.18 | 11.03 | 7.51 | 0.68 |
| **T** | 30.37 | 5.07 | 0.17 | 7.77 | 8.72 | 1.12 |
| **CRPT1** | 37.42 | 4.83 | 0.13 | 10.63 | 8.17 | 0.77 |
| **CRPT2** | 49.43 | 4.08 | 0.08 | 12.29 | 7.50 | 0.61 |
| **CRT** | 44.84 | 4.08 | 0.09 | 9.53 | 7.79 | 0.82 |
| **N3** | 35.88 | 9.09 | 0.25 | 9.03 | 11.60 | 1.28 |
| **MMFX** | 16.61 | 2.25 | 0.14 | 2.51 | 4.03 | 1.61 |
| **2205** | 0.13 | 0.11 | 0.85 | 0.04 | 0.08 | 2.00 |
| **2205p** | 0.09 | 0.08 | 0.89 | 0.02 | 0.02 | 1.00 |
| **2101(1)** | 2.39 | 0.87 | 0.36 | 1.01 | 1.57 | 1.55 |
| **2101(1)p** | 0.17 | 0.15 | 0.88 | 0.10 | 0.30 | 3.00 |
| **2101(2)** | 3.05 | 0.70 | 0.23 | 1.45 | 1.48 | 1.02 |
| **2101(2)p** | 0.04 | 0.02 | 0.50 | 0.04 | 0.01 | 0.25 |

*** Steel type →** N and N3: conventional, normalized steel, T: Thermex-treated conventional steel, CRPT1: Thermex- treated microalloyed steel with a high phosphorus content (0.117%), CRPT2: Thermex-treated microalloyed steel with a high phosphorus content (0.100%), CRT: Thermex treated microalloyed steel with normal phosphorus content (0.017%), 2101(1) and 2101(2): duplex stainless steel (21% chromium, 1% nickel), 2205: duplex stainless steel (25% chromium, 5% nickel), p: pickled.

**Table E.6 –** Ratio of corrosion rates and total corrosion losses between the cracked beam test (at week 70) and the rapid macrocell test with bare bars in 6.04 m ion NaCl and simulated concrete pore solution.

| Steel type * | Corrosion rates | | | Total corrosion losses | | |
|---|---|---|---|---|---|---|
| | Macrocell 6.04 m | Cracked beam | Ratio CB/macrocell | Macrocell 6.04 m | Cracked beam | Ratio CB/macrocell |
| **N3** | 25.46 | 9.09 | 0.36 | 9.63 | 11.60 | 1.20 |
| **2205** | 2.47 | 0.11 | 0.04 | 0.49 | 0.08 | 0.16 |
| **2205p** | 0.28 | 0.08 | 0.29 | 0.03 | 0.02 | 0.67 |
| **2101(1)** | 13.61 | 0.87 | 0.06 | 3.84 | 1.57 | 0.41 |
| **2101(1)p** | 4.46 | 0.15 | 0.03 | 1.70 | 0.30 | 0.18 |
| **2101(2)** | 11.04 | 0.70 | 0.06 | 3.43 | 1.48 | 0.43 |
| **2101(2)p** | 0.96 | 0.02 | 0.02 | 0.17 | 0.01 | 0.06 |

*** Steel type →** N3: conventional, normalized steel, 2101(1) and 2101(2): duplex stainless steel (21% chromium, 1% nickel), 2205: duplex stainless steel (25% chromium, 5% nickel), p: pickled.

**Table E.7 –** Ratio of corrosion rates and total corrosion losses between the cracked beam test (at week 96) and the rapid macrocell test with bare bars in 6.04 m ion NaCl and simulated concrete pore solution.

| Steel type * | Corrosion rates | | | Total corrosion losses | | |
|---|---|---|---|---|---|---|
| | Macrocell 6.04 m | Cracked beam | Ratio CB/macrocell | Macrocell 6.04 m | Cracked beam | Ratio CB/macrocell |
| **N3** | 25.46 | 1.41 | 0.06 | 9.63 | 13.87 | 1.44 |
| **2205** | 2.47 | 0.37 | 0.15 | 0.49 | 0.24 | 0.49 |
| **2205p** | 0.28 | 0.01 | 0.04 | 0.03 | 0.02 | 0.67 |
| **2101(1)** | 13.61 | 1.57 | 0.12 | 3.84 | 2.17 | 0.57 |
| **2101(1)p** | 4.46 | 2.45 | 0.55 | 1.70 | 1.13 | 0.66 |
| **2101(2)** | 11.04 | 0.63 | 0.06 | 3.43 | 1.83 | 0.53 |
| **2101(2)p** | 0.96 | 0.02 | 0.02 | 0.17 | 0.02 | 0.12 |

*** Steel type** → N3: conventional, normalized steel, 2101(1) and 2101(2): duplex stainless steel (21% chromium, 1% nickel), 2205: duplex stainless steel (25% chromium, 5% nickel), p: pickled.

**Table E.8 –** Ratio of corrosion rates and total corrosion losses between the cracked beam test and the rapid macrocell test with mortar-wrapped specimens in 1.6 m ion NaCl and simulated concrete pore solution.

| Steel type * | Corrosion rates | | | Total corrosion losses | | |
|---|---|---|---|---|---|---|
| | Macrocell mortar-wrapped | Cracked beam | Ratio CB/macrocell | Macrocell mortar-wrapped | Cracked beam | Ratio CB/macrocell |
| **N3** | 17.7 | 9.09 | 0.51 | 5.46 | 11.6 | 2.12 |
| **MMFX** | 10.59 | 2.25 | 0.21 | 1.37 | 4.03 | 2.94 |
| **2205** | 0.03 | 0.11 | 3.67 | 0.03 | 0.08 | 2.67 |
| **2205p** | 0.06 | 0.08 | 1.33 | 0.03 | 0.02 | 0.67 |
| **2101(1)** | 8.68 | 0.87 | 0.10 | 0.99 | 1.57 | 1.59 |
| **2101(1)p** | 0.02 | 0.15 | 7.50 | 0.01 | 0.3 | 30.00 |
| **2101(2)** | 5.11 | 0.7 | 0.14 | 0.8 | 1.48 | 1.85 |
| **2101(2)p** | 0.11 | 0.02 | 0.18 | 0.03 | 0.01 | 0.33 |
| **ECR** | 4.2 | 1.79 | 0.43 | 0.32 | 2.26 | 7.06 |

*** Steel type** → N and N3: conventional, normalized steel, T: Thermex-treated conventional steel, CRPT1: Thermex- treated microalloyed steel with a high phosphorus content (0.117%), CRPT2: Thermex-treated microalloyed steel with a high phosphorus content (0.100%), CRT: Thermex treated microalloyed steel with normal phosphorus content (0.017%), MMFX, MMFX microcomposite steel, ECR: epoxy-coated steel, 2101(1) and 2101(2): duplex stainless steel (21% chromium, 1% nickel), 2205: duplex stainless steel (25% chromium, 5% nickel), p: pickled.

**Table E.9 –** Ratio of corrosion rates and total corrosion losses between the cracked beam test and the Southern Exposure test.

| Steel type * | Corrosion rates | | | Total corrosion losses | | |
|---|---|---|---|---|---|---|
| | Southern Exposure | Cracked beam | Ratio CB/SE | Southern Exposure | Cracked beam | Ratio CB/SE |
| **N** | 4.07 | 7.34 | 1.80 | 5.78 | 7.51 | 1.30 |
| **T** | 9.76 | 5.07 | 0.52 | 5.92 | 8.72 | 1.47 |
| **CRPT1** | 4.14 | 4.83 | 1.17 | 4.34 | 8.17 | 1.88 |
| **CRPT2** | 6.43 | 4.08 | 0.63 | 6.50 | 7.50 | 1.15 |
| **CRT** | 4.14 | 4.08 | 0.99 | 5.18 | 7.79 | 1.50 |
| **N3** | 9.05 | 9.09 | 1.00 | 7.30 | 11.60 | 1.59 |
| **MMFX** | 2.44 | 2.25 | 0.92 | 1.89 | 4.03 | 2.13 |
| **2205** | 0.02 | 0.11 | 5.50 | 0.06 | 0.08 | 1.33 |
| **2205p** | 0.02 | 0.08 | 4.00 | 0.02 | 0.02 | 1.00 |
| **2101(1)** | 3.16 | 0.87 | 0.28 | 2.55 | 1.57 | 0.62 |
| **2101(1)p** | 0.85 | 0.15 | 0.18 | 0.21 | 0.30 | 1.43 |
| **2101(2)** | 0.35 | 0.70 | 2.00 | 0.19 | 1.48 | 7.79 |
| **2101(2)p** | 0.00 | 0.02 | - | 0.01 | 0.01 | 1.00 |
| **ECR** | 0.99 | 1.79 | 1.81 | 0.47 | 2.26 | 4.81 |

*** Steel type** → N and N3: conventional, normalized steel, T: Thermex-treated conventional steel, CRPT1: Thermex- treated microalloyed steel with a high phosphorus content (0.117%), CRPT2: Thermex-treated microalloyed steel with a high phosphorus content (0.100%), CRT: Thermex treated microalloyed steel with normal phosphorus content (0.017%), MMFX, MMFX microcomposite steel, ECR: epoxy-coated steel, 2101(1) and 2101(2): duplex stainless steel (21% chromium, 1% nickel), 2205: duplex stainless steel (25% chromium, 5% nickel), p: pickled.